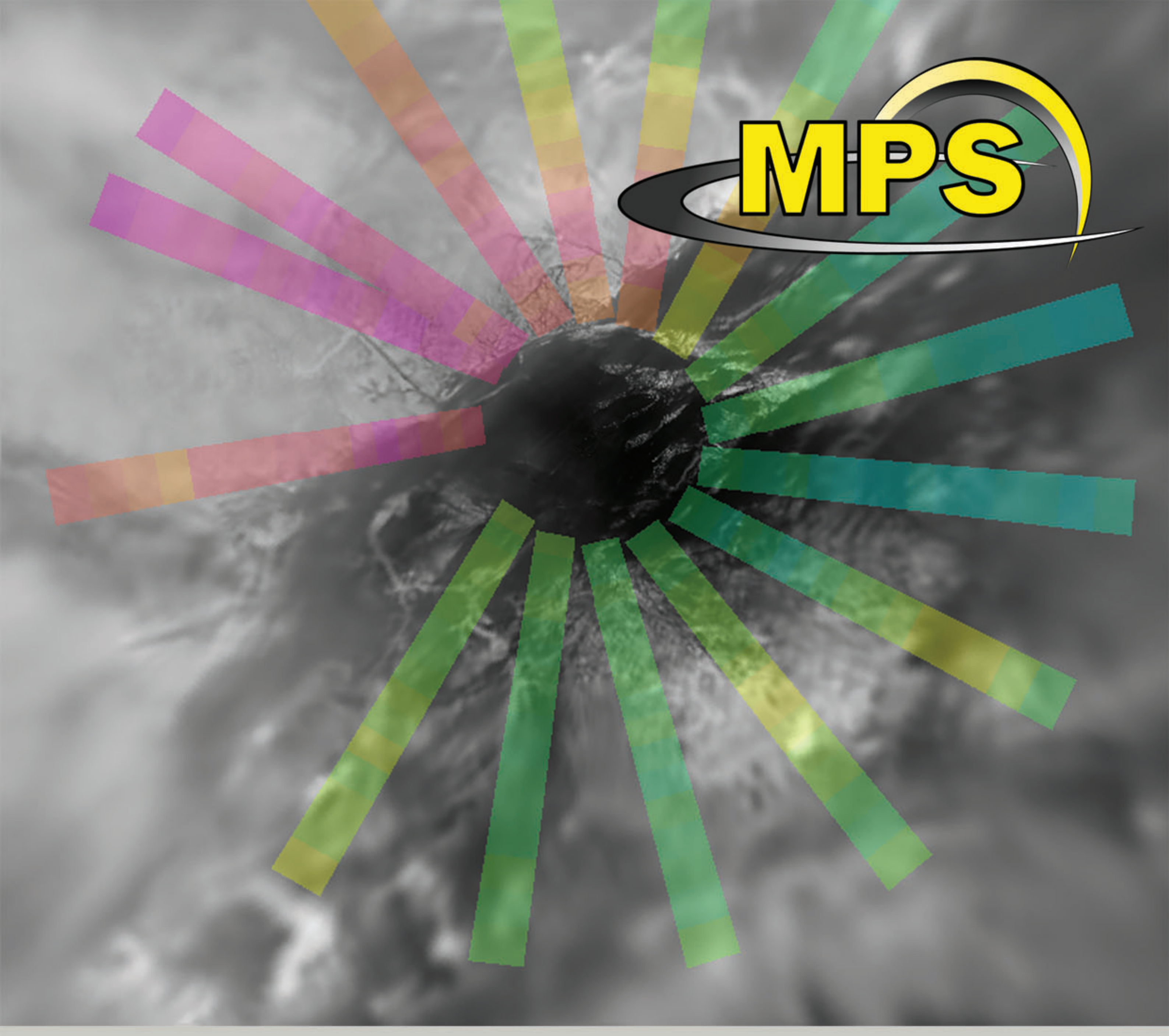

Max-Planck-Institut für Sonnensystemforschung Report 2004/2005

MAX-PLANCK-GESELLSCHAFT

MAX–PLANCK–INSTITUT FÜR SONNENSYSTEMFORSCHUNG

KATLENBURG–LINDAU

Report
für die Jahre 2004 und 2005

Herausgegeben von der Institutsleitung:	*Prof. Dr. Ulrich R. Christensen*
	Prof. Dr. Sami K. Solanki
	Prof. Dr. Vytenis M. Vasyliūnas

Redaktion:	*Dr. Johannes Wicht* *Dr. Patrick W. Daly* *Gerlinde Bierwirth*
Koordinatoren des wissenschaftlichen Teils:	*Dr. Hermann Böhnhardt* *Prof. Dr. Jörg Büchner* *Dr. Axel Korth* *Dr. Norbert Krupp*

Abbildung auf dem Frontumschlag:

Das schwarz-weiss Bild zeigt ein von der DISR-Kamera an Bord des ESA-lander Huygens aufgenommenes Panorama des Saturnmondes Titan. Darüber projeziert sind Streifen, deren Farbe die relative Intensität aus zwei Methan-Bändern im nahen Infrarot wiedergibt. Die optischen Komponenten der DISR-Kamera wurden am MPS unter der Leitung von Dr. H. U. Keller entwickelt und gebaut (siehe auch Seite 114).

Quellen: ESA, NASA, University of Arizona, MPS

Picture on the Cover:

A panorama of Titan's surface acquired by the DISR camera aboard the ESA Huygens lander. Overlaid are footprints of the visible spectrometer with false colours coding for the ratio of intensities in two methane windows. The DISR focal plane was built by an MPS team led by Dr. H. U. Keller (see also page 114).

Source: ESA, NASA, University of Arizona, MPS

Abbildung auf dem Rückumschlag:

Leistungsfähige moderne Labors und Werkstätten sind ein wichtiger Bestandteil des MPS. Dort integrieren und prüfen hochqualifizierte Mitarbeiter die empfindlichen Weltraumexperimente unter Reinraumbedingungen.

Picture on the Back:

Well-equipped modern laboratories and workshops are an important part of the MPS where highly qualified staff tests and assembles the very sensitive space experiments under clean-room conditions.

Erschienen im September 2006.

Anschrift:

Max-Planck-Institut für Sonnensystemforschung
Max-Planck-Straße 2
37191 Katlenburg-Lindau
Deutschland
Tel.: +49-(0) 5556-979-0
Fax: +49-(0) 5556-979-240
http://www.mps.mpg.de

Inhalt/Contents

Solar Transition region and corona

Solar wind and heliosphere

Past solar activity and Sun-Earth relations

Status of ongoing and future solar missions

Stars and extrasolar Systems

Fundamental Science

2 *Planeten, ihre natürlichen Satelliten und Kometen / Planets, their moons and comets*

Numerical simulation of planetary interiors

Terrestrial planets research – Mercury

Terrestrial planets research – Venus

Terrestrial planets research – Moon

Terrestrial planets research – Mars

General studies

3 Atmosphäre, Ionosphäre und Magnetosphäre der Erde / Terrestrial Atmosphere, Ionosphere, Magnetosphere

III Selbständige Nachwuchsgruppe Helio- und Asteroseismologie / Independent Junior Research Group of the Max Planck Society "Helio- and Asteroseismology"

IV International Max Planck Research School

V Rechenzentrum, Elektroniklabor, Mechanik, Haustechnik und Ausbildung / Computer Centre, Electronic Laboratory, Mechanics, Physical Plant and Education

VI Personelle Gliederung / Personnel

VII Wissenschaftliche Zusammenarbeit / Scientific Collaboration

VIII Berichte, Vorträge und Veröffentlichungen / Reports, Talks and Publications

I. **Allgemeines zum Institut**/Institute Overview

Gegenstand und Methoden der Forschung / Subject and Methods of Research

Die verschiedenen Objekte des Sonnensystems bilden den Gegenstand der Forschung am MPS. Ein großes Forschungsgebiet betrifft die Sonne, ihre Atmosphäre, das vom Sonnenwind beeinflusste interplanetare Medium, sowie den Einfluss der schwankenden solaren Partikel- und Wellenstrahlung auf die Erde und auf andere Planeten. Das zweite große Forschungsthema befasst sich mit dem Inneren, den Oberflächen, Atmosphären, Ionosphären und Magnetosphären der Planeten, ihrer Monde, sowie von Kometen und Asteroiden.

Eine wichtige Rolle spielt die Auswertung von Bildern und Spektren, die mit Instrumenten auf Raumsonden oder von erdgebundenen Teleskopen gewonnen werden. Damit werden die Sonne, Planeten (insbesondere Mars und Venus), Monde (Titan), Kometen und andere Kleinkörper erforscht. Die Korona der Sonne wird mit optischen Instrumenten im gesamten Spektralbereich vom Sichtbaren bis zum weichen Röntgenlicht vom Weltraum aus beobachtet, und ihre Plasmaeigenschaften werden mit spektroskopischen Methoden diagnostiziert. Die untere Atmosphäre der Sonne (die Photosphäre und Chromosphäre) wird anhand von spektropolarimetrischen Messungen sowohl vom Boden wie auch vom Weltraum aus untersucht. Dabei geht es vor allem um die Untersuchung des solaren Magnetfeldes, welches eine grundlegende Rolle für eine Vielzahl solarer Phänomene spielt. Ein neues Arbeitsgebiet ist die Untersuchung des Sonneninneren durch Analyse von beobachteten Schwingungen an ihrer Oberfläche (Helioseismologie). Geologische Vorgänge und die mineralogische Zusammensetzung an den Oberflächen planetarer Körper, sowie die Eigenschaften von Planetenatmosphären werden durch abbildende und spektrometrische Verfahren im sichtbaren Spektrum und nahen Infrarotbereich untersucht. In-situ-Methoden zur chemischen Untersuchung von Kometen- und Planetenoberflächen, sowie geophysikalische Untersuchungen des Planeteninneren werden in Zukunft eine Rolle spielen.

In den Magnetosphären der Erde und anderer Planeten, im Sonnenwind und in der Umgebung von Kometen werden Teilchen und Wellen von Instrumenten auf Raumsonden in-situ gemessen. Die chemische Zusammensetzung, die räumliche Verteilung der Teilchen sowie das Studium von Transportvorgängen und Beschleunigungsprozessen stehen dabei im Vordergrund. Bei der überwiegend experimentell ausgerichteten Arbeitsweise des Instituts spielt die Entwicklung und der Bau von Instrumenten und die Gewinnung und Auswertung von Messdaten eine Hauptrolle. Diese Aktivitäten werden jedoch intensiv von theoretischen Arbeiten und der Bildung von physikalischen Modellen begleitet. Das Schwergewicht liegt hierbei auf der numerischen Simulation in den Bereichen planetare und solare Dynamos, atmosphärische Zirkulationsmodelle, MHD-Prozesse in der Konvektionszone und Atmosphäre der Sonne, Physik ionosphärischer und magnetosphärischer Plasmen, Konvektionsströmungen im Gesteinsmantel terrestrischer Planeten und in den Gashüllen der Riesenplaneten.

The various objects of the solar system form the subject of research at MPS. One important area of research includes the Sun, its atmosphere, the interplanetary medium filled with solar wind, as well as the influence of the variable radiation of solar particles and waves on the Earth and other planets. The second major research field involves the interiors, surfaces, atmospheres, ionospheres, and magnetospheres of the planets and their moons, as well as those of comets and asteroids.

The analysis of images and spectra obtained from instruments on board spacecraft or from ground-based telescopes, play an important role for the exploration of the Sun, the planets (especially Mars and Venus), moons (Titan), comets, and other small bodies. The solar corona is observed with optical instruments in space in the entire spectral range from visible to soft x-rays, and their plasma properties are analysed by spectroscopic methods. The Sun's lower atmosphere (the photosphere and chromosphere) is investigated by means of spectral polarisation measurements, both from the ground and from space. In this case, it is the solar magnetic field that is of interest, which plays a fundamental role in a multitude of solar phenomena. A new field of endeavour is the study of the solar interior by analysing the observed oscillations on the surface (helioseismology). Geological processes and mineralogical composition on the surfaces *of planetary bodies, as well as the properties of the atmospheres of planets are investigated with imaging and spectrometric techniques in visible and near infrared regions. In-situ methods for chemical analysis if cometary and planetary surfaces, as well as geophysical investigations of the interiors of planets will play an important role in the future.*

In the magnetospheres of the Earth and other planets, in the solar wind and in the neighbourhood of comets, particles and waves are measured in-situ from space-borne instruments. The chemical composition, the spatial distribution of particles, and the study of transport mechanisms and energisation processes are at the forefront. As the Institute is primarily involved in experimental investigations, the development and construction of instruments together with the analysis of acquired data play a major role. These activities are accompanied by intensive theoretical efforts and the creation of physical models. Emphasis here lies in numerical simulations of the fields of planetary and solar dynamos, atmospheric circulation models, MHD processes in the convection zone and solar atmosphere, the physics of ionospheric and magnetospheric plasmas, convection currents in the solid mantle of terrestrial planets and in the gas envelopes of the giant planets.

Struktur und Leitung des Instituts / Structure and Management of the Institute

Auf Beschluss des Senats der MPG war das Institut seit dem 6. Juni 1991 in zwei Abteilungen organisiert: der von Dr.-Ing. H. Rosenbauer geleiteten Abteilung experimentelle Planetenphysik und einer Allgemeinen Abteilung, der die übrigen Direktoren kollegial vorstanden.

Mit der Emeritierung von Dr.-Ing. H. Rosenbauer am 30. Juni 2004 wurde das Institut neu strukturiert und in drei Abteilungen gegliedert: der Abteilung Sonne und Heliosphäre unter den Leitung von Prof. Dr. S. K. Solanki, der Abteilung Planeten und Kometen unter der Leitung von Prof. Dr. U. R. Christensen, sowie der Abteilung Magnetosphäre unter der Leitung von Prof. Dr. V. M. Vasyliūnas. Am 1. September 2005 wurde das Institut um die Selbständige Nachwuchsgruppe Helio- und Asteroseismologie der MPG erweitert. Eine technische Abteilung und die Verwaltung sind zentral organisiert und stehen allen Abteilungen zur Verfügung. Die zentralen technischen Einrichtungen umfassen eine Mechanische Abteilung, bestehend aus Konstruktion und Werkstätten, ein Entwicklungslabor für Elektronik, ein Rechenzentrum und eine Fachbibliothek.

Im Rahmen der Umstrukturierungen wurde das Institut am 1. Juli 2004 von Max-Planck-Institut für Aeronomie (MPAE) in Max-Planck-Institut für Sonnensystemforschung (MPS) umbenannt.

Das Institut wurde durch das Gesamtkollegium der Direktoren Prof. Dr. U. R. Christensen, Dr.-Ing. H. Rosenbauer (bis 30. Juni 2004), Prof. Dr. S. K. Solanki und Prof. Dr. V. M. Vasyliūnas gemeinschaftlich geleitet.

Geschäftsführender Direktor war bis zum 31. Dezember 2004 Prof. Dr. S. K. Solanki. Er wurde in dieser Funktion von Prof. Dr. U. R. Christensen abgelöst.

Das Kollegium wird in seiner Arbeit durch einen technischen Geschäftsführer (Dr. I. Pardowitz), einen Verwaltungsleiter (A. Poprawa), und einen Direktionsberaterkreis unterstützt. Letzterer besteht aus drei Mitarbeitern des wissenschaftlich-technischen Bereiches, die von allen Mitarbeitern des Instituts für eine einjährige Amtsperiode gewählt werden.

Für die einzelnen Forschungsvorhaben werden jeweils Projektgruppen gebildet, die nach Abschluss des Projektes wieder aufgelöst werden. Die Initiative zur Aufnahme eines Projektes und zur Gründung einer entsprechenden Arbeitsgruppe kann jeder Wissenschaftler im Institut ergreifen.

According to a decision of the MPG senate the institute was structured into two departments starting June 6, 1991: a department for general planetary physics headed by Dr.-Ing. H. Rosenbauer, and a general department that was jointly managed by the other institute directors.

Following the retirement of Dr.-Ing. H. Rosenbauer at June 30, 2004 the institute was reorganized into three departments: the department Sun and Heliosphere headed by Prof. Dr. S. K. Solanki, the department Planets and Comets headed by Prof. Dr. U. R. Christensen, and the department Magnetosphere headed by Prof. Dr. V. M. Vasyliūnas. In addition, the Independent Junior Research Group of the Max Planck Society "Helio- and Asteroseismology" was created on September 1, 2005. A technical department and the administration are centrally organized and serve all research departments. The technical department comprises a mechanical department, including design office and workshop, an electronic laboratory, a computing center, and a library.

In line with the reorganization, the institute was renamed from Max Planck Institute for Aeronomy (MPAE) to Max Planck Institute for Solar System Reseach (MPS) on the first of July 2004.

The institute was jointly managed by the directors Prof. Dr. U. R. Christensen, Dr.-Ing. H. Rosenbauer (until June 30, 2004), Prof. Dr. S. K. Solanki, and Prof. Dr. V. M. Vasyliūnas (general board of directors).

Prof. Dr. S. K. Solanki served as managing director until December 31, 2004 and was superseded by Prof. Dr. U. R. Christensen.

The board of directors is assisted by a technical manager (Dr. I. Pardowitz), the head of administration (A. Proprawa), and a director's advisory committee. The latter consists of three members of the scientific-technical staff who are elected for a one-year period by the complete staff.

A dedicated project group is formed for the duration of each research project. Every institute member can take the initiative to start a new project and to form the corresponding group.

Emeritierung Dr.-Ing. Helmut Rosenbauer / Retirement Dr.-Ing. Helmut Rosenbauer

Zum 30. Juni 2004 wurde Dr. Helmut Rosenbauer emeritiert. Die von ihm über viele Jahre geleitete Abteilung für experimentelle Planetenphysik wurde gleichzeitig aufgelöst. Die meisten der verbliebenen Mitarbeiter setzen ihre Arbeit in der Abteilung Planeten und Kometen fort. Die wissenschaftlichen Berichte der Arbeiten in Abteilung Rosenbauer im Zeitraum 1.1. – 30.6.2004 wurden aus diesem Grunde in den entsprechenden Abschnitt Planeten, ihre natürlichen Satelliten und Kometen (Seite 78) eingereiht.

Nach zehn Jahren am Max-Planck-Institut für Extraterrestrische Physik in Garching wurde Dr. Rosenbauer 1977 als Direktor an das Max-Planck-Institut für Aeronomie berufen. Dort übernahm er ab dem 6. Juni 1991 die Leitung der neu gegründeten Abteilung für Experimentelle Planetenphysik.

Dr. Rosenbauers Verdienste in der experimentellen Weltraumphysik sind zu zahlreich, um sie hier eingehend zu würdigen. Sein Erfolg basiert nicht zuletzt darauf, dass sich in ihm tiefes wissenschaftliches Verständnis und hohe Ingenieurskunst vereinen. Dieser seltenen Kombination entsprangen raffinierte und erfindungsreiche Instrumententwicklungen, die zum Erfolg vieler Weltraummissionen beigetragen haben: HEOS, HELIOS, Ulysses, GIOTTO und Phobos 1 sind nur einige Beispiele. In den letzten zehn Jahre vor seiner Emeritierung hat er die Entwicklung des ROSETTA-Landers wesentlich getragen und so dieses ehrgeizige Projekt erst ermöglicht.

Das MPS schätzt sich glücklich, dass Dr. Ing. Helmut Rosenbauer dem Institut weiter mit Rat und Tat zur Seite steht.

Dr. Helmut Rosenbauer retired on June 30, 2004, and the Department for Experimental Planetary Physics which he headed for many years, was simultaneously dissolved. The majority of his remaining colleagues continue their work within the Department of Planets and Comets. For this reason, the scientific reports for the Department Rosenbauer for the period January 1 to June 30, 2004 appear in the chapter on Planets and Comets (page 81).

After ten years at the Max Planck Institute for Extraterrestrial Physics in Garching, Dr. Rosenbauer was appointed director of the Max Planck Institute for Aeronomy in 1977. There, on June 6, 1991, he became head of the newly founded department for Experimental Planetary Physics.

Dr. Rosenbauer's accomplishments in experimental space physics are too numerous to fully acknowledge in this limited space. His success depends to no small measure on his being able to bring together a fundamental understanding for science with an enormous knowledge of the art of engineering. This rare combination has led to many refined and innovative instrument designs and to their success on numerous space missions: HEOS, HELIOS, Ulysses, GIOTTO, and Phobos 1 to name only some examples. In the past ten years before his retirement, he contributed decisively to the development of the ROSETTA lander, making this very ambitious project possible in the first place.

The MPS appreciates very much that Dr. Ing. Helmut Rosenbauer is still available to this Institute with all his experience and devotion.

Personelle Entwicklung / Personnel Development

In den Jahren 2004 und 2005 hat sich die Zahl der Mitarbeiterinnen und Mitarbeiter des Instituts entsprechend dem Sozialplan verändert.

Die Zahl der Planstellen verringerte sich bis Ende Dezember 2005 auf 113. Davon waren 28 mit Wissenschaftlern besetzt. Die Zahl der am Institut wissenschaftlich Tätigen war jedoch mit Einbeziehung der aus Mitteln des BMBF finanzierten Wissenschaftler und der Doktoranden beträchtlich größer und betrug am 31. Dezember 2005 etwa 130.

Mitarbeiter, die nach dem Sozialplan ausgeschieden sind:

2004: Herbert Ellendorff, Peter Fahlbusch, Hans-Joachim Gebhardt, Monika Majunke, Wolfgang Neumann, Waltraut Reich

2005: Waltherus Boogaerts, Hans-Adolf Heinrichs, Horst Heise, Renate Heitkamp, Karin Kellner, Renate Meusel, Ulrich Strohmeyer, Volker Thiel, Walter Wächter, Hans-Dieter Waitz

In den Ruhestand traten:

2004: Bernhard Bleckert, Dr. Jürgen Klostermeyer, Rosemarie Röttger, Helmut Schild

2005: Dr. Reinhard Borchers, Prof. Dr. Klaus Jockers, Dr. Erling Nielsen, Dr. Michael L. Richards, Prof. Dr. Konrad Sauer

---

During the years 2004 and 2005 the number of institute staff was reduced according to the social plan.

The number of permanent positions decreased to 113 by the end of December 2005. Of these 28 were filled by scientists. The number of people working scientifically, through BMBF-financed scientists and through Ph.D. students, was nevertheless substantially greater, consisting of 130 on 31st December 2005.

Staff members who have left according to the social plan are:

2004: Herbert Ellendorff, Peter Fahlbusch, Hans-Joachim Gebhardt, Monika Majunke, Wolfgang Neumann, Waltraut Reich

2005: Waltherus Boogaerts, Hans-Adolf Heinrichs, Horst Heise, Renate Heitkamp, Karin Kellner, Renate Meusel, Ulrich Strohmeyer, Volker Thiel, Walter Wächter, Hans-Dieter Waitz

The following have retired:

2004: Bernhard Bleckert, Dr. Jürgen Klostermeyer, Rosemarie Röttger, Helmut Schild

2005: Dr. Reinhard Borchers, Prof. Dr. Klaus Jockers, Dr. Erling Nielsen, Dr. Michael L. Richards, Prof. Dr. Konrad Sauer

Das Kuratorium des Instituts / Board of Trustees of the Institute

Dem Kuratorium des Instituts gehörten in den Jahren 2004 und 2005 die folgenden Mitglieder an:

Helge Engelhardt, Ministerialdirigent im BMBF (Bundesministerium für Bildung und Forschung), Bonn;

Prof. Dr. Klaus J. Fricke, Universitäts-Sternwarte, Göttingen;

Dr. Thomas Galinski, Raumfahrtmanagement Extraterrestrik DLR, Bonn;

Prof. Dr. Martin C.E. Huber, Küsnacht, Schweiz;

Prof. Dr. Reiner Kree, Vizepräsident der Universität Göttingen;

Dr. Josef Lange, Staatssekretär im Niedersächsischen Ministerium für Wissenschaft und Kultur, Hannover;

Andreas Lindenthal, Earth Observation, Navigation and Science, EADS Astrium GmbH, Friedrichshafen;

Prof. Dr. F. Jochen Litterst, Präsident der TU Braunschweig;

Prof. Dr. Oskar von der Lühe, Kiepenheuer-Institut für Sonnenphysik, Freiburg;

Frau Erika Mann, Mitglied des Europäischen Parlaments, Hannover;

Dr. Fritz Merkle, OHB-System GmbH, Bremen;

Thomas Oppermann, Mitglied des Niedersächsischen Landtags, Göttingen.

Das Kuratorium tagte am 10. November 2004 in Lindau.

The following were members of the board of trustees of the institute in the years 2004 and 2005:

Helge Endelhardt, Ministerialdirigent, BMBF (German Federal Ministry for Education and Research), Bonn;

Prof. Dr. Klaus J. Fricke, University Observatory, Göttingen;

Dr. Thomas Galinski, DLR (German space agency), Bonn;

Prof. Dr. Martin C.E. Huber, Küsnacht, Schweiz;

Prof. Dr. Reiner Kree, Vice President, University Göttingen;

Dr. Josef Lange, permanent secretary in the Lower Saxony Ministry for Science and Culture, Hannover;

The board of trustees met on 10 November 2004 in Lindau.

Der Fachbeirat des Instituts / Scientific Advisory Board of the Institute

Im Jahr 2001 wurde vom Präsidenten der Max-Planck-Gesellschaft ein neuer Fachbeirat für das Institut berufen. In den Jahren 2001 – 2006 gehören dem Fachbeirat die folgenden Mitglieder an:

Prof. Dr. D. Crisp, Pasadena, CA, USA;
Prof. Dr. G. Hensler, Wien, Österreich;
Dr. L.J. Lanzerotti, Murray Hill, NJ, USA;
Prof. Dr. Ph. Lognonné, Saint Maur, Frankreich;
Prof. Dr. E.R. Priest, St. Andrews, Großbritannien;
Prof. Dr. R. Rosner, Chicago, IL, USA;
Prof. Dr. D.J. Southwood, Paris, Frankreich;
Prof. Dr. D.J. Stevenson, Pasadena, CA, USA.

Im Berichtszeitraum fand die Zusammenkunft des Fachbeirats vom 8. – 9. November 2004 im MPS in Lindau statt.

In 2001 a new advisory board for the institute was appointed by the President of the Max Planck Society. During the years 2001 – 2006 the following were members of the scientific advisory board:

Prof. Dr. D. Crisp, Pasadena, CA, USA;
Prof. Dr. G. Hensler, Vienna, Austria;
Dr. L.J. Lanzerotti, Murray Hill, NJ, USA;
Prof. Dr. Ph. Lognonné, Saint Maur, France;
Prof. Dr. E.R. Priest, St. Andrews, UK;
Prof. Dr. R. Rosner, Chicago, IL, USA;
Prof. Dr. D.J. Southwood, Paris, France;
Prof. Dr. D.J. Stevenson, Pasadena, CA, USA.

During the period of this report the advisory board met in Lindau from 8 – 9 November 2004.

Für das Institut aufgewendete Mittel / Institute Resources

Die vom Bund und den Ländern getragene und durch die Generalverwaltung der Max-Planck-Gesellschaft zugeteilte Grundausstattung des Instituts an Personal- und Sachmitteln betrug im Jahre 2004 8,7 Millionen EURO für Personal und 2,6 Millionen EURO für Sachen. An Investitionsmitteln (Geräte mit Preisen über 5.000 EURO) wurden 1,4 Millionen EURO bewilligt. Für das Jahr 2005 lauten diese Zahlen: 8,5 Millionen EURO für Personal, 3,1 Millionen EURO für Sachausgaben und 0,4 Millionen EURO für Investitionen.

Besondere Forschungsvorhaben sind durch das BMBF (Bundesministerium für Bildung und Forschung) und die ESA (European Space Agency) gefördert worden. Vom BMBF (DLR) erhielt das Institut 2004 insgesamt 5,2 Millionen EURO und 2005 7,9 Millionen EURO. Die entsprechenden Beträge der ESA waren 0,9 Millionen EURO und 0,7 Millionen EURO.

Für diese Förderungen, ohne die viele experimentelle Forschungsvorhaben nicht durchführbar gewesen wären, möchten wir auch an dieser Stelle ausdrücklich danken.

The basic funding of the institute, from the federal and state governments and allocated through the administrative headquarters of the Max Planck Society, amounted to 8.7 million EURO for personnel and 2.6 million EURO for materials in 2004. Capital investment funds (equipment over 5000 EURO) of 1.4 million EURO were approved. For 2005 the figures are: 8.5 million EURO for personnel, 3.1 million EURO for materials, and 0.4 million EURO for capital investment.

Special research needs were funded by BMBF (German Federal Ministry for Education and Research) and ESA (European Space Agency). From BMBF (DLR) the institute received 5,2 million EURO in 2004 and 7.9 million EURO in 2005. The corresponding sums from ESA were 0.9 million EURO and 0.7 million EURO.

For this financial assistance, without which many experimental research programmes would not be possible, we wish to express our gratitude.

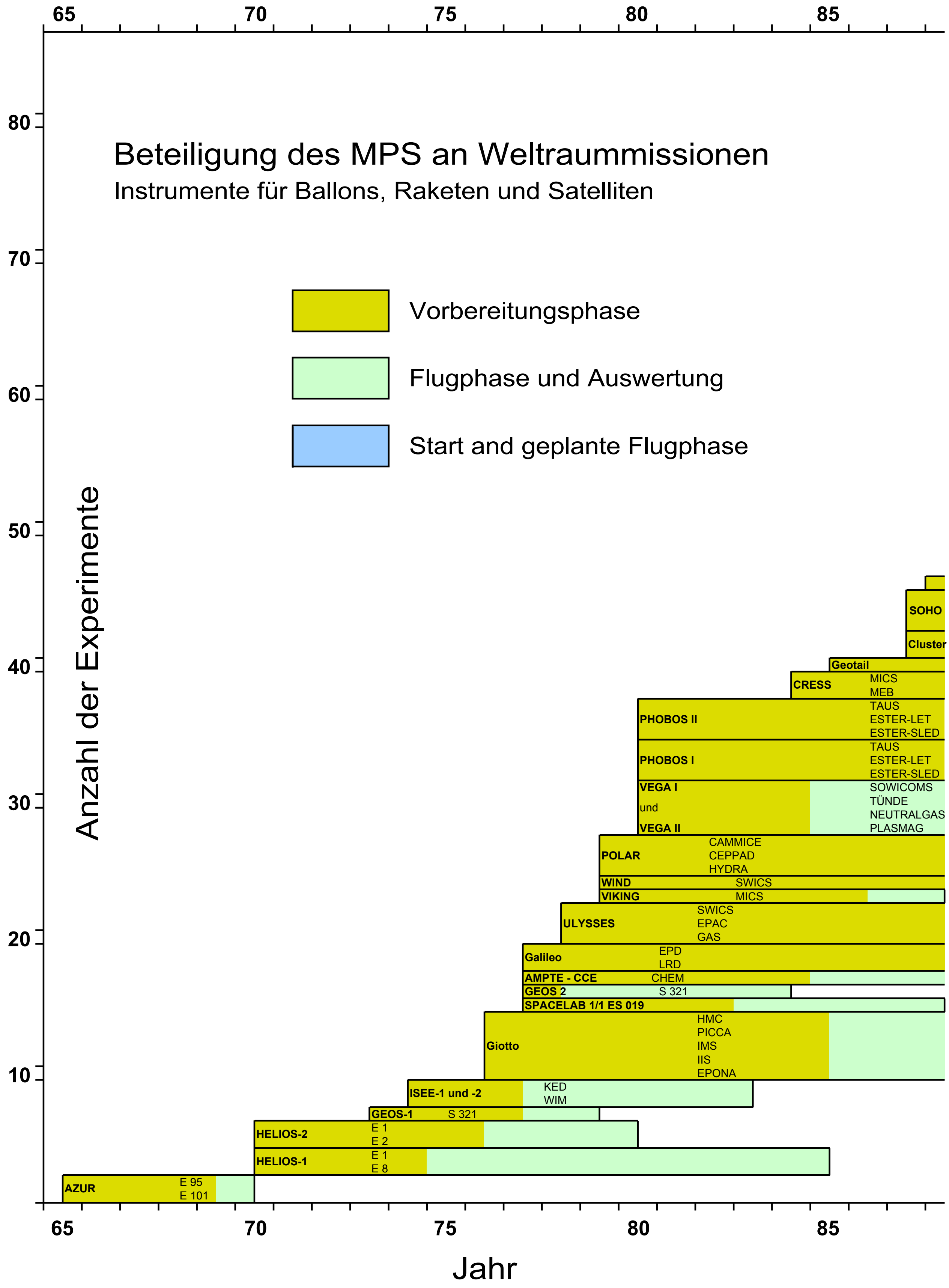

Auflistung der Missionen unter Beteiligung des MPS. Dargestellt ist die Dauer der verschiedenen Projektphasen (farbcodiert) einzelner Instrumente. Kurze Beschreibungen findet man in den einzelnen Jahres- bzw. Tätigkeitsberichten des MPS.

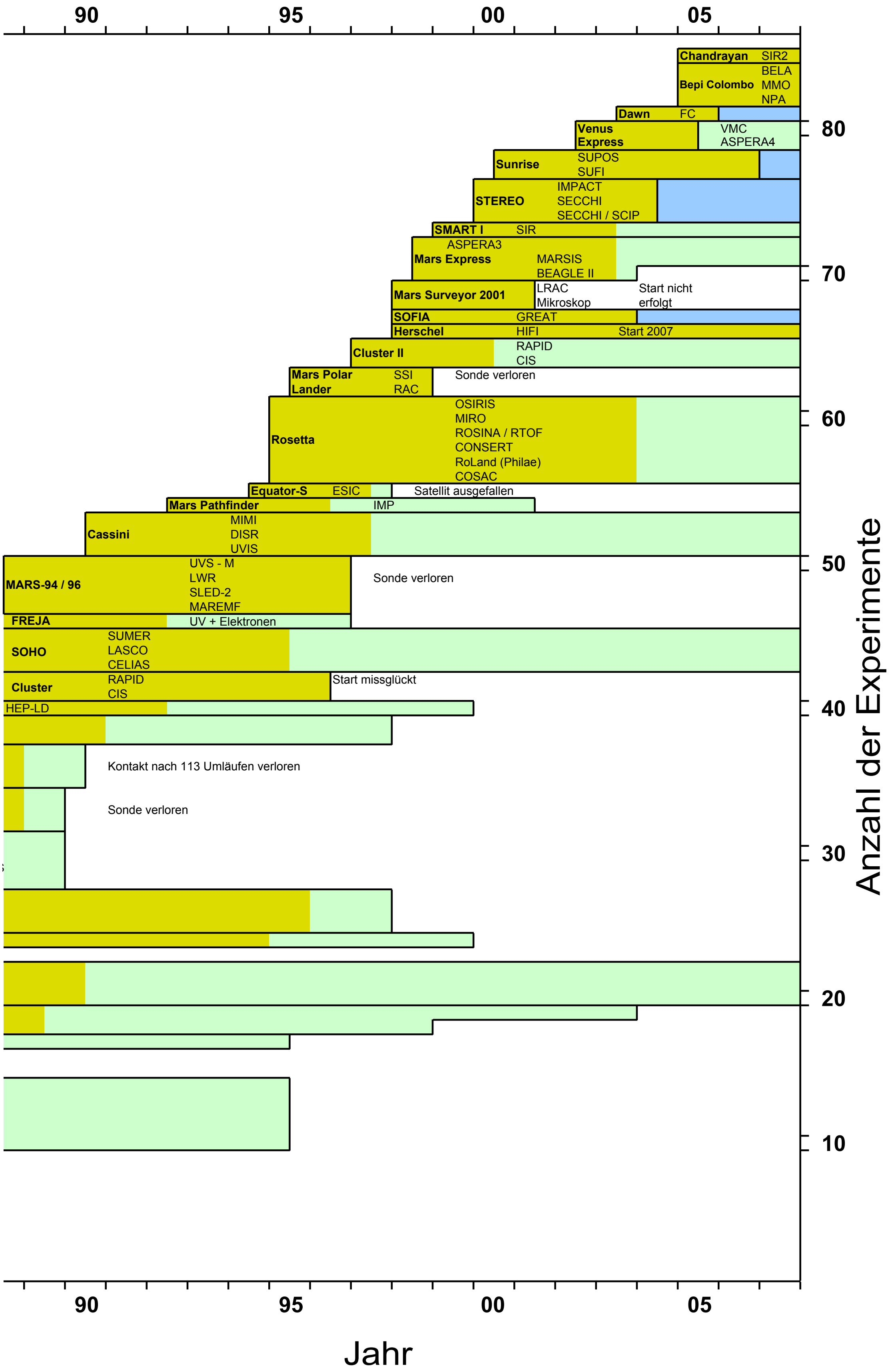

List of missions with MPS participation. The different project phases of each instruments are shown colour-coded. Short descriptions of these instruments can be found in the annual reports of the MPS.

II. **Wissenschaftliche Arbeiten**/Scientific Projects

1. Sonne und Heliosphäre/Sun and Heliosphere

Schwerpunktthema:

Woher kommt der Sonnenwind? – Neuigkeiten über die Quellregionen des Sonnenwindes in der Korona der Sonne

(E. Marsch)

(English version see page 16)

Drei Hauptarten von Sonnenwind

Wo und wie der Sonnenwind in der Sonnenatmosphäre entsteht, bleibt selbst nach Jahrzehnten der Sonnenforschung vom Weltraum aus eine der Schlüsselfragen der modernen Sonnenphysik. Allgemein gesprochen kann man sagen, dass der Sonnenwind weitgehend durch das Magnetfeld der Sonne bestimmt wird, und dass er auf vielerlei Weise auf die magnetische Aktivität und damit einhergehende Veränderungen des photosphärischen Magnetfeldes reagiert, welches wiederum das Magnetfeld der Korona bestimmt und damit auch das interplanetare Magnetfeld und die Sonnenwindströme in der ganzen Heliosphäre. Offensichtlich sind also die Quellen des Sonnenwindes durch das koronale Magnetfeld bestimmt, und sein Ursprung ist aufs Engste verknüpft mit und beeinflusst von der Struktur und Aktivität des magnetischen Netzwerkes und der solaren Übergangszone.

In diesem Beitrag werden wir neue Erkenntnisse zum Ursprung des Sonnenwindes diskutieren, wobei die Betonung auf der physikalischen Natur der Quellregionen liegen soll, so wie sie aus den Mustern der extremen ultravioletten Strahlung von der Sonnenscheibe und in der Korona sichtbar werden, und ebenso in den Bildern von Koronagraphen. Wir geben einen kurzen Überblick über Plasmaeigenschaften und Magnetfeldstrukturen in den Quellregionen des Sonnenwindes. Die Art des Sonnenwindes wird festgelegt durch die Randbedingungen in der unteren Korona. Diese kann weitgehend geschlossen sein (in Streamern und Bögen), oder vorübergehend offen (bei eruptiven Filamenten/Protuberanzen and Flussröhren), oder andauernd offen (in koronalen Trichtern und Löchern). Die Quellen des Sonnenwindes sollen hier untersucht werden, insbesondere bei kleinen Skalen und aus dem Blickwinkel des Magnetfeldes.

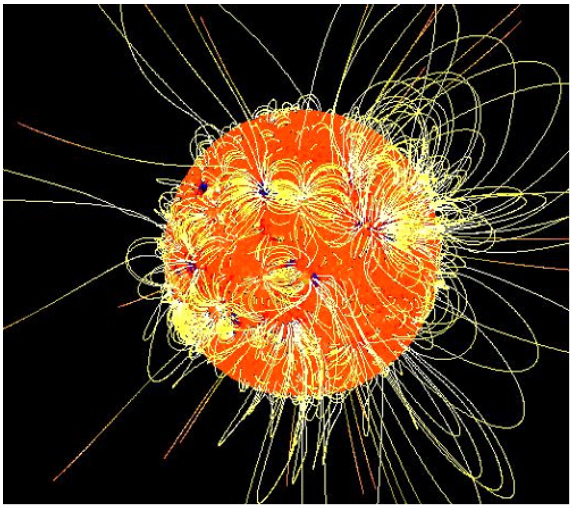

Abb. 1: Das koronale Magnetfeld wie aus einem photosphärischen Magnetogramm berechnet durch eine Potentialfeldextrapolation. Die geschlossenen Magnetfeldschleifen entsprechen bi-polaren Aktivitätsgebieten, oder sie überbrücken weit getrennte Regionen von entgegengesetzter magnetischer Polarität, wohingegen die geraden Linien das koronale Magnetfeld darstellen, das zur Heliosphäre hin offen ist und dem magnetischen Fluss entspricht, der vom Sonnenwind fortgetragen wird (nach Wiegelmann and Solanki (2004b)).

Wir wissen seit langem, dass es als Resultat von sich verändernden Randbedingungen in der Korona drei grundlegende Arten von Sonnenwind gibt: Schnelle Ströme aus großen Koronalöchern; langsame Ströme aus kleinen Koronalöchern und Aktivitätsgebieten, oder aus den Randschichten der koronalen Streamer; und die variablen, vorübergehenden Ströme bei koronalen Massenauswürfen (koronalen Massenauswürfen). Transiente Ereignisse gehen oftmals einher mit eruptiven Filamenten und Plasmoiden austretend aus den Spitzen der Streamers, oder mit Plasmaejektionen von Aktivitätsgebieten, die durch austretenden magnetischen Fluss oder Rekonnexion angetrieben werden. Die koronalen Massenauswürfee selbst, oder ihre interplanetaren Manifestationen, werden hier nicht angesprochen aber später kurz betrachtet. Die Hauptarten von Sonnenwind sind eng verknüpft mit der Struktur und Aktivität des koronalen Magnetfeldes, welches sich mit dem Sonnenzyklus verändert.

Die großskalige Korona und ihr Magnetfeld

Das koronale Magnetfeld ist noch nie direkt gemessen worden, aber es kann mit Hilfe von Extrapolationstechniken konstruiert werden, z.B. mit Hilfe von Potentialfeldern, kraftfreien Feldern oder magnetohydrodynamischen Methoden. Ein typisches Resultat, das mit der Potentialfeld-Methode gewonnen wurde, ist in Abb. 1 gezeigt, welche die offenen und geschlossenen Feldlinien des globalen Magnetfeldes der Korona illustriert. Ein Aktivitätsgebiet besteht im wesentlichen aus geschlossenen Bögen (Schleifen), in dem dichtes Plasma eingeschlossen werden kann. Ein Aktivitätsgebiet gibt deshalb helle Strahlung ab und ist deutlich sichtbar im Ultravioletten und Röntgenlicht. Im Gegensatz dazu kann das großräumig offene Magnetfeld selbst dünnes Plasma nicht festhalten, das deshalb freikommen und expandieren kann in Gestalt des Sonnenwindes. Daher erscheinen die Regionen mit offenem Feld dunkel. Sie wurden Koronalöcher genannt, denn ihre Strahlung ist vergleichsweise gering. Diese wesentlichen Eigenschaften der Korona sind klar in jedem der ultravioletten Bilder zu erkennen, die regelmäßig von SOHO aufgenommen werden.

Das Magnetfeld der Sonne bestimmt das Strömungsmuster des Sonnenwindes und die Struktur der ganzen Korona. Ihr Magnetfeld entwickelt sich langsam mit wachsendem Abstand von der Sonne in das heliosphärische (interplanetare) Magnetfeld. Ab einer gewissen Höhe, die gewöhnlich zwischen zwei und drei Sonnenradien angenommen wird, werden die Feldlinien im Wesentlichen gerade und, in ihn eingefroren, vom Sonnenwind davongetragen. Die entsprechende magnetische Quellfläche stellt man sich als virtuelle Kugeloberfläche vor, von der aus das äußere koronale Magnetfeld hauptsächlich radial gerichtet ist. Bei der Potentialfeld-Methode extrapoliert man das Magnetfeld der Sonne, so wie es in der Photosphäre gemessen wurde, in die Korona, wobei man fordert, dass das Feld in der Korona frei von elektrischen Strömen ist. Im realistischeren Modell des kraftfreien Feldes werden elektrische Ströme in Betracht gezogen, aber man nimmt an, dass sie in der Korona nur entlang der Feldlinien fließen. Die Polarität des Feldes ändert sich beim Durchgang durch die Stromschichten, und im besonderen durch die heliosphärische Stromschicht, die während des solaren Minimums mit dem äquatorialen Streamer-Gürtel verbunden ist. Dann erstreckt sich die heliosphärische Stromschicht als flache Scheibe weit in den interplanetaren Raum hinaus.

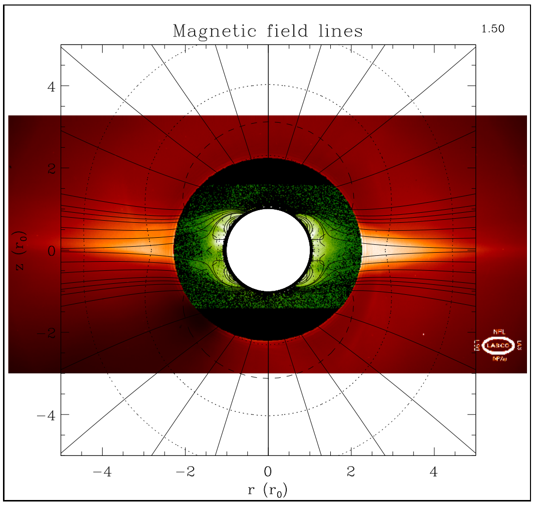

Abb. 2: Die sehr symmetrische Korona bei minimaler Sonnenaktivität und ihr zugehöriges Magnetfeld. Den Magnetfeldlinien überlagert sind Bilder der Korona, die von LASCO aufgenommen wurden (in der grünen koronalen Eisenlinie und im sichtbaren Licht) und ausgedehnte polare Koronalöcher zeigen sowie eine helle Stromschicht bei niedrigen Breiten, die mit dem äquatorialen Streamer-Gürtel zusammenfällt (nach Forsyth und Marsch, 1999).

Die Struktur der Korona ist am einfachsten während minimaler Aktivität, wenn das Feld gut als Überlagerung eines Dipols mit einem Quadrupol und einer Komponente von der Stromschicht herrührend dargestellt werden kann. Diese Korona vom Minimum-Typ ist in Abb. 2 illustriert. Die drei-dimensionale Struktur des Sonnenwindes wurde von den beiden Missionen Helios und Ulysses gemeinsam erschlossen. Die globale Struktur des Sonnenwindes und ihre Veränderungen im Verlaufe des Sonnenzyklus wurden vollständig erst von Ulysses aufgezeigt, welcher bestätigte dass der Hochgeschwindigkeitssonnenwind in den polaren Koronalöchern entsteht und über den Polen im solaren Minimum vorherrscht, wenn der langsame Sonnenwind vom Streamer-Gürtel kommend bei niedrigen Breiten dominiert. Das Magnetfeld wird zum Multipol-Feld in Richtung maximaler Sonnenaktivität, und die Quellen des Sonnenwindes ändern sich entsprechend in ihren Lagen auf der Sonne und räumlichen Ausdehnungen. Ebenso wird das Strömungsmuster des Sonnenwindes komplexer und variabler.

Die sich verändernde Sonnenkorona und der dazugehörige Sonnenwind werden in Abb. 3 gezeigt, die im oberen Teil eine Reihe von Koronabildern präsentiert und im unteren die Sonnenwindgeschwindigkeit als Funktion der Zeit und heliographischen Breite. Deutlich zu sehen ist der Übergang von einer Minimum-Typ Korona um 1995 herum zu einer Maximum-Typ Korona um 1999. Er wird begleitet von einem auffallenden Übergang von stetig schnellem in

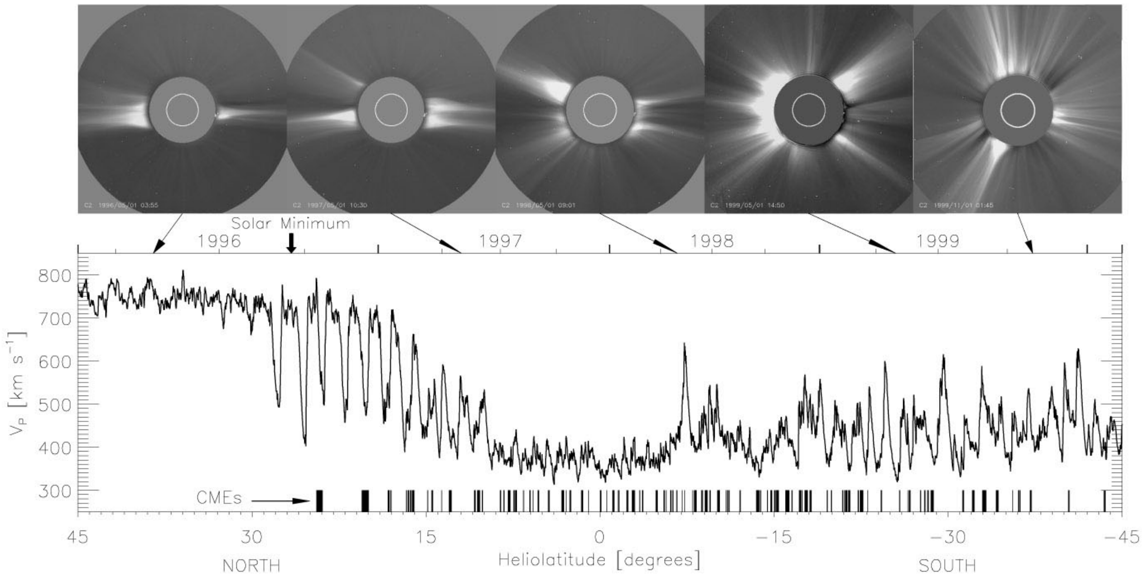

Abb. 3: Die Veränderungen der Sonnenkorona (oben) im Verlaufe des Sonnenzyklus und die entsprechenden Variationen im Strömungsmuster des Sonnenwindes (unten) als Funktion der Zeit oder heliographischen Breite entlang des Orbits des Ulysses Raumfahrzeugs. Man beachte die wiederkehrenden Ströme nach dem Minimum. Das Auftreten von koronalen Massenauswürfen ist durch kleine senkrechte Balken an der unteren Skala angezeigt (nach McComas *et al.*, 2000).

unstetig langsamen Wind. Die Oszillationen von wiederkehrenden Strömen zwischen 1996 und 1997 haben ihren Grund in der Rotation der Sonne, die in dieser Zeit zu raschen Wechseln des Raumfahrzeuges hinein in die und heraus aus der heliosphärischen Stromschicht führte, beziehungsweise rein in das offene und raus aus dem offenen Magnetfeld (der Heliosphäre), das eng mit den polaren Koronalöchern auf der Sonne zusammen hing. Diese Wechsel verursachten periodische Variation zwischen schnellen und langsamen Strömen. Am unteren Rand der Abbildung ist auch das Auftreten von koronalen Massenauswürfen angezeigt.

Neben den stetigen Sonnenwindströmen stellen die koronalen Massenauswürfe einen anderen Typ von (einem variablen und sporadischen) Sonnenwind (oder besser Sonnensturm) dar. Was die Rate ihres Auftretens angeht, so tendieren koronale Massenauswürfe dazu sich (mit einer Häufigkeitsrate von etwa drei pro Tag) um das Maximum der Sonnenaktivität zu häufen, wenn die Korona stark magnetisch strukturiert ist und eine komplexe Multi-Pol-Struktur hat. Koronale Massenauswürfe treten in zwei Haupttypen auf, als schnelle und langsame, wenngleich diese grobe Einteilung nicht eindeutig ist. Eine beträchtliche Anzahl (etwa 30% oder mehr) von koronalen Massenauswürfen entstehen aus großen eruptive Protuberanzen, deren Überreste noch als Arkaden nach der Eruption auf der Sonne zu sehen sind. Für koronale Massenauswürfe sind die Energie-Anforderungen und Beschleunigungs-Mechanismen noch weniger verstanden als für die normalen Sonnenwindströme. Auch sind die Bedingungen für das Plasma extremer für die vorübergehenden koronalen Massenauswürfe als die stationären Ströme, denn die Dichte des Plasma in koronalen Massenauswürfen ist oftmals viel höher, und die Geschwindigkeit kann leicht ein Vielfaches der mittleren Sonnenwindgeschwindigkeit erreichen.

Kehren wir wieder zum stetigen Sonnenwind zurück und rufen uns ins Gedächtnis, dass er aus zwei Hauptkomponenten besteht: schnelle, dünne und gleichmäßige Ströme, und langsame, dichte und variable Ströme. Die globalen Zuordnungen des schnellen Windes zu großen Koronalöchern und des langsamen zum Streamer-Gürtel, oder auch den Grenzregionen zwischen geschlossenen und offenen Magnetfeldern und kleinen Koronalöchern, sind seit langem etabliert.

Es gibt verschiedene Techniken den Sonnenwind auf die Sonne zurück abzubilden, um so seine Quellen in der Korona zu identifizieren. Erst kürzlich wurde, was in Bildern im weichen Röntgenlicht als schmale Koronalöcher erschien, untersucht und als mögliche Quellen des langsamen Sonnenwindes erkannt. Mit Hilfe von in-situ Sonnenwinddaten von Raumsonden nahe der Erde wurde gefunden, dass der langsame Sonnenwind auch aus kleinen Koronalöchern in der Nähe von Aktivitätsgebieten ausströmen kann.

Jedoch ist es keine leichte Aufgabe, den in-situ gemessenen Sonnenwind zu seinen genauen Quellen bei kleineren Skalen auf der Sonne zurückzuverfolgen. Aber nun werden wir einige neuere Resultate zeigen, in denen die Quellen durch eine kombinierte Analyse an Hand von Doppler-Verschiebungen und Intensitäten ultravioletter Emissionslinien zusammen mit dem koronalen Magnetfeld identifiziert wurden. Es wird aus gemessenen Magnetogrammen konstruiert und kann dann zu allen relevanten Höhen über der Photosphäre extrapoliert werden.

Sonnenwind aus Trichtern und Koronalöchern

In mehreren neueren Studien analysierten wir detaillierte Beobachtungen von äquatorialen Koronalöchern und untersuchten die klein-skaligen Strukturen des Magnetfeldes in den Quellregionen des schnellen Sonnenwindes. Wir verglichen direkt die Dopplergramme und Plasma-Strömungsgeschwindigkeit, wie sie vom SUMER (Solar Ultraviolet Measurements of Emitted Radiation) Instrument auf SOHO gemessen wurden, mit dem koronalen Magnetfeld, wie es aus photosphärischen Magnetogrammen am Boden des Koronaloches mit Hilfe der Potential oder kraftfreien Magnetfeld-Extrapolation berechnet wurde. In den untersuchten Fällen kombinierten wir so spektroskopische Daten mit dem dreidimensionalen Magnetfeld, eine Methode, die ein klareres Bild der Plasmabedingungen und Strömungsmuster ergibt, wie sie in der Korona vorherrschen.

In Abb. 4 zeigen wir eine Dopplerkarte eines Teils eines äquatorialen Koronaloches, wobei die Doppler Verschiebungen sich über den Bereich von ± 20 km s^{-1} erstrecken, und Linien des extrapolierten Magnetfeldes, die projiziert wurden zum Vergleich mit dem Dopplerverschiebungsmuster. Die geschlossenen Feldlinien sind in gelb gemalt und die offenen in rot-braun. Ein Areal von $250'' \times 300''$ auf der Sonnenscheibe wird gezeigt. Es umfasst einen großen Teil des Koronaloches und seiner Grenzbereiche. Bei genauem Anschauen der Abb. 4 findet man, dass fast überall in dieser Koronaloch-Region nur Blauverschiebungen auftreten, d.h. das Plasma strömt aufwärts entlang der Sichtlinie mit typischen Geschwindigkeiten von bis zu 10 km s^{-1}. Es gibt kaum irgendwelche signifikanten Rotverschiebungen. In den gelben Bereichen mit geschlossenen Magnetfeldschleifen ist das Plasma nahezu in Ruhe.

Diese Ergebnisse wurden untermauert durch eine Analyse der genauen Quellenregionen des schnellen Sonnenwindes, der aus einem polaren Koronaloch ausströmte. Wiederum wurden als Quellen die sogenannten koronalen Trichter identifiziert, d.h. die expandierenden offenen Strukturen des Magnetfeldes, die in den Rändern des magnetischen Netzwerkes verwurzelt sind. Diese neuen Resultate ergänzen die früheren Arbeiten und bestätigten weiter, dass das, was später der schnelle Sonnenwind wird, in den Trichtern bei Höhen über der Photosphäre zwischen 5 Mm (Megameter) und 20 Mm zu strömen anfängt.

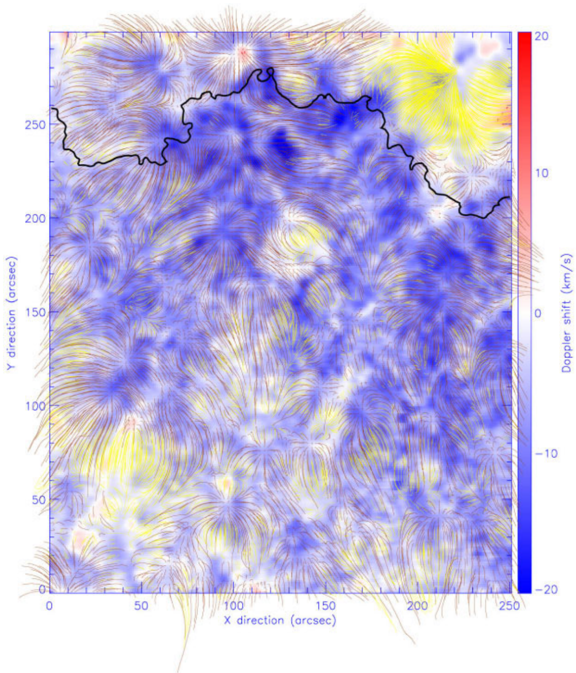

Abb. 4: Karte der Dopplerverschiebungen der Ne VIII (77 nm) Emissionslinie zusammen mit den Projektionen der extrapolierten koronalen Magnetfeldlinien. Gelb bedeutet hier geschlossene und rot-braun offene Feldlinien. Ein Bereich von $250'' \times 300''$ auf der Sonnenscheibe wird gezeigt, der einen Teil von einem äquatorialen Koronaloch und den Gebieten an seiner Grenze (angedeutet durch die dunkle Linie) umfasst. Man beachte den gleichmäßig gelben Bereich in der oberen rechten Ecke, der außerhalb des Koronaloches liegt und zu geschlossenen Magnetfeldbögen gehört. Die spinnenartigen Strukturen offenen Flusses in der oberen linken Ecke fallen mit blauen Farbflecken zusammen und weisen daher auf beträchtliches Ausströmen des koronalen Plasmas in dieser Region mit offenem Magnetfeld hin. Es gibt auch viele Feldlinien welche gelbe Flecken überbrücken, die zum geschlossenen magnetischen Teppich gehören, mit Fluss der auf die Nähe zur Sonnenoberfläche beschränkt ist (nach Wiegelmann *et al.* (2005d)).

Die neuen Entdeckungen werden in Abb. 5 illustriert. Im oberen Bild werden in zwei Ebenen bei Höhen von 0 und 20 Mm die farbkodierten Karten der Magnetfeldstärke gezeigt. Die Regionen mit Ausströmgeschwindigkeiten von mehr als 7 km s^{-1} sind durch schraffierte Flecken angedeutet, die mit offenen, unipolaren und starken Magnetfeldern zusammenfallen, welche die Trichter darstellen. Unsere neuen Er-

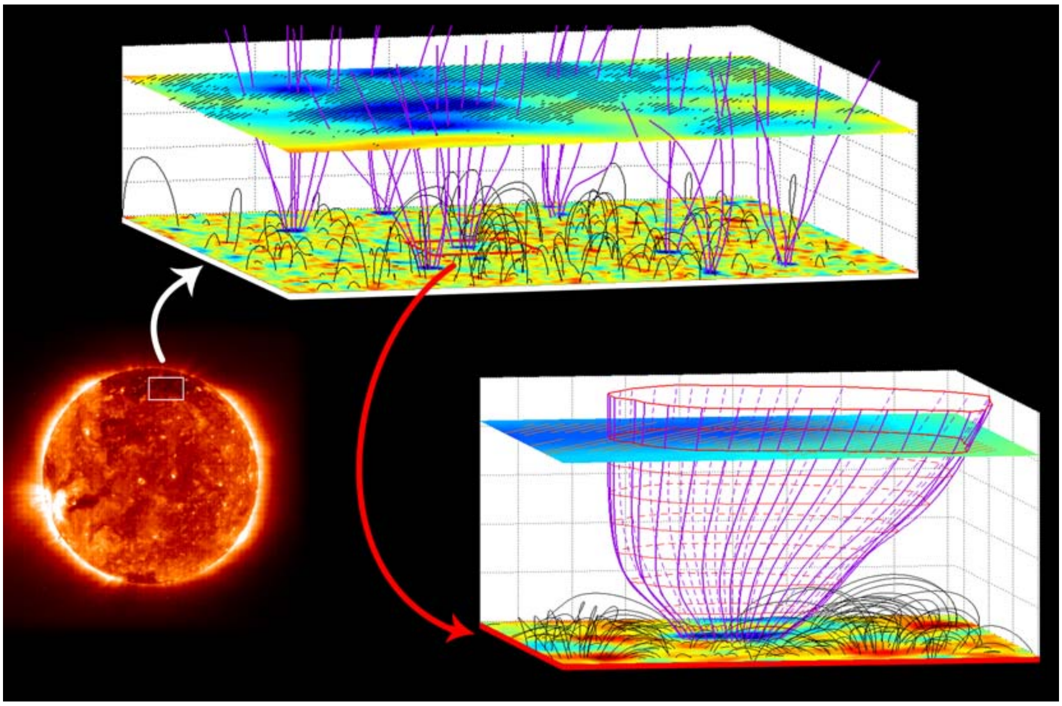

Abb. 5: In der linken unteren Ecke sieht man ein ultraviolettes Bild der ganzen Sonne mit einem großen polaren Koronaloch, von dem ein Ausschnitt mit einer ausgewählten Quellregion des schnellen Sonnenwindes durch einen weißen Kasten angedeutet ist. Die Quellen wurden als magnetische Trichter (oberes Bild) im Koronaloch identifiziert. Die magnetische Feldstärke wird in zwei Ebenen bei 4 Mm (Megameter) und 20 Mm gezeigt. Die schraffierten Bereiche zeigen an, wo die Ausströmgeschwindigkeit der Neon Ionen größer als 7 km s^{-1} ist. Offenes Magnetfeld ist durch schwarze Linien angedeutet und geschlossene Bögen durch magenta-farbige Linien. Sie erreichen kaum die Höhe von 10 Mm. Das untere rechte Bild zeigt einen einzelen Trichter, so wie er durch Feldextrapolation konstruiert wurde. Der Querschnitt des Trichters ist eingeschnürt durch die vielen benachbarten Magnetfeldbögen, die ihn stark zusammendrücken (nach Tu *et al.* (2005a)).

gebnisse erhielten wir dadurch, dass wir im Detail die Doppler-Geschwindigkeiten mit den Intensitätskarten verschiedener Spektrallinien verglichen. Speziell die Ne^{7+} Ionen strahlen hauptsächlich bei ungefähr 20 Mm, wo sie mit etwa 10 km s^{-1} aufwärts strömen, während C^{3+} Ionen ohne im Mittel zu strömen im Wesentlichen bei 5 Mm abstrahlen. Die Interpretation von alledem ist, dass wir den Sonnenwind in der Entstehung entdeckt und als seine Quellen die magnetisch offenen Trichter identifiziert haben.

Diese Beobachtungen passen gut zum folgenden Szenarium der ursprünglichen Beschleunigung des Sonnenwindes: Die Übergangszone in Koronalöchern wird von Magnetfeldschleifen unterschiedlicher Größe erreicht, oft mit Höhen niedriger als 5 Mm. Die Konvektion der Supergranulen in der Photosphäre hält ihre Fußpunkte in Bewegung und überführt so kinetische in magnetische Energie, die sich in den Magnetfeldschleifen ansammelt. Diese stoßen schließlich mit einem Trichter starker Magnetfeldkonzentration zusammen und verbinden sich dabei durch Rekonnexion mit dem schon vorhandenen offenen Magnetfeld. Das Plasma der Magnetfeldschleifen wird so frei gesetzt, und das kann zu Auf- und Abströmungen führen. Schlussendlich wird ein Teil des Plasmas aus den sich verbindenden Magnetfeldschleifen in die offene Korona gebracht. In der unteren Übergangszone unterhalb von 5 Mm haben wir hauptsächlich einen horizontalen Austausch von Masse und Energie zwischen benachbarten Flussröhren, der durch die supergranulare Bewegung angetrieben wird. Oberhalb von 5 Mm oder höher, wo die Rekonnexion zwischen den Feldlinien von Trichtern und umliegenden Magnetfeldschleifen langsam aufhört, wird der vertikale Transport bedeutender als der horizontale, und dann fängt die Beschleunigung des Sonnenwindes richtig an.

Am MPS in Lindau durchgeführte numerische Simulationen ergaben, dass hierfür tatsächlich die magnetische Rekonnexion zwischen niedrigen Bögen und Trichtern verantwortlich sein kann. Abb. 6 zeigt die in der Simulation erhaltenen Gebiete verschiedener Plasmageschwindigkeit. Die auf den Betrachter zugerichteten Plasmaströmungen sind blau dargestellt, und die in Richtung zur Sonne in rot (Farbskala in km/s), mit Geschwindigkeitswerten wie sie bei Messungen der Dopplerverschiebun in etwa gefunden werden.

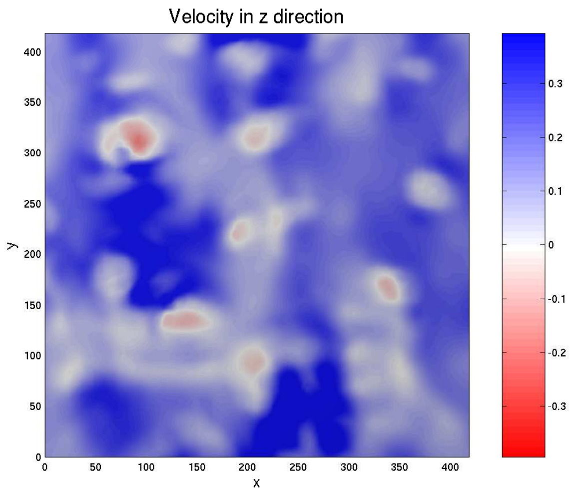

Abb. 6: Am MPS in Lindau durchgeführte numerische Simulationen ergaben, dass hierfür tatsächlich die magnetische Rekonnexion zwischen niedrigen Bögen und Trichtern für die anfängliche Beschleunigung des Sonnenwindes verantwortlich sein kann. Die Abbildung zeigt die in der Simulation erhaltenen Gebiete verschiedener Plasmageschwindigkeiten. Die auf den Betrachter zugerichteten Plasmaströmungen sind blau dargestellt, und die in Richtung zur Sonne in rot (Farbskala in km/s) (Büchner and Nikutowski, 2005).

Sonnenwind aus aktiven Gebieten?

Wie schon oben bemerkt wurden erst jüngst Aktivitätsgebiete nahe beim Sonnenmaximum klar als Quellregionen des langsamen Sonnenwindes erkannt. So wurde zum Beispiel die magnetische Topologie einiger Aktivitätsgebiete in Verbindung mit Bildern im extremen Ultraviolett (EUV) und Röntgenlicht untersucht. Synoptische Karten der Korona wurden verwendet, um die erschlossenen Quellen des Sonnenwindes von der magnetischen Quellfläche runter in die Photosphäre abzubilden. In den meisten Fällen wurde eine dunkle Furche, wie sie typisch ist für ein schmales Koronaloch, in den EUV Bildern entdeckt, was auf ein offenes Magnetfeld hinwies. Mehrere verschiedene Quellregionen (Aktivitätsgebiete und Koronalöcher) des Sonnenwindes konnten so klar identifiziert werden. Die in-situ Daten der Ladungszusammensetzung des Sonnenwindes, der zu diesen Regionen gehört, weist auf hohe Koronatemperaturen der schweren Ionen hin, ein Resultat das konsistent ist mit dem Schluss, dass ein Aktivitätsgebiet in der Tat eine echte Quelle von Sonnenwind sein kann.

Wir haben ebenfalls Aktivitätsgebiete in Verbindung mit ihrem aus einer Extrapolation gewonnenen koronalen Magnetfeld und zusammen mit den Dopplerverschiebungen und Bildern im EUV studiert. Auf diese Weise konnten wir feststellen, dass die dunklen (in der ultravioletten Strahlung) Regionen in der Nachbarschaft von geschlossenen Magnetfeldschleifen eines Aktivitätsgebiets tatsächlich magnetisch offen sein können. Sie zeigen offensichtlich in heißen koronalen Emissionslinien auch starke Aufwärtsströmungen. Ein Beispiel dafür ist in Abb. 7 gezeigt, in der das kraftfreie Magnetfeld eines aktiven Gebietes, das mit einem Sonnenfleck assoziert ist, dargestellt wird. Wir fanden, dass das Plasma im Sonnenfleck deutlich aufwärts strömte mit einer Geschwindigkeit von einigen 10 km s^{-1}. In den anliegenden geschlossenen Magnetfeldschleifen wurden hauptsächlich Abwärtsströmungen beobachtet. Ob sich diese wirklich in die obere Korona fortsetzen, musste für dieses Aktivitätsgebiet offen bleiben, aber es ist wahrscheinlich.

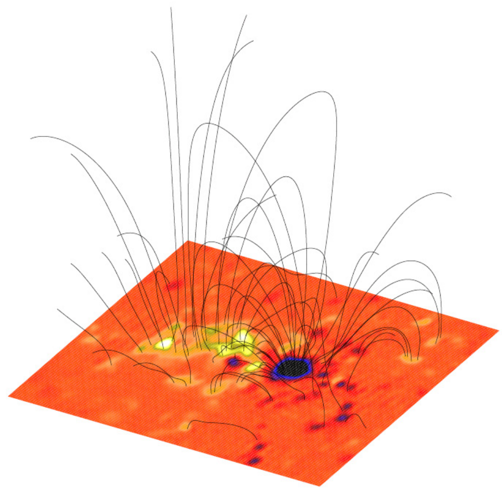

Abb. 7: Die Topologie des koronalen Magnetfelds in drei Dimensionen für ein bipolares aktives Gebiet. Nur solche Feldlinien sind über der Sonnenoberfläche dargestellt, für die in der Photosphäre $B_z > 50$ G war. Die Farbkodierung gibt die Feldstärke wieder. Eine entsprechende Karte der Dopplerverschiebung wird in der nachfolgenden Abb. 43 dieses Jahresberichts präsentiert (nach Marsch *et al.* (2004b)).

Wir können schlussfolgern, dass der Sonnenwind gelegentlich von der aktiven Sonne kommt, d.h. von Aktivitätsgebieten und ihren benachbarten kleinen Koronalöchern. Wieviele solcher Regionen im Sonnenmaximum mit dem langsamen Sonnenwind einhergehen bleibt zu untersuchen. Offen ist auch die Frage, ob der Sonnenwind in der ruhigen (weder assoziert mit einem Aktivitätsgebiet noch Koronaloch) Korona, die hauptsächlich aus geschlossenen Magnetfeldschleifen unterschiedlicher Größe besteht, entstehen kann.

Sonnenwind von der ruhigen Sonne?

Aus den Korrelationen zwischen der Stärke der solaren ultravioletten Strahlung und der vertikalen Komponente des Magnetfeldes, wie man sie aus der Extra-

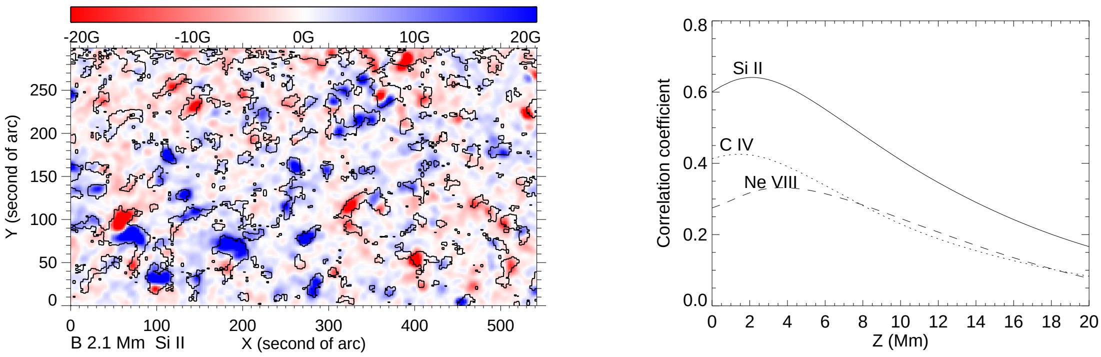

Abb. 8: Links: Magnetfeldstärke in Farbkodierung mit den überlagerten Kontouren der Si II Strahlungsstärke in einer Region der unteren Korona für die ruhige Sonne. Man beachte die deutliche Korrelation zwischen Magnetfeldstärke und Linienintensität. Hohe Intensität ist in starken Feldern konzentriert. Rechts: Die Korrelationshöhe, welche die mittlere Höhe der Strahlungsquelle angibt, für drei ultraviolette Linien wie angezeigt. Die effektive Höhe der Übergangszone ergibt sich zu nur etwa 2 Mm (nach Tu *et al.* (2005b)).

polation von photosphärischen Magnetogrammen zu verschiedenen Höhen erhält, läßt sich ungefähr die Emissionshöhe der Strahlung bestimmen, nämlich indem man die Höhe feststellt, wo der Korrelationskoeffizient zwischen Strahlungs- und Magnetfeld-Stärke sein Maximum hat. Auf diese Weise wurden für die ruhige Sonne die Korrelationshöhen für Si II bei 2.1 Mm, C IV bei 1.4 Mm, und Ne VIII bei 3.7 Mm bestimmt. Die Dicke der Übergangszone wurde so bei nur 2 Mm festgelegt. Die entsprechenden Profile der Korrelationshöhen werden im rechten Bild der Abb. 8 dargestellt, welche im linken Bild auch die zugehörige Karte des Magnetfeldes bei 2.1 Mm zeigt, wobei hier die Kontourlinien der Silizium-Linienintensität überlagert sind. Sie fallen mit den Gebieten großer Stärke des Übergangszonen-Magnetfeldes zusammen.

Ein Vergleich der extrapolierten Feldlinien mit den Dopplerverschiebungen von Ne VIII zeigt, dass schwache Blauverschiebungen von ungefähr 5 km s^{-1} in nur wenigen kleinen Gebieten mit hoher Feldstärke auftreten. Einige der geschlossenen Feldlinien mögen Höhen von bis zu 10 Mm erreichen. Kleine Blauverschiebungen treten sowohl in geschlossenen bipolaren Regionen als auch in offenen unipolaren Gebieten auf. Ob diese Aufwärtsströmungen eine Quelle des Sonnenwindes darstellen bleibt ungewiss. Die untere Übergangszone scheint in der Form eines Teppichs magnetischer Schleifen unterschiedlicher Größe stark strukturiert zu sein. Die meiste beobachtete ultraviolette Strahlung kommt ganz sicher von solchen Magnetfeldschleifen. Es ist jedoch unklar, wieviel offener magnetischer Fluss zwischen den geschlossenen Feldern in der ruhigen Sonne existiert, und wie dort der langsame Sonnenwind entstehen könnte.

Zusammenfassung

Wir haben eine knappen Überblick gegeben über den Ursprung des Sonnenwindes in der Korona und die Quellen der schnellen und langsamen Ströme. Offensichtlich ist das Magnetfeld der Hauptakteur bei den relevanten physikalischen Prozessen, denn es gibt der Korona ihre Gestalt und bestimmt die Eigenschaften und Dynamik des Sonnenwindes bei seiner Entstehung. Die Topologie und Aktivität des Magnetfelds sind die Schlüssel zum Verständnis dafür, wie der Sonnenwind in der Korona seinen Anfang nimmt. Da der Betrag des radialen magnetischen Flusses bei 1 AE zu allen Zeiten und über die ganze Himmelskugel als in etwa konstant gemessen wird, muss es zu jedem Zeitpunkt des Sonnenzyklus einen konstanten Anteil von offenem magnetischen Fluss in der Korona geben. So wie das Magnetfeld der Sonne sich systematisch im Verlaufe des Zyklus verändert, von einer einfachen Dipol- zur komplexen Multipol-Struktur, verändern sich die Quellen des Sonnenwindes, und dementsprechend variiert auch der Sonnenwind selbst. Plasma und Energie müssen laufend für ihn angeliefert werden, durch das magnetische Netzwerk in die Übergangszone und die untere Korona hinein. Rekonnexion im magnetischen Netzwerk scheint bei dieser Nachlieferung eine wesentliche Rolle zu spielen, wie numerische Simulationen bestätigten.

Zusammenfassend können wir sagen:

- Das koronale Magnetfeld auf allen Skalen bestimmt den Ursprung und die Entwicklung des Sonnenwindes in Raum und Zeit.

- Es gibt drei Arten von Sonnenwind: stetige schnelle Ströme, variable langsame Ströme und vorübergehende koronale Massenauswürfe.

- Die schnellen Ströme scheinen im Aktivitätsminimum ihren Ursprung in den Trichtern der polaren Koronalöcher zu haben, aber in anderen Phasen des Aktivitätszyklus auch in den Trichtern der äquatorialen Koronalöcher bei niedrigen Breiten.
- Die langsamen Sonnenwindströme kommen im Aktivitätsminimum hauptsächlich von den Streamern und ihren Grenzgebieten, während sie im Aktivitätsmaximum ihren Ursprung überall auf der Sonne in kleinen Koronalöchern und in der Nähe von Aktivitätsgebieten haben können.

Highlight:

Where does the solar wind come from? – News on the source regions of the solar wind in the Sun's corona

(E. Marsch)

Three main types of solar wind

Where and how the solar wind originates in the solar atmosphere remains, even after decades of solar research from space, one of the vital and key questions of modern solar physics. Generally speaking, the solar wind is largely determined by the Sun's magnetic field, and it responds in various ways to solar magnetic activity and the accompanying changes in the photospheric magnetic field, which in turn determines the coronal magnetic field and therewith the interplanetary magnetic field and solar-wind stream structure in the entire heliosphere. Apparently, the sources of the solar wind are defined by the coronal magnetic field, and the origin of the solar wind is closely linked with and influenced by the structure and activity of the magnetic network and the solar transition region.

In this highlight article we will discuss some new results on the origin of the solar wind, with emphasis on the physical nature of its source regions, which become evident in the solar extreme ultraviolet (EUV) emission patterns from the solar disk and in the corona, and from coronagraph images. The plasma characteristics and magnetic structures of the solar wind source regions are briefly reviewed. The solar-wind type is determined by the boundary conditions in the lower corona. It may be mostly closed (in streamers and loops), or transiently open (in eruptive prominences and flux tubes) or lastingly open (in coronal funnels and holes). The sources of the fast solar wind in particular will be discussed, especially at small scales and from the magnetic field point of view.

We have known for a long time that, as the result of varying boundary conditions in the corona, there exist three basic types of solar wind: Fast streams from large coronal holes; slow streams from small coronal holes and active regions, or from the boundary layers of coronal streamers; and the variable transient flows such as coronal mass ejections. The transients are often associated with eruptive prominences, plasmoids stemming from the top of streamers, or ejections from active regions that are driven through magnetic flux emergence and reconnection. Coronal mass ejections themselves, or their interplanetary manifestations, will be not discussed here but briefly considered later. The basic types of solar wind are closely associated with the structure and the activity of the coronal magnetic field that changes over the solar cycle.

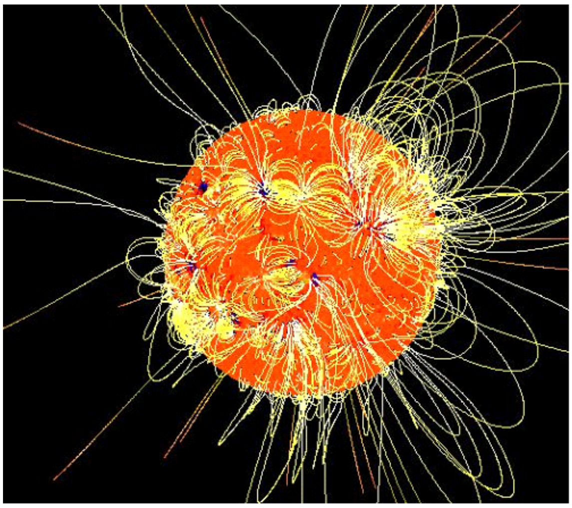

Fig. 1: The coronal magnetic field as obtained by a potential-field extrapolation from photospheric magnetograms. The closed magnetic loops mainly correspond to bipolar active regions, or they may also bridge widely separated regions of opposite polarity, whereas the straight lines illustrate the coronal magnetic field that is open to the heliosphere, and thus corresponds to the magnetic flux carried away by the solar wind (after Wiegelmann and Solanki (2004b)).

The large-scale solar corona and its magnetic field

The coronal magnetic field has never been measured directly, but it can be constructed by the help of extrapolation techniques, e.g. using potential-field, force-free-field or magnetohydrodynamic methods. A typical result obtained by a potential-field extrapolation is given in Fig. 1, which illustrates the open and closed field lines of the global coronal magnetic field. An active region mainly consists of closed magnetic loops, in which dense plasma can be confined. Therefore, the active region causes bright emission and is clearly visible in ultraviolet and X rays. In contrast, the large-scale open magnetic field cannot even hold tenuous plasma, which can therefore escape freely in the form of the solar wind. Hence the open-field regions appear dark. They were named coronal holes since their emission is comparatively low. These main coronal features are obvious in any of the ultraviolet images that regularly are obtained by SOHO.

The solar magnetic field determines the solar wind flow pattern and the structure of the entire corona. Its magnetic field gradually evolves with increasing distance from the Sun into the heliospheric (interplanetary) magnetic field. At some height, which usually is assumed to range between two and three solar radii, the field essentially becomes straight and is carried away, while being frozen into it, by the solar wind. The related magnetic source surface is considered a virtual sphere from which on the outer coronal field is mainly radial. In the potential-field model one extrapolates the solar magnetic field, as it was measured in the photosphere, into the corona, while postulating that the coronal field is free of currents. In the more realistic force-free-field model, electric currents are considered but assumed to flow along field lines only in the corona. The field polarity changes across current sheets, and in particular through the heliospheric current sheet which during solar minimum is linked with the equatorial streamer belt. Then the heliospheric current sheet extends as a flat disk far out into interplanetary space.

The structure of the solar corona is most simple around minimum activity, where the field can well be modeled by a superposition of dipolar, quadrupolar, and current-sheet-related components. This minimum-type corona is illustrated in Fig. 2. The three-dimensional structure of the solar wind was revealed together by the Helios and Ulysses missions. The global structure of the solar wind and its variation over the solar cycle were fully established by Ulysses, which confirmed that high-speed solar wind originating in the polar coronal holes prevailed over the poles in solar minimum, when slow wind coming from the streamer belt dominated at low latitudes. The magnetic field becomes multipolar towards solar maximum activity, and the solar wind source regions accordingly change in their locations on the Sun and spatial extents. Similarly, the solar wind flow pattern becomes more complex and variable.

The changing solar corona and associated solar wind are shown in Fig. 3, which presents a sequence of coronal images in the top panel and shows the solar wind speed in the bottom panel versus time and heliographic latitude. The transition from a minimum-type corona around 1995 to a maximum-type near 1999 is obvious and accompanied with a striking transition from steady fast to variable slow solar wind. The recurrent stream oscillations between 1996 and 1997 were due to solar rotation, which in that period caused rapid transitions of the spacecraft into and out of the heliospheric current sheet, respectively into and out of the open magnetic field (of the heliosphere) that was closely related with the polar coronal holes on the Sun. These changes resulted in a periodic variation between fast and slow flows. At the bottom of the panel, the occurrence times of coronal mass ejections are also indicated.

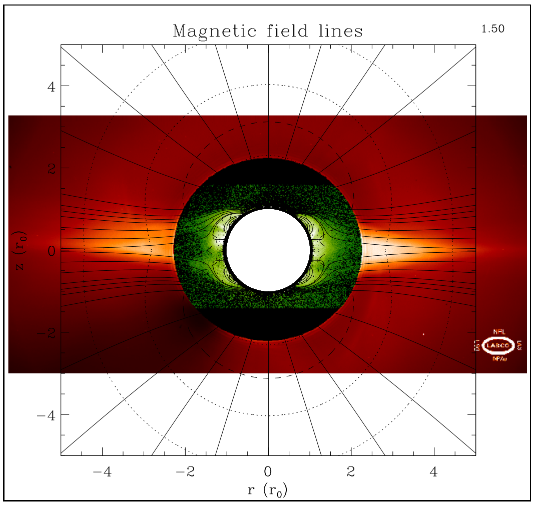

Fig. 2: The highly symmetric solar corona at minimum solar activity and the associated coronal magnetic field. Superposed on the model field lines are coronal images obtained from LASCO (in the green coronal iron line and white light), which indicate the wide dark polar coronal holes and the low-latitude bright current sheet coinciding with the narrow equatorial streamer belt. It appears as elongation on both sides of the Sun (after Forsyth and Marsch, 1999).

In addition to the steady streams, the coronal mass ejections represent the other basic type of (variable and sporadic) solar wind (or better solar storms). Concerning their ocurrence rate, the coronal mass ejections tend to accumulate (with an occurrence rate of about three per day) around maximum solar activity, when the corona is highly magnetically structured and of complex multi-polar nature. They seem to come in two main types, as slow and fast coronal mass ejections, although this rough classification is not unique. A sizable fraction (about 30% or more) of the coronal mass ejections have a large eruptive prominence at their origin, the remnants of which can still be observed as post-eruptive arcades. For coronal mass ejections the energy requirements and acceleration mechanisms are even less understood than for

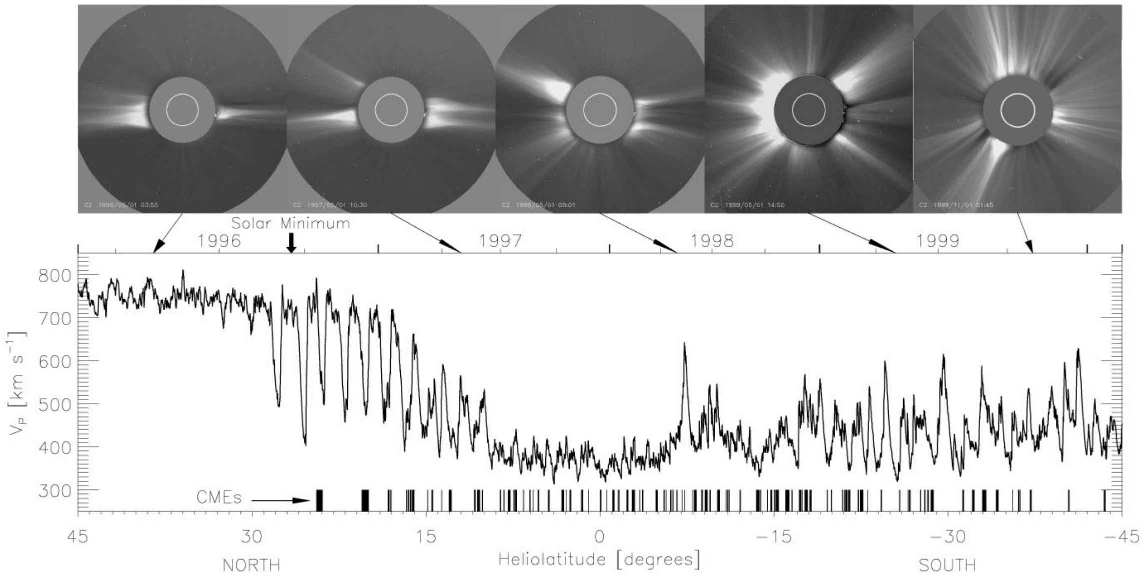

Fig. 3: The changes of the solar corona (top) over the solar cycle and the corresponding variations in the solar wind flow pattern (bottom) as a function of time or heliographic latitude along the Ulysses spacecraft orbit. Note the recurrent streams after minimum. The occurrence of coronal mass ejections is marked by the small vertical bars attached to the bottom scale (after McComas *et al.*, 2000).

the steady solar wind streams. The constraints on the plasma are also more extreme for a transient coronal mass ejection than for a steady wind stream, as the coronal mass ejection plasma density is often much higher, and its flow speed may easily reach a multiple of the average solar-wind speed.

Returning to the steady solar wind, we recall that it consists of two major components: fast, tenuous, and uniform flows, and slow, dense, and variable flows. The global associations of the fast solar wind with large coronal holes and of the slow solar wind with the streamer belt, or often the boundaries between closed and open magnetic fields and small coronal holes are long well established.

There are various techniques of mapping solar wind flows back to the Sun in order to identify their sources in the corona. Recently, what appeared to be narrow coronal holes in soft X-ray images for example, were studied and identified to be the possible sources of the slow solar wind. By using solar wind in-situ data from near-Earth spacecraft, it was also found that slow streams can emanate from small coronal holes in the vicinity of active regions.

Yet, tracing the in-situ measured solar wind back to its detailed sources at smaller scales on the Sun is not an easy task. But, here we will now present some new results, in which the sources were identified through a combined analysis of Doppler shifts and radiances of ultraviolet emission lines together with the coronal magnetic field. It is constructed from measured magnetograms and can then be extrapolated to all relevant heights above the photosphere.

Solar wind from funnels and coronal holes

In several recent studies we analysed detailed observations of equatorial coronal holes and investigated the small-scale magnetic field structures in the source regions of the fast solar wind. We directly compared the Dopplergrams and the plasma flow velocity, as obtained by the SUMER (Solar Ultraviolet Measurements of Emitted Radiation) instrument on SOHO, with the coronal magnetic field, as constructed from photospheric magnetograms at the bottom of the coronal hole via either potential or force-free magnetic-field extrapolation. In the cases studied, we thus combined spectroscopic data with the three dimensional magnetic field, an approach that provided a clearer physical picture of the plasma conditions and flow pattern prevailing in the corona.

In Fig. 4 we present a Dopplermap of a part of an equatorial coronal hole, with the Doppler shift over the range of ± 20 km s^{-1}, and the extrapolated magnetic field lines shown in projection for comparison with the Dopplershift pattern. The closed field lines are drawn in yellow and the open ones in red-brown colour. An area of $250'' \times 300''$ on the solar disk is shown, covering a large fraction of the coronal hole and its boundary regions. Detailed inspection of Fig. 4 indicates that we find almost everywhere in this coronal hole region blue shifts, i.e. plasma outflow along the line of sight at flow speeds of typically up to 10 km s^{-1}. There are hardly any significant redshifts. In the yellow domains, with closed magnetic loops, the plasma is nearly at rest.

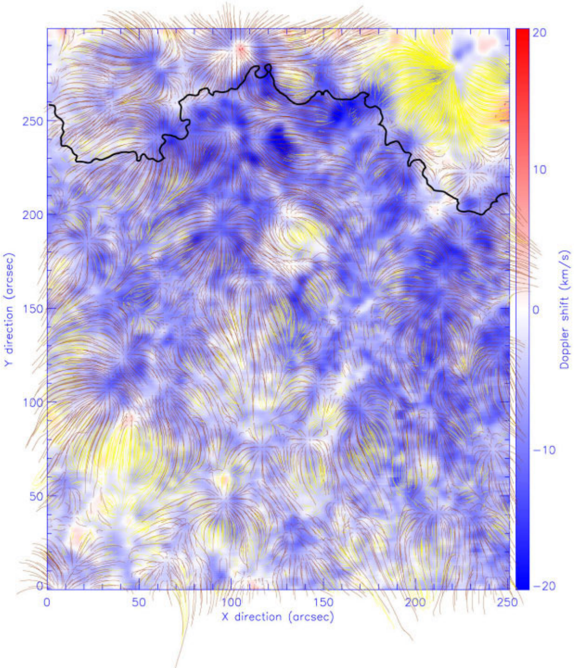

Fig. 4: Map of the Doppler shift of the Ne VIII (77 nm) emission line, together with the projections of the extrapolated coronal magnetic field lines. Here yellow means closed and red-brown open field lines. An area of $250'' \times 300''$ on the solar disk is shown, covering a fraction of an equatorial coronal hole and its boundary (indicated by the dark line) regions. Note the uniformly yellow domain in the top right corner, which lies outside the coronal hole and corresponds to closed loops. The cross-shaped spines of open flux in the top left corner coincide with blue patches and thus indicate sizable coronal plasma outflow in this open field domain. There are many open field lines overarching the yellow patches, corresponding to the closed-field carpet, with magnetic flux being confined to near the Sun's surface (after Wiegelmann *et al.* (2005d)).

These findings were corroborated by an analysis of the detailed source regions of the fast solar wind emanating in a polar coronal hole. The sources were again found to be identical with the so-called coronal funnels, i.e. with the expanding open magnetic field structures that are rooted in the magnetic network lanes. The new results complemented the earlier work and further established that what becomes the fast solar wind starts flowing out of the corona at heights above the photosphere between 5 Mm (Megameter) and 20 Mm in the funnels.

The new findings are illustrated in Fig. 5, which in the top panel shows in two planes at heights of 0 and 20 Mm the colour-coded maps of the magnetic field strength. Regions with outflow speed larger than 7 km s^{-1} are indicated by the hatched patches that coincide with the open, unipolar and strong magnetic fields representing the funnels. Our novel results were obtained by a detailed correlation of the Doppler-velocity and radiance maps of different spectral lines. Specifically, Ne^{7+} ions were found to mostly radiate around 20 Mm, where they have outflow speeds of about 10 km s^{-1}, whereas C^{3+} ions with no average flow speed mainly radiate around 5 Mm. The interpretation of all this is that the nascent solar wind was detected, and its sources identified as the magnetically open coronal funnels.

These observations correspond well to the following scenario of the original acceleration of the fast solar wind: The transition region in coronal holes is reached by magnetic loops of different sizes, mostly with a height of less than 5 Mm. The supergranular convection in the photosphere keeps the feet of the loops moving and thus transfers kinetic energy to magnetic energy that is stored in the loops. They may finally collide with a funnel and thereby reconnect the with pre-existing open field. Plasma of the loops is thus released, and this may lead to both upflows and downflows. Ultimately, parts of the plasma contained in reconnecting loops are brought into the open corona. In the lower transition region below about 5 Mm, we mainly have horizontal exchange of mass and energy between neighbouring flux tubes, which is driven by supergranular motion. Above 5 Mm or higher, where reconnection between field lines of funnels and surrounding loops gradually ceases, vertical transport will become more important than horizontal, and the radial acceleration of the solar wind will actually start.

Numerical simulations carried out at the MPS in Lindau revealed that for this the magnetic reconnection between low-rising loops and funnels can in fact be responsible. Fig. 6 shows the regions of different plasma velocity as obtained in the simulation. The plasma flows in the direction of the observer are shown in blue and toward the Sun in red (colour scale in km/s), with velocity values as they are about found in measurements of the Doppler shift.

Solar wind from active regions?

As already mentioned above, it is only recently that active regions near solar maximum were clearly identified as the source regions of slow solar wind. For example, the magnetic topology of several active regions was investigated in connection with EUV and X-ray

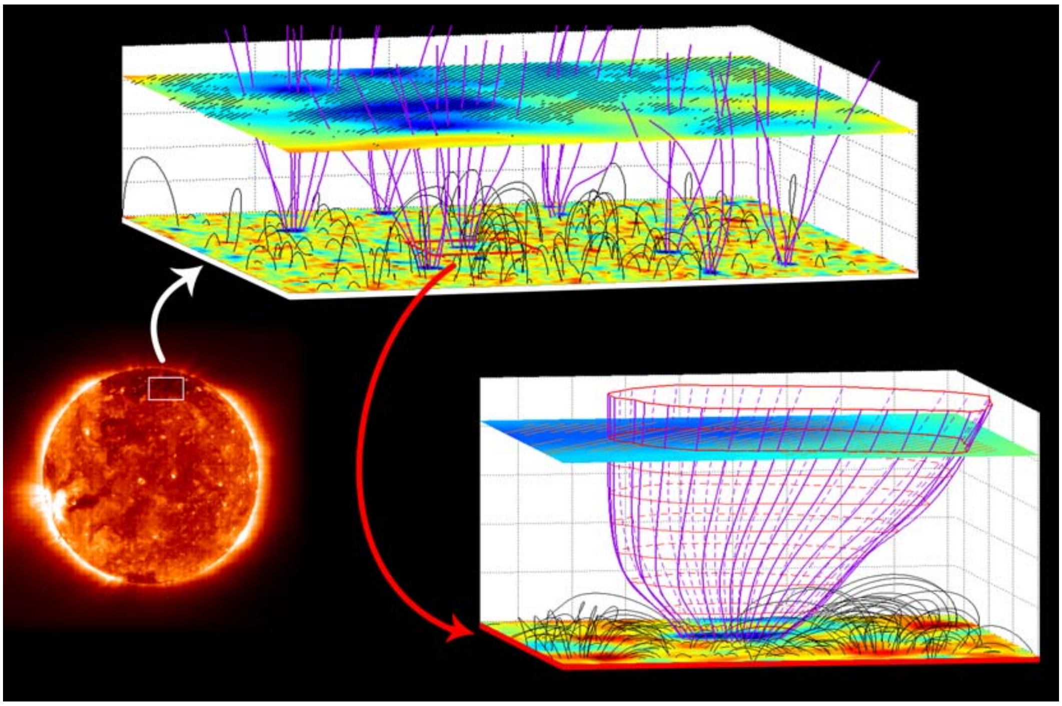

Fig. 5: In the bottom left corner there is an ultraviolet image of the full Sun with a large polar coronal hole, of which a segment with selected source regions of the fast solar wind is indicated by a white box. The sources were found to be the magnetic funnels (top panel) in the coronal hole. The magnetic field magnitude is shown in two planes at 4 Mm and 20 Mm. The hatched areas indicate outflow speeds of neon ions larger than 7 km s^{-1}. The open field is indicated by black lines, and the closed loops are shown in magenta colour. They hardly reach a height of 10 Mm. The bottom right panel shows a single funnel as constructed by means of the coronal field extrapolation. The funnel's cross area is constricted by multiple adjacent loops pushing strongly against it (after Tu *et al.* (2005a)).

images. Synoptic coronal maps were employed for mapping the inferred sources of the solar wind from the magnetic source surface down to the photosphere. In most cases, a dark lane, as it is familiar for the small coronal holes, was seen in the EUV images, thus suggesting an open magnetic field. Several different solar wind sources (active regions and coronal holes) could thus clearly be identified. The in-situ charge composition data of the solar wind associated with these regions indicates high coronal temperatures of the heavy ions, a result that is consistent with the inference that an active region can indeed be a genuine source of solar wind.

We have also studied active regions in connection with their coronal magnetic field as obtained by extrapolation and together with EUV Doppler shifts and images. Thus we could establish that the dark (in ultraviolet emission) areas adjacent to the closed active region loops can indeed be magnetically open, and apparently reveal strong upflows in hot coronal emission lines. One example is shown in Fig. 7, where the force-free model magnetic field of active region associated with a sunspot is shown. The plasma was found to clearly stream upward in the sunspot with a speed of several 10 km s^{-1}. In the adjacent closed loops mostly downflows were observed. Whether the upflows actually continue into the upper corona for this active region remained unclear, but it appears to be likely.

In conclusion, solar wind can at times come from the active Sun, i.e. from active regions and their small neighbouring coronal holes. How many such regions during solar maximum are associated with slow solar wind remains to be investigated. The question still is open if the solar wind can originate in the quiet (i.e. being neither associated with an active region nor a coronal hole) corona, which mainly consists of closed magnetic loops of different sizes.

Solar wind from the quiet Sun?

From correlations between the radiance of the solar ultraviolet emission and the vertical magnetic field component, as obtained by extrapolation from photospheric magnetograms to different heights, one can roughly determine the correlation height of the emission source, namely by identifying the altitude at which the correlation coefficient between the radiance and field strength has its maximum. In this way it was found that for a quiet-Sun region the correlation

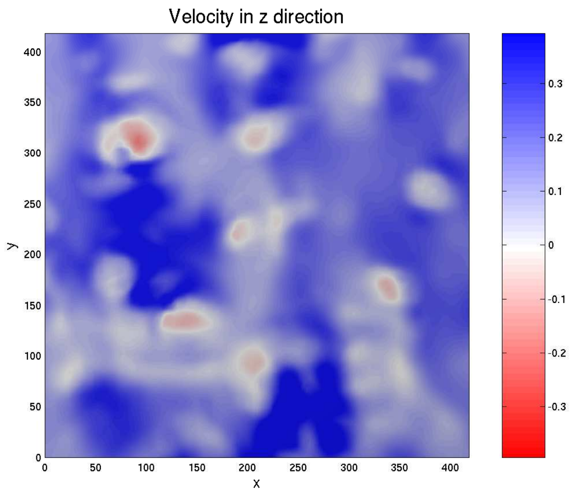

Fig. 6: Numerical simulations carried out at the MPS in Lindau revealed that the magnetic reconnection between low-rising loops and funnels can in fact be responsible for the initial solar wind acceleration. This figure shows the regions of different plasma velocity as obtained in the simulation. The plasma flows in the direction of the observer are shown in blue and toward the Sun in red (colour scale in km/s) (Büchner and Nikutowski, 2005).

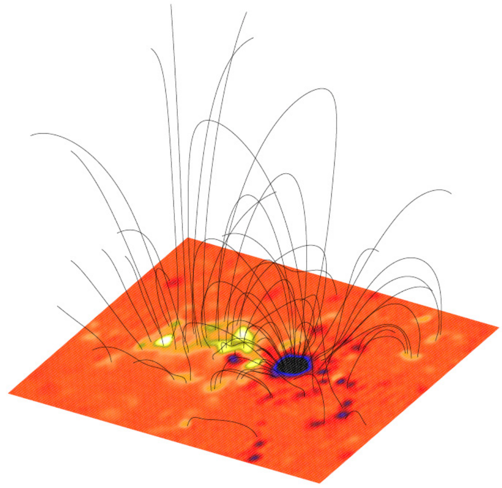

Fig. 7: The coronal magnetic field topology in three dimensions for the bipolar active region. Only field lines above the solar surface with $B_z > 50$ G on the photosphere are plotted. The colour coding represents the magnetic field strength. A corresponding Doppler-shift map is presented in the subsequent Fig. 43 of this annual report (after Marsch *et al.* (2004b)).

height for Si II was near 2.1 Mm, C IV at 1.4 Mm, and Ne VIII at 3.7 Mm. The thickness of the quiet-Sun transition region was thus determined to be only about 2 Mm. The respective correlation height profiles are illustrated in the right panel of Fig. 8, which also shows on its left side the related magnetic-field map at 2.1 Mm, with the superimposed contours of the silicon-line radiance. These contours coincide with regions of a strong transition region magnetic field.

A comparison between the extrapolated field lines and the Dopplershifts of Ne VIII indicates that weak blueshifts of about 5 km s^{-1} occur in a few small regions with strong magnetic fields. Some of the closed field lines may reach as high as 10 Mm. Weak blueshifts also appear in both closed bi-polar regions and open unipolar regions. Whether these outflows correspond to a solar wind source, or are related with mass supply to the myriad of coronal loops, remains unresolved. The lower transition region appears to be highly structured by a carpet of magnetic loops of different sizes. Most of the observed ultraviolet radiation certainly comes from such loops. However, it is unclear how much open magnetic flux exists in between such closed loops in the quiet corona, and how the slow solar wind could originate from there.

Obviously, the magnetic field is the main player in the relevant physical processes, since it shapes the solar corona and thus defines the properties and dynamics of the nascent solar wind. The field topology and activity are the keys to understand how the solar wind originates in the corona. Since the magnitude of the radial magnetic flux at 1 AU is measured to be almost constant over the full sphere and at any time, there must be a constant fraction of open magnetic flux in the lower corona at any time of the solar cycle. As the Sun's magnetic field varies systematically over the solar cycle, from a simple dipolar structure to a complex multipolar structure, so do the solar wind sources, and correspondingly varies the solar wind itself. Its plasma and energy have continuously to be supplied through the magnetic network into the transition region and lower corona. Reconnection in the magnetic network appears to play a main role in this supply, as confirmed by numerical simulations.

Summary

We have briefly reviewed the coronal origin of the solar wind and the sources of the fast and slow streams.

In summary we may say:

- The coronal magnetic field at all scales determines the origin and evolution of the solar wind in space and time.
- The solar wind comes in three types, as steady fast streams, variable slow flows and transient coronal mass ejections.
- The fast streams in solar activity minimum appear to originate in the funnels of the polar coro-

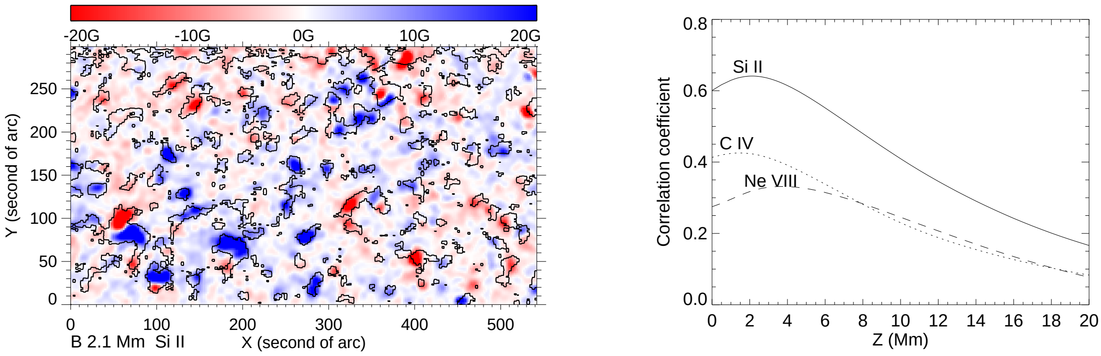

Fig. 8: Left: Magnetic field intensity colour-coded with superimposed contours of the Si II radiance for a quiet-Sun region of the lower solar corona. Note the clear correlation between field strength and line intensity. The high radiances are concentrated in the strong fields. Right: Correlation heights, defining the mean altitude of the emission region, for three ultraviolet lines as indicated. The effective transition region height is found to be only about 2 Mm (after Tu *et al.* (2005b)).

nal holes, but in other phases of the activity cycle also from the funnels of the low-latitude equatorial coronal holes.

- The slow streams in solar activity minimum mainly come from streamers and their boundaries, whereas in activity maximum they can originate all over the Sun in small coronal holes and near active regions.

Wissenschaftliche Einzelberichte/ *Individual scientific reports*

(nur in Englisch)

Solar interior, photosphere and chromosphere

Nonlinear dynamo saturation

The Sun's magnetic field, which is generated by dynamo action in the convection zone, has a total energy which is thought to be comparable with the kinetic energy of the differential rotation near the tachocline. The maintenance of such strong magnetic fields by dynamo action, especially in highly conducting plasmas, is not well understood. In order to understand some of the fundamental issues, we have studied some dynamos which saturate with almost equal magnetic and kinetic energies (Alfvénic solutions).

The Archontis dynamo is the best studied example of this type of dynamo (see Fig. 9). The velocity is driven by the spatially periodic force, in addition to the Lorentz, pressure, and viscous forces, and is periodic in all three spatial dimensions. In the non-magnetic case, and with small diffusivities, this forcing produces turbulence. Given a weak seed magnetic field, however, dynamo action occurs and the flow is driven to a stable time-independent equilibrium with almost equal magnetic and kinetic energies.

Important for this dynamo is the fact that the streamlines are chaotic. That is to say they are extremely efficient at stretching and twisting the streamlines, and the accompanying figure partly explains why this is the case. The figure shows some topologically important features of the flow in one of the periodic cubes: blue balls show the location of stagnation points (which are also magnetic null points); the black and orange lines are streamlines connecting the stagnation points; the green, yellow and red show surfaces of streamlines which connect to the central stagnation point. The black streamlines connect with stagnation points in pairs, and the yellow surface is bounded by a pair of such black streamlines. The red streamlines lie between black streamlines connecting different stagnation points, as do the green. Because the flow is incompressible as the second stagnation point is approached the yellow streamlines go in the opposite direction to the red and green streamlines. The red and green streamlines are then brought together. The important point is that streamlines which were originally close together (red and yellow or green and yellow) are efficiently separated and streamlines which were originally separated (green and red) are pushed together.

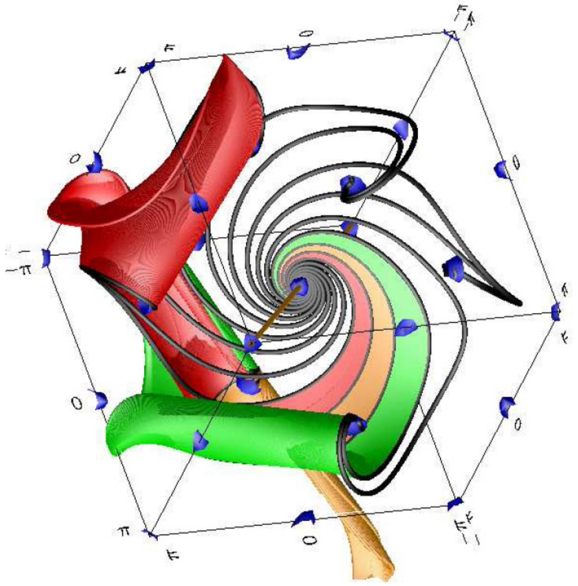

Fig. 9: This image shows the topology of the one and two-dimensional manifolds associated with a stagnation point of the Archontis dynamo. The Archontis dynamo is the first known example of a dynamo which, at low resistivity and viscosity, is Alfvénic when it saturates (i.e. the flow everywhere is at the local Alfvén speed).

The importance of this type of action is captured by the phrase "stretch, twist and fold".

The Archontis dynamo is far from unique: we have shown that many such Alfvénic solutions exist, although we have not been able to show they are all stable. The issues raised by this class of dynamo relate both to astrophysical dynamo action and magnetohydrodynamic turbulence.

(R. Cameron in collaboration with David Galloway (University of Sydney))

Magnetic flux emergence in the solar photosphere

The most prominent magnetic structures on the surface of the Sun are bipolar active regions. These magnetic complexes comprise of a hierarchy of magnetic structures of different sizes, the largest of which are sunspots. Observations indicate that the appearance of active regions on the solar surface result from the emergence of bundles of magnetic flux from the underlying convection zone.

The aim of this project is to study the magnetic flux emergence process by carrying out 3-dimensional, radiative magnetohydrodynamic (MHD) simulations. In the simulations, an initially buoyant magnetic flux tube is introduced into the near-surface layers of the convection zone. Subject to the buoyancy force, the flux tube rises towards the photosphere. Fig. 10 shows an example of an arched magnetic flux tube emerging into the photosphere.

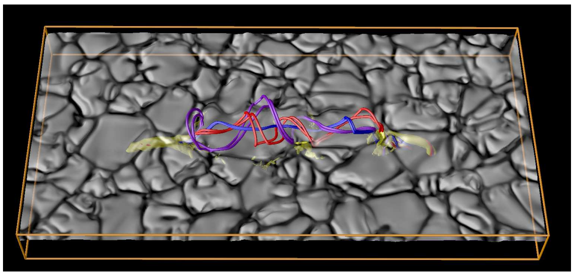

Fig. 10: The emergence of a twisted, arched magnetic flux loop from the convection zone into the photosphere. The greyscale indicates the vertical velocity (within the range ± 3 km s^{-1}, upflows bright, downflows dark) at the base of the photosphere. The subsurface trunks of the arched flux tube are indicated by the yellow isosurfaces of $|B| = 2000$ G. The winding of the field lines around the axis of the tube indicates its inherent twist.

Our simulations highlight the importance of magneto-convection on the evolution of the magnetic flux tube. The external convective flow field has an important influence on the morphology of the emerging magnetic field. Depending on the initial properties of the flux tube (e.g. field strength, twist, entropy etc.), its emergence can disturb the local granulation pattern. The observational signatures associated with emerging magnetic flux in our simulations are in qualitative and quantitative agreement with observational studies of emerging flux regions.

(M. C. M. Cheung and M. Schüssler in collaboration with F. Moreno-Insertis (Instituto de Astrofísica de Canarias, Spain))

Simulation of solar pores

Pores are dark magnetic features at on the solar surface, similar to sunspots except they lack a penumbra. Using the *MURaM* code, we have carried out realistic radiation MHD simulations of pore-sized magnetic flux concentrations. Starting with already established pores, we have followed their development and decay in the course of time. Fig. 11 shows three snapshots from the simulation, which cover about one hour simulated time.

We have compared the simulations with observational results from other authors. As an example, Fig. 12 shows the profiles of the temperature and density (averaged over the pore) as a function of continuum optical depth in comparison with observations .

(R. Cameron, M. Schüssler, A. Vögler)

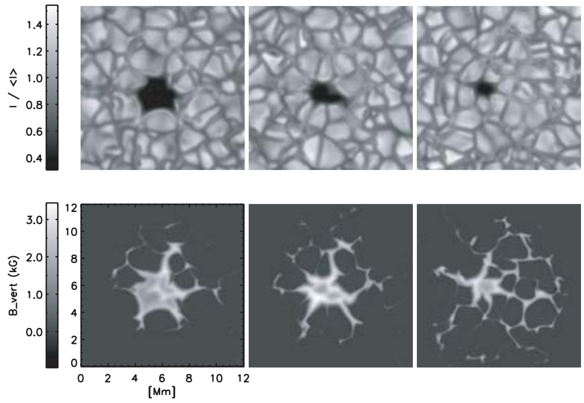

Fig. 11: Snapshots showing the decay of a pore. Upper row: brightness images, lower row: strength of the vertical component of the magnetic field.

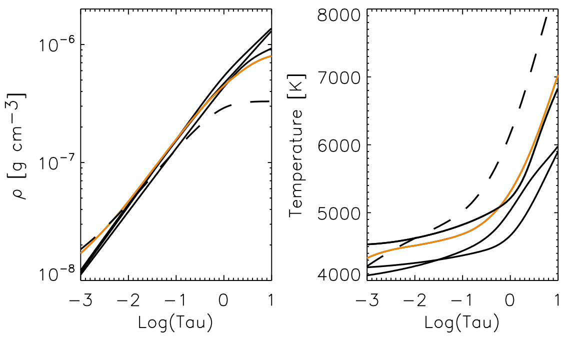

Fig. 12: Comparison of the average optical-depth profiles of density (left) and temperature (right) from three simulations of pores of different sizes (orange lines) with observational results (solid black lines) by P. Sütterlin (A&A, 333, 305; 1998). The dashed line shows the quiet-Sun temperature profile).

Modelling of solar mesogranulation

Mesogranulation is a pattern of horizontal flows in the solar photosphere at scales of 4 – 10 Mm, intermediate between granulation (the convection pattern carrying the energy) and supergranulation (outlining the magnetic network). The physical nature of mesogranulation and whether it has a preferred scale are open questions. Proposed explanations range from a genuine convection pattern to collective phenomena of granulation cells.

We have constructed highly idealized one- and two-dimensional granulation models employing different cell-interaction rules in order to analyze the conditions for the emergence of mesogranular patterns (Fig. 13). We analyze our synthetic patterns in a similar way as done in observational studies (e.g., by employing local correlation tracking). We find that the so-defined mesogranular cells naturally appear in such multicell systems as a pattern of longer-lived downflows to-

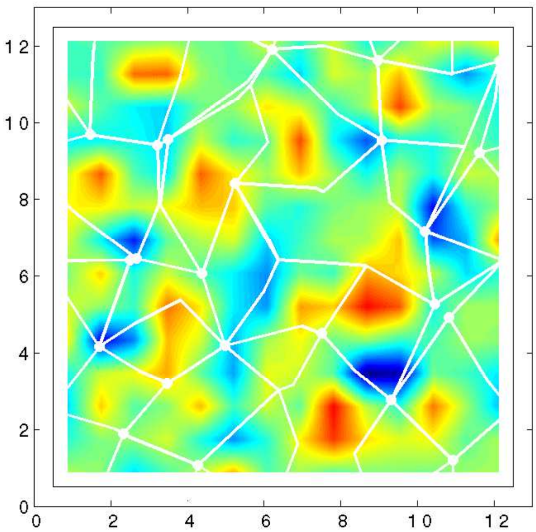

Fig. 13: Mesogranulation cells in a map of (time-averaged) horizontal flow divergence determined from the motions of an underlying system of triangular granules (not shown). Red colour indicates positive divergence (horizontal expansion), blue colour mean negative divergence. Lengths are given in units of the average granule size. The white lines show long-lived granular downflow lanes (lifetime > 1 hour). The correspondence between the divergence pattern and the long-lived downflow lanes indicates a purely statistical origin of the mesogranular pattern.

gether with the associated average horizontal flows. The spatial scale of the pattern grows with increasing averaging time, indicating that it does not represent an intrinsic scale of the system. On the other hand, the statistical properties of the mesocells (size and lifetime) do not strongly depend on the local granule interaction rules (including purely random cases). These results support the interpretation of mesogranulation as a purely statistical phenomenon due to the lifetime distribution of granular downflows.

(L. Matloch, R. Cameron, D. Schmitt, M. Schüssler)

Decay of a mixed-polarity magnetic field

The cancellation and decay of a mixed-polarity field in the solar photosphere are not well understood since the relevant processes operate on small length scales. We have carried out realistic radiation MHD simulations with the *MURaM* code to follow the evolution of an initially vertical field of mixed polarity (2×2 'checkerboard' pattern). An early phase of the simulation is shown in Fig. 14. We find that the exponential decay rate for the magnetic energy is well approximated by the conventional estimate for the turbulent magnetic diffusivity, namely $\eta \simeq U \cdot L/3 \approx 3 \cdot 10^{12}\,\mathrm{cm^2{\cdot}s^{-1}}$ with $U \simeq 1\mathrm{km{\cdot}s^{-1}}$ and $L \simeq 1\,\mathrm{Mm}$, which are typical values for granulation.

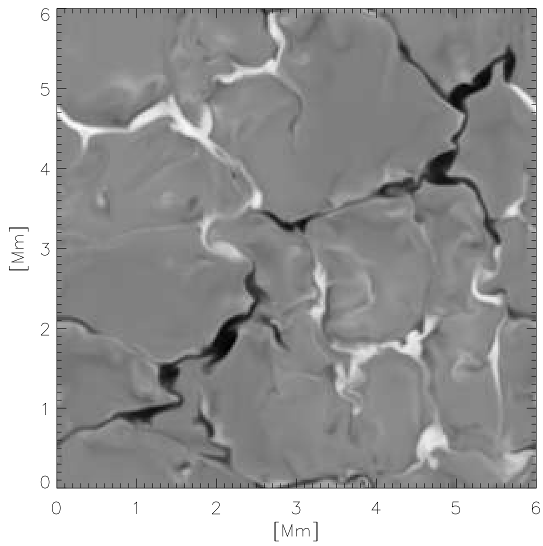

Fig. 14: Early phase of the decay of a mixed-polarity field. Shown is the strength of the vertical magnetic field on a horizontal plane in the simulation box located near the visible surface. The grey scale covers fields between about $+1500$ G (white) and -1500 G (black).

The decay (cancellation) of magnetic flux threading the surface layers layers is mainly caused by reconnection of opposite-polarity field in current sheets in the upper photosphere. The resulting $\cap$-loops and $\cup$-loops are then drawn downward and upward, respectively, by the magnetic tension forces and eventually leave the computational box through the lower and upper boundaries. Observationally, such a cancellation event corresponds to the retraction of a $\cap$-loop through the visible layers.

(A. Vögler, R. Cameron, M. Schüssler)

Magneto-convection in a sunspot umbra

The dark central part of a sunspot, the umbra, emits only 10 – 20% of the average energy flux outside sunspots, owing to the suppression of vigorous convective flows by the strong magnetic field.

However, even this strongly diminished energy flux cannot be carried by radiation alone below the umbral photosphere, so that some form of reduced convective energy transport is required. The observation of umbral dots, relatively bright features of sub-arcsecond size embedded in the dark umbral background, has often been taken as a signature of such convective energy transport, being either in the form of overstable oscillations ('elevator convection') in thin vertical columns or as intrusions from below of non-magnetic plasma into a shallow cluster-type sunspot. We have used our *MURaM* code to carry out the first realistic simulations of 3-D radiative magneto-convection in a sunspot umbra with full radiative transfer and partial ionization effects.

We find that the convective energy transport is dominated by narrow upflow plumes with downflows at their sides, which become almost field-free near the surface layers (see Fig. 15). The strong external magnetic field forces the plumes to assume a cusp-like shape in their top parts, where the upflowing plasma loses its buoyancy. The resulting bright features in intensity images correspond well (in terms of brightness, size, and lifetime) to the observed umbral dots in the central parts of sunspot umbrae. Most of the simulated umbral dots have an elongated form with a central dark lane. Above the cusp, most plumes show narrow upflow jets, which are driven by the pressure of the piled-up plasma below. The large velocities and low field strengths in the plumes are effectively screened from spectroscopic observation because the surfaces of equal optical depth are locally elevated, so that spectral lines are largely formed above the cusp. Our simulations demonstrate that nearly field-free upflow plumes and umbral dots are a natural result of convection in a strong, initially monolithic magnetic field.

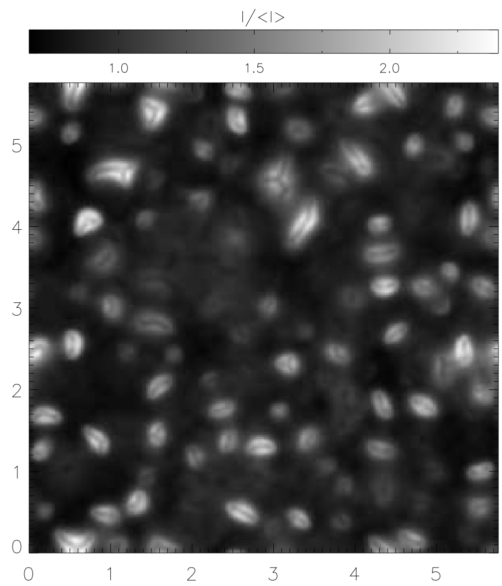

Fig. 15: Vertically emerging intensity (brightness) from the simulation box. The length unit is Mm. The vertical magnetic field has a (horizontally averaged) strength of 2500 G. The bright features in the intensity image can be identified with umbral dots. They are caused by strong upflows in regions of significantly reduced magnetic field. Their brightness, size, and lifetime correspond well to observational results. The dark lane in many of the umbral dots is caused by cooler, stagnant matter located in the cusp-shaped top parts of the upflow plumes.

(M. Schüssler, A. Vögler)

Using simulations of magnetoconvection to estimate the magnetic flux in the internetwork quiet-Sun

The amount of magnetic flux in the quiet Sun is a subject of considerable debate, with different techniques giving different results. We have made use of realistic solar magneto-convection simulations including the photospheric layers to study the polarization of the Zeeman-sensitive Fe I photospheric spectral lines at 6301.5 and 6302.5 Å in the visible and at 15 648 and 15 652 Å in the infrared. This provides a novel technique to set limits on the spatially averaged field strength, $\langle B \rangle$, and thus the magnetic flux in the quiet Sun. The Stokes spectra are synthesized in a series of snapshots with a mixed-polarity magnetic field whose average unsigned strength varies from $\langle B \rangle$ = 10 to 140 G. The effects of limited spatial resolution and of the amount of magnetic flux in the simulation box on the Stokes profile shapes, amplitudes and shifts are discussed. The synthetic spectra show many properties in common with those observed in quiet solar regions. In particular, the simulations reproduce the width and depth of spatially averaged Stokes I profiles and the amplitude and area asymmetries of Stokes V profiles, as well as the abundance of the irregular-shaped Stokes V profiles.

A direct comparison of the amplitudes of Stokes spectra of the Fe I 630 nm and 1.56 μm lines produced by these MHD simulations with simultaneous observations of the quiet Sun shows that the probability distribution function of Stokes V amplitudes depends sensitively on $\langle B \rangle$. We find that the Stokes V amplitudes of both infrared and visible observations are best reproduced by the simulation snapshot with $\langle B \rangle$ = 20 G. Our analysis also reveals that in observations with 1″ resolution, up to 2/3 of the magnetic flux can remain undetected.

(S. K. Solanki, A. Vögler and S. Shelyag, in collaboration with E.V. Khomenko, M. J. Martínez González, M. Collados and B. Ruiz Cobo (Instituto de Astrofísica de Canarias, Tenerife, Spain) and C. Beck (Kiepenheuer-Institut für Sonnenphysik, Freiburg))

Spectro-polarimetric diagnostics of radiation MHD simulations

In order to compare the results of realistic 3-D simulations of a mixed-polarity region in the solar photosphere with observational results, we have calculated synthetic spectra of the Stokes parameters on the basis of the simulation results. We have also tested the quality of inversion procedures by feeding the synthetic spectra into a Milne-Eddington inversion code and comparing the results (magnetic field, temperature, etc.) with the original data from the simulation. In performing such a test, the degradation of the observations by the finite aperture of the optical device, by seeing effects in the terrestrial atmosphere, and by detector noise have to be taken into account. In order to to quantify how well the structure of the magnetized solar atmosphere can be determined from such a degraded data, we have convolved the synthetic Stokes maps with the point spread function corresponding to the optical system as well as with the spectral filter function and added noise of various amplitudes. The resulting maps of Stokes profiles were used as input for the inversion code and the resulting parameters of the solar atmosphere were compared with the original structure from the MHD simulation.

(L. Yelles-Chaouche, A. Lagg, M. Schüssler, S. K. Solanki)

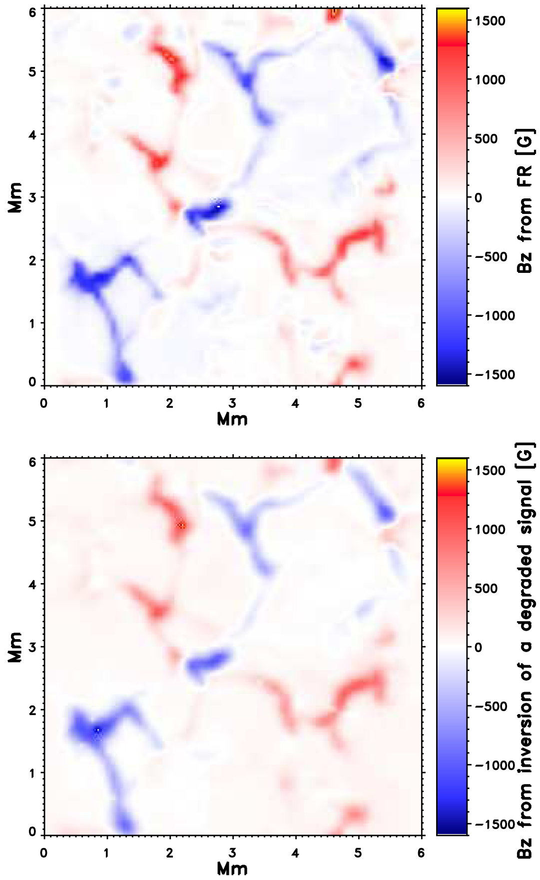

Fig. 16: Maps of the vertical component of the magnetic field on a horizontal plane of the simulation box. Upper panel: Values from the simulation (height average weighted with the Stokes response function for the spectral line FeI 6173 Å). Lower panel: Result of a Milne-Eddington inversion of degraded synthetic Stokes profiles of the same spectral line (point spread function: width = 150 km, filter function: width = 50 mÅ, six wavelength points, noise: signal/noise = 1000). Apart from missing the very weak fields and underestimating the strongest small-scale flux concentrations, the inversion works remarkably well.

High spatial resolution imaging of photospheric bright points

High-resolution simultaneous observations of the Sun in three spectral bands, the blue continuum (436.4 nm), the G band (430.5 nm) and the violet CN band-head (387.9 nm), have been carried out with the 1-m Swedish Solar Telescope (SST). The unprecedented high spatial resolution of better than 0.18 arcsec, which corresponds to 130 km on the Sun, of the solar images in all three spectral bands was achieved by means of the Joint Phase Diverse Speckle image reconstruction method (see Fig. 16). Our investigation of the intensity contrast of photospheric bright points (BP – a class of small-scale bright structures, which show enhanced contrast in the G band as compared to that in the continuum) in the obtained filtergrams of active regions at disc centre showed that:

- On average over all bright points in the 27×43 arcsec^2 filtergram triplet the contrast of the BP intensity relative to intensity of the quiet Sun is 1.4 times higher in the blue CN band-head than that in the G band and it is 3.4 times higher in the blue CN band-head than that in the blue continuum. Similarly, in the G band the contrast of bright points is on average 2.4 times higher than in the blue continuum. This is in reasonable agreement with earlier theoretical predictions, but contradicts more recent simulations by Uitenbroek and Tritschler.

- The ratio of the bright points contrast in the blue CN band-head to that in the G band decreases with increasing continuum intensity of the bright points. The minimum value of this ratio is 1.25 for the brightest BPs.

The significantly higher contrast seen in the violet CN band-head compared with the G-band makes the former a promising wavelength band for solar high resolution studies, although there are factors making contemporary high-resolution ground-based solar observations in this wavelength more complex than in the G band.

(V. Zakharov, A. Gandorfer, S. K. Solanki)

High resolution spectra of photospheric bright points

High-resolution spectra of small-scale magnetic activity manifestations in the solar photosphere were obtained simultaneously in the blue CN band-head

(387.588−388.473 nm) and in a blue spectral band (436.1−436.9 nm) containing absorption lines of CH with the spectrograph installed on the SST (see Fig. 17). These are the first high resolution spectra of the CN band-head. These data have the advantage that they allow individual spectral lines to be analyzed. The data analysis yielded that:

- At the disc centre, the change of the line-core depression in BPs relatively to the quiet Sun of a CN spectral line (λ = 387.844 nm vacuum) is on average 1.28 stronger than that of a CH spectral line (λ = 387.829 nm vacuum). In faculae at μ = 0.65 and at μ = 0.56 these values are 1.32 and 1.46, respectively.
- At the disc centre the CN line-core intensity for the same spectral lines has higher BP contrast than the contrast in the CH line-core by a factor of 1.9. The ratio decreases with increasing continuum intensity, becoming 1.5 for the brightest BPs. This trend is similar to that obtained from filtergram observations although the data are not directly comparable (individual spectral lines vs. broad spectral bands).

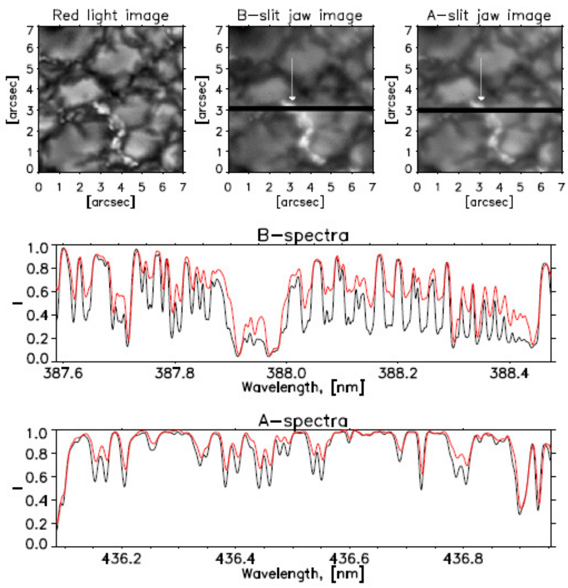

Fig. 17: Spectra of quiet Sun (black lines) and of bright points (red lines) in the CN band head (middle panel) and in a region containing CH lines (lower panel), showing the reduced line core depression in the bright point.

A detailed synthesis of the spectra at these wavelengths using 3-D MHD simulations and a direct comparison with observed data would be of considerable interest. In particular, an inversion of observed CH and CN spectral lines is desirable.

(V. Zakharov, A. Gandorfer, S. K. Solanki)

Systematic exploration of the *second solar spectrum* near the atmospheric cut-off

To investigate the *second solar spectrum* in the wavelength interval below 316 nm down to the atmospheric cut-off the Zurich Imaging Polarimeter ZIMPOL II has been attached to the largest solar telescope, the 1.5 m McMath-Pierce facility on Kitt Peak (Arizona). We were able to observe the linear polarization in the wavelength range from 305 nm to 316 nm. The strong atmospheric extinction due to ozone, starting around 310 nm renders high precision spectropolarimetry more and more difficult, and limits the accuracy of the obtained results. By careful analysis of different systematic error sources like polarized and unpolarized straylight inside the spectrograph, we could derive confidence levels for our data.

(A. Gandorfer in collaboration with D. Gisler (Institute of Astronomy, ETH Zürich))

Systematic exploration of the *second solar spectrum* in the near UV

The linearly polarised spectrum, which can be observed at the solar limb, has been referred to as the *second solar spectrum*. It shows a remarkable spectral structuring (see Fig. 18), since different physical processes contribute to its formation. In the absence of magnetic fields, scattering is the primary source of polarisation, which can be altered by magnetic fields via the Hanle effect, which allows measurement of magnetic fields not directly accessible to the Zeeman effect. Before the Hanle effect can be efficiently used for solar magnetic field diagnostics we have to explore and understand the wealth of spectral structures in the *second solar spectrum*. The observation of the *second solar spectrum* requires highly sensitive spectropolarimetry in combination with very high spectral resolution. Therefore the Zurich Imaging Polarimeter ZIMPOL II has been used at the largest solar telescope, the 1.5 m McMath-Pierce facility on Kitt Peak (Arizona). A complete survey of the scattering polarisation could be completed in the wavelength interval from 7000 Å down to 3160 Å. With the recent publication of Vol. 3 of a series of books, the dataset is now completely accessible to the science community to serve as a reference for future observations and to guide theoretical studies in this rapidly evolving field of solar science.

(A. Gandorfer)

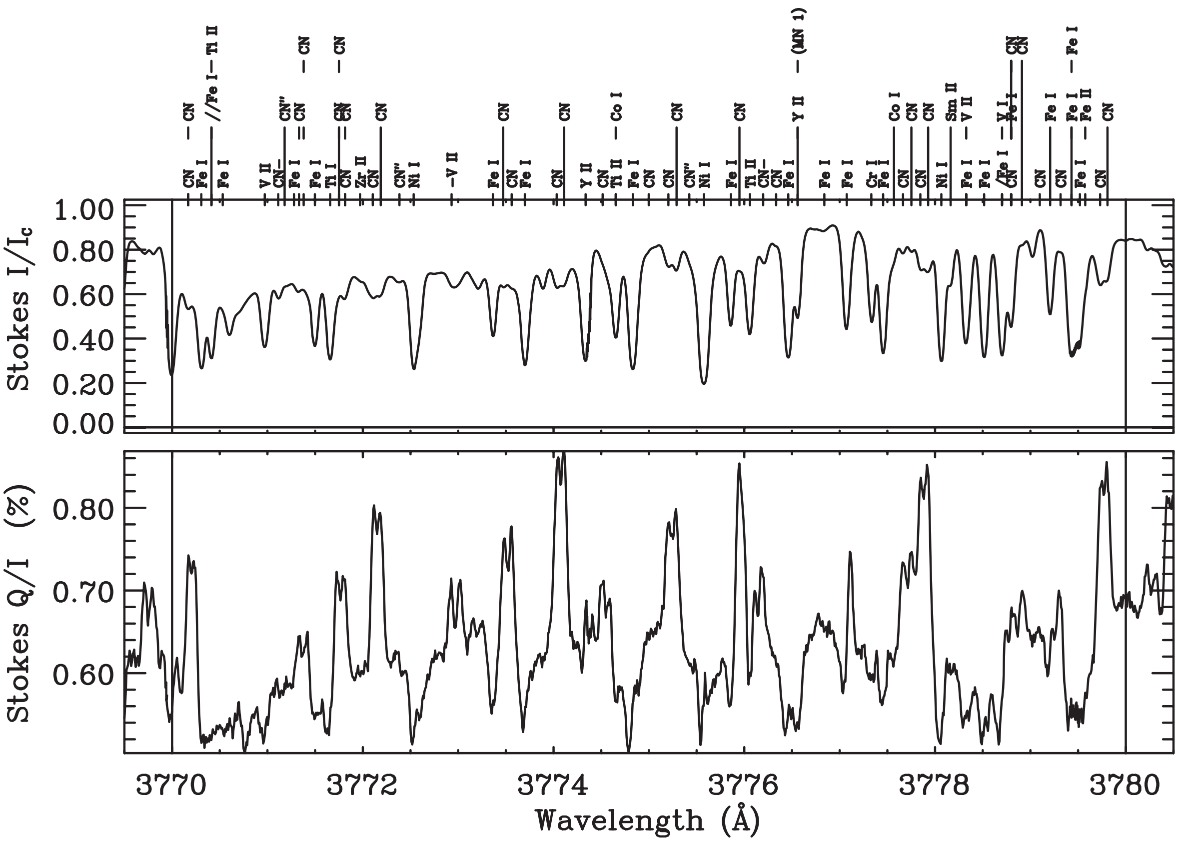

Fig. 18: Fraunhofer (upper panel) and second solar spectrum (lower panel) around 377nm showing strong polarisation due to resonance scattering at the CN molecule.

Ground Based Solar Observations (GBSO)

Supersonic flows in the solar chromosphere

We present spectropolarimetric observations of 13 active and 3 quiet-Sun regions in the chromospheric He I triplet taken with the Tenerife Infrared Polarimeter (TIP). By inverting the Stokes profiles of the He I 1083.0 nm multiplet lines we have obtained the full magnetic vector and the line-of-sight velocity. We have seen that supersonic downflows are a surprisingly common feature in almost all scanned solar regions, independently of whether they contain strong magnetic fields (active regions) or only weak fields (quiet-Sun). Multiple velocity components can often be distinguished, two being most common – a high speed downflow component and a second component almost at rest – but also three are seen in some cases. Line-of-sight velocities of the order of 30 km s^{-1} (Mach number $M_a = 2.9$) turn out to be quite common and are generally found in several locations of most scanned regions. Strongly supersonic downflows up to 60 km s^{-1} (Mach number $M_a = 5.8$), where a third component is necessary to fit the chromospheric He I 1083.0 nm line profiles (see Fig. 19), are observed in some cases. Although less common, supersonic downflow velocities of the order of 30 km s^{-1} are also observed in quiet-Sun regions scanned close to disk centre. Supersonic upflows are also present in some active regions, but are rarer.

(R. Aznar Cuadrado, S. K. Solanki, A. Lagg)

The uncombed structure of the chromosphere

A detailed knowledge of the magnetic structure of the chromosphere is essential for the understanding of the coupling between the photosphere and the corona. The measurement of the chromospheric magnetic field poses a challenge to the observers: low gas densities and low magnetic field strengths lead to very weak and difficult to interpret observational signatures, usually the presence of polarized radiation caused by the Zeeman effect.

Highly sensitive spectropolarimetric observations in the chromospheric He I line (1083.0 nm) made with the new TIP camera (Tenerife Infrared Polarimeter) mounted at the German Vacuum Tower Telescope were analyzed with a sophisticated technique, based on the solution of the radiative transfer equation and a genetic inversion algorithm. A relatively common fea-

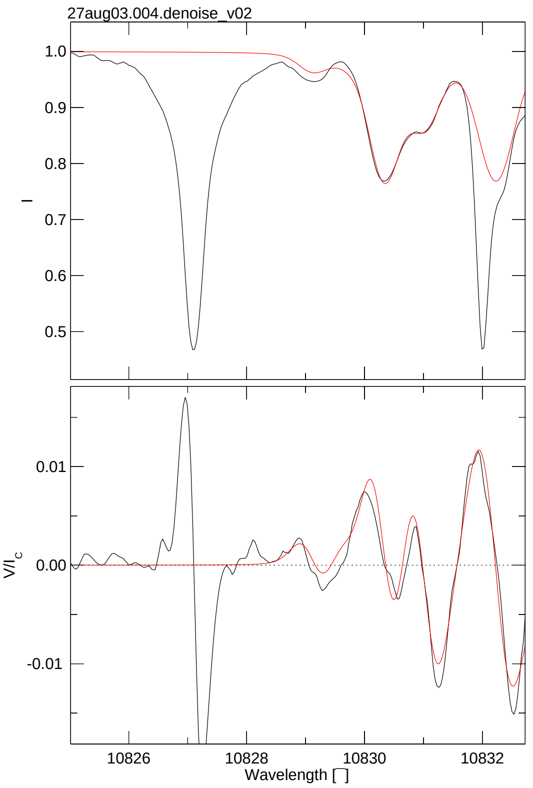

Fig. 19: Stokes I and V profiles showing three atmospheric components, each containing magnetic field, obtained in NOAA 10436.

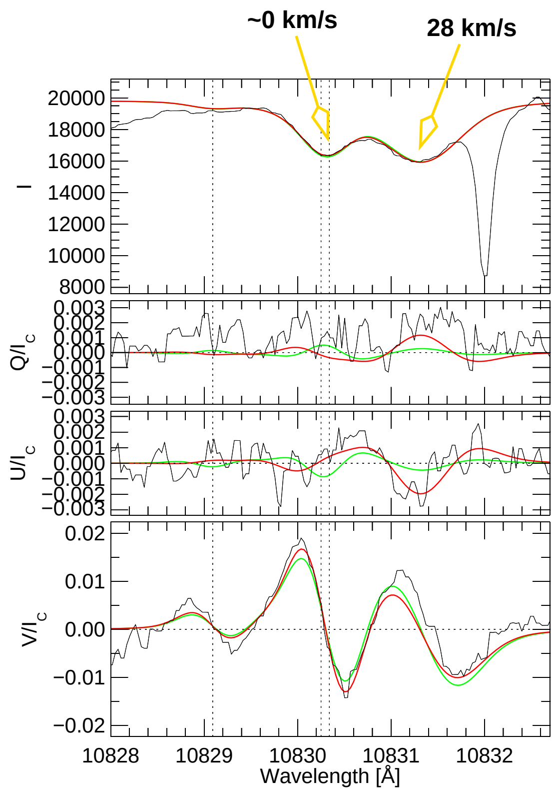

Fig. 20: Stokes profiles showing two distinct magnetic components. The observed profiles are shown in black, the fits in red (two independent magnetic components, $B_{slow} = 725$ G, $\gamma_{slow} = 30^\circ$ and $B_{fast} = 1194$ G, $\gamma_{fast} = 68^\circ$) and green (2 magnetic components with coupled magnetic field $B_{slow} = B_{fast} = 642$ G, $\gamma_{slow} = \gamma_{fast} = 61^\circ$). The two components are shifted by 28 km s^{-1} relative to each other. The fit involving two independent magnetic components reproduces the observed Stokes vector better.

ture in this He I line is the presence of two atmospheric components within the resolution element of the telescope ($\approx 1''$), shifted by wavelengths corresponding to velocities of up to 60 km s^{-1}. We were for the first time able to determine the magnetic field vector for the two components independently (see Fig. 20).

The genetic inversion algorithm (PIKAIA) reliably retrieves the atmospheric parameters, magnetic field strength and direction, if the separation of the two components is larger than 10 km s^{-1}, and if the components are of comparable strength. It was not possible to reproduce the observed Stokes profiles satisfactorily by assuming the same magnetic field parameters for both atmospheric components (see green line in Fig. 20). Only under the assumption of two independent magnetic components were we able to fit the observed profiles (red line in Fig. 20). The derived magnetic topology is sketched in Fig. 21. The differently inclined magnetic field points to a similar structure as the uncombed fields in the penumbrae of sunspots.

In a time series at the footpoint of a magnetic arcade spanning over a site of flux emergence we were also able to investigate the evolution of this magnetic configuration. We found it to be quite stable over the duration of the time series (73 minutes). Since the typical time to empty a loop filled with gas by drainage is in the order of 20 minutes, subsequent upward transport of material is needed to maintain the high downflow velocities over this time interval. The downflow is therefore most likely the consequence of mass upflow correlated with the emergence of magnetic flux tubes at the solar photosphere. The presence of the uncombed magnetic structure remains a riddle, however.

(A. Lagg, S. K. Solanki, R. Aznar Cuadrado, C. Sasso, J. Woch, N. Krupp)

Signature of current sheets as seen by TIP at VTT in the He I *multiplet at 1083.0 nm*

Electric current sheets are sharp boundaries separating regions of opposite magnetic polarity. Hence, a minimum of the magnetic field should be present at that boundary. A large jump of the magnetic field in-

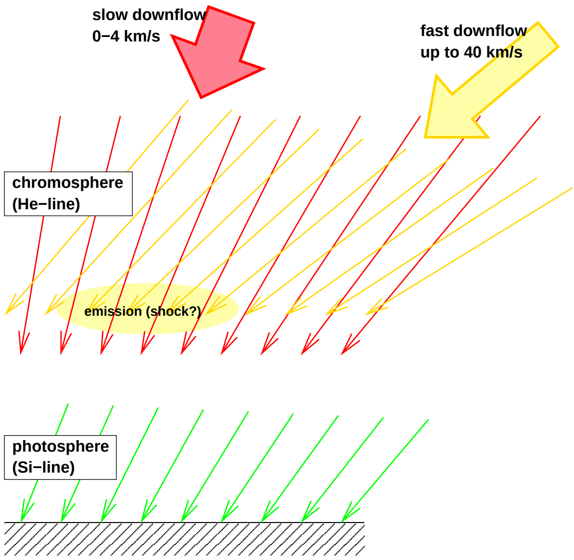

Fig. 21: Sketch of the magnetic field topology at a loop footpoint. The "uncombed model" is indicated by the different inclination angle between the field lines harbouring the rapid downflows (yellow) and the surrounding field lines (red) in the upper chromosphere. The photospheric field obtained from the inversion of the Si I line at 1082.7 nm is indicated by the green arrows. The inclination angles of the arrows represent the measured magnetic field direction.

clination angle between the two regions (ideally close to 180°) is also necessary. The azimuthal direction of the magnetic field vector is generally parallel to the current sheet. The first two requirements for a current sheet to be present can be detected by means of the analysis of the Stokes V profile, while the azimuthal angle of the magnetic field is only measurable through the inversion of the Stokes profiles revealing the full magnetic vector (i.e. Stokes Q and U are also necessary). Infrared spectropolarimetric observations were obtained with the Tenerife Infrared Polarimeter (TIP) at the German Vacuum Tower Telescope (VTT) of the Spanish observatory of Izaña, Tenerife. The observations taken in the chromospheric He I 1083.0 nm multiplet were used to create maps in the Stokes parameters I, Q, U and V. A number of active regions have been scanned. A technique to invert Stokes profiles of the He I 1083.0 nm multiplet lines was applied in order to obtain the full magnetic vector and the line-of-sight velocity. The retrieval of the full magnetic vector is important in order to detect current sheets. From a total of roughly 12 scanned active regions, only 3 showed strong evidence for a current sheet (see Fig. 22 for an example), indicating that detectable current sheets are not very common. The optimal configuration for this detection is when the current sheet is pointing towards the observer. Hence, the detection of current sheets is limited by geometric effects, i.e., current sheets are more likely to be detectable when the line-of-sight is in the direction of the plane of the current sheet. This could mean that current sheets may be more common than our analysis suggests.

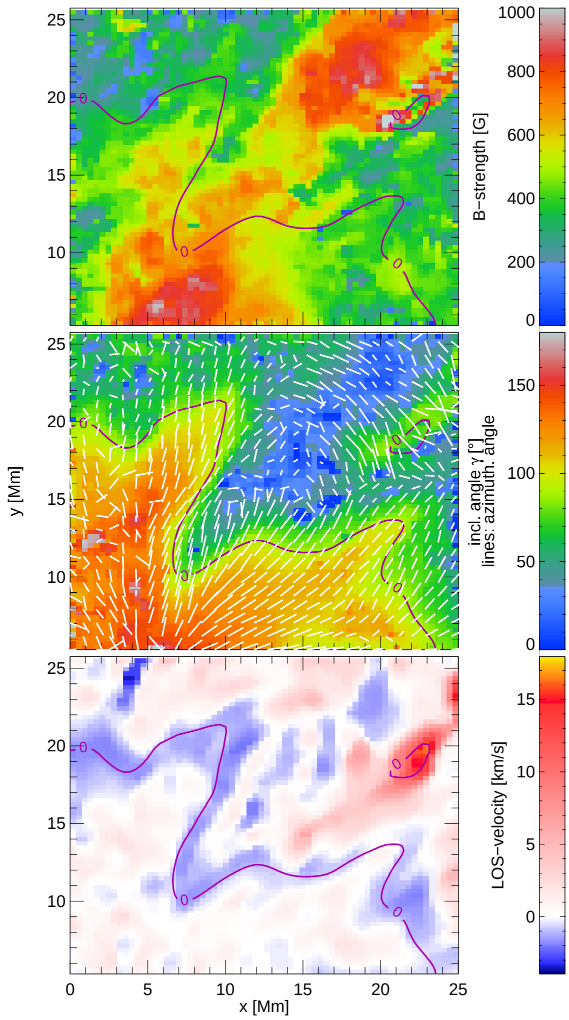

Fig. 22: Atmospheric parameters, magnetic field strength (top) and orientation (inclination: colour coded, azimuth: white lines), and line-of-sight velocity (bottom) around the position of a current sheet. The polarity inversion line (change of sign in Stokes V) is indicated by the magenta contour line.

(R. Aznar Cuadrado, S. K. Solanki, A. Lagg, R. M. Thomas)

The influence of the Paschen-Back effect on chromospheric magnetic field measurements

The Paschen-Back effect influences the Zeeman sublevels of the He I multiplet at 1083.0 nm, leading to changes in strength and in position of the Zeeman components of these lines. We analysed the influence of the Paschen-Back effect on the Stokes profiles of the He I 1083.0 nm multiplet lines, estimating its relevance using synthetic profiles and investigating its influence on the inversion of a spectropolarimetric scan of an emerging active region obtained with the Tenerife Infrared Polarimeter (TIP) at the German Vacuum Tower Telescope (VTT). We found that taking into account the incomplete Paschen-Back effect into our inversions code, on average 16% higher field strength values are obtained (Fig. 23), while other atmospheric parameters are affected less significantly. We show also that this effect is not the main cause for the blue-red area asymmetry exhibited by many He I 1083.0 Stokes V-profiles. The fact that the area asymmetry of the observed V-profiles is considerably stronger than of the synthetic V-profiles indicates that some other effect drives the area asymmetry more strongly than the Paschen-Back effect. The main candidate is gradients of atmospheric parameters like magnetic field vector and the velocity, over the formation height range of these lines.

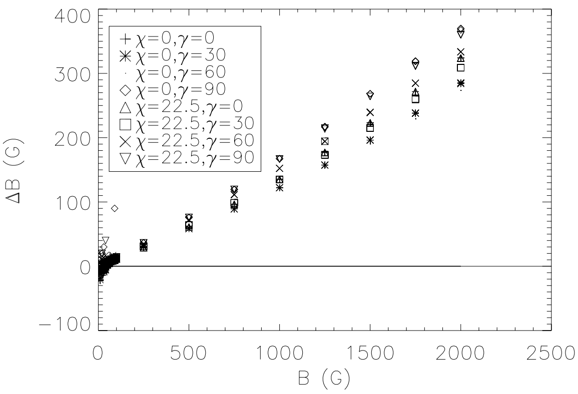

Fig. 23: Difference between the values of the magnetic field strength for a synthetic profile computed including incomplete Paschen-Back splitting (IPBS) and the ones obtained from the linear Zeeman splitting (LZS) inversion of this synthetic IPBS profile (ΔB), as a function of the magnetic field strength of the synthetic profile for different inclination (γ) and azimuthal angles (χ) of the magnetic field vector (in degrees). The retrieved values for magnetic field deviate significantly from the correct values (horizontal solid line).

(C. Sasso, A. Lagg, S. K. Solanki, R. Aznar-Cuadrado)

On the fine structure of sunspot penumbrae and the Evershed effect

Sunspot penumbrae exhibit prominent fine structure. Different interpretations of spectropolarimetric observations suggest different, sometimes contradictory, properties of this fine structure. We have analyzed polarized profiles of different spectral lines within the context of different models of the penumbral fine structure. Thus we show that the results of inversions of penumbral infrared profiles based on one-component models with gradients of the atmospheric parameters and two-component models without gradients are compatible with each other (see Fig. 24). Our analysis reconciles the results of previous investigations and provides further support for the picture that sunspot penumbrae are composed of penumbral flux tubes embedded in a magnetic background. The magnetic field in the tubes is more horizontal and weaker than that of the background atmosphere. While the tubes carry most of the Evershed flow, the background is essentially at rest. We notice also that the magnetic field strength in the flux tubes drops much more slowly with radial distance than the background field.

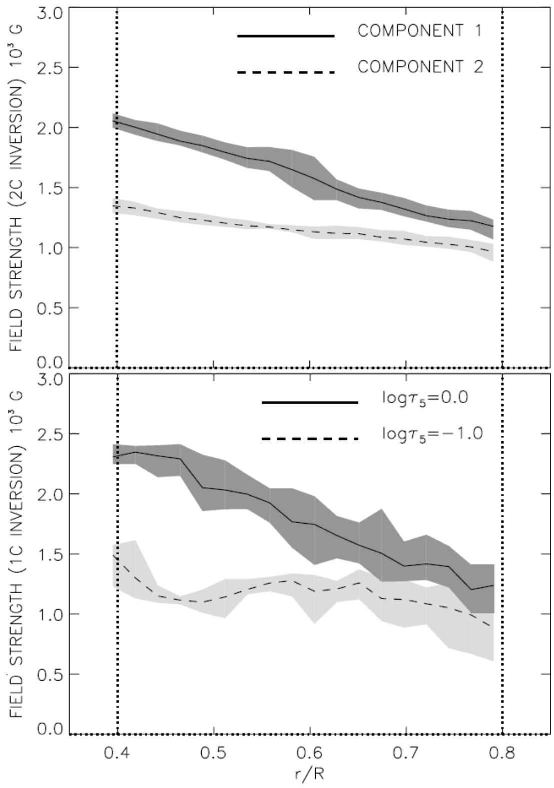

Fig. 24: Radial variation of the magnetic field strength in a sunspot. The results of the 1-component inversions with gradients (bottom panel) leads to similar results as the 2-component inversion without gradients (top panel). For the 1-component inversions we extract the values at $\log\tau = 0$ (solid lines) and $\log\tau = -1$ (dashed lines). In the 2-component inversion component #1 (solid line) represents the background whereas component #2 (dashed line) represents a flux tube.

In a next step we investigate the fine structure of the sunspot penumbra by means of a model that allows for a flux tube in horizontal pressure balance with the magnetic background atmosphere in which it is embedded. We apply this model to spectropolarimetric observations of two neutral iron lines at 1.56 μm and invert several radial cuts in the penumbra of the same sunspot at two different heliocentric angles. In the inner part of the penumbra we find hot flux tubes that are somewhat inclined to the horizontal. They become gradually more horizontal and cooler with increasing radial distance. This is accompanied by an increase in the velocity of the plasma and a decrease of the gas pressure difference between flux tube and the background component. At large radial distances the flow speed exceeds the critical speed and evidence is found for the formation of a shock front. These results are in good agreement with simulations of the penumbral fine structure and provide strong support for the siphon flow as the physical mechanism driving the Evershed flow.

(J. M. Borrero, S. K. Solanki, A. Lagg, S. K. Mathew in collaboration with L. R. Bellot Rubio (Kiepenheuer Institut für Sonnenphysik) and M. Collados (Instituto de Astrofisica de Canarias))

The molecular Zeeman effect in the Paschen-Back regime

Molecular transitions are a far more sensitive probe of the cool parts of the solar photosphere and cool-star atmospheres than atomic lines. However, the reaction of molecular lines to a magnetic field is only very incompletely known. In contrast to atomic lines many diatomic molecules present in the atmospheres of the Sun and cool stars exhibit the Paschen-Back effect at field strengths typical of sunspots and active cool stars. We have produced a complete theoretical description of the molecular Paschen-Back effect in Hund's cases (a), (b) and all cases intermediate to them. This is an extension of previous work carried out by us on the linear Zeeman effect in diatomic molecules. This description allowed us to compute the splitting of levels of any multiplicity and the transitions between them. We also introduced a generalized description of the effective magnetic Landé factor applicable not just in the Zeeman regime, but also in the Paschen-Back regime. We found that in the regime of the partial Paschen-Back effect strongly asymmetric Stokes profiles are produced, whose strengths and asymmetries depend sensitively on the magnetic field. In the regime of the complete Paschen-Back effect the profiles become symmetric again (although they may be strongly shifted). The strength of the forbidden and satellite transitions increases rapidly with field strength in the partial Paschen-Back regime, while the strength of the main branch transitions decreases. These signatures hold promise to form the basis of new diagnostics of solar and stellar magnetic fields.

(S. K. Solanki in collaboration with S. V. Berdyugina and D. M. Fluri (ETH Zürich, Switzerland) and P. A. Braun (St.-Petersburg University, Russia))

The dynamics of the solar chromosphere: millimeter–interferometer observations and comparison with model predictions

The nature of the solar chromosphere is a topic of intense debate, with a major uncertainty being the role played by chromospheric dynamics in shaping this layer of the solar atmosphere. Visible and UV atomic line observations of the chromosphere suffer from the fact that they are practically blind to potentially significant amounts of cool gas in a dynamic chromosphere. Observations at millimeter wavelengths have the advantage that they sample both the hot and the cool gas. Up to now, however, no time series with an acceptable spatial resolution has been available.

We have obtained interferometer observations of the Sun at a wavelength of 3.5 mm (frequency of 85 GHz) with the 10-element Berkeley-Illinois-Maryland Array (BIMA). With these data we have constructed two-dimensional maps of the solar chromosphere with a resolution of 10″, which represents the highest spatial resolution achieved so far at this wavelength for non-flare solar observations.

Fourier and wavelet analyses of the BIMA data reveal intensity oscillations with RMS brightness temperature amplitudes of 50 – 150 K in the frequency range 1.5 – 8 mHz. There is a tendency toward short period oscillations in the quiet-Sun internetwork and longer periods in active regions and the network (see Fig. 25), which agrees with the results obtained at other wavelengths. Most of the oscillations are short wave trains lasting for typically 1 – 3 wave periods.

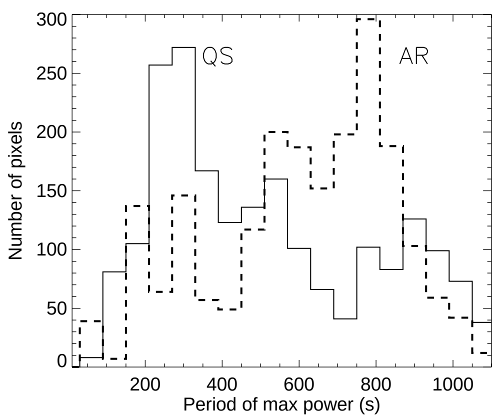

Fig. 25: Histograms of the period of maximum Fourier power for the QS (solid line) and active region data (dashed line). For each pixel the period with most significance in the power spectrum is determined and at this period the pixel is included in the distribution.

Due to the limited spatial resolution of 10″, a direct comparison of the observational data with the predictions of the radiation hydrodynamic simulations of Carlsson & Stein (hereafter CS) exhibits large differences. In particular, the RMS of the brightness temperature is nearly an order of magnitude larger in the model (∼800 K at 3 mm) than in the observations (∼100 K). Thus an accurate comparison requires a description of the influence of the spatial smearing on the parameters of chromospheric dynamics.

We are able to obtain reasonable agreement between the observed millimeter oscillations and those predicted by the CS model if we assume that the coherence length of oscillating elements is of the order of 1″. This supports the picture that the chromosphere is highly dynamic and contains significant fractions of both hot and cold gas. This work has demonstrated the usefulness of millimeter wavelength observations for uncovering the nature of the solar chromosphere, but unfortunately, the currently available spatial resolution of 10″ hinders a final answer to the question on the structure of the chromosphere. It will have to await observations with higher spatial and partly temporal resolution, which may come from the Combined Array for Research in Millimeter-wave Astronomy (CARMA), but in particular from the Atacama Large Millimeter Array (ALMA).

(M. Loukitcheva and S. K. Solanki in collaboration with S. White (University of Maryland, College Park, USA))

Inferring plasma flow velocities from photospheric field measurements

The vertical and horizontal motion of magnetized plasma in the photosphere might be crucial for understanding the solar atmospheric dynamics. It should, therefore, be used as an input parameter for dynamic models of the solar atmosphere. Unfortunately, the motion cannot be determined directly. Hence, it has to be estimated using other measured quantities. We used three methods to estimate the photospheric motion from vector magnetic field observations: local correlation tracking (LCT), a combination of induction equation and the LCT method (ILCT) and Minimum Energy Fit (MEF). These methods were applied to different active regions and the results were compared. The goal of this study is to obtain reliable photospheric plasma flows velocities to be used as an input parameter for solar coronal models and to study the influence of the photospheric motion in the evolution of the plasma and magnetic field of active regions associated with flares and CMEs.

Fig. 26 shows the results of the application of the methods to AR9077, between July 13, 2000 (02:50 UT) and July 14 (10:25 UT). The last one correspond to the peak of activity of the famous 'Bastille day' flare. The first and second panels show the horizontal and vertical components of the velocity field obtained by ILCT, respectively. The third and fourth panel show the corresponding MEF results. Fig. 26 depicts also with the horizontal and vertical velocity results the normal component of the magnetic field and the contour plot of the normal component of the magnetic field, respectively. The results obtained by ILCT and MEF for the horizontal motion show the characteristics of the evolution of the main polarity regions, as described in many papers. The main positive-polarity region fragments into two new positive-polarity regions. The negative polarity southward of this main positive-polarity also splits. One part of it moves northwest squeezing the positive-polarity region. The values obtained for the modulus of the horizontal velocity are of the order of the daily averaged values. The obtained pattern of vertical velocities obtained by the MEF method show high values in some points of the field of view. These values occur mostly in regions where the magnetic field normal component is weak. The variation of the normal component of the magnetic field calculated using the resulting velocity fields and the vertical component of the induction equation provided similar results for both methods. The results are comparable with the variation obtained using the measurements of the magnetic field.

(J. Büchner, J. C. Santos, B. Nikutowski, M. V. Alves, and H. Zhang)

Solar Transition region and corona

The structure and dynamics of the lower transition region as inferred from observations in the hydrogen Lyman-α line

The hydrogen Lyman lines dominate the Vacuum UltraViolet (VUV) radiance spectrum of the Sun. The resonance (α) line at 121.6 nm, in particular, dominates the solar radiative losses in the temperature regime between 8 000 K and 30 000 K. Hence, H I Ly-α is the most important line formed in the lower transition region and upper chromosphere. This is the region where the expansion of the photospheric magnetic field takes place, and it is important for studies of the coupling of the solar outer atmosphere with the underlying photosphere. Surprisingly, the H I Ly-α has so far been relatively rarely observed and analysed, so

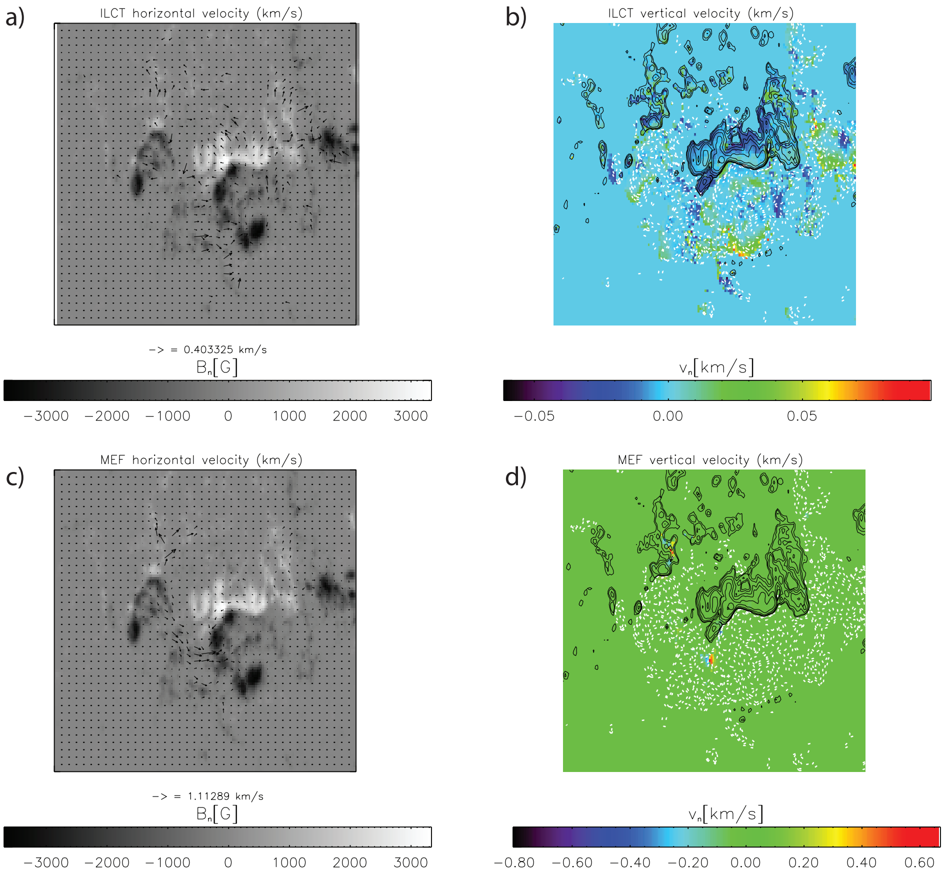

Fig. 26: Results of ILCT and MEF methods for the horizontal velocity component and the vertical component of the plasma flow velocity. a) Horizontal component of the velocity field (arrows) obtained by ILCT method and normal component of the photosperic magnetic field; b) vertical component of the velocity field obtained by ILCT method and contour lines of the normal component of the photospheric magnetic field; c) results from MEF method for the horizontal component of the velocity (arrows) and vertical component of the magnetic field; d) vertical component of the velocity field obtained by MEF method and contour lines of the vertical magnetic field.

that many of the characteristics of solar features seen in this line are not well known.

Using the SUMER spectrograph aboard SOHO, we have built simultaneous raster scans in H I Ly-α and in the optically thin Si III 120.6 nm line ($T = 60\,000$ K). The images look quite similar at the SUMER spatial resolution of 1.5″ (see Fig. 27). This result shows that the integrated H I Ly-α radiance is a good diagnostic of the lower transition region. The radiance frequency distribution of the H I Ly-α line is fairly well represented by a lognormal function, although the fit is not as good as in the case of mid-transition-region lines. The average size of network structures, when seen in H I Ly-α, is consistent with the size obtained in other lines that form at similar temperatures, but larger than in the lines formed around 10^5 K. The H I Ly-α radiance clearly shows the presence of the 3-min internetwork oscillations, while oscillations with larger periods seem to be present in the network. Above the limb, the variability is dominated by spicules and macrospicules. Several of them show a quick ($\approx$ 100 s) raise up to around 30″ to 40″, followed by a slower fall back (200 to 300 s). An indication of a periodicity of about 10 minutes is also present.

The high spectral resolution of SUMER, orbiting around the first Lagrangian point, allows us to study in detail the H I Ly-α profile without the contamination of geocoronal emission. Quiet-Sun profiles, averaged over areas ranging from cell centres to bright network, show that the relative amplitude of the central reversal becomes smaller with increasing line radiance.

High-spatial-resolution profiles show a high degree of variability, revealing the signatures of transition-region explosive events.

Due to the very high count rates achievable even with short (around 1 s) exposure times, the H I Ly-α allows the evolution and dynamics of the different features characterising the lower transition-region to be stud-

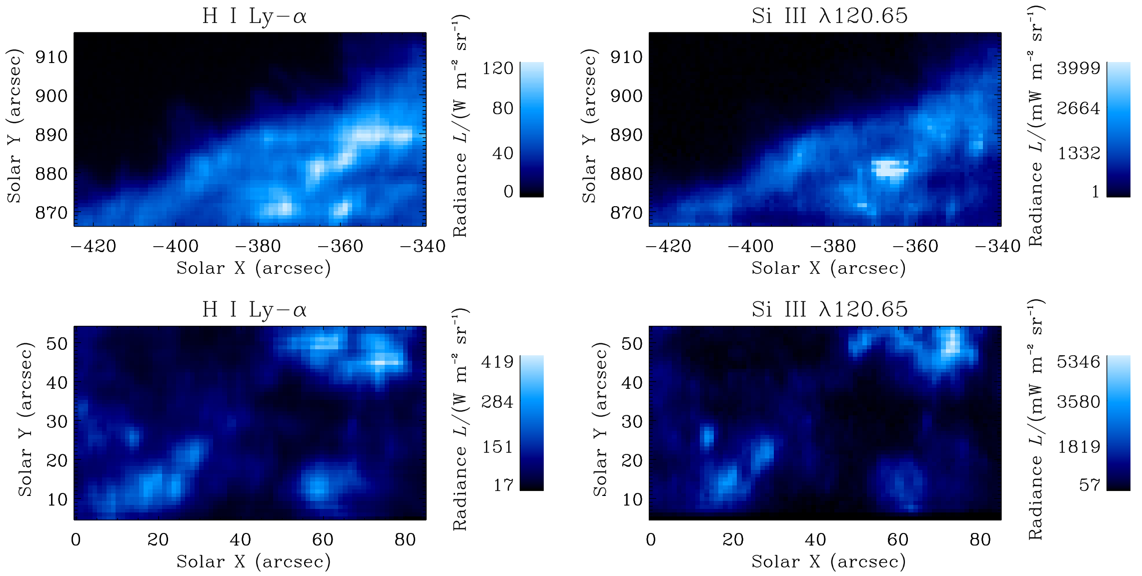

Fig. 27: Square-root radiance images of the north-east limb (top row) and of a quiet region near Sun centre (bottom row). The H I Ly-α and Si III images are simultaneous in time and space, and appear remarkably similar despite the large optical thickness of H I Ly-α. Above the limb, solar spicules are better seen in H I Ly-α. The bottom-right Si III image is displayed with a maximum value of the line radiance of 4 W m^{-2} sr^{-1}, in order to better reveal structures at the limb.

ied with unprecedented detail. Its diagnostic potential should be utilised in future missions such as Solar Orbiter.

(L. Teriaca, U. Schühle, S. K. Solanki, W. Curdt, E. Marsch)

Solar prominence parameters derived from SUMER hydrogen Lyman-α spectra

We derive the thermodynamic propierties of a prominence from a SUMER raster in the H I Lyman-α 121.57 nm line by comparing the observed spectra with synthetic ones obtained using 2-D fine structure models of vertical threads in magnetohydrostatic equilibrium (see Fig. 28). Starting with a grid of 18 models, we found the model producing a profile similar to the chosen observed profile. By varying the input model parameters (central temperature T_0, boundary pressure p_0 and temperature T_{Tr}, horizontal magnetic field at the centre of the thread $B_x(0)$, central column mass and turbulent velocity v_t as a function of the sound speed c_s) we obtained synthetic H I Lyman-α profiles which are in good agreement with the observed ones. In this way we are able to determine the structure of the magnetic dip and the thermodynamic parameters of the observed prominence.

(L. Teriaca, U. Schühle in collaboration with S. Gunár and P. Heinzel (Astronomical Institute, Academy of Sciences, Ondrejov, Czech Republic))

On the nature of the broad solar emission near 117 nm

Spectral observations of the Sun in the vacuum-ultraviolet wavelength range by SUMER on SOHO led to the discovery of unusual emission features at 116.70 nm and 117.05 nm on either side of the He I 58.43 nm line (see Fig. 29). This resonance line is seen in the second order of diffraction, whereas the broad features are recorded in the first order with the SUMER spectrometer. In its spectra both orders are superimposed. Two less pronounced broad emissions can be detected at 117.27 nm and near 117.85 nm. After rejecting various possibilities of an instrumental cause, the emissions are studied in different solar regions. Most of the measurements, in particular those related to the limb-brightening characteristics, indicate that they are not part of the background continuum. An assembly of spectrally-unresolved atomic or ionic emission lines might be contributing to the feature at 117.05 nm, but no such lines are known near 116.7 nm. It is concluded that we detect genuine radiation, the generation of which is not understood. A two-photon emission process, parametric frequency down conversion, and molecular emissions are briefly considered as causes, but a final conclusion could not be reached. The observations was published by Wilhelm *et al.* (2005b) together with a request for an identification.

In the meantime, an answer to this request has been communicated by Avrett, Kurucz and Loeser (A&A,

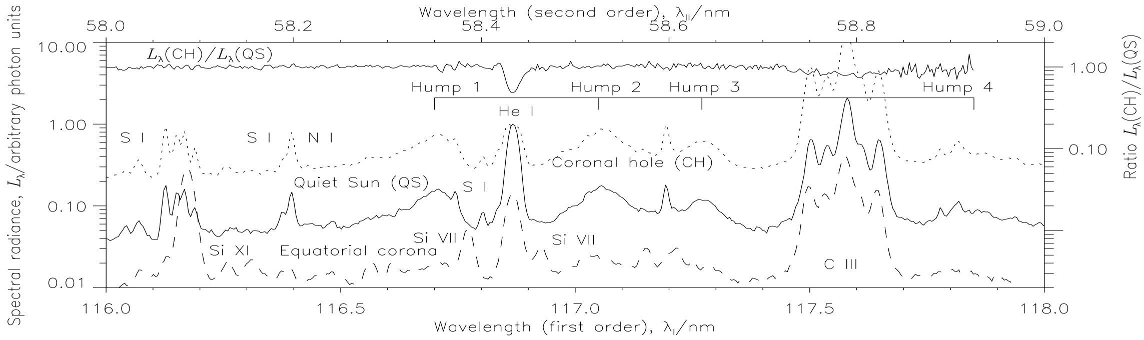

Fig. 29: Spectra of the Sun from 116 nm to 118 nm in the first order and 58 nm to 59 nm in the second order. The quiet-Sun (QS) spectrum was observed near the centre of the Sun on 28 April 1996, and the polar coronal-hole spectrum on 5 June 1996. The data of the equatorial corona $\approx 30''$ above the west limb are shown for 25 June 1996. Also shown (with a scale on the right-hand side) is the spectral radiance ratio, L_λ(CH)/L_λ(QS), measured on 7 March 1999, when sections of the SUMER slit covered both regions.

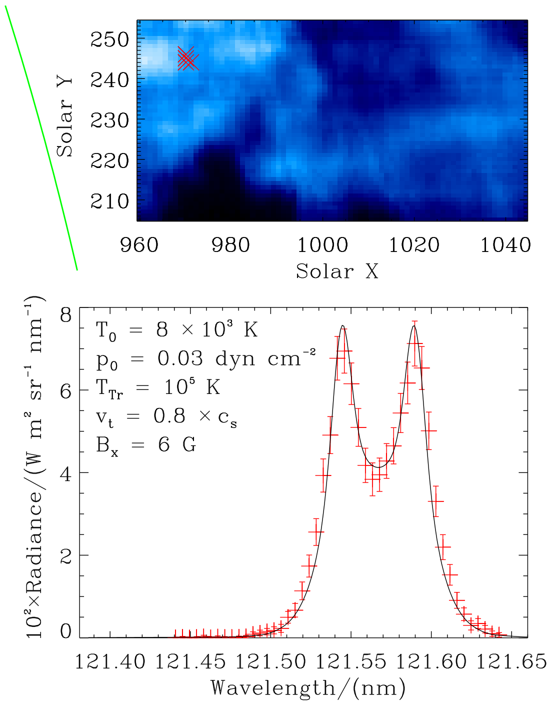

Fig. 28: Top panel: Square-root radiance map of the observed prominence. The green line marks the position of the solar limb. The red marks indicate the positions of the four spectra averaged to obtain the profile shown in the bottom panel. Bottom panel: Observed data points (red) together with the synthetic profile (black) obtained with the labelled parameters.

in press) with an explanation of the broad emission features based on the identification as auto-ionization lines of neutral sulfur. In agreement with the original observations, they stem from the low chromosphere, and can be utilized as diagnostics of the physical conditions in that region.

(K. Wilhelm, W. Curdt, M. Hilchenbach, E. Marsch in collaboration with P. Lemaire (IAS, Paris), J.-L. Bertaux (Service d'Aeronomie, Paris), S. D. Jordan (NASA-GSFC, Washington), U. Feldman (NRL, Washington))

A new 3-D magnetic null-point reconnection model of EUV- Bright Points

Recently, by means of a singular value decomposition (SVD) of the photospheric magnetic fields below EUV Bright Points (BPs), we had found that the presence and motion of weaker magnetic polarities additionally to the well-known bi-polar structure, usually associated with EUV- and X-ray BPs, seems to be essential to understand the observed energization (see the last MPAe bi-annual report 2002-2003, pages 24-25).

In order to better understand the mechanism of BP heating we have developed a model, which bases on the observed photospheric magnetic fields and the motion of the polarities below BPs. Our model describes the magnetic coupling between photosphere, chromosphere and corona considering the interaction of plasma and neutral gas in the chromosphere, where collisions dominate, implying friction between plasma and neutral gas as well as their thermal contact. We basically solve the coupled MHD-neutral gas equations. The model is initialized by observed longitudinal photospheric magnetic fields which are extrapolated to the corona by solving the force-free field equation $\nabla \times \mathbf{B} = \alpha \mathbf{B}$. For the sake of modelling we had to develop an extrapolation methods which also satisfies MHD boundary conditions. For an appropriate Fourier expansion one needs periodicity in the solar photospheric x and y directions. Choosing a MHD-compatible symmetry condition for B_z at the x and y boundaries of the system, we constructed a periodic domain $-L_x \leq x \leq L_x$, $-L_y \leq y \leq L_y$ four times as large as the original region ($0 \leq x \leq L_x$, $0 \leq y \leq L_y$). This region is fully periodic and the total magnetic flux through it is balanced to a high degree. We then "fill" this observation-based initial force-free solar magnetic configuration with plasma and neutral gas in accordance with the VAL model. As a boundary condition we also utilize the cross-field plasma motion derived from the observations of time-dependent photospheric magnetograms.

Applying this model to the BP observation of October 17-18th, 1996 (see the last MPAe bi-annual report 2002-2003, pages 24-25) we found that enhanced perpendicular currents form, but not above the main two polarities neither between them as predicted by traditional models. Instead deviations for force-freeness occur at the side-position, where, indeed, the actual BP was observed. The physical mechanism of this new physical mechanism of Bright Point heating is illustrated by Fig. 30. The Figure depicts iso-surfaces of enhanced currents and the magnetic field structure for field lines closely encountering a 3-D magnetic null. While the enhanced chromospheric currents (the chromosphere is located below a height of 2 where the transition region is located in the model's normalization) are immediately dissipated in the highly resistive chromospheric plasma, the current structure, which extends through the transition region into the less collisional corona, can accumulate magnetic energy. The accumulated energy is released by reconnection in the following way: while the footpoint motion permanently drives magnetic flux though the current sheet, the magnetic connection of the footpoints changes discontinuously from the strong opposite polarity region to a neighboring opposite polarity region. As one can see in Fig. 30 nearby started field lines discontinuously change their connectivity through the current sheet. The dynamics of this process can be seen by watching its animation on the web (see http://www.mps.mpg.de/~buechner).

The reconnection process is also the height-localized. The reason for this is the stratification of the solar atmospheric density which drops in the transition region. This latter leads to an enhancement of the current carrier velocity which, finally, exceeds a threshold of current instabilities causing collisionless dissipation (the so called "anomalous resistivity"), necessary for reconnection.

(J. Büchner, B. Nikutowski in collaboration with A. Otto (Fairbanks))

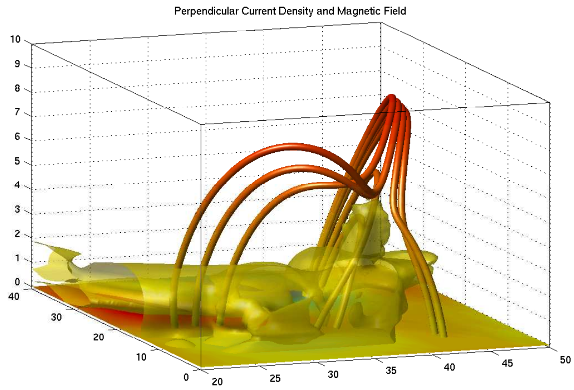

Fig. 30: Modelled magnetic field and current concentrations around a magnetic null point in the region of an EUV-Bright Point observed on October 17th-18th, 1996 by EIT (SOHO).

On the network structures in solar equatorial coronal holes

By combining the solar observations made by SUMER and MDI aboard SOHO, we studied the fine structures of the magnetic network in an equatorial coronal hole, in particular with respect to possible correlations between the ultraviolet line parameters (such as radiance, Doppler shift and width) and the measured photospheric magnetic field. Some typical observations are presented in Fig. 31. The base regions of coronal holes when seen in chromospheric spectral lines with low formation temperatures do generally have similar properties as the normal quiet-Sun regions. Small bright patches with sizes of about two to ten seconds of arc are the dominant features in the network as well as in cell interiors. With increasing formation temperature, these features become more diffuse and have enlarged sizes. Loop-like structures are the most prominent features in the transition region. In coronal holes, many of these structures seem to have one footpoint rooted in the intra-network and to extend into the cell interiors.

The Doppler shifts of the C II and O VI lines are measured relative to the chromospheric lines of O I, while the Lyβ line is referenced to its average position due to the lack of reliable reference lines in its spectral neighbourhood. In Dopplergrams of the O VI line at 1032 Å, there are also fine structures with apparent blue shifts, but on average they are red shifted. Structures with blue shifts have usually also broader line widths. They seem to represent plasma above large concentrations of unipolar magnetic field, without obvious bipolar photospheric magnetic features nearby.

(L. D. Xia, E. Marsch, K. Wilhelm)

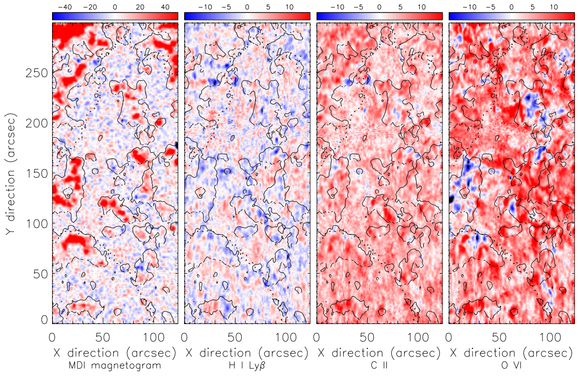

Fig. 31: Partial images of a CH in magnetogram and line shift. From left to right: The MDI magnetogram (units: gauss), and three Dopplergrams in H I Lyβ, C II and O VI (units: km/s). The equatorial CH was observed on 11 March 1999 between 12:09 and 13:09 UTC. All figures are overlaid by contours of the continuum emission observed simultaneously in order to outline the network region ($\approx$ 33 % of the CH area is occupied by the network). The positive magnetic field is plotted in red colour, while the negative in blue.

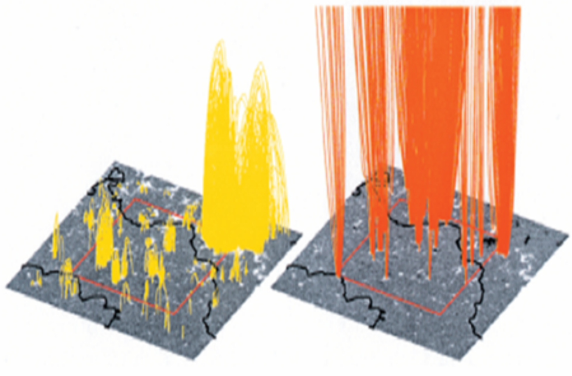

Fig. 32: Magnetic structures in a coronal hole. The gray-coding shows the field strength in the photosphere. The black line gives roughly the boundary of the coronal hole. The field of view for SUMER is marked as a red rectangle in both panels. The magnetic field was constructed from a MDI magnetogram. Left figure: mostly closed loops at various scales. Only closed magnetic field lines with $B \geq 30$ G are shown. Right figure: Only open fields with large photospheric values, $B \geq 100$ G. The open flux is bundled in narrow funnels and originates in stronger fields concentrated at small-scale footpoints.

Links between magnetic fields and plasma flows in a coronal hole

We compare the small-scale features visible in the Ne VIII Doppler-shift map (not shown here explicitly) of an equatorial coronal hole (CH) as observed by SUMER with the small-scale structures of the magnetic field as constructed from a simultaneous photospheric magnetogram by a potential magnetic-field extrapolation. The combined data set is analysed with respect to the small-scale flows of coronal matter, which means that the Ne VIII Doppler-shift used as tracer of the plasma flow is investigated in close connection with the ambient magnetic field. The magnetic structures found in the CH are shown in Fig. 32. Unipolar open-field coronal funnels prevail in the CH, but some small closed-field regions in this largely open CH are also found in the coronal volume considered. The Doppler-shift patterns are found to be clearly linked with the field topology.

The results of this phenomenological correlative study are discussed with the intention to understand how the magnetic field determines mass supply to the extended CH, and with respect to the role played by the field in guiding plasma flows at all scales resolved.

(T. Wiegelmann, L. D. Xia, E. Marsch)

Plasma acceleration due to transition region reconnection

Modern observations allow to diagnose plasma acceleration in the solar atmosphere. A most probable energy source for these acceleration processes is the photospheric motion, powered by the sub-photospheric plasma convection. Among others magnetic reconnection is a major possible mechanism for the observed plasma acceleration. In order to understand, where and how reconnection can accelerate solar plasma, we developed a fully three-dimensional dissipative MHD simulation approach based on observed photospheric magnetic fields and plasma motion. Our model starts with a force-free extrapolation of the longitudinal photospheric magnetic fields and with a stratified equilibrium distribution of the chromospheric-coronal plasma. Heat conduction, radiation cooling and gravity are neglected in the present version of the model. The applied photospheric boundary conditions do not consider magnetic flux emerging from or submerging to the solar interior. The horizontal photospheric plasma motion drives the chromospheric and coronal plasma dynamics. The resulting currents are generated not only parallel, but also perpendicular to the magnetic field. Using plasma-microphysical results we consider an anomalous resistivity that is switched on as soon as the local current density exceeds a critical value. As a result we obtain plasma acceleration mainly in the transition region between chromosphere and corona, where the plasma density decreases and plasma collisions become less efficient. The resulting vertical plasma velocities (see Fig. 33) are consistent with those observed for the same photospheric boundary conditions.

(J. Büchner, B. Nikutowski in collaboration with A. Otto (Fairbanks))

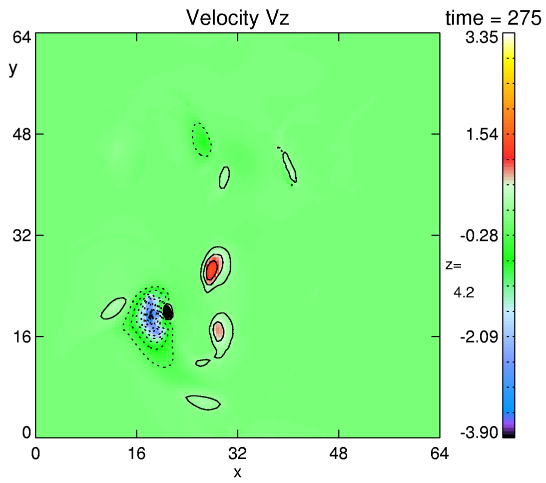

Fig. 33: Vertical plasma velocities in the lower corona due to reconnection in the transition region below.

Doppler-shift oscillations in coronal loops

Hot coronal loop Doppler-shift oscillations were discovered by SUMER in 2002. Studies of their oscillation characteristics, in particular their wave speeds and phase shifts between velocity and intensity oscillations, suggest that they are slow mode standing waves.

We have now looked in more detail at the evolution of the spectral line profiles in the initial phase of the oscillations, when they get excited. In particular the evolution of the spectral line profiles reveals insights into the triggering mechanism of these oscillations. In many events, about 50%, the oscillations are triggered by a pulse of hot plasma flowing through the loop from one footpoint (Fig. 34). The events start with the appearance of a highly shifted component in the wing of a background component. This highly shifted component reaches its maximum shift and intensity almost simultaneously, which is consistent with the signature of a pulse of ejected hot plasma, as seen by a slit spectrometer.

The signature of strong ejected hot flows suggests that the excitation of standing slow mode waves in the coronal loops is by a pulse of hot plasma at or near one footpoint and not by chromospheric evaporation. Such an excitation model is also supported by the fact that the initiation of hot loop oscillations has been associated with X-ray brightening at one footpoint.

(T. J. Wang, D. Innes, S. K. Solanki, W. Curdt)

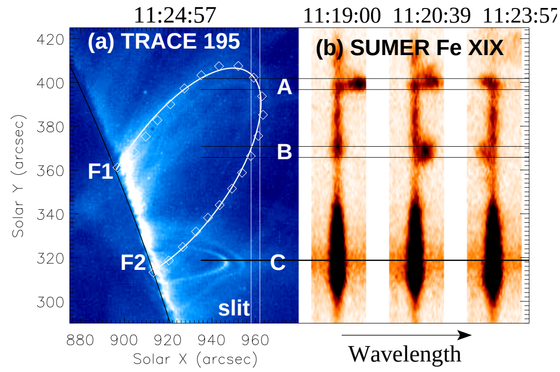

Fig. 34: Observations of the initial stages of a hot loop oscillation event on 17 April 2002. (a) TRACE image. A coronal loop (outlined with diamonds) is fit with a circular model (white curve). The SUMER slit is indicated by two vertical lines, and positions of two cuts (denoted A and B) are marked. (b) Spectra along the slit in the Fe XIX lines at three times during the event onset phase. Note the presence of a second component of the line profile at location A. The other leg of the loop (location B) reacts later to the initial pulse.

Vertical oscillations of a coronal loop observed by TRACE

Various wave modes have been found in coronal loops. One of the most widely studied is a kink mode, a horizontal transverse oscillation, in which the loop sways from side to side. This oscillation is clearly seen in on-disk data gathered by TRACE. In this study, we discovered the first observational evidence for a vertical loop oscillation, which exhibits alternately expanding and shrinking motions in a loop seen at the solar limb (see Fig. 35).

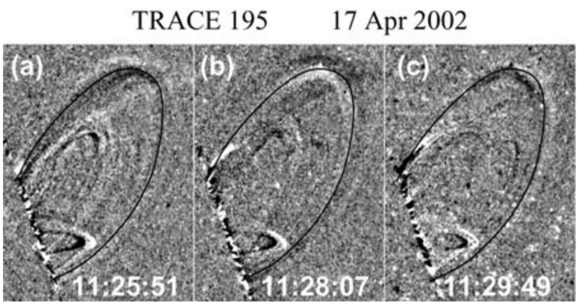

Fig. 35: (a)-(c) Running difference images with an interval of ~2 min. Black indicates where the loop was in the earlier image and white where it has moved to. The initial position of the loop prior to the oscillations is represented by a solid curve.

Based on the derived 3-D geometry of an oscillating loop seen in the 195Å bandpass, we simulate these two kinds of global kink modes and find that only the vertical oscillations produce a signature in the difference images that is in agreement with the observations. In a curved loop vertical and horizontal oscillations are quite distinct from each other and have different properties.

We also find that the oscillating loop is associated with intensity variations. Based on the measured displacement amplitude, the simulation predicts an intensity variation of about 13% due to density changes produced by the change in loop length. The observed intensity changes have the same sign, but are considerably larger than these predictions. This suggests that these oscillations are compressible.

(T. J. Wang and S. K. Solanki)

Numerical simulations of vertical oscillations in a solar coronal loop

Vertical oscillations of coronal loops (i.e. kink oscillations polarized vertically) were recently observed in TRACE data. In the work described here we considered the impulsive excitation of fast vertical kink standing waves in a solar coronal loop that is embedded in a potential arcade (Fig. 36). The two-dimensional numerical model we implemented includes the effects of field line curvature and nonlinearity on the excitation and damping of standing fast magnetosonic waves. The effect of gravity is not included, however. The results of the numerical simulations revealed wave signatures which are reminiscent of TRACE observations.

A pulse launched below a loop is in general found to excite multiple wave modes, in particular a vertical oscillation with many properties of a kink mode, fast mode oscillations and a slow mode pulse (or two slow mode pulses, depending on the location of the original pulse). The main emphasis of our analysis lay on the vertical kink oscillations. From our parametric studies we deduced that wave periods and attenuation times of the excited waves depend on the position below the loop summit, as well as the width of the pulse. Wider pulses launched closer to a foot-point and to the loop apex trigger wave packets of longer period waves which are more strongly attenuated. A perturbed loop does not return to its initial state but is stretched instead, with its apex shifted upwards. As a result, the perturbations propagate along the stretched loop, so that stronger and wider pulses which stretch a loop more lead to longer period oscillations.

A pulse located near one of the foot-points is found to excite a distortion mode leading to asymmetric oscillations which are distinct from the vertical or horizontal kink modes that have been identified in TRACE data. We predict that such a distortion mode should also be present in TRACE data. We also found strong

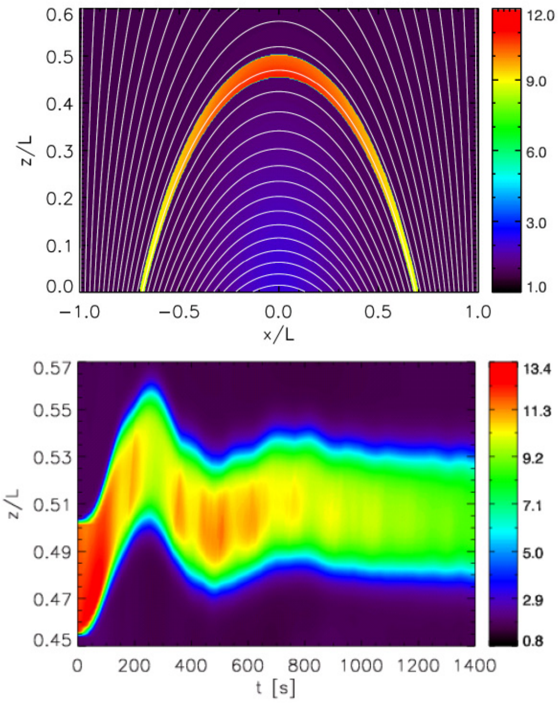

Fig. 36: Upper frame: Configuration of the simulated loop (region with higher density; colour scale) at the moment that a pulse launched below it begins to reach it. Magnetic field lines are shown as solid white lines. Lower frame: Time signature of the mass density (colour scale) along a vertical cut through the loop's apex. L is chosen to be 100 Mm.

evidence that the rapid damping of the vertical oscillations, seen both in the observations and the numerical simulations, is due to wave leakage from the loop in the form of fast waves.

(S. K. Solanki, T. J. Wang in collaboration with M. Selwa, K. Murawski (UMCS Lublin, Poland), U. Shumlak (University of Washington, Seattle, USA), and G. Toth (University of Michigan, Ann Arbor, USA))

Excitation and damping of slow magnetosonic standing waves in a solar coronal loop

Standing slow magnetosonic waves in solar coronal loops were detected by the MPS solar group using the SUMER instrument on board SOHO. The observations show that these waves are impulsively excited and that a standing oscillation is set up rather quickly. We have carried out the first theoretical investigation of the excitation of these waves. The one-dimensional numerical model we implemented includes the effects of nonlinearity and, optionally, thermal conduction, heating, and cooling of the solar plasma. We numerically evaluated excitation and damping times of a standing wave in hot coronal loops on the basis of a parametric study. Results of the numerical simulations reveal that initially launched pulses mainly trigger the fundamental mode. Its first harmonic is excited if the initial pulse is located very close to the loop's apex. The parametric study shows that these standing waves are excited in a dozen or so wave periods corresponding roughly to 13 min and that they are strongly damped over a similar time-scale. The time over which the oscillations are excited corresponds roughly to the observed excitation time. However, due to the fact that the length of the loop in the numerical simulation is shorter than in the observations, the number of wave periods is larger.

(S. K. Solanki in collaboration with M. Selwa and K. Murawski (UMCS Lublin, Poland))

Shock wave driven by an expanding system of loops

We have analyzed a Coronal Mass Ejection (CME) observed by the UltraViolet Coronagraph Spectrometer (UVCS) and the Large Angle Spectroscopic Coronagraph (LASCO) operating on board the SOHO spacecraft. Emission of unusually hot material was recorded by UVCS propagating in front of an opening system of loops generated by the CME. The evolution of the UVCS structure is highly correlated to the evolution of the opening loop. The data reveal excess broadening of the O VI doublet lines and a strong enhancement in the intensity of the Si XII λ520.66 and λ499.37 lines due to the motion of the expanding hot gas. The hot gas emission seems to be due to a shock wave propagating in front of a very fast gas bubble traveling along the opening loop system.

(N.-E. Raouafi, S. K. Solanki, B. Inhester, M. Mierla in collaboration with S. Mancuso and C. Benna (Osservatorio Astronomico di Torino), G. Stenborg (NASA GSFC), and J. P. Delaboudinière (IAS, Orsay))

Using direct observations of magnetic loops to test magnetic field extrapolations

We compare direct observations of magnetic loops in a newly developed active region with the magnetic field extrapolated from a photospheric magnetogram. This is the first time that the 3-D-structure of the magnetic field is available to test the extrapolations. We compare the observations with potential fields, linear force-free fields and non-linear force free fields (see Fig. 37). Our results show that a potential field extrapolation is not suitable for a reconstruction of the magnetic field in a newly developed active region. The inclusion of field line parallel electric currents, the so called force-free approach, provides much better results. The non-linear force-free approach reproduces the observations better than the linear force-free approximation, although no free parameters are available in the former case. This clearly demonstrates that even while emerging magnetic loops already possess significant shear.

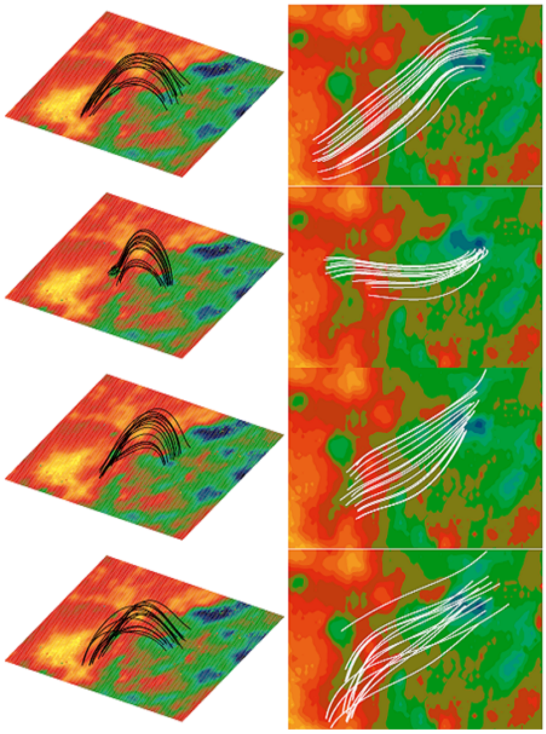

Fig. 37: Top: Original observed loops. Second row: potential fields, Third row: linear force-free fields, Bottom: nonlinear force-free fields.

(T. Wiegelmann, A. Lagg, S. K. Solanki, B. Inhester, J. Woch)

How to use magnetic field information for coronal loop identification

The structure of the solar corona is dominated by the magnetic field because the magnetic pressure is about four orders of magnitude higher than the plasma pressure. Due to the high conductivity the emitting coronal plasma (visible e.g. in SOHO/EIT) outlines the magnetic field lines. The intensity gradient of the emitting plasma structures is significantly lower parallel to the magnetic field lines than in the perpendicular direction. Consequently information regarding the coronal magnetic field can be used for the interpretation of coronal plasma structures. We extrapolate the coronal magnetic field from photospheric magnetic field measurements into the corona. The extrapolation method depends on assumptions regarding coronal currents, e.g. potential fields (current free) or force-free fields (current parallel to magnetic field). As a next step we project the reconstructed 3-D magnetic field lines on an EIT-image and compare with the emitting plasma structures. Coronal loops are identified as closed magnetic field lines with a high emissivity in EIT and a small gradient of the emissivity along the magnetic field (see Fig. 38).

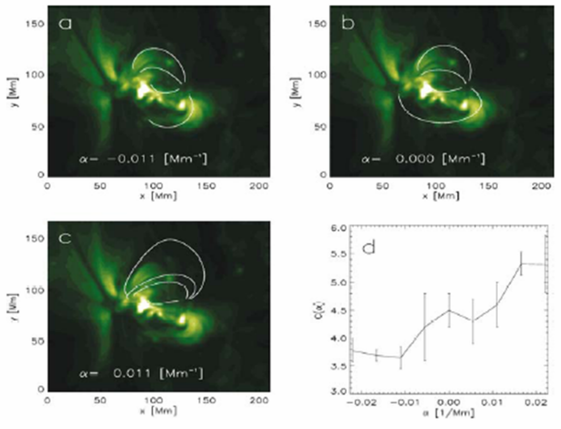

Fig. 38: EIT picture of AR 7953 and projections of linear force-free magnetic field lines. The field lines have been computed with the help of our loop identification method. It is obvious from the pictures that a linear force-free model with a negative value of $\alpha = -0.011 Mm^{-1}$ (panel a) fits the EIT-image better than a potential field (panel b) or a linear force-free field with a positive value of $\alpha = 0.011 Mm^{-1}$ (panel c). Panel d) rates the quantitative agreement of the magnetic field model and EIT-image as a function of the force-free parameter α. The smaller the value of C, the better the agreement of magnetic field and EIT emission.

(T. Wiegelmann, B. Inhester, A. Lagg, S. K. Solanki)

The SUMER Spectral Atlas of Solar Coronal features

The solar corona cannot be seen with the naked eye except for rare eclipse observations, when it becomes visible for several minutes. The nature of the corona remained for long time unexplained, despite the many attempts to determine it, which began around the middle of the 19th century. Spectroscopic observations in the visible had shown that the coronal light is composed of discrete emission lines of which the most prominent are the “red” and the “green” lines. In spite of the enormous progress in atomic physics and the systematic research in laboratories all over the world all attempts to identify the coronal lines as known laboratory spectral lines failed. In desperation some scientists postulated the presence in the solar corona of an element “coronium” lighter than hydrogen to which they attributed the coronal emission.

The first major breakthrough in coronal research occurred in 1939, when Grotrian suggested that the coronal line emission is due to forbidden transitions in highly ionized atoms. By studying energy levels of Cl-like iron (Fe^{9+}) that were derived by Edlèn from laboratory-generated spectra, he noticed a coincidence between the difference of levels within the ground configuration and one of the unidentified coronal lines. Motivated by Grotrian’s suggestion, Edlèn in 1943 succeeded identifying additional lines as transitions within the ground configuration of several other highly ionized atoms. Confident in the identifications he concluded that the coronal emission must emerge from million-degree plasmas. This identification was the starting point of modern coronal physics. It took, however, another decade until space-borne instruments became available and the full dimension of Edlèn’s discovery became apparent.

An EUV spectral atlas of the Solar Corona between 670 and 1609 Å has been derived from observations obtained with the SUMER spectrograph on SOHO. The atlas contains off-disc spectra of the quiescent corona, the corona above a coronal hole, the active corona and the flaring corona. The physical parameters of the coronal plasma are very different from those in the lower solar atmosphere, so the coronal spectrum includes a number of emission lines, which are difficult to observe elsewhere. Most of the lines in the spectrum have been identified (see Fig. 39), some of them for the first time. 40% of the coronal emission lines still remain unidentified. The present atlas (Curdt *et al.*, 2004) complements the disk atlas (Curdt *et al.*, 2001). It represents the most comprehensive and accurate line list for the solar corona in this wavelength range. Wavelengths are given with an uncertainty of typically ≃30 mÅ and spectral radiances are determined with a relative uncertainty of 0.15 to 0.40 (1σ). This atlas also provides an excellent reference for astrophysical applications.

Element	4+	5+	6+	7+	8+	9+	10+	11+	12+	13+	14+	15+	16+	17+	18+	19+	20+	21+	22+
N	x																		
O		x																	
F																			
Ne		x	x	x															
Na			x	x	x	x													
Mg		x	x	x	x	x	x												
Al			x	x	x	x	x												
Si		x	x	x	x	x	x	x	x										
P					x														
S		x	x	x	x	x	x	x	x										
Cl			x				x	x											
Ar			x	x	x		x	x	x										
K					x		x	x	x										
Ca			x	x	x	x		x	x	x	x								
Sc																			
Ti											x	x							
V																			
Cr						x	x					x	x	x		x			
Mn													x	x		x	x		
Fe			x	x		x	x	x					x	x	x	x	x	x	x
Co								x	x						x				
Ni										x	x				x		x		x

Fig. 39: Alltogether, 504 emission lines have been found with clear coronal origin. 60% of these lines have been identified or reconfirmed – including several new identifications –- from 90 ions.

(W. Curdt, E. Landi)

Nonlinear force-free coronal magnetic fields

A good knowledge of the coronal magnetic field is necessary to understand and predict basic processes like coronal mass ejections and flares. Coronal magnetic fields are assumed to be force-free, because the magnetic pressure is about four orders of magnitudes higher than the plasma pressure. Further popular simplifications are potential (current free) fields and linear force free fields. Potential fields and linear force-free fields do not contain free energy and are a poor approximation for active region fields prior to an eruption. Consequently we use a nonlinear force-free coronal magnetic field model, which has to obey the equations

$$(\nabla \times \mathbf{B}) \times \mathbf{B} = \mathbf{0}, \tag{1}$$
$$\nabla \cdot \mathbf{B} = 0. \tag{2}$$

We solve (1) and (2) by minimizing the functional

$$L = \int_V \left[B^{-2} \, |(\nabla \times \mathbf{B}) \times \mathbf{B}|^2 + |\nabla \cdot \mathbf{B}|^2 \right] \, d^3x, \tag{3}$$

where an observed preprocessed vector magnetogram specifies the photospheric boundary conditions (see Fig. 40). Other methods to solve (1) and (2) exist, but a recent comparison of six different nonlinear force-free extrapolation codes revealed that minimizing the functional (3) is the fastest and most accurate currently available method.

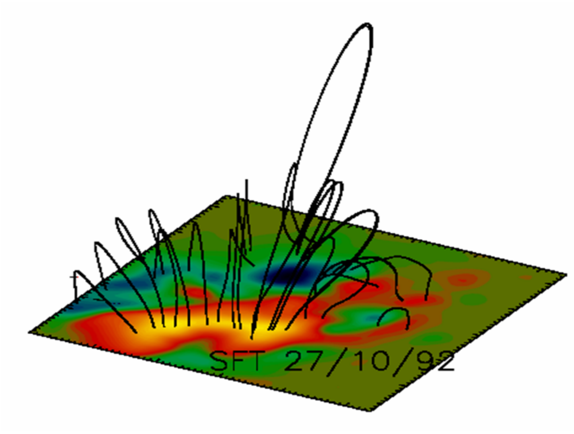

Fig. 40: Active Region AR7321: Nonlinear force-free magnetic field extrapolation with vector magnetogram data from the Solar Flare Telescope in Tokyo.

(T. Wiegelmann, B. Inhester)

Alternative algorithms for force-free field extrapolation

We have compared the performance of two alternative algorithms which aim to reconstruct a force-free magnetic field given suitable boundary conditions on the solar surface. For this comparison, we have implemented both algorithms on the same finite element grid using Whitney forms to describe the fields within the grid cells. The additional use of conjugate gradient and multigrid iterations results in quite effective codes for the reconstruction.

The two algorithms tested were the Grad-Rubin algorithm, a non-linear iteration scheme and the Wheatland-Sturrock-Roumeliotis algorithm based on a variational approach. Both algorithms perform well for the reconstruction of known analytic force-free fields when exact boundary conditions are supplied. For more general boundary conditions the Wheatland-Sturrock-Roumeliotis approach has some difficulties because it requires an overdetermined set of boundary informations which may include inconsistencies with the force-free constraints. The Grad-Rubin code on the other hand has been reported to lack convergence for strong current densities.

For the example we have investigated, however, the maximum current density achieved in a converging reconstruction seems to be not far from the limit beyond which a force free field cannot exist anymore, given the normal magnetic field intensity on the boundary (Fig. 41). We speculate therefore that the lack of convergence observed by other authors may have physical reasons rather than being due to an inadequacy of the algorithm.

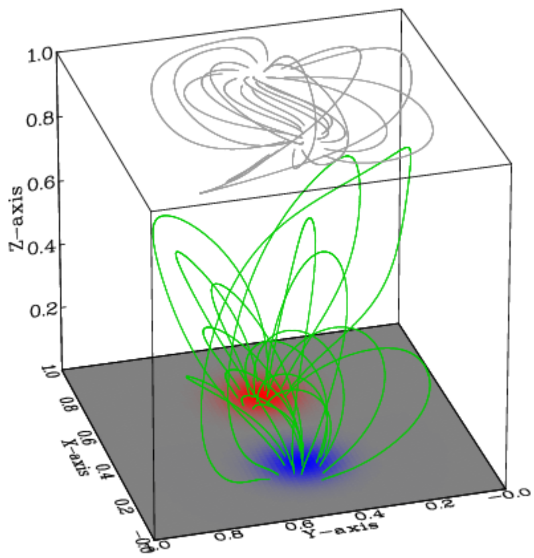

Fig. 41: An example of a force-free magnetic field reconstruction in the case of a simple antisymmetric twisted bipolar region on the solar surface

(B. Inhester, T. Wiegelmann)

Physically consistent non-force-free chromospheric and coronal magnetic fields

Photosphere, chromosphere and corona are coupled by the solar magnetic field. Since direct measurements of chromospheric and coronal magnetic fields usually are not available, in most investigations of the solar atmospheric magnetic field one mathematically extrapolate the photospheric magnetic field to chromosphere and corona. In order to solve the mathematical problem the assumption of force-free fields is used. This excludes Lorentz-forces, i.e. the force-free extrapolation approach neglects major physical processes which correspond to, e.g., coronal heating or solar plasma acceleration. In order to investigate the consequences of this limitation of the force-free approach we compared the force-free current components of extrapolated magnetic fields with those, obtained after taking into account the physical Lorentz forces. For this sake we carried out coronal plasma simulations based on measured photospheric fields and inferred plasma motions. We considered four cases - one of a directly observed chromospheric current sheet, one of an observed EUV bright point, a coronal hole and of one active region. The perturbation of the initial equilibrium situation by plasma motion generates currents in the chromosphere and corona. We diagnosed the relative strength of the perpendicular currents, causing Lorentz forces, and force-free parallel currents. We find that after the plasma motion has started perpendicular currents immediately build up. Fig. 42 shows, for the first case considered, a perpendicular current sheet, observed in the chromosphere by Solanki *et al.* (2004), the resulting isosurface of a constant perpendicular current density (in brown colors) causing Lorentz forces and distort the magnetic field structure around the current sheet indicated by yellow field lines. The strongest deviation from the force-free field was obtained, however, in the active region case, which was analyzed for the time period before an observed eruption. In dependence on the collisionless resistivity which we switched on after when the parallel current carrier velocity exceeded a certain threshold, reconnection, however, can reduce the accumulated current energy. Generally speaking, the action of perpendicular currents always has to be taken into account if one wants to quantitatively investigate the consequences of the magnetic coupling between photosphere and corona for the energetics and dynamics of the solar atmosphere.

(J. Büchner, B. Nikutowski)

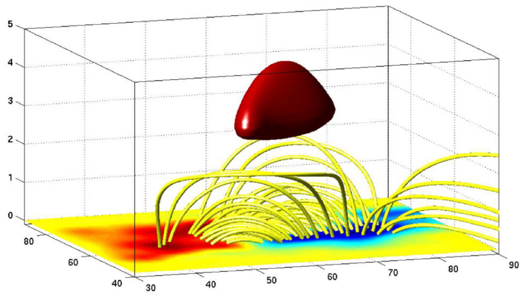

Fig. 42: Simulated chromospheric perpendicular current sheet, based on observations by Solanki *et al.* (2004). The resulting isosurface of a constant perpendicular current density (in brown colours) that causes Lorentz forces and distorts the magnetic field structure around the current sheet indicated by yellow field lines.

Coronal plasma flows and magnetic fields in solar active regions

During the early days of the SOHO mission, the SUMER spectrometer observed a few active regions connected with sunspots on the Sun and took their images and spectra in various ultraviolet emission lines. In addition to these spectroscopic data magnetograms of the photospheric footpoint regions of the active region loops were available from the Michelson Doppler Imager (MDI) on SOHO and the National Solar Observatory/Kitt Peak, data which were used to construct the coronal magnetic field of the active regions by force-free-field extrapolation. The combined data set was analysed with respect to the large-scale circulation of coronal matter, which means that the Dopplershifts of various lines used as tracers of the plasma flow were investigated in close connection with the ambient magnetic field, which was found to be either closed or open in the coronal volume considered.

Close inspection of the Fig. 43 shows that the region of the bipolar active region with negative field polarity (blue contours) indicates outflow in the area corresponding to the visible sunspot, where correspondingly the magnetic field lines form a compact bundle, whereas the region of positive polarity mostly shows downflows, is widely spread and consist of a group of spotty fields (yellow contours on the left), which are at the origin of open as well as closed field lines. There are two dark red and blue Dopplershift domains in the location of the sunspot proper, separated by rather sharp boundaries between these regions of up and down flows.

We also estimated the coronal currents in the active region, and discussed the results of this correlative study with the perspective to understand coronal heating and mass supply to the extended corona, and with respect

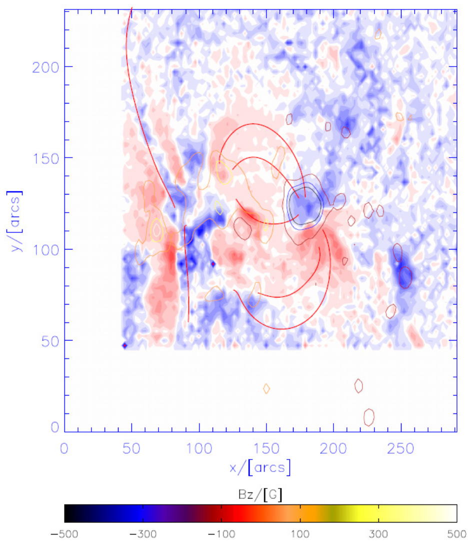

Fig. 43: SUMER Dopplergram (with colour scale in km s^{-1} on the right bar) in Ne VIII (λ 77 nm) and a two-dimensional projection of some reconstructed magnetic field lines (with the force-free-field parameter $\alpha = -1.1\ 10^{-8} m^{-1}$). Additional contours (colour bar at the bottom) of the magnetic field strength are drawn on the photosphere.

to the role played by the field in guiding and constraining plasma flows. Our study clearly illustrated the future need for simultaneous measurements on all scales of the (vector) magnetic field and of the plasma by means of imaging and spectroscopy. Only through such a combined effort can further progress be expected in understanding the dynamics and energetics of the active corona.

(E. Marsch, T. Wiegelmann, L. D. Xia)

Locating current concentrations in the solar corona

Reconnection is thought to release magnetic energy in the solar atmosphere. However, where and how is still under investigation. Before one can understand and predict the consequences of reconnection one has, first, to find out, where it takes place. Different sites were suggested: regions of vanishing magnetic field – magnetic nulls, separatrices – surfaces through nulls of different sign or bald patches, separators – the lines of intersection of separatrices, quasi-separatrix layers (QSL) and hyperbolic flux tubes, all peculiar regions in the topology of current-free (potential) magnetic fields. But, in the first place, reconnection needs dissipation. In the hot, collisionless solar corona the dissipation due to Spitzer-Härm binary collisions does not suffice to provide the necessary dissipation, e.g., of currents. Hence, it is necessary to find out were in the complex coronal structure the dissipation can become enhanced, e.g., due to high current concentrations. Numerical simulations are appropriate to locate such current concentrations.

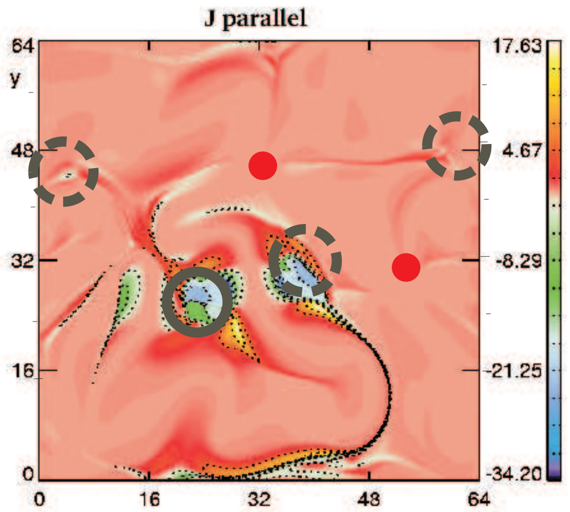

Fig. 44: Simulated parallel current densities, integrated along the magnetic field lines. The red dots indicate the positions of two chromospheric magnetic nulls located just above the photosphere. The black solid and dashed circles show the approximate size and location of the main magnetic flux concentrations in the field of view, the same line style means the same polarity.

For observed potential reconnection sites we located current concentrations by numerically simulating the dynamic response of the corona to the photospheric plasma motion. Fig. 44 depicts the resulting, integrated along the magnetic field, parallel current densities, mapped to their photospheric footpoints. Further, we compared the resulting locations of current concentrations with those predicted by different methods characterizing the magnetic field complexity and topology. Fig. 45, for example, depicts the squashing factor Q, which is the symmetrized norm of the mapping of a shift of a photospheric footpoint of a field line to the shift vector of the magnetically conjugate footpoint. Large Q correspond to the presence of QSL. We calculated Q for the magnetic field above the same photospheric area as the one, for which the simulation was carried out that revealed the current concentration shown in Fig. 44. The colour coding depicts the logarithm of the squashing factors. As in Fig. 44 the red dots indicate the positions of two chromospheric magnetic nulls located just above the photosphere. The black solid and dashed circles show the approximate size and location of the main magnetic flux concentrations in the field of view, the same line style means the same polarity. Note that the magnetic nulls are located just above the photosphere, while no coronal nulls were found in this area. Comparing the photospheric footprints of the parallel current concentrations (Fig. 44) with the location of QSL (large squashing factors Q, see Fig. 45), where the magnetic connectivity changes strongly, we found that the current sheet location correlates with QSL only, if below the QSL a photospheric plasma motion was applied as a boundary condition. Also, the strongest currents are generated not in regions of the largest squashing factors, i.e. near separatrices, i.e. near magnetic nulls, but in regions of large squashing, where additionally energy inflow from the photosphere was took place. Hence, in order to predict current locations in the corona one has always to combine the calculation, e.g., of the squashing factor with some information about the photospheric energy.

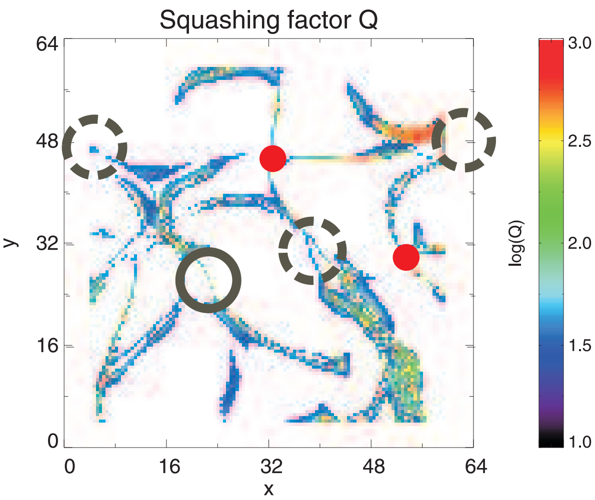

Fig. 45: Squashing factor Q for the same photospheric area as shown in Fig. 44. The colour coding depicts the logarithm of the squashing factors. The red dots indicate the positions of two chromospheric magnetic nulls located just above the photosphere. The black solid and dashed circles show the approximate size and location of the main magnetic flux concentrations in the field of view, the same line style means the same polarity.

(J. Büchner)

Vector tomography for the reconstruction of the coronal magnetic field

The magnetic field contains the dominant energy per unit volume in the solar corona and therefore plays an important role in most coronal processes. However, the coronal magnetic field cannot be measured directly but is often extrapolated from magnetic surface measurements. These extrapolations are prone to errors at greater distances from the surface and in presence of strong electric currents in the corona.

Some information about the coronal magnetic field can, however, be obtained by spectropolarimetric observations of the Zeeman and Hanle effect on coronal infrared lines. The Hanle effect observations of long-lived forbidden coronal lines provide roughly the orientation of the coronal magnetic field in the plane of the sky while the Zeeman effect observation yield the line-of-sight component of the field. Especially the latter type of measurements are very difficult and have only recently been performed successfully.

We have investigated whether a tomographic reconstruction based on these observations allows us to obtain a reliable model of the vector magnetic field in the corona. The inversion problem is strongly ill-posed. To improve the condition of the inversion we make explicit use of the divergence-free constraint of the magnetic field besides the fact that the field has to comply with the spectropolarimetric line observations. The use of the divergence-free condition requires the additional knowledge of the solar surface magnetic field which is, however, observed regularly. A full dataset for the inversion includes therefore the surface magnetic field and coronagraph line observations of all four Stokes components during half a solar rotation. The spatial and temporal resolution of these observations influence the resolution that can be achieved in the magnetic field reconstruction.

In our test inversion calculations we have demonstrated that with our new method we can reproduce details of the magnetic field which cannot be obtained by mere extrapolation of the surface fields. Zeeman effect or Hanle effect observations alone are not enough to yield a reliable reconstruction because the individual observations do not fully constrain the coronal magnetic field.

Further tests still need to be done to investigate the robustness of our inversion with respect to noise and data gaps. On the other hand additional stabilising constraints, like the requirement for the field to be force-free have not been exploited yet.

(B. Inhester, M. Kramar, S. K. Solanki)

The widths of vacuum-ultraviolet spectral lines in the equatorial solar corona observed with CDS and SUMER

Observations of the solar equatorial corona between heights of 36 Mm and 184 Mm above the limb obtained by the SOHO spectrometers CDS and SUMER in December 2003 are presented and discussed with special emphasis on the widths of the spectral lines Mg X at 62.50 nm, Al XI at 55.00 nm and 56.82 nm, Ca X at 55.78 nm, and Si XI at 58.09 nm. SUMER observed, in addition, the lines Mg X 60.98 nm, Ca X 57.40 nm, Fe XII 124.20 nm, Fe XVII 115.31 nm, and Ca XIII 113.37 nm. The Si XII 52.11 nm line was only observed by CDS. A different behaviour of the line width of Mg X 62.50 nm as a function of height above the limb had been found in studies carried out independently with both instruments at different times. It is the aim of this joint investigation to (a) study instrumental effects on line-width results; and (b) provide a thorough analysis of line profiles with altitude for the new campaign. No line width decrease with height was observed with the exception of the hot Fe XVII 115.31 nm observed above an active region.

(K. Wilhelm, L. Teriaca in collaboration with A. Fludra, R. A. Harrison, C. D. Pike (Rutherford Appleton Laboratory, Didcot, UK) and with B. N. Dwivedi (Banaras Hindu University, Varanasi, India))

Coronal heating by transition region reconnection

Plasma waves and magnetic reconnection are the main mechanisms thought to explain the heating of the solar corona. We addressed the question about the driver of reconnection in the quiet-Sun and of the location, where it heats the corona. As a driver we considered the photospheric plasma motion determined by using the MDI line-of sight magnetic field information for a local correlation tracking analysis. We numerically simulated the consequent formation of non-force-free currents in chromosphere and corona. Based on plasma-physical results we switched on, in places where the current carrier velocity exceeds a certain critical level, an anomalous plasma resistivity which allows reconnection. Both the current carrier velocity (due to the decreasing plasma density) and the threshold of a instability which drives anomalous resistivity, grow with height, the latter slower due to its square-root dependence on temperature. Hence, there might be a characteristic height range, where the current carrier velocity might exceed the threshold of current instability. Our simulations showed that the most favorable region for reconnection is located near the transition region and the attached lower corona, following a flux tube, strongly driven by the photospheric plasma motion at its footpoint. Fig. 46 depicts the simulated chromospheric and coronal magnetic field and the region of enhanced current carrier velocity as it is driven by the footpoint motion of the flux tube, taken from observations.

(J. Büchner, B. Nikutowski in collaboration with A. Otto (Fairbanks))

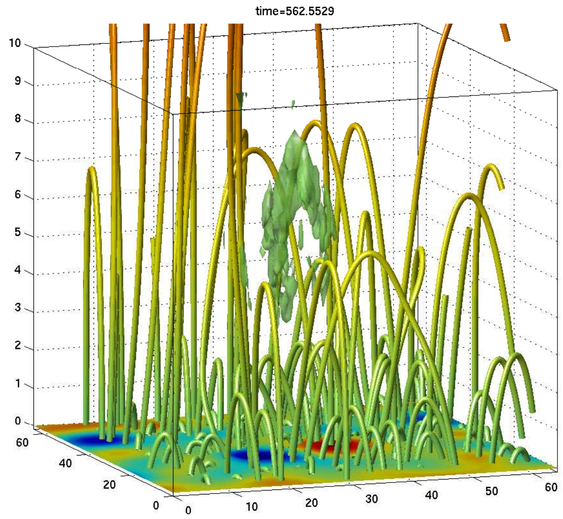

Fig. 46: Simulated chromospheric and coronal magnetic field and region of enhanced current carrier velocity, driven by the footpoint motion of the flux tube, taken from observations. The scales are given in Mm.

A nanoflare model of quiet Sun EUV emission

Nanoflares have been proposed as the main source of heating of the solar corona. However, detecting them directly has so far proved elusive, and extrapolating to them from the properties of larger brightenings (microflares and flares) generally gives too few of them to be relevant for coronal heating. Here we take the approach of statistically modelling light curves representative of the quiet Sun as seen in EUV radiation. The basic assumption is that all quiet-Sun EUV emission is due to micro- and nanoflares, whose radiative energies display a power-law distribution. Thus, the quasi-constant background radiation is, in this model, assumed to be produced by the overlap of many weak brightenings. The free parameters of the model are constrained by requiring the simulated time series to simultaneously reproduce the lognormal probability distribution function of the intensity in transition region and coronal spectral lines, as well as the power spectra obtained from the light curves emitted by these lines. We show that these distributions and spectra can be reproduced by a simple model, which assumes that the radiance is produced by a stochastic (micro-, nanoflaring) process. A good statistical match of the measurements is obtained for a steep power-law distribution of nanoflare energies, with power-law exponent $\alpha > 2$ (see Fig. 47). This is consistent with the requirement that the dominant heat input to the corona is provided by nanoflares.

(S. K. Solanki in collaboration with A. Pauluhn (Paul Scherrer Institut, Switzerland))

Waves and turbulence in the solar corona

As chapter in the book *The Sun and the Heliosphere as an Integrated System*, a short review was written about

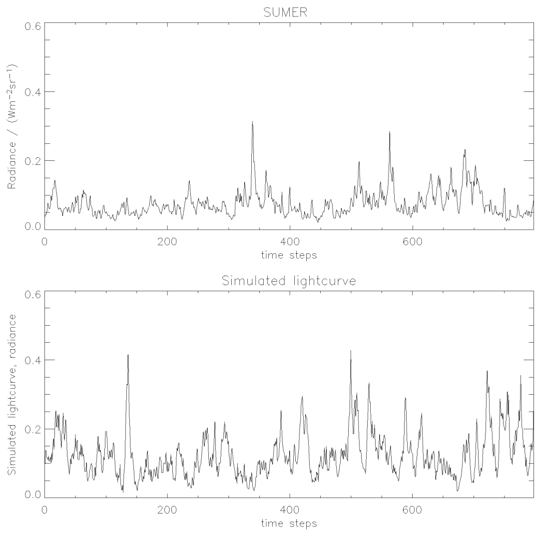

Fig. 47: SUMER time series of a quiet-Sun cell interior recorded in the transition region O VI line at 79.0 nm (upper frame), and a corresponding simulated spectrum with power law exponent of the nanoflare energy distribution, $\alpha = 2.5$ (lower frame). Note the similarity between the two light curves.

waves and turbulence in the solar corona. The content of the article was summarized in the abstract reading:

In the solar corona (and solar wind) waves and turbulence occur at all scales ranging from the particles' gyroradii to the size of a solar radius (or even to an astronomical unit). A concise review of some new observations and theories of waves in the Sun's atmosphere and corona is given, with the focus being on coronal waves that are magnetically confined to loops, as well as on waves in the open coronal funnels and holes. In the corona all kinds of kinetic (plasma) waves and fluid (magnetohydrodynamic) waves, at wavelengths that may range from the size of a loop (about several Mm) down to the inertial lengths of a coronal ion (about a km), are believed to play a key role in the transport of mechanical energy from the chromosphere to the Sun's outer corona and wind, and through the dissipation of wave energy in heating and sustaining the solar corona. Recent evidence obtained from spectroscopy of lines emitted by coronal ions points to cyclotron resonance absorption as a possible cause of the observed emission-line broadenings. Novel remote-sensing solar observations reveal low-frequency loop oscillations of the type expected from MHD theory. They appear to be excited by magnetic activity and are strongly damped. Kinetic models of the corona indicate the importance of wave-particle interactions, which may hold the key to understand coronal particle acceleration and heating by high-frequency waves.

(E. Marsch)

Plasma waves and instabilities in a coronal funnel within the multi-fluid description

We studied the wave propagation in the low-β plasma of a coronal funnel, using a collisionless multi-fluid model. Neglecting the electron inertia, this model allowed us to take into account ion-cyclotron wave effects absent in the MHD model. First we performed a Fourier plane-wave analysis, and then numerically solved the dispersion relations for a two- and three-fluid model. Thus the local wave dispersion properties for representative parameters of the corona could be calculated. The crossings of the dispersion branches were found to generate mode couplings. We also considered alpha particles (α) as a third, aside from protons (p) and electrons (e), particle population. A realistic two-dimensional funnel model was used to define the open magnetic field in the a polar coronal hole.

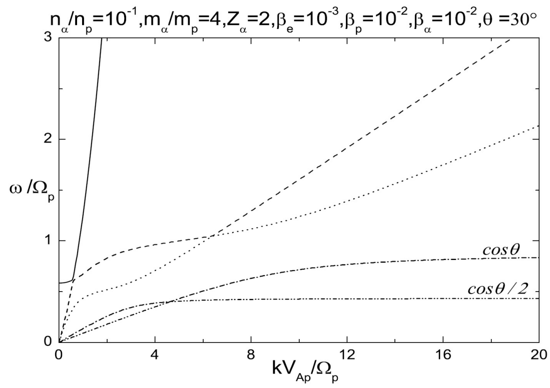

Fig. 48: Dispersion relations in a coronal funnel for a three-fluid plasma. Five dispersion curves for oblique wave propagation ($\theta = 30°$) are shown. The quantities ω and k are normalized, respectively, to Ω_p and Ω_p/V_{Ap}, where Ω_p is the proton cyclotron frequency and V_{Ap} the proton Alfvén speed. From top left to bottom right we have the magnetosonic, the two Alfvén waves, and the two slow mode waves. Typical plasma parameters are given at the top.

As Fig. 48 shows, the oblique slow mode reveals a resonance frequency at $\omega \approx \Omega_p cos\theta$. Five modes exist in the three-fluid model. They are subject to mode conversion and show the appearance of a cut-off frequency and additional resonance. The numerical results indicate that the free energy provided by a heavy ion beam can excite waves through ion-cyclotron and Cherenkov resonance, and may thus lead to plasma instability. In particular, the absorption and dissipation near the resonance frequencies of the minor heavy ions play an important role in coronal heating by waves.

(R. Mecheri, E. Marsch)

Kinetic aspects of coronal ion heating

In order to understand coronal heating, the microphysics of the dissipation at small scales of various forms of mechanical, electric and magnetic energy (contained in waves, turbulence and nonuniform flows and currents) must be addressed. In fluid treatments this difficult problem is often circumvented by enhancing artificially the dissipation, e.g. through an increase of the Coulomb collision rates for the corona, and by thus lowering the Reynolds number by many orders of magnitude.

In two invited contributions to the *SOHO 15* and *Solar Wind 11* conferences, we critically reviewed the basic assumptions underlying collisional transport theory, discussed the related ion heating rates, and then also described collisionless alternatives. We further elucidated the kinetic aspects of coronal heating in association with Landau and cyclotron resonant damping of plasma waves, and discussed results numerically obtained by solving the Vlasov equation.

Kinetic processes are important in the solar corona and solar wind, because the plasma is tenuous, multicomponent and nonuniform. Owing to weak collisionality, there is a lasting influence of the coronal boundary conditions on the interplanetary solar wind, which are reflected in its microscopic state.

Solar wind ions, once being beyond their sonic critical point and detached from the Sun, behave very differently than electrons. The ion velocity distributions are prone to sizable distortions in phase space and strongly shaped by wave-particle interactions in the turbulent wind. Two typical examples in fast wind are given in Fig. 49. The pertinent traits of these non-thermal distributions are the core temperature anisotropy and the beam travelling faster than the local Alfvén speed. The origin of these features in the solar corona remains still unclear.

(E. Marsch)

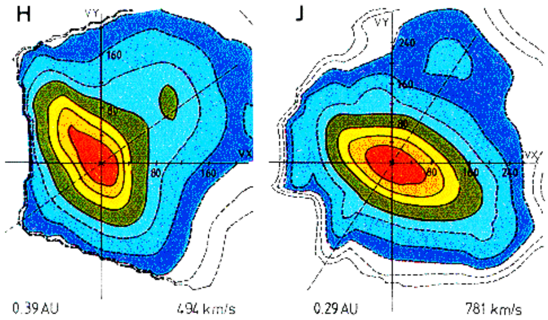

Fig. 49: Proton velocity distribution functions in the fast solar wind as measured by the plasma instrument on the Helios spacecraft at 0.3 AU (right) and 0.4 AU (left). The isodensity contours in velocity space range from the maximum down to the one percent level. Note the core temperature anisotropy and the beam.

A new conservative unsplit method for a numerical solution of the Vlasov equation for solar applications

If one wants to understand and predict the consequences of plasma processes taking place in the hot, dilute, collisionless, strongly magnetized solar corona one has to solve essentially kinetic physical problems. Since the resulting dynamical processes are, as a rule, strongly nonlinear, analytic methods most of the time fail and numerical simulation is appropriate. In order to resolve the important in collisionless plasmas phase space effects a direct solution of the Vlasov equation is desired. Since existing splitting methods are not synchronous and non-conserving in principle, they add a too large amount of numerical dissipation to *ab initio* solve the most urgent problems, e.g., of energy dissipation causing corona heating, of collisionless resistivity and heat conduction. In order to address these numerical challenges adequately by means of modern massively parallel computers we have developed a new conservative method for solving the Vlasov equation without using any splitting technique. Our code ultimately maintains the positivity of the distribution function and avoids any un-physical oscillations which usually lead to numerical instabilities. Based on a finite volume conservative discretization of the Vlasov equation in its conservative form we implemented a highly accurate second order upwind scheme. We avoid un-physical oscillations and their possible numerical instability by applying a flux-limiter in the second order. The scaling of the code on massively parallel computers is excellent, 75% on 128 processors. A validation of our new Vlasov solver by considering a standard ion-acoustic instability revealed a weak growth of the relative numerical entropy for fixed grids which we further improved by applying a stretched grid approach around the main resonances. The performance of the code can be judged upon, e.g., looking at Fig. 50, where Str denotes the stretching factor and the numbers correspond to the number of mesh points in the velocity- and in the spatial dimension. The Figure shows that the relative numerical entropy growth is limited to about 0.1 even for very long run times.

(N. Elkina, J. Büchner)

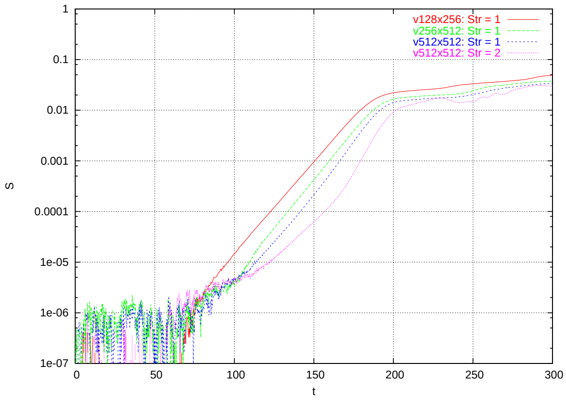

Fig. 50: Relative entropy evolution in the ion-acoustic instability simulation for high resolution fixed grids and a lower overall resolution stretched grid.

Kinetic physics of electron and ion heating by solar coronal currents

The mechanism of heating the solar corona to temperatures of the order of 10^6 K is a still unresolved issue. One of the hypotheses is heating by DC currents, which are driven by the photospheric plasma motion. Since binary collisions are too inefficient to dissipate currents in the corona, microscopic instabilities will have to generate fluctuating electric fields which might irreversibly energize electrons and ions in the corona. By means of an *ab initio* kinetic approach we investigated the question whether current-driven nonlinear field perturbations will heat preferably ions or electrons and at which rate.

The linear stability theory of isothermal current-driven space plasmas predicts an ion-acoustic instability if the relative drift velocity of the current-carrying particles exceeds a certain threshold, which, generally speaking, depends on the plasma parameters. The spectrum of waves, excited by a marginal instability, is very narrow. Hence, the wave power at saturation and the resulting heat transfer rate due to wave-particle interaction cannot be obtained by means of a quasi-linear, weak turbulence approach and the nonlinear single-mode theory provides too small saturation amplitudes. To solve the nonlinear problem we applied our newly developed unsplit conservative Eulerian Vlasov code to simulate the heating of the strongly magnetized current-driven coronal plasma in a 1D1V (one spatial, one velocity space direction) kinetic approach. Instead of periodic boundary conditions, traditionally used in simulations since they are simpler to treat, we implemented open boundaries which allowed us to maintain the current constant. We found that the nonlinear saturated state of the coronal plasma are dominated by the formation of coherent phase space structures. Fig. 51 depicts the consequences for coronal plasma heating: Most of the energy, transferred to the electric field fluctuations (see the heating rate, shown against the time axis, by a solid blue line) leads to electron heating (the electron heating rate ν^e_{heat} is depicted by a green dashed line), while the ions are heated much, by an order of magnitude less efficiently (the ion heating rate ν^i_{heat} is depicted by the red dash-dotted line).

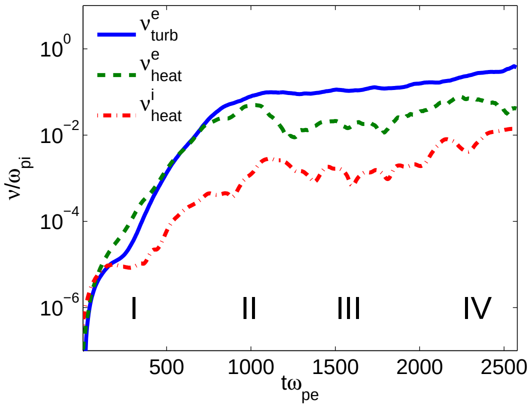

Fig. 51: Kinetically simulated effective turbulence energy transfer rate ν^e_{turb} (blue solid line) electron- (ν^e_{heat}, green dashed line) and ion- (ν^i_{heat}, red dash-dotted line) heating rates.

(J. Büchner, N. Elkina)

Helium Line Formation and Abundance in a Solar Active Region

Despite the high Helium abundance in the universe, its photospheric solar abundance ([He]= N_{He}/N_H) is unknown. The inversion of helioseismic data leads to values of [He], in the convection zone, in the range 0.078 – 0.08. Direct measurements of [He] in the inner solar atmosphere are available only for the corona where, at R≈ $1.1R_\odot$, values between 0.05 and 0.08 are found. An average value of 0.05 is found *in-situ* in the fast solar wind. Detailed theoretical calculations including diffusion effects seem to confirm that [He] undergoes strong changes from the chromosphere to the lower corona before stabilizing at the values observed in the solar wind. Therefore, it would be very important to determine [He] at chromospheric and transition region (TR) levels directly from line profiles. Simultaneous ground-based and CDS/SOHO spectroheliograms of the same active region have been acquired in several spectral lines (Ca II K, Hα, Na I D, He I 10830, 5876, 584, and He II 304 Å). The EUV radiation at λ < 500 Å and in the range 260 < λ < 340 Å has also been measured at the same time. These simultaneous observations allow us to build semi-empirical models of the chromosphere and low

TR of an active region, taking into account the estimated total number of photoionizing photons impinging on the target active region and their spectral distribution. We obtained a model that matches very well all the observed line profiles, using a standard value for the He abundance ([He]=0.1) and a modified distribution of microturbulence. For this model we study the influence of the coronal radiation on the computed helium lines. We find that, even in an active region, the incident coronal radiation has a limited effect on the UV He lines, while it is of fundamental importance for the D3 and 10830 Å lines. Finally, we build two more models, assuming values of He abundance [He]=0.07 and 1.5, only in the region where temperatures are $> 1 \times 10^4$ K. This region, between chromosphere and TR, has been indicated as a good candidate for processes that might be responsible for strong variations of [He]. The set of our observables can still be well reproduced in both cases, changing the atmospheric structure mainly in the low TR. This implies that, to choose between different values of [He], it is necessary to constrain the transition region with different observables, independent of the He lines.

(L. Teriaca in collaboration with P. J. D. Mauas (Instituto de Astronomía y Física del Espacio, Buenos Aires, Argentina), V. Andretta (INAF-Osservatorio Astronomico di Capodimonte, Napoli, Italy), A. Falchi, G. Cauzzi (INAF-Osservatorio Astrofisico di Arcetri, Firenze, Italy), R. Falciani (Universitá di Firenze, Italy))

RHESSI Images and spectra of two small flares

We studied the evolution of two small flares (GOES class C2 and C1) that developed in the same active region with different morphological characteristics: one is extended and the other is compact. We analyzed the accuracy and the consistency of different algorithms implemented in RHESSI software to reconstruct the image of the emitting sources, for energies between 3 and 12 keV. We found that all tested algorithms give consistent results for the peak position while the other parameters can differ at most by a factor 2. *Pixon* and *Forward-fit* generally converge to similar results but *Pixon* is more reliable for reconstructing a complex source. We investigated the spectral characteristics of the two flares during their evolution in the 3 – 25 keV energy band. We found that a single thermal model of the photon spectrum is inadequate to fit the observations and we needed to add either a non-thermal model or a hot thermal one. The non-thermal and the double thermal fits are comparable. If we assume a non-thermal model, the non-thermal energy is always higher than the thermal one. Only during the very final decay phase a single thermal model fits fairly well the observed spectrum.

(L. Maltagliati, L. Teriaca in collaboration with A. Falchi (INAF-Osservatorio Astrofisico di Arcetri, Firenze, Italy))

Dynamics and evolution of an eruptive flare

Flares arise from the sudden release (through magnetic reconnection) of free magnetic energy stored in the corona in non-potential configurations. The energy is then transported down to the chromosphere along the magnetic field lines by accelerated particles and/or by a thermal conduction front. Hydrodynamic simulations indicate that, for sufficiently high energy fluxes, the evaporation is explosive and leads to downflows in the chromosphere and upflows of very hot plasma that is injected into the corona to fill coronal loops. Although this general picture seems well established, the details of some of the key processes assumed to take place remain to be verified. The CDS spectrograph aboard SOHO, facilities at the Sacramento Peak Solar Observatory, and the TRACE and RHESSI spacecrafts were used to obtain multiwavelength observations of a C2.3 two-ribbon flare. CDS spectroheliograms in the Fe XIX, Fe XVI, O V and He I lines allows us to determine the velocity field at different heights/temperatures during the flare and to compare them with the chromospheric velocity fields deduced from Hα image differences. TRACE images in the 17.1 nm band greatly help in determining the morphology and the evolution of the flaring structures. During the impulsive phase a strong blue-shifted Fe XIX component (-250 km s^{-1}) is observed at the footpoints of the flaring loop system (see Fig. 52), together with a red-shifted emission of O V and He I lines (20 km s^{-1}). In one footpoint simultaneous Hα data are also available and we find, at the same time and location, downflows with an inferred velocity between 4 and 10 km s^{-1}. We also verify that the "instantaneous" momenta of the oppositely directed flows detected in Fe XIX and Hα are equal within one order of magnitude. These signatures are in general agreement with the scenario of explosive chromospheric evaporation. Combining RHESSI and CDS data after the coronal upflows have ceased, we prove that, independently from the filling factor, an essential contribution to the density of the post-flare loop system is supplied from evaporated chromospheric material. Finally, we consider the cooling of this loop system, that becomes successively visible in progressively colder signatures during the gradual phase. We show that the observed cooling behaviour can be obtained assuming a coronal filling factor of ≈ 0.2 to 0.5.

(L. Teriaca, L. Maltagliati in collaboration with A.

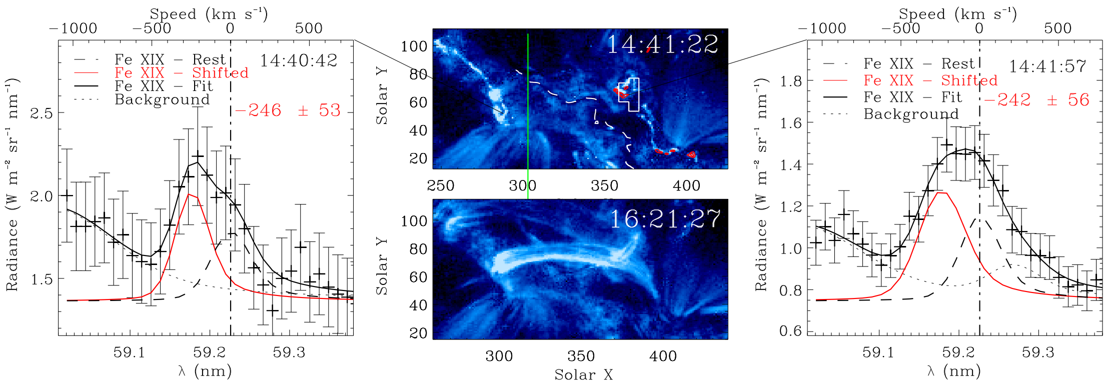

Fig. 52: Large upflows are observed in the Fe XIX line profiles aquired at the flaring kernels visible in the 14:41 UTC TRACE image. These are the footpoints of a large loop system that cools down to the ≈1 MK formation temperature of the Fe IX - X lines of the 17.1 nm TRACE bandpass in about one hour. In the 14:41 UTC TRACE image, the green line indicates the east edge of the Hα FOV while the red contours show dowflowing speeds of 4 and 7 km s^{-1} detected in Hα. The white dashed line shows the location of the magnetic neutral line. The Fe XIX profile on the right panel was obtained integrating over the area within white solid lines in the 14:41 UTC image while the profile on the left panel is obtained integrating over three CDS pixels.

Falchi, G. Cauzzi (INAF-Osservatorio Astrofisico di Arcetri, Firenze, Italy) and R. Falciani (Universitá di Firenze, Italy))

Using LASCO-C1 spectroscopy for coronal diagnostics

The LASCO-C1 telescope was designed to perform spectral analysis of coronal structures by means of a tunable Fabry Pérot interferometer acquiring images at different wavelengths (see Fig. 53). Results from spectral scans of the Fe XIV 5303 Å green coronal emission line are presented. Physical quantities like the ion temperature (line widths), and the flow velocity along the line of sight (Doppler shifts) are obtained over the entire corona.

(M. Mierla, R. Schwenn, L. Teriaca, B. Podlipnik in collaboration with G. Stenborg at NASA-GSFC, Greenbelt, USA)

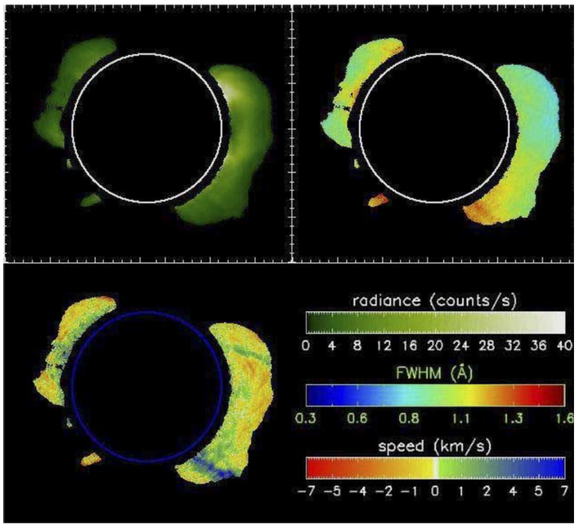

Fig. 53: Maps of radiance (upper left), speed (lower left) and line width (upper right) as deduced from fitting the Fe XIV emission line profiles acquired on 28th March 1998. Negative speed values represent plasma moving away from the observer.

Is a velocity distribution anisotropy in the solar corona really needed?

Coronagraphic spectral observations carried out with the UltraViolet Coronagraph Spectrometer (UVCS) on SOHO show extremely broad spectral lines of O VI in coronal holes above the solar poles, while Doppler dimming measurements of these lines suggest that they appear relatively narrow to the radiation coming from lower in the corona. These observations are usually interpreted in terms of a highly anisotropic velocity distribution in the solar corona. This anisotropy is taken to provide evidence for ion-cyclotron waves and has major implications for heating the coronal hole plasma and accelerating the fast solar wind.

We have examined the influence of the density stratification on the interpretation of such observations. In particular, we investigated spectral line profiles emitted in the corona by employing an analytical 2-D model of the large scale coronal magnetic field and solar wind. We concentrated on the polar coronal holes and took into account the integration along the line of sight. We found that at distances greater than 1 $R_\odot$ from the solar surface the widths of the emitted lines are significantly affected by the details of the adopted electron density profiles. In particular, the densities deduced from SOHO data (Doyle *et al.*, 1999) result in O VI profiles whose widths and intensity ratio are relatively close to the values observed by UVCS/SOHO, although only isotropic velocity distributions are employed (see Fig. 54).

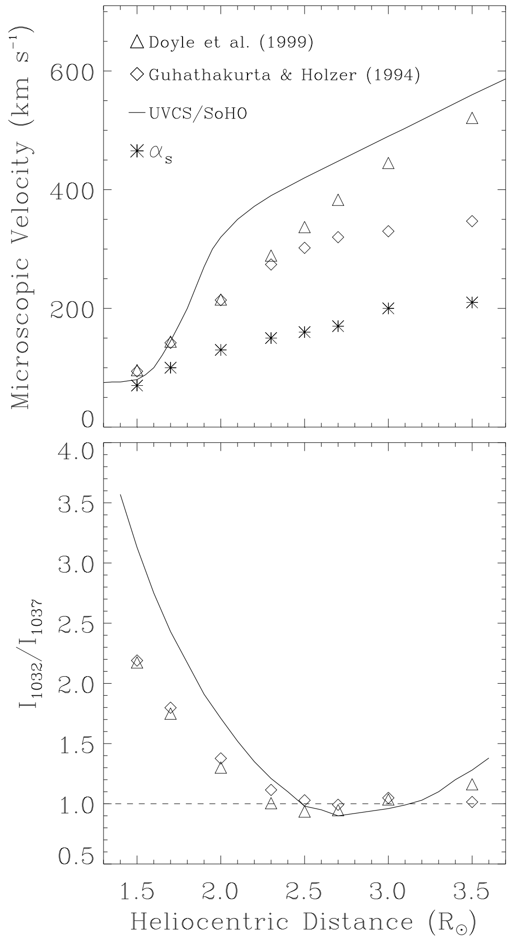

Fig. 54: Computed O VI 103 nm doublet line width (upper frame) and line ratio (lower frame) plotted vs. height. Different symbols represent outputs of calculations with different density profiles. These values are to be compared with values observed by UVCS (solid lines). Note the relatively good agreement between the computations based on the density model of Doyle *et al.* (1999) and the observation.

The Lyα and Mg X profiles are also well reproduced. Hence we expect that the magnitude of anisotropy of the velocity distribution deduced from UVCS data depends strongly on the adopted density profile. The role played by ion-cyclotron waves may, therefore, need to be reconsidered.

(N.-E. Raouafi, S. K. Solanki)

Solar wind and heliosphere

Source regions of the solar wind

The solar wind has been an essential topic in space physics, ever since it was in 1951 inferred from cometary observations and predicted from coronal models. Its properties were then analysed through in-situ observations. But even after five decades of spacecraft exploration and theoretical modelling, the exact source of the solar wind in the solar atmosphere remains a mystery.

Outflow in the magnetic funnels of a coronal hole

In a paper in *Science*, we now established that the solar wind starts flowing out of the corona at heights above the photosphere between 5 Mm and 20 Mm in magnetic funnels (see Fig. 55). This result was obtained by a detailed correlation of the Doppler-velocity and radiance maps of various spectral lines emitted by different ions with the force-free magnetic field as extrapolated from photospheric magnetograms to different altitudes in the corona. Specifically, we found that Ne^{7+} ions mostly radiate around 20 Mm, where they have outflow speeds of about 10 km/s, whereas C^{3+} ions with no average flow speed mainly radiate around 5 Mm. Based on these results, a new scenario for understanding the solar wind origin was suggested.

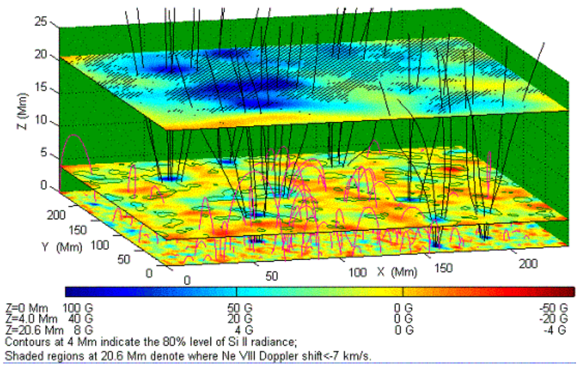

Fig. 55: Magnetic field structures in the 3-D solar atmosphere. The black solid curves illustrate open and the red ones closed field lines. Since the magnetic field strength decreases with increasing height (Z) in the corona, the scales on the colour bars differ for different Z. In the plane inserted at 4 Mm, we compare the Si II radiance with the extrapolated vertical magnetic field component, B_z. The contours delineate the 80% level of the Si II radiance. In the plane inserted at 20.6 Mm we compare the Ne VIII Doppler shifts with the extrapolated B_z. The shaded areas indicate where the Ne^{7+} outflow speed is larger than 7 km/s.

Solar wind mass and energy supply through funnels

Considering the estimated height of solar wind origin, the shape and size of funnels and loops, and the Doppler shifts of C^{3+} as identified from the SUMER and MDI data, we suggested a new scenario for the solar wind formation. Fig. 56 describes this model in detail. In this scenario the photospheric supergranular convection is the main driver of the solar wind. The advected side loops of the funnels with sizes of several megameter are the main carriers of the energy and plasma for the solar wind.

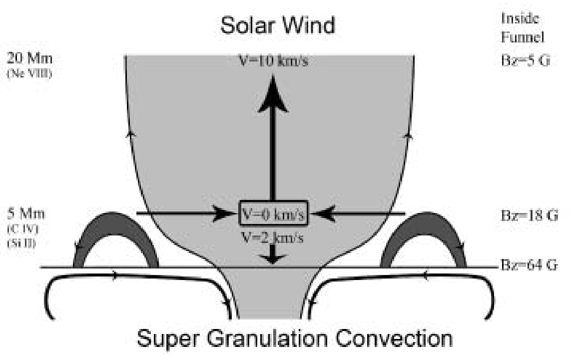

Fig. 56: Sketch to illustrate the scenario of the solar wind origin and mass supply. The plot is drawn to show that supergranulation convection is the driver of solar wind outflow in coronal funnels. The sizes and shapes of the funnels and loops shown in the figure are drawn according to the real size of the magnetic structures.

Previously, it was believed that the solar wind possibly originated in the ionization layer of the hydrogen atom, only slightly above the photosphere. However, the Doppler shift of the emission line of the carbon ions shows that a significant solar wind bulk flow has not yet occurred at a height of 5 Mm. The solar wind matter is considered to be supplied by plasma stemming from small adjacent magnetic loops with a few Mm in height. By magnetic reconnection, driven by the supergranular convection, the plasma in magnetic side loops is fed into the funnels. Part of this plasma is accelerated in the funnel and may finally form the solar wind.

Correlation heights of the sources of solar ultraviolet emission lines in a quiet-Sun region

The radiance and Doppler-velocity maps of the emission lines of Si II, C IV and Ne VIII obtained in a quiet region of the Sun by SUMER are found to be correlated with the vertical component, B_z, of the magnetic field vector as extrapolated, by means of a force-free field model, from the photospheric magnetic field. With increasing vertical height, each of the correlation coefficients initially increases to a maximum value before it decreases again. The altitude corresponding to this maximum is called correlation height. For the data sets selected from a quiet-Sun region, the correlation heights of Si II and C IV are near 2 Mm, and for Ne VIII near 4 Mm. At their correlation heights the averaged square root of the radiance of the lines of Si II and C IV, considered as a proxy of the plasma density, has a linear relationship with B_z. This is illustrated in Fig. 57 which supports the empirical concept that the quiet solar transition region is thin.

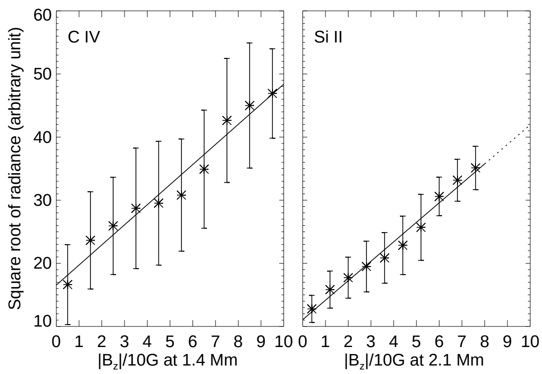

Fig. 57: Dependence of the square root of the radiances of the C IV and Si II lines on B_z. The asterisks show the averages of the square root of the radiance in each bin as a function of B_z. The uncertainties show the corresponding standard deviations of the averages. The solid lines represent linear fits to the averages.

(E. Marsch and K. Wilhelm in collaboration with C.-Y. Tu (Peking University, China) and with L. D. Xia (University of Science and Technology, Hefei, China))

Acceleration of the fast solar wind by reconnection

We carried out computer simulations of the plasma dynamics above a polar coronal hole observed by SOHO on September 21, 1996. We started the simulation with the observed line-of-sight components of the photospheric magnetic fields and the derived photospheric plasma motion. The cross-field motion of the magnetized plasma causes currents flowing both parallel (force-free) and perpendicular to the magnetic field. We address the physics of current dissipation by applying threshold and dependence of finite resistivity on macroscopic plasma parameters according to the results of kinetic investigations of the collisionless dissipation. In particular we link the collisionless resistivity and the current carrier velocity as obtained by the MHD model. For the observed polar coronal hole we investigated the interaction between low rising loops and funnel-shaped magnetic fields rooted in the supergranule boundary. The resulting reconnection heats the plasma at the funnel-loop interfaces and accelerates it to the initial velocities larger than 10 km/s. The accelerated plasma flows change their direction around the source region of the fast solar wind above a coronal hole as shown in Fig. 58.

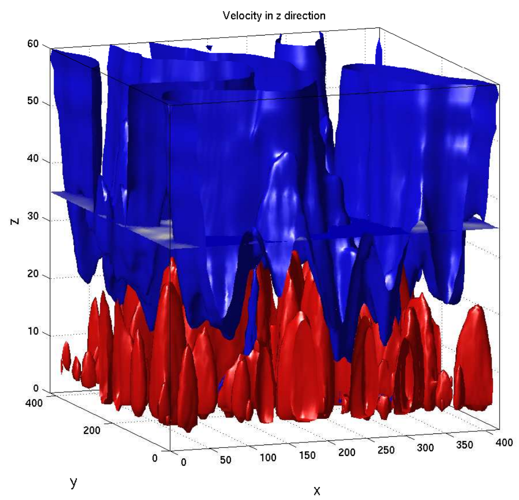

Fig. 58: Isosurfaces of upward (blue) and downward (red) accelerated plasma flow velocities changing their sign around the source region of the fast solar wind above a coronal hole. These results were obtained by the simulation of reconnection above an observed coronal hole. The linear scales are given in Mm.

(J. Büchner, B. Nikutowski)

Radial evolution of solar wind electrons between 0.3 and 1.5 AU

The observed electron distribution functions of the solar wind exhibit three different components: a thermal core and a supra-thermal halo, which are always present at all pitch angles, and a sharply magnetic-field aligned "strahl" which usually moves away from the Sun. Whereas Coulomb collisions can explain the relative isotropy of the core population, the origin of the halo population, and more specifically of its sunward-directed part, are not well understood. We studied the radial evolution of the electron velocity distribution functions in the fast solar wind between 0.3 and 1.5 AU (see Fig. 59). For this purpose, we combined data obtained separately by the Helios, Wind and Ulysses spacecraft.

We first computed the average distributions over distance and normalized them to 1 AU, to remove the effects of solar wind expansion. Then we modeled separately the core, halo and strahl components to compute their relative number densities or fractions of the total electron density. While the core fractional density remained roughly constant with radial distance,

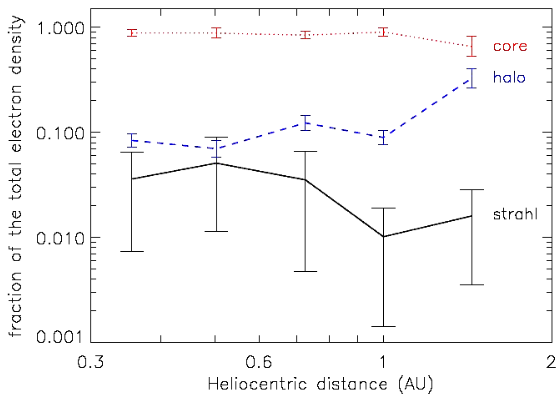

Fig. 59: Radial variations of the relative number densities of the core (red), halo (blue) and strahl (black) electrons in the solar wind. The core fractional density remains roughly constant over the whole radial range. While they are about equal between 0.3 AU and 0.5 AU, beyond 0.5 AU the halo and strahl fractional densities vary oppositely with radial distance. This suggests that a significant number of strahl electrons are scattered into the halo electron population.

we found that the halo and strahl fractional densities varied in an opposite way. The relative number of halo electrons increased, while that of strahl electrons decreased with distance. This is evidence that the electron halo population partly consists of electrons that have been scattered out of the strahl.

(E. Marsch in collaboration with M. Maksimovic (Observatoire de Paris-Meudon, France))

Kinetic properties of proton velocity distributions in fast solar wind

Resonant diffusion plateaus

In a collisionless plasma, such as the fast solar wind, wave-particle interaction plays the decisive role in determining the shape of particle velocity distribution functions (VDFs). We provided convincing observational evidence for cyclotron-resonant absorption of Alfvén/cyclotron waves, which propagate outward from the Sun along the interplanetary magnetic field, by the fast solar wind protons. According to quasi-linear theory the protons thereby diffuse in velocity space, a process leading to the formation of diffusion plateaus in their VDF as shown in Fig. 60. In this respect, we investigated a large number of data from several distinct fast solar wind streams between 0.3 and 1 AU. The measurements were made on Helios 2 during solar minimum in 1976. The cyclotron-resonant absorption of Alfvén waves and the associated pitch-angle diffusion naturally explain the observed thermal anisotropy in the core of the proton VDFs.

(M. Heuer and E. Marsch)

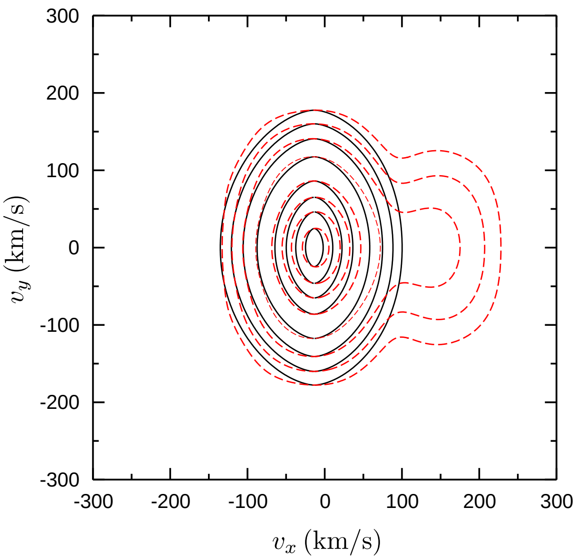

Fig. 60: Contours (in red dashes) of a symmetrized measured proton velocity distribution. The diffusion plateaus (in black continuous lines) are superimposed, and have the same v_y-intercepts with the ordinate in the center of the core as the measured contours.

Dependence of the beam drift velocity on the core plasma beta

A distinct correlation, between the proton core plasma beta and the proton beam drift speed in units of the local Alfvén speed, was found in high-speed solar wind data obtained by the Helios 2 spacecraft in 1976. This empirical relation reads: $v_d/v_A = (2.16 \pm 0.03)\beta_{\parallel c}^{(0.281\pm0.008)}$, for the range $\beta_{\parallel c} = 0.1$ to 0.6, where $\beta_{\parallel c}$ is the proton core plasma beta determined from the proton core thermal velocity component parallel to the magnetic field, v_d is the proton beam drift speed relative to the core, and v_A is the local Alfvén speed. This result places a tight constraint on the theoretical models which describe the formation of the proton beam in the fast solar wind. It was also found that most of the observed proton beam distributions were stable with respect to the electromagnetic beam instability. The results of this analysis are summarized in Fig. 61, which also gives, for comparison with the data, several theoretical thresholds for instabilities.

(E. Marsch in collaboration with C.-Y. Tu and Z.-R. Qin (Peking University, China))

On the core temperature anisotropy

We analysed the temperature anisotropy of the VDFs of the protons measured by the Helios spacecraft in fast solar wind. We concentrated on data obtained during the primary mission, including the first perihelion passage, of Helios 2 in a distance range between 0.98

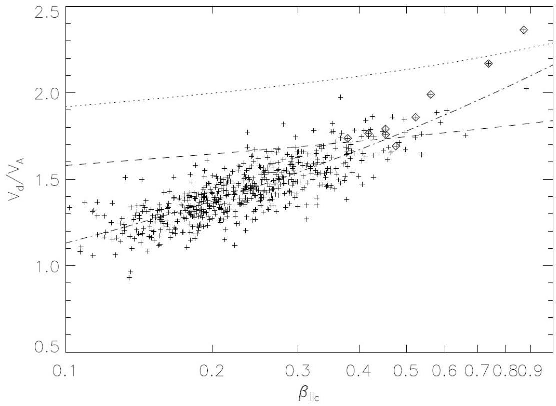

Fig. 61: Beam drift speed versus plasma beta. Each cross point represents a single Helios 2 (at 40.5-s cadence) plasma measurement of the proton beam drift speed plotted against the core plasma beta, $\beta_{\parallel c}$. The dash-dot line shows the result of a linear least-squares fit to the logarithm of the observed data points. The dotted line and the dashed line show the theoretical threshold of the Alfvén I instability with a constant ratio of the proton beam relative density, for values of 0.05 (top) and 0.2 (bottom line). The maximum instability growth rate at the threshold is $\gamma_m/\Omega_p = 0.01$.

and 0.29 AU for the days 23 to 114 of the year 1976. The main goal was to provide solid statistical evidence on the relation between the proton core anisotropy and core plasma beta, which play a key role in the regulation of the shape of the core. It is formed by resonant interactions between ion-cyclotron waves and protons, as described by the quasilinear theory of pitch-angle diffusion. Particular attention in our analysis of the VDF was paid to the symmetry axis, which can be determined by the directions of either the magnetic field, proton heat flux or alpha-proton relative drift. We analysed in detail the core part of the proton VDF, thereby avoiding carefully a possible influence of the proton beam component. The results are presented in Fig. 62, which gives, for comparison with the data, relevant thresholds from plasma instabilities.

(E. Marsch in collaboration with X.-Z. Ao and C.-Y. Tu (Peking University, China))

Freezing-in temperature profiles in ICMEs

We have used data from the Solar Wind Ion Composition Spectrometer (SWICS) and the magnetometer on Ulysses to investigate Coronal Mass Ejections (CMEs). Magnetic clouds (MCs) represent nearly one third of all the interplanetary coronal mass ejections (ICMEs) seen by Ulysses. Among the many open questions regarding their origin and evolution, one of the most challenging scientific problems is to gain insights into their internal structure. Furthermore, a still

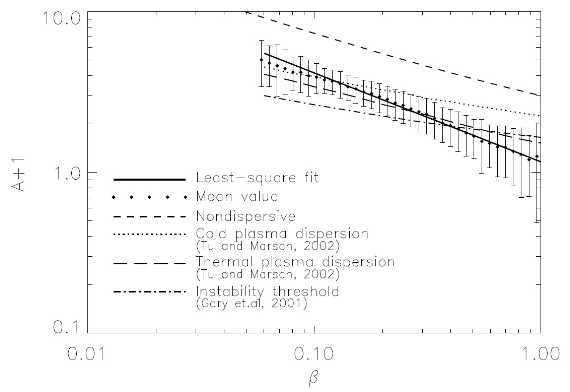

Fig. 62: Comparison of the measured proton core temperature ratio, $T_{\perp c}/T_{\parallel c} = A + 1$, with theoretical predictions. This empirical ratio is plotted versus the plasma beta, β, based on the core only. A least-squares fit to the binned data with variance bars is also given, together with several lines indicating various A-β relations as published in the literature.

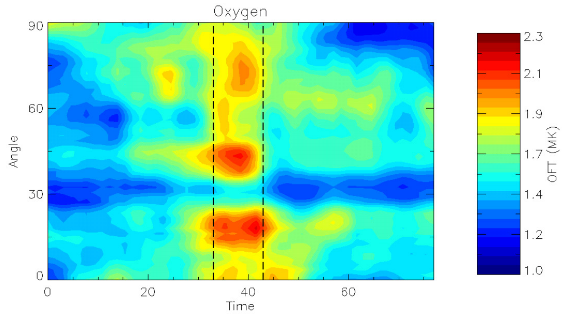

Fig. 63: Filled contour plot showing the Ulysses Magnetic Cloud events ordered by attitude angle and time (unity is 3 hours). Colour represents oxygen freezing-in temperature. The dashed lines represent the average flux rope size.

outstanding question is whether cloud and non-cloud ICMEs represent different kinds of mass ejections. The ionization level of the solar wind plasma serves as a robust tool to characterize the different types of solar wind. We have used charge states of heavy ions to infer the temperatures in the source region of ICMEs. MCs show increased temperatures with respect to non-cloud ICMEs and surrounding solar wind. By combining these data with a magnetic field model, insights into the internal structure of magnetic clouds can be provided. We fitted a non-force-free, elliptical CME magnetic field model to about 40 MC events observed by Ulysses. One of the parameters obtained after fitting the data is the azimuthal angle between the spacecraft path inside the MC and the flux rope axis (attitude angle, with 90° corresponding to a cut through the flux rope center). Based on a kind of superimposed epoch method, Fig. 63 shows the variation of the oxygen freezing-in temperature versus the attitude angle for the MC events.

The high temperatures are clearly confined to the flux rope region. There is no clear difference between the trailing and the leading solar wind, nevertheless lower temperatures cover a larger region in the trailing zone. Regarding the attitude angle, there is no clustering of high temperatures at 90° as it would have been expected if one considers that the hottest material will be found near the center of the cloud and not at its sides. At low angles, the high temperatures appear more spread and not so well confined as at higher angles. Also carbon and iron ions show a clear temperature enhancement in the flux rope region. However, differences in the profiles are found, pointing to a distinctive temperature history of MCs in the low corona, since the various elements freeze-in at different heights. The processes heating the plasma seem to act differently as the CME rises, since the profile for oxygen shows larger differences with the surrounding solar wind when compared with carbon and iron.

(L. Rodriguez, J. Woch, N. Krupp)

Observations of Energetic Neutral Atoms and their Implications on Modeling the Heliosheath

Since 1996, energetic hydrogen and helium atoms (ENAs) have been identified and their fluxes are monitored by the High-Energy Suprathermal Time-of-Flight sensor (HSTOF) of the Charge, Element, and Isotope Analysis System (CELIAS) on the Solar and Heliospheric Observatory (SOHO) near the Lagrangian point L1. Potential sources of ENAs in the heliosphere are CIRs, solar energetic particle events, pre-accelerated pickup ions as well as low-energy (up to few hundred keV) anomalous cosmic ray (ACR) ions in the outer heliosphere, close to and beyond the solar wind termination shock. ENAs, neutralized via charge transfer reactions, can penetrate into the inner solar system, unaffected by the interplanetary magnetic field. The observed ENA fluxes set limits on potential theories of the dominant sources of the energetic neutral atoms and on the modelling parameters of the heliospheric plasma simulations.

ENA fluxes of energetic hydrogen and helium atoms are plotted with respect to observation direction in the apex direction of the heliosphere for 28 to 58 keV/nuc energy/mass (Fig. 64) and 58 to 88 keV/nuc energy/mass (Fig. 65). To improve statistics, observed ENA fluxes are binned. Still, the counting statistics is poor, as revealed by the 1σ statistical error bars. ENH flux time variations might to be rather higher than ENHe flux time variations, but this is not statistically significant.

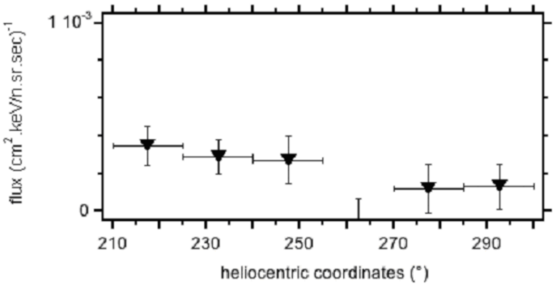

Fig. 64: Fluxes of energetic neutral helium (ENHe) in the 28 to 58 keV/nuc energy/mass range plotted versus the heliocentric coordinates in the region between 210° and 300°. Bars refer to 1 statistical flux errors and 15° bins.

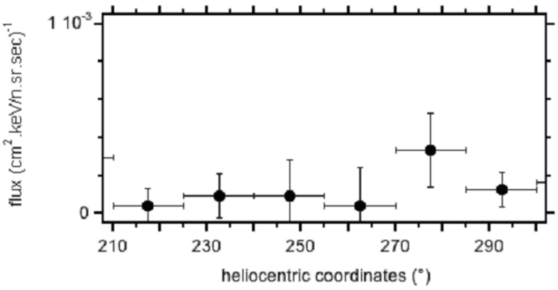

Fig. 65: Fluxes of energetic neutral hydrogen (ENH) in the 58 to 88 keV/nuc energy/mass range plotted versus the heliocentric coordinates in the region between 210° and 300°. Bars refer to 1 statistical flux errors and 15° bins.

The ENH and ENHe observations of SOHO/CELIAS/HSTOF do reveal a variation pattern of the apex and tail directions of the heliosphere, i.e. the observed ENH and ENHe fluxes are higher from the tail direction while the fluxes from the apex direction are only just above the detection threshold, only significant on the lowest statistical level (1σ). As the observation of ENAs constitutes an integral observation along the line of sight, one does not expect large variations from year to year, however, the observed fluxes in the ecliptic plane do not support nor exclude the possibility of such variations.

If other ENA sources, as outlined above, would have contributed to the observed ENA fluxes to a different extent than our previous estimates implied, the ENA flux observations would have to be interpreted rather as upper flux limits for the ACR contribution towards the observed ENA fluxes than as ACR- ENA fluxes. Models of the heliosphere and the heliosheath should subsequently predict heliospheric ACR- ENA fluxes smaller or equal to ENA fluxes observed with SOHO/CELIAS/HSTOF in the last decade.

(M. Hilchenbach in collaboration with A. Czechowski (Polish Academy of Sciences, Poland) and K. C. Hsieh (University of Arizona, USA))

Past solar activity and Sun-Earth relations

Meteorites, cosmogenic nuclides and past solar activity

Long-term solar activity is usually estimated from cosmogenic isotopes measured in terrestrial archives, in particular ^{10}Be in polar ice and ^{14}C in tree rings. Such an approach suffers, however, from uncertainties due to the sensitivity of the data to climate, geomagnetic field, reservoir exchange, etc. An independent and direct measure of the cosmic ray flux near the Earth is provided by the activity of the cosmogenic isotope ^{44}Ti in meteorites fallen during the past 250 years. This isotope (half life 59 years) is produced by galactic cosmic rays impinging on the meteorite. Its production stops once the meteorite has fallen. Measurements of ^{44}Ti activity in meteorites with a known time of fall allow a weighted average of the solar modulation in the roughly 100 years prior to the fall to be determined completely independently from terrestrial influences. In our work we aimed at verifying earlier reconstructions of galactic cosmic ray modulation based on sunspot number and cosmogenic isotopes. We showed that a model based on the sunspot number record is consistent with the data on ^{44}Ti activity in meteorites (see Fig. 66). Specifically, the ^{44}Ti measurements support a doubling of the Sun's open magnetic flux in the last century. We also demonstrated that the ^{44}Ti data can distinguish between various reconstructions of past solar activity based on ^{14}C, allowing realistic models to be identified and provide an independent estimate of the deposition factor of ^{10}Be. The ^{44}Ti data currently available are already able to rule out one ^{14}C-based reconstruction. As the measurements become finer in the coming years, the sensitivity of this independent diagnostic will continue to increase.

(S. K. Solanki in collaboration with I. G. Usoskin (Sodankylä Geophysical Observatory, Finland), C. Taricco (University of Torino, Italy), N. Bhandari (Basic Sciences Research Institute, Ahmedabad, India), and G. A. Kovaltsov (Ioffe Physical-Technical Institute, St. Petersburg, Russia))

Do cosmogenic isotope data harbour the signature of solar proton events?

The concentration of cosmogenic isotopes in terrestrial archives is determined mainly by the flux of galatic cosmic rays, modulated by the magnetic field of the Sun (open magnetic flux) and of the Earth. There may, however, also be a contribution of solar energetic particle events to such concentrations. We have

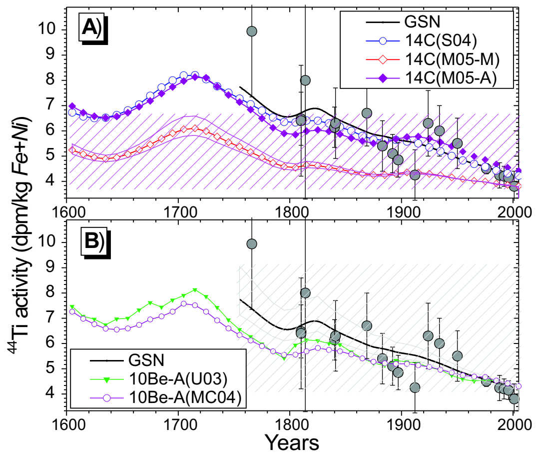

Fig. 66: ^{44}Ti activity in stony meteorites as a function of time of fall. Large dots with error bars depict measurements (Taricco *et al.*, J. Geophys. Res., in press) in meteorites fallen in 1766-2001. Curves correspond to the theoretically expected ^{44}Ti activity based on different reconstructions of the solar modulation parameter Φ which determines the level of cosmic ray flux modulation by solar activity. These reconstructions are due to the MPS group based on sunspot numbers (GSN), on ^{14}C [14C(SO4)] and ^{10}Be [10Be-A(U03)], but also due to other groups based on ^{10}Be [McCracken *et al.*: 10Be-A(MC04)] and ^{14}C [Muscheler *et al.*: 14C(M05-M) and 14C(M05-A)]. Note that the main reconstruction by Muscheler *et al.*, which shows a large enhancement in solar activity around 1780, is not consistent with the ^{44}Ti data. Uncertainties in the absolute values of the ^{44}Ti production rate include both the measurement errors and model uncertainties.

studied the production of cosmogenic ^{10}Be and ^{14}C in the atmosphere. The solar particle effect is found to be negligible in most ^{14}C data. Exceptional, extreme events may be detectable in high-resolution ^{14}C data, however. Although the overall effect is small in ^{10}Be data, strong events could well contribute, notably on the inter-annual time scale. In combination with the 11-year solar modulation of galatic cosmic rays, it may lead to an intermittent 5.5-year periodicity, which is seen in high resolution ^{10}Be data. We have identified ten episodes during the interval 1750-1950 when ^{10}Be may hold signatures of strong solar proton events. Thus, including such events in physics-based reconstructions of ^{10}Be production increases their correspondence with the Dye-3 data set. This opens a new possibility to study extreme solar particle events in the past using high resolution cosmogenic isotope data.

(S. K. Solanki in collaboration with I. G. Usoskin (Sodankylä Geophysical Observatory, Finland), G. A. Kovaltsov (Ioffe Physical-Technical Institute, St. Petersburg, Russia), J. Beer (EAWG Dübendorf, Switzerland), and B. Kromer (Institut für Umweltphysik, Heidelberg))

Reconstruction of solar irradiance since 1700

Observations of total solar irradiance are availble only since 1978, so that they cannot provide any reliable information on longer-term secular trends. Originally, stellar evidence was invoked for a secular change in irradiance. This evidence has recently been questioned. The aim of this research is to understand the physical mechanisms responsible for solar brightness variations and to carry out quantitative modelling of variations of the surface magnetic flux and total solar irradiance. In a first step the magnetic flux and irradiance since the Maunder minimum (a time of extended lack of sunspots which coincided with the little ice age) have been reconstructed using a simple, but consistent physical model. By using all available data on total and open magnetic flux and total irradiance the cycle-averaged increase in the total solar irradiance since the Maunder minimum could be estimated to be approximately 0.1%.

(L. A. Balmaceda, N. A. Krivova, S. K. Solanki)

A cross-calibrated sunspot area time series since 1874

A complete and homogeneous historical record of sunspot areas is a valuable proxy of solar variability and has been widely used, e.g., to study the characteristics of the solar cycle or to reconstruct total and spectral irradiance at earlier times. The Royal Greenwich Observatory (RGO) regularly measured this and other related parameters between 1874 and 1976. After that records from a row of different observatories are available. These, however, show systematic differences and often have significant gaps. We compare the data from different observatories when they overlap and determine the corresponding calibration factors. Using these data we compile a complete and cross-calibrated time series. The Greenwich data set is used as a basis until 1976, the Russian data (a compilation of observations made at stations in the former USSR) between 1977 and 1985 and data compiled by the USAF network since 1986. Other data sets (Rome, Yunnan, Catania) are used to fill in the remaining gaps. This combination provides a set of observations almost free of gaps after 1976, which correlates relatively well with the sunspot number record. The new composite sunspot areas record will serve as the basis for various models, e.g. of solar irradiance variations.

(L. A. Balmaceda, S. K. Solanki, N. A. Krivova)

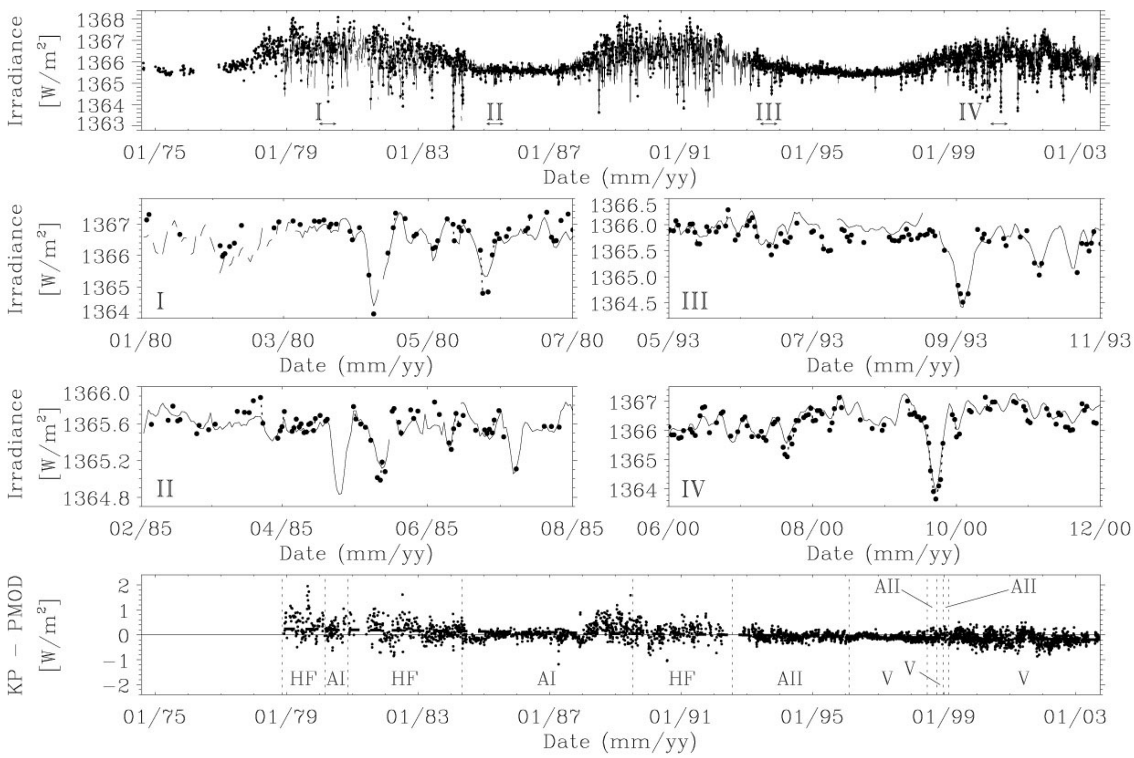

Fig. 67: Composite record of total solar irradiance (solid line) and reconstructed daily TSI (filled circles, connected by the dotted curve when there are no data gaps) from the minimum prior to cycle 21 to the declining phase of cycle 23 (*top panel*). The 4 smaller panels show enlargements of four shorter intervals at different activity levels. The times corresponding to these zoom-ins are marked in the top panel by the double-headed arrows under the roman numerals. The *bottom panel* shows the difference between the reconstructed total solar irradiance based on KP data and the PMOD composite measurements. The solid line indicates difference = 0, the dashed line is a regression. The dotted vertical lines indicate periods when data sets from the radiometers HF, AI & AII (ACRIM I & II) and V (VIRGO) were used for the irradiance composite.

Reconstruction of solar total irradiance back to 1974: identifying the cause of irradiance variations

The Sun's total irradiance is known to vary by about 1 W m^{-2} over the solar activity cycle. Due to the potential importance of this parameter for global climate change on Earth, an identification of the source of this variability is of considerable importance. For cycle 23 we had shown in an earlier investigation that over 90% of the irradiance variations are due to the evolution of the surface magnetic field. However, it has been argued in the literature that cycles 22 and 23 were different in that cycle 23 shows a similar variation in total solar irradiance (TSI) as cycle 22, although according to solar activity indices (e.g. sunspot number, or total magnetic flux) cycle 23 was weaker than cycle 22. Therefore it is important to extend the accurate reconstruction of solar irradiance over as long a period of time as possible.

Magnetograms and continuum images recorded at the National Solar Observatory (NSO) Kitt Peak allow such reconstructions back to 1974. In a first step we have compared and intercalibrated the magnetograms and continuum images recorded at the NSO Kitt Peak with the Spectro-Polarimeter (NSO-SPM) to those from the MDI (Michelson Doppler Interferometer) instrument on board SOHO which were earlier used for cycle 23. We have demonstrated that NSO-SPM data, available since 1992, can be employed to reconstruct TSI variations with almost the same accuracy as earlier shown for MDI data.

Next, using also data obtained by the older and lower quality NSO 512-channel magnetograph, we have extended the reconstruction back to the year 1974, i.e. over nealy 3 activity cycles. The reconstructed irradiance is compared with three composites of total solar irradiance measurements, which combine the measurements carried out by radiometers flying on different space platforms. A good correspondence is found with the total solar irradiance composite from PMOD/WRC, with no bias between the three cycles on time scales longer than the solar rotation period (Fig. 67). This suggests that the same driver, namely the evolution of the magnetic flux at the solar surface, is causing the irradiance variations over the whole pe-

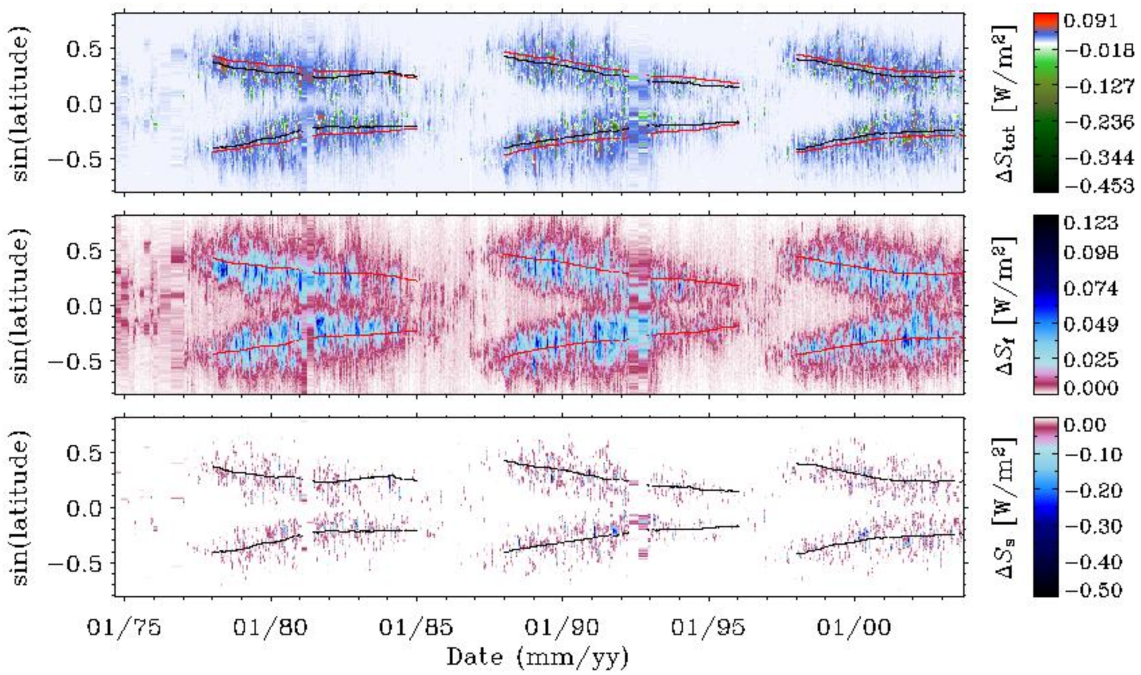

Fig. 68: Butterfly diagram for variations of the total solar irradiance relative to the quiet-Sun, ΔS_{tot}, reconstructed from NSO-512 data for 1734 days between 1974 and 1992 and NSO-SPM data for 2055 days between 1992 and 2003, i.e. from the minimum of cycle 21 to the declining phase of cycle 23 (*top panel*). The other two panels show the same but for the irradiance coming from faculae (*middle panel*) and sunspots (*bottom panel*) separately. The red and black curves are the 2-year running means of the corresponding mean latitudes. The y-axes are linear in $\sin(l)$. The colour bars on the right indicate the absolute scale of irradiance variations relative to the quiet-Sun (i.e. the irradiance of the quiet Sun corresponds to 0 W/m^2 on this scale).

riod of time that measurements exist.

(T. Wenzler, S. K. Solanki, N. A. Krivova, in collaboration with C. Fröhlich (Physikalisches Meteorologisches Observatorium Davos))

Statistical analysis of solar activity indices

We have carried out a statistical study of the daily total solar irradiance in cycles 21 – 23 reconstructed using the NSO Kitt Peak magnetograms and intensity images obtained between 1974 and 2003. Based on this analysis we have identified the contributions of different magnetic features on the solar surface to the variations of the total solar irradiance and evaluated the ratio of umbral to sunspot area. We have also created a butterfly diagram of the solar irradiance, which is shown in Fig. 68.

We have also studied the latitude distribution of solar activity as presented by sunspot positions and areas using the five lowest statistical moments of the latitudinal distribution of all complete sunspot cycles since 1874 and compared these moments with each other. Remarkable correlations are found between some of the moments. The same analysis when applied to different dynamo models reveals significant differences between the models and demonstrates that such moments are a powerful diagnostic to distinguish between rival dynamo models. Such an analysis also provides the possibility for improved estimates of the butterfly diagram for earlier times when only sunspot numbers were available and hence to improve activity and irradiance reconstructions for the period between the Maunder minimum and 1874 when sunspot positions were also recorded.

(T. Wenzler, S. K. Solanki, D. Schmitt, N. A. Krivova)

Reconstruction of solar UV irradiance in cycle 23

Solar irradiance variations show a strong wavelength dependence. Whereas the total solar irradiance varies by about 0.1% over the solar cycle, variations at wavelengths around the Ly-α emission line near 121.6 nm reach up to 100%. These variations may have a significant impact on the Earth's climate system. Being almost completely absorbed in the upper atmosphere, solar UV radiation below 300 nm affects stratospheric chemistry and controls production and destruction of ozone.

In spite of considerable progress in modelling the irradiance variations longwards of about 200 – 300 nm the agreement with SUSIM measurements has in the past been unsatisfactory. We show that after correcting for the exposure dependent degradation of the SUSIM channels sampling irradiance at $\lambda > 240$ nm (making use of the Mg II core-to-wing ratio) the agreement between model and measurement is significantly improved.

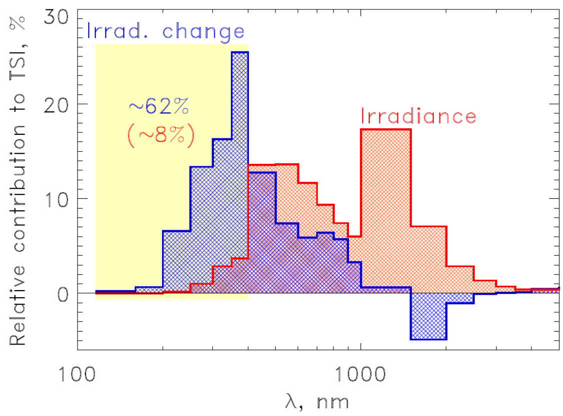

Fig. 69: The relative contribution of different wavelength ranges to the total solar irradiance (red histogram) and its solar cycle variations (blue histogram). About 60% of the total irradiance variations over the solar cycle are produced at wavelengths shorter than 400 nm (marked by the light yellow area), whereas the contribution of this spectral range to the total irradiance is only around 8%. Note different size of bins: about 40 nm below 200 nm, 50 nm between 200 nm and 400 nm, 100 nm between 400 and 1000 nm and 500 nm at yet longer wavelengths.

At shorter wavelengths the LTE approximation often made in such models fails, which makes a reconstruction of the solar UV irradiance a rather intricate problem. We choose an alternative approach and use the observed SUSIM UV spectra to extrapolate available models to shorter wavelengths. The model reproduces observed solar cycle variations of the irradiance at wavelengths down to 115 nm and indicates an important role of UV irradiance variability: up to 60% of the total irradiance variations over the solar cycle might be produced at wavelengths below 400 nm (see Fig. 69). This implies the need for more research into the effects of solar irradiance variations on stratospheric chemistry and the propagation of such disturbances into the troposphere.

(N. A. Krivova, S. K. Solanki, in collaboration with L. Floyd (Interferometrics Inc., Herndon, USA))

On the size distribution of sunspot groups in the Greenwich sunspot record 1874-1976

Sunspots are the largest and the best studied photospheric magnetic structures. It is therefore surprising that their size distribution is only partly known. The distribution of their sizes at a random time within their lifetime has previously been shown to follow a log-normal function. For many purposes, however, it is of greater interest to know the distribution of their maximum sizes, since a sunspot's size varies strongly in the course of its lifetime. We have, therefore, investigated the size distribution of the maximum areas in addition to the instantaneous distribution of areas of sunspot groups using the Greenwich sunspot group record spanning the interval 1874 – 1976. Both distributions are found to be well described by log-normal functions. Using a simple model taking into account the evolution of a sunspot's area with time we can transform the maximum area distribution into the instantaneous area distribution if the sunspot area decay rates are also distributed log-normally. For single-valued decay rates the resulting snapshot distribution is incompatible with the observations. The current analysis therefore supports the results of Howard (1992, Sol. Phys., 137, 51) and Martínez Pillet *et al.* (1993, A&A, 274, 521), who found that decay rates are log-normally distributed.

(I. Baumann and S. K. Solanki)

Reconstruction of sunspot activity in the Holocene from terrestrial records of ^{14}C

The sunspot number record is one of the longest running scientific time series and is of great interest for solar, stellar and climate research, as well as for the physics of magnetic field generation in astrophysical systems in general. Direct observations of sunspot numbers are available for four centuries, but for many purposes much longer series are required. We have carried out reconstructions of the sunspot number covering up to 11,400 years, which are based on dendrochronologically dated ^{14}C concentrations. Our method combines physical models for the whole chain of processes connecting the ^{14}C concentration with the sunspot number.

The cosmogenic isotope ^{14}C is produced in the terrestrial atmosphere by cosmic-ray induced spallation of oxygen and nitrogen nuclei and deposited in tree rings, which allow a precise dating. Since the cosmic ray flux is modulated by solar activity, the ^{14}C concentration measured in tree rings serves as a proxy for past solar activity. Using physical models we have provided the first *quantitative* reconstruction of past solar activity (sunspot numbers) from ^{14}C data. To this end, we have inverted a model we had previously derived to compute the concentration of cosmogenic isotopes starting from sunspot number: from the ^{14}C data we first determine the cosmic ray flux, which in turn depends on the strength of the heliospheric magnetic flux (open coronal source flux of the Sun); the latter is then used to infer the sunspot number.

According to the reconstructions, the level of solar activity present during the last 70 years is exceptional. In the course of the whole reconstructed time series, the Sun spent only about 8% of the time at a similarly high level of magnetic activity, and most of the earlier periods of similarly high activity were shorter than the current episode. The statistics suggest that the current period of high solar activity will probably come to an end within the coming 2 – 3 decades.

Fig. 70 shows the time series of the sunspot number reconstructed from the ^{14}C record. The result indicates that, throughout the whole interval covered, periods of high solar activity (cycle-averaged sunspot number exceeding a value of 50 over an extended period of time) are quite rare. These results have potential implications for the present discussion about the level of the solar contribution to global warming.

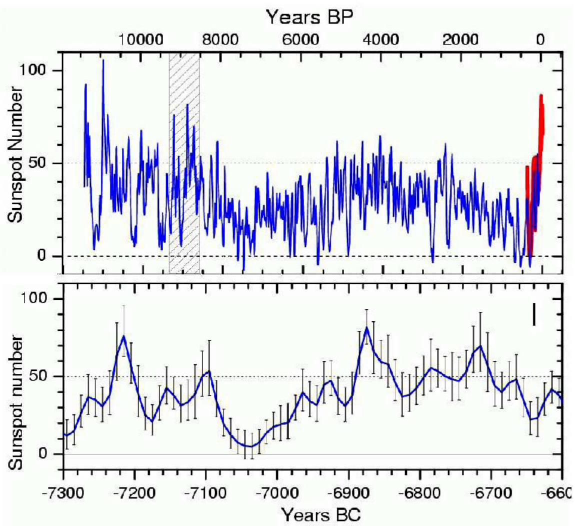

Fig. 70: *Upper panel:* 10-year averaged sunspot number reconstructed from Δ^{14}C data since 9500 BC (blue curve) and 10-year averaged group sunspot number obtained from direct telescopic observations since 1610 (red curve). The horizontal dotted line marks the threshold above which we consider the Sun to be exceptionally active. The chosen threshold of 50 corresponds to 1.3 standard deviations above the mean. *Lower panel:* a detail from the full time series of reconstructed sunspot numbers with expanded temporal scale. The chosen interval (corresponding to the shaded part of the upper panel) exhibits three episodes of high solar activity and a grand minimum. The error bars indicate the total uncertainty of the reconstruction.

An important quantity that affects the reconstructed sunspot number is the geomagnetic dipole moment. Besides carrying out a reconstruction with a widely used time series of the virtual axial dipole moment available through the whole Holocene, we have also employed a more recent compilation of the dipole moment reaching back to 7000 BP. The new series, which displays lower values of the dipole moment in the past, leads to somewhat higher values of the reconstructed sunspot number (by approximately 1σ on average), but does not change the main conclusions.

(S. K. Solanki, M. Schüssler in collaboration with I. Usoskin (University of Oulu, Finland), B. Kromer (Institut für Umweltphysik, Heidelberger Akademie der Wissenschaften), J. Beer (EAWAG, Dübendorf, Switzerland), and M. Korte (GeoForschungsZentrum Potsdam))

Status of ongoing and future solar missions

The SUMER instrument on SOHO

During the last years the Solar Ultraviolet Measurements of Emitted Radiation (SUMER) spectrograph has been operated only in campaign mode with 4 to 6 observational blocks per year. The pointing was selected preferably to off-limb targets. This policy was a reaction to extrapolations showing that otherwise the instrument would reach the overall limit of accumulated photons seen by the detectors much too early. While this measure was very successfull in extending the expected rest life time, it came out as a surprise that what at first glance could be interpreted as a restriction was more a change of scientific objectives - focussing now on new questions - rather than a drawback (cf., the highlight 'Coronal Seismology' on page 12 of the 2002/2003 report).

In June 2004, however, an unexpected problem with detector 'A' started: multiple rows of the active detector array were accumulated into single rows just like an artificial binning (recently, a similar effect was reported by the UVCS team, the UVCS instrument on *SOHO* is equipped with identical, SUMER-type detectors). Since this degradation was progressing also during no-activity periods, the data-taking policy was changed again, and now observations with high photon loads were allowed for detector 'A'. This opened new opportunities for joint observations with ground-based observatories focussing on chromospheric science. Even raster scans in the very bright H I Lyman-α emission line at 1215 Å were performed for the very first time (cf., article 'The structure and dynamics ...' by Teriaca *et al.* in this volume).

Detector 'B', which was only used occasionally, is fully operational. It was kept as a resource to be used for joint observations with the Japanese-US-UK mission *Solar-B* scheduled for launch in September 2006, and the NASA mission *Solar Dynamics Observatory (SDO)* scheduled for launch in August 2008.

The scientific analysis of SUMER spectra continues almost untouched despite of the instrumental restrictions mentioned here. The level of peer-reviewed publications using SUMER data is unchanged and reaches high values of about 40 papers per year.

(W. Curdt, U. Schühle, K. Wilhelm)

LASCO (Large Angle and Spectrometric COronagraph on SOHO)

Again, for another 2 years, the LASCO telescopes C2 and C3 worked almost without any non-scheduled interruption, as did the SOHO spacecraft as a whole. Not even the slightest signs of degradation are visible.

By the end of 2005, solar activity has almost reached minimum conditions. For several days, the Sun has already been completely spotless, and the number of flares and CMEs has never before been that low. On the other hand, because of these low rates associations between solar transients and effects at the Earth can now more easily and uniquely be done. This helped us to improve our prediction tool further and develop an easy-to-use IDL program (G. Munoz and A. Dallago) for practical space weather forecasting. We applied it several times and found that it performed significantly better than other schemes.

The spectral data obtained with the LASCO-C1 instrument were evaluated by M. Mierla (see separate report) and showed very promising results.

(R. Schwenn, G. Munoz, M. Mierla, B. Podlipnik)

MICA (Mirror Coronagraph for Argentina)

The MICA telescope is a ground-based coronagraph located at 2400 m altitude on the Precordillera de los Andes near San Juan, Argentina. MICA and the H-alpha telescope HASTA installed by MPE Garching have been taking images of the Sun and the corona almost everyday. The team of the Observatorio Astronómico Félix Aguilar (OAFA) in San Juan is operating the instruments and takes care of their maintenance. In fact, the responsibility for the instruments, the operations and data management has been shifted gradually to the Argentinean side. Our colleagues from San Juan began a major refurbishment of both instruments, for general cleaning, exchange of aged filters, software updates etc.

In November 2005 the Third El Leoncito Summer School was held with 20 students from Brazil, Argentina, and Chile attending. R. Schwenn gave a lecture series "Introduction to Physics of the Heliosphere".

(R. Schwenn and B. Podlipnik in collaboration with IAFE Buenos Aires Argentina and OAFA San Juan University, San Juan, Argentina)

The NASA STEREO Mission

The aim of the NASA STEREO mission is to observe the genesis, the eruption and interplanetary propagatation of coronal mass ejections (CME) (see Fig. 71). These are eruptive releases of some 10^9 tons of coronal plasma warped in a helically twisted magnetic field. Imbedded in the solar wind these plasma clouds then drift away from the Sun with speeds of up to 1000 km/s. On their front side, individual solar wind particles may be accelerated by shocks to energies of several 100 MeV. If the Earth's magnetosphere happens to be hit by such a CME, strong deformations of the Earth's magnetosphere along with inductive electric fields and currents may result which could cause serious damage to Earth orbiting satellites.

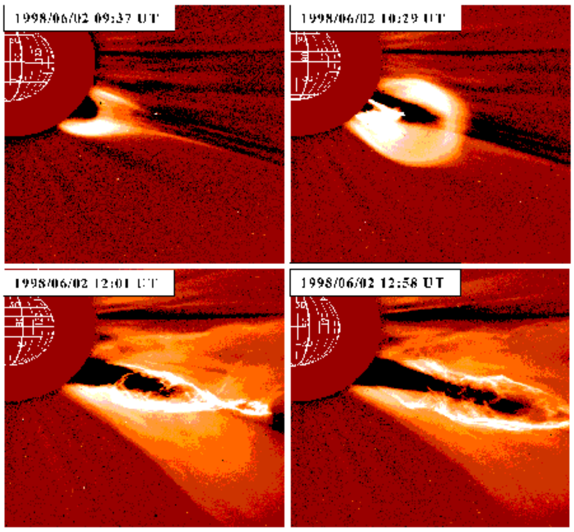

Fig. 71: A coronal mass ejection as observed with the LASCO/SOHO coronagraph. The Sun is occulted behind the $\sim 2\ R_\odot$ wide disk in the upper left.

Unfortunately, single view observations made of CMEs in the past did not allow to resolve the three-dimensional coronal magnetic field conditions expected to trigger the ejections nor could reliable predictions be made about their propagation direction. These shortcomings are intended to be overcome by the STEREO mission.

This mission (see Fig. 72) comprises two almost identical space crafts which will be launched in July 2006 into orbits surrounding the Sun. Their respective orbit period will be slightly slower (STEREO B) and faster (STEREO A) than the Earth's period such that they respectively lagg and lead the Earth in heliospheric longitude on average by 22° per year.

The spacecrafts are equipped with a set of telescopes and particle instruments, which will provide for the first time a stereoscopic view of the Sun and the surrounding heliosphere and measure in-situ the plasma and energetic particles emitted from the Sun and from propagating CMEs. The MPS contributes to two of the four spacecraft instruments, to the particle detector IMPACT and the solar telescope set SECCHI.

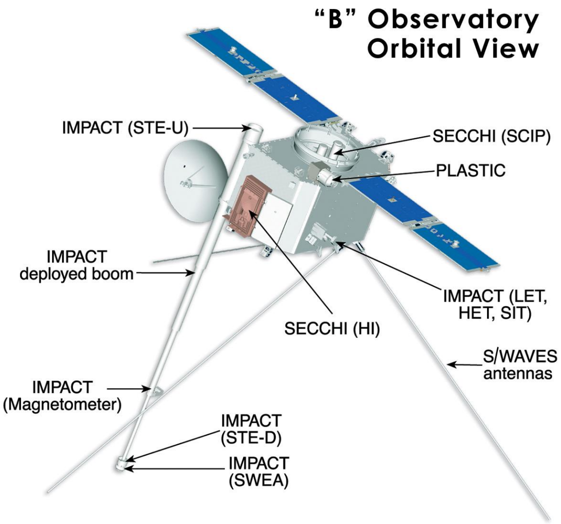

Fig. 72: One of the STEREO spacecrafts and its instrumentation in an approximate view from Earth. The Sun's position is in upward direction.

The IMPACT instrument

The name of the instrument is an acronym for 'In-situ Measurements of Particles and CME Transients'. It consists of seven particle spectrometers which measure the three-dimensional distribution of energetic electrons (up to 20 keV) and of energetic ions (up to 100 MeV) and discriminates ion masses up to the mass of the Fe atom. The spectrometers are supplemented by a magnetometer which measures the ambient solar wind magnetic field.

The institute's contribution to this instrument is the A/D conversion electronics for the suprathermal ion telescope (SIT) (see Fig. 73). A special feature of the electronics is a fast 'constant-fraction' discriminator with a temporal resolution of 1.2 ns. The device has been delivered early in 2005 and has passed all tests and calibration experiments successfully.

The SIT telescope will measure the energy and the direction of ions in the range from 0.1 to 100 MeV per nucleon. With the help of heliospheric magnetic field models, the orbits of these particles will be mapped back to their acceleration sites in the vicinity of the CME cloud.

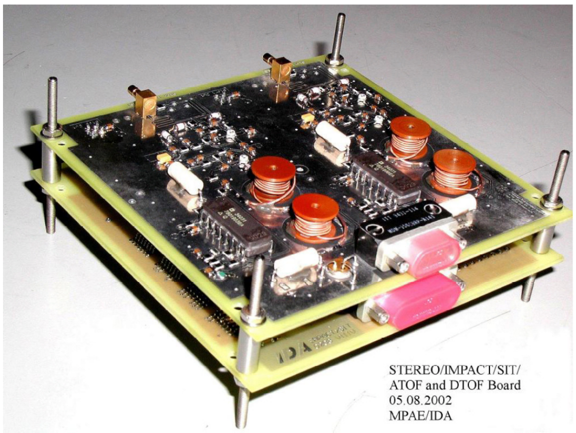

Fig. 73: The SIT A/D converter electronics board built at MPS

The SECCHII instrument

The SECCHI instrument is a set of five telescopes: an EUV instrument which observes the Sun in four EUV wavelengths, two stacked coronagraphs and two heliospheric imagers with an almost 2π field of view.

The institute has contributed to this instrument the six entrance apertures for the EUV telescopes and coronagraphs (see Fig. 74). Being a heritage of similar devices built for SOHO instruments, these new aperture doors had to meet much higher mechanical stresses. They were delivered in fall 2004 and successfully integrated and tested in 2005.

In preparartion for the STEREO observations, the CME shape and topology and their projection onto coronagraph images in dependence on the CME eruption site on the Sun has been investigated. In another study, relationships between magnetic field topologies as deduced from, e.g., post-eruptive magnetic arcades and CMEs were determined.

Once in operation, the two STEREO spacecrafts will enable for the first time continuous and simultaneous observations of all these phenomena from two different vantage points in space. This allows to reconstruct the three-dimensional structure and evolution of the coronal magnetic field. A further part of the institute's contribution to the STEREO project consists

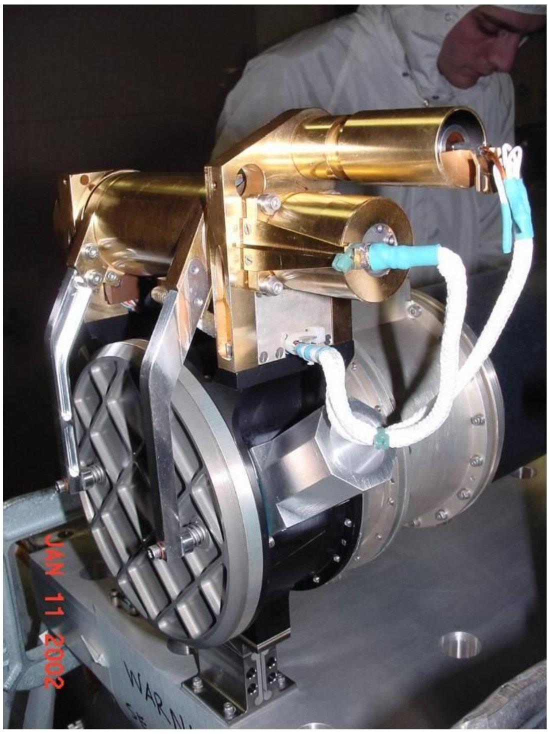

Fig. 74: One of MPS's aperture doors on a test stand

of software tools for the three-dimensional analysis of the SECCHI data by means of stereoscopic and tomographic algorithms. The three-dimensional reconstruction is a deeply ill-posed problem. However, experiments with artificial data have shown, that the information about the magnetic field can greatly improve the outcome of these reconstructions. The software contributions we are working on are threefold:
• Modelling of the coronal magnetic field from photospheric surface observations,
• Stereoscopic reconstruction of active region loops from EUV observations,
• Tomographic inversion of white-light coronagraph observations to obtain the 3-D density distribution of the corona.
To some extent these tools interact with each other. The magnetic field information has turned out to be the key information to be exchanged. For this reason a major effort has gone during the last two years into the magnetic field modelling part.

The STEREO project at the MPS is supported by the Bundesministerium für Bildung und Forschung (BMBF) and the Deutsches Zentrum für Luft- und Raumfahrt (BMBF) under contract number 50 OC 0501.

(V. Bothmer, H. Cremades, W. Deutsch, O. Hawacker, K. Heerlein, B. Inhester, A. Korth, U. Mall, H. Oberländer, B. Podlipnik, R. Schwenn, D. Triphathi, T. Wiegelmann)

SUNRISE: A balloon-borne telescope for high-resolution observations of the Sun

The central aim of SUNRISE is to understand the structure and dynamics of the magnetic field in the solar atmosphere. The magnetic field is the source of solar activity, controls the space environment of the Earth and causes the variability of solar irradiance, which may be a significant driver of long-term changes of the terrestrial climate. Interacting with the convective flow field, the magnetic field in the solar photosphere develops intense field concentrations on scales below 100 km, which are crucial for the dynamics and energetics of the whole solar atmosphere. These spatial scales cannot be studied systematically from the ground because of image distortion by turbulence in the lower atmosphere of the Earth.

The balloon-borne SUNRISE telescope will, for the first time, provide measurements of the magnetic structure of the solar atmosphere on its intrinsic spatial and temporal scales. These measurements will directly attack basic problems:

- What are the origin and the properties of the intermittent magnetic structure?
- How is the magnetic field brought to and removed from the solar surface?
- How does the field provide momentum and energy for the outer solar atmosphere?
- How does the magnetic field variation modify the solar brightness?

These questions are of fundamental importance, not only for understanding the influence of solar activity on the human environment but also for astrophysics in general. The universe abounds with objects that are dominated by magnetohydrodynamical and plasma processes, but of all astronomical objects only the Sun offers the possibility to directly and quantitatively investigate these processes with sufficient resolution.

SUNRISE is a light-weight solar telescope with 1 m aperture and instrumentation for spectro-polarimetric observations of the solar atmosphere on the intrinsic spatial scale of its magnetic structure. The telescope will be operated in long-duration stratospheric balloon flights at 35 km to 40 km altitude in order to obtain diffraction-limited image quality and to study the UV spectral region down to 220 nm, which is not accessible from ground.

The SUNRISE telescope is a classical Gregory design with a parabolic main mirror (M1) and an elliptical secondary mirror (M2). A carbon fiber Serrurier trusswork keeps M1 and M2 parallel under any gravitational deformation of the structure. After reflecting off M2, the light passes through a central hole in M1 onto two flat folding mirrors feeding the instruments mounted inside a dedicated structure on top of the telescope central frame (see Fig. 75). The attitude control and Sun pointing of the telescope is maintained by a gondola system with azimuth and elevation drives (see Fig. 76). The gondola provides the electrical power via solar panels and serves as mounting platform for system and instrument electronics. Acquired data are stored onboard in two large-capacity hard-disk arrays.

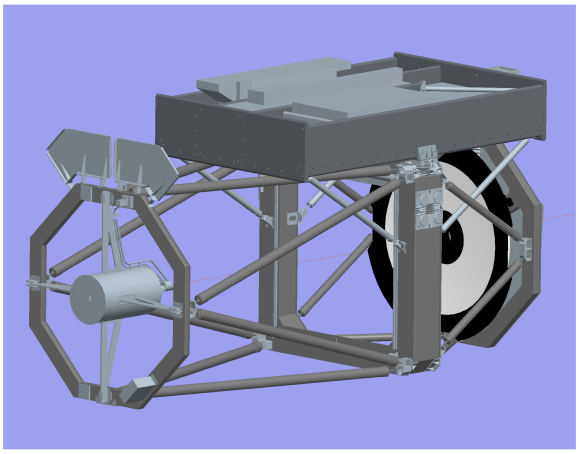

Fig. 75: The SUNRISE telescope with its science instrumentation ontop.

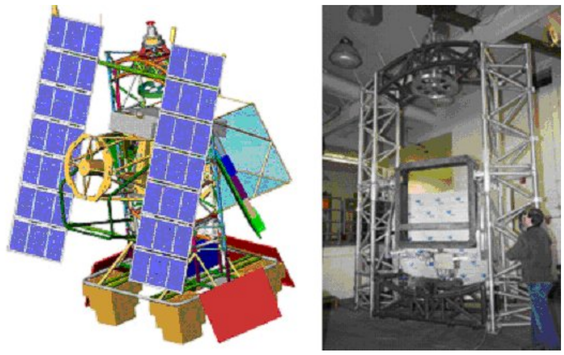

Fig. 76: Right: The SUNRISE instrument in flight configuration with telescope, gondola structure, solar panels and crush pads (to reduce landing shocks). Left: Assembled gondola structure elements with telescope central frame dummy (courtesy by HAO/NCAR).

SUNRISE features two innovative elements: 1) the telescope is actively kept aligned and focused in flight by re-positioning the secondary and the two fold mirrors. For this, the image quality is permanently checked by a wavefront sensor, which creates control signals for the closed-loop telescope alignment. 2) Residual image jitter due to gondola pointing errors and micro-vibration is cancelled by a high-speed steering mirror in front of the science instrumentation controlled by a correlation tracker.

The focal plane instrumentation consists of an Image Stabilisation and Light Distribution module ISLiD, a filter imager (SUFI: SUNRISE Filter Imager) for high-resolution images in the visible and the UV, which will provide diffraction-limited spatial resolution down to 0.05 arcsec at 220 nm, corresponding to 35 km on the Sun, a magnetograph (IMaX: Imaging Magnetograph Experiment) providing two-dimensional maps of the full magnetic field vector and the line-of-sight velocity, and a spectrograph-polarimeter (SUPOS: SUNRISE Polarimetric Spectrograph) for high-precision measurements of the four Stokes parameters.

SUNRISE is a project led by MPS, with participation of the Kiepenheuer-Institut für Sonnenphysik (KIS), Freiburg, the High Altitude Observatory (HAO), Boulder, the Lockheed-Martin Solar and Astrophysics Lab. (LMSAL), Palo Alto, and a Spanish consortium led by the Instituto de Astrofisica de Canarias (IAC), Teneriffa.

MPS is responsible for system design aspects, the main telescope (subcontracted to industry), the instruments ISLiD, SUFI and the post focus instrumentation structure, as well as for the central computer and data storage units. The experiment has sucessfully passed the initial preliminary design and study phases. All components are either in the detailed design phase or already in the manufacturing phase (see Fig. 76). The first long-duration balloon flight of about 2 weeks will take place from either ESRANGE / Sweden in summer 2009 or from Antarctica in winter 2009/2010. A test flight of the gondola system is planned for 2007.

(S. K. Solanki, P. Barthol, A. Gandorfer and the MPS engineering team in cooperation with teams led by W. Schmidt (KIS), B. W. Lites (HAO), A. M. Title (LMSAL), and V. Martinez Pillet (IAC))

KuaFu, A Sun-Earth-System Explorer Project

Mission description

The KuaFu project (named after a chinese mythodological figure, see Fig. 77) is a new space science mission selected by China's National Space Administration (CNSA), upon advice by and in close collaboration with a group of European scientists under the lead of R. Schwenn from MPS. It will be an essential element of the International Living With a Star (ILWS) programme. The scientific goal of KuaFu is to study globally the complex Sun-Earth system. The mission is designed to observe the complete chain of disturbances from the solar atmosphere to geospace, including solar flares, Coronal Mass Ejections (CMEs), interplanetary clouds, shock waves, and their respective geo-effects, such as magnetospheric sub-storms, magnetic storms, and aurora activities.

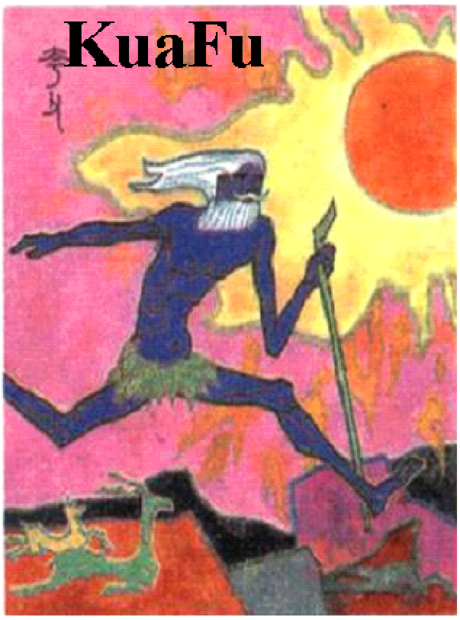

Fig. 77: KuaFu as shown here on a Chinese stamp is the hero of an old Chinese myth. He tried to catch the Sun and to enter it. As he became terribly thirsty he went to drink in the Yellow River and Wei river, but all water was not enough for him. So he turned northward to the sea. Before he could reach it he still died of thirst. His stick was lost in the wild field and then grew into a forest.

The KuaFu mission consists of three spacecraft:

- KuaFu-A will be located near the L1 Lagrangean point and have solar instruments to continuously observe the solar disk in ultraviolet emission (including Lyman alpha), to register CMEs in white light and Lyman alpha radiation, and to measure in-situ radio waves, the solar wind plasma, the local magnetic field, and solar energetic particles. Another remote-sensing instrument will observe the solar hard X-ray and Gamma-ray spectrum.
- KuaFu-B1 and KuaFu-B2 will be in polar Earth orbits that enable continuous observations to be made of the northern hemisphere auroral oval and the ring current, as well as systematic observations of the conjugate aurora. KuaFu B will also carry a limited suite of in situ instruments, including a magnetometer and charged particle detectors.

In the development of the scientific concept of the whole mission, R. Schwenn, E. Marsch and E. Donovan (Canada) made major contributions. An assessment study of the mission was performed and a detailed report was reviewed under the arrangement made with the ILWS steering committee. KuaFu was thereby rated between excellent and very good. ESA's Solar System Working Group (SSWG) found the KuaFu mission concept good and noted a widespread interest within the relevant scientific community in Europe. The SSWG therefore endorsed the payload participation by national agencies in the KuaFu mission. It may start at the next solar maximum (planned launch in 2012), with an initial mission lifetime of two to three years.

Possible MPS participation in KuaFu

German scientists designed and suggested three important instruments for KuaFu A. Among them is the far/extreme ultraviolet (FUV/EUV) Disk Imager (EDI) proposed by U. Schühle and E. Marsch. It will obtain solar disk images in both, the comparatively cold Lyman-alpha emission line and the hot 19.5 nm line, and will thus permit the first observations of the origin and development of CMEs from the upper chromosphere and transition region into the lower corona. S. Solanki has further suggested to try making the first ever direct observation of the coronal magnetic field, by using the Lyman-alpha line polarization.

(R. Schwenn and E. Marsch in collaboration with C.-Y. Tu (Peking University, China), E. Donovan (University of Calgary, Canada), J.-S. Wang (Meteorology Administration of China), L.-D. Xia (University of Science and Technology of China), Y.-W. Zhang (DFH Satellite Co. LTD, China).)

SOLAR ORBITER, A high-resolution mission to the Sun and inner heliosphere

Science goals, assessment studies and orbit design

The Solar Orbiter mission was conceived and proposed by a European team led by MPS scientists. After a successful first assessment study, it was selected by the ESA executive in September 2000 as ESA's next solar physics mission. In the following years the mission went through many ups and downs, concerning its status in the science programme of ESA. However, the past two years brought substantial progress, and the mission was reconfirmed as an essential part of the present science program. The Payload Definition Document (PDD) was released in August 2005. The Science Management Plan of Solar Orbiter was also approved by the Solar System Working Group in 2005. The ESA Space Science Advisory Committee again reviewed the mission, which then was confirmed by the Science Programme Committee (SPC) for a launch in 2015.

The comprehensive assessment study carried out in 2005 by ESA with the help of industry had the following goals: Consolidation of the science requirements, definition of the mission requirements enabling the spacecraft platform design, identification and selection of the optimal mission profiles, a further maturing and specification of the reference payload, preliminary definition of flight segment design (by industry), confirmation of overall feasibility and potential technology development needs, preliminary definition of ground segment and mission operations requirements, identification of the BepiColombo commonalities, and finally the assessment of the overall development risks and estimation of the cost at completion.

Turning now to the science, the Solar Orbiter will provide, at very high spatial and temporal resolution, novel observations of the solar atmosphere and unexplored inner heliosphere. The science goals of the Solar Orbiter with a combination of remote-sensing and in-situ instruments are, for the first time, to

- determine the properties, dynamics and interactions of plasma, fields and particles in the near-Sun heliosphere,
- investigate the links between the solar surface, corona and inner heliosphere,
- explore, at all latitudes, the energetics, dynamics and fine-scale structure of the Sun's magnetized atmosphere,
- probe the solar dynamo by observing the Sun's high-latitude field, flows and seismic waves.

The Solar Orbiter scientific requirements define the basic characteristics of the mission, in terms of orbital parameters, launch windows and payload mass. The celestial constellation of Sun, Venus and Earth leads to a launch window of three weeks in every 19 months. The science-phase orbits can be reached using either high specific impulse (solar electric) or low specific impulse (chemical) propulsion. A strategy using chemical propulsion and planetary gravity assists is now baselined. Chemical propulsion has a lower development risk, but means a longer cruise phase. The (ballistic) mission using chemical propulsion and being launched in 2015 has the best mass margins. The ecliptic projection of the Solar Orbiter trajectory is shown in Fig. 78.

The selected orbit assures that the spacecraft design is thermally feasible. The total mass of the Solar Orbiter is compatible with a Soyuz-Fregat 2-1b launch. The launch date is currently baselined in May 2015, with a backup opportunity in January 2017, and the cruise phase will last 3.4 years. The mission exploits gravity assist manoeuvres at Venus and Earth. In the science

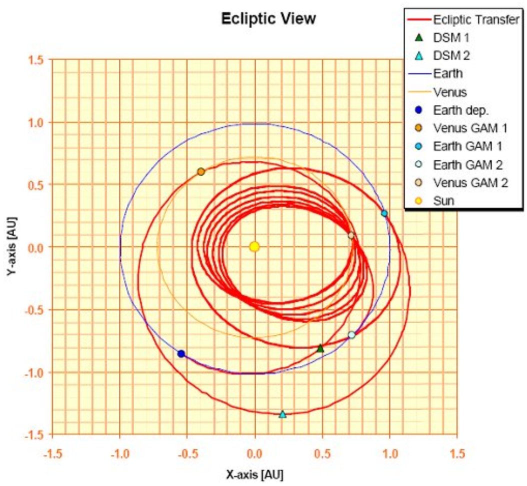

Fig. 78: Orbit design of Solar Orbiter: Ecliptic projection of the spacecraft trajectory.

phase we have a 3:2 resonant orbit with Venus and a period of 149.8 days. The total mission duration, including the extended phase, will be 10 years. The minimum perihelion distance will be 48 solar radii (corresponding to 0.22 AU), and the maximum solar latitude 34° (in the extended phase).

The Solar Orbiter will, through its novel orbital design, for the first time

- explore the uncharted innermost regions of our solar system,
- study the Sun from close-up (48 solar radii or 0.22 AU),
- fly by the Sun tuned to its rotation and examine the solar surface and the space above from a co-rotating vantage point,
- provide images of the Sun's polar regions from heliographic latitudes up to 34°.

These four important new aspects to the Solar Orbiter mission will allow unique science investigations to be performed. The near-Sun interplanetary measurements together with simultaneous remote-sensing observations of the Sun will permit us to disentangle spatial and temporal variations during the co-rotational phases. They will help us to understand the characteristics of the solar wind and energetic particles in close linkage with the plasma conditions in their source regions on the Sun. By approaching as close as 48 solar radii, the Solar Orbiter will view the solar atmosphere with unprecedented spatial resolution. Over extended periods the Solar Orbiter will deliver the first images of the polar regions and the side of the Sun not visible from Earth.

The Solar Orbiter mission will have variable transmission phases, the durations of which vary with distance from Earth. Three scientific observation periods (each ten days long) are considered per S/C revolution about the Sun, with the strategy that these periods are centred on the passages through maximum southern and northern latitude and perihelion. The spacecraft will be 3-axis stabilised and always Sun-pointed. Given the extreme thermal conditions at 48 solar radii (20 solar constants), the thermal design of the spacecraft has been considered in detail during the assessment study, and viable solutions for the instrumentation have been identified (see Fig. 79).

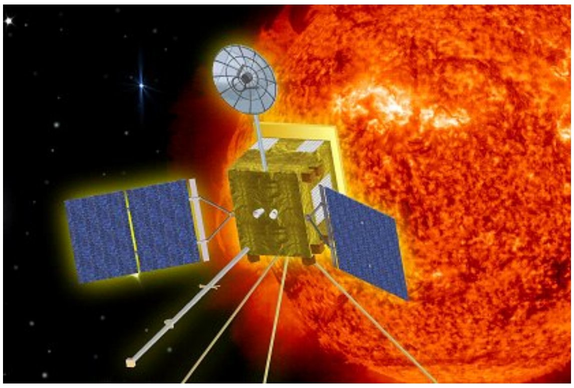

Fig. 79: Industrial concept of the Solar Orbiter spacecraft, with its major components (various antennas, solar arrays, main body). The remote-sensing instruments are looking through the heat shield (yellow plate) at the front towards the Sun.

Payload and programmatic issues

Over the years, the MPS has been a major player in the design of Solar Orbiter and its objectives, and has continued this role in various groups. The Payload Working Group (PWG) was established by ESA in 2002 with the task to address payload-related issues, study instrument feasibility, and to produce the Payload Definition Document (PDD, delivered to ESA in May/June 2003). A Science Definition Team (SDT) was also appointed by ESA (Chair: E. Marsch) to review the scientific goals and to help in writing the Science Requirements Document (SRD), the final version of which was issued in March 2005.

Future milestones of the mission are: In May 2006 the mission workplan will be presented to ESA's SPC. In the middle of 2006 a call for letters of intent to propose will be issued, and the Announcement of Opportunity (AO) release is expected in spring 2007. With the SPC approval of the payload in 2008 the definition phase (lasting 18 months) of the mission will start. In 2010 the implementation phase will begin.

The Solar Orbiter will achieve its wide-ranging aims with a suite of sophisticated instruments, which are optimised to meet the main solar and heliospheric science objectives. The baseline payload presently has a total mass of 168 kg, a power consumption of 170 W, and a telemetry rate of about 90 kbs. The remote-sensing suite consists of five instruments:

- Visible Light Imager and Magnetograph (VIM)
- EUV Imager (EUI, encompassing 3 telescopes)
- EUV Spectrometer (EUS)
- Coronagraph (COR)
- Spectrometer Telescope Imaging X-rays (STIX)

Our institute intends to participate in this mission with key instrumentation for imaging and spectroscopy in visible and extreme ultraviolet light. The three instruments of main interest to MPS are the VIM, EUI, and EUS, which are described below in separate sections.

There always was strong European as well as US support in the PWG and SDT activities, in anticipation of some US-led instrumentation as NASA contribution to the mission. Solar Orbiter was highlighted as important for the US community in a number of documents, such as the Sun-Earth connection Roadmap and the Decadal report of the National Science Foundation. Solar Orbiter will be ESA's prime contribution to the ongoing International Living with a Star (ILWS) programme, which involves NASA, ESA, RSA, the Japanese, Chinese, Indian and other space agencies.

(E. Marsch)

The Solar Orbiter EUS instrument

Of the four top mission goals of the Solar Orbiter, as described in the previous section on page 69, the first three require EUV spectroscopy. The Extreme Ultraviolet imaging Spectrograph (EUS) is a high-resolution telescope/spectroscope designed to reach ambitious performance parameters such as a spatial resolution of 150 km and a spectral resolution good enough to resolve Dopplershifts of 1 km/s over a wide temperature range. Three spectral bands are foreseen to cover the entire range of temperatures of the solar atmosphere: the 116-126-nm band with the bright H I Ly-α line, the 95-105-nm band with the O VI doublett, and the 70-80-nm band with the Ne VIII doublett. The latter will be particularly suited to observe the emanating solar wind at higher latitudes, a capabiliy unique to Solar Orbiter.

The consortium forming now around the CDS and SUMER teams involved in the SOHO (Solar and Heliospheric Observatory) mission will be led by the Rutherford-Appleton-Laboratory (UK) and will

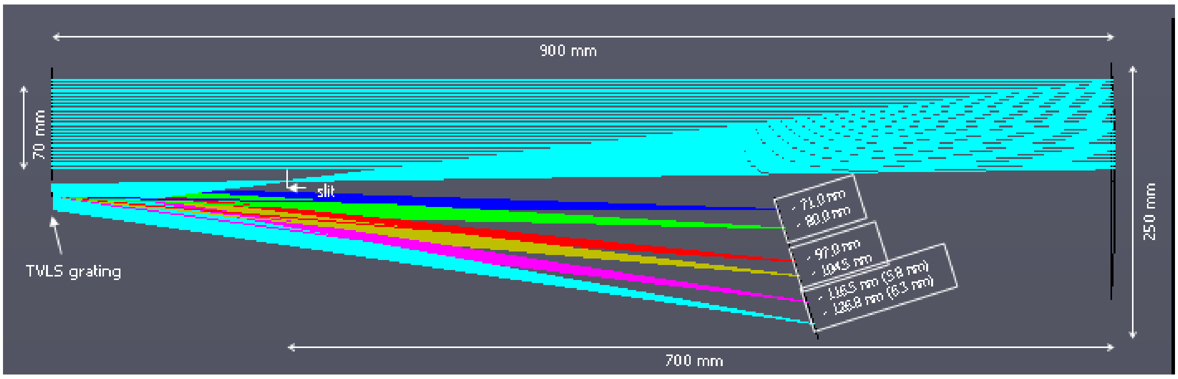

Fig. 80: The proposed EUS optical design

greatly benefit from the SOHO heritage. Severe limitations in mass and power require a simple design, and the instrument will be built with a two-mirror optic (cf., Fig. 80). The collimator will also act as the dispersion element and carry a toroidal variable line space grating (TVLS).

(W. Curdt, U. Schühle, L. Teriaca)

The Solar Orbiter EUI instrument

The Solar Orbiter EUI instrument is a package of filter telescopes for quasi-monochromatic imaging of the solar corona in selected spectral emission lines. The lines are selected to cover the base of the corona as well as higher regimes at temperatures above 1 million degrees. The primary goals of this instrument are

- To provide EUV images with at least a factor 2 higher spatial resolution than currently available, in order to reveal the fine-scale structure of coronal features,
- To provide full-disc EUV images of the Sun in order to reveal the global structure and irradiance of inaccessible regions such as the ffar sideöf the Sun and the polar regions,
- To study the connection between in situ and remote sensing observations.

Providing both high spatial resolution and a full-disc field of view, would pose very challenging technical problems if a single telescope design should fulfil these requirements. This led to the design of a package consisting of a High Resolution Imager (HRI) with 3 telescopes operating in different wavelength bands and a Full Sun Imager (FSI) based on a single telescope with a larger field of view. To image the lower temperature regime of the corona, the chromosphere and the lower transition region, a telescope with a spectral band centered at the Lyman-α line is best suited to follow dynamic features with the high cadence needed at small spatial scales. One of the HRI chanels shall therefore be a telescope using the hydrogen 121.6-nm line, the most intense line of the solar emission spectrum in the VUV. An optical study has been made to verify that a two-mirror (Gregory) design can fulfil the performance requirements within the boundary conditions given by the Solar Orbiter Payload Definition Document (PDD). The aperture size of the telescope will be dictated by the resolution attainable within the diffraction limitation. Such an instrument can be built with current technology, but nevertheless ways have been investigated to limit the heat input into such an instrument during the close approach to the Sun. We also started to develop imaging detectors that are specifically sensitive at the wavelength of hydrogen Lyman-α. A radiometric model calculation has shown that such an instrument will allow us to image the base of the solar corona with unprecedented speed and signal-to-noise ratio. MPS has committed itself to build the Lyman-α telescope as part of the EUI-HRI instrument.

(U. Schühle, W. Curdt, E. Marsch, S. Solanki, L. Teriaca)

The Solar Orbiter VIM instrument

The Visible Light Imager and Magnetograph (VIM) is a primary instrument of the remote sensing package of ESAs Solar Orbiter mission. A consortium for implementation of VIM, led by the MPS, has been established.

VIM is based on two optical telescopes – a High Resolution Telescope (HRT) and a Full Disk Telescope (FDT) – as well as a Filtergraph Optics (FO) alternately coupled to the telescopes (see Fig. 81). This design allows measuring magnetic and velocity fields at the photospheric level by scanning across a magnetically sensitive spectral line. The FOV of the HRT is approximately $1000'' \times 1000''$ which corresponds to 150 × 150 Mm^2 at minimum perihelion distance. Its spatial resolution is 150 km on the Sun. Powerful on-board data reduction (Milne-Eddington RTE inversion) provides a data flow compatible with science requirements and telemetry rates. The MPS contribution consists of a full opto-mechanical design of the instrument and simulations of the instrumental performance and data.

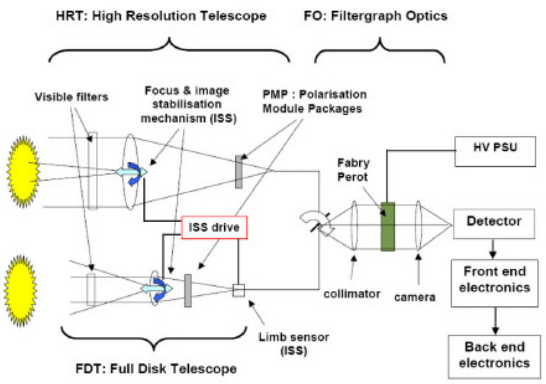

Fig. 81: Functional diagram of the VIM instrument

VIM will carry out full-disk and high-resolution observations simultaneously with all science instruments on Solar Orbiter and, thus, will give rise to study an ample variety of solar phenomena with hitherto unprecedented detail. The major science topics are:

- Magnetic coupling science: Photospheric vector-magnetograms will allow 3-D field extrapolations into the transition region and corona.
- Polar view: Helioseismic and magnetic field measurements at the Sun's polar regions will provide crucial constraints on the solar dynamo theories.
- Stereoscopy: Simultaneous observation from different viewpoints (co-ordinated with near-Earth-orbit instruments) will establish a stereographic view of photospheric structures. VIM will provide even data from the Sun's backside.
- Co-rotation: Long-term observations of structures from almost non-variable vantage points will be enabled during perihelion passages.
- Helioseismology: VIM will continuously provide high-cadence velocity maps, excellently suitable for both local and global helioseismic studies of sub-surface flows and magnetic field structures.

(A. Gandorfer, H. Hartwig, J. Hirzberger, A. Lagg, U. Schühle, S. K. Solanki, J. Woch, L. Yelles Chaouche in collaboration with T. Appourchaux (IAS, Paris), M. Sigwarth (KIS, Freiburg), V. Martínez Pillet (IAC, Tenerife) and others)

Stars and extrasolar Systems

Magnetic flux transport on active cool stars

Rapidly rotating cool stars with outer convection zones typically show a much higher degree of magnetic activity as the Sun. Moreover, the 'starspots' and magnetic field structures that are observed by (Zeeman) Doppler imaging are much larger than the corresponding structures on the Sun. Many such active stars show prominent long-lived magnetic features on the polar caps, but also a wide latitude distribution of more transient magnetic structures.

In order to investigate the evolution and lifetime of magnetic regions on active stars, we have carried out numerical simulations of the evolution of the radial magnetic flux on the stellar surface under the influence of surface flows (differential rotation, meridional flow) and turbulent diffusion. We start from a (freshly emerged) bipolar magnetic region and vary its initial size, latitude, tilt angle with respect to latitude circles, and substructure. Using the observed differential rotation profiles for stars we find that the lifetimes of our simulated bipolar magnetic regions in low and mid latitudes (i.e., the time until the field strength everywhere falls below a threshold value) (see Fig. 82) correspond well to the observed values.

The lifetimes of high-latitude magnetic regions is increased by a local convergence of the meridional flow and by a large tilt angle, favoring the formation of a unipolar magnetic cap. Its roughly circular form then minimizes the effect of the rotational shear. Therefore, the lifetime of such a region is increased by a factor of about two as compared to the case without tilt.

(E. Işık, M. Schüssler, S. K. Solanki)

Large-scale magnetic field of the G8 dwarf ξ Bootis A

The G8 dwarf ξ Bootis A (ξ Boo A) has long been known as a magnetically active late-type dwarf star, but little was known about the large-scale structure of the field. We investigated the magnetic geometry of this star from spectropolarimetric observations obtained in 2003 with the MuSiCoS échelle spectropolarimeter at the Télescope Bernard Lyot (Observatoire du Pic du Midi, France). We repeatedly detected a photospheric magnetic field, with periodic variations

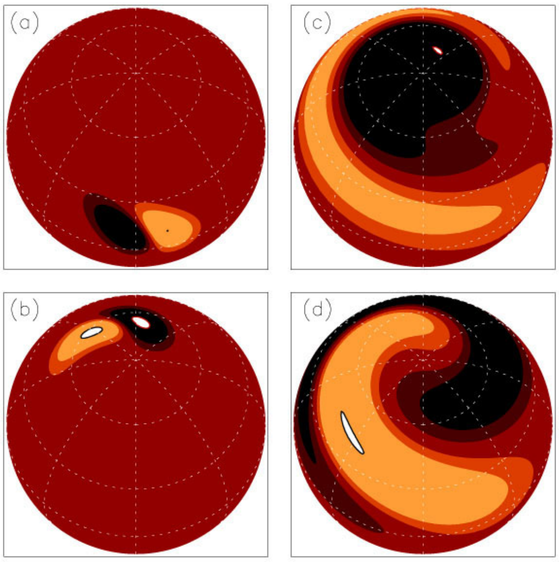

Fig. 82: Magnetic field distribution on a star of solar radius. Shown is the instant when the field strength of the bipolar regions are about to fall under a detection threshold. Black and yellow show opposite magnetic polarities. White regions covered by black contours indicate the regions still above the threshold. a,b): solar-like magnetic regions in low (a) and high (b) latitudes, respectively, 61 days after their emergence. c,d): Very large stellar magnetic regions with an initial tilt with respect to the equator (c) and without tilt (d), after 219 and 123 days, respectively.

consistent with rotational modulation. Circularly polarized (Stokes V) line profiles present a systematic asymmetry, showing up as an excess in amplitude and area of the blue lobe of the profiles. Direct modelling of Stokes V profiles suggested that the global magnetic field is composed of two main components, with an inclined dipole and a large-scale toroidal field. We derived a dipole intensity of about 40 G, with an inclination of 35° of the dipole with respect to the rotation axis. The toroidal field strength is of the order of 120 G. A noticeable evolution of the field geometry was observed over the 40 nights of our observation window and resulted in an increase in field strength and dipole inclination.

This study is the first step of a long-term monitoring of ξ Boo A and other active solar-type stars, with the aim of investigating secular fluctuations of stellar magnetic geometries induced by activity cycles.

(P. Petit in collaboration with J.-F. Donati, M. Aurière, F. Lignières, D. Mouillet, F. Paletou, N. Toqué (Laboratoire d'Astrophysique de Toulouse-Tarbes, Observatoire Midi-Pyrénées), J. D. Landstreet (University of Western Ontario, London, Canada), S. Marsden (ETH Zürich, Switzerland), and G. A. Wade (Royal Military College of Canada, Kingston, Ontario, Canada))

The binary IM Pegasi, the guide star for the *Gravity Probe B* mission

The spectroscopic binary system IM Pegasi (HR 8703) was chosen as the guide star for the NASA-Stanford relativity gyroscope mission Gravity Probe B. Given its central role for the mission, it is important to learn as much as possible about this binary. In support of this mission, high-resolution echelle spectra of IM Peg were obtained on an almost nightly basis. Applying the technique of least-squares deconvolution, we achieved line profiles with a very high signal-to-noise ratio line profiles and detected the orbit of the secondary of the system. This was the first detection of the secondary. Combining almost 700 new radial velocity measurements of both the primary and secondary of the system with previous measurements, we derived improved orbital parameters of the IM Peg system. Using these estimates along with the previously determined range of orbital inclination angles for the system, we found that the primary of IM Peg is a giant of mass $1.8 \pm 0.2 M_\odot$, while the secondary is a dwarf of mass $1.0 \pm 0.1 M_\odot$.

(P. Petit in collaboration with S. C. Marsden and S. V. Berdyugina (ETH Zürich, Switzerland) and 10 others)

Fundamental parameters and granulation properties of Alpha Centauri A and B

The study of convection (granulation) on cool-stars is hampered by the fact that stellar surfaces in general cannot be spatially resolved, so that practically only the line bisector is available as a diagnostic. Properties of stellar granulation are obtained by inverting spectra of the late-type stars α Centauri A and B. Our inversions, the first of their kind, are based on a multi-component model of the stellar photosphere and take into account the center-to-limb variation and rotational broadening. The different atmospheric components describe the areas harboring up-, down- and horizontal flows. The inversions are constrained by fitting not only the flux profiles, but also their line bisectors, and by using a simple mass conservation scheme. The inversions return the properties of convection at the stellar surface, including the stratification of the thermodynamic parameters, as well as fundamental parameters such as the gravitational acceleration, $v \sin i$ and the element abundances. For α Cen A (G2V) the derived stratifications of the temperature and convective velocity are very similar to the Sun, while for α Cen B (K1V) we find similar up- and down-flow velocities, but lower horizontal speeds and a reduced overshoot. The latter is consistent with the smaller scale height of the atmosphere, while mass conservation arguments taken with the lower horizontal speed imply that the granules on α Cen B are smaller than on the Sun. Both these properties are in good agreement with the hydrodynamic simulation of Nordlund & Dravins (1990, A&A, 228, 155). The inversions also return the fundamental parameters ($T_{\rm eff}$, $\log g$, abundances, $v \sin i$, etc.) of the two stars, which do not strongly depend on the details of the inversion. These values are on the whole in good agreement with literature values. However, *importantly*, the element abundances are 0.1 to 0.15 dex lower when a 2- or 3-component inversion is carried out than with a 1-component inversion.

(S. K. Solanki in collaboration with C. Frutiger (ETH Zürich, Switzerland) and G. Mathys (European Southern Observatory, Chile))

Numerical modelling of extrasolar planetary magnetospheres

Since 1995 approximately 126 extrasolar planets have been discovered. In contrast to the solar system, with Mercury as the closest planet to the Sun, about 36% of the planets around main-sequence stars have been found within Mercury's semi-major axis of 0.387 AU, the closest being located only 0.0225 AU away from its star. Shkolnik et al. (2003) reported on planet induced chromospheric heating for one of the stars (HD 179949 with planet at 0.045 AU). The observed "hot spot" is assumed to be related to some kind of magnetic interaction between star and planet.

We used this hint to search for possible star-extrasolar planetary interaction mechanisms. The "hot spot" observation in the HD 179949 system does not only hint at the existence of a planetary magnetic field. It also favors our earlier results, that the close-in extrasolar planets may be located within sub-Alfvénic stellar winds ((see the bi-annual report 2002 – 2003 of the Max-Planck-Institut für Aeronomie). We had obtained those results by modelling the stellar wind regime for planets closer to their star than 0.6 AU on the basis of the solar wind models of Parker (1958) and Weber & Davis (1967).

Now, in order to gain more insight into the implications of these special stellar wind regimes for star – planetary interaction processes, we have started to simulate the interaction of a planetary magnetosphere with the stellar wind. For this purpose we adapted a code which previously was used to investigate solar wind – planetary and – cometary interactions. Our code numerically integrates the equations of resistive magnetohydrodynamics (MHD) on a 3-dimensional cartesian grid. As an initial configuration we compute the Weber & Davis stellar wind solution, which yields stellar wind density, velocity, gas pressure and magnetic field. Moreover, we add a dipolar magnetic field for the planet. We then integrate until a stationary state is reached. Fig. 83 is an example for magnetic field lines connected to the planet υ And b (a star at 0.0597 AU with a stellar mass 1.37 $M_\odot$ and a radius of 1.45 $R_\odot$). In our model the magnetic field strength at the base of the stellar corona was set to $5 \cdot 10^{-4}$ T and the coronal temperature to $2.0 \cdot 10^6$ K. Furthermore the corona was assumed to be isothermal. Our preliminary simulation results already indicate that, indeed, an efficient magnetic interaction is possible between an extrasolar planet and its star.

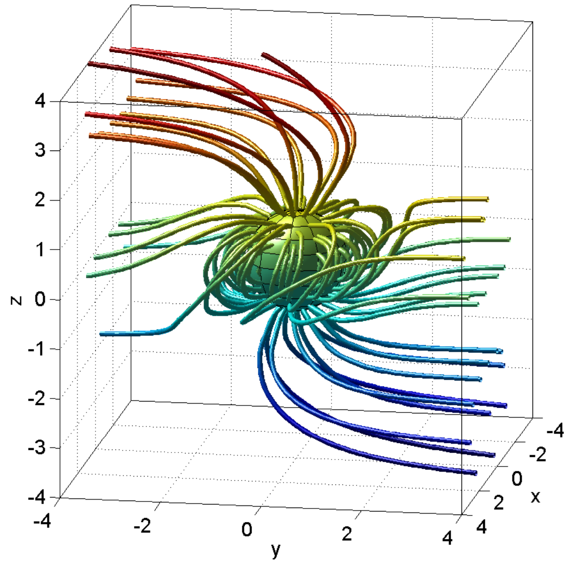

Fig. 83: Simulated magnetic field structure for an interaction of the star υ And b with its observed first planet. The sphere in the center of the box indicates the planet, whose radius was taken to be equal to Jupiter's radius. The origin of the coordinate system is the center of the planet, while the y-axis connects it to the star. The planetary magnetic dipole moment is aligned with the z-axis. The initial stellar wind consists of mainly radial and azimuthal velocity and magnetic field components according to the Weber & Davis stellar wind solution.

(S. Preusse, A. Kopp, J. Büchner in collaboration with U. Motschmann, TU Braunschweig)

Current systems of extrasolar planets

Since their discovery starting 1995 more than 100 extrasolar planets were recognized. Observations of these systems are so difficult that only a few details are known. Many of the planetary systems are very different to our Solar System, e.g. with gaseous giant planets very close to their stars. If Mercury, the innermost planet of the Solar System, has a semi-major axis of about 0.387 AU. This is about 17 times larger than the semi-major axis of OGLE-TR-56 b, the closest of today's known planets. OGLE-TR-56 b is only

4.4 stellar radii away from its star. In the Solar System such small distances exist only between planets and their moons, e.g. between Jupiter and it's moon Io. A strong electromagnetic interaction takes place between Io and Jupiter. With this in mind we investigated, by means of numerical plasma simulations, whether extrasolar planetary systems with planets at such extremely small orbital distances could act like Io and Jupiter.

Fig. 84 illustrates our findings: The yellow circle to the left of the figure is the star. The white circle in the figure presents a planet of Jupiter size. The distance between both is 0.0225 AU. What you see is a cut perpendicular to the ecliptic of the system. We simulated the interaction of an assumed planetary magnetic field with the stellar wind. It's flow direction is indicated with the yellow arrows.

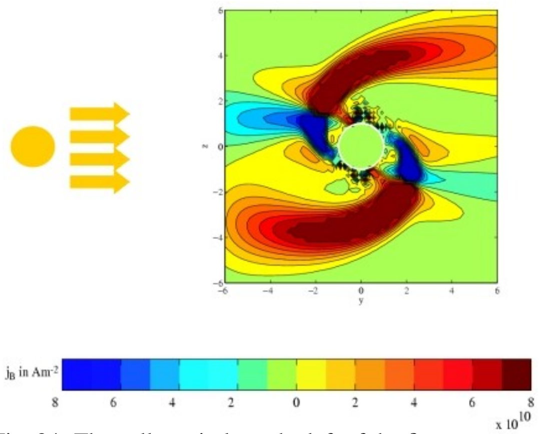

Fig. 84: The yellow circle to the left of the figure represents a star. The white circle in the figure represents an exoplanet of Jupiter size at a distance of 0.0225 AU. Shown is, in a cut perpendicular to the ecliptic plane of the system, the simulated interaction of an assumed planetary magnetic field with the stellar wind. The flow direction of the stellar wind is indicated by yellow arrows.

Due to the interaction currents start to flow. The colour indicates the magnetic field-aligned currents. The upper part of the current system is carried by the stellar wind into the interplanetary space, i.e. to the right. But, strikingly, the lower part seems to be connected with the star. This only happens if the planet is close enough to the star so that the stellar wind shows special properties. This is why we do not find this for the planets in the Solar System. However, a more detailed look into the Solar System reveals a similar behaviour of Io and Jupiter. Both are connected with a current system, but in this case both parts of the current system are involved. This leads e.g. to strong radiation events which we can observe as bright footpoints in the Jovian aurora or as radio emissions.

(S. Preusse, J. Büchner, and U. Motschmann)

Fundamental Science

The relativistic energy spectrum of hydrogen

The method originally used by Dirac in 1928 to derive his famous equation for a single electron is here applied to the two-particle system electron plus proton, considered as an elementary fermion, to obtain a relativistic two-particle Dirac-Breit-type Hamiltonian for the hydrogen atom. This problem can be solved exactly. Thus the relativistic energy levels of the hydrogen atom as a system bound by the static Coulomb force are obtained. The radial part of the resulting Hamiltonian operates in a four-dimensional space describing particles, respectively antiparticles, i. e. electron and positron as well as proton and antiproton. The spin of a particle is described by the normal two-component Pauli spinor, and therefore standard theoretical tools for dealing with angular-momentum coupling can be exploited. Thus the exact eigenfunctions of the spin-orbit-coupling operators for a relativistic binary system can be calculated. The classical energy states of the hydrogen atom are retained in the appropriate non-relativistic limit, in particular the energy levels resulting from Schrödinger's equation. The exact energy spectrum shows the expected dependence on the reduced mass of the two-particle system, and thus describes the recoil of the core properly. The fine structure of the hydrogen spectrum arises from a dependence of the energy levels upon the quantum number of the total angular momentum.

(E. Marsch)

Observational Astronomy and Gravity: Spectropolarimetric measurements for exploring couplings of electromagnetic fields to gravity

The center of interest of our work are nonminimal couplings between electromagnetic and gravitational fields, motivated by current assumptions about new physics in unified quantum theories of gravity. As a consequence of a violation of the Einstein equivalence principle, these couplings influence the polarization state of light passing through a gravitational field and result in a depolarization of light emitted from extended astrophysical sources. Therefore, such violations of the Einstein equivalence principle are directly accessible to observations.

In this context we have shown that the Poincaré gauge theory exhibits gravity-induced birefringence under the assumption of a specific non-minimal coupling between electromagnetism and gravity. This significantly extends the range of theories of gravity explicitely displaying this effect. Furthermore we gave for the first time an explicit expression for the induced phase shift between two orthogonal polarization modes within the Poincaré framework. By using white dwarf polarimetric data we constrained the essential coupling constant responsible for this effect.

In addition we investigated the transport of polarized electromagnetic radiation in a Riemann-Cartan spacetime with torsion. While general relativity features a Riemannian spacetime where photons propagate along geodesics, the trajectories of test particles in a Riemann-Cartan spacetime are in general neither autoparallels nor extremals. Therefore the correct transport equations for polarized radiation in non-Riemannian spacetimes are based on a post-geodesic flow vector field defined on a Riemann-Cartan manifold which reduces to the familiar Riemannian flow in case of a vanishing spin density. The resulting transport equations which we derived provide the starting point for innovative tests of alternative theories of gravity.

(O. Preuss, S. K. Solanki in collaboration with F. W. Hehl, University of Cologne)

2. Planeten, ihre natürlichen Satelliten und Kometen/ *Planets, their moons and comets*

Schwerpunktthema:

Planetare Dynamos

(U. Christensen, J. Wicht, M. Fränz)

(English version see page 81)

Fast alle Planeten in unserem Sonnensystem besitzen oder besaßen ein Magnetfeld. Die Verschiedenartigkeit der Felder lässt auf unterschiedliche dynamische Vorgänge in den Planeten schließen. Ihre Erforschung mittels Planetenmissionen und Computersimulationen ist darum ein wichtiges Werkzeug, das uns Einblicke in die inneren Vorgänge der Himmelskörper ermöglicht. Diese kurze Einführung bietet einen Einblick in die Aktivitäten am MPS und legt den Schwerpunkt auf Computermodelle, bei denen in den letzten Jahren große Fortschritte erzielt wurden.

Das Magnetfeld der Erde

Das Magnetfeld der Erde wird seit vier Jahrhunderten mit zunehmender Präzision vermessen. Aufgrund seiner Bedeutung für die Navigation begann man recht früh, seine Richtung zu kartieren. Heute vermessen drei Forschungssatelliten das geomagnetische Feld mit nie gekannter Präzision (Abb. 85). Im Wesentlichen entspricht es dem Feld eines leicht gegen die Rotationsachse geneigten Stabmagneten, dem klassischen Dipolfeld. Genauer betrachtet lassen sich jedoch auch Beiträge höherer Multipole identifizieren, die zu einer komplexeren Struktur führen. Wir wissen auch, dass sich das Erdmagnetfeld im Zeitraum von Jahrzehnten bis Jahrhunderten merklich verändert. Besonders auffällig ist, dass der Dipolanteil in den letzten 150 Jahren um etwa 10% schwächer geworden ist. Setzt sich dieser Trend fort, so wäre der Dipolanteil in etwa 2000 Jahren ganz verschwunden. Paläomagnetische Untersuchungen an magnetisierten Gesteinen erlauben es, die Kenntnis über das Erdmagnetfeld bis in die ferne geologische Vergangenheit auszudehnen. Kleine Mengen von eingelagerten ferromagnetischen Mineralen konservieren Richtung und Stärke des bei der Bildung des Gesteins herrschenden Erdmagnetfeldes. Gesteine aus verschiedenen Epochen der Erdgeschichte bilden ein weit zurück reichendes geomagnetisches Archiv. Dieses Archiv belegt, dass sich das Magnetfeld im Laufe der Erdgeschichte viele Male umgepolt hat. Umpolungen sind jedoch kurze, seltene Ereignisse. Sie dauern typischerweise nur einige tausend Jahre, während Perioden mit einer stabilen Dipolrichtung mehrere hunderttausend Jahre andauern können.

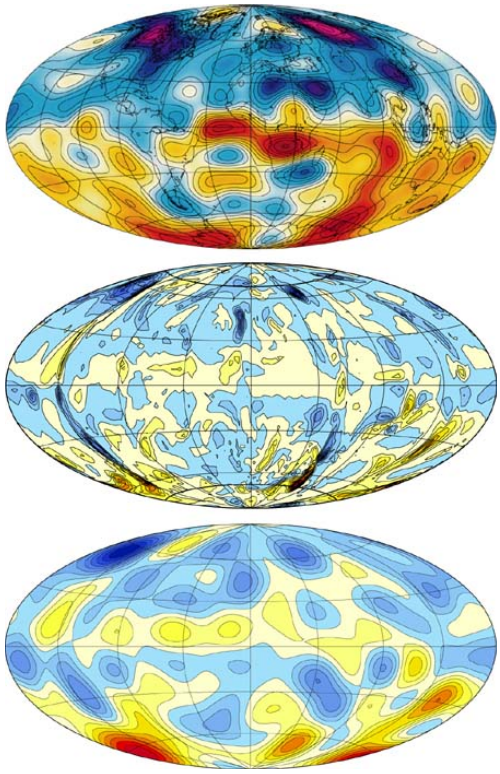

Abb. 85: Das obere Bild zeigt die Vertikalkomponente des Erdmagnetfeldes im Jahr 1990 an der Grenze des Erdkerns, berechnet aus Beobachtungen an der Oberfläche und von Satelliten aus. Strukturen mit Ausdehnungen kleiner als 3000 km werden nicht gezeigt, da sie sich nicht aus den Daten berechnen lassen. Die Beiträge höherer Multipole sind an der Kerngrenze viel stärker als auf der Erdoberfläche. Das mittlere Bild zeigt das Magnetfeld eines Dynamomodells in voller Auflösung. Es enthält zahlreiche kleinräumige Strukturen. Dasselbe Magnetfeld ist im unteren Bild so geglättet, dass seine Auflösung der des Erdmagnetfeldes im oberen Bild entspricht. In ihrer Struktur ähneln sich diese beiden Bilder stark.

Magnetfelder anderer Planeten

Unbemannte Raumsonden haben gezeigt, dass Magnetismus ein im Planetensystem häufiges, aber kein allgemeines Phänomen ist. Unsere planetaren Nachbarn, Venus und Mars, besitzen kein globales Magnetfeld. Die starke Magnetisierung von sehr alten Teilen der Marskruste legt aber nahe, dass der Planet in seiner Frühgeschichte ein starkes inneres Magnetfeld besaß. Beim kleinen Merkur fand man unerwarteter Weise ein Dipolfeld, allerdings ist die Feldstärke an der Planetenoberfläche hundert Mal schwächer als bei der Erde. Jupiters Magnetfeld hingegen ist etwa zehnmal stärker als das der Erde, die Neigung des Dipols gegen die Rotationsachse beträgt jedoch bei beiden Planeten etwa 10°. Saturns Magnetfeld wiederum ist zwar ähnlich stark wie das der Erde, Dipolachse und Rotationsachse scheinen jedoch überein zu stimmen, zudem ist das gesamte Magnetfeld fast rotationssymmetrisch. Auch die Felder von Uranus und Neptun haben eine ähnliche Struktur, werden aber nicht vom Dipolanteil dominiert, zudem ist der Dipol stark gegen die Rotationsachse gekippt.

Der Dynamo

Wie entsteht das Magnetfeld der Erde und der übrigen Planeten? Was bestimmt seine Stärke? Lassen sich die Eigenschaften der verschiedenen Magnetfelder im Detail verstehen? Im 20. Jahrhundert hat sich in einem langwierigen Prozess die Dynamotheorie zur Erklärung natürlicher Magnetfelder im Kosmos durchgesetzt. Im Inneren der Planeten gibt es fluide und elektrisch gut leitende Regionen. Bei der Erde und den anderen erdähnlichen Planeten ist es der flüssige Eisenkern, in Jupiter und Saturn Wasserstoff in seiner metallischen Hochdruckform, und im Inneren von Uranus und Neptun ein Gemisch aus Wasser, Ammoniak und anderen Komponenten, das bei hoher Temperatur und hohem Druck eine gute Ionenleitfähigkeit aufweist. Fließt ein solches Medium in einem bereits vorhandenen Magnetfeld, so werden durch elektromagnetische Induktion elektrische Ströme erzeugt. Wenn das mit diesen Strömen verbundene Magnetfeld gerade das zur Induktion benötigte Feld reproduziert, spricht man von einem selbst-erhaltenden Dynamo. Angetrieben werden die Fließbewegungen durch Konvektion, also durch thermische oder chemische Dichteunterschiede in der Dynamoregion. Alle Generatoren wie auch der Fahrraddynamo beruhen auf dem gleichen Prinzip, funktionieren aber nur wegen der zweckmäßigen Anordnung des elektrischen Leiters, etwa in Form von Spulen. Die Kerne der Planeten stellen dagegen nahezu homogen leitende Kugeln oder Kugelschalen dar. Die verschiedenen Teile des Dynamos sind sozusagen kurzgeschlossen. Ob solche homogenen Dynamos überhaupt funktionieren können, war längere Zeit unklar. Erst um 1960 wurden die ersten theoretischen Beispiele für funktionierende homogene Dynamos gefunden. Weitere 35 Jahre mussten vergehen, bis die ersten realistischen Computersimulationen für den Geodynamo publiziert wurden. Seit zehn Jahren befindet sich die Modellierung planetarer Dynamos in einer raschen Entwicklung, zu der Arbeiten am MPS einen wesentlichen Anteil geleistet haben. Die meisten numerischen Simulationen beziehen sich auf den Geodynamo, da das Erdmagnetfeld am besten bekannt ist. Verschiedene seiner Eigenschaften werden von den Modellen gut reproduziert. Abb. 85 zeigt, dass über den dominierenden Dipolanteil hinaus viele Details denen des Erdmagnetfeldes nahe kommen. Auch die zeitlichen Variationen des geomagnetischen Feldes, von Schwankungen im Bereich von Jahrhunderten bis hin zu Umpolungen, werden von einigen Modellen überzeugend wiedergegeben.

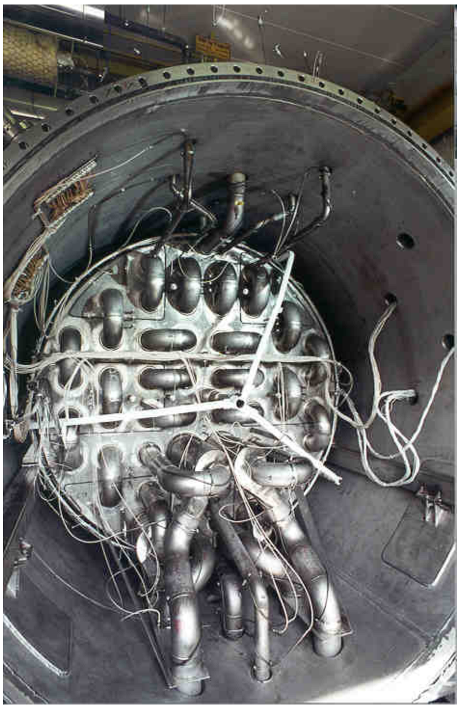

Abb. 86: Das Karlsruher Dynamoexperiment. Flüssiges Natrium wird durch ein System von Stahlröhren gepumpt. Die elektrische Leitfähigkeit der zylinderförmigen Anordnung ist nahezu homogen. Bei hoher Pumpleistung entsteht ein selbst erhaltendes Magnetfeld, das um ein vielfaches stärker ist als das Erdmagnetfeld.

Skalierung zum Erfolg

Die Erfolge der Simulationen sind etwas überraschend, da die Computermodelle mit einigen unrealistischen Annahmen arbeiten müssen. Beispielsweise wird eine um viele Größenordnungen zu hohe Zähigkeit angenommen, um die kleinräumigen turbulenten Wirbel in der Strömung zu unterdrücken, die sich auf den in heutigen Computern realisierbaren Modellgittern nicht darstellen lassen. Andererseits wissen wir, dass die Viskosität in den Dynamoregionen der Planeten vernachlässigbar klein ist. Kann es sein, dass manche Eigenschaften der Modelle nur durch einen glücklichen Zufall mit der Beobachtung überein stimmen, während man anderen Aspekten vielleicht nicht trauen kann? Um diese Frage zu klären wird am MPS in umfangreichen Modellserien untersucht, wie sich die charakteristischen Eigenschaften des Dynamos mit den Kontrollparametern ändern. Dabei zeigt sich, dass die Viskosität, obwohl sie viel zu groß gewählt wurde, keinen entscheidenden Einfluss auf die Magnetfelderzeugung hat. Eine wichtige Kenngröße ist der Energiebedarf eines homogenen Dynamos. Die Vielzahl der Modelle erlaubte es, hierfür ein Gesetz aufzustellen, das sich an Hand des Karlsruher Dynamoexperiments verifizieren ließ (siehe Abb. 86). Dieses Experiment arbeitet mit flüssigem Natrium, dessen Viskosität der des flüssigen Eisens im Erdkern ähnelt. Die gute Übereinstimmung des Energiebedarfs des Karlsruher Dynamos mit der Vorhersage aus den Modellen legt nahe, dass die Turbulenz in der Natriumströmung keine wesentliche Rolle spielt. Für den Geodynamo sagt das Gesetz einen Energiebedarf in Höhe von 200 – 500 GW voraus, soviel wie einige Hundert Kraftwerke erzeugen. Dies ist deutlich weniger als in früheren Abschätzungen und lässt sich mühelos aus der langsamen Abkühlung des Erdkerns gewinnen. Besondere Energiequellen sind nicht nötig. Was bestimmt die Stärke des erzeugten Magnetfeldes? Das ist eine der Schlüsselfragen der Dynamotheorie. Bisher wurde meist angenommen, dass das Magnetfeld gerade so stark wird, dass sich die elektromagnetische Kraft und die rotationsbedingte Corioliskraft die Waage halten. Unsere Modellergebnisse bestätigen dies nicht. Vielmehr legen sie nahe, dass der zur Verfügung stehende Energiefluss die magnetische Feldstärke kontrolliert. Wenn man diese Regel auf die Planeten Erde und Jupiter anwendet, bei denen sich die Energieflüsse abschätzen lassen, ergeben sich plausible Feldstärken im Inneren der jeweiligen Dynamoregion. Beim Jupiter liegt sie um einen Faktor acht höher als bei der Erde, in Übereinstimmung mit der etwa zehn Mal höheren Feldstärke an der Oberfläche jenes Planeten.

Saturn ist anders

Für den Saturn ist die Übereinstimmung weniger gut. Die nahezu achsensymmetrische Struktur des Magnetfeldes, die unlängst von der Cassini-Mission bestätigt wurde, lässt vermuten, dass hier ein anderer Typ von Dynamo am Werke sein könnte, denn ein so einfaches Feld ist untypisch für konvektionsgetriebene Dynamos. Unsere Simulationen zeigen, dass differentielle Rotation hier die Antwort sein könnte. Abb. 87 zeigt das Magnetfeld, das entsteht, wenn man die innere Begrenzung der Dynamoregion schneller rotieren lässt als die äußere. Wie das Feld des Saturns ist es sehr achsensymmetrisch und einfach strukturiert. Während im Computermodell die unterschiedlichen Rotationsraten einfach vorgegeben werden, ist nicht völlig klar,

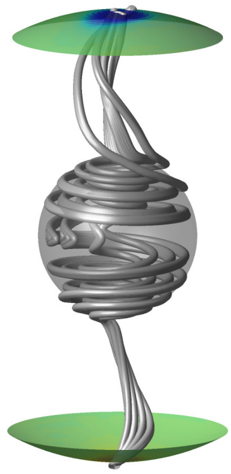

Abb. 87: Magnetische Feldlinien in einem Dynamomodell, in dem die Strömung durch differentielle Rotation zwischen der inneren Begrenzung und der äußeren Begrenzung getrieben wird (von letzterer werden nur die Polkappen dargestellt). Die Magnetfeldlinien entweichen aus der Dynamoregion hauptsächlich in zwei eng begrenzten magnetischen Flussbündeln an den Polen. Das Magnetfeld im Außenraum ist dadurch sehr stark achsensymmetrisch, so wie es im Fall des Planeten Saturn beobachtet wird.

welcher Effekt differentielle Rotation in Saturn verursachen könnte. Ein möglicher Kandidat ist ein Heliumregen, der Drehimpuls aus der oberen Atmosphäre in tiefere Regionen transportiert. Differentielle Rotation ist auch der Mechanismus, der die im Bau befindlichen Dynamoexperimente der nächsten Generation antreiben soll. Die Simulation dieser Experimente war das primäre Ziel unserer Rechnungen. Das Modell für den Saturndynamo ergab sich gewissermaßen als Nebenprodukt.

Das Magnetfeld als Schutzschild

Wir sind noch ein gutes Stück von dem Ziel entfernt, die vielfältigen Erscheinungsformen des planetaren Magnetismus qualitativ und quantitativ vollständig erklären zu können. Numerische Simulationen spielen inzwischen aber eine entscheidende Rolle auf dem Weg dorthin. Die planetaren Magnetfelder haben eine wichtige Funktion – sie halten die energiereiche Partikelstrahlung des Sonnenwindes ab, welche unter anderem eine Gefahr für technische Systeme darstellt. In Gebieten wie dem Südatlantik, wo das Erdmagnetfeld relativ schwach ist und seine Stärke langsam weiter abnimmt, sind Satelliten bei heftigen Eruptionen auf der Sonne einer stark erhöhten Strahlenbelastung ausgesetzt. Da der Marsdynamo vor langer Zeit aufgehört hat zu arbeiten, kann der Sonnenwind ungehindert auf die Atmosphäre des Planeten prallen und Bestandteile der oberen Atmosphäre erodieren. Dies be-

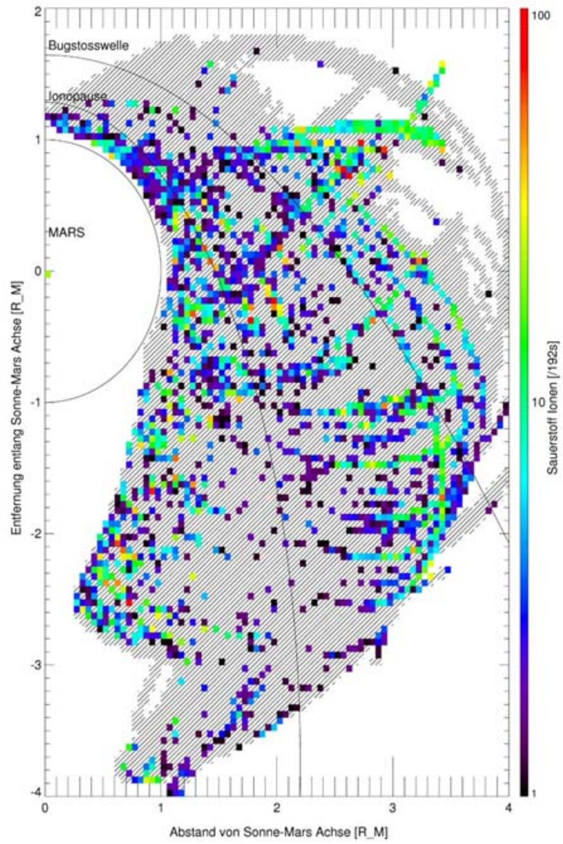

Abb. 88: Einfach geladene Sauerstoff-Ionen im Mars-nahen Weltraum beobachtet vom Aspera-3 Experiment auf dem europäischen Mars Express Satelliten. Gezeigt werden mittlere Zählraten von O+-Ionen in Abhängigkeit von Sonnenrichtung (oben) und Abstand von Mars. Die Hilfslinien bezeichnen die Bugstoßwelle des Sonnenwindes und die Grenzschicht der Ionosphäre (Ionopause) des Mars. Der Abfluss von atmosphärischen Ionen erfolgt im Schatten des Mars und entlang der Ionopause.

legen Messungen von Partikelsensoren auf der Mars Express-Mission, die mit Beteiligung des MPS gebaut wurden (Abb. 88). Ein Magnetfeld kann also entscheidend für die langfristige Entwicklung von Planetenatmosphären und somit für das Entstehen lebensfreundlicher Umweltbedingungen sein.

Highlight:

Planetary dynamos

(U. Christensen, J. Wicht, M. Fränz)

Nearly all the planets in our solar system possess a magnetic field or had one some time in the past. The diversity of the planetary fields reflects interesting differences in interior dynamics. Their exploration by space missions or computer simulations is an important tool to provide insight into the otherwise shielded planetary interiors. This short introduction gives an overview of activities at the MPS concentrating mainly on computer models, where considerable progress was achieved during the past years.

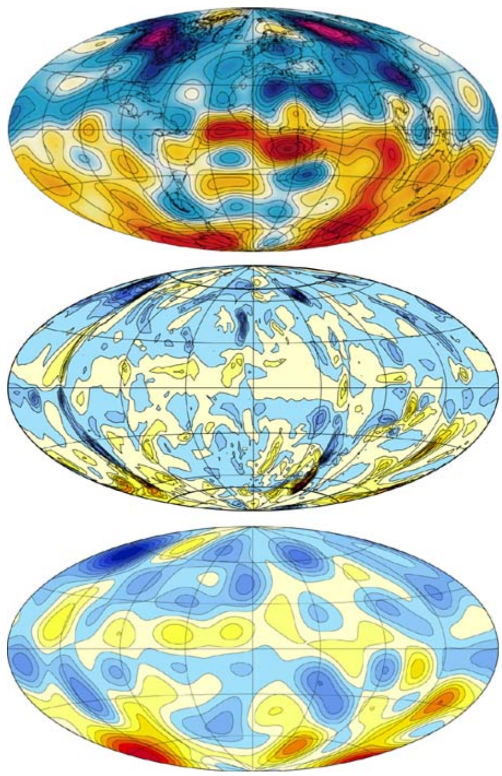

Fig. 85: The upper panel shows a model of the vertical component of the geomagnetic field in the year 1990 on the top of the Earth's core based on surface and satellite measurements. Structures smaller than 3000 km can not be resolved, they are shielded by the mantle magnetization. Higher multipole contributions grow with depth and are therefore much more pronounced than on Earth's surface. The middle panel shows the respective field in a dynamo simulation, note the many small scale contributions. These are filtered away in the lower panel mimicking the shielding by mantle magnetization. A comparison with the 1990 geomagnetic field reveals many similarities.

Earth's magnetic field

The geomagnetic field has been measured for more than four centuries with increasing precision. Maps of magnetic field direction were compiled early on because of the prime importance for navigation. Today three geomagnetic satellites continuously measure Earth's magnetic field with previously unknown precision. Fig. 85 shows the vertical magnetic field at the core surface in the year 1990. The geomagnetic field is very similar to the field of a bar magnet that is somewhat tilted against the planet's rotation axis, i.e. a classical dipole field. When looking closer, higher multipole contributions can be identified leading to a more complex field structure. We also know that Earth's magnetic field is changing significantly on time scales from decades to centuries. Most notably, the dipole contribution has decreased by about 10% during the last 150 years. Should this trend continue, the dipole will have vanished within the next two millennia. Paleomagnetic examination of magnetized rocks allows us to extend our knowledge of the geomagnetic field into the far geological past. Small grains of embedded ferromagnetic minerals conserve field strength and direction at the time when the rock was formed. Samples from different epochs form a geomagnetic archive reaching far back into Earth's history. The archive proves that the magnetic field has reversed its direction several hundred times. These reversals are rare and short events that are separated by long time spans of stable polarity. Reversals last some thousand years while the polarity can remain stable for some hundred thousand years on end.

Other planets

Unmanned spacecraft have shown that planetary magnetism is a wide spread but not general phenomenon in our solar system. Our planetary neighbours Venus and Mars have no global magnetic fields. Strong magnetization of very old parts of the Martian crust suggests that the planet must have had a strong internal magnetic field early in its history. Unexpectedly, the small planet Mercury has a dipole field, but it is 100 times smaller the Earth's magnetic field on the planet's surface. Jupiter's magnetic field, on the other hand, is ten times stronger than the geomagnetic field, but the tilt of the dipole contributions is very similar, about 10 degree. Saturn's magnetic field strength is comparable to Earth. However, dipole and rotation axis seem to be aligned, moreover the field is very much axisymmetric and rather simple. Uranus and Neptune have similar magnetic fields that are not dominated by the dipole component. In addition, the dipole is strongly tilted with respect to the rotation axis.

The dynamo

Where do Earth's magnetic field and the fields of the other plants come from? What determines the field strength? Why do some planets have different fields while the fields of other planets are so similar? In a long process the dynamo theory has become the accepted explanation for the natural magnetic fields of astrophysical objects. Fluid and electrically conducting regions in the interior of the planets are a prerequisite for the dynamo mechanism to work. These are the fluid iron cores found in Earth and other terrestrial planets, the electrically conducting high pressure phase of hydrogen in Jupiter and Saturn, and a mixture of water, ammonia, and other components in Uranus and Neptune, that is a good ion conductor provided temperature and pressure are high enough. When such an electrically conducting medium flows through an already existing magnetic field, a physical process called electromagnetic induction drives electric current. These currents in turn produce a magnetic field. The dynamo is called self-exciting provided the newly produced field can substitute the originally present inducing field. The fluid flow is generally driven by convection, which means by thermal or chemical density difference in the dynamo region. All electricity producing generators or dynamos rely on the same principle. These technical dynamos work because the electrically conducting parts are arranged in an appropriate way, for example wounded in an electrical coil. This is certainly not the case with planetary dynamos and their generally homogeneous conducting regions that have the shape of a sphere or spherical shell. The different parts of the dynamo seem to from a short-circuit here. Whether such a dynamo could work at all was unclear until the first theoretical examples were found around 1960. Additional 35 years had to pass until the first realistic computer simulations of the geodynamo were published. But since then modelling of planetary dynamos has advanced considerably notably due to the research preformed at MPS. Most of the numerical dynamo simulations try to model the geodynamo since the Earth's magnetic field is well known. Many of its properties can be reproduced convincingly as demonstrated by Fig. 85 that compares the geomagnetic field for 1990 with a numerical solution. In addition, time variations of the geomagnetic field including secular variations and reversals can be modeled successfully.

Scaling to success

The success of the numerical simulations is somewhat surprising since the computer models have to work with several unrealistic assumptions. For example, the fluid viscosity is several orders of magnitude too large

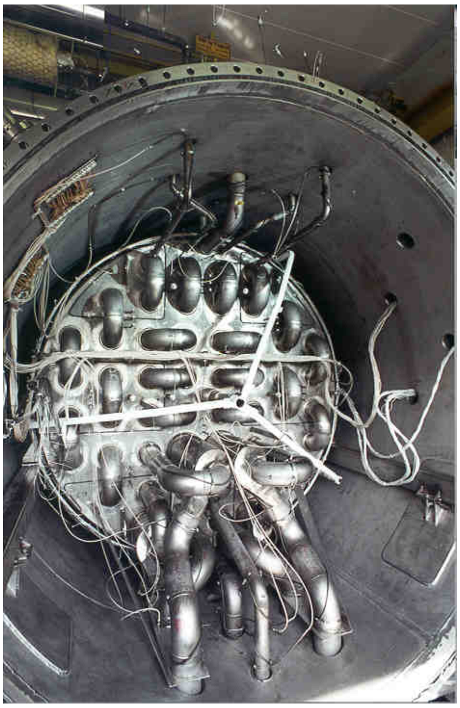

Fig. 86: The dynamo experiment that has been performed in Karlsruhe. Liquide sodium is pumped through a specially designed system of tubes. The electrical conductivity is nearly homogeneous once the cylinder is flooded with sodium. When the liquid is pumped sufficiently fast through the system the created magnetic field is many times stronger than the geomagnetic field.

to suppress small scale convective eddies that can not be resolved on today's computers. On the other hand, we know that viscosity is negligible in the dynamo region of the planets. Is the good agreement of simulations and observations simply a lucky coincidence? Could we trust other aspects of the simulations? To answer these questions the MPS has explored a large suit of simulations in order to find out how the solution properties depend on the control parameters. The results demonstrate that the fluid viscosity, though being too large, has no significant influence on the magnetic field production. Another important and interesting quantity is the power requirement of a homogeneous dynamo. The large number of numerical models allowed us to derive scaling laws that could be verified with the Karlsruhe dynamo experiment (see Fig. 86). This experiment works with liquid sodium whose viscosity is very similar to that of liquid iron in the Earth's core. The good agreement of power requirement in the model simulations and the experiment suggest that the small scale turbulence is of minor importance. The scaling law predicts that the geodynamo needs about 200 – 500 GW which is the output of some hundreds of today's biggest power plants. This is significantly less that previous estimates suggested and could simply be provided by the secular cooling of Earth's core. No additional power sources are required. What determines the strength of the magnetic field produced by a homogeneous dynamo? This is one of the key questions in dynamo theory. Previously it has been assumed that the magnetic field is exactly so strong that electromagnetic force and Coriolis force acting on a fluid parcel are in balance. Our model results tell a different story, here the magnetic field strength is controlled by the available energy flux. If we apply this rule to the planets where estimates of this energy flux are available we get two plausible estimates in the interior of the respective dynamo regions. The magnetic field in Jupiter is eight times stronger than the field in Earth's core. This is in good agreement with the fact that Jupiter's surface field is about ten times stronger than the geomagnetic field.

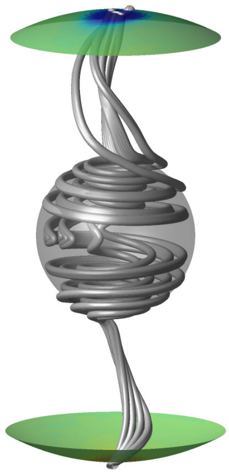

Fig. 87: Magnetic fieldlines in a dynamo model that is driven by a differential rotation between inner(grey) and outer boundary (only polar caps shown). The magnetic field lines are wound up by the faster rotation of the inner boundary and leave the shell through two confined patches at the poles. Like Saturn's magnetic field the solution is very axisymmetric and simple.

Saturn is different

The agreement is less convincing for Saturn. The nearly perfectly axisymmetric field structure that has recently been confirmed by Cassini measurements suggests that the dynamo working within Saturn could be of a different type. Such a simple magnetic field is not at all typical for convection driven dynamos. Our numerical simulations demonstrate that a dynamo driven by differential rotation could be the answer here. Fig. 87 shows the magnetic field that is produced when the inner boundary of the dynamo region is rotating faster than the outer. Like on Saturn, the field is very axisymmetric and of simply structure. While we can simple impose the differential rotation in our computer model it is less clear what could be the source for the shear in Jupiter. One possible candidate is helium rain transporting angular momentum from the upper atmosphere into deeper regions. Differential rotation is also the mechanism that will drive the second generation dynamo experiments currently being built. The simulations of these experiments was our primary goal while the Saturn dynamos came as a byproduct.

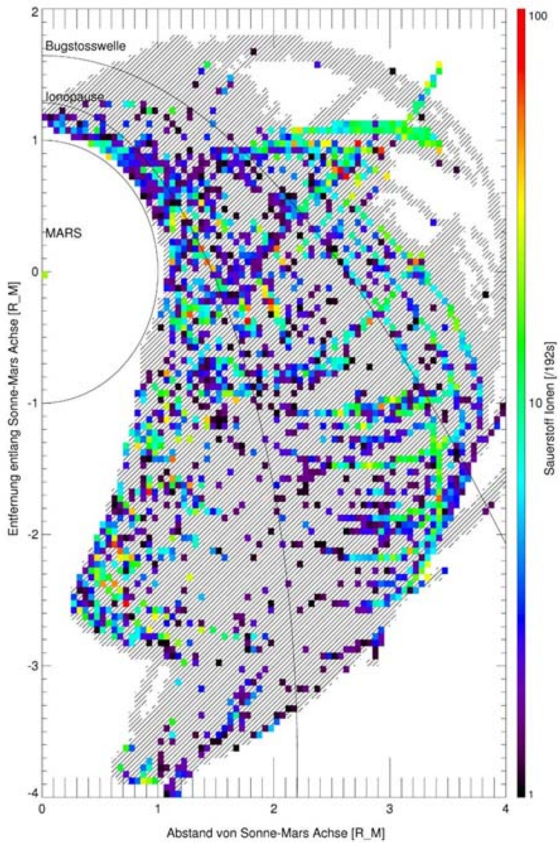

Fig. 88: Singly ionized oxygen close to Mars as measured by the Aspera-3 experiment on Mars Express. The figure shows the dependence of colour-coded O+ ions counts on solar direction and distance from Mars. Thin black lines indicate the bow shock of the solar wind and the boundary to the ionopause. The eroding of oxygen ions occurs on the night side along the ionopause.

The magnetic shield

We are far from understanding all the qualitative and quantitative aspects of planetary magnetism. Numerical simulations play a vital part here. Magnetic fields shield the planetary surface from the high energy solar particle radiation called the solar wind. This radiation is a threat for technical systems. Above the south Atlantic, where the magnetic field is particularly weak, increased radiation during solar eruptions is already harming satellites in Earth orbit. Since the dynamo in Mars has ceased its operation in the early planetary history, the solar wind can directly reach and erode the atmosphere. This is demonstrated by measurements from the particle sensor on Mars Express that has partly been built in the MPS (see Fig. 88). A shielding magnetic field is essential for the long-term evolution of a planetary atmosphere and can therefore be decisive for a habitable environment.

Wissenschaftliche Einzelberichte/
Individual scientific reports

(nur in Englisch)

Numerical simulation of planetary interiors

Scaling laws for dynamos in rotating spherical shells and application to planetary magnetic fields

Recent numerical dynamo models do remarkably well in reproducing the properties of the Earth's magnetic field, but the theoretical understanding of the dynamos has not progressed at the same pace. This work is part of a program to derive universal scaling laws for planetary dynamos. These laws relate basic properties of the dynamo, such as the characteristic flow velocity, heat transport efficiency, and magnetic field strength to the basic control parameters. The latter represent factors such as rotation rate, vigor of convection, and material parameters such as viscosity and electrical conductivity. We analyze the results of an extensive set of numerical dynamo models in rotating spherical shells, varying all relevant control parameters by at least two orders of magnitude. Convection is driven by a fixed temperature contrast between rigid boundaries. There are two distinct classes of solutions with strong and weak dipole contributions to the magnetic field, respectively. Non-dipolar dynamos are found when inertia plays a significant role in the force balance. In the dipolar regime the critical magnetic Reynolds number for self-sustained dynamos is of order 50, independent of the magnetic Prandtl number Pm. However, dynamos at low Pm exist only at sufficiently low Ekman number E. For dynamos in the dipolar regime we attempt to establish scaling laws that fit our numerical results. Assuming that diffusive effects do not play a primary role, we introduce non-dimensional parameters that are independent of any diffusivity. These are a modified Rayleigh number based on heat (or buoyancy) flux $Ra^{\star}_{Q}$, the Rossby number Ro measuring the flow velocity, the Lorentz number Lo measuring magnetic field strength, and a modified Nusselt number $Nu^{\star}$ for the advected heat flow. To first approximation, all our dynamo results can be collapsed into simple power-law dependencies on the modified Rayleigh number, with approximate exponents of 2/5, 1/2 and 1/3 for the Rossby number, modified Nusselt number and Lorentz number (see Fig. 89), respectively. Residual dependencies on the parameters related to diffusion (E, Pm, Prandtl number Pr) are weak, but may be significant in case of the magnetic Prandtl number.

Our scaling laws are in agreement with the assumption that the magnetic field strength is controlled by the available power and not necessarily by a force balance. The Elsässer number, which is the conventional measure for the ratio of Lorentz force to Coriolis force, is found to vary widely. We try to assess the relative importance of the various forces by studying sources and sinks of enstrophy (squared vorticity). In general Coriolis and buoyancy forces are of the same order, inertia and viscous forces make smaller and variable contributions, and the Lorentz force is highly variable. Ignoring a possible weak dependence on the Prandtl number or the Ekman number, a surprising prediction is that the magnetic field strength is independent both of conductivity and of rotation rate and is basically controlled by the buoyancy flux. Estimating the buoyancy flux in the Earth's core using our Rossby number scaling and a typical velocity inferred from geomagnetic secular variations, we predict a small growth rate of about 0.1 mm/yr and old age (3.5 Gyr) of the Earth's inner core. For this buoyancy flux, the scaling law for the Lorentz number predicts a magnetic field strength inside the core of 1.2 mT, which is somewhat low compared to other estimates, but still reasonable. From the observed excess luminosity of Jupiter, we predict a field of 8 mT in the dynamo region of this planet, in agreement with Jupiter's external field being

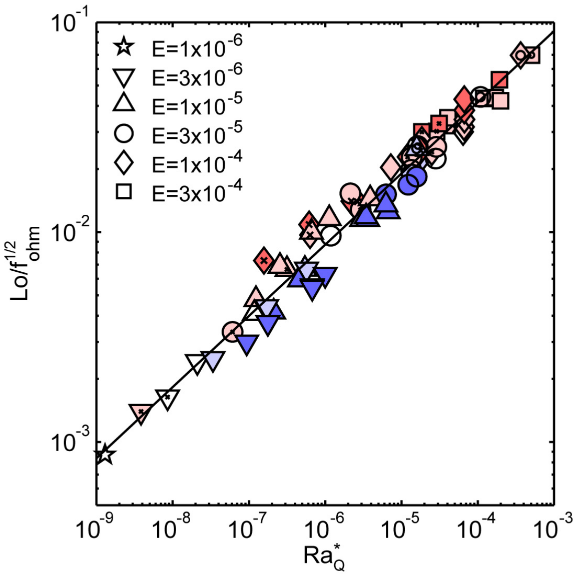

Fig. 89: Lorentz number (non-dimensional magnetic field strength) corrected for the fraction of ohmic dissipation versus modified Rayleigh number for 71 dynamo models that generate a dipole-dominated magnetic field. The Ekman number is indicated by the shape of the symbol, the magnetic Prandtl number is colour-coded ($Pm > 3$ dark red, $1 < Pm \leq 3$ light red, $Pm = 1$ white, $0.3 \leq Pm < 1$ light blue, $Pm < 0.3$ dark blue). Prandtl numbers other than one are indicated by a large cross (Pr=10), small cross (Pr=3), small circle (Pr=0.3) or large circle (Pr=0.1) inside the main symbol.

ten times stronger than that of the Earth. For Saturn, the predicted field strength seems too high in comparison to the observed external field. Mercury's very weak internal field cannot be explained by a very low buoyancy flux, because this would lead to a subcritical magnetic Reynolds number. Perhaps Earth and Jupiter represent one class of dynamos, while particular conditions in Mercury and Saturn lead to a different ratio of internal to external field strength.

(U. Christensen in collaboration with J. Aubert (IPGP Paris))

Steady zonal flows in spherical shell dynamos

The Earth's magnetic field and its time derivative contain evidence for the existence of fairly time independent, axisymmetric flows in the longitudinal direction. These zonal flows exist in various layers of several geophysical objects: They can be observed, for instance, in the atmosphere, the oceans, as well as on the surface, and possibly the interior of large fluid planets like Jupiter and Saturn. Numerical simulations of convective dynamos in an Earth-like geometry (Aubert, 2005) reveal a fairly robust zonal flow pattern (see Fig. 90). They co-exist with lines of magnetic force

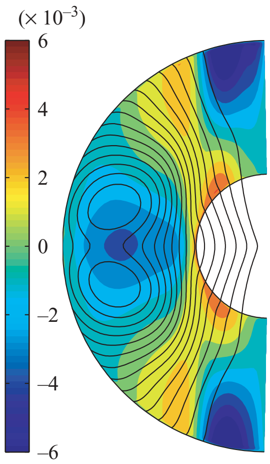

Fig. 90: Colour-coded time average zonal flow and magnetic field lines in a dynamo simulation (yellow to red colours (blue) mark prograde (retrograde) zonal flow speeds in arbitrary units).

under a law of minimal interaction known in astrophysics as Ferraro's law of co-rotation. A power budget allows to derive a scaling law for their amplitude, which depends solely on the buoyancy flux, a geophysically well-constrained parameter. Applied to the Earth's outer core, the law predicts the correct amplitude for the huge polar vortices present in the tangent cylinder of the core.

(J. Aubert)

Tests of core flow imaging methods with numerical dynamo models

We test the quality of a new method for imaging the fluid flow at the surface of the Earth's core using the observed geomagnetic secular variation and assuming that the magnetic flux is frozen into the fluid. The method incorporates constraints on flow helicity. We use synthetic magnetic secular variation data from 3-D self-consistent numerical dynamo models. Comparison of the inverted flow with the dynamo flow reveals that our imaging method recovers a significant part of the large-scale features, both in pattern and in magnitude. The dynamo flow is characterized by high-latitude vortices, some equatorial symmetry, columnar convection, and a significant amount of flow along radial magnetic field contours. Our inversion method correctly images these aspects of the flow. The correlation coefficient between the dynamo velocity and the imaged velocity exceeds a value of 0.5 in cases with large-scale flow and magnetic field pattern, but degrades substantially in more complex cases especially when the scale of the secular variation is small. The magnitude of the imaged velocity depends on the a priori-assumed ratio k of tangential divergence to radial vorticity, in some resemblance to the damping parameter in spectral inversion methods, but different k-values do not result in increasing data misfits. Including tangential magnetic diffusion in core flow inversion improves the quality of the imaged velocity pattern. However, effects of unmodeled radial diffusion and magnetic field truncation are not recovered well and may cause severe artifacts in the imaged velocities.

(U. Christensen in collaboration with H. Amit and P. Olson (Johns Hopkins University))

Inverse magnetic field patches at the top of Earth's core

The Earth's magnetic field varies on many different time scales. Changes over periods of years, decades, centuries, or millenia are called secular variation and are directly connected to the fluid flow in Earth's outer core. Fig. 91 shows a comparison of the geomagnetic field on the core surface for the year 1990 with the field from a dynamo simulation. These fields are not only similar in their overall structure, but also several smaller features agree nicely.

Recently, regions of inverse field direction on the core surface received considerable attention. These are patches where the radial field direction is inverse to the direction of the dominating dipole field. Particularly prominent are the patches underneath southern

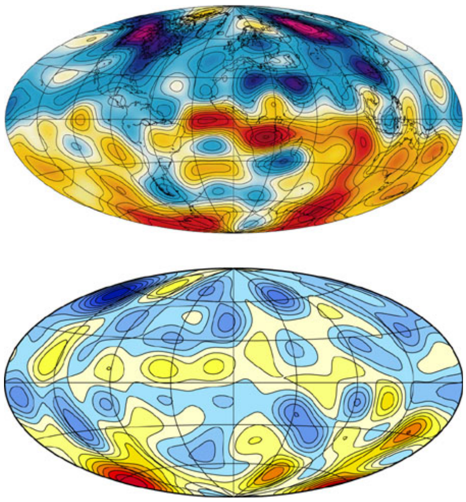

Fig. 91: Comparison of the radial geomagnetic field for 1990 at core surface with the field from a dynamo simulation. The geomagnetic field is an average from the 1980 field based on Magsat data and the 2000 field based on Oerstedt data and was published by Gaultier Hulot and coworkers (2002). Magsat and Oerstedt are sattelites.

Africa and close to the north pole. Growth and wander of these regions can explain the considerable decrease in dipole strength that has been observed, about 10% in the last 150 years. There are speculations that the geomagnetic field might undergo a reversal in the next 2 millennia.

However, computer simulations show that such inverse patches are normal contributions to the magnetic field and its secular variation. They grow and decay on time scales of some centuries due to variations in the convective upstream in Earth's outer core. Plume-like features produce patches in the polar region, while sheet like outreaches of convective rolls are responsible for the equatorial counterparts. Neither are necessarily precursors to field reversals.

Unfortunately, our knowledge of the Earth's magnetic field in historic times is quite scarce. Only for the last four centuries do we have the spatial resolution suffitient to identify inverse patches. Dynamo simulations are thus essential for classifying this phenomenon. Paleomagnetic models reaching back several millennia confirm that Earth's dipole strength is varying considerable on longer time scales. They show that today's dipole decay is indeed nothing special and that the dipole strength still lies above average.

(J. Wicht)

Reversal rate in a dynamo model

The slowest time scales in the geodynamo process are connected to magnetic reversals and variations in the reversal rate. Changes in Earth's mantle likely cause variations over several tens of million years. But the reverals rate also varies considerably on time scales of some million years. We employ computer simulations to explore these variations in a dynamo model. A particularly simple model has been selected where magnetic field and flow are fairly large scale so that a reasonable long time interval could be afforded. The solutions are nevertheless fully 3-D, self-consistent chaotic and very Earth-like. We succeeded to simulate more than 100 reversals that where analysed statistically.

Reversals seem to obey a Poisson statistics, i.e. each reversal is essentially independent from all others. This is in accordance with analysis of paleomagnetic data and compliant with the fact that reverals are seperated by time intervals much longer than the reversals process itself. Exceptionally strong variations in the convective flow seem to trigger the reversal process in the model. Flow amplitudes vary stochastically, very rarely reaching the necessary vigour long enough to cause a reversal. This is the reason why reversals are so rare and why the reversal rate varies so strongly. Valet and coauthors (2005) suggest that there is a correlation between reversal rate and dipole strength during the last two million years of Earth's history. Reversals are more likely to occur when the dipole is weak. Such a correlation cannot be found in the simulation that contains many more reversals than the analysed paleomagnetic data set.

(J. Wicht in collaboration with C. Constable (SCRIPS, San-Diego))

Joint geodynamical and seismological modelling of the Eifel plume

During the Eifel-Plume Project, 250 temporary and permanent seismic stations distributed in an array roughly 400 km x 400 km, centered in the volcanic Eifel region in Germany, have recorded travel times of teleseismic events for a period of six months. The tomographic inversion of P-wave residuals has revealed a columnar low-velocity anomaly in the Earth's upper mantle below the volcanic Eifel region extending to at least 400 km depth. In this study we have explored whether a geodynamically consistent model of a mantle plume can explain the observed traveltime residuals. We have used a three-dimensional mantle convection code with temperature and pressure-dependent viscosity to generate a suite of model plumes that rise from the transition zone and spread below a stationary or drifting lithospheric plate. We have used ray-tracing to calculate synthetic traveltimes and varied the plume location, radius, temperature and the rate and direction of plate motion in order to fit the observed traveltimes. Our results show a fair correlation between synthetic and observed traveltime residuals (see Fig. 92).

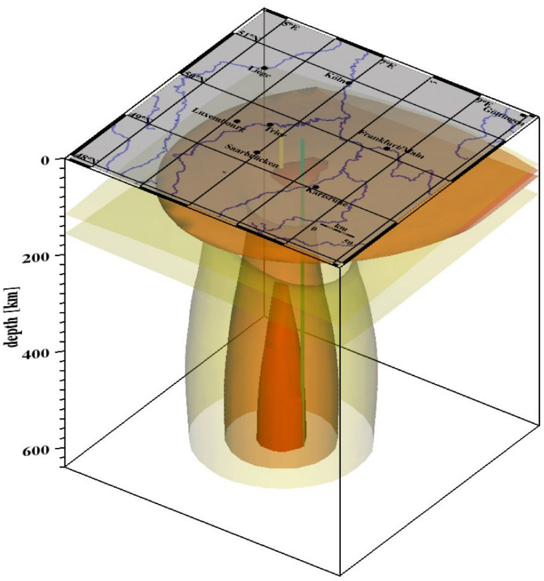

Fig. 92: Geodynamical computer model of the plume underneath the Eifel that has been observed seismically. Faster than normal travel times are shown in red contours.

The presence of additional structures in the lithosphere and upper mantle of the Eifel region that are not covered by a simple plume model prevents a perfect fit of the observed seismological data and may bias to some degree the derived plume parameters. The travel time anomalies are mainly caused by the plume stem with smaller contributions from the plume head. Models with and without an axisymmetric plume head below the lithosphere fit the data almost equally well and we conclude that the absence of a plume head in tomographic images does not rule out its existence. In the best fitting model the plume stem has a radius of 60 km and rises about 50 km to the SW of the quaternary volcanic field below a lithosphere that is slowly moving in the NNE direction. The temperature of the plume and its flux cannot be constrained tightly from our model results, but combining them with other constraints we estimate an excess temperature of 200° C and a buoyancy flux of 500 – 1000 kg/s. Our new approach of interpreting seismic data directly with a geodynamical model, without first going through a tomographic inversion, can bypass some of the problems of the latter, such as smearing of structures or creating artefacts in regions poorly covered with crossing rays. It introduces geodynamical consistency and plausibility of the inferred structure as additional a priori information. It will work well when the modeled structure stands out as the dominant one in the mantle volume under consideration. For the Eifel plume this condition is marginally satisfied.

(U. Wüllner, U. Christensen, in collaboration with M. Jordan (University of Utah))

Effect of a cratonic lithospheric root on plume melting

The formation of Large Igneous Provinces on Earth, which is associated with the rise of diapiric heads of starting mantle plumes, has often occurred near the margins of cratonic lithosphere. Previous numerical models of plume-lithosphere interaction and decompression melting modeled the lithosphere as a rigid lid of mostly uniform thickness. We have calculated a three-dimensional numerical model of a starting mantle plume, consisting of a diapiric head and a trailing conduit, which interacts with a moving lithospheric plate of non-uniform thickness. We study in particular the effect of a lithospheric root on plume flow and partial melting. The plume is deflected away from the root, preferentially in the upstream direction of plate motion. The presence of a root facilitates a threefold enhancement in the melting rate by restricting the horizontal spreading of plume material and the diffusion of the thermal anomaly in comparison with the model having no root. The large melting rate is sustained for a longer time when depletion buoyancy of the residue plays a role. Our model does not require an excessively high plume temperature or compositionally heterogeneous plume head and reproduces the characteristics of melting rates and melt volumes seen in flood basalt, volcanic provinces and the trailing hotspot tracks. The model also explains the occurrence of volcanism of different ages at a given location as a result of initial melting in the upstream region and its subsequent passage over the plume conduit due to plate motion.

(A. Manglik, U. Christensen)

Mean-field view on geodynamo models

Many features of the Earth's magnetic field have been successfully reproduced by nonlinear three-dimensional simulations of the magnetohydrodynamics (MHD) in the Earth's core. Although some model parameters do not reach realistic values, the simulations exhibit a dipole dominated magnetic field. In addition, the time dependence of the dipole moment, including secular variation, excursions and reversals, resembles the observed Earth's magnetic field.

Despite this success in the case of the geodynamo, global dynamo calculations applied to various other astronomical objects make use of mean-field theory.

Its idea is based on a scale separation where attention is focused only on large-scale mean fields. Whether a mean-field model shows dynamo action or not depends strongly on the mean electromotive force.

Since both approaches are available in the case of the geodynamo, a detailed comparison of mean-field theory with direct numerical simulations can be done for the first time. One aim of our work is to get an estimate of the validity and reliability of mean-field theory. On the other hand, mean-field concepts help to improve the conceptual understanding of the geodynamo.

Using an azimuthal average and defining mean fields as the axisymmetric parts of the actual magnetic field, we calculated the mean-field coefficients with the fluid velocity taken from the direct numerical simulations. Two different methods have been applied. While the first, numerical one does not use intrinsic approximations, the second, analytical one is based on the first-order smoothing approximation. There is satisfying agreement of the results of both methods for sufficiently slow fluid motions.

A comparison is made between direct numerical simulations of magnetohydrodynamic processes in a rotating spherical shell and their mean-field description (see Fig. 93). In the investigated example of rotating magnetoconvection the mean magnetic field from the numerical simulation is well reproduced on the mean-field level. For a quasi-steady geodynamo model a discrepancy occurs, which is probably a consequence of the neglect of higher-order derivatives of the mean magnetic field in the mean electromotive force.

At higher excitations geodynamo models of the same type show highly time-dependent fluid motions and magnetic fields. The coefficients determining the mean electromotive force fluctuate then considerably in space and time but on the average their profiles resemble those of their counterparts in the quasi-steady case.

(M. Schrinner, U. Christensen, D. Schmitt, in cooperation with K.-H. Rädler and M. Rheinhardt (Potsdam))

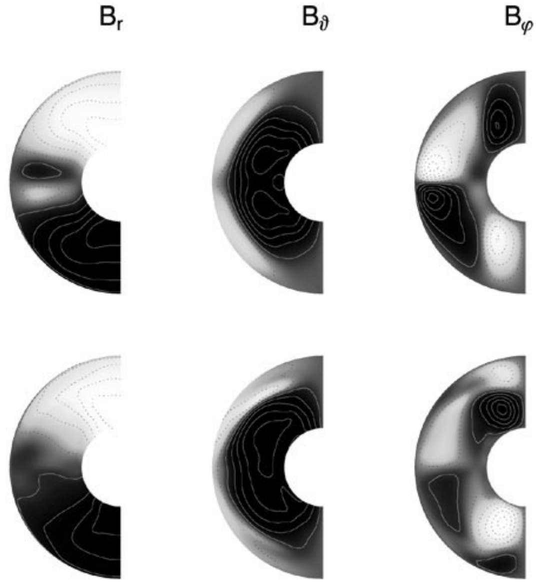

Fig. 93: The mean magnetic field components in a direct numerical dynamo simulation (upper panel) and in the corresponding mean-field model (lower panel). For each component the grey scale (white – negative, black – positive values) in the meridional plane is separately adjusted to its maximum modulus.

Terrestrial planets research – Mercury

Thermal evolution models for Mercury

The internal structure of Mercury is not well known at the moment. The extremly high density of the planet suggests a big iron core. But the available data give no insight whether this big iron core is completely liquid or solid or at least partially solid. But the structure of the core is important for different dynamo mechanisms. During the Mariner 10 flybys a weak magnetic field of Mercury was observed and it is an open question which mechanism produces this magnetic field. Thermal evolution models for the mantle of Mercury can provide important information about the interior structure and give some hints for the magnetic field.

We use a 3-D numerical convection code which includes the effects of freezing out a solid inner core. The viscosity is depth-dependent and varies with the horizontally averaged temperature following an Arrhenius term. According to changes in the temperature the viscosity varies with time and allows to simulate the thickening of the lithosphere. The model also includes the cooling of the core. Its temperature is determined by the heat given to the mantle. Effects like latent heat or gravitational energy which are related to the growth of an inner core reduce the cooling of the core.

First 3-D results show that Mercury has a solid inner core. The size of this inner core strongly depends on the exact melting conditions of iron with a small sulfur content (0.5 – 5%) which are not well known yet. After 4.5 Ga the radius of the inner core is in the range between 575 km und 1440 km or 30% and 76% of the core radius also depending of the assumed convection strength. The size is also controlled by the starting temperature conditions of the core. In a very hot core at the beginning the growth of an inner core is delayed which results in smaller inner cores. While

the solid inner core from pure iron is freezing out, the liquid shell gets enriched in buoyant sulfur which can start chemical convection. This chemical convection can be an energy source for driving a dynamo in the liquid outer shell of the core. Here further investigations on the buoyancy flux and the possible strength of the magnetic field are needed. A thermally driven dynamo can be ruled out in all simulations because the heat flux out of core which is transported by the mantle is to low too allow for thermal convection in the core.
The convection pattern in the simulations is dominated by cold downwellings and is very small scaled. The convection pattern together with the observed thermal anomalies at the core mantle boundary can give hints to a possible realisation of a thermoelectric dynamo in Mercury which was suggested by Stevenson (1987).
The temperature profile in the mercurian mantle is dominated by a very thick upper thermal boundary layer. The thickness of the lithosphere after 4.5 Ga is about 300 km.
New data from upcoming missions like BepiColombo can give important information to restrict the model assumptions and, together with the models, lead to a more complete understandig of the interior of Mercury.

(M. Buske, U. Christensen)

The BepiColombo mission to Mercury

BepiColombo is an ESA-JAXA/ISAS mission to the planet Mercury (Fig. 94). It consists of two spacecraft. The Mercury Magnetospheric Orbiter (MMO) is built by the the japanese space agency JAXA/ISAS and the Mercury Planetary Orbiter (MPO) is provided by ESA. Currently the launch of both spacecraft onboard one Sojus rocket is foreseen for August 2013, arriving at Mercury in 2019.

MPS is involved in preparing instruments for both spacecraft. On MPO the institute is providing major parts for the BEpi Colombo Laser Altimeter (BELA) and for the Planetary Ion CAMera (PICAM) of the SERENA instrument (SERENA = Search for Exospheric Refilling and Emitted Natural Abundances). On the MMO MPS is involved in the Mass Spectrum Analyser (MSA) of the (Mercury Plasma Particle Experiment (MPPE)

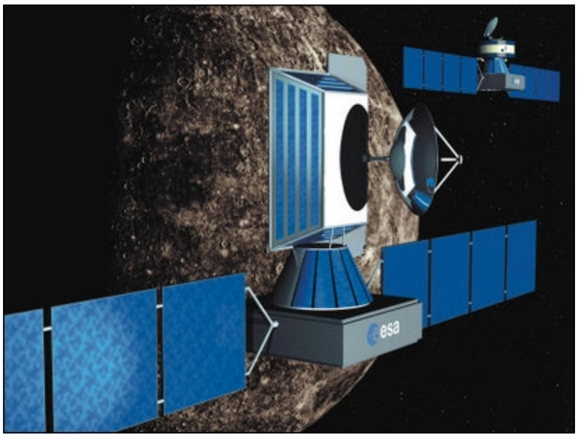

Fig. 94: Artistic view of Bepi Colombo arriving at Mercury in 2019.

The Laser Altimeter for the BepiColombo to Mercury

In the framework of the ESA Mission BepiColombo, a Mercury planetary orbiter, our institute is part of an international team for the development of the laser-altimeter BELA for mapping Mercury's surface and analysing its interior. The institute's contributions and responsibilities are the development of a space qualified laser with 50 mJ pulse energy and 3 nsec pulse width as well as the preparation of parts of data analysis algorithms together with the international BELA team. In September 2005 the "proof of concept" of the laser was presented to ESA and in November BELA was finally accepted as part of the science payload of BepiColombo by ESA. The laser development is carried out in the frame of industrial contracts, our institute is responsible for the science specifications, space qualification and management.

(U. Christensen, C. Koch, H. Fischer, R. Roll, M. Hilchenbach)

Particle Packages on the BepiColombo mission to Mercury

On both BepiColombo spacecraft MPS is involved in the neutral and charged particle spectrometers. The institute is responsible for the high voltage power supplies of the MSA sensor of the MPPE package on the MMO spacecraft and for parts of the PICAM electronics for the SERENA instrument on MPO. The science goal of both instruments is the investigation of the plasma environment of Mercury, the interaction of the solar wind with the surface of Mercury, and the global configuration and dynamics of Mercury's magnetosphere.

After the final selection of the instruments the first breadboard models have been started.

(N. Krupp, J. Woch, H. Fischer, A. Loose, U. Bührke in collaboration with the CETP, Paris, France; ISAS, Tokio, Japan; IWF, Graz, Österreich)

Simulation for the Bepi Colombo laser altimeter – extracting time dependent variations of the topography

ESA's BepiColombo mission will be launched in 2013 and carry onboard the laser altimeter BELA to Mercury. After a five year journey in the inner solar system, the spacecraft will be orbiting the planet and the BELA instrument will measure the distance towards the planetary surface. Mercury's topography will be modelled from the resulting data set in terms of spherical harmonic functions. In our study, we investigate if time-dependent variations of the topography, resulting from solar tides and the physical libration can be recovered. Knowledge of tidal Love number h_2 and the librations amplitude provides constraints on the internal structure of the planet.

We find that the Love number and libration can be determined within a few percent for a continuous coverage of the entire planet over at least two Mercury years. Since the satellite is in an elliptical orbit and thermal restrictions limit the continuous operation of the instrument, data gaps will be inevitable. Therefore simulations are carried out to investigate if topography and time-dependent variations can still be extracted under the envisaged operational conditions. If data are obtained only below a specific spacecraft altitude, topography and the time-dependent variations can still be recovered with somewhat larger uncertainty. In practice, slightly more than half of the planetary surface along the orbit is observed during each pass. A preliminary result is that the data coverage of the pole areas and therefore overlapping data-sets are essential.

We find that data weighting factors are essential tools for accurate topography modelling with respect to regular and irregular data gaps. The input topography, errors of the spherical harmonics for the nominal satellite orbit and for the great data gap due to the elliptical orbit are shown in Fig. 95. The accuracy of the parameter determination will be a function of the surface's point density. The time dependent variations and the impact of data gaps will be further investigated with future simulations and models inverting the data sets up to a high order of the spherical harmonics analysis.

(C. Koch, U. Christensen, M. Hilchenbach)

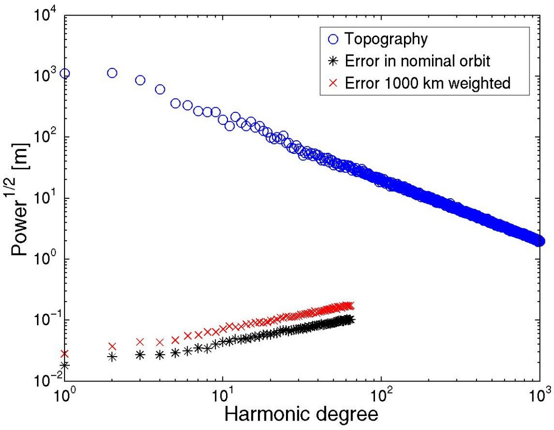

Fig. 95: Input topography (top) and errors for topology inversion (middle and bottom)

Terrestrial planets research – Venus

Venus Express – the first European mission to planet Venus

Venus Express (Fig. 96) is the first European mission to planet Venus. It re-uses the Mars Express spacecraft with minor modifications mainly needed to cope with the harsh thermal environment at Venus. The mission aims at global investigation of the Venus atmosphere and plasma environment and will address some important aspects of the surface physics from orbit. In particular, Venus Express will focus on investigation of the structure, composition, and dynamics of the Venus atmosphere, escape processes and interaction of the atmosphere with the solar wind. The suite of spectrometers and imaging instruments, radio science experiment, and plasma package onboard the Venus Express spacecraft are capable of addressing the mission goals. Scientific payload consists of seven instruments. Five of them were inherited from the Mars Express and Rosetta projects. Two instruments were designed and built specifically for Venus Express.

Fig. 96: Artists rendering of Venus Express at its destination.

The spacecraft was launched on November 9, 2005 from Baykonur (Kazakhstan) by the Russian Sojuz-Fregat launcher. It reached Venus on April 11, 2006. Venus Express carries out observations from a polar 24-hour orbit. They include nadir and limb observations during pericentre passes, off-pericentre global monitoring, solar, stellar and Earth radio occultation, as well as bi-static radar sounding of the surface and solar corona studies. These observations are consolidated in the Science Activity Plan developed in a coordinated way to optimize the payload activity, maximize the overall mission science return, and to fit into the available mission budgets. In 3 Earth years (4 Venus sidereal days) of operations Venus Express will return about 1 Terabits of scientific data. Telecommunications with the Earth will be performed via a newly built ESA antenna in Cebreros (Spain), while another ground station in New Norcia (Australia) and NASA DSN antennae will support the radio science experiment. In comparison to earlier missions to the planet, Venus Express will take advantage of state-of-the-art remote sensing and in situ observation techniques and the capable and versatile spacecraft.

(D. Titov)

Venus Monitoring Camera for the Venus Express mission

The Venus Express mission aims at a global investigation of the Venus atmosphere, plasma environment, and some surface properties from orbit. The instruments PFS and SPICAV inherited from the Mars Express mission and VIRTIS from Rosetta form a powerful spectrometric and spectro-imaging payload suite. Venus Monitoring Camera (VMC) – a miniature wide-angle camera with 17.5° field of view – was specifically designed and built to complement these experiments and provide imaging context for the mission (Fig. 97). The figure shows the VMC instrument with one side of the box taken off.

VMC will take images of Venus in four narrow band filters centered at 365, 513, 965, and 1000 nm all sharing one CCD detector. Spatial resolution on the cloud tops will range from 0.2 km/px in pericentre to 45 km/px in apocentre where full the Venus disc will be in the field of view. VMC will significantly contribute to the study of cloud structure and morphology, atmospheric dynamics, and surface imaging. The UV channel will be used to investigate the distribution and nature of the unknown UV absorber, to determine the wind field at the cloud tops (70 km) by tracking UV features, and to study wave phenomena. The night side observations in the near-infrared filter at 1000 nm, which is centered at the atmospheric transparency "window", will provide for the first time thermal imaging of the Venus surface from orbit. These observations will determine spatial distribution of surface temperature and will search for active volcanoes. This channel will also yield global wind field in the main cloud deck (50 km) by tracking near-IR features. The other near-IR channel (965 nm) centered at the absorption band of atmospheric water will investigate H_2O spatial distribution at the cloud tops on the day side and in the lower 10 km at night. The visible channel at 513 nm was designed to map the O_2 airglow and its variability on the night side. The VMC images and movies of the cloud motions Venus atmosphere will be of significant interest for the public outreach programme.

Fig. 97: The Venus Monitoring Camera for the Venus Express mission.

The tests in cruise included the observations of stars, Venus, and Earth-Moon system and stray light tests. They demonstrated good performance of the instrument. Fig. 98 shows false colour image of the Earth and Moon taken by VMC from a distance of 3.5 Mio km. Both planets were only few VMC pixels across. The visible and UV channels were strongly overexposed.

The VMC instrument was designed and manufactured in cooperation with the Institute of Computer and Communication Network Engineering (IDA, Technical University, Braunschweig) and the Institute for Planetary Exploration (DLR, Berlin) with the MPS being the PI institute.

(W. Markiewicz (PI), D. Titov, H. U. Keller, H. Perplies, I. Szemerey, I. Sebastian, M. Wedemeier, R. Moissl)

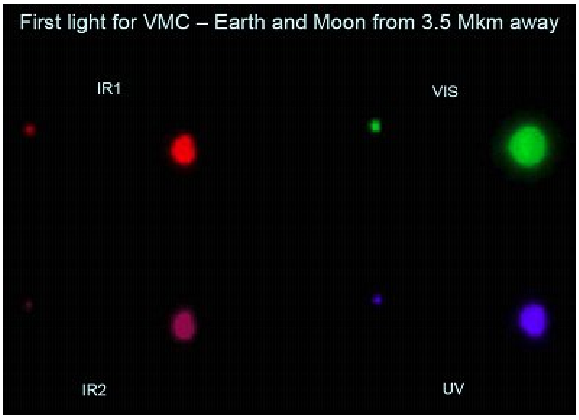

Fig. 98: False colour image of the Earth and Moon taken by VMC from a distance of 3.5 Mio km.

The Plasma Environment of Venus – Venus Express Aspera-4

On 9 November 2005 the Venus Express spacecraft was launched and reached the planet on 11 April 2006. One of the goals of the mission is the investigation of the ionosphere of Venus at solar minimum. Our current knowledge of the Venus ionosphere is based on the Pioneer Venus Orbiter which operated more than 20 years ago at solar maximum. It showed that the ionosphere has a very fragmented structure (Fig.99). At solar minimum the reduced solar radiation will probably result in a much weaker ionosphere. How this will influence the interaction of solar wind ions with the atmosphere is unknown. The Aspera-4 instrument on board Venus Express measures ions and energetic neutrals while the spacecraft is orbiting the planet. It will determine the structure of the ionosphere and the total escape rate of atoms from the planet. This information can then be used to model the atmospheric history of Venus.

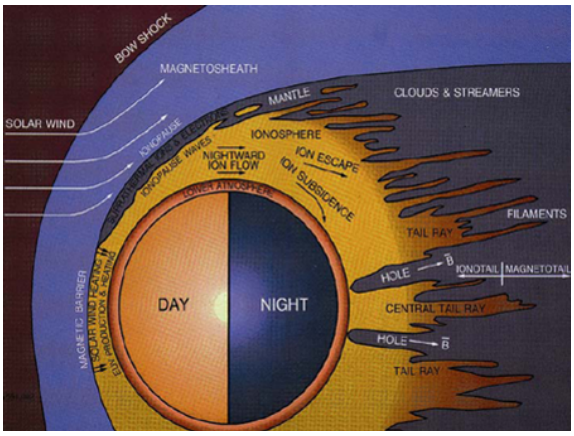

Fig. 99: Structure of the ionosphere of Venus after Brace and Kliore (1991).

(M. Fränz, E. Dubinin, J. Woch, N. Krupp)

Terrestrial planets research – Moon

SIR-2 – a NIR spectrometer for the first Indian mission into interplanetary space

Lunar science is undergoing something of a renaissance. The recent success of ESA's SMART-1 mission, a renewed interest in returning astronauts from the USA to the Moon, and the stated long-term space goals of newcomer nations, such as China, India and Japan, have put lunar science back into the limelight.

The ESA SMART-1 technology mission to the Moon, launched on 27 September 2003, carries a prototype light-weight instrument developed by the MPS for Solar System Research to test the concept for a spot spectrometer to map the lunar mineralogical composition in the NIR range.

To make the transition from instrument technology development to science, MPS participated in the Indian Space Agency's (ISRO) announcement of the first Indian Mission into interplanetary space. ISRO will send its first interplanetary spacecraft, Chandryaan-1, to the Moon (Fig. 100).

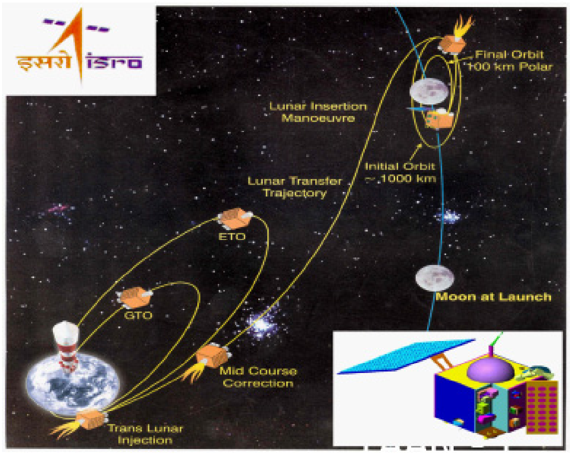

Fig. 100: The Chandrayaan-1 mission concept to the Moon.

The purpose of the baseline science mission is to fly a lunar polar orbiter at an altitude of 100 km for two years. The main scientific objective of the mission is high resolution remote sensing in the visible, near IR, low energy X-rays and high energy X-rays.

The mission goals include:

1. Preparing a 3-D atlas with a spatial and altitude resolution of 5 – 10 m;
2. Chemical mapping of the global surface for the main rock forming elements Mg, Si, Al, Ca, Fe, Ti at a 10-km resolution;

3. Mineralogical maps of the Moon at high resolution;
4. Mapping of high Z elements, such as 222Rn, U, Th, Gd, at a 20-km resolution.

These photogeological, mineralogical, and chemical maps would allow one to distinguish between different geological units, in order to study the formation of the Moon by (1) giant impact, the partial melting which formed a magma ocean and solidified crust,(2) the late heavy bombardment by large planetesimals which formed basins, and (3) the evolution of mare volcanism.

In the framework of this mission we are developing and building in-house an upgraded, highly compact, monolithic grating, near-infrared spectrometer based on SIR, flown on ESA's SMART-1 mission, covering a wavelength range from 0.9 to 2.4 μm. SIR-2 is intended to accomplish a highly integrated study of the lunar mineralogy, together with two further optical instruments from a lunar polar circular orbit, thereby extending the wavelength range of Chandrayaan-1's Hyper Spectral Imager into the extended near-infrared region. This much wider range covering the 1- and 2-μm absorption band is a necessary condition to be able to distinguish unambiguously between the major lunar minerals, thereby making this instrument far superior compared to older spectrometers using 1.7-μm cutoff detectors. SIR-2 has a spectral resolution of 6 nm/pixel and an angular resolution of 2.2 millirad.

SIR-2 will address the surface-related aspects of lunar science in five broad categories:

- Analyze in unprecedented detail the lunar surface in various geological/mineralogical and topographical units;
- Study the vertical distribution of crustal material;
- Investigate the process of basin, maria and crater formation on the Moon;
- Explore "Space Weathering" processes of the lunar surface;
- Survey mineral lunar resources for future landing sites and exploration.

(U. Mall and A. Nathues)

Terrestrial planets research – Mars

The Martian magnetosphere and ion escape

The solar wind interaction with Mars leads to the formation of the induced magnetosphere which is strongly depleted in solar wind particles. Fig. 101 shows the map of median electron fluxes with energy $E_e = 40 - 60$ eV based on the observations carried out by ASPERA-3 over 2 years of Mars Express operation near Mars. The position of the magnetospheric boundary is controlled by the solar wind ram pressure as well as by local crustal magnetization and direction of the interplanetary magnetic field. Solar wind drives the magnetospheric plasma of planetary origin into a global motion providing the induced escape of oxygen and carbon dioxide at Mars. Fluxes of planetary plasma are mainly confined within the induced magnetosphere.

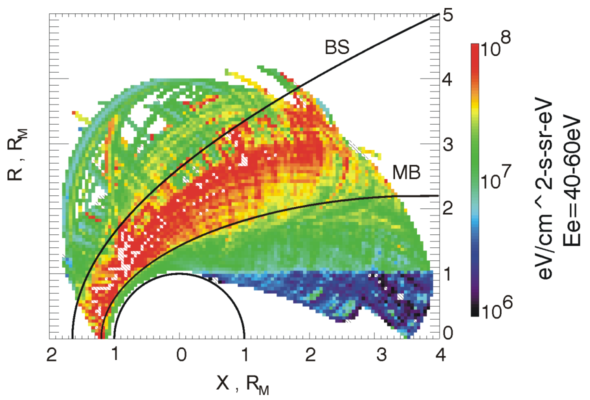

Fig. 101: Map of median electron fluxes ($E_e = 40 - 60$ eV)in cylindrical coordinates. These electrons display clearly the positions of the bow shock (BS), the magnetospheric boundary (MB) and a magnetospheric cavity void of solar wind electrons.

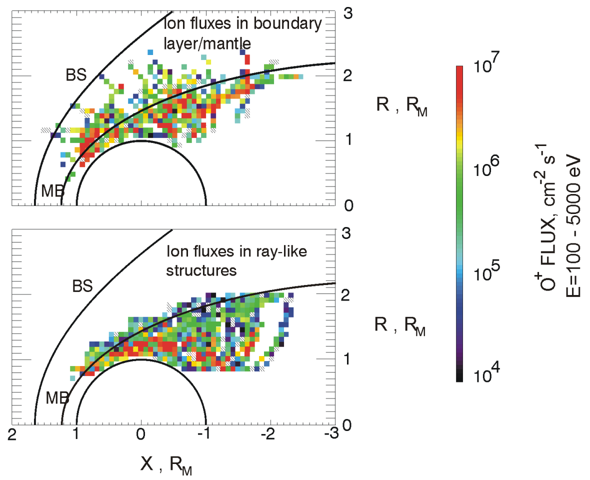

Fig. 102: Maps of oxygen ion fluxes in cylindrical coordinates in the boundary layer and 'rays' which form the main channels for ion escape.

Fig. 102 depicts the fluxes of oxygen ions originated from the extended Martian atmosphere. Two main channels for escaping planetary ions are readily identified, the boundary layer/mantle adjacent to the magnetospheric boundary and ray-like structures centered

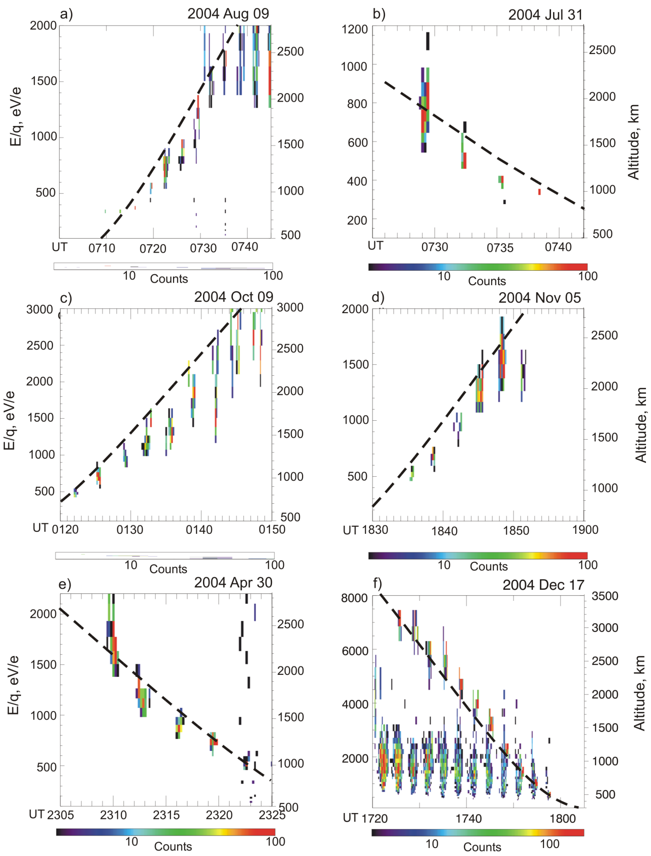

Fig. 103: Energy-time spectrograms of the ion beams on several Mars Express orbits. Dashed curves depict the altitude of the spacecraft above the Mars surface.

close to the wake boundary. The third important channel, plasma sheet is not well explored yet because of power constraints of the spacecraft in the optical planetary shadow.

(E. Dubinin, M. Fränz, J. Woch)

Ion extraction from Mars

Observations made by the ASPERA-3 experiment onboard the Mars Express spacecraft found within the Martian magnetosphere beams of planetary ions energy linearly increasing with altitude (Fig. 103). A such dependence suggests ion acceleration in the electric fields. The values of the electric field evaluated from ion energization occur close to the typical values of the interplanetary motional electric field that imply an effective penetration of the solar wind electric field deep into magnetosphere or generation of large fields within the magnetosphere. The existence of large electric fields extracting planetary ions explains an effective scavenging of oxygen and carbon dioxide from Mars.

(E. Dubinin, M. Fränz, J. Woch)

Ray structures near Mars

The ASPERA-3 experiment onboard the Mars Express spacecraft observed near the wake boundary a spatially narrow ray-like plasma structure stretched into the tail. This structure is composed of magnetosheath-like (but with higher temperature) electrons and planetary ions (Fig. 104). Analysis of proxy magnetic field configurations inferred from the Mars Global Surveyor data and corresponding to the Mars Express orbits suggests that such rays are formed due to magnetic field tensions generated by draping interplanetary magnetic field lines slipping around the planet and pushing a planetary plasma into the tail. Such a mechanism suggests a strong asymmetry in plasma intrusion and, correspondingly, an asymmetry of ion scavenging controlled by the orientation of the IMF (interplanetary magnetic field) (Fig. 105).

(E. Dubinin, M. Fränz, J. Woch)

Ionospheric photoelectrons at Mars

Spectra of photoelectrons at Mars contain the characteristic “discrete spectral lines” in the energy range 20 – 30 eV due to enhanced solar radiation in the He^+

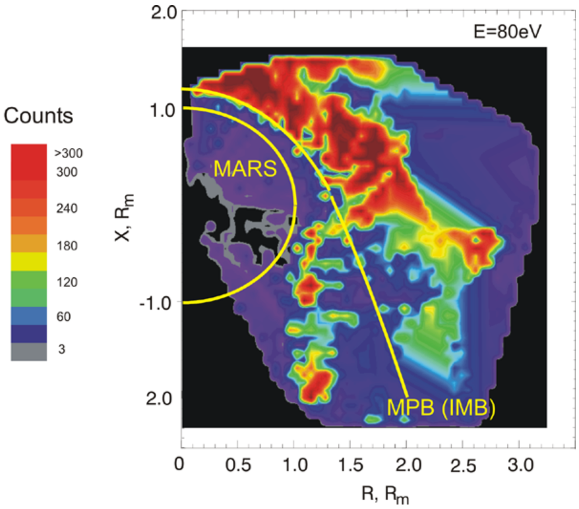

Fig. 104: Image of the electron fluxes at a fixed energy (E_e = 80 eV) near Mars in cylindrical coordinates (~50 Mars Express orbits). MPB denotes the magnetic pileup boundary found from the Mars Global Surveyor observations. A ray-like structure near the wake is clearly displayed.

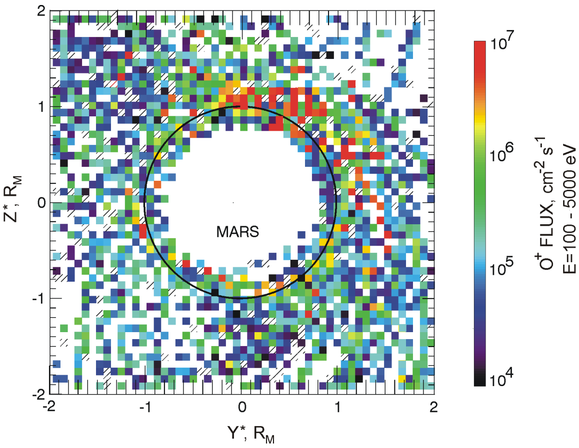

Fig. 105: Image of the O^+ fluxes on the Mars Express orbits at which the ray structures were observed. The data are presented in the IMF coordinate system determined by the IMF orientation. The Y^* and Z^* axes are along the interplanetary magnetic (electric) fields, respectively. A clustering of ray-events near the "northern magnetic poleïs in a reasonable agreement with asymmetry of the pile up of the magnetic field.

emission at 30.4 nm. These peaks are used as tracers of ionospheric plasma at Mars. The ASPERA-3 observations onboard Mars Express have shown that photoelectrons can be detected at large distances from the planet (Fig. 106). They are often observed close to the nominal magnetospheric boundary, implying an important role of the ionospheric plasma as an obstacle to solar wind. The main mechanisms responsible for the transport of ionospheric plasma to the tail are the bulk motion driven by the solar wind/ionosphere interaction and "upward" motion along the magnetic field lines and, particularly, along the reconnected crustal field lines which are stretched into the tail (analog of polar wind). The observations demonstrate the essential losses of the ionospheric matter due to the direct exposure of the Martian ionosphere to solar wind.

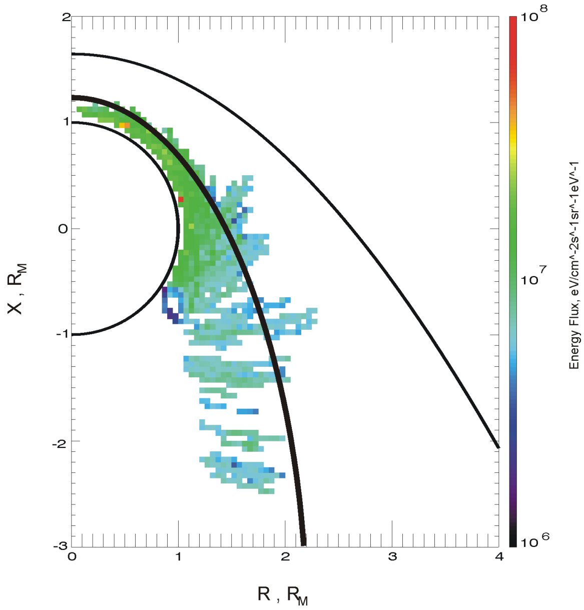

Fig. 106: Sites in cylindrical coordinates where the ionospheric photoelectrons were observed. Nominal positions of the bow shock and magnetospheric boundary are given. Colour shows energy fluxes of photoelectrons centered near the CO_2-peaks (δE_e=5 eV)

(E. Dubinin, M. Fränz, J. Woch)

Three-dimensional hybrid modelling of the solar wind/Mars interaction

Influence of solar UV flux on solar wind induced escape of planetary ions at Mars was studied by using a three-dimensional multi-species global hybrid model developed at CETP – Centre d'Etude des Environnements Terrestre et Planétaires (France) (Modolo *et al.*, 2005). The model describing dynamics of the main ion species (H^+, He^{++}, O^+, O_2^+) is in reasonable agreement with the observations made by Mars Express and Mars Global Surveyor. Fig. 107 shows how the interplanetary magnetic field lines are draped around the planet, creating the induced magnetosphere with two magnetic field lobes separated by the plasma sheet. The results show a transition from the solar wind dominated plasma to the planetary plasma at the magnetic pile up boundary. The motional electric field of the solar wind flow creates a strong asymmetry in the Martian plasma environment. The fluxes of escaping planetary ions strongly depend on solar activity while the position of the main boundaries are much less sensitive to solar UV. Total escape fluxes of H^+

ions at solar minimum (maximum) are estimated as $\sim 4.3 \times 10^{25} s^{-1}$ and $1.1 \times 10^{25} s^{-1}$, respectively. The corresponding escape fluxes of oxygen ions are $\sim 0.5 \times 10^{24} s^{-1}$ and $\sim 2.4 \times 10^{24} s^{-1}$.

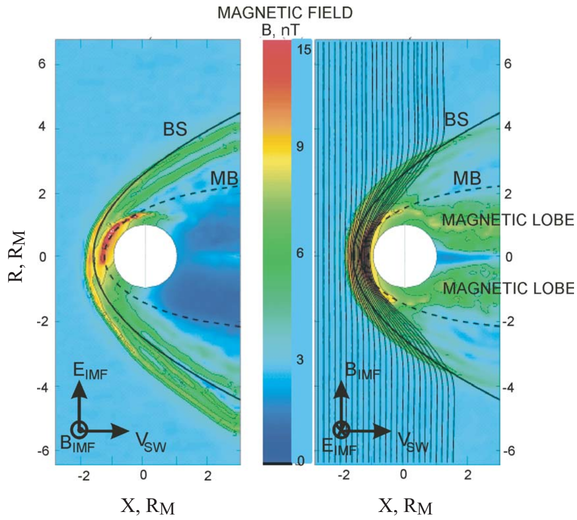

Fig. 107: Maps of the magnetic field strength in two different planes. Magnetic pile up boundary (MPB) discovered by Mars Global Surveyor which correlates with the magnetospheric boundary (MB) is reproduced in 3-D hybrid simulations. Asymmetry caused by the interplanetary electric field is revealed.

(E. Dubinin in collaboration with G. Chanteur and R. Modolo (CETP, Velizy, France))

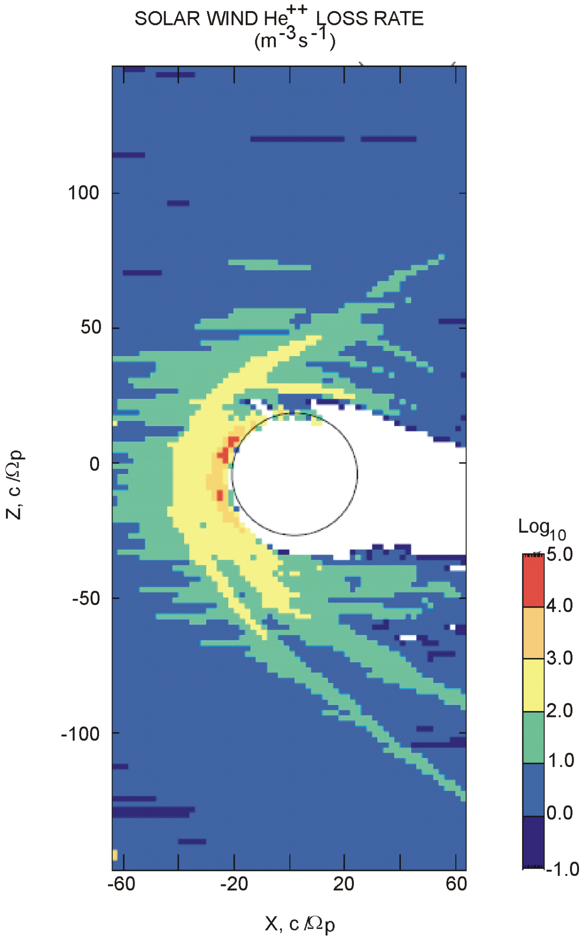

Fig. 108: Map of loss rate of solar wind ions He^{++} which are transformed to He^{+} ions and He atoms as a result of charge exchange processes. The distances are normalized to the proton inertial length.

(E. Dubinin, M. Fränz in collaboration with G. Chanteur and R. Modolo (CETP, Velizy, France))

Capture of solar wind He^{++} ions by the Martian exosphere

It was thought that losses of helium at Mars are balanced by the interior outgassing. However the recent observations and theoretical estimates (Krasnopolsky and Gladstone, 2005) show that radioactive decay of U and Th with subsequent outgassing can explain only 1/3 of the losses. It is suggested that the remaining helium is captured from solar wind due to charge exchange of α-particles in the Martian exosphere. Researchers at CETP (France) developed a consistent multi-species three-dimensional hybrid model of the interaction of the solar wind consisting of protons, α-particles and electrons with Mars provides a tool to calculate for the first time consistently the deposition of solar wind helium into the Martian atmosphere. During solar minimum activity a total loss of α-particles due to charge exchange with hydrogen and oxygen atoms is about of $6.8 \times 10^{23}\ s^{-1}$. This value can explain a 'deficit' of helium sources at Mars. Fig. 108 shows a map of He^{++} loss rate in the plane containing the solar wind speed (X-axis) and the interplanetary electric field $-V_{sw} \times B_{IMF}$ (Z-axis).

Plasma shielding above Mars crustal fields – Mars Express ASPERA-3 observations

In 1996 remnant magnetic fields were discovered in the Martian crust by the magnetometer on board the Mars Global Surveyor (MGS) spacecraft. Since then it has been discussed how these crustal fields influence the interaction of the solar wind with the Martian ionosphere. Using data (Fig. 109) of the ASPERA-3 instrument on board the European Mars Express spacecraft we investigated the effect of the Martian crustal fields on electrons intruding from the magnetosheath. For the crustal field strength we used published data obtained by the Mars Global Surveyor MAG/ER instrument for a fixed altitude of 400 km. On the nightside of the planet the crustal fields efficiently shield the ionosphere from intruding electrons (Fränz *et al.*,

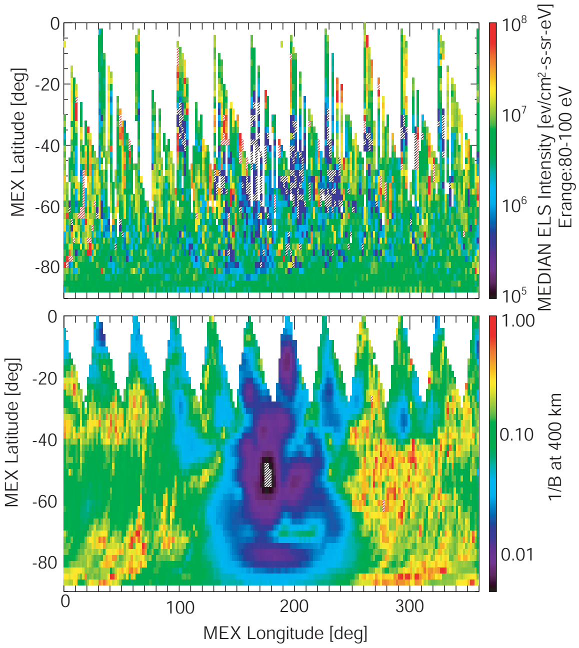

Fig. 109: Top: Median energy flux of 80 – 100 eV electrons measured by the electron sensor of the Mars Express (MEX) ASPERA-3 instrument below 800 km altitude on the nightside for all orbits between 1 Feb 2004 and 1 Mar 2005 as a function of Mars planetocentric eastern longitude and latitude. Bottom: Inverse of the total crustal field strength [1/nT] at 400 km altitude from MGS data.

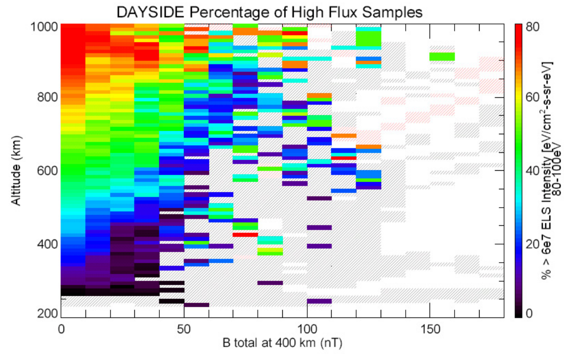

Fig. 110: Energy flux of 80 – 100 eV electrons measured by the electron sensor of the Mars Express ASPERA-3 instrument for all orbits between 1 Feb 2004 and 1 Mar 2005 as a function of total crustal field strength at 400 km altitude and Mars Express spacecraft altitude for the dayside. Shown are the percentages of samples above $6 \cdot 10^7$eV/(cm^2 s sr eV).

Icarus, **182**, 406–412, 2006).

(M. Fränz, E. Roussos, E. Dubinin, J. Woch)

Plasma intrusion above Mars crustal fields – Mars Express ASPERA-3 observations

On the dayside of Mars the magnetosheath is pressed against the ionosphere and the interplanetary magnetic field is deviated forming the Magnetic Pile-Up Boundary (MPB). This boundary also builds a barrier for magnetosheath electrons. We used statistics on 13 months of 80 – 100 eV electron observations to show that the electron intrusion altitude determined by a probability measure is approximately linearly dependent on the total field strength at 400 km altitude (Fig.110). We showed that on the dayside the mean electron intrusion altitude describes the location of the MPB such that we can quantify the effect of the crustal fields on the MPB (Fränz *et al.*, Icarus, **182**, 406–412, 2006).

(M. Fränz, E. Roussos, E. Dubinin, J. Woch)

Martian aerosols and HRSC stereo images

HRSC is the stereo camera of Mars Express, Europe's mission to Mars. Since the beginning of 2004 the camera has mapped a large fraction of the red planet in stereo and in colour at resolutions of 15 – 50 meters. Digital terrain models, routinely derived from the stereo information, have a similar resolution, both in the horizontal and in the vertical. The mission still continues, and now is in the first extended phase.

Since the time of Viking it is well known that the Martian atmosphere contains large amounts of dust and other aerosols that invoke a strong diffuse illumination onto the surface. The spectral characteristics of the diffuse illumination reflect the optical properties of the aerosols and are different from that of the direct solar illumination. Interpreting spectral observations of the surface requires careful analysis of this atmospheric effect. The required analysis yields, at the same time, information on the compositions and properties of the aerosols. HRSC stereo imagery offers a unique and powerful tool to study the Martian atmosphere.

The magnitude of atmospheric effects in the first place depends on the optical depths of the atmosphere. Optical depths can be measured from HRSC stereo imagery with the so-called stereo method; the nadir view has a shorter atmospheric path than the forward and backward ones and thus, given that the atmosphere usually displays little contrast, differences in contrast between the images yield a measure of the optical depth. We have developed, and extensively tested, software based on this method. Our analysis of HRSC images shows that the total optical depth of the atmosphere strongly depends on the altitude of the surface. On average the airborne dust appears to have the same scale-height as the atmosphere itself, probably meaning that the dust is more or less well mixed. However, locally we found strong deviations.

By now, our analysis of HRSC images has made it clear that aerosol properties show important differences from place to place and from time to time. For example, during early 2004 the average airborne dust-particle over Gusev crater probably was considerably larger than that some years earlier near the Pathfinder landing-site. Another example: most limb scans show thin whitish or bluish hazes above altitudes of about 50 km. Such hazes are highly variable and localized, but typically may have optical depths of order 0.01, as compared to 0.5, or often even much more, for the airborne dust. Somewhat surprisingly, it appears that these very thin high altitude hazes significantly increase the albedo of the planet. The likely reason is that high altitude hazes contain small, and probably icy, particles that show strong backscattering. As an effect, the high hazes directly reflect a lot of sunlight back into space. In contrast, the airborne dust sends most of the scattered solar radiation towards the surface.

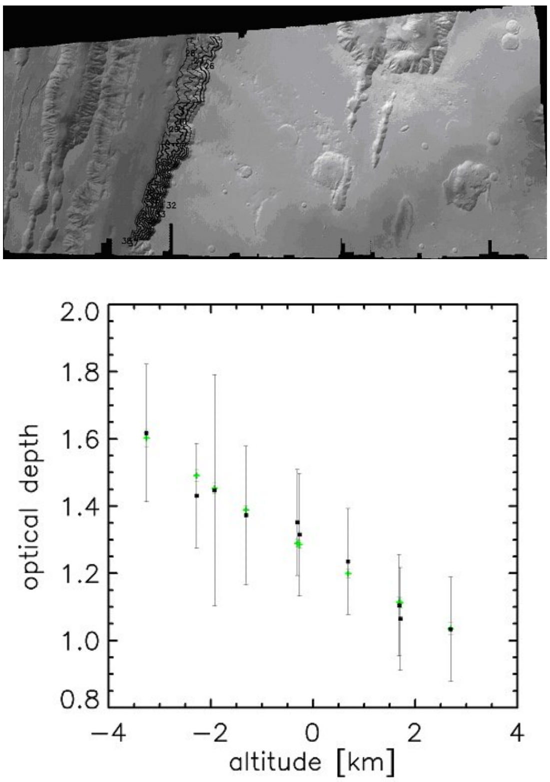

Fig. 111: On the Norhern slopes of Vallis Marineris the optical depths show a very clear correlation with the altitude of the surface. Black: measured optical depths with one sigma errors. Green: the result of a linear-log fit on the measured points. This fit yields a scale-height for the airborne dust of 14.0 km +1.3 -1.1 km, which is similar to that of the atmosphere itself.

(N. M. Hoekzema, W. J. Markiewicz, L. Petrova, H. U. Keller)

Lee wave clouds in the Martian atmosphere: observations by HRSC

Lee wave clouds are a well-known phenomenon in the Earth's atmosphere. Usually they show up as large and dense clouds that hover over the tops of the mountains. They can prevail for long periods of time, and, even if there are very strong winds, they usually are almost stationary. Lee wave clouds are formed by vertical deflection of winds on a topographic obstacle; the air is forced to oscillate in the lee of the obstacle. In the crest of the wave, air rises up to the cooler region where condensation occurs due to adiabatic cooling. In this way, often a regular train of elongated clouds forms. This train of clouds is aligned orthogonal to the prevailing wind if the obstacle is a mountain range or an isolated mountain.

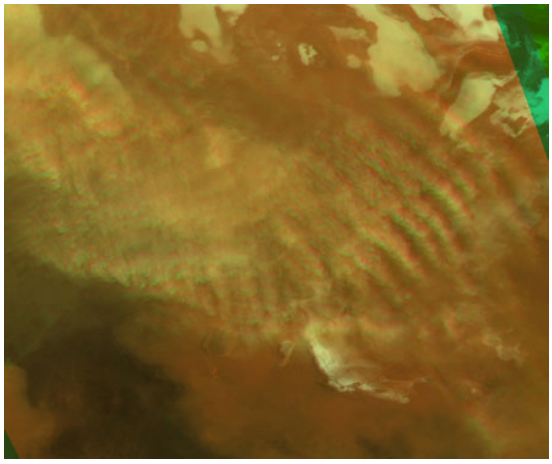

Fig. 112: Subsection of HRSC image from orbit 1096 of Mars Express. It shows distinct lee wave cloud over North polar cap.

In the Martian atmosphere lee wave clouds were observed for the first time by Mariner 9. They were subsequently regularly detected by Viking Orbiter and Mars Global Surveyor. The High Resolution Stereo Camera (HRSC) onboard Mars Express has atmospheric observations as one of the priorities of its scientific program. From the beginning of the mission it has detected quite a number of clouds in the Martian atmosphere. Several of them are lee wave clouds in the middle latitudes and in the polar regions. These polar lee wave clouds appear superimposed on the haze and streak clouds. The wavelength, height and propagation characteristics of lee waves are mostly determined by the velocity of driving wind and the obstacle dimensions. Other critical parameters include atmospheric temperature and moisture in the flow. There is a simple connection between the wavelength of produced lee wave and the velocity of horizontal wind. If the lee wave structure is distinct enough to measure its wavelength, it can be used for estimation of wind

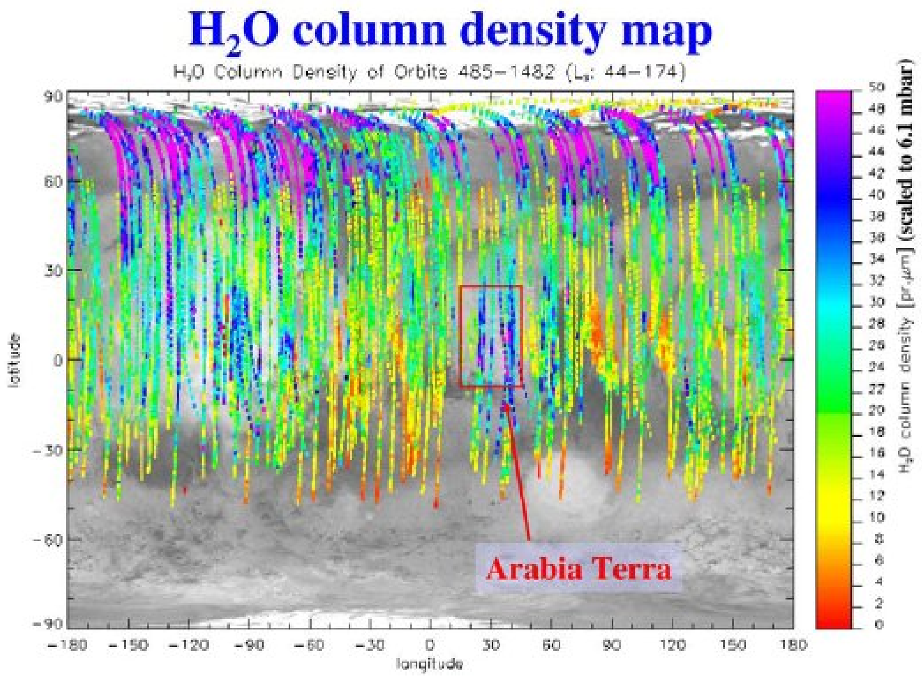

Fig. 113: Global distribution of atmospheric water during the Northern spring and summer derived from the PFS spectra in the 2.56 m H_2O band.

speed over the area. Wind speed inferred from several HRSC lee wave images is in the range 24.5 – 25.2 m/s. This result is in agreement with measurements of Martian wind speed from Hubble Space Telescope and estimates from dust devil motion.

Combination of physical properties of lee wave clouds and stereo imaging techniques of HRSC gives us the possibility to measure height of these clouds in the atmosphere (Fig. 112). Height of clouds marks height of ice condensed level which is of big interest for understanding of atmospheric processes on Mars. As an example we calculated height of lee wave cloud from the image taken during orbit 1107 of Mars Express, which appeared to be 5.2 km above Martian surface.

(G. Portyankina, W. J. Markiewicz)

Monitoring the atmospheric water on Mars by the PFS and OMEGA experiments onboard Mars Express

The abundance of atmospheric water on Mars strongly varies with latitude, season, location, and local time. This indicates that the trace gas is involved in a number of physical and chemical processes which are not completely understood. One of the primary goals of the ESA Mars Express orbiter mission to Mars is to study the water cycle on the planet. Three experiments onboard Mars Express – high-resolution spectrometer PFS, imaging spectrometer OMEGA, and solar occultation spectrometer SPICAM – have been monitoring the abundance of atmospheric water for about two years. MPS is involved in the analysis of data from PFS and OMEGA experiment.

Fig. 113 shows the global distribution of atmospheric water on Mars derived from the PFS measurements in the Northern spring-summer season. Strong increase of water abundance in high northern latitudes is caused by the sublimation of the seasonal polar cap. There are also two local maxima at low latitudes. One of them is located above Arabia Terra and coincides with the region of enhanced subsurface water content observed by the neutron detector HEND on the Odyssey spacecraft. The other one corresponds to the Tharsis region.

The OMEGA experiment confirmed strong enhancement of the water mixing ratio above the volcanoes (Fig. 114) – the anomaly first discovered by the ISM/Phobos mapping spectrometer. The increase in mixing ratio combined with the pressure drop on the volcanoes results in H_2O column density equal to that above the lowlands. Such behaviour suggests that the atmospheric water is not uniformly mixed with altitude but is rather confined to a shallow layer close to the surface, and its abundance is governed by the exchange with regolith.

(M. Tschimmel, L. Maltagliati, D. Titov)

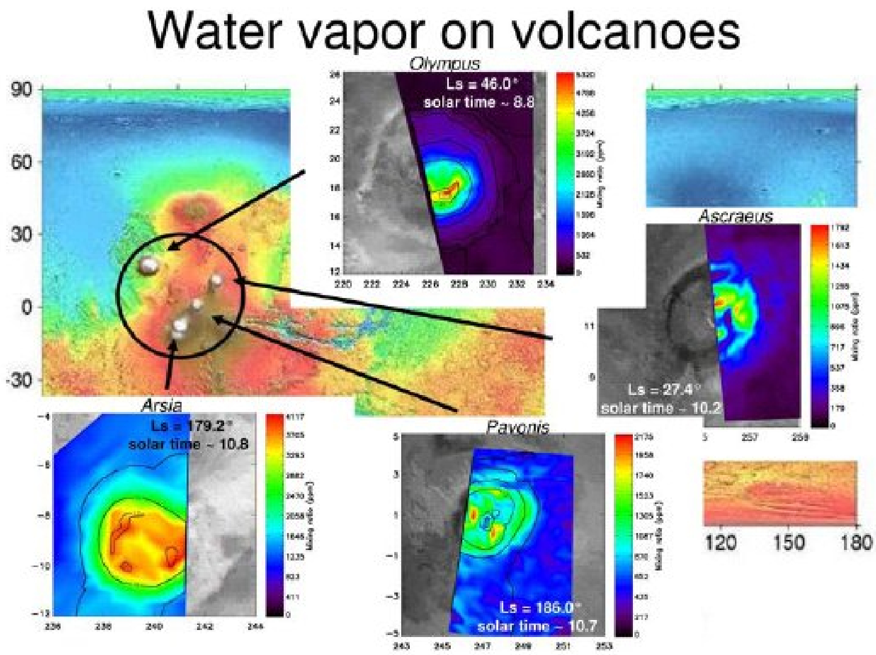

Fig. 114: Maps of atmospheric water mixing ratio in the vicinity of Martian volcanoes derived from the OMEGA imaging spectrometry.

Modelling of the Martian atmosphere with MAOAM

MAOAM – (the former MART-ACC, see annual report 2002 – 2003) describes the dynamics and chemistry of the Martian atmosphere from ground to above 100 km altitude. The basic idea of the project is to create a tool that helps to interpret data to be provided by future experiments sounding the atmosphere from ground up to the thermosphere. Especially submillimeter instruments have the capability to highly resolve the Martian Atmosphere in this entire altitude range. We are involved in the submillimeter instruments Herschel-HIFI and SOFIA-GREAT (see this issue) and hope to get access to the new ground-based submillimeter facilities APEX and ALMA. Furthermore we have been involved in the ESA study of the Submillimeter Wave Instrument (SWI), a potential payload for the ExoMars Orbiter. Among others, this instrument would provide highly accurate temperature and Doppler wind data (see Fig. 115).

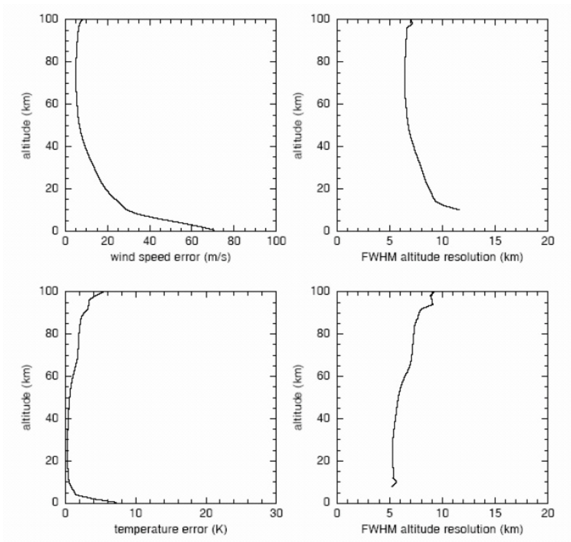

Fig. 115: SWI temperature and Doppler wind retrieval simulations: Errors and vertical resolution.

Progress in the model development: A detailed description of the Martian GCM (General Circulation Model) status can be found in Hartogh *et al.* (2005). Compared to the 2003 version called Mart-ACC, a number to changes have been performed. A brief listing of the changes follows:

- The numerical stability has been improved in a number of steps including optimization of the time integration scheme, the introduction of a staggered vertical grid, a vertically varying horizontal diffusion and an update of the convective adjustment scheme.
- The smoothed topography used in Mart-ACC has been replaced by the MOLA (Mars Orbiter Laser Altimeter)topography. Currently, our model works with the full topography at all reso-

lutions.

- The surface physics has been improved by a new parameterization which is based on the calculations of the energy balance on the surface. It uses the available measurements (TES – Thermal Emission Spectrometer) of the surface thermal inertia and the albedo map.

- The radiation scheme has been changed using a new non-LTE heating/cooling rate scheme representing an optimized version of the ALI-ARMS code by our co-workers A. Kutepov and A. Feofilov. Simultaneous with the model refurbishment a dust radiation scheme adapted from the Japanese CCSR/NIES general circulation model (Kuroda *et al.*, 2005). The dust scheme was validated on Submillimeter Astronomy Satellite (SWAS) data of the 2003 global dust storm on Mars. The Mart-ACC gravity wave parameterization has been replaced by a scheme of Medvedev and Klaassen, coupled for the first time with orographic sources of gravity waves.

- A new MAOAM chemistry-transport-module (CTM) has been developed and tested. Fig. 116 shows first results on the diurnal variation of ozone in the Martian atmosphere.

- The model code consists of parts written in FORTRAN and C. The structure of the code has been completely redesigned to a user friendlier version. At the same time multi-processor capability has been implemented and tested on a 48 - processor Opteron Cluster.

One of the first results of MAOAM was that the meridional circulation of the Martian atmosphere is driven by eddies rather than the hemispheric thermal contrast, as derived by other models. Related to this, MAOAM finds stronger winter polar warmings (see Fig. 117).

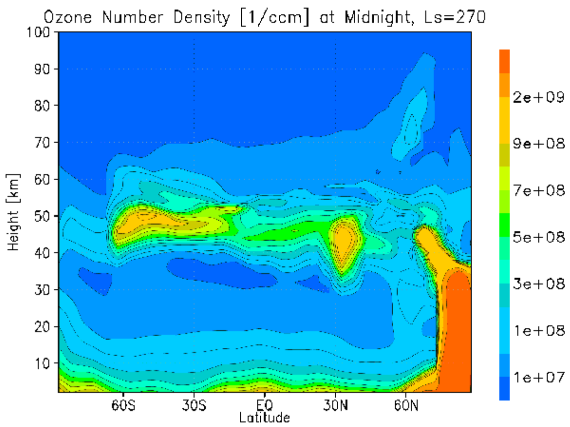

Fig. 116: Ozone number density at midnight during Northern winter solstice.

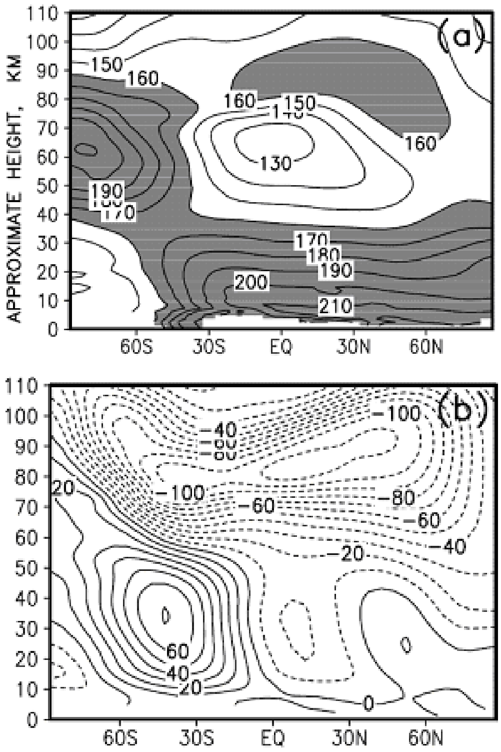

Fig. 117: (a) Zonally averaged temperature and (b) zonal wind simulated for Ls = 90. The shaded area in (a) denotes the temperatures above 160 K

(P. Hartogh, A. Medvedev, T. Kuroda, C. Jarchow, R. Saito, G. Sonnemann, G. Villanueva in collaboration with U. Berger and M. Grygalashvyly (IAP Kühlungsborn), A. Feofilov and A. Kutepov (University of Munich), and H. Elbern (University of Cologne))

Mars climate simulator

Like the Earth, Mars has polar ice caps. From satellite observation we know that the Martian polar regions show structures, the so-called polar layer deposits, which lead to the assumption of periodic climate changes of the polar caps. To understand how the layered deposits and the ice-caps evolve during Mars' strong orbit driven climate variations, numerical simulation of the involved physical systems atmosphere and ice-sheet are necessary. The climates at different orbit conditions are constructed with a General Circulation Model (GCM) of the Martian Atmosphere. To understand the behaviour of the Martian ice caps at different climatic conditions a model is needed to simulate the ice physics. SICOPOLIS, a polythermal ice-sheet model, is used for this purpose.

With the help of the coupled models, we have been able to show that the ice caps show different behaviour at distinct obliquities. A strong inclination of the rota-

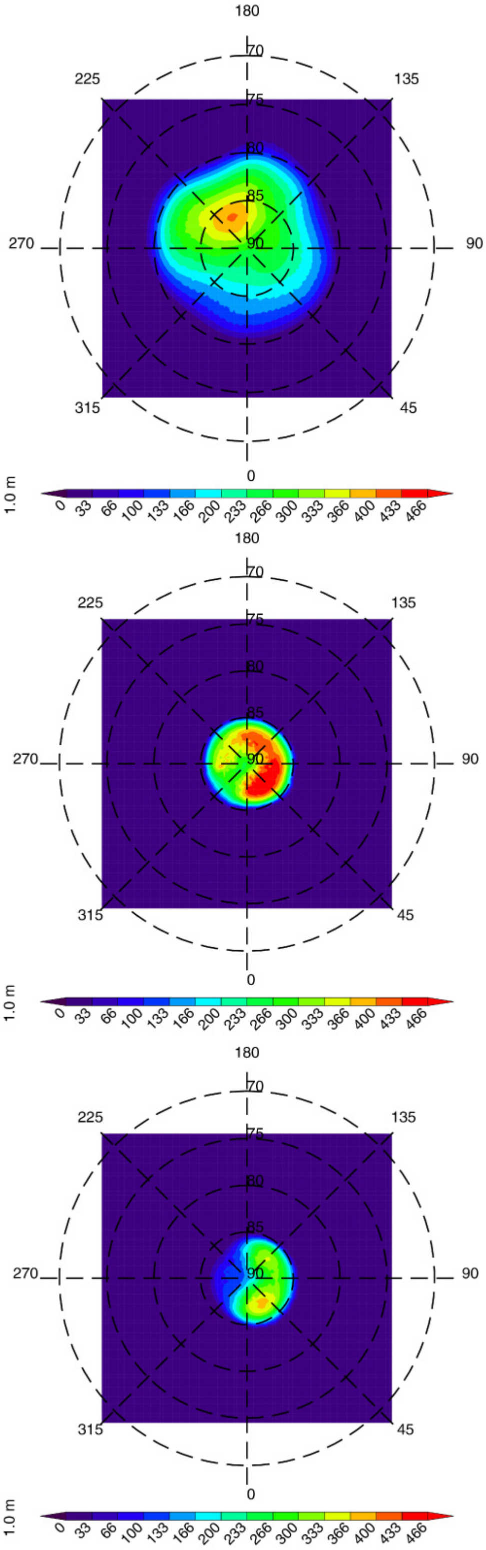

Fig. 118: Height of the ice-sheet after 5 Ma, starting the integration from the present day topography for three different obliquities: (a) 15°, (b) 25.2° and (c) 35°.

tion axis leads to a strong ablation during the summer month through the higher insolation. This seemingly counterbalances the increased polward transports of humidity in the warmer polar atmosphere. Further it was found that through the albedo feedback, it is easier to sustain an ice-cap at high obliquities than to create a new one. The model results show that an obliquity angle of no more than about 18° is needed to start the build-up of a new north polar cap. This work was done in cooperation with the partners at the universities of Sapporo and Hamburg.

(O. J. Stenzel, R. A. Mahajan, B. Grieger, H. U. Keller)

Thermal evolution models for Mars

The volcanism on Mars is concentrated in only two regions, in the Elysium region and much more prominent in the Tharsis region. Together with strong anomalies in the gravity field and the areoid these observations lead to the assumption that thermal convection in the martian mantle differs from that in the Earth's mantle and that the convection pattern could be dominated by only two strong plumes under Tharsis and Elysium.

A possible reason for this strong reduction to only a few plumes can be the endothermic phase transition in the mineral structure from γ-spinel to perovskite and magnesiowüstite, which may appear in Mars close to the core-mantle boundary (cmb) (Harder and Christensen, 1996).

An existing 3-D numerical convection code has been adopted to the specific features on Mars and extended to allow for more realistic simulations of the thermal evolution of the planet. We include the endothermic phase boundary from γ-spinel to perovskite and magnesiowüstite close to the cmb. The viscosity is depth-dependent and varies with the horizontally averaged temperature following an Arrhenius term. This viscosity law allows us to model the evolution of the lithosphere and takes into account that the convection strength decreases with time due to the viscosity increase, which has an important influence on the cooling rate of the system. The model also includes the cooling of the core. Its cooling rate is proportional to the heat flux into the mantle. In extended models we investigate the influence of a depth-dependent thermal expansivity α and the depth-dependence of the thermal conductivity λ which varies with the horizontally averaged temperature. The effects of these additional depth-dependencies on the thermal evolution and the convection pattern are worked out. The simulations were carried out in both the Boussinesq- and the extended Boussinesq-approximation.

The combination of both additional depth-dependencies shows a strong reduction in the number of upwellings. The influence of the endothermic phase transition from γ-spinel to perovskite and magnesiowüstite on the convection pattern and the thermal evolution is reduced. A complete model which also includes the exothermic phase transitions leads again to a convection pattern with two upwellings which could explain the concentrated volcanism on Mars today. Both depth-dependent parameters α and λ increase the heat flux at the cmb in the beginning of the evolution. In combination the early heat flux out of the core is probably high enough to allow for thermal convection in the core and for a thermally driven dynamo. This early active dynamo could be the reason for the strong magnetisation of the old part of the martian crust. Today the heat flux is too low to allow for a thermally driven dynamo. The comparison of the interpolated temperature structure in the core with the melting conditions of iron with 10% to 14% sulfur demonstrates that Mars has not yet frozen out an inner core. The martian core is completly liquid and does not allow for chemical convection as a driving mechanism for a dynamo today. The failure of both a thermally and a chemically driven dynamo in Mars can explain the lack of a global martian magnetic field today.

(M. Buske, U. Christensen)

Outer planets research – Jupiter

Banded flows in Jupiter's Atmosphere

Motion in the outer gas envelopes of Jupiter and Saturn is dominated by strong east- and westward blowing winds. The fastest wind is an eastward jet at the equator, followed by weaker jets of alternating directions in the northern and southern hemispheres. This wind pattern is reflected in the banded cloud structure on Jupiter.

Former simulations of convection in the gas envelopes successfully replicate some of the jets and the general wind speed but fail to reproduce the correct number of jets and some other details of the wind structure. New simulations performed by Heimpel *et al.* (2005) (see Fig. 119) come much closer to the real wind pattern by assuming more realistic parameters, in particular a shallower outer convective envelope.

Analysis of the jets on Jupiter and in the simulations show that their width is governed by the so-called Rhines-length scale. Energy in transfered by an inverse cascade from small turbulent eddies to larger scales. This cascade stops at the Rhines scale where the planetary curvature becomes influential, diverting the energy into the zonal jets (Heimpel *et al.*, 2005).

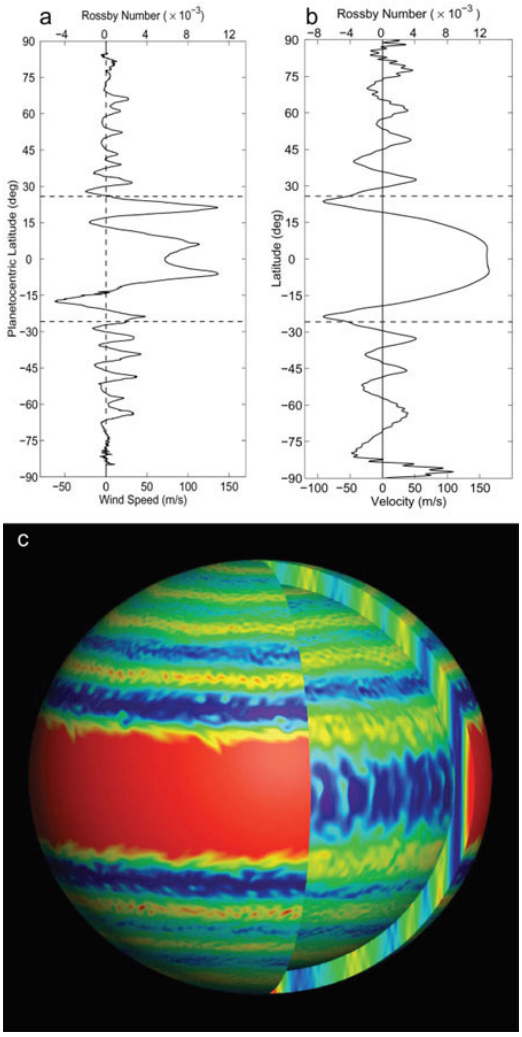

Fig. 119: Simulation of the convection in Jupiter's outer molecular gas envelope. Panels **a** and **b** compare Jupiter's wind profile as measured by the Cassini spacecraft with the profile in the computer simulation. Panel **c** shows eastward (red) and westward (blue) blowing winds in the simulation at the outer and inner boundary and a meridional cut.

(J. Wicht in collaboration with M. Heimpel (University of Alberta) and J. Aurnou (UCLA))

Multi-jets in rotating thermal convection

Studies of rapidly rotating convection in spherical shells have several applications in planetary science. The present work is focused on numerical models of enclosed liquid planetary cores. In addition, the work has implications for experiments on rotating convection.

Ideally, the model would be a Boussinesq, possibly anelastic, spherical shell. However, numerical 3-D simulations of rapidly rotating convection soon become too expensive at high rotation rates. The rotation rate is measured by the Ekman number Ek, the ratio between the viscous force and the Coriolis force. Fig. 120a shows the zonal flow in a strongly non-linear Boussinesq simulation close to the present practical limit of Ek. Due to the outer viscous boundary layer, multiple jets, i.e., more than 2, have developed outside the tangent cylinder. Kinematic dynamos using this new type of time-dependent flows have been shown to produce magnetic fields with a strong toroidal component. This is due to an increased ω-effect steming from the increased shear by the multi-jets. In addition, at higher Ek, it has been shown that well-developed convection inside the tangent cylinder may result in self-consistent dynamo solutions with a moderate Lorentz force. Thus these results seem to suggest a scenario for obtaining magnetic fields with a strong toroidal component at very low Ek.

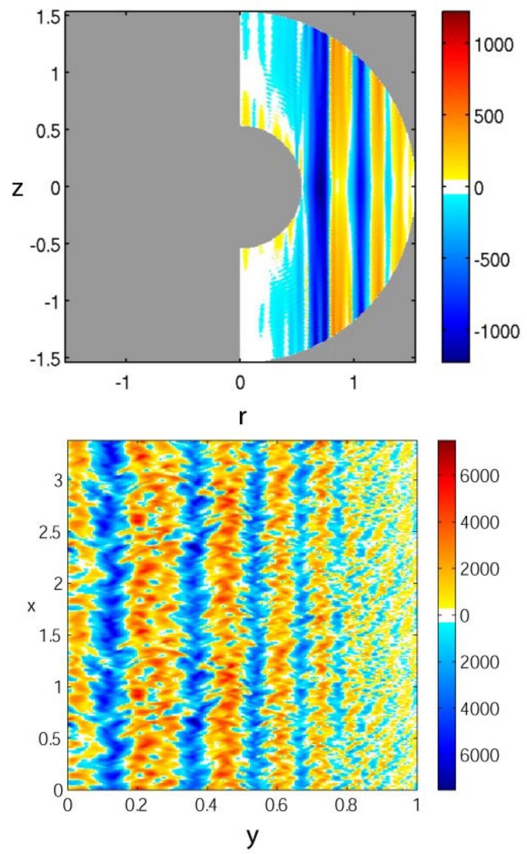

Fig. 120: Non-magnetic convection. (*a*) Snapshot of the zonal flow $< u_\phi >_\phi$ in a spherical shell rotating about the vertical axis. Ek $= 1.78 \times 10^{-6}$. (*b*) Snapshot of u_x in a 2-D model. The model plane represents the equatorial plane outside the tangent cylinder in a spherical shell. Ek $= 1 \times 10^{-7}$.

The practical limit to 3-D models may be circumvented by taking advantage of the weak dependence on the coordinate along the rotation axis. Several quasi-geostrophic models of convection outside the tangent cylinder exist in the literature. The present work is a further development of the 2-D models by Busse. A rotating duct has non-slip top and bottom boundaries with variable curvature. The problems resulting from a streamfunction representation of the flow have been solved. In one limit the model reduces to the classical annulus. In another limit the model geometry closely resembles the spherical shell. A strongly non-linear solution in the latter model is shown in Fig. 120b. The jets drift towards the inner boundary. The number of jets scales as Ek$^{-1/4}$ in accordance with the theory of Rhines (1975).

(J. Rotvig)

Models of convection in the gas giants including density stratification

Denstity increases significantly towards the interior of the giant planets gas envelopes. Most simulations that model convection within these envelopes nevertheless assume homogeneous density for simplicity. As a first step towards more realistic dynamical models we include density stratification but neglect adiabatic and viscous heating. Furthermore, we restrict ourselves to mildly supercritical convection to closely explore density stratification effects. When taking into account the possible density dependence of physical properties (like thermal conductivity or viscosity) key parameters like the Rayleigh number become depth dependent. As a result, convection close to onset may be confined to a certain depth range, either close to the inner boundary or close to the outer boundary depending on the assumed model. Likewise, densitiy stratification leads to generally smaller scales and a compressed bifurcation scenario, i.e. more complex and chaotic solutions are reached at smaller supercritical Rayleigh numbers when density stratification is increased. While the shape of convective rolls aligned with the rotation axis is generally retained, the flow amplitude can increase significantly towards the exterior. This would mean that the jet stream observed on the gas planets' surfaces represent much smaller interior flow amplitudes.

(D. Tortorella, U. Christensen, and J. Wicht)

In-situ observations of the Jovian magnetosphere

The Jupiter in-situ research at MPS in the years 2004/2005 was based on the data analysis mainly from the Energetic Particles Detector (EPD) on board the

Galileo spacecraft, which was the first spacecraft orbiting an outer planet. EPD was partly built at the institute and consists of two double-headed detector systems. EPD uses typical dE/dx versus E telescope and Time-Of-Flight techniques to separate different ion species and electrons in an energy range between tens of keV and several MeV. The whole instrument is mounted on top of a turntable so that its rotation combined with the spacecraft spin allows measurements from all directions in the three dimensional space.

Jovian plasma sheet morphology

Measurements of energetic ions and magnetic field data in the Jovian magnetosphere were used to identify 500 encounters of the equatorial plasma disc during the first 25 orbits of the Galileo spacecraft. It was found that a well-defined periodicity in the two data sets exists out to distances of 110 jovian radii. These periodic signatures display a large variability in the location of the peaks in the ion fluxes, interpreted as changes of the plasma sheet geometry during the encounters. Fig. 121 schematically shows a possible interpretation.

(N. Krupp, A. Lagg in collaboration with Applied Physics Laboratory/The Johns Hopkins University, USA; University of California Los Angeles, USA; Boston University, USA)

Evolution of an electron pitch angle distribution in the inner Jovian magnetosphere

Energetic electrons observations in the inner to middle Jovian magnetosphere have established a distinct transition from a pancake distribution close to the planet to a bi-directional distribution further out as an intrinsic feature of the Jovian magnetosphere. One possible mechanism causing such a distinct and localised boundary is pitch angle scattering. In particular, by simulating the evolution of an electron pitch angle distribution assuming conservation of first and second adiabatic invariants, the results can be compared with the observed distributions and discussed in the context of global particle transport in the Jovian magnetosphere.

In Fig. 122 the simulated and actually measured electron flux is compared. The simulation of the evolution of an electron pitch angle distribution with radial distance showed that conserving the first and second adiabatic invariants leads an electron population with a bi-directional pitch angle distribution in the current sheet region into a pancake distribution in the dipolar region, in the same radial range as observed by measurements.

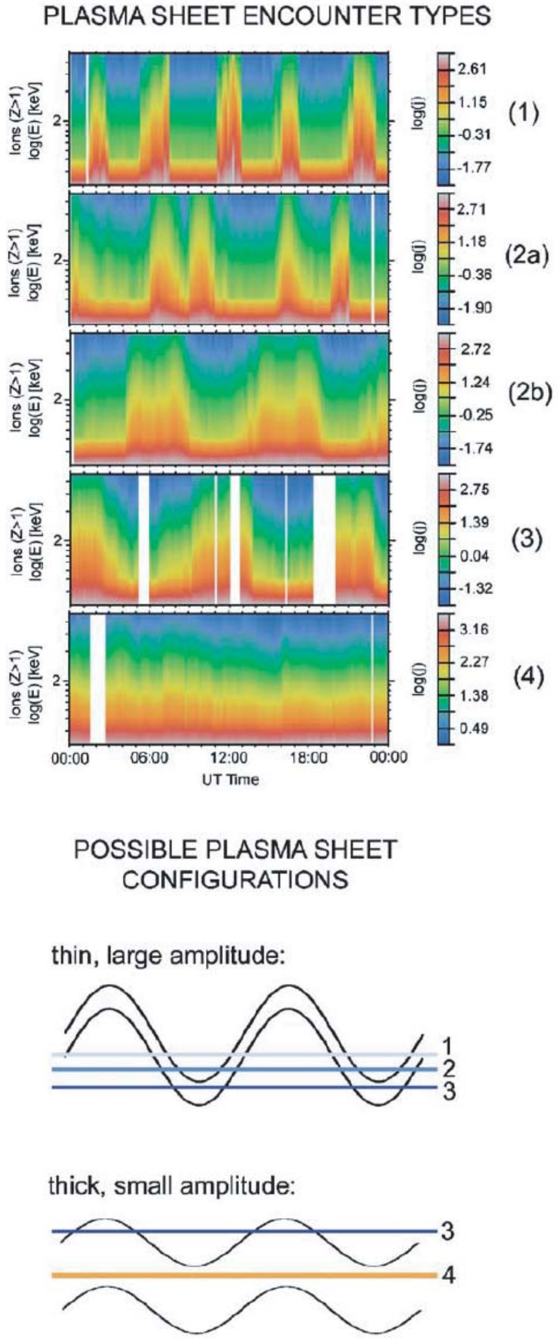

Fig. 121: Schematic showing the interpretation of various plasma sheet encounter signatures as changes in sheet configuration and mean location with respect to the spacecraft. Top: Examples of the types of signatures discussed in this paper displayed as omni-directional ion energy spectra. Bottom: Schematic illustrating the effect of vertical displacement of the plasma sheet relative to the spacecraft trajectory. Labeled lines are spacecraft trajectories that would give rise to the signatures on the left. The top right illustrates signatures resulting from an encounter with a plasma sheet having an oscillation amplitude larger than its thickness, while the bottom right shows those resulting from a sheet having a greater thickness than oscillation amplitude.

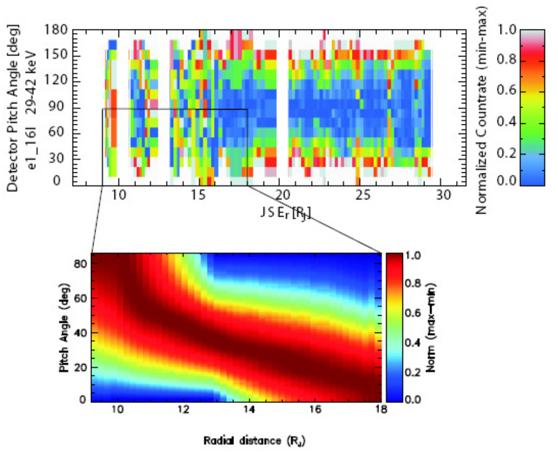

Fig. 122: Normalised pitch angle distribution. The upper panel shows the measured normalised distribution during the outbound passage of the C3 orbit of Galileo, for the e1 channel (29 keV to 42 keV). In the lower panel the simulated normalised pitch angle distribution is shown in the radial range from 10 R_J to 18 R_J (R_J (Jupiters radius) = 71492 km). In both cases the colour code indicates the particle flux, normalised to the maximum and minimum of each bin.

(A. Tomas, J. Woch, N. Krupp, A. Lagg in collaboration with Imperial College London, UK; University of Iowa, USA; Applied Physics Laboratory/The Johns Hopkins University, USA; University of California Los Angeles, USA; Technical University Braunschweig)

Quasi-periodic dynamics of the Jovian magnetosphere

Quasi-periodic modulations with a time period of several days were observed in most regions of the Jovian magnetosphere covered by the Galileo spacecraft. Each individual cycle of these modulations represents a global reconfiguration of the Jovian magnetosphere. The reconfiguration process in the magnetotail consists of a transition from a quiet state to a disturbed state. The initial loading phase is characterized by plasma convection at a moderate speed in the corotational direction and by a gradual stretching of the Jovian plasma sheet configuration (as seen from radial and azimuthal magnetic field components as well as the sulfur energy spectral index changes in Fig. 123).

In the release phase, reconnection through a thinned current sheet leads to radially inward and outward plasma flows and the ejection of plasmoids. In order to explain these periodical modulations a simple conceptual model was developed. It assumes that the ion-mass loading from internal plasma sources and the fast planetary rotation causes magnetotail field line stretching due to centrifugal forces. This leads to the

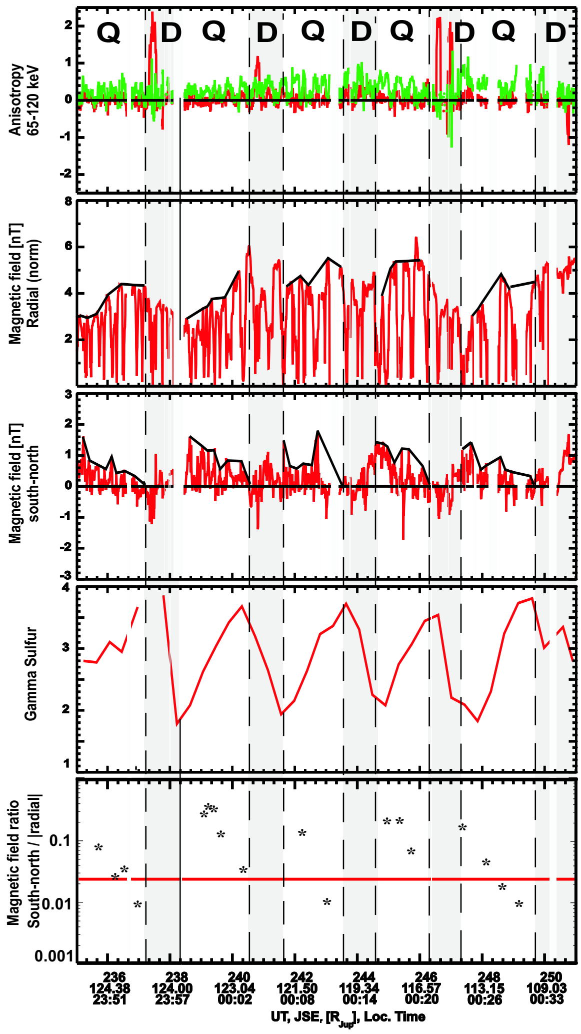

Fig. 123: An example of the periodic modulations of first order anisotropies, magnetic field, the sulfur energy spectral index γ and the ratio of the south-north magnetic field component in the current sheet crossing to the absolute value of the radial magnetic field component for the time interval DOY 235, 00:00 to DOY 251, 00:00 in 1998. First order anisotropies in the radial (black, positive is outward) and corotational direction (grey) (first panel); the absolute value of the radial magnetic field component, the black line presents the rough envelope (transient events are neglected) (second panel); the south-north component of the magnetic field, the black lines show again the envelope (third panel); the sulfur energy spectral index γ, 10-hour-averages (fourth panel); the ratio of the south-north magnetic field component in the current sheet crossing to the absolute value of the radial magnetic field component, the red line shows the threshold for the ion tearing instability (fifth panel). The time interval DOY 235, 00:00 to DOY 251, 00:00 in 1998 (orbit E16) is shown. The dashed lines indicate times at which the Jovian magnetotail transits from a quiet to disturbed state or vice versa.

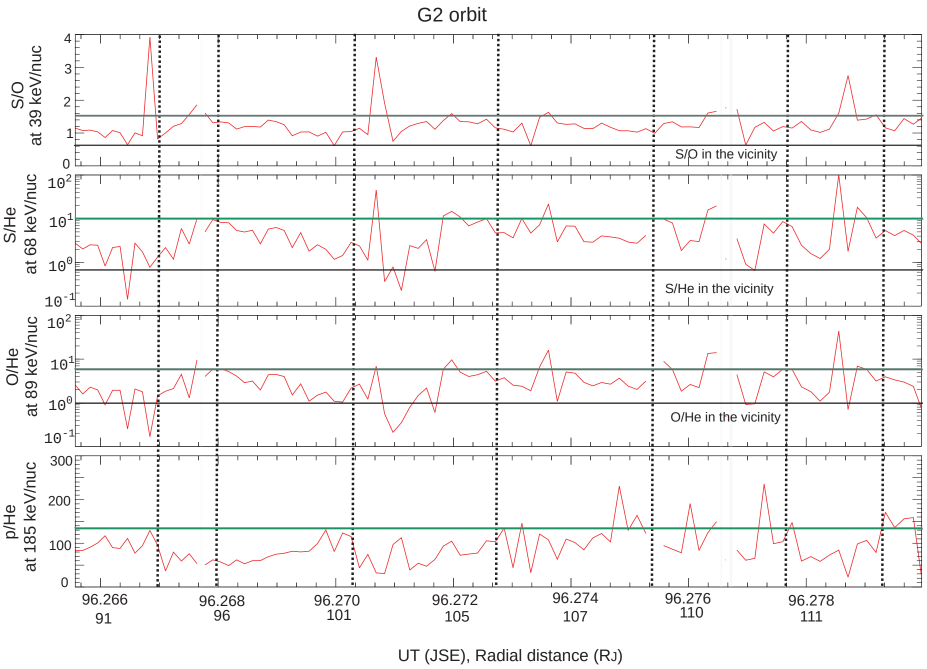

Fig. 124: S/O, S/He, O/He and p/He ion abundance ratios (from top to bottom) as a function of radial distance for the time interval 1996, day 265 to day 280 (along the G2 Galileo orbit). The observed values are plotted in red, the black horizontal lines indicate the level of the ratio in the vicinity and the horizontal green lines the values derived by the accelerated spectra according to the model, with input parameters based on magnetic field observations. The vertical dashed lines indicate the onset of the reconfiguration events.

development of a magnetotail configuration favoring magnetic reconnection. It is shown that the condition for the onset of a tearing mode instability is satisfied just before each disturbed period of the reconfiguration process. Thus, it is suggested that the tearing instability may cause both plasmoid formation and their release with continuing mass loading, leading to renewed stretching of tail field lines. The model yields that the intrinsic time constant of the Jovian reconfiguration process depends on internal parameters like the mass-loading rate and the initial mass density during loading phase which is affected by the external solar wind conditions. This model shows that the suggested intrinsic mechanism can explain the observed modulations of several days of the Jovian reconfiguration process.

(E. Kronberg, J. Woch, N. Krupp, A. Lagg in collaboration with Applied Physics Laboratory/The Johns Hopkins University, USA; Technical University Braunschweig, Imperial College London, UK)

Energetic particle composition during substorm-like events in the Jovian magnetotail.

Based on the first 15 orbits of the Galileo spacecraft the composition of the energetic ion population of the Jovian magnetosphere was studied on a global scale. Analyzing data from the Energetic Particles Detector onboard Galileo, we investigate the relative ion abundance ratios of S/O, S/He, O/He and p/He at various energy/nucleon. Prominent enhancements of S/O, S/He and O/He abundance ratios are observed in the predawn sector associated with substorm-like events in the magnetotail. During these reconfiguration events frequent small-scale variations of the south-north component of the magnetic field are present. Acceleration by such magnetic field variations is examined as a possible mechanism for particle energization in that region. When the time scale of the magnetic field variation is comparable to the particle gyro period the particle is accelerated by the induced electric field. Based on magnetic field observations it is shown that during the Jovian substorms sulfur and oxygen ions are more effectively energized than helium and protons, generating the observed ion abundances.

Fig. 124 shows an example of enhanced ion composition along a region of the G2 orbit where many reconfiguration events are present, the observed values (red) as well as the modeled (green) are plotted together for comparison.

(A. Radioti, J. Woch, N. Krupp, A. Lagg in collaboration with Applied Physics Laboratory/The Johns Hopkins University, USA; Technical University Braunschweig)

Dust stream measurements from Ulysses' 2nd Jupiter encounter

The Ulysses spacecraft has been orbiting the Sun on a highly inclined ellipse ($i = 79°$, perihelion distance 1.3 AU, aphelion distance 5.4 AU) since it encountered Jupiter in 1992. During this Jupiter flyby within 2 AU of the planet the impact ionisation dust detector on board discovered periodic burst-like streams of dust particles emanating from the jovian system (E. Grün *et al.*, Nature, **362**, 428–430, 1993). In February 2004 Ulysses had its second flyby at Jupiter at 0.8 AU distance from the planet. 28 dust streams were measured between November 2002 and August 2005 while the spacecraft was within 4 AU of the planet, scanning jovigraphic latitudes from $+75°$ to $-25°$. The highest dust fluxes were measured in mid 2004 at the passage of the jovian equatorial plane when more than 2000 impacts per day were measured (Fig. 125). The data show clear signatures for dust particle interaction with the solar wind driven interplanetary magnetic field (H. Krüger *et al.*, Planetary and Space Science, in press, 2006). At high jovigraphic latitudes, the impact rates show a periodicity of 26 days, closely matching the solar rotation period, while at the jovian equator the streams fluctuate with twice this period. The 14-day subharmonic streams alternate in arrival direction and are correlated with the pointing of the interplanetary magnetic field.

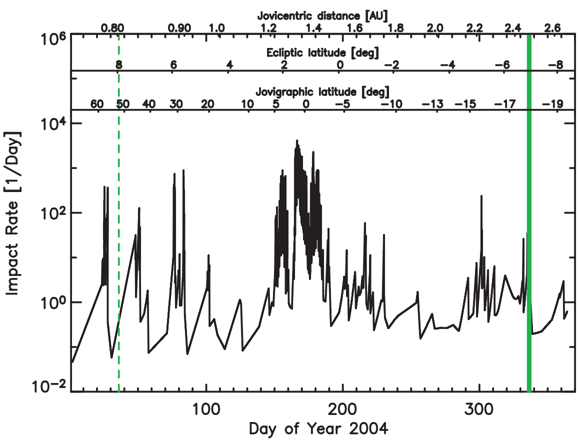

Fig. 125: Impact rate of dust stream particles measured in 2004. A vertical dashed line shows Jupiter closest approach in February and the shaded area indicates a short period in late November 2004 when the dust instrument was switched off.

(H. Krüger in collaboration with E. Grün (MPI für Kernphysik, Heidelberg))

Outer planets research – Saturn – Magnetosphere

A differential-rotation dynamo for Saturn?

Today's computational resources do not allow us to simulate planetary dynamos with realistic parameters. In particular the viscosity is several orders of magnitude higher in the numerical models than would be realistic. This higher viscosity is essential to damp small scale flows than cannot be resolved. Are these small scales important for the magnetic field production? We simply don't know. And unfortunately, we have no means to answer this question for the geodynamo, because we know so little about the dynamics in the Earth's core.

Laboratory experiments are essential here. They bridge the wide gap between simulations and reality, since they can run with fluids whose physical properties are significantly more realistic. Viscosity and electrical conductivity of liquid sodium, the fluid preferably used in dynamo experiment, are close to the properties of the liquid iron in the Earth's outer core. The dynamo group at the LGIT (Laboratoire de Géophysique Interne et Tectonophysique) in Grenoble, France, and the laboratory of Dan Lathrop at the University of Maryland are working on a new generation of dynamo experiments. These are based on the spherical Couette setup: Differential rotation of an inner sphere and the outer boundary drives a fluid flow in the liquid sodium that fills the cavity. If the differential rotation is large enough, non-axisymmetric flow instabilities grow that bear some similarity with convective columns in rotating spherical shells. The computer simulations show that these instabilities can drive a dynamo. According to these results, in particular the experiment designed by Dan Lathrop seems powerful enough to actually work as a dynamo.

Magnetic fields produced by this type of dynamo are surprisingly axisymmetric due to the stong winding of fieldlines by the rotating inner boundary (see Fig. 126). We suggest that such a mechanism could be responsible for Saturn's highly axisymmetric and simple magnetic field that has puzzeled researchers for a long time. Helium precipitation carrying angular momentum into Saturn's interior is a conceivable source for differential rotation within the planet.

(J. Wicht in collaboration with P. Olson (Johns-Hopkins University) and D. Lathrop (University of Maryland))

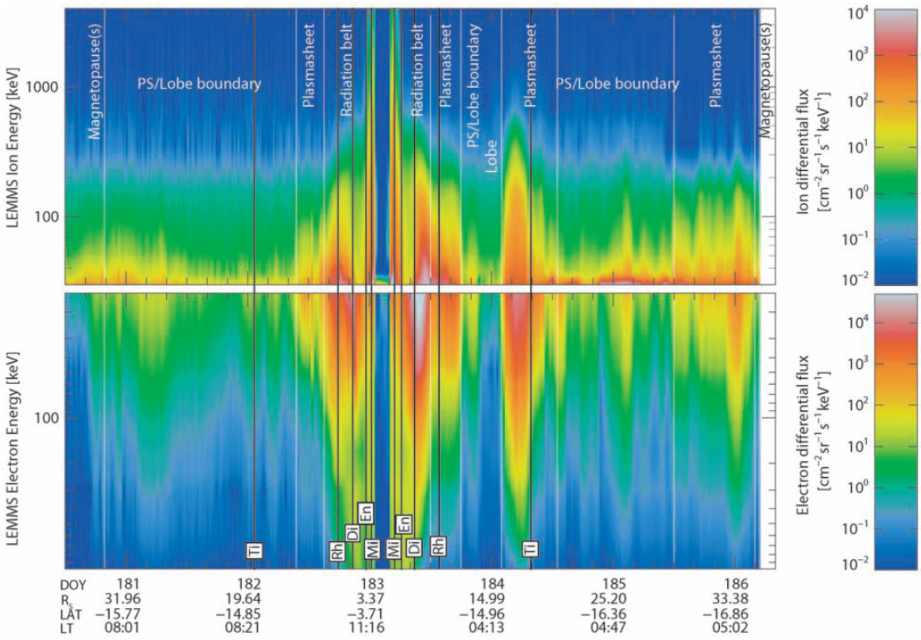

Fig. 127: Dynamic spectrogram (energy vs. time) of LEMMS ions and electron intensities. Colour-coded is the intensity of ions (top panel) and electrons (bottom panel). Electron energy is plotted increasing downward, ion energy increasing upward for a better comparison.

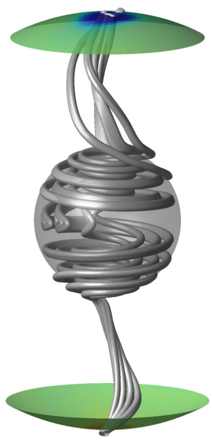

Fig. 126: Magnetic fieldlines in the spherical-Couette dynamo.

In-situ observations of the Saturnian magnetosphere

The Saturn in-situ research at MPS is based on data from instruments onboard the Cassini spacecraft which went into orbit around Saturn on July 1, 2004. MPS built the Low Energy Magnetospheric Measurement System LEMMS, one out of three detectors of the Magnetospheric Imaging Instrument MIMI. The institute was also involved in the Hydrogen Deuterium Absorption Cell HDAC which is part of the Ultraviolet Imaging Spectrograph UVIS.

Global configuration and dynamics of the Saturnian magnetosphere

MIMI onboard the Cassini spacecraft has been observing the Saturnian magnetosphere since July 1, 2004. Until the end of 2005, the spacecraft performed 21 revolutions around the ring planet, predominantly in the morning and the predawn local time sector of the magnetosphere.

Fig. 127 shows a dynamic spectrogram of energetic ions and electrons measured by MIMI/LEMMS during the insertion orbit. Different magnetospheric regions (lobe, plasma sheet, radiation belts) could be identified. The study of the Saturnian plasma sheet is crucial to understand the dynamics of the whole Saturnian system. The analysis of MIMI/LEMMS data in combination with magnetic field data revealed that periodic changes at the planetary rotation period of 10 hours and about 40 minutes are observed. Currently the reason is not yet fully understood since the rotation and magnetic axis of saturn are aligned with each other.

Fig. 128 shows one of the best examples measured along the outbound path of Cassini's orbit B in December 2005. For almost 6 days the electron intensities and total magnetic field varied periodically. One possible explanation was discussed in terms of a magnetic anomaly at a given longitude pushing the spacecraft on different field lines with different par-

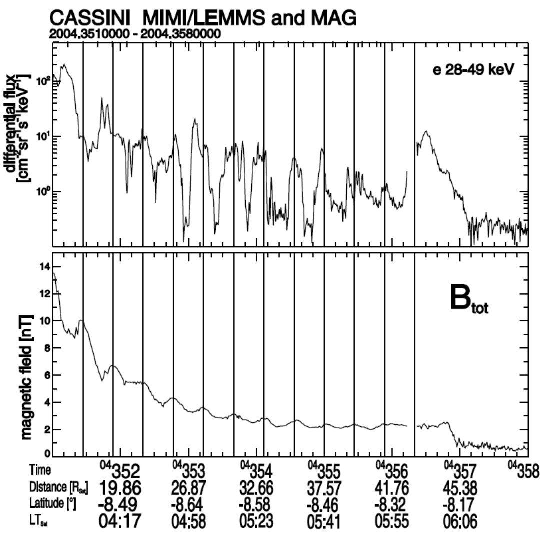

Fig. 128: Total magnetic field and intensities of electrons during the outbound portion of Cassini's orbit B around Saturn in December 2005. Vertical lines are drawn every 10 hours 40 minutes (planetary rotation period).

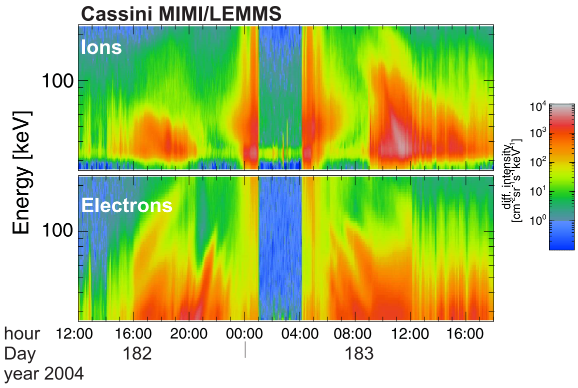

Fig. 129: Energy-time spectrograms during the Saturn insertion orbit. The colour-coded intensities of electrons and ions clearly show a strong dispersion of arrival times at the spcecraft.

ticle distributions every rotation. Other explanations such as periodic substorms or other dynamic changes in the Saturnian magnetotail are also discussed. The measurements of the MIMI instrument inside the Saturnian magnetosphere also allowed the study of so-called particle injections in great detail. Those dynamic planetward injections of energetic particles confined in azimuth have been observed at Earth as well as in Jupiter's magnetosphere. Now with MIMI/LEMMS it was possible to detect them at Saturn as well. During an injection event, hot plasma from a region further out in the magnetosphere is injected into an inner region, azimuthally drifting around the planet. Injections are observable in the opposite energy-time dispersion of ions and electrons arriving at the spacecraft with a characteristic delay in time, dependent on their charge and initial energy. The disperion theory applied to the observations at Saturn required an additional term in the Saturn case to explain the unexpected change in the ion arrival profile. This additional term took the radial motion of the plasma into account.

Fig. 129 gives one example of a series of injections seen in the energy spectrograms as time dispersed features.

(N. Krupp, A. Lagg, J. Woch, G. H. Jones, E. Roussos in collaboration with the Applied Physics Laboratory/ The Johns Hopkins University, USA; University of Maryland, USA; Imperial College London, UK; Fundamental Technologies, USA; Centre d'Etude Spatiale Rayonnement, Toulouse, France)

Microsignatures caused by the interaction of plasma and the icy satellites of Saturn

Within 9 R_S from the center of Saturn (1 R_S = 60287 km) seven moons with a diameter greater than 100 km orbit the planet in almost circular and equatorial orbits. These moons interact continuously with the trapped plasma of the radiation belts. As most of these moons are electromagnetically inert, they absorb plasma effectively, resulting in very characteristic depletions, mainly in the electron population. The kinematics of those electron "holes" (termed microsignatures), is similar to the one of the electrons before their depletion on the moon's surface. Therefore by studying the position of these signatures in the magnetosphere, with respect to the position of the moon that caused them, we can get direct information about the electron flow pattern in the radiation belts. In addition, the study of the refilling of the microsignatures gives us a direct estimate of the diffusion rates in the radiation belts. Using data from LEMMS, we studied the electron absorption signatures of the moon Tethys, in the energy range of 20 – 100 keV, observed in the first six orbits of Cassini around Saturn.

Fig. 130 shows one of the many Tethys microsignatures found. In total, 11 out of 12 crossings of the regions magnetically connected to Tethys's orbit revealed the moon's electron absorption signatures. The detection and analysis of double microsignatures (as seen in Fig. 130) has shown that Tethys's microsignatures persist in the magnetosphere for long periods. This qualitatively suggested low diffusion rates and was in agreement with our estimate of a radial diffusion coefficient of $10^{-9} R_S^2/s$, that resulted from the modelling of a single absorption event. Furthermore, the study of the position of the microsignatures with respect to Tethys's orbit revealed that the electron

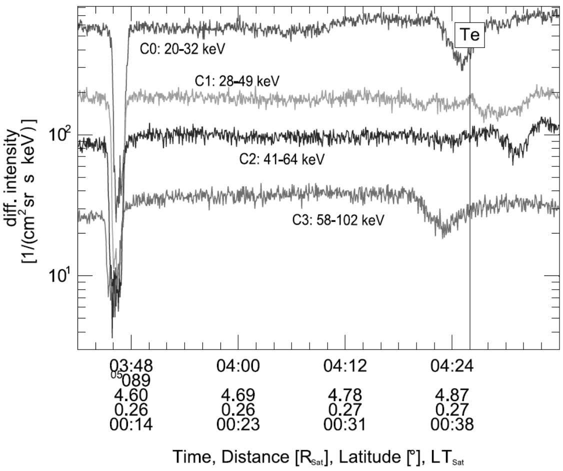

Fig. 130: Multiple microsignatures in four electron channels of LEMMS seen during Tethys's L-shell crossing on day 89 of 2005. The sharp absorption feature at 3:46, as well as the features around 4:26, are associated with Tethys. The vertical line at 4:26 indicates the time for the expected Tethys L-shell crossing.

flow pattern deviates significantly from axisymmetry. It was found that the direction of this deviation correlates strongly with local time, in a way that it is consistent with the effects of an interplanetary convective electric field at Saturn. This was a surprising result, as Saturn's magnetosphere is thought to be corotation dominated, with the effects of the interplanetary convective field appearing only at large radial distances in the magnetosphere of Saturn.

Microsignatures in the wake of the 500 km-wide moon Enceladus were also studied. In mid-2005, this body was discovered by several Cassini instruments to be an active source of neutral gas and dust, and is thought very likely to be the dominant source of Saturn's tenuous E-ring. Most charged particles travel around Saturn in the same direction as the moons orbit, but at higher velocities. This forms a wake that leads Enceladus's motion around Saturn. The exception to this behaviour is the population of energetic electrons, which, above a certain energy, actually travels around Saturn in the opposite direction, and hence forms a wake that trails Enceladus's orbital motion. LEMMS was therefore able to sense two populations of microsignatures: all positively-charged particles and low-energy electrons on one side of the moon, and high energy electrons on the other. The high-energy electron population behaved approximately as expected, with their microsignatures gradually filling in with diffused magnetospheric particles as they moved away from Enceladus. The low energy electrons did not behave like this: the signatures varied in depth and width, and did not follow a predictable pattern. We assign this behaviour to the plume of gas and dust released by Enceladus. As the low-energy electron microsignatures varied, we strongly suspect that this is a result of variability in the activity of the plume itself over a period of days or weeks.

High-energy ion signatures were also studied. These particles form a deep, persistent wake that extends all the way around Saturn, centered on the orbit of Enceladus. This wake, termed a macrosignature, can be attributed to the very short orbital period of these particles: before the wake can be refilled by magnetospheric plasma, the particles again encounter the moon, thus continuously retaining the presence of the drop in energetic positively-charged particles in this region.

(E. Roussos, N. Krupp, G. H. Jones, A. Lagg, J. Woch in collaboration with Applied Physics Laboratory/The Johns Hopkins University, USA; Technical University of Braunschweig; Imperial College London, UK)

Outer planets research – Saturn – Moons

Disk-integrated photometric and polarimetric observations of Saturn's major satellites

Although the opposition phenomena observed in brightness and polarization for the surfaces of various astronomical objects and laboratory samples have been under intense study for many years, their explanation is still far from being complete. The shadow hiding and coherent backscattering mechanisms are discussed most frequently in this connection. Different scattering mechanisms such as interference and interaction between scatterers in the near field may influence brightness and polarization of complex ensembles of particles as well. To enlarge the data base on polarization measurements of high albedo icy surfaces at small phase angles we have embarked on a ground-based observational program to measure the integrated polarization of Saturn's major satellites Enceladus, Tethys, Dione, Rhea, Titan and Iapetus as a function of phase angles in the range available from Earth of 0° to about 5°. The measurements of Titan do not refer to its surface. They are done for intercomparison with the recent space observations of this satellite. The observations were conducted at the 2m-telescope of the National Observatory of the Institute of Astronomy of the Bulgarian Academy of Sciences on Mount Rojen from 3 – 17 January (small phase angles) and from 25 November – 8 December 2005 ("large" phase angles). Some preliminary results for the satellites Enceladus and Dione are shown in Fig. 132. Measurements at intermediate phase angles are still missing. Therefore

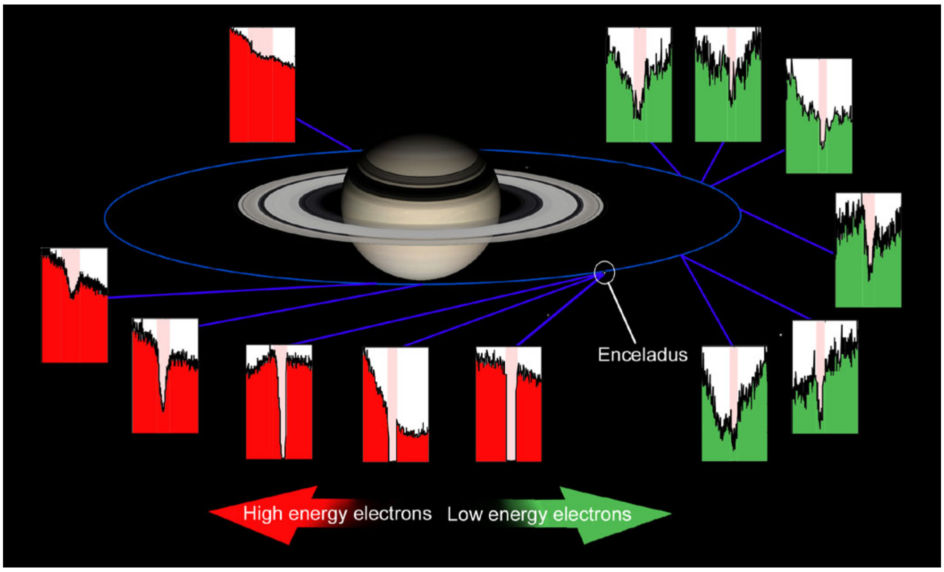

Fig. 131: Electron flux measurements made by LEMMS are shown here in normalized counts plotted against distance from Saturn. The red panels show that high energy electrons behave as expected. The behaviour of the low energy electrons (green) does not however fit a fixed pattern. High energy electrons pass straight through Enceladus's plume, while low energy electrons are sensitive to Enceladus's varying environment.

we cannot draw conclusions on the contribution of different scattering mechanisms to the polarization yet.

The work was supported by grant 436 RUS 113/684/0-2 of the Deusche Forschungsgemeinschaft in the framework of the priority program 1115 "Mars and the terrestrial planets".

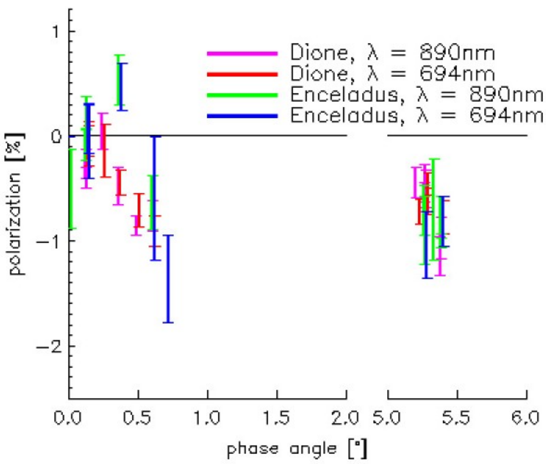

Fig. 132: Phase curves of polarization of Saturn's satellites Enceladus and Dione at 694 and 890 nm.

(K. Jockers, I. Kulyk)

Cassini UVIS/HDAC observations of Titan's exosphere during the 9th Titan encounter

Cassini UVIS/HDAC is a Lyman α photometer with Hydrogen/Deuterium cells, which is designed to measure Deuterium (121.533 nm) and Hydrogen (121.567 nm) Lyman alpha emissions from Titan and Saturn. HDAC works as a very narrow absorption filter. The incident Lyman alpha emission is absorbed by hydrogen (deuterium) atoms from hydrogen (deuterium) molecules dissociated by heated filament. The strength of the absorption can be controlled by the power heating the filament. This and the variation of the Doppler velocity (near zero) allow us to deconvolute the profile of the incident Lyman alpha line and the D/H ratio in Titan.

A measurement sequence was performed with HDAC during the Cassini T9 encounter on Dec 26, 2005. Fig. 133 shows the data taken around the closest approach (17:52 – 19:18 (UTC)). During this period the distance between Titan and the spacecraft changed from 30,000 km to 13,000 km. The phase angle changed from 30 – 110°. Lyman alpha emission was detected at a brightness level of 500 ~700 [R]. The Doppler velocity changed from -4.7 km/s to -5.0 km/s. Line profile sweeping was successful. We are developing a remote sensing program for retrieval of the hydrogen altitude distribution and retrieval of exospheric temperature of Titan.

(Y. Ito, H. U. Keller, A. Korth)

Microscopic properties of Titan's surface from Huygens/DISR images

After its descent through Titan's atmosphere the Huygens probe landed on a plain which resembled a

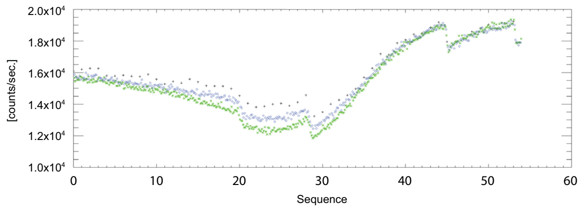

Fig. 133: HDAC observations during the T9 closest approach. HDAC modulated signal can be clearly seen in the data. The black cross, blue square and green asterisk denote background data, the data when Hydrogen cell is switched on and the data when both (Hydrogen and Deuterium) cells are switched on.

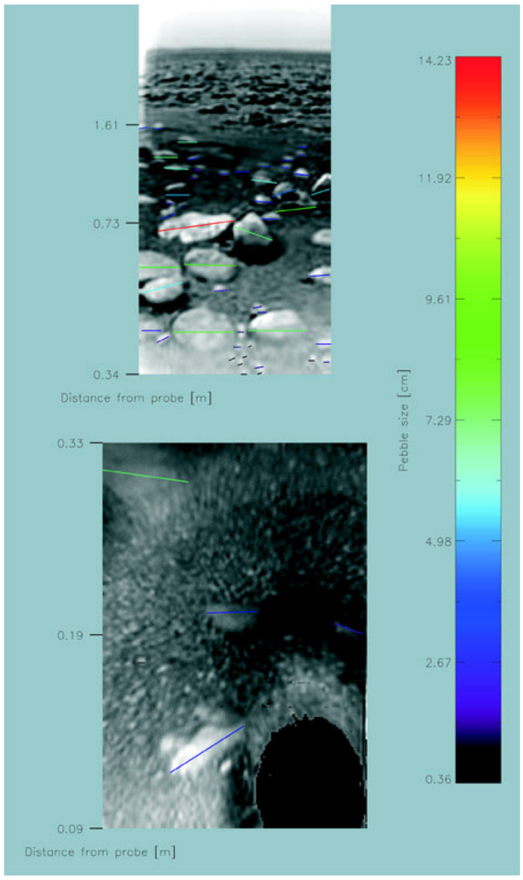

Fig. 134: Composite of DISR surface images taken with the sideward looking imager (top) and the medium resolution imager (bottom). Data from the high resolution imager were not used because it was out of focus due to the close proximity to the surface. The sizes of the pebbles and horizontal distances from the probe are marked.

lakebed surrounded by hills Tomasko *et al.* (2005). In the following hours the three cameras (sideward looking imager, medium resolution imager, and high resolution imager) of the Descent Imager/Spectral Radiometer (DISR) took several dozen images of the same surface spot. The resolution of those images of a few millimeters exceeds the best resolution achieved during descent by more than two orders of magnitude.

While the surface at the landing site does not contain any liquids at present, it is covered by pebbles of several millimeters to 15 cm in size (Fig. 134). It is likely that the pebbles are mostly made of water ice. Their size distribution (in terms of surface coverage) shows a peak at sizes between 5 and 15 cm (Fig. 135). Few smaller and no larger pebbles are seen.

The size distribution of the pebbles is different from that of stones seen on other solar system objects like Mars or asteroid Eros. However, it is similar to that of stones transported by terrestrial rivers or by flash floods in a regime where the flow entrains material up to a certain threshold size. We conclude that the pebbles seen on the surface have been transported by a liquid flooding into the lowland where the Huygens probe landed. The interpretation is supported by images taken during descent. They show a network of channels which are interpreted as dry riverbeds Tomasko *et al.* (2005).

In the cold environment on Titan (surface temperature about 90 K) methane can exist in the solid, liquid, and gaseous state, similar to water on Earth. Assuming that water ice pebbles were transported by liquid methane, the flow velocity was on the order of 1 m/s.

(M. Küppers, R. Kramm, H. U. Keller)

Determining the reflectance properties of Titan's surface

Retrieving the properties of Titan's surface is of paramount importance to understanding this mysterious world. The Descent Imager / Spectral Radiometer (DISR) aboard Huygens amassed a wealth of data during its descent through Titan's atmosphere in January last year. More specifically, the Downward Looking Visual and Infrared Spectrometers (DLVS/DLIS) viewed the surface with increasing clarity as the probe approached landing (Fig. 136). Because the atmosphere strongly absorbs at certain wavelengths due to haze and methane, we must take care to disentangle atmospheric from surface contributions. Spectra acquired by the DLVS show that in the visible wavelength range the atmosphere contributes to the observed intensity all the way to the surface. However, the DLIS spectra reveal that in near-infrared a methane windows in atmospheric absorption appears to be minor below 4 km, which allows for the determination of the surface bi-directional reflectance distribution function (BRDF). The BRDF shows a relative increase of intensity towards lower phase angles that is approximately constant with wavelength.

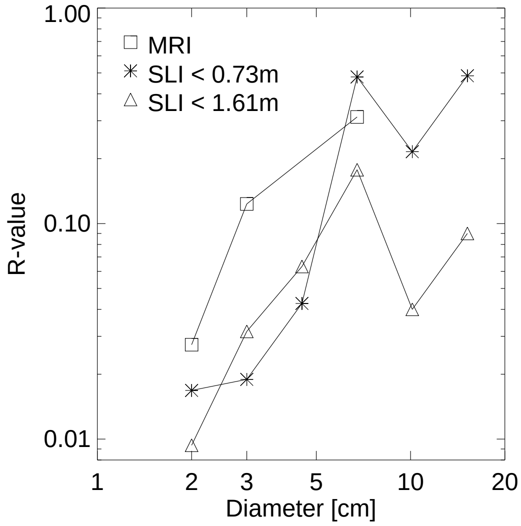

Fig. 135: Size distribution of the pebbles larger than 1.6 cm. The quantity R is proportional to the fraction of the surface area covered by pebbles of a given size.

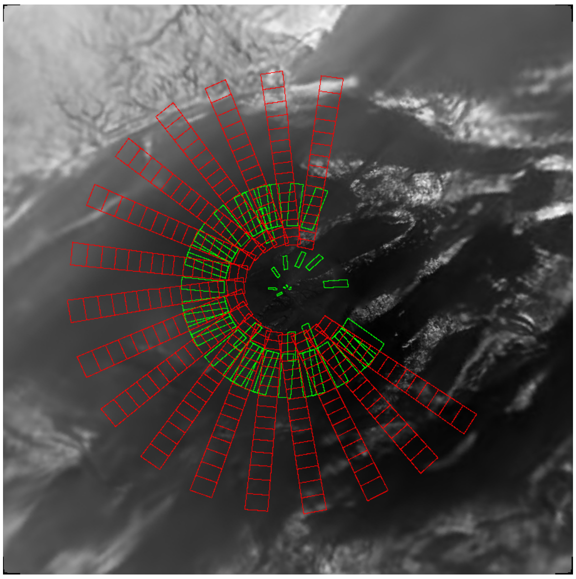

Fig. 136: The area covered by the second spectrophotometric map in gnomonic projection (10 × 10 km). The DLVS and DLIS footprints are overlayed in red and green, respectively. The MNS and VLNS mode DLIS footprints are also shown for reference.

We attempt to model the surface BRDF, using a twofold approach. The images acquired by DISR after landing show a surface strewn with rounded rocks, presumably composed of water ice. By simulating how the Sun casts shadows on various idealized surfaces (Fig. 137) we determine that the macroscopic shadow hiding contribution is most likely minimal (Fig. 138). The next step in our investigation is to model scattering by the icy soil.

(S. E. Schröder, M. Küppers, H. U. Keller)

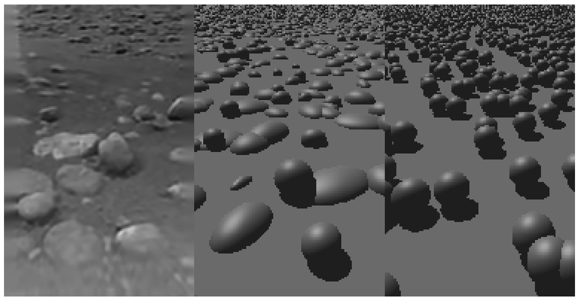

Fig. 137: Titan's surface and two simulated surfaces as seen from the probe's perspective after landing, all displayed at the same image resolution. The Huygens SLI view (left) is shown with a realistic (middle) and an idealized (right) simulated surface, covered with identical spheres. The simulations are supposed to reflect observations in the near-IR methane bands, and therefore the shadows are much more pronounced than in the SLI image. Note that the latter was highly compressed before being transmitted, degrading the resolution.

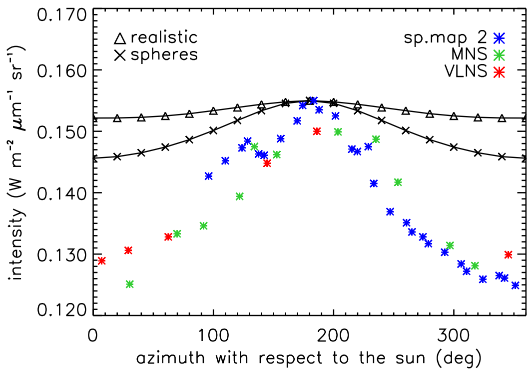

Fig. 138: Simulations of the macroscopic shadow hiding effect compared to observations at 1.28 μm. Shown in black is the relative intensity of the two surfaces in Fig. 137 as it would be observed by the DLIS for a full probe rotation, scaled to match the maximum of the low altitude observations. The colored data points are observations by the DLIS below 4 km altitude, operating in different modes (Spectrophotometric Map 2, Medium Near Surface, and Very Low Near Surface mode).

Topographic shading in Huygens/DISR images of Titan's surface

During the descent of the Huygens probe in January 2005, its Descent Imager/Spectral Radiometer (DISR) has taken the first close up images of Titan's surface Tomasko *et al.* (2005). No *obvious* topographic shading is visible in the images. This was attributed to the fact that the illumination on Titan is very diffuse. However, even a completely isotropic illumination would imply topographic shading. This is due to the fact that any significant terrain obscures a part of the sky, with the fraction of obscured sky varying from place to place. Moreover, although diffuse illumination is dominant in the visible wavelength range on Titan, it is concentrated in a pronounced solar aureole, cf. Fig. 139. I.e., the illumination is far from being isotropic and exhibits quite a prefered direction Grieger (2005).

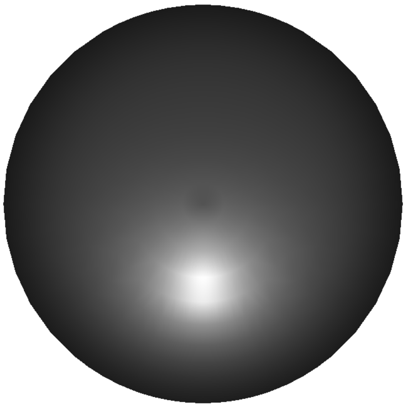

Fig. 139: Diffuse radiance from Titan's sky in the DISR imager wavelength range. The zenith is in the center, the horizon is at the limb. Note the pronounced solar aureole.

The optical properties of the aerosols in Titan's atmosphere have been retrieved from upward and downward looking measurements of DISR visible and infrared spectrometers Tomasko *et al.* (2005). Based on these retrievals, we have conducted radiative transfer computations for a set of wavelengths in the response window of the panchromatic DISR imagers. By integrating the computed radiances over wavelength weighted with the imager response function, we are able to model the atmospheric radiance as seen by the imagers. This modelled radiance is then used to correct the images for the atmospheric contribution, cf. Fig. 140. While DISR images of the river bed area originally exhibit a contrast of only a few per cent, the corrected contrast of true surface brightness is about 20%.

Based on the surface illumination implied by the modelled radiance, cf. Fig. 139, we have rendered various digital terrain models to investigate the contribution of topographic shading to the observed contrast. We find that a moderate terrain with slopes of up to 25° yields surface brightness variations which are comparable in magnitude to the observations. An elevation model of a Titan river bed that can reproduce the observed brightness profile without assuming local variations in surface albedo, i.e., without any "dark stuff" in the river bed, is presented in Fig. 141. The river bed is about 100 m wide and 20 m deep. The actual river is possibly much narrower, may be only a few meters wide.

(B. Grieger, Y. Skorov, H. U. Keller)

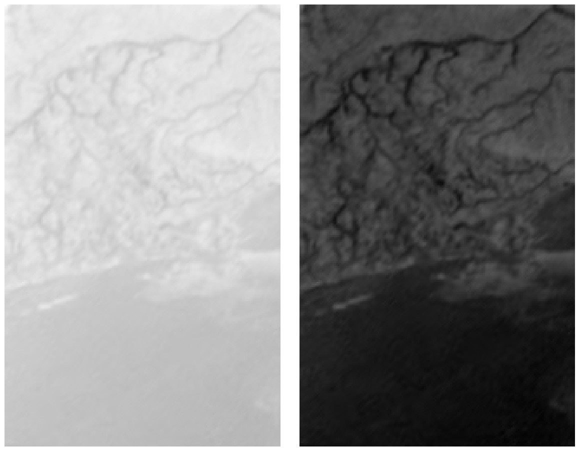

Fig. 140: Original image *(left)* and image corrected for atmospheric effects *(right)*, both in the same gray scale.

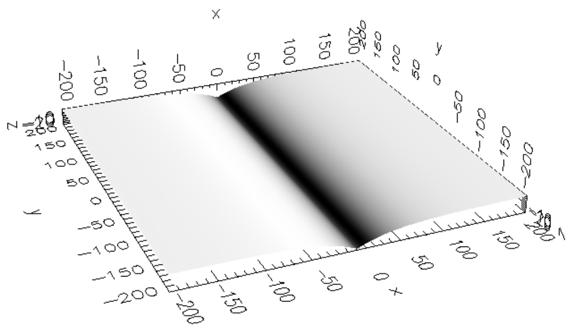

Fig. 141: Elevation model of a Titan river bed (topography not exaggerated), rendered according to Titan sky illumination, cf. Fig. 139. The direction of the sun is 17° counterclockwise of the $+x$-direction. Constant surface albedo is assumed. The resultant brightness profile across the river bed is consistent with observations, cf. Fig. 140.

Cometary research

Comet 2P/Encke: Observations in the visual and submillimeter range during its November 2003 apparition: Dust polarization, HCN and CN

Comet 2P/Encke is the short-periodic comet with the smallest known perihelion distance q = 0.33 AU and with a period of 3.28 years. It does not display a tail. Instead a so-called "fan" is observed, a broad feature on the solar side of the comet forming an angle with the solar direction. Because comet Encke orbits at rather close distance from the Sun, it is probably the most evolved comet known. The ISO satellite revealed that the dust grains of this comet are large and merge into a so-called dust trail, extending along the orbit of the comet. These large grains are invisible in the visual wavelength range.

We have observed comet Encke in the optical and submillimeter wavelength ranges during its November 2003 apparition. The submillimeter observations were conducted with two heterodyne receivers combined with the high resolution chirp transformer spectrometer (CTS) of MPS and two acousto-optical spectrometers (AOS) at the 10m Heinrich-Hertz-Telescope of Steward Observatory and MPI für Radioastronomie on Mount Graham, Arizona, USA. High-resolution profiles of the 4 – 3 (354.505 GHz) and 3 – 2 (265.886 GHz) rotational lines of HCN were obtained. For the optical observations the Two-Channel Focal Reducer of MPS was used at the 2m-telescope of the National Astronomical Observatory of the Institute of Astronomy of the Bulgarian Academy of Sciences on Mount Rojen, Bulgaria. The comet was imaged with narrow-band filters centered on the emission of the CN 0–0 band at 388 nm, the 0–7–0 band of NH_2 at 662 nm and a dust continuum at 642 nm. In addition, we used the four-beam Wollaston imaging polarimeter of MPS to obtain polarization maps in the 662 nm and 642nm filters. The NH_2 and CN molecules emit discrete molecular bands but the dust scatters the solar spectrum as a quasi-continuum. In the CN band the dust continuum is negligible but a contribution of dust continuum is present in the 662 nm filter as well as faint molecular lines contribute to the light transmitted by the 642nm filter. Making use of the fact that the polarization of NH_2 is a characteristics of the molecule and therefore should not depend on the location within the cometary coma we were able to separate dust and NH_2 in the cometary images. The resulting images are shown in Fig. 142. Comet Encke does not have a dust tail. In the visual range its dust forms an almost circular cloud around the nucleus. The fan is visible only in the CN and NH_2 images, i.e. it consists of molecular gas.

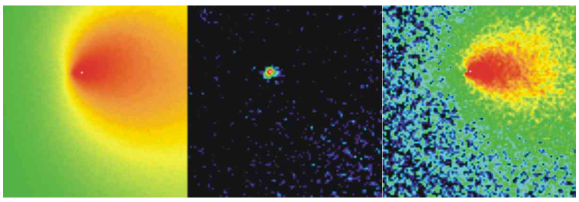

Fig. 142: Comet 2P/Encke: Left: CN. Center: Dust. Right: NH_2. The Sun is to the lower right. Note absence of dust tail. Comet Encke's fan is visible only in the distribution of the molecules. The width of the imaged field corresponds to $\approx$ 20,000 km at the comet.

Polarization

During our observations the phase angle comet–Sun–observer ranged from 91 – 105°. At these angles the linear polarization of NH_2 averaged over our filter passband amounts to $\approx$ 7%. The dust polarization however, when corrected for the effect of molecular emissions, is larger than 30%. (Levasseur-Regourd *et al.*, A&A, **313**, 327, 1996) have suggested a division of comets into two polarimetric classes with one class having in the visual wavelength range a maximum polarization $<$ 20% and the other one having maximum polarization $\geq$ 30%. The comets in the class of low polarization usually lack an infrared (15μm) silicate feature, which indicates that their dust particles are of large size. The dust continuum of the comets of low polarization is much weaker than that of the comets in the high polarization class. This is because larger dust particles scatter solar radiation less effectively. Comet Encke, because of its large dust grains, should belong to the low polarization class. Like other comets in this class also comet Encke has a weak dust continuum. The degree of linear polarization, if measured with the usual diaphragm size of $\approx 10^4$ km at the comet and not corrected for the low polarization of the molecular gas indeed turns out to be low. If one, however, properly corrects for the presence of molecular gas, the polarization is as high as in the class of high polarization. It therefore appears that the so-called low polarization class advocated by Levasseur-Regourd is caused by ignoring the contribution of molecular emission and therefore is an artifact. Whether the comet displays a strong silicate feature (i.e. its dust grains are small) or not, the dust polarization is high. This conclusion is in accordance with the theoretical prediction by aggregate models of cometary grains (Petrova *et al.*, 2004) and with the high polarization observed in the remnant of the dissolved comet D/1999 S4 (LINEAR) which consisted of large grains only.

CN and HCN

The CN images and the HCN line profiles were compared with Monte Carlo models of the outflow of gas from an active region and of the dissociation of HCN into H and CN. The following results were obtained: The outgassing from the nucleus of comet 2P/Encke mainly occurs from a limited active area but some isotropic outgassing is also present. The location of the optical CN jet is consistent with the pole position derived by (Sekanina, Astron. J., **95**, 911–924, 1988), but the co-latitude of the source is significantly smaller (8° versus 35°). The nucleus rotation period of $\approx$ 11 hours derived by (Y.R. Fernandez *et al.*, Icarus, **175**, 194–214, 2005) is confirmed. The observed radio lines of HCN reveal a gas expansion velocity of the coma = 1.1 km s^{-1}. This agrees with the results of comet Borrelly obtained by (Bockelée-Morvan *et al.*, Icarus, **167**, 113–128, 2004). The HCN line profiles are consistent with the position of axis and co-latitude of the active region derived from the CN observations. The observed modulation of the HCN production rate can be explained by the longitude of the active source derived from the CN images but the amplitude of the modulation is rather high. We presently investigate the cause of the strong modulation. The CN production rate is somewhat higher than the HCN production rate. Within the systematic errors present in the production rate determinations HCN can possibly still be the sole parent of CN. But the life time of the CN parent derived from our data is 16400 s at 1 AU, significantly less than the theoretical values of 31900 s for high solar activity and 79400 s for low solar activity. This speaks in favour of another CN parent. But during the time of the observations several strong flares occurred on the Sun, the radiation of which may have reduced the life time of HCN.

(K. Jockers, S. Szutowicz, G. Villanueva, N. Kiselev, T. Bonev, P. Hartogh)

Cometary research – ROSETTA

MPS Instrumentation and Subsystem Contributions for ESA's ROSETTA Mission

On 2 March 2004 ESA's ROSETTA mission was launched by an Ariane rocket from Kourou/French Guiana with a delay of about one year. This delay has forced ESA to change the scientific targets for ROSETTA, since the ones the mission was originally planned and designed for were out of reach for the new launch date. The new prime target is the Jupiter family comet 67P/Churyumov-Gerasimenko. The spacecraft will arrive at this comet in early 2014 and will perform scientific measurements of the object in orbit around the comet for about 1 1/2 years throughout the perihelion passage of the comet. In late 2014 the ROSETTA lander PHILAE is expected to touch down on the cometary nucleus and to perform scientific measurements at the surface and of samples taken from the surface layers. On its way to the comet ROSETTA will fly-by two asteroids (2867 Steins in 2008 and 21 Lutetia in 2010) and it will perform three swing-bys at Earth and one at Mars.

The MPS is responsible for various scientific instruments or hardware contributions to such instruments onboard ROSETTA, i.e. for COSIMA and OSIRIS as principle investigator responsibility and for CONSERT, MIRO and ROSINA-RTOF with co-investigator contributions, all equipment onboard the ROSETTA spacecraft itself. Furthermore, MPS is also responsible for the COSAC experiment and various subsystems onboard the ROSETTA lander PHILAE.

(H. Böhnhardt)

CONSERT on board ROSETTA

CONSERT (= COmet Nucleus Sounding Experiment by Radio-wave Transmission) is a 90 MHz radio wave experiment in the ROSETTA mission launched by ESA in 2004.

CONSERT will probe the interior of a comet with radio waves to reveal its structure and electrical properties: permittivity, absorption, correlation length of signal (planetesimal size), and volume scattering coefficient.

In the ROSETTA mission a spacecraft will orbit the cometary nucleus, and another spacecraft, a lander, will settle on its surface. 90 MHz radio waves will be transmitted through the comet between the two spacecrafts. As the relative position of the lander and orbiter will vary with time owing to the motions of the orbiter and the (possibly) rotating comet, the cometary interior will be swept by radio waves. Thus, the mean permittivity among a ray path can be determined as a function of aspect angle, and that variation is a measure of the spatial inhomogeneity of the internal structure of the comet.

MPS is responsible for the CONSERT antenna on the orbiter and on the lander. The low mass allocated to the experiment means that no mechanically or electronically steerable narrow antenna main lobe can be contemplated. The antennas must be fixed on both spacecrafts, and have a wide antenna lobe centered on the comet, such that the whole comet is illuminated; this will ensure the best possible signal intensity on the direct ray between orbiter and lander.

The orbiter antenna is two crossed half-wave dipoles placed 0.3 wavelength above two reflectors. The normal of the plane of the dipoles is directed towards the comet.

The lander antenna consists of two quarter-wave monopoles placed on the lower part of the lander body, and extending 'horizontal' away from the body in the deployed position. During launch and cruise phase the monopoles are folded back along the body.

After launch of ROSETTA the CONSERT orbiter antenna was successfully deployed. The antenna on the lander will be deployed when the lander legs are extended after separation from the spacecraft. The CONSERT experiment was then commissioned and the operations verified. Since then every 6 months a status verification has been carried out, where the orbiter and lander electronics are separately tested followed by an orbiter/lander time synchronization test (ping-pong using the CONSERT antennas). The communication between orbiter and lander has so far been via umbilical cord. These tests have shown that the experiment has not changed since commissioning.

(E. Nielsen)

COSAC on board ROSETTA

COSAC onboard of the ROSETTA lander PHILAE will measure the volatile component of cometary surface samples by means of mass spectroscopy and gas chromatography (GC). After successful launch of ROSETTA the commissioning phase of COSAC was performed which proved the functionality of the instrument. It does not seem to have suffered during launch nor during the prolonged stay in Kourou prior to launch.

Two passive payload check-outs were performed afterwards. Both delivered meaningful house-keeping values for COSAC which is presumably in a healthy state.

On collaboration with Cyril Szopa (Service d'Aeronomie, Paris), a calibration campaign of the COSAC GC was performed. The outcome was an improved performance in the GC MS mode which will be useful for the measurement at the comet. Fig. 143 shows the data produced by a combined measurement.

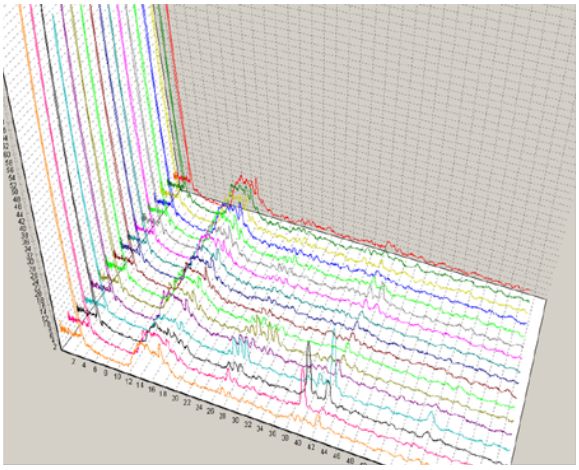

Fig. 143: The image shows a set of mass spectra accumulated for 16 s each and displayed on a time axis. The sample was a test mixture and was injected into the flight spare unit of COSAC operated in a vacuum tank at MPS.

(F. Goesmann, R. Roll, H. Fischer, O. Küchemann, H. Rosenbauer)

COSIMA on board ROSETTA

Since April 2003, our institute is the new home of COSIMA, another Rosetta PI instrument and a cometary secondary ion mass analyser (SIMS). The purpose of the COSIMA instrument is to analyse the cometary dust in the vicinity of the comet's nucleus on its approach to perihelion. COSIMA was not only developed, but would not have been possible without its PI, J. Kissel, who joined our institute in April 2003. He guided the instrument and the COSIMA team successfully through the instrument definition and development phase to the first successful operation of a SIMS instrument in space in 2004 (onboard of the ROSETTA spacecraft). Following his retirement, the COSIMA PI responsibilities were transfered in May 2005 to M. Hilchenbach by the international COSIMA team. The institute will be involved, together with the COSIMA team, in the calibration of the ground reference model, operation of the flight model and preparation for the science phase in the vicinity of the comet in 2014/2015.

(M. Hilchenbach, J. Kissel, H. Krüger, H. Fischer, C. Tubiana, H. Böhnhardt)

MIRO on board ROSETTA

The scientific objectives of MIRO (Microwave Instrument for the ROSETTA Orbiter) are to characterise the abundances of major volatile species and key isotopic ratios of the comet, to study the processes controlling the outgassing in the surface layer of the nucleus and the development of the inner coma, to globally characterise the nucleus subsurface to depth of a few centimetres or more, and to search for low gas levels in the asteroid environment. MIRO (Fig. 144) is a heterodyne spectrometer detecting the molecular and surface emissions at 0.5 and 1.6 mm wavelength. MIRO is the first of a new class of instruments, resembling miniaturised radio telescope. The key component of MIRO is the Chirp Transform Spectrometer (CTS), which has been developed at the MPS and is a worldwide unique equipment in terms of power consumption and mass per spectrometer channel.

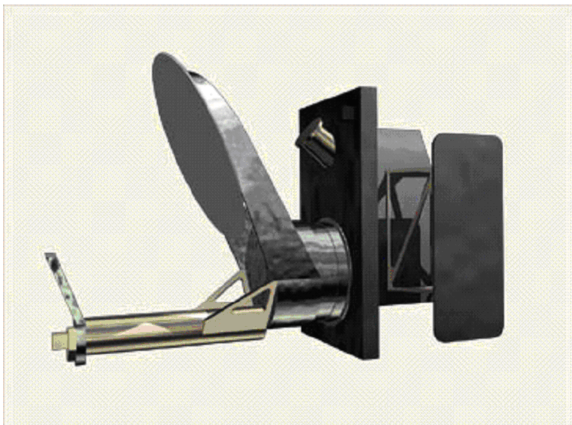

Fig. 144: The MIRO instrument

During the commissioning phase after the launch of ROSETTA in March 2004 it turned out that all MIRO subsystems worked without any problems. The antenna pattern has been determined. One year later, during the Earth flyby in March 2005 MIRO provided water vapour data of the terrestrial thermosphere and mesosphere. MIRO also participated in the Deep Impact observation in July 2005. However, since the amount of water ejected during the impact was much smaller than expected, MIRO could provide just an upper limit of the number of water molecules, produced by this cratering experiment which is in line with observations of the Submillimeter Astronomy Satellite (SWAS) and Odin.

(P. Hartogh, C. Jarchow, L. Song, E. Steinmetz)

OSIRIS on board ROSETTA

OSIRIS (Optical, Spectroscopic,and Infrared Remote Imaging System) is the scientific imaging system on Rosetta. It comprises a narrow angle camera (NAC) with an image scale of $\approx 18.8\mu$rad/pixel, and a wide angle camera (WAC) with a scale of $\approx 99\mu$rad/pixel. Both cameras are equipped with 2048 x 2048 pixel CCD detectors. 12 (NAC) and 14 (WAC) discrete filters allow us to extract light from selected wavelength regions between 245 nm and 1000 nm.

After Rosetta had been launched on 2 March 2004, OSIRIS was commissioned in seven slots between March 2004 and June 2005. Operations included mechanism tests, instrument calibration, alignment between the boresights of the different remote sensing instruments on Rosetta, and checking for interference between OSIRIS and other instruments. During commissioning, the bright comets C/2002 T7 (LINEAR) and C/2004 Q2 (Machholz) were observed on 1 May 2004 and 20 January 2005, respectively. The images showed the good performance of the cameras surpassing the instrument requirements.

Since March 2005 the instrument health has been monitored every 6 months. The instrument proved to be in good health.

The first scientific observations with OSIRIS were conducted during a monitoring campaign of comet 9P/ Tempel 1 around the Deep Impact event. On 4 July 2005, the NASA mission Deep Impact fired a projectile into the comet. A crater formed and material was ejected from the comet. The cloud of ejected material was observed by the Deep Impact spacecraft and by many earth-based and some space-based observatories. Among those, Rosetta was in a privileged position because it could observe 9P/ Tempel continuously for more than two weeks.

OSIRIS monitored the comet's production of dust and ice. Immediately after the impact a steep increase in brightness was measured with the "orange" filter of the NAC, which mainly measures reflected radiation from the cometary dust (Fig. 145). Using certain assumptions about the physical properties of the dust grains ejected from the comet, the mass of the dust ejected by the impact could be estimated. The dominant non-refractory constituent of the comet is water ice. The ice sublimates and is dissociated in the cometary coma by solar radiation. The content of water vapour in the cloud of material ejected by the impact was measured with the WAC, using a filter that measures fluorescence emission from OH, the principal dissociation product of water (Fig. 146). The resulting dust/ice mass ratio in the comet was estimated to be significantly larger than one (Küppers *et al.*, 2005).

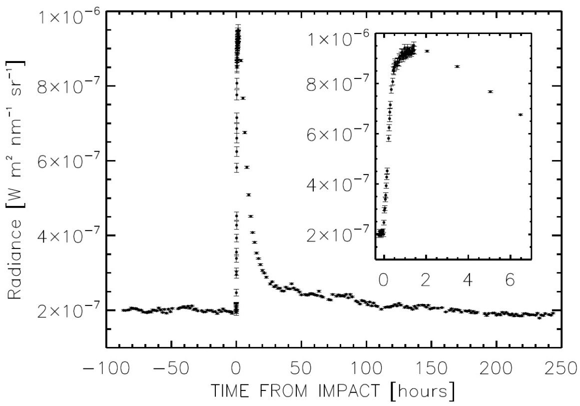

Fig. 145: Brightening of the dust from comet 9P/ Tempel 1 during the Deep Impact event. The radiance from the comet in a circular field of 3000 km radius centered on the nucleus is shown as a function of time relative to the impact. The increase in the first 90 minutes is caused by the dust produced by the impact. The decrease after a few hours is caused by material leaving the circular field and can be used to estimate the dust velocity.

The lightcurve of the impact (Fig. 145) was used to derive the outflow velocity of the dust. The mean velocity of $\approx$ 160 m/s was much larger than typical for impact ejecta. It was concluded from the data that much of the material left the nucleus as "icy grains", a mixture of dust and ice. The grains were heated in the coma when they were exposed to sunlight and sublimated. The dust was then accelerated by the hot water vapour molecules. Furthermore, the increase of the cross section of the dust due to fragmentation of icy grains contributes to the brightness increase seen in Fig. 145 in the first 40 minutes after the impact (Keller *et al.*, 2005).

OSIRIS will be active on several occasions before ROSETTA will arrive at its main target, comet

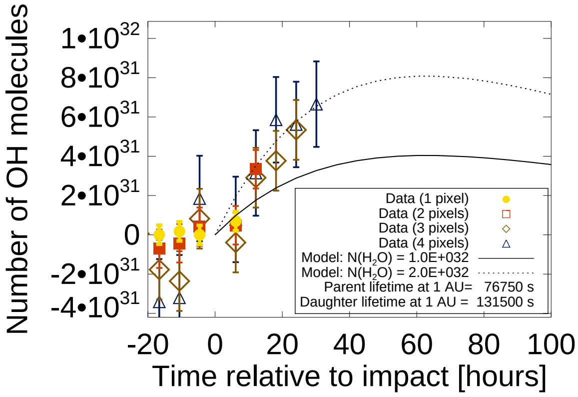

Fig. 146: Number of OH molecules in the coma of the comet. Circular fields with radii between 31,200 km (1 pixel) and 125,000 km (4 pixels) have been used. The median number of molecules measured pre-impact has been subtracted. The solid and the dashed line are models which represent the minimum and maximum number of water molecules created by the impact, respectively.

Churyumov-Gerasimenko, in 2014. The most important observing opportunities are the Mars swing-by in February 2007, two Earth swing-bys in November 2007 and November 2009, and flybys of asteroids Steins (September 2008) and Lutetia (July 2010).

(H. U. Keller, I. Büttner, S. F. Hviid, R. Kramm, O. Küchemann, M. Küppers, M. Rengel, H. Sierks)

ROSINA on board ROSETTA

ROSINA's (Rosetta Orbiter Spectrometer for Ion and Neutral Analysis) primary objective is to determine the elemental, isotopic, and molecular composition of the comet's atmosphere and ionosphere when the ROSETTA spacecraft has arrived at the comet in 2014. ROSINA has unprecedented capabilities including a very wide mass range (1 amu to >300 amu), a very high mass resolution (m/dm > 3000, i.e. it is capable to resolve CO from N_2 and ^{13}C from ^{12}CH), and a very wide dynamic range and high sensitivity, as well as the ability to determine cometary gas velocities, and temperatures. ROSINA consists of two mass spectrometers, a double focusing mass spectrometer (DFMS) and a reflectron type time-of-flight mass spectrometer (RTOF) for neutral and primary ions with complementary capabilities and a pressure sensor (COPS).

Since the successful launch of ROSETTA on March 2, 2004, several commissioning phases were conducted for checkout of different parts of the ROSINA instrument. The high voltage power supply of RTOF shows occasionally discharges which can lead to high currents on a low voltage power line. It is almost certain that this problem will remain and thus additional control software and careful planning is required for a successful full operation of this instrument at the comet.

Currently the ROSINA spare unit, which is identical to the ROSINA flight unit, stays in a vacuum container at the University of Bern and is used for failure investigation, for calibration measurements, software upgrades and tests. It is further used for developing data analysis software to analyse the spectra in various measurement modes.

(A. Korth, U. Mall, K. Heerlein, A. Loose, B. Dabrowski)

The ROSETTA Lander PHILAE

Extensive testing of the ROSETTA lander PHILAE have shown that all subsystems supervised by the MPS work perfectly. These tests have been performed during the commissioning phase after launch of the spacecraft in March 2004. Subsequent checkouts are scheduled to take place twice per year to check the state of each subsystem, e.g.

- Complex landing gear including the damping mechanism
- MSS device to separate lander and orbiter and to push PHILAE into the landing orbit
- Power supply system PSS for the lander
- Harpoon system to anchor the lander at the cometary surface
- Hardware for the command and data management system

Spare reference systems are available for each subsystem. Tests of the PHILAE subsystems are generally performed using the ground reference model at the DLR in Köln-Wahn. The fully functional systems at the MPS are used for planning and qualifying the checks as well as other activities, for training purposes, and for exploring the system behaviour in detail and before hand. Individual lander instruments and subsystems can be replaced by software models. The MPS has also built a thermal vacuum chamber where reference systems are stored for long time and performance test, shortly before PHILAE landing.

(R. Roll, O. Küchemann, H. Fischer, W. Kühne, H. Böhnhardt, I. Szemerey, H. Rosenbauer, H. Timpl, M. Richards, R. Enge, M. Sperling)

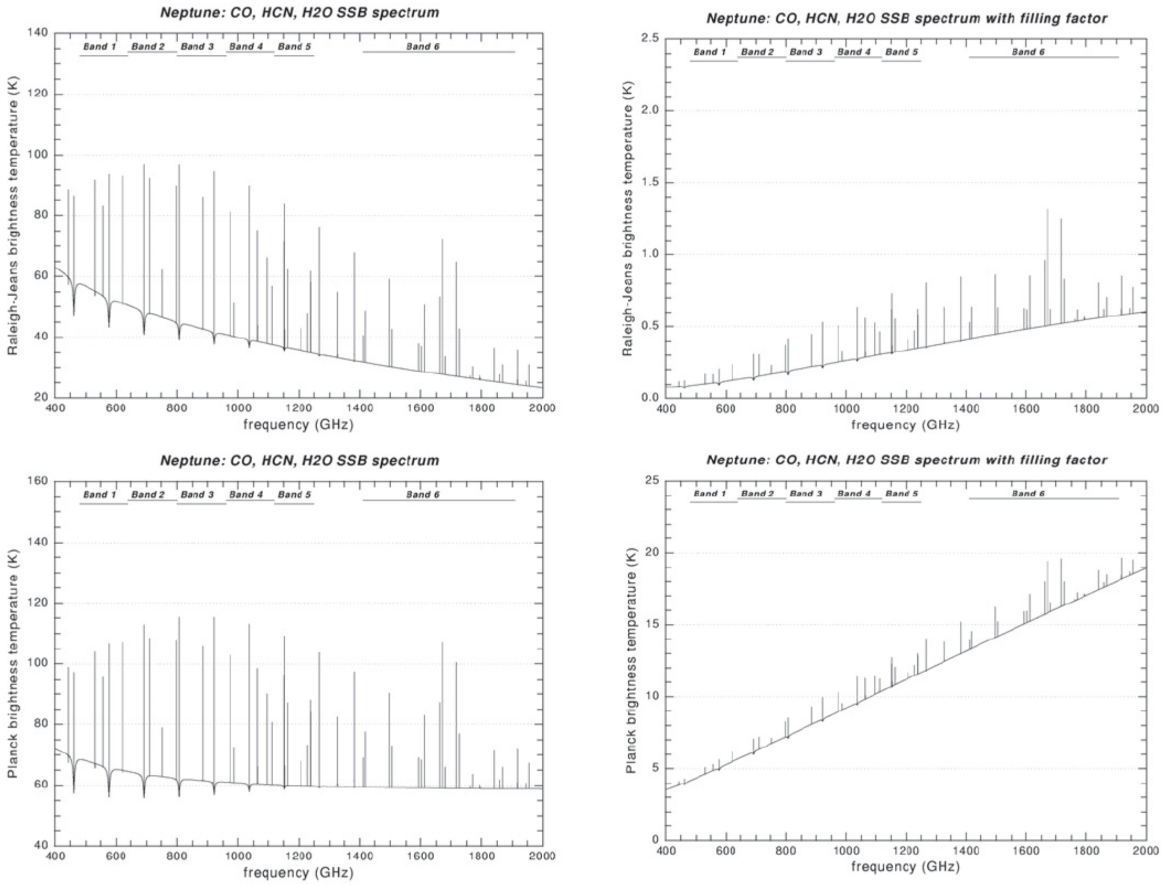

Fig. 147: Simulation of the submillimmeter spectrum of Neptune in the HIFI frequency range. Stratospheric lines are in emission. Left panel: Rayleigh-Jeans and Planck brightness temperatures of Neptune's disk. Right panel: including Herschel's beam dilution. Rayleigh-Jeans brightness temperatures are required in order to determine the signal-to-noise ratio for a given observation time.

Research on minor bodies

Herschel Space Observatory (former Far Infrared Space Telescope – FIRST)

The Herschel Space Observatory will perform photometry and spectroscopy in the 60 – 670 μm range. It will have a radiatively cooled telescope and carry a science payload complement of three instruments housed inside a superfluid helium cryostat. It will be operated as an observatory for a minimum of three years following launch and transit into an orbit around the Lagrangian point L2 in the year 2007.

The key science objectives emphasise especially the formation of stars and galaxies, and the interrelation between the two, but also include the physics of the interstellar medium, astrochemistry and solar system studies.
The three instruments on the Herschel Space Observatory are PACS (Photodetector Array Camera & Spectrometer, SPIRE (Spectral and Photometric Imaging Receiver) and HIFI (Heterodyne Instrument for the Far-Infrared).

HIFI

For solar system research, HIFI will focus on the exploration of planetary and cometary atmospheres. A core program has proposed guaranteed time to investigate the external water of the four giant planets (Fig. 147) and Titan in combination with PACS and SPIRE and to repeat these measurements over the mission lifetime in order to get knowledge about a possible temporal variability. Another program will be dedicated to the Martian atmosphere. It is proposed to monitor the water vapour and to determine accurately it's isotopic ratios. A number of specific species (O_2, O_3, OH, H_2 and H_2O_2) will be searched for. In addition a deep line survey over the whole HIFI spectral range is prepared. Furthermore, it is proposed to study water in a significant sample of comets over a large range of heliocentric distances. The topics are: evolution of water and kinematics by observing the 557 GHz water line; water excitation and physical conditions by observing several water lines; the deuterium isotopic ratio by searching for HDO.

The MPS hardware involvement in HIFI started in 2000 and concerns the Wide Band Spectrometer (WBS) Readout Electronic (WBE) and the WBS Intermediate Frequency Processor (WBI) (see Fig. 148). The flight unit has been delivered in late 2005.

Fig. 148: HIFI-WBS subsystem during EMC-test. Left: WBO (optical unit). Right: WBE (electronic unit) and WBI (intermediate frequency processor).

(P. Hartogh, C. Jarchow, P. Börner, H. Bitterlich, W. Boogaerts, M. Küppers, A. Loose, C. Römer, L. Song, H. Schüddekopf, E. Steinmetz, U. Strohmeyer)

Stratospheric Observatory for Infrared Astronomy (SOFIA)

SOFIA will offer astronomers a unique platform, providing regular access to the entire MIR/FIR and submillimeter wavelength range between 5 μm and 600 μm.
As demonstrated by the KAO (Kuiper Airborne Observatory), IRAS (Infrared Astronomical Satellite) and ISO (Infrared Space Observatory), infrared and submillimeter radiation characterizes a multitude of rich and varied physical processes, and reveals astronomical phenomena occurring in otherwise hidden regions of the cosmos. SOFIA will exploit and extend this scientific legacy by means of sensitive, high spectral and spatial resolution observations spanning the infrared and submillimeter domain. Topics to be addressed by SOFIA users include:

- Composition and structure of planetary atmospheres and rings, and comets.
- Interstellar cloud physics and star formation in our galaxy.
- Proto-planetary disks and planet formation in nearby star systems.
- Origin and evolution of biogenic atoms, molecules, and solids.
- Star formation, dynamics, and chemical content of other galaxies.
- The dynamic activity in the center of the Milky Way.
- Ultra-luminous IR Galaxies (ULIRGS) as a key component of the early universe.

German Receiver for THz Astronomy (GREAT)

GREAT (Fig. 149) has been developed in cooperation with MPIfR in Bonn (PI), the University of Cologne and DLR-WS in Berlin-Adlershof. It will operate in three bands between 1.4 and 5 THz. The MPS contribution is to deliver 4 high resolution Chirp Transform Spectrometers (CTS) and the local oscillator unit (LOU) for the intermediate frequency processor (IFP). One CTS unit and the IFP have been delivered. Due to delays of the SOFIA mission the delivery of the remaining 3 CTS units has been postponed. Since GREAT will be able to measure water vapour in space we plan to determine vertical water vapour profiles in the atmospheres of Mars and the giant planets, investigate its isotopic ratios and seasonal variation. Furthermore, we will work on cometary observations, again mainly of water and its isotopes. Part of the anticipated work should be understood as a preparation of and support for the Herschel Space Observatory.

(P. Hartogh, G. Villanueva, M. Clement, C. Jarchow, C. Römer, E. Steinmetz)

General studies

Deep Impact at comet 9P/Tempel 1: Exploring the dust component

The team of collaborators participated in the worldwide campaign to observe the Deep Impact target comet 9P/Tempel 1 in 2005 (Fig. 150). A regular monitoring program was performed at the Calar Alto 2.2 m telescope over 6 months before the event and at the MPG/ESO 2.2 m telescope for one month thereafter. The measurements characterize the dust and gas evolution of the comet that peaked about 60 – 80 days before perihelion. As of mid February 2005 a porcupine structure of several mostly straight jet-like features evolved in the coma that did not change much in geometry and relative intensity over the long orbit arc of the comet observed. The porcupine structure is interpreted as due to embedded fans produced by 3 – 4 active regions on the rotating nucleus and can be modeled by a rotation axis that is close to be perpendicular to the orbital plane of the comet. An arclet structure appeared in the coma on 14 June 2005 due to an outburst of the nucleus. Abundance ratios of vari-

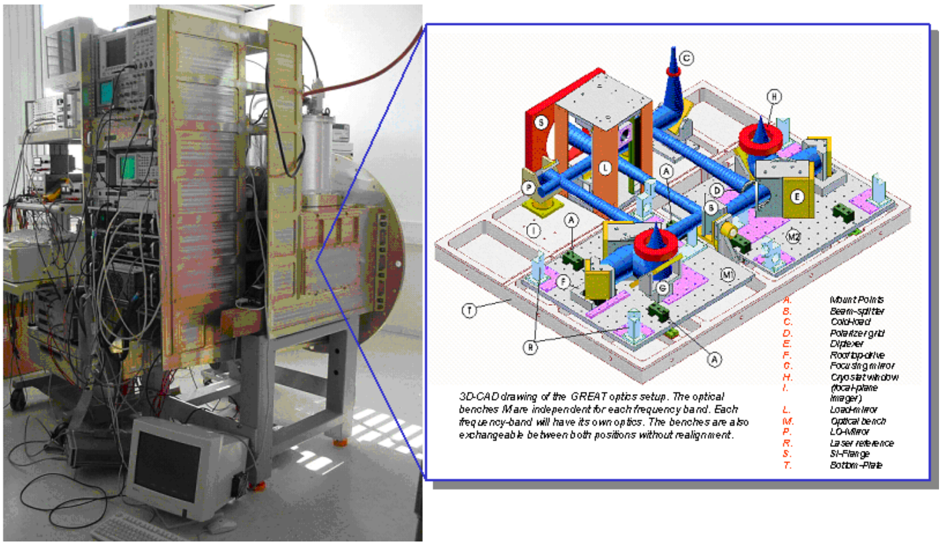

Fig. 149: GREAT – “End-to-End” test

ous coma gases indicate that the comet is classified as “typical” in terms of C_2 abundances.

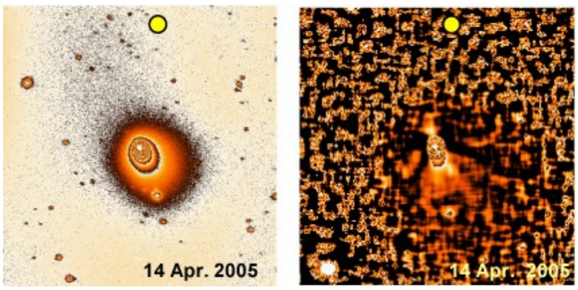

Fig. 150: Comet 9P/Tempel 1 observed with the CAFOS instrument at the MPG 2.2 m telescope at Calar Alto, Spain. Left: isophote image of the comet showing mostly the distribution of dust in the coma. Right: computer enhanced coma structures showing the porcupine structure of embedded fans produced by 3 – 4 active regions on the rotating nucleus. The Sun position is indicated by a filled yellow circle. Background objects appear slightly trailed. North is up and East to the left.

During the week of impact the comet was observed by the team with various telescopes at Calar Alto and at ESO Chile. The ejecta cloud from the impact expanded at an average speed of ∼200 m/s during the first hours after the event (Fig. 151). It reached a stagnation distance of ∼30000 km about 3 days after impact. The pre-impact dust jet and fan activity remained undisturbed after impact. This jet activity can be traced to a few 100 km nucleus distance. No obvious signatures of a new active region produced by the impact, were found. The overall dust production during impact compares to about 10 h of normal activity. The dust temperature rose from about 280 – 290 K before to 330 K one day after the event and returned to pre-impact level the day thereafter. The dust reflected sunlight was found to be linearly polarized at about 7% in the visible and near-IR wavelength regions. This polarization did not change with distance from the nucleus in the very inner coma. Circular polarization of the dust was not detected. The nucleus signal can be isolated in high-spatial resolution adaptive optics images.

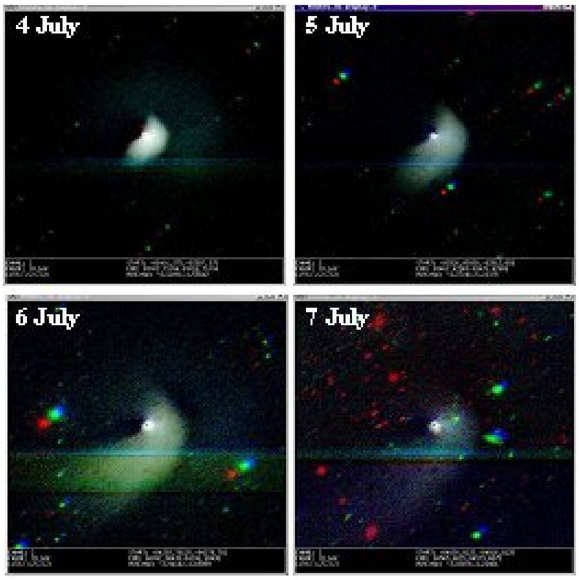

Fig. 151: The expansion of the dust ejecta cloud from the Deep Impact event, observed with the FORS2 instrument at the ESO VLT observatory in Paranal, Chile. The images show the cloud on 4 days after impact. The normal coma pattern is subtracted. The images are composites from individual exposures of the comet taken through B, V, and R filters. North is up and East is to the left.

(H. Böhnhardt)

Comet observations with the Submillimeter Telescope (SMT)

We started a program to observe emission lines from the gas coma of bright comets. The goal is to investigate differences in molecular abundances between comets from different regions in the solar system and to study physical processes in the coma.

At the Submillimeter Telescope (SMT) at Mt. Graham, Arizona, in May 1994 we observed comets 2001/Q4 (NEAT) and 2002/T7 (LINEAR). Both comets are dynamically new, they most likely visited the inner solar system for the first time. We detected emissions of HCN, CS, CH_3OH, HNC, and H_2CO (Fig. 152). CO emission was searched for, but not found. In January 2005 comet 2004/Q2 (Machholz) was observed. Additionally to the molecules found in 2001/Q4 (NEAT) and 2002/T7 (LINEAR), we detected CO and the isotope $H^{13}CN$.

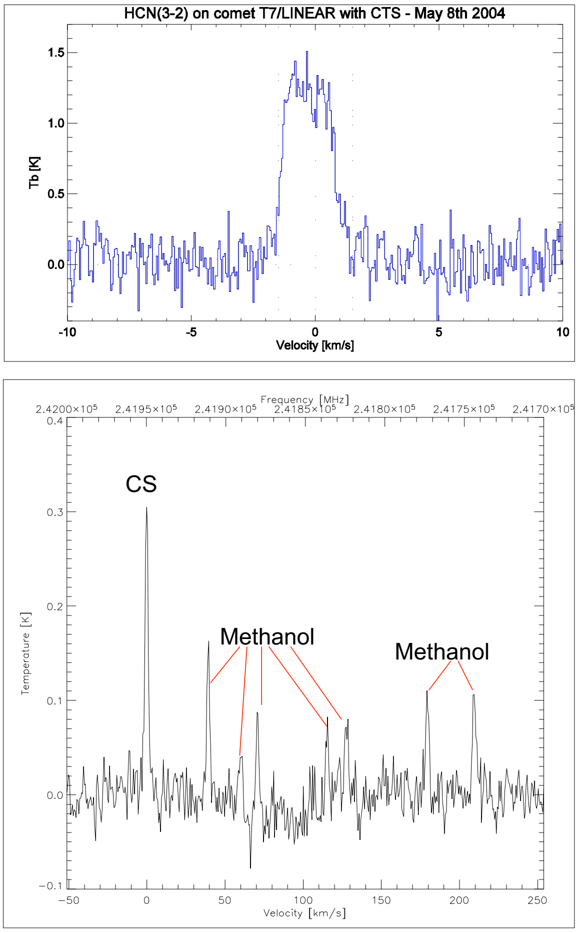

Fig. 152: Spectra of comet 2002 T7/LINEAR in emissions of HCN (top) and CS and CH_3OH (bottom). Intensity is given as a function of radial velocity. On the bottom panel the velocity scale refers to CS molecules only.

Considering also previous observations of several comets by other groups, the results show evidence of a depletion of CO in dynamically new comets. A possible explanation could be connected to the history of these comets: Statistically, they have most likely visited the outer solar system (>5 AU from the Sun) several times. CO is more volatile than the other observed molecules and may have partly evaporated during the previous visits. More observations of dynamically new comets are needed to confirm our results.

(M. Küppers, P. Hartogh, G. Villanueva)

Spitzer and ESO observations of Oort Cloud Comets during their sojourns through the Solar System

Fig. 153: Comet C/2004 B1 (LINEAR) on 10 July 2005, observed with the EMMI instrument at the 3.5 m ESO NTT telescope in La Silla, Chile. The image shows colour coded coma isophotes. The comet appears comma-shaped with a tail extension into sun direction. Background objects are trailed due to the telescope tracking at cometary velocity. The image displays about 250000 x 250000 km at the comet. North is up and East to the left.

This program investigates the interplay between dust grain properties and activity with heliocentric distance in Oort Cloud comets. Spitzer and ground-based observations at various solar distance pre- and postperihelion of two already discovered Oort Cloud comets, C/2004 B1 (LINEAR) (Fig. 153) and C/2003 T4 (LINEAR) (Fig. 154), plus one to two comets not yet discovered will be measured to constrain and compare the grain properties in the comae during three stages of cometary activity: distant activity (5 – 7 AU), coma onset (4 – 6 AU) and vigorous activity (3 – 4 AU). Somewhat unexpectedly, ESO observations of the two comets above revealed that C/2003 T4 was split in at least two pieces in summer 2005, while C/2004 B1 showed a prominent comma-shape coma and tail phenomenon that might be due to emission of heavy dust grains over the past ∼ 1 1/2 years before observations.

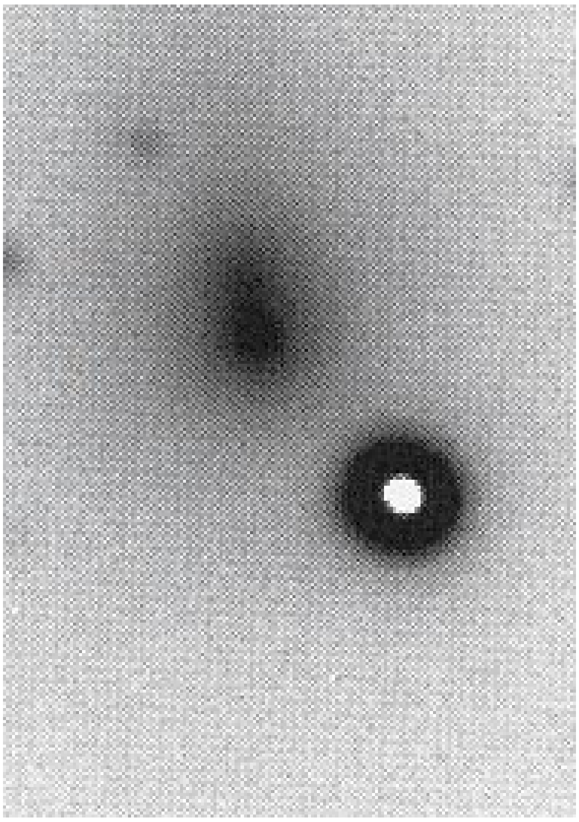

Fig. 154: Comet C/2003 T4 (LINEAR) observed on 10 July 2005 with the EMMI instrument at the 3.5 m ESO NTT telescope in La Silla, Chile. The comet appears split with the secondary component about 1.5 arcsec to the north of the primary one. The dark/white object in the lower image part is a background star as are a few more fainter objects towards North of the comet.

(H. Böhnhardt)

Surface exploration of Kuiper Belt Objects

One part of the project measures – using FORS1 at the ESO VLT – the linear polarization and opposition surge of Kuiper Belt Objects (KBOs) and Centaurs over the maximum phase angle range observable from Earth. So far and for the first time, three objects were observed and analysed by polarimetric measurements: the Plutino 28978, the classical disk object 50000 Quaoar and the Centaur 2060 Chiron. All three objects show negative polarization. 2060 Chiron has the deepest polarization minimum (∼1.5%); for 28978 Ixion (Fig. 155) the negative linear polarization increases rapidly with phase angle while for 50000 Quaoar the polarization is relatively small (∼0.6%) and nearly constant with phase angle. For all three objects, modelling results, invoking numerical descriptions of shadowing and coherent backscattering effects and further measurement results on the albedo and surface chemistry of the objects, suggest that the surface contains an areal mixture of at least two components with different single-scatterer albedos and photon mean-free paths.

The other part of the project focuses on the detection of surface ices on Pluto and its moon Charon. L and M band observations have been obtained using the adaptive optics instrument NACO at the ESO VLT and resolving for the first time the spectra of both objects in this wavelength region.

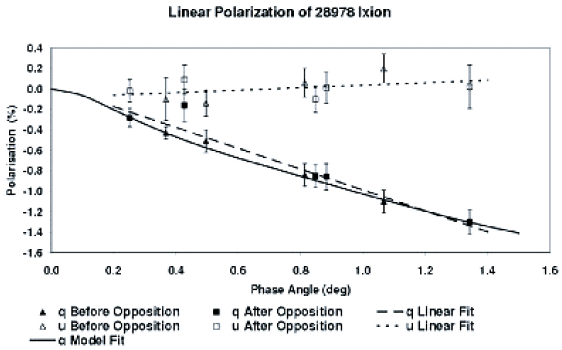

Fig. 155: The linear polarization of 28978 Ixion vs phase angle obtained with the FORS1 instrument at the ESO VLT in Paranal, Chile. Filled symbols: measurements of Stokes Q, open symbols: measurements of Stokes U. Broken and dotted lines indicate linear fits to the observations, the solid line shows the best fit by a light scattering model.

(H. Böhnhardt)

The YORP effect in asteroid (54509) 2000PH5

The thermal YORP-effect may either spin-up or spin-down irregularly shaped asteroids, explaining several puzzling observations of asteroidal rotation. We have found that linking high precision lightcurves of the fast-spinning neath-Earth asteroid 2000PH5 may allow a first precise measurement of this effect as it occurs. In 2003 and 2004 we obtained photometry of 2000PH5 with several telescopes including the ESO VLT and the 2.2 m Calar Alto telescope; these data indicate the discovery of a YORP acceleration at a rate of about 0.001 s/year. Some uncertainty persists as we need to discount stochastic events which required further photometry observations of the object in 2005 (using among others the Calar Alto 2.2 m and 3.5 m telescopes).

(H. Böhnhardt)

Regolith on atmosphereless bodies of the solar system – modelling by aggregates and derivation of a vector radiative transfer equation for dense media

In recent years an increased number of images and spectra of the surfaces of atmosphereless bodies of the solar system (satellites and asteroids) has become available from space missions. In addition ground-based observations allow us to study the phase dependence of the integrated brightness and polarization of the radiation scattered by these bodies. In order to derive the properties of the regolith ("rubble") covering their surface from such observations, an adequate theory of the light scattered by the regolith is needed.

Up to now, most theoretical models of the light scattering by densely packed random media are based on a solution of the vector radiative transfer equation (VRTE) for the Stokes vector which is strictly valid only for sparse media (SM), i.e. for media described by individual scatterers separated far enough to allow the assumption that the electromagnetic wave impinging on spatially separated scatterers is a homogeneous plane wave. Such an approach neglects the effects of correlation between individual particles present in a dense medium (DM) and of wave inhomogeneities. Interference effects between scattered waves are much more important in DM than in SM and, except for the coherent backscattering effect, usually not considered in the SM-VRTE. We have studied the scattering in DM along different lines of research.

In a first step, we have investigated aggregates consisting of spheres in terms of their scattering characteristics and studied how these depend on aggregate structure and on the properties of the constituent particles Petrova *et al.* (2004); Tishkovets *et al.* (2004). Our study is based on an interpretation in terms of successive orders of scattering, in particular on the analysis of the contribution of the interference and near-field effects. Such an approach allowed us to explain and interrelate the main peculiarities of the angular dependence of the intensity and polarization displayed by aggregates. Of special interest are the aggregates showing a so-called negative branch of linear polarization of light scattered into angles close to the backscattering direction. It has been shown that the enhancement of intensity and the negative polarization in this angular range are mainly caused by the interference of multiply scattered waves as well as by near-field effects. If the number of particles in the aggregate is large enough and its size is comparable to the wavelength, the backscattering enhancement is caused by the particles in the surface layers of the aggregate, where the radiation field is mostly homogeneous, while the negative branch is mainly generated by the deeper layers of particles, where the radiation field is inhomogeneous with chaotic changes of amplitudes and phases. This results in a rather weak dependence of the negative polarization on particle location in the deeper layers of the aggregate and on particle number but not on packing density. Some pecularities in the polarization behaviour of complex structures allow us to look at such aggregates like a kind of "mini-regolith", if they are larger than the wavelength in size. However, so far it has not been possible to study aggregates of size considerably larger than the wavelength.

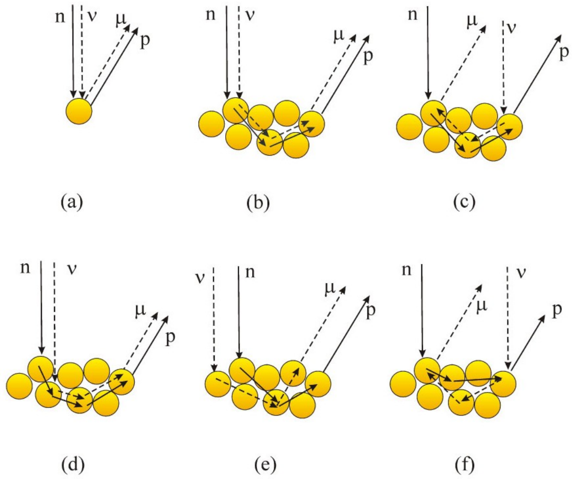

Fig. 156: Diagrams of scattering in a dense medium. Solid lines correspond to a wave with initial polarization n and scattered polarization p. Dashed lines correspond to the complex conjugate wave with corresponding polarizations ν and μ. (a) and (b): Ladder diagrams (incoherent scattering), (c): Cyclical diagram (interference between waves propagating along oppositely directed light paths causing the coherent opposition effects), (d) and (e): Examples of generalization of (b) for the interference between different scattering orders and between waves scattered by neighbouring particles (possible only in a dense medium with particles of size comparable to or less than the wavelength). (f): Example of generalization of (c) for the interference of waves scattered by neighbouring particles.

In the framework of the aggregate model, the behaviour of polarization phase curves observed for both, comets and asteroidal regolith surfaces, can be explained. The modelling carried out confirms that cometary dust particles are larger than the wavelength. However, the grains forming the cometary dust particles or the regolith (or details of the particle surface) have a size less than 0.3 -- 0.5 μm.

In a different approach we have derived a DM-VRTE for a medium consisting of monodisperse spheres. This work is based on scattering scenarios visualized by diagrams derived from the Bethe-Salpeter equation of quantum mechanics (Fig. 156). As a first approach we studied the ladder diagrams only. The derived DM-VRTE has been numerically solved. The results show the expected influence of particle correlation and wave inhomogeneity effects in the framework of ladder diagrams for a not too strongly absorbing medium.

In the future it will be necessary to include other scattering scenarios into the DM-VRTE. For scenario (c) this will be possible only to second scattering order, which is not satisfactory for a dense medium. But there is hope that it will be possible to include scenarios (d) and (e) which are responsible for the wide negative branch of polarization commonly observed in asteroids and cometary dust.

The work was supported by grant 436 RUS 113/684/0-2 of the Deusche Forschungsgemeinschaft in the framework of the priority program 1115 “Mars and the terrestrial planets”.

(K. Jockers, E. V. Petrova, V. P. Tishkovets)

3. Atmosphäre, Ionosphäre und Magnetosphäre der Erde/ *Terrestrial Atmosphere, Ionosphere, Magnetosphere*

Schwerpunktthema:

Erforschung der mittleren Atmosphäre mit Mikrowellen

(P. Hartogh)

(English version see page 135)

Die Entdeckung des Ozonlochs hat die mittlere Atmosphäre seit der zweiten Hälfte der 80er Jahre in den Blickpunkt einer breiten Öffentlichkeit gerückt und international Ozonforschungsprogramme angestoßen. Auch das Projekt WASPAM (WAsserdampf und SPurengase in der Atmosphäre mit Mikrowellen) verdankt seine Existenz dem deutschen Ozonforschungsprogramm. Es stellte sich alsbald heraus, dass das Ozonloch ein Resultat aus sehr niedrigen Temperaturen in der unteren polaren Winter–Stratosphäre und der damit einhergehenden Bildung von PSCs (Polar Stratospheric Clouds) und dem gleichzeitigen Anstieg von Fluor-Chlor Kohlenwasserstoffen (FCKWs) ist. FCKWs werden in der Stratosphäre photolysiert und damit Halogene freigesetzt. Mikrowellenmessungen in der Antarktis zeigten eine Antikorrelation zwischen Ozon und Chloroxid und ließen vermuten, dass Chlor eine wichtige Rolle in der Ozonzerstörung spielt. Je nach Tiefe der Temperatur bestehen PSCs aus Salpetersäurehydraten und/oder Wassereis (PSC Typ I und II). In der Ozonzerstörung spielen sie eine doppelte Rolle. Einerseits wird die Effizienz des katalytischen ClOx-Zyklus auf Wolkenpartikeln drastisch erhöht (heterogene Chemie), anderseits bedeutet die Salpetersäurewolkenbildung eine Abnahme des gasförmigen Stickstoffs in der unteren Stratosphäre.

Um dieselbe besser zu verstehen, bzw. deren Auswirkung zu analysieren, war eine der ersten Aufgaben des WASPAM Experimentes Senken (und Quellen) von Chlor zu identifizieren. So wurden Anfang der 90er Jahre insgesamt ca. 50 Messflüge mit einem Submillimeterwellenspektrometer (dem ersten seiner Art) an Bord des DLR Forschungsjets D-CMET hauptsächlich in polaren Breiten durchgeführt und Salzsäure und insbesondere Chlornitrat als Senken identifiziert. Ein Mangel an gasförmiger Salpetersäure führt also zwangsläufig zu einer Anreicherung der Stratosphäre mit Chlorgas. Umso effizienter findet dann im polaren Frühjahr, ausgelöst durch die ersten Lichtstrahlen der Sonne, die Chloraktivierung und damit die photochemische Zerstörung des Ozons statt. Die wichtigsten Mechanismen der Ozonlochentstehung sind seit den frühen 90er Jahren bekannt. Es stellte sich heraus, dass die bereits 1974 von Rowland und Molina benannten schädlichen Einflüsse der FCKWs noch wesentlich schwerer wogen als berechnet. Beide erhielten zusammen mit Paul Crutzen im Jahre 1995 den Nobelpreis für Chemie.

Die Menschheit nimmt in vielfältiger Weise Einfluss auf die mittlere Atmosphäre. Die Produktion von FCKWs und das damit einhergehende Ozonloch ist nur ein Beispiel. Im Jahre 2000 erschien der Report WCRP-113 (World Climate Research Programme) der WMO (World Meterological Organisation) bekannter unter dem Namen SPARC – WAVAS (Stratospheric Processes and their Role in Climate – Water Vapour Assessment) an dessen Entstehung auch die Mikowellengruppe beteiligt war. Obwohl von der Öffentlichkeit kaum wahrgenommen, war das Ergebnis dieser Studie nicht minder brisant: Zwischen 1950 und 2000 hat der Wasserdampfgehalt der mittleren Atmosphäre je nach Höhenbereich zwischen 10% und 20% pro Dekade zugenommen (vgl. stratosphärisches Ozon: Globale Abnahme 2 – 3% pro Dekade). Da neben dem ClOx – auch der katalytische HOx – Zyklus für die Ozonzerstörung verantwortlich ist (dessen Quellgas Wasserdampf darstellt) und mehr Wasserdampf auch zu vermehrter Bildung von PSCs führt, stellt sich die Frage, wie groß der Anteil des Wasserdampfes am weiter fortschreitenden globalen Ozonabbau ist. Modellrechnungen beschränken sich gegenwärtig auf die Frage, ob ansteigender stratosphärischer Wasserdampf die Erholung der Ozonschicht hinauszögern könnte. Erste Ergebnisse zeigen, dass die für Ende dieser Dekade vorausgesagte Umkehr des negativen stratosphärischen Ozontrends um mindestens 30 Jahre verzögert werden kann, sollte der positive Wasserdampftrend weiter anhalten.

Was ist eigentlich der Grund für den Wasserdampfanstieg der mittleren Atmosphäre? Etwa die Hälfte lässt sich auf den anthropogenen Anstieg von Methan zurückführen (in Zahlen: 0,55 ppm zwischen 1950 und 2000). Das Spurengas Methan entsteht hauptsächlich mikrobiologisch beim anaeroben Abbau organischen Materials z.B. in Feuchtgebieten wie Moore, Sümpfe oder Reisfelder aber auch im Pansen von Wiederkäuern sowie in Mülldeponien und Altablagerungen. Durch menschliche Aktivitäten wird auch fossiles Methan freigesetzt: bei der Erdöl-, Erdgas- und Kohleförderung. Methan wird durch Oxidation in Wasserdampf umgewandelt. Die Ursache für die andere Hälfte des Wasserdampfanstiegs konnte noch nicht eindeutig identifiziert werden. Wasserdampf wird in erster Linie durch die tropische Tropopause mit ihren sehr niedrigen Temperaturen in die Stratosphäre eingetragen. Diese “Kühlfalle” dehydriert die aufsteigenden Luftmassen auf Werte knapp über 4 ppm (d.h. auf ein zehntausendstel des tropischen Bodenwertes). Eine Erhöhung der tropischen Troposphärentemperatur zwischen 1950 und 2000 wäre also ein Kandidat für erhöhten Wasserdampfeintrag. Allerdings konnte ein solcher Anstieg nicht beobachtet werden. Der Dehydrierungsprozess, bereits 1946 von Dobson vorgeschlagen ist in seiner Komplexität bis heute nicht verstanden und deshalb Gegenstand intensiver Forschungen. Mikrowellenspektrometer werden dabei zukünftig eine wichtige Rolle spielen. Um den Einzelbeitrag der beiden Wasserdampfquellen der mittleren Atmosphäre besser charakterisieren und separieren zu können ist es notwendig, die Fortpflanzung des Wasserdampfanstiegs möglichst bis an die “Oberkante” der mittleren Atmosphäre, d.h. die Mesopause, zu bestimmen. Die Mikrowellenfernerkundung ist die einzige Meßmethode, die das sowohl von Satelliten als auch vom Boden aus leisten kann. Bereits in den 80er Jahren wurden am MPS sporadisch Wasserdampfmessungen im cm- und Millimeterwellenbereich durchgeführt. Die dabei gewonnenen Erfahrungen flossen in vollautomatische Spektrometer ein, die neben Wasserdampf auch Ozon messen. Seit 1994 sind diese Instrumente im Dauerbetrieb und beobachten die mittlere Atmosphäre von Lindau und Nordnorwegen (69°N, 10°O) aus. Unser Instrument wird dort im ALOMAR Observatorium (Artic Lidar Observatory for Middle Atmospheric Research) auf der Insel Andoya betrieben. Messungen unseres 22 GHz Wasserdampfspektrometers in Lindau zeigen ein Sommermaximum in etwa 65 km Höhe, dass im Wesentlichen auf die Oxidation von Methan zurückzuführen ist (Abb. 157).

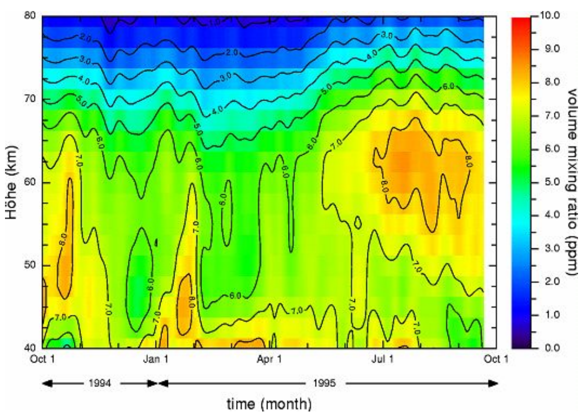

Abb. 157: Wasserdampf Jahresgang über Lindau.

Zum Vergleich ist in Abb. 158 der mit unserem Mikrowellenspektrometer gemessene Jahresgang auf der norwegischen Insel Andoya nördlich des Polarkreises dargestellt. Wir sehen ebenfalls einen stark ausgeprägten Jahresgang mit Sommermaximum und Winterminimum. Jedoch gibt es eine Reihe gravierender Unterschiede: Das Sommermaximum ist zweigeteilt, mit Gewicht auf ca. 45 km Höhe und tritt fast 2 Monate später auf als in Lindau. Das Verhältnis Maximum/Minimum ist in der polaren Mesosphäre weit größer als in Lindau. Der Anstieg zum Sommermaximum beginnt in Lindau bereits im Februar, auf Andoya fast 3 Monate später. Viele weitere Detailabweichungen sind auf die unterschiedliche geographische Position zurückzuführen.

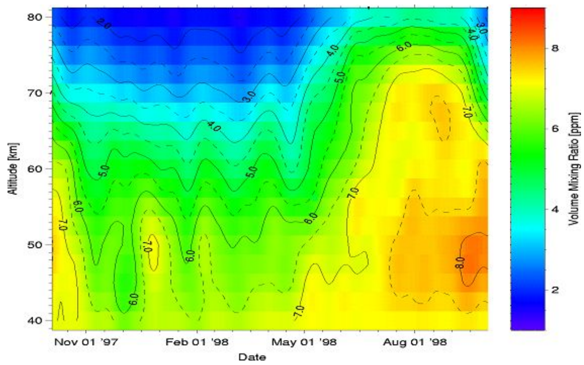

Abb. 158: Wasserdampf Jahresgang über Andoya.

Die Modellierung dieser Unterschiede erfordert neben der Beschreibung der atmosphärischen Zirkulation und Dynamik auch die Kenntnis der Atmosphärenchemie. Moderne Allgemeine Zirkulationsmodelle mit interaktiv gekoppelter Chemie beschreiben nicht nur Klimatologie der mittleren Atmosphäre und die Wechselwirkung zwischen Chemie und Dynamik, sie können darüber hinaus im Idealfall unter Zuhilfenahme von Datenassimilationstechniken die beobachteten Eigenschaften bis ins Detail simulieren. Voraussetzung ist, dass für den Simulationszeitraum ausreihend (möglichst globale) Daten zur Verfügung stehen. Wertvolle Quellen für Temperatur- und Winddaten sind ECMWF (European Centre for Medium Term Weather Forecast, Reading, UK) und NCEP (National Center for Environmental Prediction). Obwohl die vertikale Ausdehnung dieser Daten meist nicht über die mittlere Stratosphäre hinausgeht und somit die untere Randbedingung der Modelle darstellen, lässt sich damit der Zustand der gesamten mittleren Atmosphäre erstaunlich gut modellieren. Die Analyse der Modellrechnungen liefert dann z.B. die raumzeitliche Variation von Betrag und Richtung des Vertikalwindes als Hauptursache für die unterschiedlich ausgeprägten Jahresgänge des Wasserdampfs in mittleren und hohen Breiten.

Auch sporadisch auftretende Phänomene lassen sich anhand des Modells besser verstehen. Abb. 159 stellt einen zeitlich hochaufgelösten Abschnitt (Februar

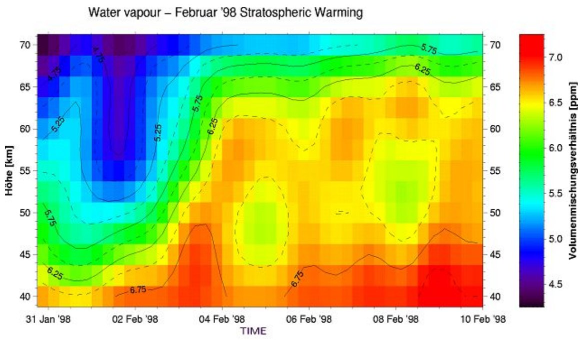

Abb. 159: Wasserdampf Mischungsverhältnisse während einer Stratosphärenerwärmung.

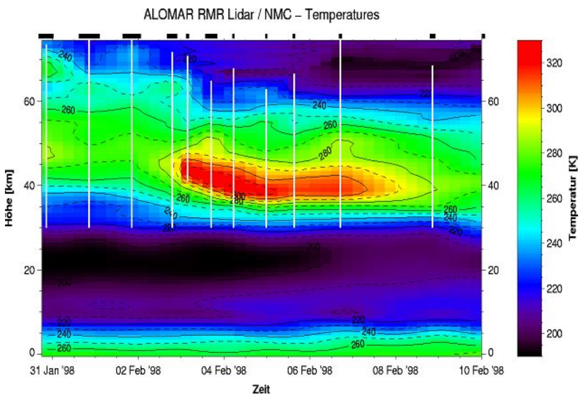

Abb. 160: Stratosphärenerwärmung über Andoya.

1998) aus Abb. 158 dar. Der ungewöhnlich starke Anstieg z.B. der 6.25 ppm Konturlinie um fast 20 km in 2 Tagen tritt während einer Stratosphärenerwärmung auf (Abb. 160). Auf den ersten Blick handelt es sich um einen Vertikaltransport des Wasserdampfes. Die Aufwärtsbewegung liegt allerdings mehr als eine Größenordnung über den Vertikalwinden, die üblicherweise in diesen nördlichen Breiten wehen. Es liegt also nahe, dass horizontaler Transport aus südlichen Breiten hier eine wichtige Rolle spielen könnte. Da aber für den betrachteten Höhenbereich keine Daten über den 3-dimensionalen Transport vorliegen, kann hier die Analyse von GCM-Rechnungen Abhilfe schaffen, oder umgekehrt die gemessenen Wasserdampfdaten als Randbedingungen für die Modellrechnungen herangezogen werden. Wasserdampf kann also als Tracer für Transportbewegungen in der mittleren Atmosphäre genutzt werden.

Wie Abb. 161 zeigt, treten besonders im Winter sporadische Ereignisse des Öfteren auf. Ob sie alle mit Stratosphärenerwärmungen einhergehen oder andere Prozesse eine Rolle spielen ist Gegenstand zukünftiger Untersuchungen. Einige weitere Strukturen in Abb. 161 sind interessant. Sowohl in 45 – 50 km als auch um 65 km herum findet man eine zweijährige Variation, die wahrscheinlich in Beziehung zu der aus der unteren Atmosphäre bekannten QBO (Quasi biannual oscillation) steht. Ob die QBO tatsächlich die Ursache ist und welche Kopplungsparameter die ausschlaggebende Rolle spielen könnten ist ebenfalls noch unklar. Schließlich fällt noch die Variation des Wasserdampfes in der oberen Mesosphäre auf (blaugefärbte Konturen). Der Beginn der Messungen in 1995 fällt in ein Sonnenfleckenminimum. Zunehmende Sonnenaktivität geht einher mit einer Vergrößerung der blauen Flächen, d.h. die Konturen des mesosphärischen Wasserdampfminimums wandern nach unten. Die in Abb. 162 aufbereiteten Wasserdampfdaten zeigen sehr schön, dass die Mesosphäre sozusagen den Übergangsbereich zwischen internen und externen Einflüssen auf die Erdatmosphäre darstellt. Wie man sieht, steigt der Wasserdampf in 47.5 und 57.5 km in der Zeit zwischen 1995 und 2001 um ca. 0.1 ppm ($\sim$2%) pro Jahr an (in Übereinstimmung mit dem allgemein beobachteten Anstieg des stratosphärischen Wasserdampfes). Gleichzeitig nimmt der Wasserdampfgehalt in größeren Höhen jedoch um ca. 0.05 ppm ($\sim$1%) pro Jahr ab. Die Ursache dieses Verhaltens liegt in der Zerstörung des Wasserdampfes durch die im Rahmen der ansteigenden Sonnenaktivität stärker werdenden UV Strahlung (Lyman-Alpha). Das Zeitintervall von 1995 bis 2001 entspricht dem Zeitraum vom Sonnenfleckenminimum zum -maximum.

Die Mesosphäre ist als Übergangsbereich zwischen internen und externen Einflüssen in den letzten Jahren zu einem Schwerpunktthema der Klimaforschung, z.B. im Rahmen des CAWSES (Climate And Weather in the Sun-Earth-System) Programms, geworden. Wie Modellrechnungen zeigen, führt die Erwärmung der Troposphäre um ein Grad zu einer Abkühlung der Mesosphäre um bis zu 5 Grad. Bedenkt man die große natürliche Variabilität der Temperatur scheint es viel versprechender zu sein, Klimaschwankungen in der Mesosphäre als in der Troposphäre nachzuweisen. In der Tat deuten verschiedene Messungen an, dass die Mesosphäre insbesondere in mittleren Breiten in den letzten Dekaden kälter geworden ist. Allerdings sollte man bedenken, dass die Genauigkeit von mesosphärischen Temperaturmessungen noch nicht das Niveau erreicht hat, das in der Troposphäre seit langer Zeit Standard ist. Abgesehen von den erst seit relativ kurzer Zeit zur Verfügung stehenden Temperaturmessungen gibt es mit bloßem Auge sichtbare Anzeichen einer Klimaänderung, nämlich die so genannten Nachtleuchtenden Wolken (NLC = Noctilucent Clouds), auch bezeichnet als polare mesosphärische Wolken (PMC), wobei letztere Bezeichnung streng genommen nicht zutrifft, da man die 82 km hohen Wolken nahezu jeden Sommer auch in Deutschland beobachten kann (Abb. 163). Man nimmt an, dass NLCs Anzeichen ei-

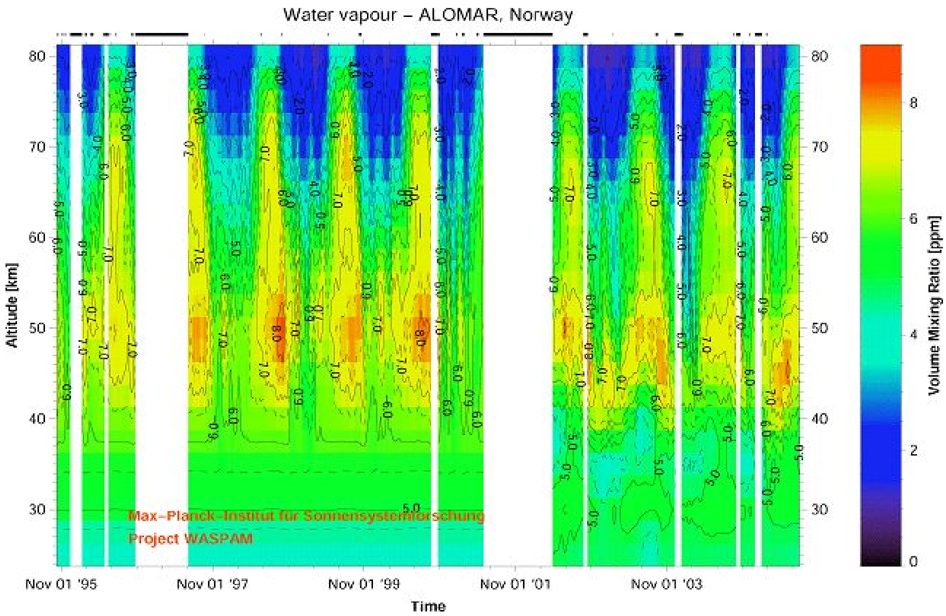

Abb. 161: Wasserdampf Mischungsverhältnisse über Andoya von 1995 bis 2005.

nes klimatischen Wandels sind, da sie offenbar erstmals Ende des 19. Jahrhunderts beobachtet wurden. Die Entstehung von NLCs setzt einen hohen Wasserdampfgehalt und sehr niedrige Temperaturen (sowie genügend Kondensationskeime) voraus. Beides gibt es nur im Sommer, und NLCs werden außerhalb der Monate Juni bis August nur sehr selten beobachtet.

Abb. 164 illustriert die Bedingungen der oberen Sommermesosphäre über Andoya. Die blauen Kurven zeigen Wasserdampf in 85 km Höhe, die grünen die Temperatur in 85 und 87.5 km (gestrichelt), die roten Kurven den Sättigungsgrad des Wasserdampfes und die schraffierten Flächen den Zeitraum in dem der Sättigungsgrad größer als 1 ist (in 85 und 87.5 km Höhe), sich also Wolken bilden können. Die schwarzen Kurven stellen die relative Häufigkeit von beobachteten Eisteilchen (Wolken) dar. Es stellt sich nun die Frage, ob sich die beobachtete Reduzierung des Wasserdampfgehaltes in verringerter NLC Aktivität wieder findet.

Neben der Häufigkeit von NLCs, ist auch deren Albedo ein wichtiges Maß für NLC-Aktivität. Letztere steigt mit größer werdenden Teilchen, bzw. Teilchendichten. Weniger Wasserdampf würde die NLC Albedo verringern. SBUV Beobachtungen zeigen jedoch, dass sich seit 1980 und offensichtlich auch zwischen 1995 und 2001 die NLC Albedo im Mittel erhöht hat (Abb. 165), was auf den ersten Blick im Gegensatz zur unseren Beobachtungen auf Andoya zu stehen scheint.

Der Konflikt löst sich auf, wenn man bedenkt, dass NLCs nur im Sommer auftreten, während die Wasserdampfdaten aus Abb. 162 das ganze Jahr umfassen. Analysiert man nur die Monate Juni bis August sieht man in der Tat einen geringen Anstieg im Wasserdampf (Abb. 166). Da im Sommer die Vertikalwinde im Mittel nach oben gerichtet sind, wird offenbar der durch die solare Lyman-Alpha Strahlung zerstörte Wasserdampf durch Transport von unten ausgeglichen. Der beobachtete NLC-Albedo Anstieg steht also im Einklang zu dem beobachteten stratosphärischen Wasserdampftrend. Daraus folgt, dass man die Variabilität der Sonnenaktivität in Lyman-Alpha im Wasserdampf der Wintermesosphäre suchen muss, dann nämlich, wenn die mittleren Vertikalwinde nach unten gerichtet sind. Weitergehende Analysen, die auch Modellrechnungen einschließen, bestätigen diese Interpretation. Betrachtet man in Abb. 161, wie weit in den Wintern 2002 und 2003 mesosphärische Wasserdampfwerte von unter 3 ppm bis in die Stratosphäre transportiert werden, stellt sich die Frage, ob es nicht doch einen Einfluss der Sonne auf den Wasserdampf der mittleren Atmosphäre im Sommer geben kann. Die sehr niedrigen Mischungsverhältnisse im Winter könnten sich transportbedingt (aufgrund der langen chemischen charakteristischen Zeiten des Wasserdampfs in diesem Höhenbereich) auch im darauf folgenden Sommer wieder finden. Die Atmosphäre hätte in diesem Fall eine verzögernde Funktion, solare Aktivitätsschwankungen würden sich erst Monate später etwa in einer veränderten Ozonkonzentration in der Stratopausenregion artikulieren. Quantitative Untersuchungen zu dieser Frage mit Hilfe eines Allgemeinen Zirkulationsmodells sind im Gange.

Oberhalb der Stratopause dominiert der katalytische HOx-Zyklus den Abbau von Ozon. Deshalb

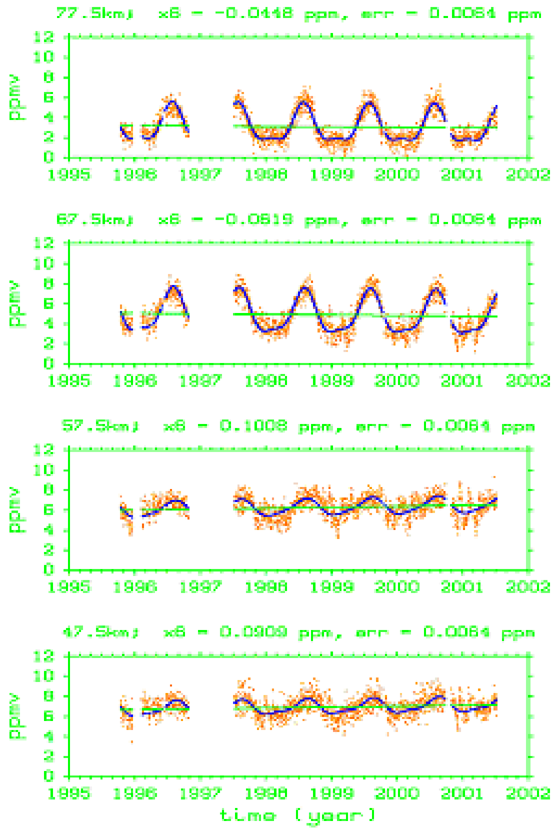

Abb. 162: Veränderungen der Wasserdampf Mischungsverhältnisse zwischen 1995 und 2001. Die orangen Punkte repräsentieren Tagesmittel des Wasserdampfgehaltes, die schwarzen Kurven Fits der halb- und ganzjährigen Komponente der Wasserdampfvariation und die grünen Kurven die Änderung des mittleren Wasserdampfgehaltes über den gesamten Meßzeitraum.

Abb. 163: NLCs im Juni 2005 (von Göttingen aus beobachtet).

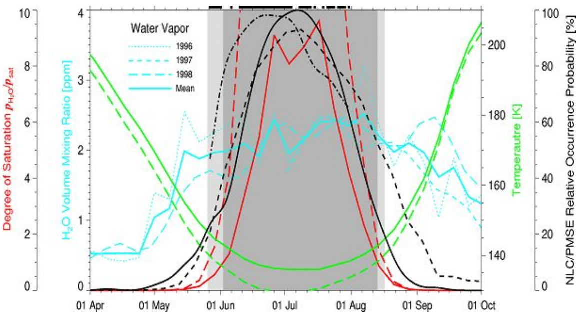

Abb. 164: Bedingungen der Sommermesosphäre über Andoya.

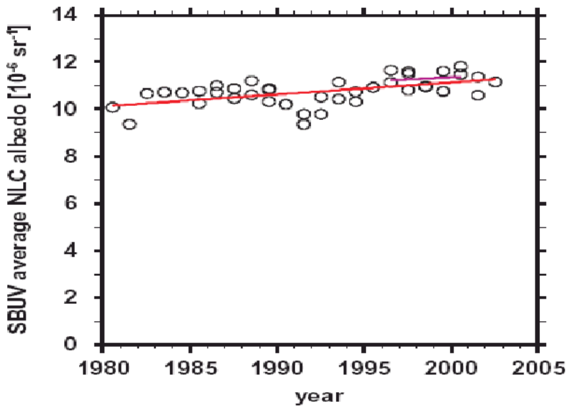

Abb. 165: SBUV Beobachtungen der NLC Albedo.

ist die genaue Kenntnis der Konzentration von Wasserdampf (das Quellgas für Hydroxylradikale) von großer Bedeutung. Grundsätzlich sind die Konzentrationen von Wasserdampf und Ozon antikorreliert. Das gilt natürlich nur solange Hydroxylradikale erzeugt werden können. Am Beispiel des tertiären Ozonmaximums (auch unter MMM = Middle Mesosphere Maximum bekannt) wurde dieser Zusammenhang quantitativ untersucht. Die Abb. 167 und Abb. 168 zeigen das von unserem 142 GHz Ozonspektrometer gemessenen MMM über Lindau und Andoya. Das MMM tritt in ca. 72 km Höhe auf, wobei in Nordnorwegen höhere Mischungsverhältnisse erreicht werden. Ferner gibt es Unterschiede im zeitlichen Verhalten der MMM-Amplitude. Während des Wintersonnenwende erreicht das MMM beispielsweise Maximalwerte über Lindau, während über Andoya ein Minimum auftritt. Die jahreszeitliche Asymmetrie ist auf den jahreszeitlichen Verlauf des Wasserdampfes zurückzuführen. Normalerweise wird Ozon in 72 km Höhe durch ungeraden Wasserstoff abgebaut. Da Wasserdampf aber einen höheren Absorptionsquerschnitt als Sauerstoff hat, ist die Eindringtiefe der Lyman-Alpha Strahlung nicht so tief wie in den für die Dissoziation des molekularen Sauerstoffs verantwortlichen Schumann-Runge Bändern, d.h. für niedrige Sonnenstandswinkel wird weniger Wasserdampf in ungeraden Wasserstoff umgewandelt und deshalb weniger Ozon zerstört. Da aber weiterhin molekularer Sauerstoff photolysiert wird, entsteht weiterhin atomarer Sauerstoff der durch Dreikörperstoffreaktion mit O_2 Ozon bildet.

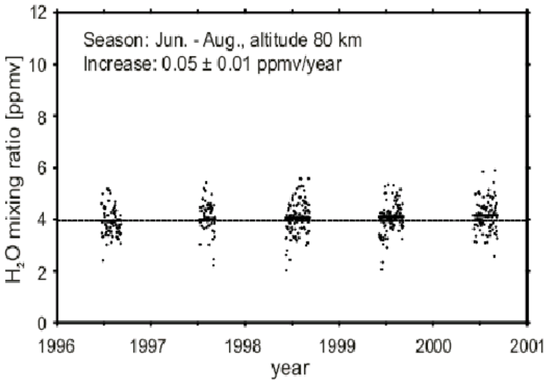

Abb. 166: Veränderungen der Wasserdampf Mischungsverhältnisse (Juni bis August) zwischen 1995 und 2001.

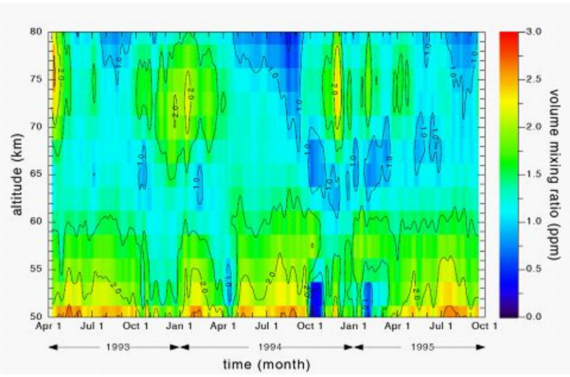

Abb. 167: MMM (Middle Mesosphere Maximum) über Lindau.

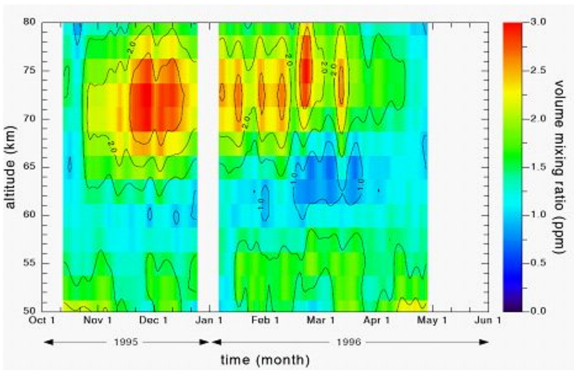

Abb. 168: MMM (Middle Mesosphere Maximum) über Andoya.

Abb. 169 zeigt das relative Verhältnis der Dissoziationsraten von Wasserdampf und Sauerstoff in 75 km Höhe als Funktion des Sonnenstandswinkels. Für Zenitwinkel von mehr als 36 Grad beginnt das Verhältnis zu fallen und erreicht bei 90 Grad sehr kleine Werte. Selbst in Lindau beträgt der Zenitwinkel der Sonne während des Wintersolstitiums 75 Grad um die Mittagszeit, d.h. die Produktionsrate von Hydroxylradikalen ist stark reduziert. Diese qualitative Beschreibung zeigt den grundlegenden Mechanismus der MMM - Entstehung auf. Die quantitative Modellierung der gemessenen Mischungsverhältnisse erfordert allerdings wesentlich detailliertere Betrachtungen, für die an dieser Stelle nicht genügend Platz zur Verfügung steht. Es sein nur kurz angedeutet, dass für große Zenitwinkel die Dissoziation von geraden Wasserstoff durch $O(^1D)$ eine wichtige Rolle zu spielen beginnt. Letztere hängt wiederum von einer Reihe anderer Parameter ab, u.a. der Ozonkonzentration, der Ozondissoziationsrate (die wiederum von der Ozonkonzentration abhängt = “Self Shielding Effect”), der Temperatur, der Dichte und natürlich spielen auch dynamische Vorgänge eine wichtige Rolle.

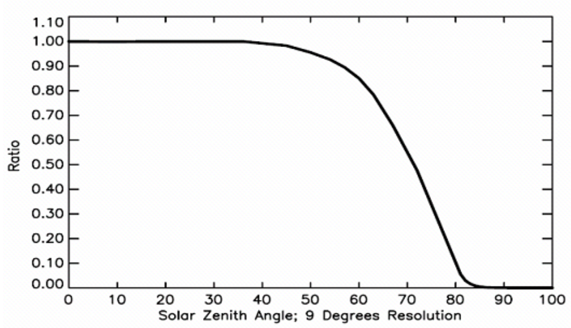

Abb. 169: Relative Dissotiationsrate von Wasserdampf und molekularem Sauerstoff in 75 km Höhe.

Es ist u.U. sehr schwierig, Beobachtungen mit Hilfe von Modellrechnungen selbstkonsistent und quantitativ zu beschreiben. Messungen sind (natürlich) dazu geeignet und notwendig, Modelldefizite aufzuzeigen. Um nur ein Beispiel zu nennen: Das Doppelmaximum im Wasserdampf (Abb. 158 und Abb. 161) konnte mit dem in unseren Arbeiten u.a. verwendeten Allgemeinen Zirkulationsmodell “COMMA-IAP” erst reproduziert werden, nachdem ein neues advektives Transportschema mit verringerter numerischer Diffusion in das Chemie-Transport Modul integriert wurde. Derartige Verbesserungen fließen in der Regel direkt in unser “Schwestermodell” MAOAM ein (siehe Seite 101), das die allgemeine Zirkulation der Marsatmosphäre beschreibt. Solange es für die meisten (potentiellen) Spurengase in der Marsatmosphäre weder gemessene Säulendichten, geschweige denn Vertikalprofile gibt, leisten unsere bodengebundene Messungen der mittleren Erdatmosphäre auf diesem Wege einen wichtigen Beitrag zur Erforschung der Marsatmosphäre und sind ein Paradebeispiel für den Nutzen der vergleichenden Planetologie.

Highlight:

Investigations of the middle atmosphere with microwaves

(P. Hartogh)

The discovery of the ozone hole initiated a large number of national and international activities on middle atmospheric research. Among others, the WASPAM (Water vapour and trace gas measurements with microwaves) project has been funded by the German ozone research program.

Rather quickly scientists found the most important mechanisms causing the ozone hole: the lower polar winter stratosphere gets so cold that ice clouds, known as Polar Stratospheric Clouds (PSCs), are formed. Photolysis of the increasing amount of Chlorofluorocarbons (CFCs) in the stratosphere releases halogens. In the late eighties, microwave observations in Antarctica found an anti-correlation of chlorine oxide and ozone which indicated the important role of this gas in the ozone depletion process. Depending on temperature, PSCs consists either of nitric acid hydrates and/or water ice (PSC types I and II). They play a double role in the depletion of ozone. Not only due they drastically enhance the efficiency of the catalytic ClOx-cycle, the forming of nitric acid clouds (PSC I) also reduces the amount of gaseous nitrogen in the lower polar stratosphere.

One of the first investigations of the WASPAM experiment was to identity the sinks (and sources) of chlorine. In the early nineties we performed about 50 flights mainly in polar regions using a submillimetre wave spectrometer onboard the D-CMET, a twin jet aircraft of DLR und identified hydrochloric acid and mainly chlorine nitrate as sinks. Thus the lack of gaseous nitric acid obviously leads to a chlorine enrichment of the stratosphere in the polar winter and a very efficient ozone destruction mechanism starts in spring once triggered by solar light.

The most important mechanisms creating the ozone hole are known since the early nineties. It turned out that CFCs are even more harmful than already predicted by Rowland and Molina back in 1974. They were rewarded the Nobel price in chemistry together with Paul Crutzen in 1995.

The ozone hole is not the only example for anthropogenic effects on the environment. In 2000 the report WCRP-113 (World Climate Research Programme) of WMO (World Meteorological Organisation) also known as SPARC-WAVAS report (Stratospheric Processes and their Role in Climate – Water Vapour Assessment) was published (including members of our microwave team in the authors list). Although not as much noticed by the public, the result of the study was as least as spectacular as the discovery of the ozone hole: between 1950 and 2000 the amount of water vapour in the stratosphere increased altitude dependent by 10% to 20% per decade (compare with the ozone decrease of about 2 – 3% per decade). An increase in water vapour not only intensivies the HOx-cycle which by itself destroys ozone, it also leads to more PSCs forming. This bears the questions about the net effect of water vapour on ozone depletion. Taking into account the reduced production of CFCs agreed upon in the Montreal protocol model calculation predicted a recovery of ozone for the end of this decade. However, under the assumption that water vapour would continuously increase this recovery may be delayed by another 30 years.

What causes the water vapour increase? About half of the increase is related to the anthropogenic increase of methane (0.55 ppm between 1950 and 2000). This trace gas methane is produced mainly by the anaerobe decomposition of organic material, for instance in moors, marshes, and rice fields, but also in the rumen of cows, solid waste disposal sites and from mining of fossil fuels (coal, oir and gas). Methane is transformed into water vapour by oxidation. The other half of the middle atmospheric water vapour increase has not been clearly identified yet. The main source of mid atmospheric water is the transport of tropospheric air through the tropical tropopause. Since the tropical tropopause is very cold, it acts as a cold trap resulting in a water content of little more than 4 ppm in the upwelling air after the dehydration process. Thus, an increase of the tropical tropopause temperature could explain the observed water vapour increase. However, such a temperature increase has not been observed. Although already proposed by Dobson in 1946, the very complex dehydration process has not been completely understood yet and is still subject to extensive research. Future microwave spectrometers will play a substantial role in this disentangle the number of physical processes involved.

In order to better characterise the two known sources of water vapour it is of great importance to determine its profile up to the highest level of the middle atmosphere, the mesopause. Microwave remote sensing is the only method capable to provide this information from ground-based as well as from satellite borne platforms.

Already in the eighties we performed sporadic water vapour measurements in the centimetre and millimetre wave range. Based on these experiences, fully automated spectrometers have been developed detecting water vapour and ozone. Since 1994 these instruments are in permanent operation and observe the middle atmosphere above Lindau and the island Andoya (69°N, 16°E) in Northern Norway at ALOMAR (Arctic Lidar Observatory for Middle Atmospheric Research).

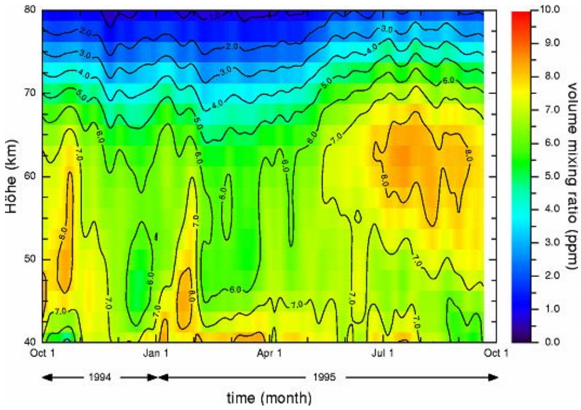

Fig. 157: Annual variation of water vapour above Lindau.

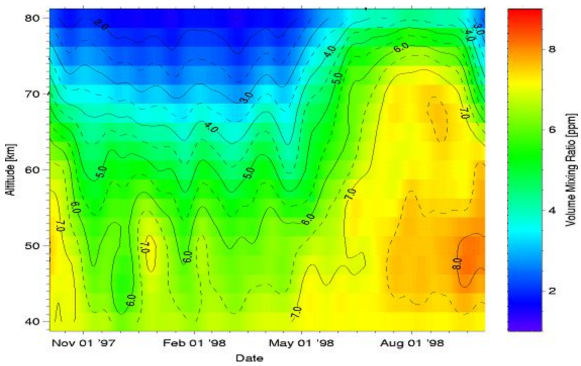

Fig. 158: Annual variation of water vapour above Andoya.

Measurements of our 22 GHz water vapour spectrometer show a pronounced annual cycle in both locations with a maximum of water vapour in summer. It appears at a height of about 65 km in Lindau (Fig. 157). In Northern Norway (Fig. 158) there is a summer maximum and winter minimum as well, however there are a number of differences: the summer maximum is separated into two peaks at 45 – 50 km and 65 to 70 km and appears about 2 month later than in Lindau. The rise of the contour lines starts about 3 month later in Northern Norway. There are many other differences related to the different geographical positions, reflecting features of the atmospheric chemistry and dynamics. Thus the modelling of these differences requires to consider both, chemistry and dynamics. Modern General Circulation Models (GCMs) with interactive coupled chemistry do not only describe the climatology of the middle atmosphere and the interaction of chemistry and dynamics. In the ideal case they are able to explain details of the observed features, provided data assimilation techniques are applied. Of course, this requires that enough data is available for the simulated period. Valuable data of temperature and wind data are for instance provided by the European Centre for Medium - Range Weather Forecasts (ECMWF) and the National Center of Environmental Predicion (NCEP). Although the vertical extension of these data generally does not include the upper stratosphere and mesosphere it is sufficient to act as lower boundary condition allowing to describe higher up processes with amazing accuracy. These model calculations find for instance that the main reason for the different annual variations of water vapour in Germany and Northern Norway is related to the spatiotemporal variation of vertical winds.

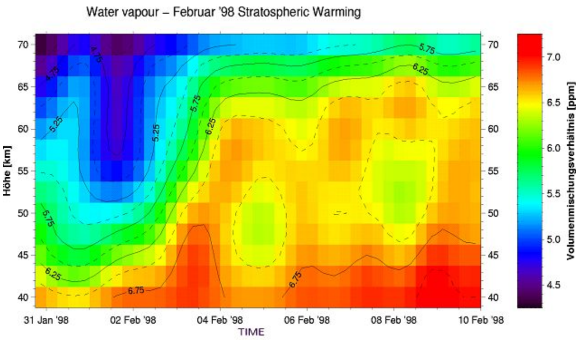

Fig. 159: Mixing rations of water vapour during a stratospheric warming.

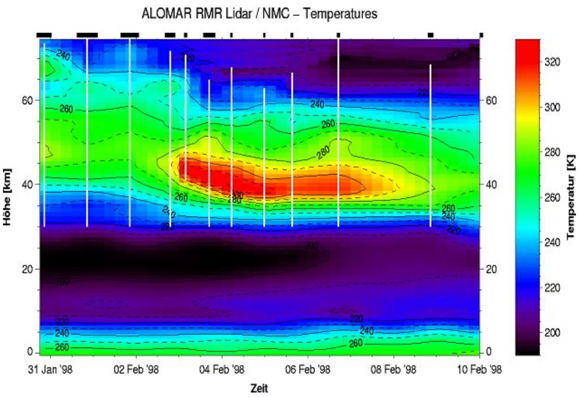

Fig. 160: Atmospheric temperatures above Andoya during a stratospheric warming.

The model also helps to better understand the sporadic phenomena appearing in the contour plots discussed above. Fig. 159 shows a temporally highly resolved episode (February 1998) of Fig. 158. The unusually strong rise, for instance, of the 6.25 ppm contour line of nearly 20 km within 2 days appears during a stratospheric warming (Fig. 160). At first glance, it looks like a vertical transport of water vapour. This upwelling, however, appears to be more than one order of magnitude quicker than the usual vertical wind in this latitude. Therefore, horizontal advection has to be considered as a possible reason. Since we do not have temperature and wind data for the altitude range,

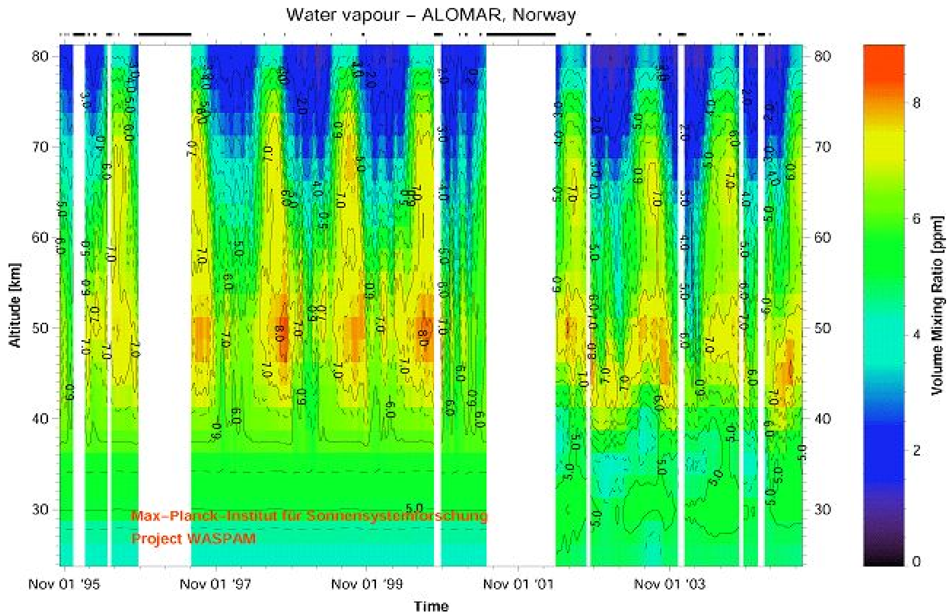

Fig. 161: Mixing ratios of water vapour above Andoya between 1995 and 2005.

the GCM helps to quantify the vertical and horizontal transport. On the other hand, our water vapour data is used to constrain the model. Generally, water vapour acts as a tracer since it is photochemically stable in the middle atmosphere. The example of the stratospheric warming however shows, that 3-dimensional measurements are preferable compared to our 1-dimensional ones. In the future, we plan experiments observing 3 directions at the same time.

Fig. 161 shows that the sporadic events and described above mainly appear in winter. Since it is not clear if all of them are related to stratospheric warmings or other processes may play a role, these events are subject for further investigations.

We find some additional interesting features. Both maxima in 45 – 50 km and around 65 km show a biannual variation which probably is related to the QBO (quasi biannual oscillation). It is interesting that the phase of these maxima in both altitudes is shifted by 180 degrees. It remains unclear whether this features are really related to the QBO nor do be understand the possible coupling mechanisms.

Finally, there is a striking feature in the upper mesosphere (blue contours). The measurements start in 1995 during a sunspot minimum. Increasing solar activity comes along with an increase of the blue areas, i.e. the contour lines migrate to lower altitudes. Fig. 162 is a good example demonstrating that the mesosphere is the transition region between internal and external influences on the atmosphere. It shows that from 1995 to 2001 water vapour increases at 47.5 and 57.5 km by about 0.1 ppm (∼2%) per year (in consistency with the generally observed increase of stratospheric water vapour). At the same time, water vapour at higher altitudes is decreasing by about 0.05 ppm (∼1%) per year, probably related to the increasing amount of photolysing solar Lyman-Alpha radiation. Note that from 1995 to 2001 the sun changed from minimum to maximum activity.

The transition region between internal and external influences mentioned above recently became a priority of climate research for instance within the framework of the CAWSES program (Climate And Weather in the Sun-Earth-System). As model calculations show, an increase of the tropospheric temperature by 1 degree C goes along with a cooling of the mesosphere by 5 degrees C. Taking into account the large natural variability of temperature it seems to be more promising to detect climate change in the mesosphere rather than in the troposphere. Indeed, a number of measurements indicate a decrease of temperature especially at mid latitudes. However, it should be kept in mind that mesospheric temperature measurements have not yet achieved the level of accuracy being standard at tropospheric heights since a long time.

Apart from mesospheric temperature records which cover a few decades there are visible indications of climate change, the so called noctilucent clouds (NLCs), also called polar mesospheric clouds (PMCs). Actually, the latter denomination is not completely apply since these 82 km high clouds can even be observed from central Germany nearly every summer (Fig. 163). Noctilucent clouds are believed to be an indication of climate change, because they have not been observed and described before end of the nineteenth

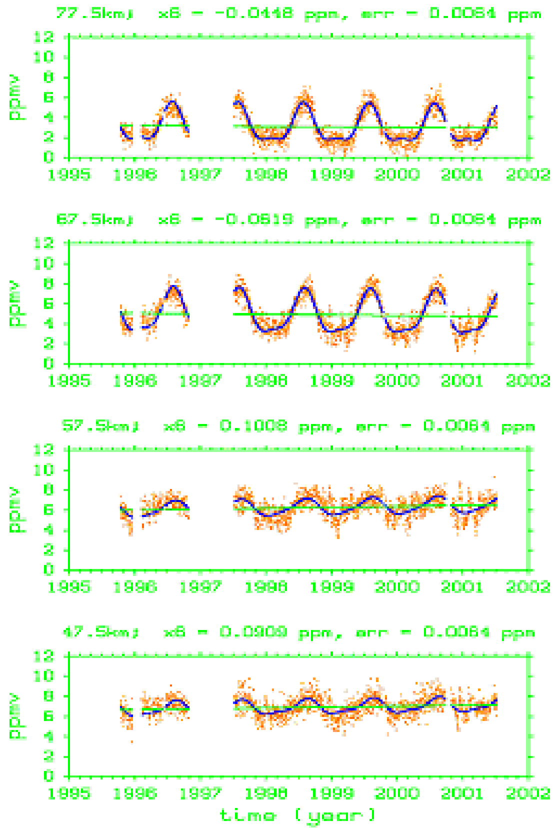

Fig. 162: Interannual variations of water vapour from 1995 to 2001. The orange dots represent diurnal averages of the water vapour content, the black curves represent fits of the annual and semi-annual component of the water vapour variation and the green curves the variation of the mean water vapour content during the observation period.

century. The formation of NLCs requires high water content, low temperatures, and enough condensation nuclei. Temperature and water vapour conditions fulfil this requirement in summer. NLCs are hardly observed before June and after August.

Fig. 163: NLCs in June 2005 (observed from Göttingen).

Fig. 164 illustrates the conditions of the upper summer mesosphere over Andoya. The blue curves show the water vapour mixing ration at 85 km, the green curves the temperature in 85 and 87.5 km (dashed), the red curves the degree of saturation of water vapour (S) and the shaded areas the time interval of S > 1 (in 85 and 87.5 km), i.e. the conditions under which clouds can form. The black curves show the relative frequency of observed ice particles (clouds). Does the observed water vapour decline translate into less NLC activity?

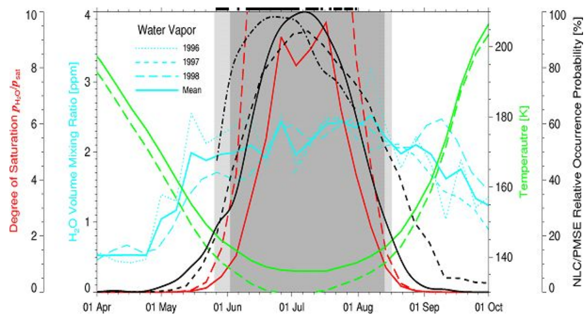

Fig. 164: Conditions of the summer mesosphere over Andoya.

Beside the relative appearance frequency of NLCs their albedo is an indication of NLC activity. The latter increases with growing particle sizes and densities. Less water should result in a smaller NLC albedo. However, SBUV observations show, in contrast to our observations, that since 1980 as well as between 1995 and 2001 the average NLC albedo increased (Fig. 165).

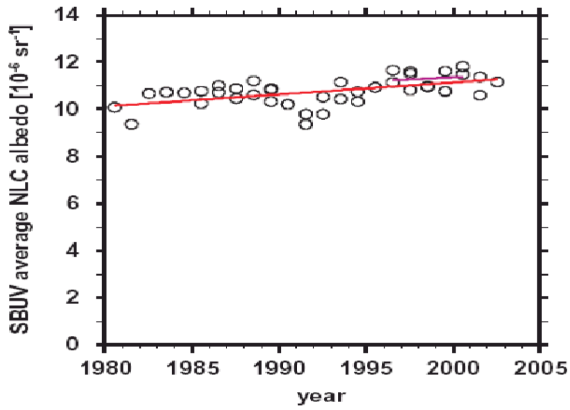

Fig. 165: SBUV observations of the NLC Albedo from 1980 to 2005.

This discrepancy can be resolved taking into account that NLCs only appear in summer while the water vapour data shown in Fig. 162 cover the whole years. Analysing only the months June to August indeed shows a slight increase instead of a decrease of water vapour in the upper mesosphere (Fig. 166). Since the medium vertical winds blow upwards in summer, the amount of water vapour destroyed by Lyman-Alpha radiation seems to get over-compensated by the water vapour rich air from below. Thus the observed NLC albedo increase is in line with the observed stratospheric water vapour increase. Since there is no decrease in the summer mesospheric water vapour, it follows that the decrease in winter, i.e. when the vertical winds point downwards, must be all the larger. A more detailed data analysis supported by GCM calculations have confirmed this interpretation. Thus, solar UV variability in summer translates into atmospheric responses in winter.

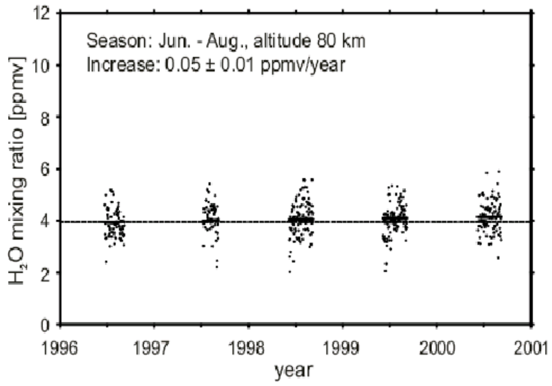

Fig. 166: Interannual variation of the water vapour mixing ratio at 80 km during the summer months.

Looking at Fig. 161 it is amazing how far the 3 ppm contour lines penetrate into the stratosphere. The questions arises, whether there is an influence on the mid atmospheric summer water vapour in the following year based on this transport. This appears to be possible due to the rather long photochemical characteristic time of water vapour in this altitude regime. With this delay solar variability could for instance translate into a decline of stratopause ozone in the following year. Presently, we investigate this question using a general circulation model.

Above the stratopause the catalytic HOx-cycle dominates ozone depletion. Thus, the exact knowledge of the amount of water vapour (the source gas of hydroxyl radicals) is of great importance. The concentrations of water vapour and ozone are basically anticorrelated. However, this is true only as long as hydroxyl radicals can be produced. We performed a quantitative analysis of this interrelationship by investigating the tertiary ozone maximum (also known as MMM, i.e. Middle Mesosphere Maximum).

Fig. 167 and Fig. 168 show the MMMs over Lindau and Andoya, detected by our ozone millimetre wave spectrometers operating at 142 GHz. The MMM appears at about 72 km altitude with higher mixing ratios in Northern Norway. Furthermore, the temporal behaviour of the MMM amplitude differs at the two locations. At Lindau maximum amplitudes appear during the winter solstice while we find a minimum at Andoya. The annual asymmetry is related to the annual variation of water vapour. Usually, ozone is depleted by odd hydrogen at 72 km altitude. Since water vapour has a larger absorption cross section than oxygen, the penetration depth of Lyman-Alpha radiation is not as deep as the radiation in the Schumann Runge bands which dissociate molecular oxygen, i.e. for large solar zenith angles less water vapour is transformed into odd hydrogen, and less ozone is depleted. Since the production of atomic oxygen by dissociation of molecular oxygen goes on, ozone is still formed by the 3-body reaction of atomic with molecular oxygen.

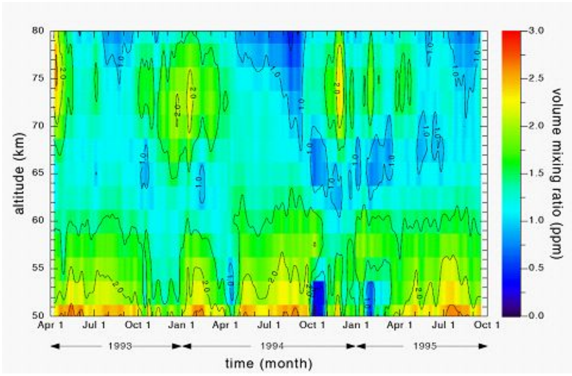

Fig. 167: Middle mesospheric maximum of ozone over Lindau.

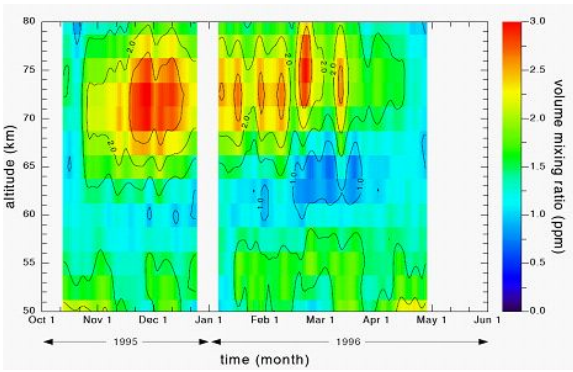

Fig. 168: Middle mesospheric maximum of ozone over Andoya.

Fig. 169 shows the relative ratio of the dissociation rates of water vapour and oxygen at 75 km as a function of the solar zenith angle. For zenith angles larger than 36 degrees the ratio starts to decline and gets very low at 90 degrees. Even at Lindau the zenith angle of the sun is as large as 75 degrees during winter solstice, i.e. the production of odd hydrogen is strongly reduced.

This qualitative description shows the basic mechanism leading to the MMM of ozone. The quantitative modelling of the measured mixing ratios of ozone, however, requires a more detailed analysis which is beyond the scope of this article. We just mention that the dissociation of even hydrogen by O(1D) becomes important for large zenith angles. This depends on a number of other parameters: among others: ozone concentration, ozone dissociation rate (which itself depends on the ozone concentration = self shielding effect), temperature, air density, and, of course, atmospheric dynamics.

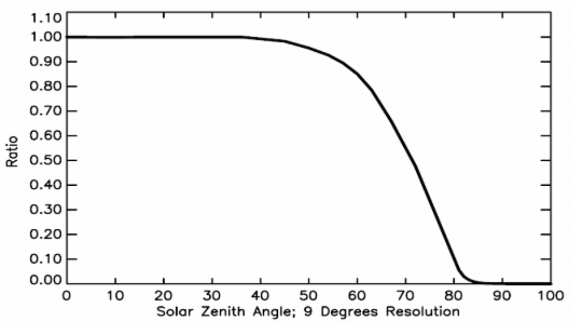

Fig. 169: Relative dissociation rates of water vapour and molecular oxygen at 75 km.

In general, it is not easy to provide self consistent quantitative model descriptions of observations. Measurements are required to constrain models and to uncover model deficits. For instance, in the beginning we were not able to model the water vapour double maximum found at Andoya (Fig. 158 and Fig. 161). Our model called, COMMA-IAP, was only capable of reproducing the double maximum after a new advective transport scheme with less numerical diffusion was introduced into the chemistry transport module. Improvements like that generally are directly implemented into our "sister model" MAOAM (see page 101) which describes the general circulation of the Martian atmosphere. As long as neither column densities nor vertical profiles are none for most of the trace gases in the Martian atmosphere ground-based observations of the Earth atmosphere provide a valuable analogy and are a good example for comparative planetology.

Wissenschaftliche Einzelberichte/
Individual scientific reports

(nur in Englisch)

The WASPAM experiment

The WASPAM (Wasserdampf- und Spurengasmessungen in der Atmosphäre mit Mikrowellen) experiment consists of cm and mm heterodyne spectrometers located in Lindau and at the Arctic Lidar Observatory for Middle Atmospheric Research (ALOMAR) in Northern Norway. These spectrometers observe mid atmospheric water vapour and ozone almost continuously since 1993/4. The microwave instruments are not only used for science purposes, but act at the same time as calibrators for new spectrometer backend developments. For instance we cross-calibrated the MIRO spectrometer backend with the well characterized WASPAM spectrometers, observing the 142 GHz rotational transition of ozone. More recently we calibrated the SOFIA spectrometer backends and performed an intercomparison campaign with the ETH Zürich FFT spectrometer, observing the 22 GHz transition of water vapour. Within the framework of the CAWSES (Climate and Weather of the Sun Earth System) research priority program of the DFG we applied successfully for a new 22 GHz water vapour system replacing the old one still operating at ALOMAR.

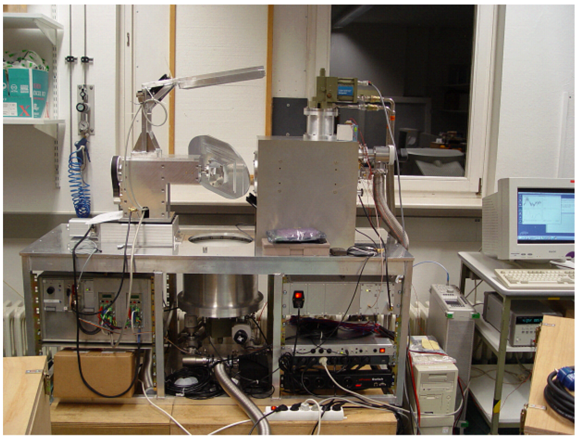

Fig. 170: New 22 GHz prototype heterodyne spectrometer

The new system is characterized by a number of improvements compared to the old one (e.g. cooled optics, dual polarization capability, more accurate baseline wobbler, integrated cooled microwave black bodies and last but not least newly developed ultra-low-noise InP high electron mobility transistor MMIC amplifiers which will be operated at 7 K rather than 20 K). Once operational the new system will be the most sensitive and advanced instrument of its kind, enabling us for instance to detect for the first time the diurnal variation of upper mesospheric water vapour and episodic water increases caused by sublimating noctilucent clouds. Several new type of components and concepts will be used in the new instrument. Therefore we developed a prototype spectrometer in order to validate the functional performance of these (see Fig. 170).

(P. Hartogh, H. Bitterlich, C. Jarchow, E. Steinmetz and L. Song with contributions from S. Weinreb (California Institute of Technology, Pasadena))

The winter anomaly of the night-to-day ratio of ozone in the middle and upper mesosphere: WASPAM observations and interpretation using a general circulation model

The photochemical system of the mesosphere is a radiation-forced nonlinear chemical oscillator, damped as a function of altitude. In altitude ranges where the chemical characteristic time is of the order of the excitation period, namely one day, the system may create nonlinear effects as for instance subharmonic oscillations. The radiative excitation is modified by the Doppler-Sonnemann effect (DSE): the time an air parcel is illuminated by the Sun depends on the zonal wind speed. Thus the latter influences the chemical reaction of the system. Especially near the mesospheric jet the zonal wind changes in a characteristic manner: the summer is dominated by easterlies, while the winter is dominated by westerlies. The latter may be modified by stratospheric warmings and modulated by planetary waves. During the easterly regime, an air parcel is moving with the Earth's rotation and the period of radiative excitation gets longer, in case of westerlies vice versa. Deviations from the 24 h period can be as large as 8 h.

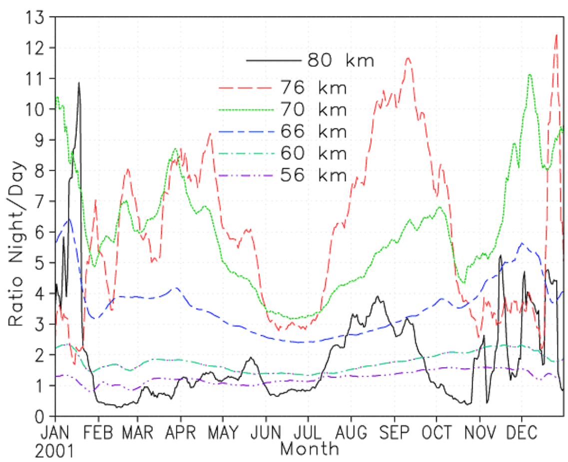

Fig. 171: Modeled ozone NDR 8-day running mean at 51.5 degree northern latitude for different altitudes.

Model calculations with COMMA-IAP (the terrestrial counterpart of MAOAM, see page 101) show that due to the DSE, ozone concentrations during night can be up to 60% enhanced compared to the situation with the zonal wind equal to zero. In contrast the daily concentrations are a little smaller. This behaviour was not expected, since the characteristic time of the chemical system appears to be just a few hours, i.e. almost an order of magnitude smaller than the diurnal period. A more detailed analysis showed however that the sunset is the crucial phase for the nighttime ozone. The chemistry during sunset is characterized by the transfer of atomic oxygen into ozone, i.e. an increase of ozone. At the same time the ozone depleting hydroxyl reactions are still active, but due to the DSE, their influence is reduced in time. A stratospheric warming may reverse the direction of the zonal wind or at least weaken it. Thus a clear signal of the stratospheric warming should appear in the night-to-day ratio (NDR) of ozone which in turn is a good indicator for dynamical processes in the mesosphere. By assimilation of ECMWF data for altitudes below 35 km it is possible to model the effect of stratospheric warmings and propagating planetary waves in the mesosphere, i.e. to describe real annual variations. Fig. 171 shows the NDR of ozone for the year 2001 (8 day running mean) at several altitude levels at 51.5 degrees north (near the geographical latitude of MPS). The winter anomaly of the ozone NDR appears clearly above 60 km. At higher altitudes the NDR is strongly fluctuating, with maximum values as high as in summer. These modulations show structural similarities with the winter anomaly of the D-layer plasma.

Fig. 172 shows WASPAM observations of mesospheric ozone over Lindau since 1998 of several hours. These data points have been smoothed using an 8 day running mean. The red curve shows the mean value of the seven year data set derived from a 14 harmonics Fourier analysis. The winter anomaly appears between 60 and 75 km. The observed NDR is larger than the modelled. The annual variations show an asymmetry, maximum values appear before the winter solstice. The largest winter/summer ratios appear at 70 km altitude (a factor of 3). The temporal variations are superposed by strong modulations. Fig. 173 shows the modelled smoothed annual variation for 2001 in 66 km altitude at different latitudes. The figure shows that the winter anomaly appears only at high and mid latitudes. Obviously there is a strong influence of the zonal wind on the NDR, however the observations indicate that the phenomenon is more complex. For future work on the one hand the highly variable temperature and its influence on the photochemistry has to be considered in more detail, taking advantage of the new interactive coupling between the chemistry and dynamics part of the model, on the other hand the transport of water vapour plays a crucial role and simultaneous 3-D measurements of its distribution are required for an improved quantitative description of the NDR.

(P. Hartogh, C. Jarchow, G. Sonnemann in collaboration with M. Grygalashvyly and U. Berger (IAP, Kühlungsborn))

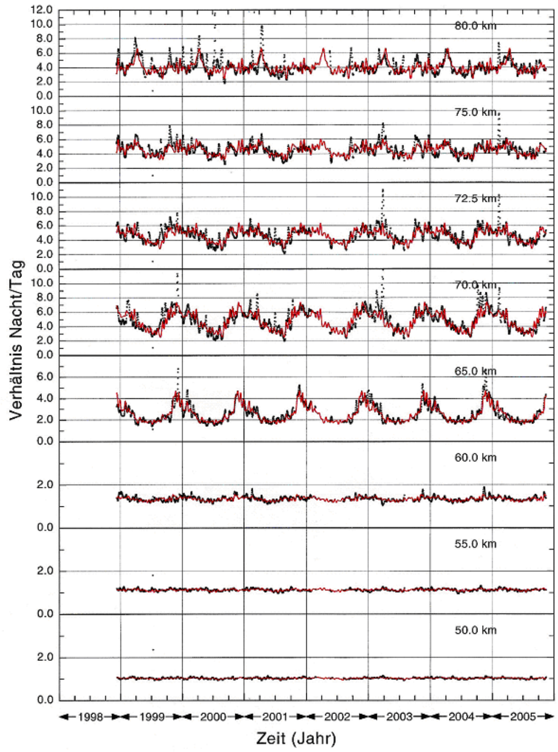

Fig. 172: WASPAM microwave observations of the NDR for 8 levels between 50 and 80 km. The black curves show the running means, the read curves the mean annual variations (see text).

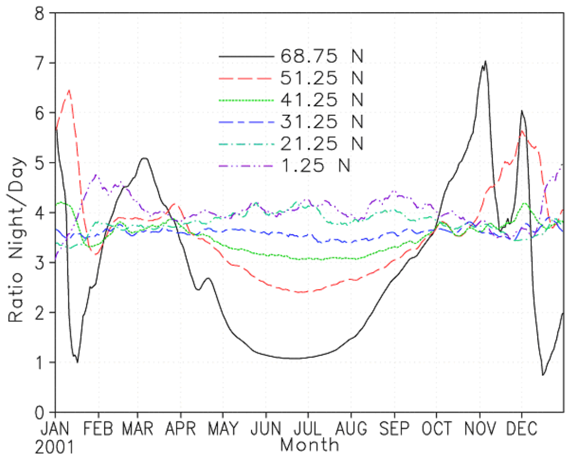

Fig. 173: Model smoothed annual variation of the ozone NDR at 66 km for several latitudes.

The Cluster Mission extended to 2009

The Cluster Mission to the Earth's magnetosphere was launched in 2000 from Baikonur and started its initial two-year operation phase in February 2001. A first extension was later granted to last until the end of 2005. At the beginning of 2005, the ESA approved a second extension, so that Cluster operations will now continue, pending spacecraft and instrument health, until the end of 2009. The spacecraft are expected to reenter during 2010.

This final extension also provides new possibilities for this already successful mission. Each of the four spacecraft carries an identical payload of 11 experiments for measuring plasma and energetic particles, electric and magnetic fields, as well as wave phenomena. During the first 4.5 years, the spacecraft were in a tetrahedron configuration of size varying from 100 to 5000 km, in order to investigate events at different scale sizes. The separation distances were altered first twice, and then later once a year.

After the manoeuvers in June–July 2005, a totally new concept was implemented: 3 of the 4 spacecraft form a large triangle of size 10 000 km, while the 4th spacecraft is in an orbit such that its distance from one of the others is adjustable from 100 to 10 000 km. Furthermore, the orientation of the large triangle can be rotated to be parallel to the geomagnetic tail during the months when the apogee is in the nightside, or perpendicular to the solar wind when the apogee is on the dayside. All these manoeuvers can be achieved with small changes to the spacecrafts' phase within the orbits, with very little fuel consumption. This new aspect of the Cluster constellation is called *multi-scaling*.

The new geometry together with the southward movement of the perigee angle allows for new studies in regions not previously accessible. In Fig. 174, the dotted lines show the original orbits with perigee near the ecliptic, while the solid lines illustrate the orbits at the end of the mission in 2009. On the nightside, the tail crossing will occur closer in than previously, at 8–10 R_E, where current disruption is expected, an important process during substorms. On the dayside, the magnetopause crossing will be closer to the subsolar point and the auroral zones will be better covered.

MPS has two major contributions to Cluster: the CIS ion spectrometer (up to ~40 keV/e) and the RAPID ion and electron imager (from ~30 keV). These instruments will be able to exploit the multi-spacecraft feature of the mission at best with the large separations which approximate the typical ion gyroradii.

(P. W. Daly, A. Korth)

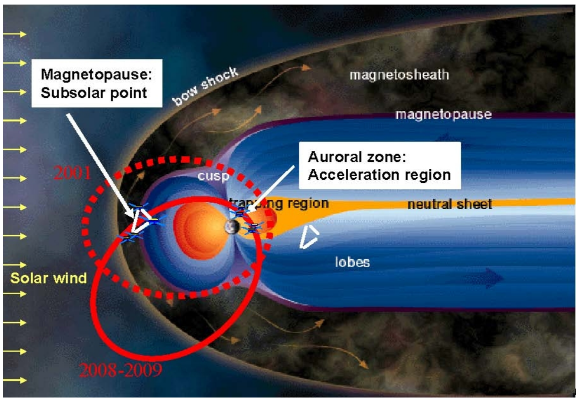

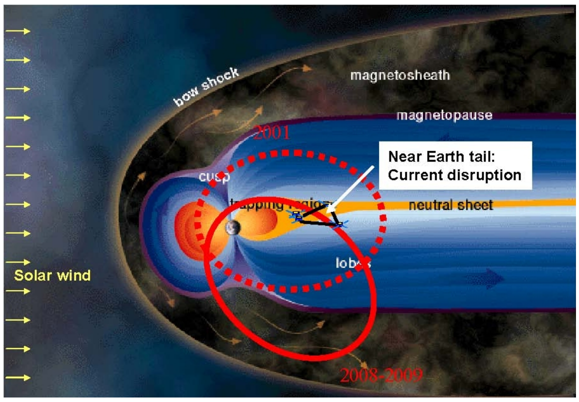

Fig. 174: New regions covered by Cluster during dayside (top) and nightside (bottom) perigees

RAPID contribution to Cluster Active Archive

The Cluster Active Archive (CAA) is the ESA contribution to the NASA *Living with a Star* Project. It is intended to be a depository of processed and validated high-resolution Cluster data, raw data, processing software, calibration data, documentation and other value added products. During the remaining Cluster operation phase (until end of 2009) plus one year, the archive is *active*, meaning it is being regularly populated with new and/or upgraded data, directly from the instrument teams. After that, it will become the long-term archive for the invaluable Cluster data set, making processed data available to the world long after the instrument teams have been dissolved and direct knowledge of the experiments is no longer at hand.

Fig. 175 shows the CAA home page at `http://caa.estec.esa.int/caa/`.

As one of 11 instruments per spacecraft RAPID (Research with Adaptive Particle Imaging Detectors) detects counts of electrons with its Imaging Electron Spectrometer (IES) and protons, helium and heavier ions with the Imaging Ion Mass Spectrometer (IIMS). The RAPID instrument is able to provide 3-D particle measurements in an energy range of 28 to 1500 keV.

Fig. 175: The CAA home page

For CAA, RAPID delivers count rates and differential fluxes of omnidirectional and 3-D data products and their standard deviations, particle flow directions and pitch angles, useful diagnostic products for expert users, caveat and instrument mode files and 6-hour overview plots.

The data processing chain for the CAA works as follows (see also Fig. 176): RAPID raw data (green blocks) are combined with Cluster housekeeping parameters to generate the intermediate binary merged science files (MSF). The RAPID team at MPS delivers MSF files, software, calibration and other support files for the final data production at CAA. These items are indicated as yellow blocks in Fig. 176. The RAPID PI software written at the MPS, which together with the various production support files converts the MSF files to the level 2 SCI files. The final CAA data products are generated the so-called Cluster Exchange Files (CEF) are produced at the CAA headquartes using the provided RAPID PI software.

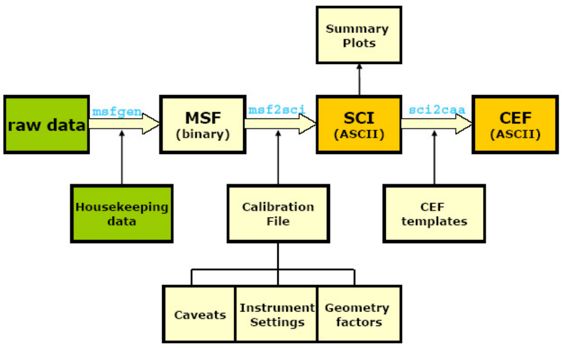

Fig. 176: The RAPID data processing chain. Green boxes indicate raw data, yellow mark steps performed by the PI institute and orange show products produced by CAA. Core software for the data production is written in blue letters.

Following the delivery schedule, the data for the first two years of operation (2001, 2002) have been ingested by the end of 2005. Afterwards, two years of data are to be delivered per year. Because of on-going improvements in the calibration and processing algorithms, it is expected to update the already ingested data sets at least once before the end of the active phase.

In addition, a RAPID data analysis software is developed as well as summary plots, which are produced at the MPS and delivered to CAA.

(P. W. Daly, S. Mühlbachler)

Cluster/RAPID observations of a modified two-stream instability in the geomagnetic tail.

In space plasma physics current sheets which separate oppositely directed magnetic fields very often play an important role in the onset of physical processes. In particular, the onset of reconnection due to current disruption is one of the most observed and studied phenomena in the terrestrial magnetosphere. Theoretical studies have shown that various types of microinstabilities can be responsible for the build up of an anomalous resistivity in the current sheet, which is reckoned as the initial point of magnetic reconnection. Recent theoretical studies have proven that the so-called modified two-stream instability (MTSI) might be most effectively operative at the neutral sheet.

The studies suggest that the plasma is MTSI unstable if (1) a relative drift of electrons and ions is present, which exceeds the Alfvén speed, and (2) this relative drift or current is in the cross-field direction. As consequences of the formation of a MTSI one expects to observe (1) a field-aligned electron beam, (2) heating of the plasma, and (3) an enhancement in the B-wave spectrum at frequencies in the range of the lower hybrid frequency (LHF).

The study presented here deals with several observations of the Cluster spacecraft on September 24, 2003 around 15:11 UT, which indicate necessary prerequisites and consequences for the formation of an MTSI. At this time the Cluster fleet was in the dusk tail plasmasheet close to the neutral line at a distance from the Earth of $\sim$16 R_E. Prime parameter data of the CIS (ion) and PEACE (electron) instruments on board the Cluster spacecraft are used to verify the drift velocities of ions and electrons, magnetic field data (FGM) to calculate the expected LHF and Alfvén velocity, and the direction of the current. The B-wave spectrum is recorded by the STAFF (magnetic fluctuations) instrument of Cluster. Finally, the differential flux distribution of electrons is observed by 3-D measurements of the electron detectors from the RAPID unit.

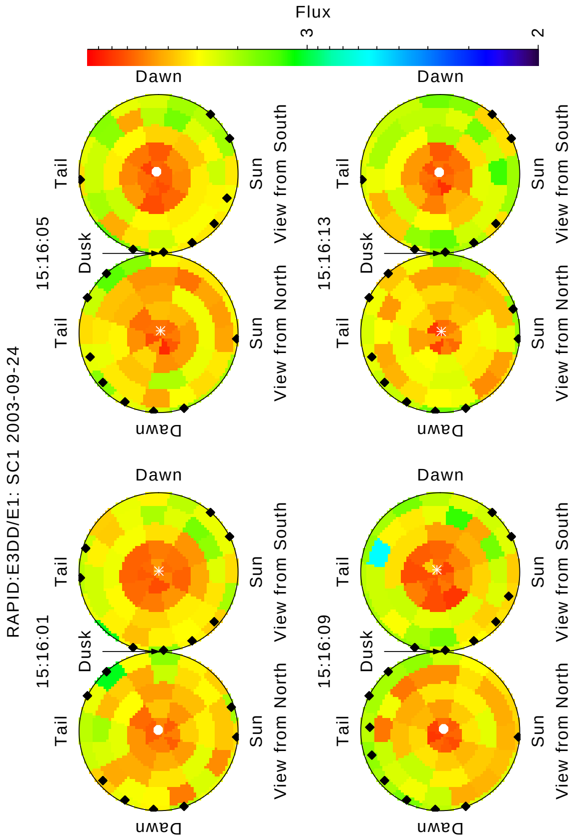

Fig. 177: A 3-D electron distribution as observed by RAPID showing a field aligned electron beam caused by the formation of a modified two-stream instability in the tail plasma sheet.

Fig. 177 shows 3-D electron distributions in a bispherical view, i.e., the left sphere is a view looking down from the GSE north axis, while the right one is from the south. Black dots indicate 90° to the magnetic field, as measured on-board in each sector, and the white dot marks the calculated direction of the positive magnetic field vector, with the white star showing the opposite direction. This snapshot of four 3-D electron differential flux distributions is taken over one spin for each of the four pairs. These observations were made ~5 minutes after a drift of electrons and ions with a velocity difference greater than the Alfvén speed is observed by CIS and PEACE instruments (see above). The flux enhancement close to the magnetic field vector indicates a field aligned electron beam, which confirms the formation of a MTSI. As another indicator the STAFF instrument records waves in the range of the LHF, which is around 10 Hz at this time. Magnetograms of College and Tixie show a huge negative bay during this event and a substorm onset between 15:50 and 16:00 UT. Thus we are able to conclude that the formation of an MTSI as observed with Cluster data in our study, might indeed be a indication point for large scale phenomena as tail reconnection and thus substorms in the terrestrial magnetosphere.

(S. Mühlbachler, P. W. Daly and colleagues from Austria, Russia, and USA)

Observations with Cluster CIS

Plasma Sheet Response Observed by Cluster during Corotating Interaction Regions

Corotating Interaction Regions (CIRs) are large scale structures in the heliosphere during the declining and minimum phase of the solar activity cycle. They are the result of the interaction of fast and slow solar wind. Streams of fast solar wind originating from coronal holes often recurred with a period of ~27 days (1 solar rotation). These streams of fast solar wind and the interplanetary field will influence the dynamics of the Earth's magnetosphere. This influence is examined in the plasma sheet activity during the September 14–28, 2003 corotating high speed stream event, in which Alfvénic fluctuations were observed. Alfvénic fluctuations are characterized by highly fluctuating velocity and magnetic fields. The study uses particle (CIS and RAPID) and magnetic field measurements from the Cluster S/C, solar wind velocity, density, and magnetic field data from ACE, Los Alamos geosynchronous orbit data, and ground based magnetic field data. The results can be summarize as follows: The appearance of continuous Alfvén waves in the IMF B_z leads to heating of the plasma sheet, to small storms, and substorm activity. Applying a wavelet analysis a high correlation was observed between the interplanetary magnetic field IMF B_z and the sunward component B_x measured with Cluster in the plasma sheet (Fig. 178).

The change of the particle pressure and the B_x component of the magnetic field in the plasma sheet are related to substorms. They are further correlated with injections at geosynchronous orbit and the H-component of ground based magnetograms. The correlation period is 2 to 4 hours.

(A. Korth, M. Fränz, E. Echer, F. Guarnieri, R. Friedel, and H. Rème)

Cluster observations of O^+ escape in the magnetotail in comparison with the ring current input rate during an intense magnetic storm

Magnetic storms are disturbances in the Earth's magnetosphere (magnetic field and plasma populations) that are well known over more than ~150 years. Their effects are easily observed in the disturbed horizontal component of the geomagnetic field measured at low-latitude observatories and are represented by the Dst index. The Dst is itself proportional to the kinetic

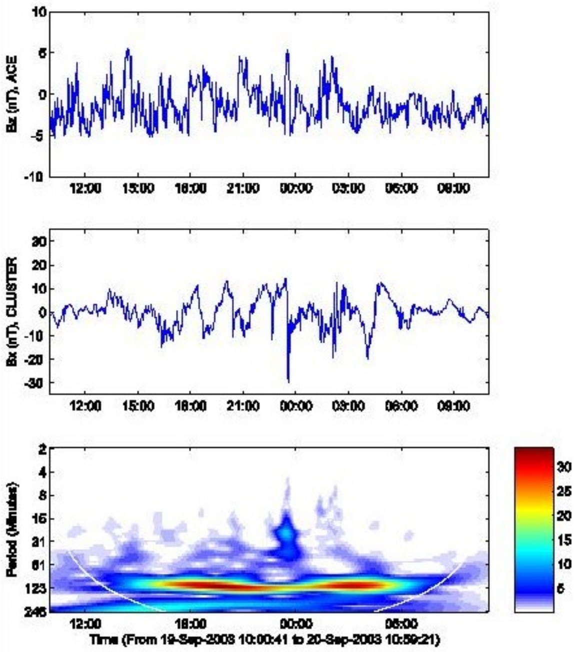

Fig. 178: Correlations between IMF B_z and Plasma sheet B_x on September 19/20, 2003

energy transported by ∼20 – 300 keV energetic particles that encircle the Earth in a westward ring current around 4 – 6. The ion composition of this ring current has contributions from both terrestrial/ionospheric and solar wind sources. The plasma sheet is a major plasma source for the storm time ring current. The origin of plasma particles in the magnetotail was initially thought to be only the solar wind, but several observations have shown that ionospheric plasma is present in the magnetotail. Observations showed that there is a O^+ and H^+ upward flow at high latitudes along magnetic field lines in the polar cusp/auroral oval region during substorms/storms. The ionospheric O^+ plasma, which escaped into the magnetotail, is observed by CIS and RAPID on the four Cluster spacecraft. An intense magnetic storm (Dst ~ -100 nT) occurred on August 17, 2001 caused by a compressed southward B_z interplanetary magnetic field (IMF) due to the passage of an interplanetary shock by the Earth. It is recognized that already during the pre-storm a lot of O^+ ions were injected into the lobes of the magnetotail. During the pre-storm period no oxygen is injected into the ring current. For this period the oxygen outflow was calculated in the tail lobe at 19 R_E distance and compared this with the oxygen flow into the ring current during the main phase of an intense storm with a strength of Dst ∼ 100 nT. A sketch of the O^+ flow into the magetotail and the ring current is given in Fig. 179.

We conclude that the O^+ escape rate into the tail is 20 times larger than the ring current input rate during an

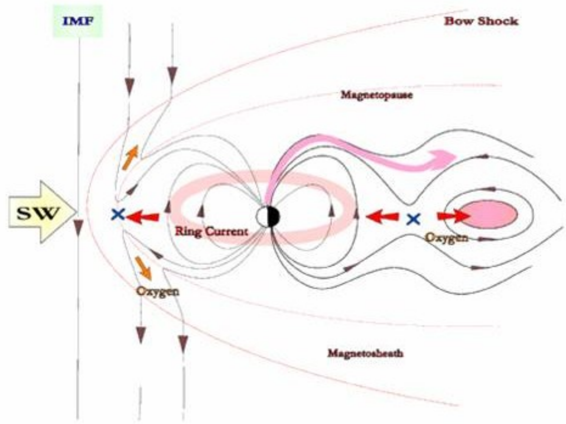

Fig. 179: Sketch of the oxygen flow inside the magnetosphere

intense magnetic storm.

(A. Korth, M. Fränz, E. Echer, F. Guarnieri, Q.-G. Zong, and P. W. Daly)

Cluster observation of LHD waves at the high-latitude magnetopause

The fine structure of the outer boundary of the Earth's magnetosphere, the magnetopause (MP), plays an important role in the magnetosheath plasma transport through the MP. Using Cluster electric and magnetic field, as well as plasma moment measurements, we studied the observation of the lower hybrid drift (LHD) waves at a thin magnetopause and estimated the diffusion rate provided by the wave-particle interactions. On March 30, 2002 the four Cluster spacecraft crossed the Earth's high-latitude magnetopause three times within 17 min. We found that all three magnetopause current sheets are nearly co-planar at the scales of the Cluster spacecraft separation. The thickness of the current sheets changes from 1 to 40 magnetosheath-proton thermal gyro-radii. The thinnest (first crossed) magnetopause current sheet is locally open to the solar wind and might be electron driven (Fig. 180).

We found the frozen-in condition of the thermal ions is violated and that the Hall term is comparable to the electric field. Substantial electrostatic wave intensities are observed at lower-hybrid frequencies on the magnetospheric side of the thinnest magnetopause current sheet. We determined that the quasi-linear diffusion rate due to lower-hybrid drift waves would not explain the formation of the adjacent boundary layer and a fast magnetopause thickening. Instead, the diffusion is enhanced due to a strongly nonlinear wave-particle interactions. We estimate the anomalous diffusion rates by calculating the correlation between the fluctuations

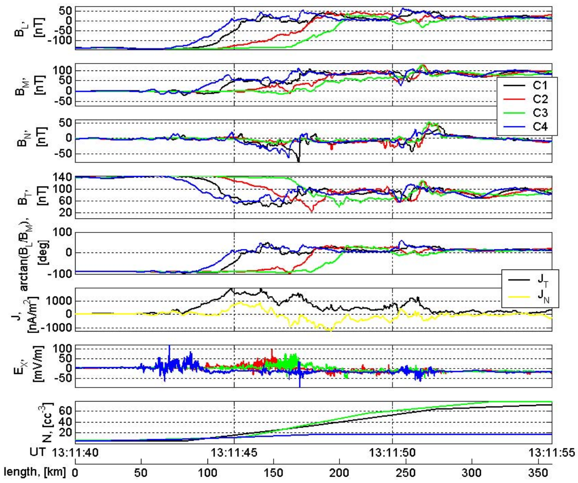

Fig. 180: Cluster observation of the magnetopause crossing on 30 March 2002, 13:11:40 – 13:11:55 UT. From top to bottom: LMN magnetic field components and total magnetic field, arctan(B_L/B_M), tangential (black) and normal (yellow) current density components, E_X electric field component (approximately along X_{GSE}), number density, length scale along normal direction. (For interpretation of the references to colors in this figure legend, the reader is referred to the web version of this article.)

of current density and magnetic field. Based on the cross-product of fluctuations of the magnetic field and current density (see Fig. 181) we estimated the cross-field diffusion rate. We found that this diffusion rate can be much higher than predicted by the quasi-linear theory ($D_{jb} \sim 10^9$ m^2/s $\gg D_{ql} \approx 5 \times 10^6$ m^2/s) and can account for the formation of the adjacent magnetopause boundary layers and eventually the fast magnetopause thickening.

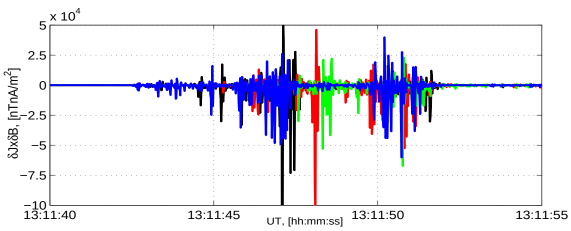

Fig. 181: Normal component of the cross-product of the magnetic and current fluctuations in the range between 4 and 33.5 Hz observed on March 30, 2002 during 13:11:40 – 13:11:55 UT by the Cluster fleet. For colour coding see legend in Fig. 180.

(E. V. Panov, J. Büchner, M. Fränz, A. Korth, Y. Khotyaintsev, B. Nikutowski, S. P. Savin, K.-H. Fornaçon, I. Dandouras, and H. Rème)

Cluster observations of magnetopause transport by ion-cyclotron waves

The transport of the magnetosheath plasma into the magnetosphere occurs through the outer boundary of the Earth's magnetosphere, the magnetopause. A possible transport mechanism is diffusion due to resonant interaction of ions with plasma waves. We used Cluster magnetic field and plasma data in order to investigate the magnetopause transport at a high-latitude thick magnetopause (MP). On May 10, 2002 the Cluster spacecraft encountered an about 450 km (five magnetosheath thermal proton gyro-radii) wide high-latitude MP. Magnetic field observations indicate the crossing of an about 130 km thick MP current sheet (CS). Proton flux measurements diagnose a dense boundary layer (BL) directly attached to the MP and an additional rare BL located earthwards from the MP (Fig. 182).

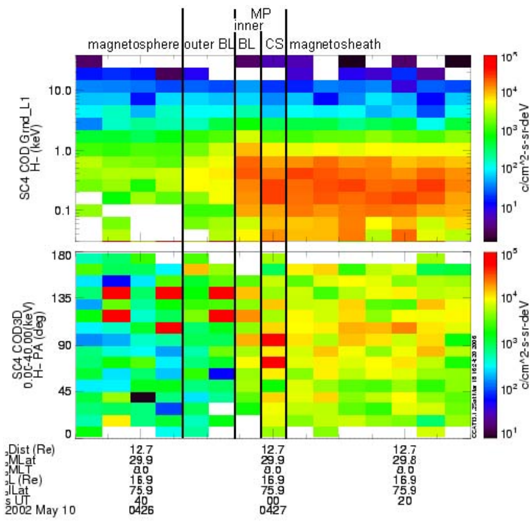

Fig. 182: Differential particle flux of protons from CIS/CODIF instrument onboard SC-4 on May 10, 2002 (top) and pitch-angle distribution of protons for SC-4 (bottom) during the time interval 4:26:30 – 4:27:30 UT.

Enhanced magnetic fluctuations are found near the local proton-cyclotron frequency Ω_{cp} (0.4 – 2 Hz). Applying the phase-differencing technique we obtained a wavelength of 150 – 250 km and the propagating direction earthward perpendicular to the MP. The presence of a transverse population inside the MP (see bottom panel in Fig. 182) with the proton velocity correspond well to the estimated phase speed of the observed waves points out on the ongoing wave-proton interaction. Based on the cross-product of fluctuations of the magnetic field and current density (Fig. 183) we estimated the cross-field diffusion rate using a random walk estimate $D_{rw} = \Delta x^2/\Delta t$. We took the spatial scale Δx equal to the ion inertial length λ_i and the time scale Δt equal to the electromagnetic input into the effective collision frequency ν (from the Vlasov theory of wave-particle interaction follows $\nu = (n_i m_i V)^{-1}(e\langle\delta n\delta\mathbf{E}\rangle + \langle\delta\mathbf{j} \times \delta\mathbf{B}\rangle))$. We found that this diffusion rate is two orders of magnitude higher than that predicted by the quasi-linear theory and enough to provide the particle flux to support the observed boundary layers: $D_{jb} \approx 2.0 \times 10^6 m^2/s \gg D_{ql} \approx 2 \times 10^4 m^2/s$. Hence, we could show that the formation of the two BLs can be understood by enhanced collisionless diffusion of magnetosheath protons due to wave-particle interaction.

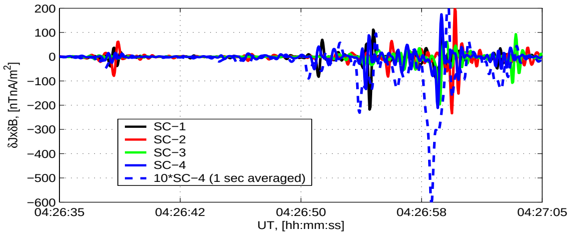

Fig. 183: Normal component of the cross-product of the magnetic and current fluctuations in the range between 0.4 and 2 Hz observed on May 10, 2002 during 4:26:35 – 4:27:05 UT by the Cluster fleet. For colour coding see legend. The dashed line shows the one second sliding window averaged value of $(\delta j \times \delta B)_N$ for SC-4 multiplied by a factor of ten for better visibility.

(E. V. Panov, J. Büchner, M. Fränz, A. Korth, S. P. Savin, K.-H. Fornaçon, I. Dandouras, and H. Rème)

Magnetic reconnection through magnetopause-like asymmetric current sheets with arbitrarily sheared magnetic fields

Magnetic reconnection is a fundamental energy release process in solar and interplanetary plasmas. Thin current sheets are a prerequisite for reconnection to take place. Since their thickness reaches kinetic scales, plasma kinetic investigations are necessary. With our especially developed Vlasov-code we investigated the influence of sheared fields on the wave-particle interactions, causing resonance current instabilities in current sheets with symmetric density profile and constant initial temperature (see the biannual report 2002 – 2003 of the Max-Planck-Institut für Aeronomie). One of the most prominent reconnection sites, the Earth's magnetopause, has currently been thoroughly investigated by the four ESA-Cluster spacecraft. However, here our previous calculations are not applicable, since plasma density and temperature change asymmetrically across the magnetopause current sheet. Also, the Cluster spacecraft often observed that at the magnetopause the magnetic field changes direction without significant variations of the field strength. We have developed a theoretical equilibrium model for such asymmetric magnetopause current sheets and have used this model as an initial condition for Vlasov-code simulations.

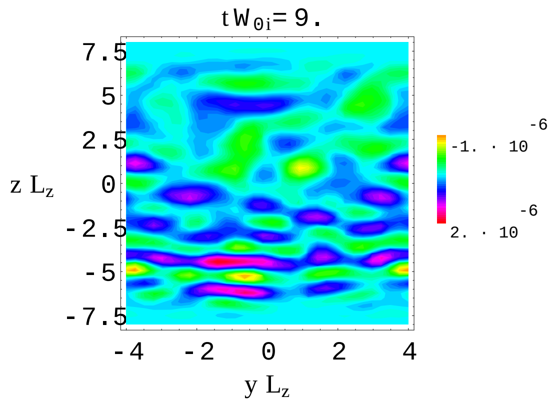

Fig. 184: 3-D Vlasov-code simulated reconnection- magnetic field B_z through the magnetopause diagnosed in the plane across the current sheet, z-axis normal to the magnetopause plane: asymmetric perturbations due to an LHD instability an the magnetospheric side.

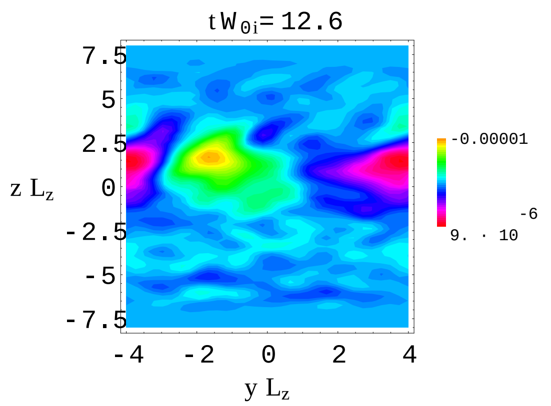

Fig. 185: 3-D Vlasov-code simulated reconnection- magnetic field B_z through the magnetopause diagnosed in the plane across the current sheet, z-axis normal to the magnetopause plane: magnetic island through the magnetopause are formed triggered by the saturated LHD waves.

We found that the lower-hybrid drift (LHD) waves form preferentially on the magnetospheric side of the current sheet (Fig. 184). Our theoretical results are in agreement with Cluster observations (electric field measurements by M. Andre *et al.*). Although the rotating-magnetic-field equilibrium meets the threshold conditions for a LHD instability locally, no spatial coherence can be obtained as in symmetric current sheets, where the waves couple to large scale plasma modulations. However, now the short LHD waves trigger a three-dimensional reconnection structure with longest possible wavelength of magnetic islands. The reconnected field has a regular island structure as shown in Fig. 185, corresponding to observed structures (so-called "Flux Transfer Events" – FTE).

(I. Silin, J. Büchner)

Forced magnetic reconnection

Using a multi-code approach, we have investigated the current sheet thinning and the onset and progress of magnetic reconnection, initiated by a temporally limited, spatially varying, inflow of magnetic flux. The thinning leads to fast magnetic reconnection, which exceeds the rates expected from tearing instability of the initial state. This study extends an earlier collaborative effort into the transition regime from thick to thin current sheets. As in the earlier study, we find that full particle, hybrid, and Hall-MHD simulations lead to the same fast reconnection rates, apparently independent of the dissipation mechanism. The reconnection rate in MHD simulations is considerably larger than in the earlier study, although still somewhat smaller than in the particle simulations. All simulations lead to surprisingly similar final states, despite differences in energy transfer and dissipation. These states are contrasted with equilibrium models derived for the same boundary perturbations. The similarity of the final states indicates that entropy conservation is satisfied similarly in fluid and kinetic approaches and that Joule dissipation plays only a minor role in the energy transfer.

(J. Büchner together with J. Birn, K. Galsgaard, M. Hesse, M. Hoshino, J. Huba, G. Lapenta, P. L. Pritchett, K. Schindler, L. Yin, T. Neukirch, and E. R. Priest)

Vlasov code simulation of anomalous resistivity

One of the outstanding open questions in space physics is that of the resistivity of collisionless plasmas, where binary collisions are inefficient and collective wave-particle interactions determine transport and dissipation. In order to obtain macroscopic transport coefficients one has to solve kinetic equations together with the Maxwell equations for the interacting electromagnetic fields, an essentially nonlinear problem. For weak turbulence the quasi-linear and other weakly nonlinear theories provide predictions for the saturated field fluctuations and the so called anomalous resistivity, the normal mode of current dissipation in collisionless space plasmas. Unfortunately, no generic anomalous resistivity expression is found yet, which could be used for a macroscopic Ohm's law description like the Spitzer – Braginski one for the case of binary collisions.

In the past the main results about anomalous resistivity caused by ion sound turbulence were obtained in the framework of weak turbulence theories and by Particle-In-Cell (PIC) kinetic plasma simulations. PIC-code simulations are, however, very noisy, they introduce artificial numerical collisions. Desired is a direct integration of the kinetic Vlasov equation for the distribution functions, which are, however, very messy. The availability of massively parallel computers led to a revival of Vlasov-code simulations. We use our newly developed conservative Vlasov equation solver (see section Sun) to recalculate the anomalous resistivity caused by the ion sound turbulence. Fig. 186 shows the resulting effective collision rate ν (upper curve), which we obtained by simulation, in comparison to the heuristic Sagdeev-type estimate (lower curve), where W_x denotes the electric field fluctuation energy, T_e the electron thermal energy and ω_{pe} the electron plasma frequency.

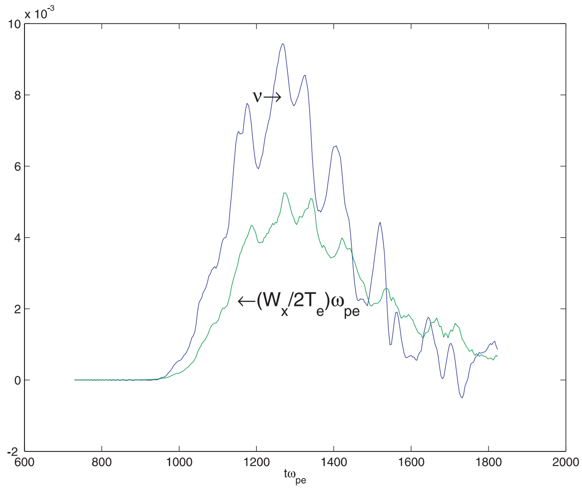

Fig. 186: Vlasov-code simulated effective collision rate ν due to ion acoustic waves (upper curve) in comparison to the heuristic Sagdeev-type estimate combining the electric field fluctuation energy (W_x), the electron thermal energy (T_e) and the electron plasma frequency (ω_{pe}; lower curve).

(J. Büchner and N. Elkina)

Magnetosheath interaction with the high latitude magnetopause

We carried out both statistical and case studies of the interaction between magnetosheath and magnetospheric plasma through the high-latitude magnetopause using Interball and Polar spacecraft data. We investigated the topology of the cusp-magnetosheath transition and the role of nonlinear disturbances in mass and energy transfer across the high-latitude magnetopause. For sunward tilts of the Earth's magnetic dipole the cusp throat is magnetically open for a direct interaction with the incident solar wind flow. This results in the creation of a turbulent boundary layer (TBL) above the indented magnetopause position, downstream of the cusp. For antisunward tilts, the cusp throat is closed by a smooth magnetopause. In this case demagnetized "plasma balls" (with a size of a few Earth radii, an occurrence rate of 25% and trapped energetic particles are present in a magnetosheath plasma channel just inside the cusp. The magnetosheath flow interacts with the "plasma balls" via reflected waves, which trigger a chaotization of up to 40% of the upstream kinetic energy. These waves propagate upstream of the TBL and initiate an amplification of the existing magnetosheath waves and their decay during downstream passage throughout the TBL. The most striking feature of the nonlinear interaction is the appearance of magnetosonic jets, accelerated up to an Alfvénic Mach number of 3. The characteristic impulsive local momentum loss is followed by decelerated Alfvénic flows and modulated by the TBL waves. The momenta are balanced on time scales of the Alfvénic flows ($1/f_A \sim 12$ min). Wave trains at $f_A \sim 1.3$ mHz are capable to synchronize the interaction between the outer and the inner boundary layers. The sonic/Alfvénic flows, bounded by current sheets, control the TBL spectral shape. They result in non-Gaussian statistical characteristics of the disturbances, indicating the fluctuation intermittency. We suggest that multi-scale TBL processes play a role due to reconnection between the solar wind and the magnetosphere. As an example Fig. 187 shows a schematics of the observation of reconnection at the high-latitude magnetopause during northward IMF conditions on 29 May 1996. Secondary micro-reconnection constitutes a necessary chain at the small-scale (ion gyroradius) edge of the TBL cascades. The thick TBL transforms the flow energy, including deceleration and heating of the flow in the open throat, "plasma ball" and the region downstream of the cusp.

(S. Savin, J. Büchner, L. Zelenyi et al.)

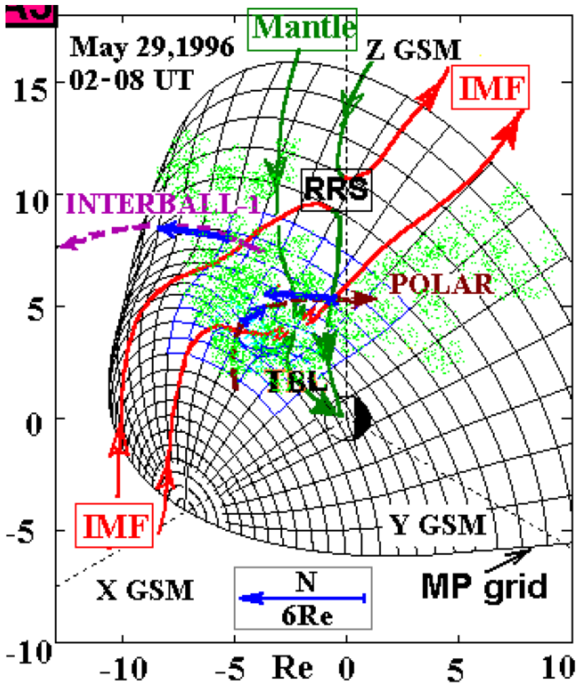

Fig. 187: Schematics of the reconnection observations at the hight-latitude magnetopause during northward IMF conditions on 29 May 1996. The black magnetopause (MP) grid is obtained by empirical models. The Polar and Interball-1 orbits are shown by the dashed brown and violet lines, respectively and the turbulent boundary layer (TBL) is depicted by green dots. The measured MP normals are marked by blue arrows (the total normal length is shown at the bottom of the figure by a blue arrow marked "N"). The draped IMF magnetic field is marked red, the magnetospheric (mantle-) field is depicited by green lines.

Quasi-adiabatic description of particles accelerated in a reconnection magnetic field geometry

We have re-investigated the properties of charged particle motion in three different regions of the Earth's magnetotail: (1) in regions were the magnetic field reverses its direction, (2) in the vicinity of an X type neutral line and (3) in the vicinity of an O type neutral line. We use the existence of the smallness of (a) the ratio of the characteristic length scales in and perpendicular to the symmetry plane and (b) of the electric fields to introduce a hierarchy of motions characteristics. Applying perturbation theory methods we derived a parameter τ which measures the mixing state of the system.

For the case of large negative τ Fig. 188 shows a typical phase portrait where P_x corresponds to the canonical momentum in the X-direction and λx is the appropriately normalized conjugate spatial variable. The curve of uncertainty, through which the character of the particle motion changes drastically and chaotic orbits arise, has the form of two straight lines $S_\pm$, parallel to the P_x axis. Three fix points can be seen, one O-type, hyperbolic fix point at the origin, where the separatrices σ cross and two elliptic type fix points $C_\pm$, encircled by closed orbits $\Gamma_\pm$.

We could show that the parameter τ describes the relative importance of the diffusion of adiabatic invariants compared to the time scale of particle acceleration in the electric field. Depending on the value of τ, the jumps of the adiabatic invariants either just disturb the distribution functions or particles become accelerated to leave the tail quickly maintaining the shape of the distribution function. In the limit of small jumps of the

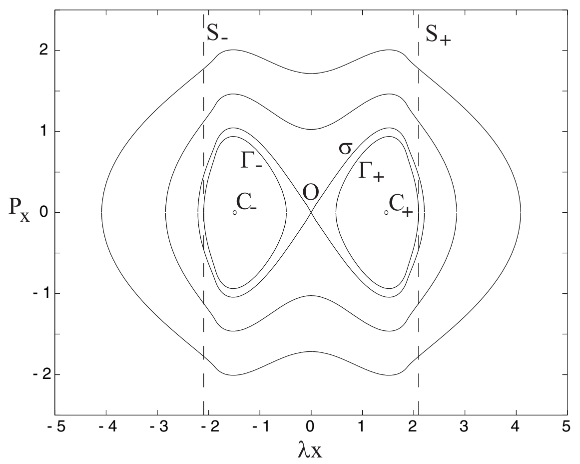

Fig. 188: Phase portrait canonical momentum in the X-direction (P_x) vs. the normalized conjugate spatial variable λx. Shown are the curves of uncertainty (two straight lines $S_\pm$), three fix points: one O-type, hyperbolic fix point at the origin, the separatrices σ, two elliptic type fix points $C_\pm$ and closed orbits $\Gamma_\pm$.

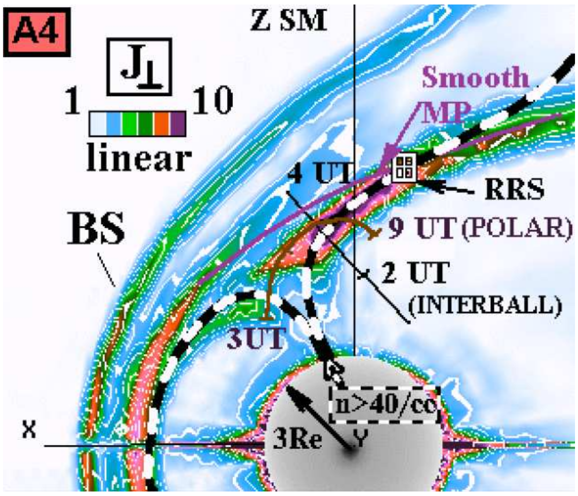

Fig. 189: Distribution of currents perpendicular to the magnetic field in the noon-meridian plane in solar-magnetospheric coordinates, depicted by a colour scale and compared with a the results of global MHD model. The projections of the Polar (brown trace) and Interball-1 (black trace) orbits onto that plane (Polar crossed this plane at 05:30 UT) are also shown. The dayside magnetopause (MP) and bow shock (BS) are seen in the current maxima at low latitudes, the higher latitude smooth MP from Sibeck *et al.* (1991) model is depicted by the violet line. The global MHD model determined "remote" (from the cusp) reconnection site (RRS) position is shown by a white squared cross. The model inward boundary of the MSH is shown by a thick black-and-white dashed line.

adiabatic invariant we obtained the equations governing the particle acceleration. We could show that for particles on long elongated "cucumber" shaped trajectories the mixing is less prominent than for the rest of the particles. Our approach illustrates the usefulness of the introduction of quasi-adiabatic invariants for the description of the particle acceleration if the guiding center theory breaks down. Our new quasi-adiabatic approach will be useful for the description of the particle acceleration in other astrophysical configurations as well.

(D. L. Vainchtein, J. Büchner, A. I. Neishtadt, and L. M. Zelenyi)

The turbulent boundary layer at the magnetosheath-cusp interface

We used Cluster, Polar and Interball spacecraft data to explore the magnetosheath-cusp interface. Fig. 189 depicts the observed distribution of currents perpendicular to the magnetic field in the noon-meridian plane in solar-magnetospheric coordinates in colour scale in comparison with global MHD model results.

Our multi-spacecraft study revealed that in 80% of the cases the interaction of the magnetosheath (MSH) flow with the high latitude magnetopause (MP) produced a turbulent boundary layer (TBL). The TBL contains wave trains with flows at approximately the Alfvén speed along field lines and "diamagnetic bubbles" with small magnetic fields inside. A comparison of our multi-point measurements with the results of a global MHD model indicates three types processes (1) large-scale (few R_E) anti-parallel merging at sites remote from the cusp, (2) medium-scale (few thousand km) local TBL-merging of fields that are anti-parallel on average and (3) small-scale (few hundred km) bursty reconnection of fluctuating magnetic fields, representing a continuous mechanism for MSH plasma inflow into the magnetosphere. The low frequency (1 -– 2 mHz) TBL fluctuations are traced throughout the magnetosheath from the post-bow shock region up to the inner magnetopause border. The resonance of these fluctuations with dayside flux tubes might provide an effective correlation for the entire dayside region of the solar wind interaction with the magnetosphere. The TBL disturbances are characterized by kinked, double-sloped wave power spectra and, most probably, three-wave cascading. Both elliptical polarization and nearly Alfvénic phase velocities with characteristic dispersion indicate the kinetic Alfvénic nature of the TBL waves. A three-wave phase coupling could effectively support the self-organization of the TBL plasma by means of coherent resonant-like structures. The estimated characteristic scale of the "resonator" is of the order of the TBL width across cusp. Inverse cascades of kinetic Alfvén waves are proposed to form the larger scale structures, which in turn synchronize all nonlinear cascades within the TBL in a self-consistent manner.

(S. Savin, J. Büchner, L. Zelenyi et al.)

Dynamic interaction of plasma flow with the hot boundary layer of a geomagnetic trap

We studied the interaction between the collisionless plasma flow and the stagnant plasma at the outer boundary of the geomagnetic trap, where the super-Alfvén subsonic laminar flow changes to a dynamic regime characterized by the formation of accelerated magnetosonic jets and decelerated Alfvénic flows. Fig. 190 shows a schematics of the observed magnetosonic waves in the magnetosheath (MS; 1.4 mHz), of the reflected MS waves (4 -- 5 mHz) and of the decay into the accelerated MS jet waves (4.4 mHz) and decelerated Alfvén waves (Alfvén; 3 mHz). The characteristic time scale of the decay process is 10 min. The nonlinear interaction of fluctuations in the initial flow with the waves reflected from an obstacle explains the observed flow chaotization. A Cherenkov resonance of the magnetosonic jet with the fluctuations between the boundary layer and the incoming flow is a possible mechanism of its formation. In the reference system of the flow the incoming particles are accelerated by the electric fields at the border of boundary layer that arise self-consistently as a result of the preceding wave–particle interactions. The inertial drift of the incoming ions in a transverse electric field increases toward the border. This explains the observed ion acceleration. The magnetosonic jets can carry up to a half of the unperturbed flow momentum, and their dynamic pressure is an order of magnitude higher than the magnetic pressure at the obstacle border. The appearance of non-equilibrium jets and the boundary-layer fluctuations are synchronized by the magnetosonic oscillations of the incoming flow at frequencies of 1 -- 2 mHz.

(S. Savin, J. Büchner, L. Zelenyi et al.)

Dynamic flow chaotization at the magnetopause

Our spacecraft observations of the high-latitude magnetopause revealed strong fluctuations in a sheared current sheet with including a dynamic equilibrium, in which nonlinear disturbances serve as an effective obstacle for 80% of the incident magnetosheath ions, providing the exchange of 10% of plasma particles with the stagnant high-beta boundary layer in the minimum field region over the polar cusps. The measured waves, reflected upstream by the boundary, undergo a three-wave interaction with magnetosonic (MS) fluctuations in the incident flow. This results in their amplification and decay, driving decelerated flows at the Alfvén speed. This impulsive momentum loss via MS-jets contributes to the average flow around the magnetosphere. The leading jet appearance is suggested to be phase-synchronized with both the initial MS fluctuations and the nonlinear cascades upstream at the magnetopause, which constitutes the wavy obstacle with multiple decays into the smaller MS-jets and Alfvénic flows. The strong dynamic pressure in the jets enables reconnection in the downstream magnetopause. The acceleration of the MS-jets is consistent with a Fermi-type mechanism, in which electric wave-trains play the role of a moving non-continuous "wall" (see Fig. 191). An estimate of the jet scales due to nonlinear Cherenkov resonances reveals 2–3 reflections of the jet before overcoming the potential barrier which agrees well with the observations.

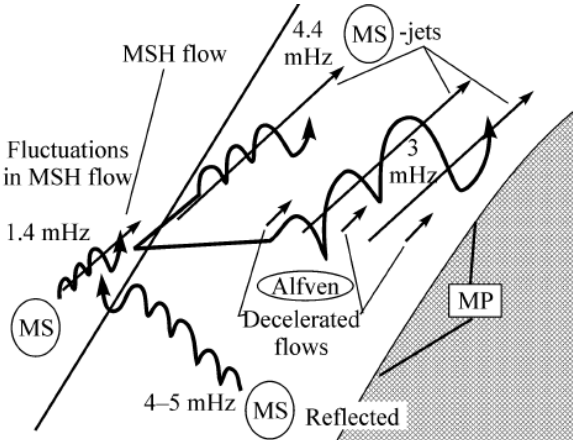

Fig. 190: Schematics of the observed magnetosonic waves in the magnetosheath (MS; 1.4 mHz), of the reflected MS waves (4 — 5 mHz) and of the decay into the accelerated MS jet waves (4.4 mHz) and decelerated Alfvén waves (Alfvén; 3 mHz).

(S. Savin, J. Büchner, L. Zelenyi et al.)

Cluster observations of anomalous collisionality due to nonlinear lower-hybrid drift (LHD) waves

We compared Cluster observations and Vlasov-code simulations of lower-hybrid-drift waves at the magnetopause in order to estimate the possibility of causing anomalous collisions by wave particle interactions. Our simulation results confirm our previous eigenmode theory concerning the electromagnetic instability at the current sheet center due to LHD waves. We have demonstrated that the electromagnetic LHD mode excited at the current sheet center can lead to significant anomalous resistivity in addition to the electrostatic turbulence at the current sheet periphery,

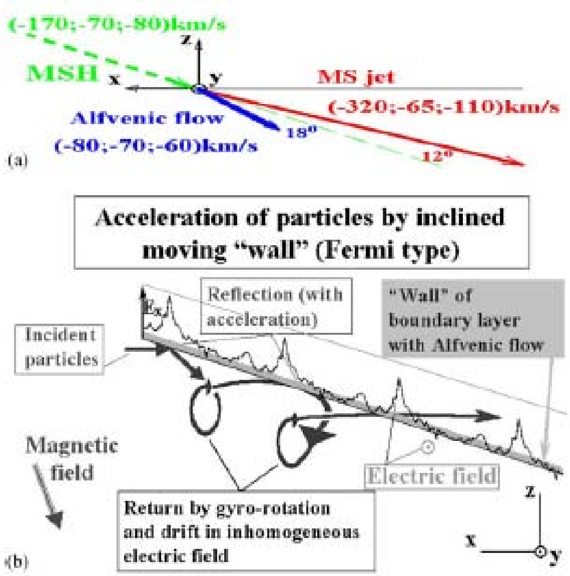

Fig. 191: Mechanism of the dynamic flow chaotization at the magnetopause: (a) Projections of flow vectors onto the XZ plane of the GSE coordinate frame; (b) schematics of Fermi acceleration of the first MS-jet by the moving "wall", i.e. the boundary of the slow Alfvénic flow.

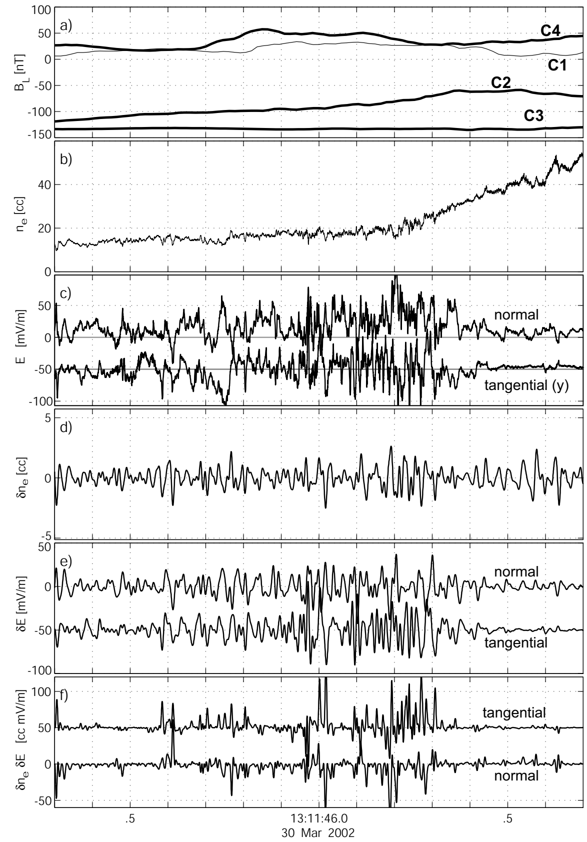

Fig. 192: Cluster observations of a thin current sheet traversal on March 30, 2002, for which we carried out our Vlasov code simulations: L-component of the magnetic field for all four Cluster spacecraft (top panel), electron density (second from top panel), normal and tangential components of the electric field density (third panel), density fluctuations (fourth panel), fluctuations of the normal and tangential components of the electric field (but last panel) and correlation of the electric field and density fluctuations, to which the anomalous collision rate is directly proportional.

and thus contribute to magnetic reconnection through thin current sheets. The LHD waves grow quite rapidly in unperturbed current sheets without magnetic islands. Thus, before other kinetic effects, such as electron inertia or electron temperature anisotropy, may become important, resistivity due to LHD waves can already play a major role in providing dissipation necessary for reconnection onset.

The results of the Vlasov simulations are in a good agreement with the estimates of the effective collision frequency and anomalous resistivity due to LHD waves at the magnetopause measured by Cluster spacecraft. Although direct measurements of plasma density, currents, and electromagnetic field fluctuations with sufficient temporal and spatial resolutions pose a formidable challenge, there is a possibility to make reliable estimates of these quantities, based on the spacecraft potential and electric and magnetic field measurements. We considered in detail one magnetopause crossing on 30 March 2002 and came up with effective collision rates of the same order as the lower-hybrid frequency f_{LH}. For this reason we used the general expression involving particle density and electric field fluctuations shown in the lowest panel of Fig. 192, to derive the effective collision frequency. Further, our Vlasov-code simulations and Cluster observations have revealed that in the case of an extremely thin current sheet electrostatic and electromagnetic LHD fluctuations provide approximately equal contributions to the effective anomalous electron collision rate, which is of the order of the lower-hybrid frequency. The anomalous resistivity based on these anomalous collisions could be significant for the solar plasma entry into the Earth magnetosphere, e.g. by magnetic reconnection.

(I. Silin, J. Büchner and A. Vaivads)

Small-scale reconnection due to lower-hybrid drift instability in current sheets with sheared fields

We investigated the consequences of a lower-hybrid drift (LHD) instability for reconnection through magnetopause-like thin current sheets in dependence on a guide magnetic field B_{y0} by means of three-dimensional Vlasov-code simulations. We found that the LHD waves are amplified by inverse resonant Landau damping on the ion flow. In current sheets separating anti-parallel magnetic fields the LHD waves can trigger global current-aligned eigenmodes, which directly couple to the tearing-mode instability. Depending on the initial conditions either small-scale three-dimensional or two-dimensional reconnection prevails. In the case of the magnetopause, however, i.e. in the presence of a guide magnetic field up to $B_{y0} = B_0$ (where B_0 is the asymptotic B_x field), the unstable LHD waves propagate obliquely to the current direction, at different angles from the opposite sides of the current sheet. For a guide field $B_{y0} = 0.25B_0$ the resulting patchy three-dimensional small-scale reconnection structure is shown at $t\Omega_{0i} = 34$ after the instability has started (Ω_{0i} is the ion cyclotron frequency) in see Fig. 193). For guide magnetic field up to $B_{y0} = B_0$ the reconnection instability grows significantly slower than in purely anti-parallel field configurations.

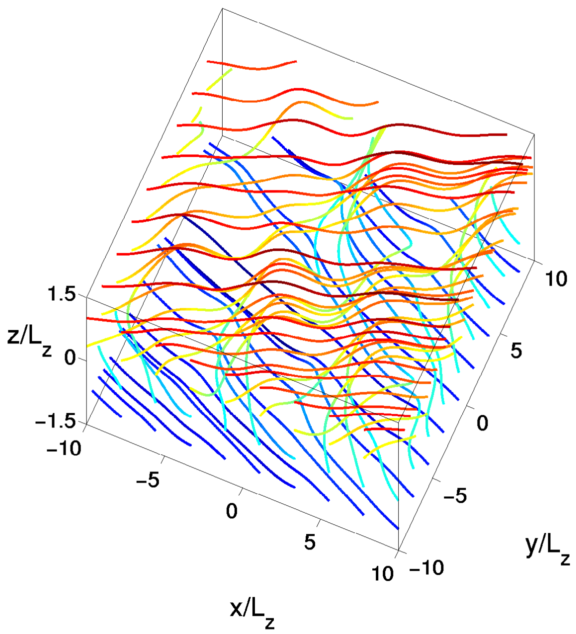

Fig. 193: Simulated magnetic field inside a thin ($r_i/L_z = 1$) current sheet with a moderate guide field component $B_{y0} = 0.25B_0$ at $t\Omega_{0i} = 34$. All lines initiate at the edges of the simulation box above, below and at the current sheet center. The colour coding depicts the position of the line along the normal to the current sheet direction (blue to red from bottom to top).

(J. Büchner and I. Silin)

Theory of coherent wave packets in different wave modes of space plasmas

Over the last few years significant progress has been made in satellite observations of wave phenomena in magnetospheric and solar wind interaction physics as a result of the successful procurement of high-time and spatial resolution measurements hitherto unavailable. These data show that strongly nonlinear processes lie behind many space plasma phenomena. One of the intriguing features of plasma turbulence is a coherent behaviour of different wave modes. Fig. 194 shows, for example, that "whistler turbulence" observed by Cluster often consists of many almost monochromatic and coherent wave packets. Another example of coherent wave structures, but at much lower frequencies is the observations of periodic 20 – 30 s magnetohydrodynamic waves upstream of the Earth's bow shock. In this spectacular case, a coherent behaviour is revealed not only in the electric and magnetic field variations, but also in a coherent large-amplitude gyration of the solar wind protons together with beam particles propagating from the shock (Fig. 195). Fig. 196 shows example of coherent wave packets observed at frequencies which are 5 orders of the magnitude higher (high frequency Langmuir waves). It is believed that the physics of all these structures is similar, inspite of a huge difference in frequencies and scales. Effective interplay between electrons and protons (whistler waves), solar wind and beam protons (low frequency Alfvén and magnetosonic waves), two different electron populations (Langmuir waves) with a periodic momentum exchange between two (or more) species mediated by magnetic or electric field stresses leads to a specific nonlinear beating effect. The exact nonlinear theory for whistlers and MHD waves in beam-plasma configurations was developed in MPS (Dubinin *et al.* (2003); Dubinin *et al.* (2004); Webb *et al.* (2005b)).

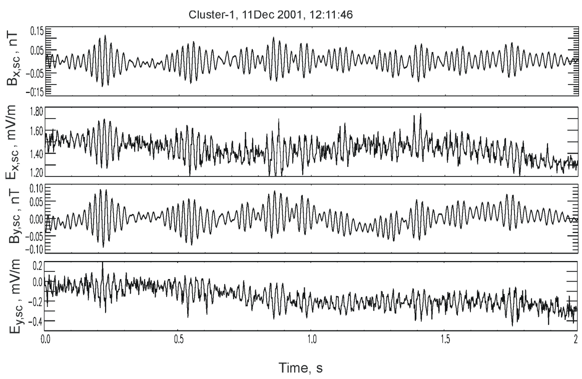

Fig. 194: Magnetic and electric field variations observed by the STAFF-SC instrument on Cluster spacecraft in a "whistler burst" within the Earth's magnetosphere.

(E. Dubinin, K. Sauer, in collaboration with J. F. McKenzie and G. Webb)

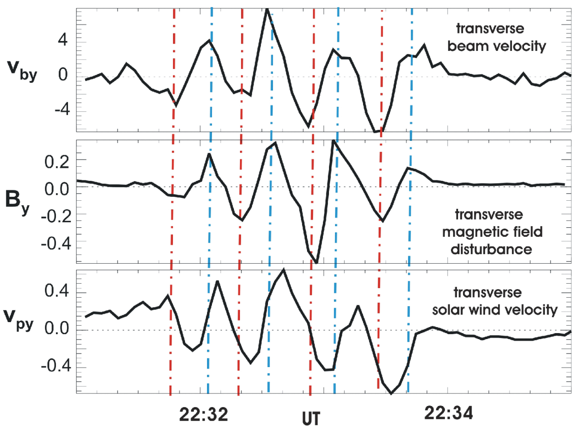

Fig. 195: From top to bottom: Variations in the transverse components of the beam ions, magnetic field and the solar wind speed observed by Cluster in the foreshock region (Sauer *et al.*, 2005). The values are normalized to the Alfvén speed and the undisturbed magnetic field strength.

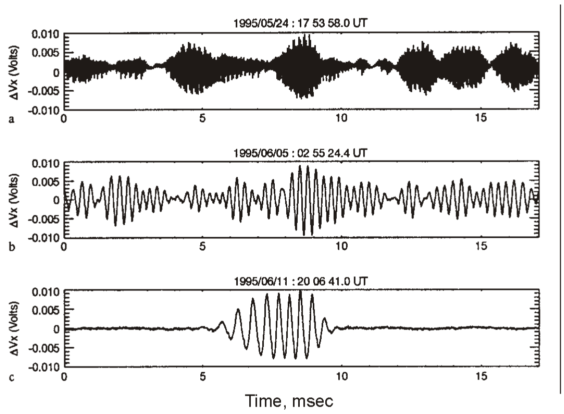

Fig. 196: Examples of wave forms of high frequency electrostatic waves observed on the WIND spacecraft (adopted from Mangeney et al., Ann. Geophys. 17, 307, 1999).

Differential ion streaming in the solar wind as an equilibrium state

An intriguing problem in solar wind research is the presence of differential streaming between the protons and minor ions. A solar wind flow made up of differentially streaming core protons and minor ions (alphas, protons) represents a nonlinear dynamic system in which the ion fluids and the electromagnetic fields generated by their motion interplay through the exchange of the momentum between ion populations mediated by the magnetic field tensions. It is shown (Dubinin *et al.*, 2005a) that a such dynamic system possesses an equilibrium state with a differential ion streaming between the core protons and ions of a beam. The minor ions move faster than the core protons. This equilibrium state is also characterized by a gyrating motion of both ion populations with a phase shift of π. The waves which act as the catalyst to equilibrium differential speeds are either Alfvén or magnetosonic waves, depending upon the beam speed. The beam ions do not "surf" on the waves but efficiently participate in the momentum exchange process between core protons, beam and electromagnetic fields.

(E. Dubinin, K. Sauer, in collaboration with J. F. McKenzie)

Theory of the Dst index and its relation to the solar wind

The Dessler-Parker-Sckopke formula for the disturbance magnetic field averaged over the Earth's surface, universally used to interpret the geomagnetic Dst index, can be generalized, by using the well known method of deriving it from the virial theorem, to include the effects of ionospheric currents. There is an added term proportional to the global integral of the vertical mechanical force that balances the vertical component of the Lorentz force $\mathbf{J} \times \mathbf{B}$ in the ionosphere; a downward mechanical force reduces, and an upward increases, the depression of the magnetic field. If the vertical component of the ionospheric Ohm's law holds exactly, the relevant force on the plasma is the collisional friction between the neutral atmosphere and the vertically flowing plasma. An equal and opposite force is exerted on the neutral atmosphere and thus appears in *its* virial theorem. The ionospheric effect on Dst can then be related to the changes of kinetic and gravitational energy contents of the neutral atmosphere; since these changes are brought about by energy input from the magnetosphere, there is an implied upper limit to the effect on Dst which in general is relatively small in comparison to the contribution of the plasma energy content in the magnetosphere. Hence the Dessler-Parker-Sckopke formula can be applied without major modification, even in the case of strong partial ring currents; the ionospheric closure currents implied by the local time asymmetry have only a relatively small effect on the globally averaged disturbance field, comparable to other sources of uncertainty. When derived from the virial theorem applied to a bounded volume (e.g. the magnetosphere bounded by the magnetopause and a cross-section of the magnetotail), the Dessler-Parker-Sckopke formula contains also several boundary surface terms which can be identified as contributions of the magnetopause (Chapman-Ferraro) and of the magnetotail currents. (Published: Vasyliūnas, 2006a)

The simple equation proposed by Burton *et al.* (J. Geophys. Res. **80**, 4204–4214, 1975) and extensively applied with considerable success for predicting the time series of the geomagnetic storm index Dst

is generally derived solely from conservation of energy, without describing the specific energization processes. More recently, numerical simulation models of ring current evolution have relied on the opposite approximation: they describe the energization and loss processes, without imposing conservation of energy. The fact that predictions of Dst by both methods agree reasonably well with each other and with observations suggests that some of the assumptions need to be reexamined. The Dessler-Parker-Sckopke theorem, in its generalized form, contains a magnetotail surface term proportional to the open magnetic flux, the time derivative of which equals the difference between the electric field integrals along the dayside and along the nightside reconnection lines. The dayside integral contributes a term to the equation for $(d/dt)Dst$ that is identical in form and (within the uncertainties) consistent in magnitude with the empirically determined source term of the Burton-McPherron-Russell equation. The success of the empirical equation in predicting Dst then implies that the remaining terms in the equation, the contribution of the nightside integral of the magnetotail term and the rate of increase of plasma energy content, sum to zero. The simplest interpretation is that the energy of ring current plasma is indeed being supplied primarily from the magnetotail by processes that involve nightside reconnection in an essential way. (Published: Vasyliūnas, 2006b)

(V. M. Vasyliūnas)

Relations between magnetic and electric fields and currents in plasmas

Fundamentally, the time derivative of the electric field is given by the displacement-current term in Maxwell's generalization of Ampère's law, and the time derivative of the electric current density is given by the generalized Ohm's law. The latter is derived by summing the accelerations of all the plasma particles and can be written exactly, with no approximations, in a (relatively simple) primitive form containing no other time derivatives. When one is dealing with time scales long compared to the inverse of the electron plasma frequency and spatial scales large compared to the electron inertial length, however, the time derivative of the current density becomes negligible in comparison to the other terms in the generalized Ohm's law, which then becomes the equation that determines the electric field itself. Thus, on all scales larger than those of electron plasma oscillations, neither the time evolution of **J** nor that of **E** can be calculated directly. Instead, **J** is determined by **B** through Ampère's law and **E** by plasma dynamics through the generalized Ohm's law. The displacement current may still be non-negligible if the Alfvén speed is comparable to or larger than the speed of light, but it no longer determines the time evolution of **E**, acting instead to modify **J**. For theories of substorms, this implies that, on time scales appropriate to substorm expansion, there is no equation from which the time evolution of the current could be calculated, independently of $\nabla \times \mathbf{B}$. Statements about change (disruption, diversion, wedge formation, etc.) of the electric current are merely descriptions of change in the magnetic field and are *not* explanations. (Published: Vasyliūnas (2005b))

Maxwell's equations allow the magnetic field **B** to be calculated if the electric current density **J** is assumed to be completely known as a function of space and time. The charged particles that constitute the current, however, are subject to Newton's laws as well, and **J** can be changed by forces acting on charged particles. Particularly in plasmas, where the concentration of charged particles is high, the effect of the electromagnetic field calculated from a given **J** on **J** itself cannot be ignored. Whereas in ordinary laboratory physics one is accustomed to take **J** as primary and **B** as derived from **J**, it is often asserted that in plasmas **B** should be viewed as primary and **J** as derived from **B** simply as $\nabla \times \mathbf{B}$. The relation between $\nabla \times \mathbf{B}$ and **J** can be investigated in the same terms and by the same method as previously applied to the MHD relation between electric field and plasma bulk flow: Vasyliūnas (2001) assume that one but not the other is present initially, and calculate what happens. The result is that, for configurations with spatial scales much larger than the electron inertial length λ_e, a given $\nabla \times \mathbf{B}$ produces the corresponding **J**, while a given **J** does not produce any $\nabla \times \mathbf{B}$ but disappears instead. The reason for this can be understood by noting that $\nabla \times \mathbf{B} \neq \mathbf{J}$ implies a time-varying electric field (displacement current) which acts to change both terms (in order to bring them toward equality); the changes of the two terms, however, proceed on different time scales, light travel time for **B** and electron plasma period for **J**, and clearly the term changing much more slowly is the one that survives. (By definition, the two time scales are equal at λ_e.) On larger scales, the evolution of **B** (and hence also of $\nabla \times \mathbf{B}$) is governed by $\nabla \times \mathbf{E}$, with **E** determined by plasma dynamics via the generalized Ohm's law; as illustrative simple examples, the formation of magnetic drift currents in the magnetosphere and of Pedersen and Hall currents in the ionosphere have been described. (Published: Vasyliūnas (2005a))

(V. M. Vasyliūnas)

III. Selbständige Nachwuchsgruppe Helio- und Asteroseismologie / Independent Junior Research Group of the Max Planck Society “Helio- and Asteroseismology”

Schwerpunktthema:

Neues Forschungsthema am MPS

(L. Gizon)

(English version see page 159)

Millionen von Pulsationsmoden, welche durch turbulente Konvektion angeregt werden, ermöglichen es Sonnenphysikern, in die Sonne hineinzusehen, ebenso wie Geophysiker den inneren Aufbau der Erde mittels Beobachtungen der seismischen Aktivität untersuchen. In den letzten zwanzig Jahren kam es durch die Helioseismologie zu einer beachtlichen Anzahl an Entdeckungen in der Physik der Sonne, der Sterne sowie im Bereich der Grundlagenphysik. Jedoch scheint das Beste noch bevorzustehen: dreidimensionale helioseismologische Verfahren bieten die Aussicht, komplexe magnetohydrodynamische Vorgänge zu erkunden und somit die Mechanismen des Sonnenzyklus aufzudecken. Gleichzeitig eröffnet sich durch die Ausweitung der seismologischen Untersuchungen auf entfernten Sternen eine neue Ära der beobachtenden Astrophysik.

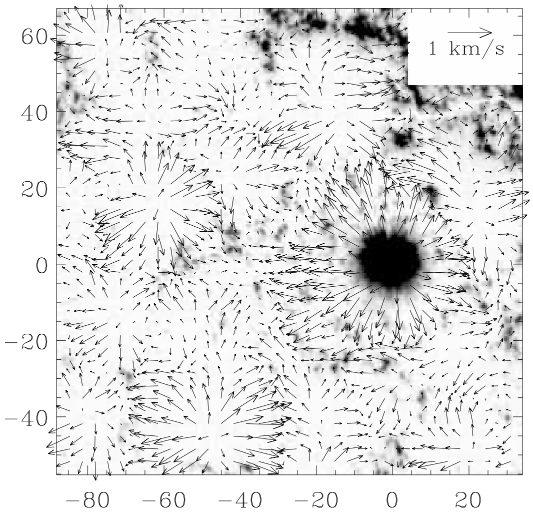

Abb. 197: Karte horizontaler Strömungen um einen Sonnenfleck bei einer Tiefe von 1 Mm unterhalb der Sonnenoberfläche. Die Strömungsgeschwindigkeiten ergeben sich aus Messungen von Anisotropien in den seismischen Laufzeiten mittels einer Methode der lokalen Helioseismologie, die als *Time-Distance* Methode bekannt ist. Um den Sonnenfleck sieht man eine Auswärtsströmung mit einer Geschwindigkeit von bis zu 500 m/s. Die Achsen bezeichnen die Abstände auf der Sonne in Mm.

Die Methoden der Helioseismologie können in zwei Klassen eingeteilt werden: global und lokal. Der eher traditionelle Ansatz der globalen Helioseismologie basiert auf der Messung der Frequenzen der einzelnen Oszillationsmoden, mit der die Suche nach einem seismologischen Sonnenmodell, dessen Eigenfrequenzen mit den beobachteten übereinstimmen, einhergeht. Damit kann der großskalige Aufbau der Sonne sowie die Rotation als Funktion der Tiefe und der heliographischen Breite angegeben werden. Ergänzend zur globalen Helioseismologie werden neue Methoden der lokalen Helioseismologie entwickelt, mit denen dreidimensionale Abbildungen des Sonneninneren gewonnen werden können. Die grundlegende Idee ist dabei, Tiefeninformationen aus der Laufzeit solarer Wellen zwischen zwei beliebigen Punkten an der Oberfläche zu gewinnen.

Die globale Helioseismologie war bei weitem die präziseste Überprüfung der Theorie des inneren Aufbaus und der Entwicklung der Sterne, die insbesondere zu einer Revision des Standardmodells der Teilchenphysik geführt hat, um das Problem der Sonnenneutrinos zu lösen. Heutzutage ist der aufregendste Aspekt der Helioseismologie die Suche nach den Zusammenhängen, die den Ursprung und die Variabilität des Magnetfelds der Sonne betreffen. Dies ist wahrscheinlich das wichtigste ungelöste Problem der Sonnenphysik. Allgemein wird angenommen, dass ein Dynamoprozess für den Zyklus des Magnetfeldes der Sonne verantwortlich ist. Entsprechend dieser Vorstellung werden Magnetfeldlinien durch innere Scherbewegungen gedehnt und verdreht. Deshalb ist es wichtig, innere Materiebewegungen, Abweichungen von der Kugelsymmetrie und deren zeitliche Variation zu kartografieren. Die globale Helioseismologie konnte hierzu weitere grundlegende Ergebnisse beisteuern, wie z.B. die Entdeckung von Bereichen rotations-

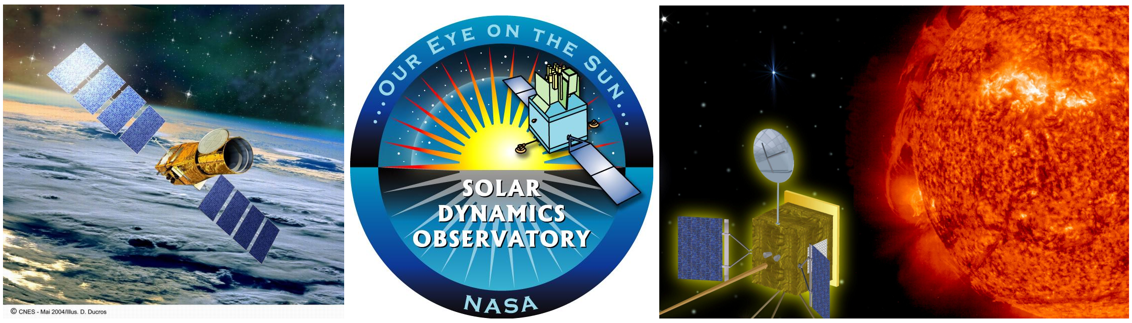

Abb. 198: Zükunftige Weltraummissionen zur Untersuchung solarer und stellarer Pulsationen: COROT (CNES/ESA), SDO (NASA), Solar Orbiter (ESA).

bedingter Scherungen im Sonneninneren, Variationen der Rotationsrate mit dem Sonnenzyklus und noch unverstandene quasi-periodische Variationen am Boden der Konvektionszone.

Es wird erwartet, dass die weiteren Fortschritte mit lokaler Helioseismologie erzielt werden. Obwohl diese noch eine recht junge Wissenschaft ist, hat sie bereits einen Mechanismus für den breitenabhängigen Transport des magnetischen Flusses erklären können, der die Dauer des Sonnenzyklus festlegen könnte. Detaillierte 3-D Karten der oberen Konvektionszone ermöglichen neue Einblicke in den Aufbau, die Entwicklung und die Gliederung aktiver Gebiete und konvektiver Strömungen. In einer weiteren Anwendung kann die lokale Helioseismologie dazu verwendet werden, Abbildungen aktiver Gebiete auf der Rückseite der Sonne zu gewinnen. In all diesen Fällen hat man inzwischen eine Vorahnung der vielfältigen Möglichkeiten erhalten, jedoch sind bessere Daten und Weiterentwicklungen der Methoden notwendig, um das volle Potential ausschöpfen zu können.

Ein wichtiger technologischer Schritt für die Helioseismologie wird mit dem HMI-Instrument auf dem Solar Dynamics Observatory der NASA erfolgen, das 2008 gestartet wird. Mit einer hohen räumlichen Auflösung über die gesamte sichtbare Sonnenhemisphäre ist HMI das erste Instrument, das speziell für lokale Helioseismologie konzipiert ist. Später, in etwa einem Jahrzehnt, soll der Solar Orbiter der ESA erstmals Informationen über den Aufbau und die Dynamik von Bereichen unterhalb der Sonnenoberfläche der Polregionen liefern. Diese neuen Beobachtungen werden weitere Verbesserungen im Bereich der Modellierung der Sonne erforderlich machen. Insbesondere werden theoretische Untersuchungen und numerische Simulationen benötigt werden, um die Wellenausbreitung in stark magnetisierten Fluiden zu verstehen. Dies ist eine Grundvoraussetzung bei der Anwendung lokaler Helioseismologie in aktiven Gebieten. Die lokale Helioseismologie befindet sich heutzutage in einer rasanten Entwicklung und verspricht viele weitere Entdeckungen. Eines der ambitioniertesten Ziele ist die direkte Abbildung des Magnetfelds im Inneren der Sonne.

Asteroseismologie ist die Untersuchung globaler Oszillationen in entfernten Sternen. Auch sie tritt in eine sehr aufregende Phase großer Entdeckungen ein. Viele Sterne, mit einem breiten Spektrum an Massen und Entwicklungszuständen, sind dafür bekannt, dass sie Schwingungen aufweisen. Aber erst in den letzten Jahren ist es mit hochentwickelten Spektrographen und großen bodengebundenen Teleskopen möglich geworden, diese Oszillationen in sonnenähnlichen Sternen nachzuweisen. Stellare Oszillationen haben ein beachtliches diagnostisches Potential und erlauben, die Masse und das Alter eines Sterns mit beispielloser Genauigkeit zu bestimmen. Derartige Kenntnisse für eine ausreichende Anzahl an Sternen wird die Untersuchung der Entwicklung von Sternen und Galaxien revolutionieren. Asteroseismologie bietet des Weiteren die Möglichkeit, den Bereich der Rotation im Inneren von Sternen einzuschränken und die Ränder von Konvektions- und Ionisationszonen festzulegen. Diese Informationen könnten dazu beitragen, die von einem Dynamo verursachten stellaren Aktivitätszyklen und den solar-stellaren Zusammenhang zu verstehen.

Diese vielversprechenden Möglichkeiten zur Untersuchung des inneren Aufbaus, der Entwicklung und der Aktivität von Sternen können vollständig realisiert werden, sobald nur für eine genügend große Anzahl von Sternen Beobachtungen verfügbar werden. Die Genauigkeit der Frequenzbestimmung von globalen stellaren Oszillationen ist jedoch sehr stark durch die verfügbare Teleskopzeit beschränkt. Das ist der Grund weshalb Weltraumteleskope, die allein diesem einen Zweck gewidmet sind, eine attraktive Lösung sind, um Langzeitbeobachtungen pulsierender Sterne zu ermöglichen. Mit dem Start der CNES-Mission COROT werden hochpräzise photometrische Messungen im Jahr 2006 erwartet. In den folgenden Jahrzehnten wird die Asteroseismologie große Fortschritte machen, insbesondere auch durch die noch anspruchsvollere NASA-Mission Kepler sowie möglicherweise mit der ESA-Mission Eddington. Ganz genau wie im Fall der Helioseismologie bedarf es eines verbesserten Verständnisses was die Oszillationen und ihre Wechselwirkung mit magnetohydrodynamischen Prozessen in Sternen betrifft.

Highlight:

New science topics at MPS

(L. Gizon)

Millions of modes of vibration, excited by turbulent convection, enable solar physicists to see inside the Sun, just as geophysicists can probe the internal structure of the Earth using records of seismic activity. Over the past twenty years, helioseismology has produced a considerable number of discoveries in solar, stellar, and fundamental physics. The best is still to come, however: three dimensional helioseismic techniques offer unique prospects for probing complex magnetohydrodynamical processes and uncovering the mechanism of the solar cycle, while the extension of seismic investigations to distant stars will open a new era of observational stellar research.

Methods of helioseismology can be divided into two classes: global and local. The more traditional technique of global helioseismology consists of measuring the frequencies of the modes of oscillation and searching for a seismic solar model whose oscillation frequencies match the observed ones. This reveals the Sun's large-scale structure and rotation as a function of depth and latitude. To complement global helioseismology, new methods of local helioseismology are being developed to make three dimensional images of the solar interior. The basic idea is to retrieve information at depth from the time it takes for solar waves to travel between any two surface locations.

Global helioseismology has provided by far the most precise tests for the theory of stellar structure and evolution, implying, in particular, a revision of the standard model of particle physics to solve the solar neutrino problem. Today, the most exciting aspect of helioseismology is the search for clues regarding the origin and variability of the Sun's magnetic field, possibly the most important unsolved problem in solar physics. The general belief is that a dynamo process is responsible for the solar magnetic cycle. According to this scenario, magnetic field lines are stretched and twisted by internal shearing motions. Therefore, it is essential to map internal mass motions, structural asphericities, and their temporal variations. Global helioseismology has already provided some fundamental results, revealing regions of rotational shear in the Sun's interior, solar-cycle variations in the rotation rate, and mysterious quasi-periodic changes at the base of the convection zone.

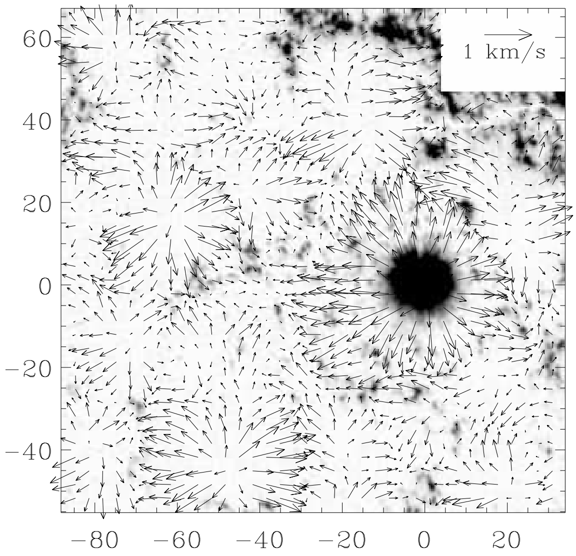

Fig. 197: Map of horizontal flows around a sunspot at a depth of 1 Mm below the surface. Flow velocities are obtained by measuring the anisotropy of seismic travel times, using a technique of local helioseismology known as time-distance. The outflow around the sunspot, with an amplitude of about 500 m/s, is called the moat. Spatial coordinates are given units of Mm.

The next advances are expected to come from local helioseismology, which, although still a young science, has already pinpointed a mechanism for the latitudinal transport of the magnetic flux that could determine the period of the solar cycle. Detailed 3-D maps of the upper convection zone provide new insights into the structure, evolution and organization of active regions and convective flows. In yet another application, local helioseismology can be used to construct maps of active regions on the far side of the Sun. These few examples illustrate the richness of the science possible with local helioseismology. In all these cases a taste of the possibilities has been provided, but better data and further developments in the technique are required to realize the full potential.

An important technological step for helioseismology will come with the HMI instrument on the Solar Dynamics Observatory of NASA to be launched in 2008. With a high spatial resolution over the entire visible solar hemisphere, HMI is the first instrument specifically designed for local helioseismology. Later, in about one decade, ESA's Solar Orbiter should give access, for the first time, to the subsurface structure and

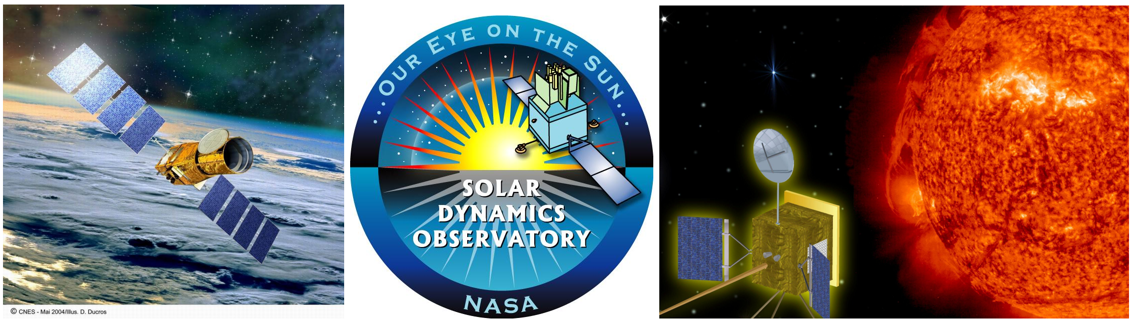

Fig. 198: Future space missions for the study of solar and stellar pulsations: COROT (CNES/ESA), SDO (NASA), Solar Orbiter (ESA).

dynamics of the Sun's polar regions. With these new observations, will come the need for improvements in solar modeling. In particular, theoretical studies and numerical simulations will be required to understand wave propagation in strongly magnetized fluids, a necessary condition for the application of local helioseismology to solar active regions. Local helioseismology is very much under development today and promises many more discoveries. Among the most ambitious goals is to directly image the magnetic field in the solar interior.

Asteroseismology, the study of global oscillations on distant stars, is entering a very exciting period of discoveries. Many stars, covering a wide range of masses and evolutionary states, are known to exhibit oscillations. Only in the last few years, however, has it been possible to detect oscillations on Sun-like stars using sophisticated spectrographs on large ground-based telescopes. Stellar oscillations have considerable diagnostic potential and allow stellar mass and age to be determined with unprecedented precision. Such knowledge for a sufficient sample of stars will revolutionize stellar evolution and galactic evolution studies. Asteroseismology has also the potential to constrain internal stellar rotation and locate the borders of convection and ionization zones . Such information would help understand dynamo-generated stellar activity cycles and the solar-stellar connection.

These exciting possibilities for the study of stellar structure, evolution, and activity will be fully realized only once observations become available for a large sample of stars. The precision on the frequencies of the global modes of stellar oscillations, however, is very much limited by available telescope time, which is why dedicated space telescopes are an attractive solution to provide long-term coverage of many types of pulsating stars. High precision photometry from space is expected in 2006 with the launch of COROT of CNES. The field of asteroseismology will make much progress in the following decades with more ambitious missions like NASA's Kepler and possibly ESA's Eddington. As in the case of helioseismology, there is a strong need to improve our understanding of the oscillations and how they interact with the magnetohydrodynamical processes in stars.

Wissenschaftliche Einzelberichte/
Individual scientific reports

(nur in Englisch)

Research on stellar oscillations is carried out at the Institute by the new Independent Junior Research Group "Helio- and Asteroseismology" of the Max Planck Society. Because this group was set up in September 2005, most of the scientific reports listed below have not appeared in print yet.

Comprehensive review of local helioseismology

A large fraction of current research in helioseismology focuses on the development of techniques of local helioseismology to produce three-dimensional maps of the subphotospheric flows and temperature inhomogeneities. We have reviewed this field of research, which is still relatively new, covering both theoretical and observational results. After a brief introduction to solar oscillations and wave propagation through inhomogeneous media, we described the main techniques of data analysis used in local helioseismology: Fourier-Hankel decomposition, ring-diagram analysis, time-distance helioseismology, helioseismic holography, and direct modeling. We discussed local helioseismology of large-scale flows, the solar-cycle dependence of these flows, perturbations associated with regions of magnetic activity, and solar supergranulation. This work is perhaps the first comprehensive review of the field of local helioseismology.

(L. Gizon in collaboration with A. Birch (CoRA, USA))

Measurements of travel times from the MDI Structure Program

Time-distance helioseismology consists of analysing of the travel times of acoustic wave packets that propagate through the solar interior. One goal is to infer flows at a precision level close to 1 m/s in the upper solar convection zone. In order to achieve this level of precision, the most critical aspect is to obtain clean measurements of seismic travel times. We used Doppler velocity maps recorded by the Michelson Doppler Imager (MDI-SOHO Structure Program) as input data. Since MDI data are available from May 1996, the temporal evolution of these flows can be studied over the last 10 years. Of particular interest are the so-called "torsional oscillations", which are bands of faster and slower rotation with an amplitude of about ± 10 m/s that migrate slowly towards the equator as the solar cycle develops (Fig. 199). These flows appear to be strongly correlated with the latitudinal distribution of sunspots and active regions. Thus, they may tell us something useful about the magnetohydrodynamical processes governing the magnetic cycle of the Sun. In addition to measuring travel times, we derived the noise correlation matrix of the travel-time measurements. Correlations in the data errors are a required input to solve the inverse problem of time-distance helioseismology, which consists of inferring internal flows from the travel-time measurements.

(M. Roth and L. Gizon, in collaboration with J. Beck (Stanford University, USA))

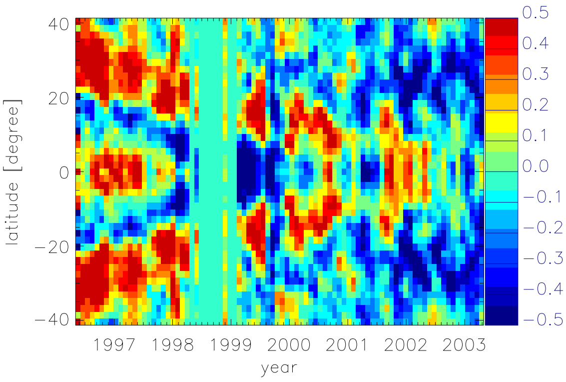

Fig. 199: Temporal evolution of banded zonal flows. The travel time shifts between waves travelling eastward and waves travelling westward are shown as a function of time and latitude. The colour bar gives the travel times in units of second. Some data are missing due to the loss of SOHO attitude in July 1998.

Travel-time shifts caused by small magnetic features

The solar surface magnetic field is dragged by convective motions into concentrations that form the quiet-Sun magnetic network. Because these magnetic features are smaller than the wavelengths of solar oscillations, they are ideal to study the response of finite-wavelength seismic travel times to point-like perturbations.

We used time-distance helioseismology to directly measure the spatial sensitivity of f-mode travel times to a point-like magnetic perturbation. Travel-time maps reveal that the sensitivity is not restricted to the geometrical ray path, is spread on elliptical and hyperbolic curves, and oscillatory (Fig. 200a). We find that these geometrical features are mostly due to finite wavelength effects and to the fact that the sources of excitation of solar oscillations are distributed over the whole solar surface. To reach this conclusion, we developed a simple phenomenological model to explain the travel-time observations. We assumed that scattering from a magnetic feature can be described

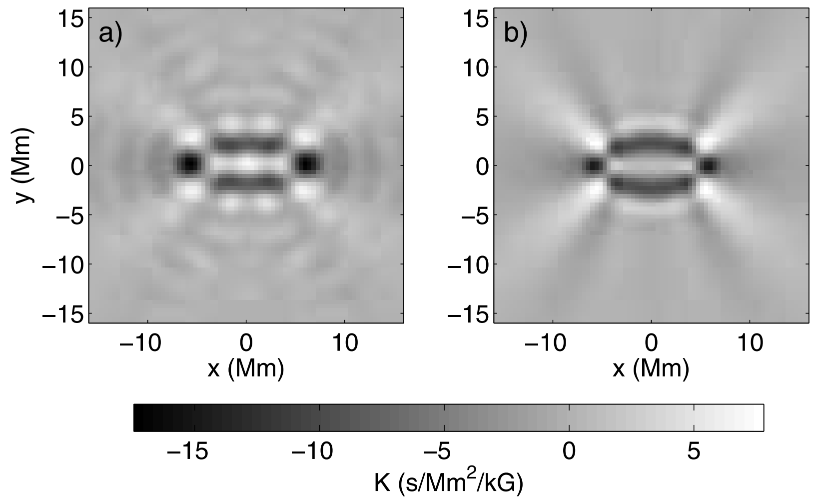

Fig. 200: Sensitivity of solar surface-wave travel times to small magnetic features. (a) Observations based on MDI data from the high-resolution field of view. A magnetic feature at position (x, y) causes a shift in the travel time measured between the two observation points (at $x = \pm 4.95$ Mm, $y = 0$). As magnetic features have a finite spatial extent, we applied a simple regularized deconvolution. The grey scale gives the shift in travel time due to a 1 kG magnetic field covering 1 Mm^2. (b) Phenomenological model for a point magnetic scatterer based on single-scattering theory. A scatterer located anywhere along an ellipse (with focii at the observation points) causes travel-time shifts of the same sign, giving rise to Fresnel zones. The hyperbolic features are due to the scattering of waves generated by distant sources.

by a combination of monopole and dipole scattering. Treating solar surface-gravity waves (f modes) as deep water waves, we computed the wave field using a single-scattering approximation, and then adjusted the complex scattering amplitudes to obtain the best match with the observations (Fig. 200b). We find that the dipole and monopole contributions are equally important.

By studying the interaction of seismic waves with localised magnetic features on the Sun, we have provided an observational confirmation of the basic banana-doughnut theory originally developed for finite-wavelength tomography of the Earth, according to which body-wave travel times are sensitive to the wave speed in a broad region surrounding the geometrical ray path. This is the first test outside the laboratory showing the relevance of scattering theory to cross-correlation travel times (laboratory tests exist for ultrasonic waves). As in Earth seismology, we suggest that finite-wavelength modelling will be essential in revealing deep structures in the solar interior.

(L. Gizon in collaboration with T. Duvall (NASA-GSFC, USA) and A. Birch (CoRA, USA))

Sensitivity of surface-wave travel times to steady flows

As shown in the previous report, interesting phenomena that exist near the solar surface leave a signature in the properties of solar surface-gravity waves. In particular, surface waves can be used to probe local flows of plasma with a variety of scales and velocities. The surface waves that are affected by the flows display a shift in their travel times: it takes less time for waves to propagate along the flow than against it. Thus, by mapping the travel-time differences between any two points on the Sun, information about the flow can be learned.

In general, the sensitivity of travel times to small perturbations in internal solar properties is described through linear sensitivity functions, also called travel-time kernels. We have calculated such kernels in the first Born approximation, which is a single-scattering approximation. Fig. 201 shows an example of a 2-D kernel which gives the sensitivity of f-mode travel times to a localized horizontal flow on the solar surface.

The next step will be to compute a collection of sensitivity kernels in order to carry out the inverse problem of time-distance helioseismology and infer solar flows from travel-time maps with high precision. With these

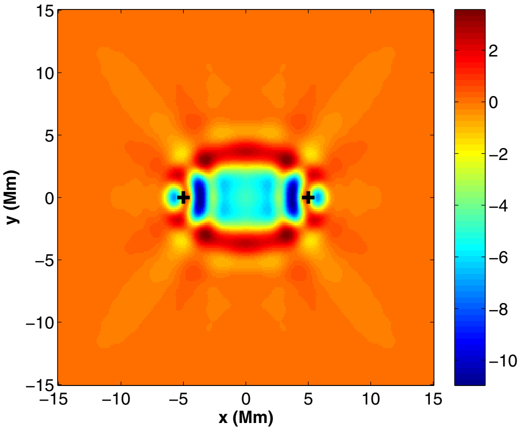

Fig. 201: A two-dimensional travel-time sensitivity kernel for flows. The observation points (crosses) have coordinates $(-5, 0)$ Mm and $(5, 0)$ Mm. Travel times are counted positive for waves that propagate from left to right. This particular kernel gives the sensitivity of f-mode travel times to a horizontal flow pointing in the x direction. For instance, a local flow located in an area of blue causes a decrease in the travel time, and one in an area of red causes an increase. The colour bar has units of s $(\mathrm{km/s})^{-1}\mathrm{Mm}^{-2}$.

kernels, we are hoping to achieve a sub-wavelength spatial resolution of about 2 Mm.

(J. Jackiewicz, L. Gizon)

Line profiles of fundamental modes of solar oscillations

We have studied the asymmetry of f-mode line profiles in the power spectrum of solar oscillations, which have received less attention than for acoustic modes (p modes). Line asymmetry is interesting as it contains information about the mechanism of wave excitation.

Using MDI-SOHO data, we find that f-mode line asymmetry is pronounced in the degree range 600-1200 and has opposite signs in velocity and intensity power spectra. One may ask if the mechanism responsible for f-mode line asymmetry can be described in simple physical terms, as is done for p modes. An argument based on wave interference (used to explain p-mode line asymmetry) has little value in the case of f modes, which do not propagate in the vertical direction. Is it at all conceivable that line asymmetry may occur from combinations of exponential wave functions? To investigate this question, we considered the propagation of a surface wave at the interface between two media with different constant densities, forced at a given height by a vertical momentum impulse. We find that, in the limit of a large density discontinuity, line asymmetry can occur when the source is situated above the interface. Although this toy model is not intended to approximate the Sun, it has the merit of demonstrating that line asymmetry can occur even for waves that do not propagate in the vertical direction, such as the f mode.

(L. Gizon)

Simulations of wave propagation in the convection zone

The propagation of waves in the near photospheric layers is being studied using numerical simulations, in order to better understand some helioseismological observations. The code we have developed follows the linear evolution of perturbations in a stratified, inhomogeneous background fluid. We have used existing granulation simulations, extended using a standard solar model atmosphere, to provide a realistic background state.

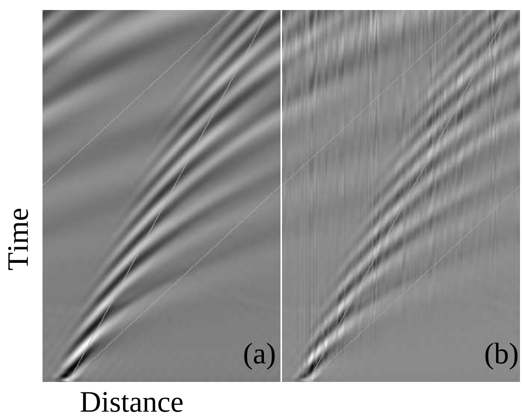

Fig. 202: The vertical velocity perturbation of an f mode propagating (a) through a horizontally uniform atmosphere and (b) when background convection is present. The box is periodic so that a wave propagating through the right boundary reappears on the left. The broken white lines show propagation with the phase and group speeds.

We are interested in the wave propagation through this atmosphere. A practical problem is that the solar atmosphere is superadiabatic beneath the solar photosphere, and so exponentially growing modes are present in the solutions. As we wish to focus on the effects of the convection on the waves, we currently modify the density so that, in the wave simulation, the atmosphere is nowhere unstable.

Fig. 202 shows two 2-D runs, with which we have tried to understand the scattering and damping of waves by the near-surface convection. Our code will be extended to three dimensions and to magnetic perturbations. Many applications are hoped for, in particular to study the interaction of solar waves with sunspots.

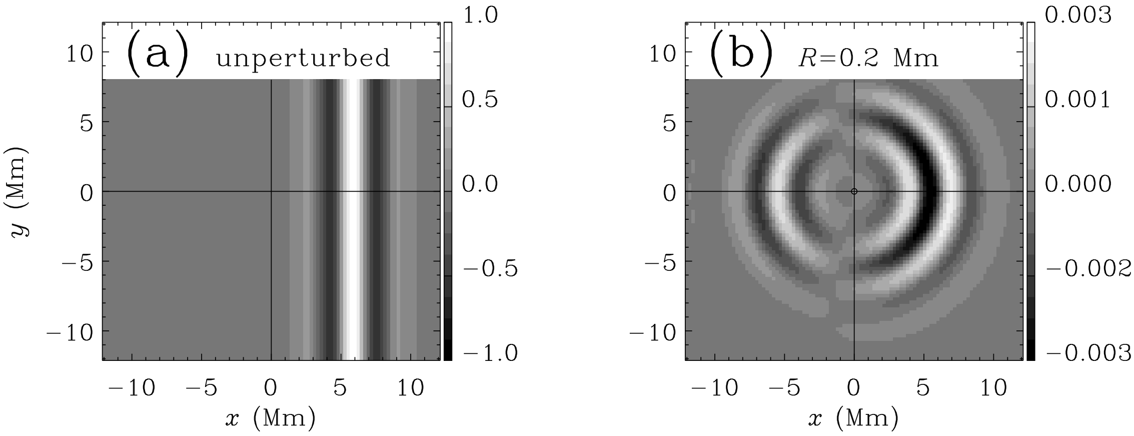

Fig. 203: Plots of the pressure field of an unperturbed (a) and scattered (b) acoustic wave packet at time $t = 8.9$ min after the incident wave packet has crossed the center of a magnetic cylinder with radius $R = 0.2$ Mm. The wave vector is normal to the axis of the cylinder and in the $+x$ direction. For this exact caculation, the ratio of the magnetic to the gas pressures is 0.13, corresponding to a 1 kG magnetic field strength at a depth of 200 km below the photosphere. The total wave field is the superposition of the unperturbed and the perturbed wave fields. Notice that there is a significant amount of backscattered energy.

(R. Cameron, L. Gizon)

Interaction of acoustic waves with a magnetic cylinder

The interaction of acoustic waves with sunspot magnetic fields is strong in the near surface layers. As a result, the effect of the magnetic field on the travel times is not expected to be small near the surface. Deeper inside the Sun, however, the ratio of the magnetic pressure to the gas pressure becomes small, and it is tempting to treat the effects of the magnetic field on the waves using perturbation theory.

With the aim of studying magnetic effects in time-distance helioseismology, we used the first-order Born approximation to compute the scattering of small amplitude acoustic plane waves by a magnetic cylinder embedded in an otherwise uniform medium. Because this simple problem has a known exact solution for arbitrary magnetic field strengths (see Fig. 203), we can study the validity of the linearization of the wavefield on the square of the magnetic field. The validity of the Born approximation is not a priori obvious since the magnetic field allows additional wave modes. We show, by comparison with the exact solution, that travel-time shifts computed in the single-scattering Born approximation are everywhere valid to first order in the ratio of the magnetic to the gas pressures. We also show that, for arbitrary magnetic field strength, the Born approximation is not valid in the limit where the radius of the magnetic cylinder tends to zero. We conclude that, for typical values of the solar magnetic field, the Born approximation should be good at depths larger than a few hundred km below the photosphere.

(L. Gizon in collaboration with S. Hanasoge (Stanford University, USA) and A. Birch (CoRA, USA))

European network for helio- and asteroseismology

HELAS is a new European network for helio- and asteroseismology, funded by the European Union for the period 2006-2010 (EU Framework Program 6). The MPS is an important component of HELAS (MR is Project Scientist, LG is Chair of the Local Helioseismology Network Activity).

The objectives of the Local Helioseismology Network Activity are to (1) coordinate and consolidate European research activities in the field of local helioseismology, exchange knowledge and share experiences; (2) identify areas for which common actions are desirable; (3) promote the exchange of data for tests, comparisons, and analysis; (4) coordinate the process of developing common software tools; (5) facilitate the preparation for the SDO and Solar Orbiter missions. Three workshops are planned and one large conference will be organized in Göttingen in 2007.

(M. Roth, L. Gizon)

IV. International Max Planck Research School on Physical Processes in the Solar System and Beyond at the Universities of Braunschweig and Göttingen

Übersicht / Overview

Die “International Max Planck Research School on Physical Processes in the Solar System and Beyond at the Universities of Braunschweig and Göttingen” wurde 2002 als gemeinsame Inititative des Max-Planck-Instituts für Sonnensystemforschung in Katlenburg-Lindau und der physikalischen Fakultäten der Universität Göttingen (Institut für Astrophysik, Institut für Geophysik) und der Technischen Universität Braunschweig (Institut für Geophysik und Extraterrestrische Physik, Institut für Theoretische Physik) gegründet. Sie bietet in- und ausländischen Studenten Gelegenheiten, auf dem Gebiet der Physik des Sonnensystems zu promovieren.

Die Schule bietet ein forschungsintensives dreijähriges Promotionsstudium. Voraussetzung ist ein Diplom oder ein Master of Science in Physik. Der Doktorgrad kann an den beteiligten Universitäten Braunschweig oder Göttingen oder an der Heimatuniversität angestrebt werden.

Das Lehrprogramm beinhaltet die gesamte Physik des Sonnensystems von der Geophysik über Planetenphysik zur Sonnenphysik. Es garantiert eine breite, interdisziplinäre und fundierte wissenschaftliche Ausbildung. Das wissenschaftliche Programm wird durch Kurse in numerischer Physik, Weltraumtechnologie und Projektmanagement ergänzt. Das Lehrangebot ist in englischer Sprache.

Die Forschungsmöglichkeiten für Doktoranden reichen von Instrumentierung und Beobachtung über Datenanalyse und -interpretation zu numerischen Simulationen und theoretischer Modellierung. Eine klare wissenschaftliche Schwerpunktbildung sorgt für eine thematische Verzahnung der einzelnen Promotionen.

In den Jahren 2004 und 2005 nahmen insgesamt 65 Doktoranden an der Schule teil, davon haben 24 ihre Promotion erfolgreich abgeschlossen. Die Teilnehmer kamen aus insgesamt 21 Ländern, 72% sind ausländischer Nationalität, 29% sind weiblich. Über 800 Bewerbungen in den ersten vier Jahren der Research School zeigen die Attraktivität dieses internationalen Programms für junge Wissenschaftler.

Am 11. November 2005 wurde die IMPRS von einer externen wissenschaftlichen Kommission begutachtet und ihre Weiterführung empfohlen.

The “International Max Planck Research School on Physical Processes in the Solar System and Beyond at the Universities of Braunschweig and Göttingen” was founded in 2002 as a joint venture of the Max Planck Institute for Solar System Research with the University of Göttingen (Institute of Astrophysics, Institute of Geophysics) and the Technical University Braunschweig (Institute of Geophysics and Extraterrestrial Physics, Institute of Theoretical Physics). The participating institutes are uniquely positioned in the fields of solar system physics and together form a center of scientific excellence in an innovative and interdisciplinary research area.

The School offers graduate students from many countries attractive conditions for education and research. A prerequisite is a diploma or masters degree in physics. The PhD degree can be obtained either from the Universities of Braunschweig or Göttingen or the home university of the student.

The program covers the full range of physics inherent in the rapidly growing field of solar system science from geophysics and planetary science to solar physics, as well as the underlying fundamental physics. It ensures a broad, interdisciplinary, and well-founded education for a career in science. The science program is complemented by training in computational physics, space technology and project management, which considerably widens the career opportunities for the students.

High-profile space missions and projects for ground-based instruments, data analysis as well as theoretical and large-scale numerical modeling provide a wide range of research possibilities for PhD students.

In 2004 and 2005 altogether 65 students took part in

Fig. 204: Unsere Studenten während einer Seminarwoche in der Evangelischen Akademie Hofgeismar im Mai 2005 / Group of students during a seminar week in the Protestant Academy Hofgeismar in May 2005

the program, from which 24 successfully finished their PhD. The students came from 21 countries, 72% were of foreign nationality, 29% were female. More than 800 applications in the first four years of operation of the Research School show the attraction of this international program for young scientists.

On 11 November 2005 an external scientific committee evaluated the IMPRS and recommended its continuation.

Vorstand / *Chair*

U. Christensen (MPS), K.-H. Glassmeier (Technische Universität Braunschweig), F. Kneer (Universität Göttingen), U. Motschmann (Technische Universität Braunschweig), S. K. Solanki (MPS, Vorsitz/Chair), A. Tilgner (Universität Göttingen), D. Schmitt (MPS, Koordinator/Coordinator)

Lehrveranstaltungen / *Lectures* 2004 – 2005

Cosmology, 2 – 5 March 2004 (Hoyng)

How to write a scientific paper, 2 March 2004 (Solanki)

Presentation skills, 3 March 2004 (Degenhardt)

How to write a grant proposal, 4 March 2004 (Glassmeier)

Data analysis and numerical methods, 18 – 21 October 2004 (Lagg, Motschmann, Schmitt, Otto)

Introduction to solar physics, 31 January – 4 February 2005 (Solanki)

Hydrodynamics, 31 January – 4 February 2005 (Ferriz Mas)

Project management, 23 – 25 May 2005 (Madauss)

Magnetospheres – Earth and outer planets, 12 – 16 September 2005 (Vasyliunas, Krupp, Daly)

Planetary atmospheres, 12 – 16 September 2005 (Titov)

Solar System Seminar, 23 seminar days with 70 talks by students and 18 tutorial talks by guests (Schmitt)

Abgeschlossene Dissertationen / *Finished PhDs*

Thorsten Bagdonat: Hybrid simulation of weak comets. Institut für Theoretische Physik, Technische Universität Braunschweig, December 2004.

Juan Manuel Borrero Santiago: The fine structure of the sunspot penumbra. Universität Göttingen, August 2004.

Itahiza Francisco Domínguez Cerdeña: Quiet Sun magnetic fields. Universitäts-Sternwarte, Universität Göttingen, July 2004.

Oleg Okunev: Observations and modeling of polar faculae on the Sun. Universitäts-Sternwarte, Universität Göttingen, September 2004.

Sergey Shelyag: Spectro-polarimetric diagnostics of magneto-convection simulations of the solar photosphere. Universität Göttingen, July 2004.

Ilya Silin: Theory and Vlasov-code simulations of thin current sheet instabilities in collisionless space plasmas. Technische Universität Braunschweig, July 2004.

Anja Stadelmann: Globale Effekte einer Erdmagnetfeldumkehr: Magnetosphärenstruktur und kosmische Teilchen. Institut für Geophysik und Extraterrestrische Physik, Technische Universität Braunschweig, November 2004.

Geronimo Villanueva: The high resolution spectrometer for SOFIA–GREAT: Instrumentation, atmospheric modeling and observations. Universität Freiburg, November 2004.

Aleksandra Andjić: Analysis of short-period waves in the solar chromosphere. Institut für Astrophysik, Universität Göttingen, July 2005.

Ingo Jens Baumann: Magnetic flux transport on the Sun. Universität Göttingen, March 2005.

María Hebe Cremades Fernández: Three-dimensional configuration and evolution of coronal mass ejections. Technische Universität Braunschweig, May 2005.

Yevgen Grynko: Light scattering by cometary dust particles with sizes large compared to the wavelength of light. Universität Göttingen, April 2005.

Michael Heuer: Kinetische Plasmaprozesse und Welle-Teilchen-Wechselwirkung von Ionen im schnellen Sonnenwind. Universität Göttingen, September 2005.

Maxim Kramar: A feasibility study of the use of vector tomography for the reconstruction of the coronal magnetic field. Universität Göttingen, September 2005.

Rupali Arunkumar Mahajan: Modelling martian polar caps. Universität Göttingen, September 2005.

Marilena Mierla: On the dynamics of the solar corona. Universität Göttingen, March 2005.

Ana Teresa Monteiro Tomás: Energetic particles in the Jovian magnetosphere and their relation to auroral emissions. Technische Universität Braunschweig, May 2005.

Ganna Portyankina: Atmosphere-surface vapour exchange and ices in the Martian polar regions. Universität Göttingen, September 2005.

Sabine Preuße: Szenarien der Plasmawechselwirkung in kurzperiodischen extrasolaren Planetensystemen. Technische Universität Braunschweig, December 2005.

Luciano Rodriguez Romboli: Internal characteristics of magnetic clouds and interplanetary coronal mass ejections. Technische Universität Braunschweig, May 2005.

Aveek Sarkar: Simulations of the Karlsruhe dynamo using the Lattice-Boltzmann method. Institut für Geophysik, Universität Göttingen, July 2005.

Martin Schrinner: Mean-field view on geodynamo models. Universität Göttingen, July 2005.

Denise Aida Tortorella: Numerical studies of thermal and compressible convection in rotating spherical shells: an application to the giant planets. Universität Göttingen, July 2005.

Durgesh Kumar Tripathi: EUV and coronagraphic observations of coronal mass ejections. Universität Göttingen, February 2005.

Laufende Dissertationen / *Ongoing PhDs*

MPS:

Balmaceda, Laura Antonia: Solar variability and solar irradiance reconstructions (Solanki).

Buske, Monika: Thermal evolution models for the Martian interior (Christensen).

Cheung, Chun Ming Mark: Magnetic flux emergence in the solar photosphere (Schüssler).

Cierpka, Kerstin: Auswertung von Fabry-Perot Daten zur Dynamik der Thermosphäre (Schlegel).

Isik, Emre: Magnetic flux generation and transport in cool stars (Schüssler).

Kolesnikov, Fedor: Vortex flows around magnetic flux tubes (Schüssler).

Kronberg, Elena: Dynamical processes in Jupiter's magnetosphere (Woch/Krupp).

Kuroda, Takeshi: Study of the Martian meteorology using general circulation models (Hartogh).

Maltagliati, Luca: Investigation of the Martian atmospheric water cycle by the OMEGA mapping spectrometer onboard Mars Express (Keller/Markiewicz/Titov).

Matloch, Lukasz: Modeling of solar mesogranulation (Schüssler/Schmitt).

Mecheri, Redouane: Coronal waves and turbulence in the multi-fluid and kinetic approach (Marsch).

Moissl, Richard: Energy transport in the upper Venus mesosphere (Keller/Markiewicz/Titov).

Muñoz Martinez, Guadalupe: Dynamics of coronal mass ejections in the interplanetary medium (Schwenn).

Paganini, Lucas: Accuracy characterization and improvement of real-time spectrometer for remote-sensing applications in radio astronomy and planets atmosphere sounding (Hartogh).

Panov, Evgeny: Thin current sheets at the Earth's magnetopause (Büchner/Korth).

Radioti, Aikaterini: Plasma composition in the magnetosphere of Jupiter (Woch/Krupp).

Roussos, Elias: Interaction of weakly or non-magnetized bodies with magnetospheric plasma and the solar wind: results from modeling and spacecraft observations (Krupp/Woch/Fränz).

Saito, Ryu: Influence of the surface on the atmospheric circulation of Mars (Hartogh).

Santos, Jean: Investigation of solar eruptions using numerical simulations (Büchner).

Sasso, Clementina: Spectro-polarimetry of the solar chromosphere in He I 1083nm (Solanki/Lagg).

Schröder, Stefan: Investigating the surface of Titan with the Descent Imager/Spectral Radiometer aboard the Huygens probe (Grieger/Küppers/Keller).

Seleznyov, Andrey: The origin of solar variability, with an application to the search for extra-solar planets (Solanki).

Semenova, Alina: Modelling of giant starspots on the poles of rapidly rotating stars (Solanki).

Tschimmel, Martin: Investigation of the atmospheric water cycle on Mars by the Planetary Fourier Spectrometer (PFS) instrument onboard the Mars Express spacecraft (Titov/Keller).

Tubiana, Cecilia: Characterization of the Rosetta Target Comet, 67P/Churyumov-Gerasimenko (Böhnhardt).

Vilenius, Esa: Analysis of near-infrared data from lunar dayside using the SIR point spectrometer onboard the SMART-1 spacecraft (Mall).

Yelles Chaouche, Lotfi: Spectro-polarimetric diagnostics of magnetic fields in solar and stellar atmospheres (Solanki/Schüssler).

Zakharov, Vasily: Solar photospheric fine-scale structure: theory and observations (Gandorfer, Solanki).

Universität Göttingen:

Bello González, Nazaret: Fine-scale structure of sunspot penumbrae (Kneer).

Blanco Rodriguez, Julian: Magnetic activity at the poles of the Sun (Kneer).

Sailer, Markus: High spatial resolution for solar observations with Multi Conjugated Adaptive Optics and Speckle reconstruction (Kneer).

Sánchez-Andrade Nuño, Bruno: Observations, analysis and interpretation with non-LTE of chromospheric structures on the Sun (Kneer).

Technische Universität Braunschweig:

Bößwetter, Alexander: Solar wind - Mars interaction (Motschmann).

von Borstel, Ingo: Dust-dust interaction processes studied in dense aerosols using a paul trap (Blum).

Constantinescu, Dragos Ovidiu: Magnetic mirror structures in the terrestrial magnetosphere (Glassmeier).

Grießmeier, Jean-Mathias: Exomagnetospheres and their interaction with the stellar wind (Motschmann).

Kleindienst, Gero: ULF waves in the Kronian magnetosphere (Glassmeier).

Narita, Yasuhito: Low frequency waves upstream and downstream of the terrestrial bow shock (Glassmeier).

Rost, Michael: Coagulation of magnetized dust under micro-gravity in variable magnetic fields (Glassmeier).

Schäfer, Sebastian: Correlated observations of magnetohydrodynamic waves as seen by Cluster and at the ground (Glassmeier).

Simon, Sven: Solar wind interaction with magnetized and unmagnetized obstacles (Motschmann).

(D. Schmitt)

V. Rechenzentrum, Elektroniklabor, Mechanik, Haustechnik und Ausbildung/ Computer Centre, Electronic Laboratory, Mechanics, Physical Plant and Education

Rechenzentrum / Computer Centre

(I. Pardowitz und Mitarbeiter)

Neugestaltung Internetauftritt

Im Zuge der Umbenennung des Instituts wurden neben der Instituts-Broschüre, Briefkopf und Visitenkarten auch der Internetauftritt in den Jahren 2004 und 2005 erneuert. Im wesentlichen wurden für die allgemeine Struktur und das Seiten-Layout die MPG Richtlinien zur Gestaltung von Webseiten übernommen. Details der Menü-Struktur und Seitenaufteilung wurden an die Institutsbedürfnisse angepasst. Die allgemeinen Seiten sind in Deutsch und Englisch verfügbar. Die Projektseiten werden standardmäßig in Englisch aber im einheitlichen Institutsformat präsentiert.

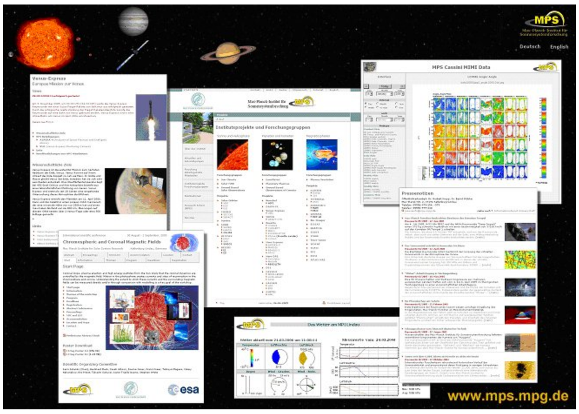

Abb. 205: Neugestaltung Internetauftritt.

Das Motto der Umgestaltung lautete: “aktuelle und lebendige Webseiten”. Die Eingangsseite präsentiert im festen Rhythmus aktuelle Meldungen, Vorträge und Pressenotizen sowie ein Monatsthema. Durch das Monatsthema wird im monatlichem Wechsel ein aktuelles wissenschaftliches Thema vorgestellt. Der Öffentlichkeit wird dabei Einblick in die aktuelle Arbeit einer Arbeitsgruppe gegeben.

Entsprechend des neuen MPS Institutskürzels wurde die Domäne “mps.mpg.de” eingeführt und die Webseiten sowie sämtliche Zugänge (E-Mail, FTP, SSH) darüber zur Verfügung gestellt.

Ausbau der Unix Rechner und Speicherkapazität

Mit den im Rahmen des MPG Grossgeräte-/EDV-Programm beantragten und bewilligten Sondermitteln wurde 2004 ein leistungsfähiges Rechnersystem zur Analyse und Visualisierung hoher Datenmengen aufgebaut.

Das Systemkonzept umfasst ein Solaris 16-Prozessor SPARC SMP-System mit 32 GByte RAM, um die hohen Rechenanforderungen der Datenauswertung abzudecken, vier Linux 4-Prozessor Systeme für rechenintensive MPI Anwendungen, zwei Linux Doppelprozessor Frontend-Rechner, und zwei Raidsysteme zur Datenspeicherung mit jeweils 2TB Kapaziät, die in die bestehende Speicherinfrastruktur integriert wurden.

Ende 2005 wurde ein weiteres Rechnersystem für das Projekt MAOAM der Planetengruppe zur Modellierung der Mars-Atmosphäre durch Bewilligung von BAR-Mitteln in Betrieb genommen. Dabei handelt es sich um drei Linux 8-Prozessor Doppelkern SMP Maschinen die für die MPI-Modellierungsprogramme mit einem Hochgeschwindigkeits-Infiniband-Switch und entsprechenden Verbindungskarten in den Knotenrechnern verbunden sind. Zur Speicherung der anfallenden Modellierungsdaten sind jeweils Raidsysteme mit 2TB Kapazität angeschlossen.

(M. Bruns, I. Pardowitz)

Ausbau der Windows Serverplatform

Eines der herausragenden Themen im MS-Windows-Umfeld betraf die Virtualisierung von Serverdiensten. Dieses im letzten Jahresbericht vorgestellte Konsolidierungskonzept wurde konsequent weiter verfolgt. Abgesehen von zwei Terminalservern wurde alte Hardware nicht wie in der Vergangenheit einfach durch neue ersetzt, sondern durch virtuelle Maschinen (VM), die auf zunächst zwei Doppelprozessor-

Maschinen (IBM x345) unter VMware ESX Server gehostet werden. Diese Farm wurde später durch eine Dell-Maschine ergänzt, die zuvor als Computerserver unter Linux im Einsatz war.

Zu den bereits Ende 2003 als VM realisierten Druck- und Webmail-Diensten kamen im Berichtszeitraum u.a. ein Domain Controller, ein File-Server, der Exchange-Server und eine weitere VM hinzu, die für die Verteilung des Virenscanners und die Authentifizierung von Benutzern zuständig ist, die sich aus dem Internet einwählen. Weiterhin ist die komplette Test- und Entwicklungsumgebung unter ESX realisiert. Insgesamt ist die ESX-Farm in der Lage ca. 20 – 25 Betriebssysteminstanzen gleichzeitig zu betreiben.

Zweiter Schwerpunkt war der Aufbau eines Speichernetzwerks (Storage Area Network, SAN), dessen Plattenspeicher von zwei IBM DS4300 mit einer Bruttokapazität von jeweils 2 TB bereitgestellt wird. Die Anbindung der Server erfolgt über zwei Fibre-Channel-Switches vom Typ Brocade Silkworm 3800. Im Vergleich zum früher üblichen direkt angeschlossenen Speicher ist ein SAN bedeutend flexibler: Neue Rechner können einfacher angeschlossen werden, und es können – entsprechende Unterstützung durch das Betriebssystem vorausgesetzt – mehrere Maschinen transparent auf die gleichen Daten zugreifen.

VMware ESX Server beispielsweise ermöglicht auf diese Weise die unterbrechungsfreie Migration einer VM von einem Host auf einen anderen. So können etwa Arbeiten an der Hardware und Software der ESX-Server ohne Beeinträchtigung des Benutzerbetriebs durchgeführt werden, und der Administrator kann die Zuordnung der virtuellen Maschinen zu den Hosts je nach Ressourcenverbrauch ebenfalls im laufenden Betrieb dynamisch anpassen.

(G. Kettmann)

Die personellen Dienstleistungen für die wissenschaftlichen Projekte spielen weiterhin neben dem Betrieb der Infrastruktur (Rechner, Netze, Peripherie) eine wichtige Rolle. Für die Projekte STARE, WIND, CELIAS und SUMER/SOHO, Ulysses, RAPID und CIS/Cluster werden regelmäßig die eingehenden Daten aufbereitet und für die weitere wissenschaftliche Analyse bereitgestellt und archiviert.

(M. Bruns, H. Michels, C. Ludwieg)

Elektroniklabor / Electronic Laboratory

(I. Pardowitz)

Die Mitarbeiter im Elektronik-Labor haben im Berichtszeitraum wieder maßgeblichen Anteil am Entstehen neuer Instrumente und der Begleitung von Instrumenten während der Flugphase gehabt. Die größten Anteile haben die Aktivitäten für die Projekte SUNRISE in der Sonnenabteilung und DAWN in der Planetenabteilung gespielt. Bei beiden Projekten hat das Institut die Systemführerschaft übernommen und ist mit wesentlichen Beiträgen beteiligt.

Daneben hat die Fertigstellung von Komponenten für HIFI, SOFIA und der VMC-Kamera sowie die Betreuung während der Flugphase von SIR und der Rosetta-Instrumente zusammen einen vergleichbar großen Anteil der personellen Dienstleistungen des Labors ausgemacht. Auch sind Arbeiten zur Vorbereitung von neuen Instrumenten wie SIR-2 auf der indischen Mission Chandraayan und den Beteiligungen an NPA und MMO für BepiColombo angelaufen.

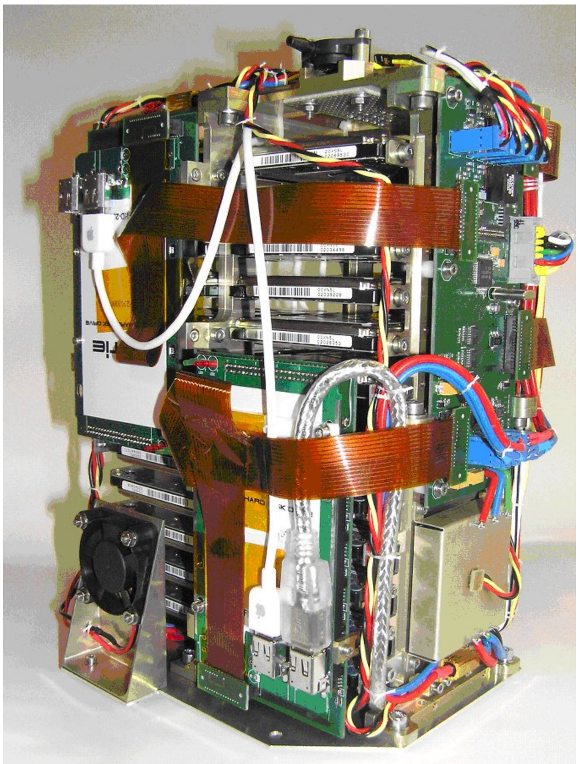

Abb. 206: Plattenstapel des SUNRISE Data Storage Subsystems.

Data Storage Subsystem für SUNRISE

Das Data Storage Subsystem (Abb. 206) für das ballongetragene Sonnenteleskop SUNRISE ist im Institut gebaut worden. Es hat eine Kapazität von 2,4 TB und dient während der Flugphase als onboard Datenspeicher. Dies ist notwendig, da die Datenleitung zum Boden bei weitem nicht ausreicht um die hohe Datenrate, die die hochauflösenden Instrumente liefern, zur Erde zu senden. Dieser Datenspeicher muss auf der einen Seite eine hohe Kapazität haben, auf der anderen Seite muss es unter den speziellen Bedingungen eines Stratosphären-Ballonfluges mit seinen speziellen Druck-, Temperatur-, Gewichts- und elektrischen Leistungsanforderungen genügen. Mit einem Gesamtgewicht von 8,6 kg, einem Verbrauch von 14 W und der Möglichkeit bei einem Druck zwischen 0 und 2000 hPa und bei Umgebungstemperaturen von -20 bis +40°C zu arbeiten wurde ein sehr guter Kompromiss zwischen den verschiedenen Anforderungen gefunden.

(G. Tomasch)

DAWN Power Conversion Unit

Das Institut lieferte für die NASA Mission DAWN die zwei Framing Cameras, die sowohl Navigationszwecken als auch wissenschaftlichen Zwecken dienen sollen. Entsprechend waren die Anforderungen an die Qualität und Zuverlässigkeit der gebauten Komponenten sehr hoch. Insbesondere an die vom Institut beigestellte Power Conversion Unit wurden extrem hohe Sicherheitsanforderungen gestellt.

Das Main-Board (Abb. 207) enthält verschiedene Filter, diskret aufgebaute Step-Down Regulatoren, mehrere Fold-Back Current Limitter sowie die Housekeeping Data Aquisition.

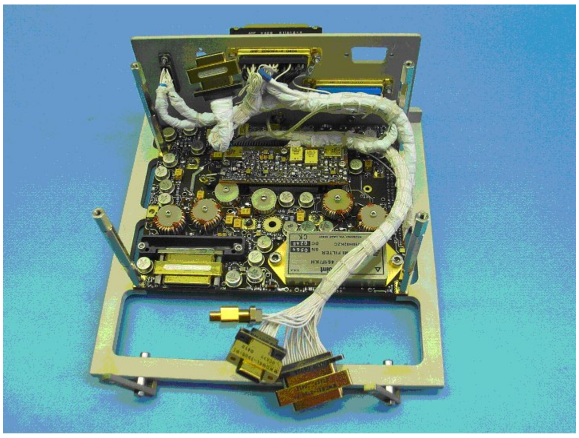

Abb. 207: Main-Board der DAWN-FC Power Conversion Unit.

Im Zentrum der Top-Side (siehe Abb. 207) sieht man ein zusätzliches Piggyback-Board, welches aus Platzgründen eingeführt wurde. Es enthält 6 elektronische Schalter für externe Heizer, Mechanismen und Kalibrationslampen mit 2 separaten Fold-Back Current Limittern.

Das Piggyback-Board wird über eine 30 polige MIL-Strip Leiste mit dem Main-Board verbunden.

Die DC/DC Converter wurden auf einem Aluminium U-Profil befestigt, welches direkt mit der Wand der E-Box verschraubt wird, um eine möglichst gute Wärmeableitung zu erreichen.

Im Inneren des U-Profils befinden sich zwei weitere Boards mit den notwendigen Common-Mode Filtern.

(R. Enge)

24 Jahre CCD-Labor am MPAE – ein Rückblick

Im Jahre 1980 wurde die Entscheidung getroffen: Eine Kamera zum Kometen Halley sollte gebaut werden, um von der Giotto-Sonde aus, dem ersten interplanetaren Projekt der ESA, unter anderem die Existenz eines Kometenkerns nachzuweisen. Der Vorschlag hierfür war von einer vorwiegend europäischen Gruppe von Wissenschaftlern unter der Leitung von H. U. Keller am MPAE erarbeitet worden.

In jener Zeit waren gerade die ersten brauchbaren elektronischen (CCD-) Bildaufnehmer verfügbar, die fast ausschließlich von Astronomen eingesetzt wurden. Diese Detektoren sollten für die Halley Multicolour Camera (HMC) eingesetzt werden.

Das CCD-Labor wurde am MPAE gegründet. Hier wurde die Elektronik für den Betrieb der Detektoren entwickelt und gefertigt. Es stellte sich bald heraus, dass jeder CCD individuell verschiedene Eigenschaften hatte. Die bestgeeigneten Detektoren wurden ausgewählt und die zugehörige Elektronik musste exakt auf den jeweiligen Detektor abgestimmt werden. Umfangreiche Messungen waren erforderlich. Als drittes Aufgabenpaket kamen die Daten- und schließlich auch die Bildverarbeitung hinzu.

1. Die erste Bildaufnehmer-Generation

Nach eingehenden Untersuchungen wurde für HMC ein CCD von Texas Instruments mit 392x584 Bildpunkten ausgewählt (Abb. 208). Dieser Detektor musste für unsere Anwendung freilich weiterentwickelt werden, um die Empfindlichkeit und die Dynamik zu verbessern, aber auch, um ihn für die Raumfahrtanwendung zu qualifizieren. Texas Instruments fertigte übrigens in dieser Zeit auch die CCDs für das Hubble Space Telescope; wir waren offensichtlich an der richtigen Adresse.

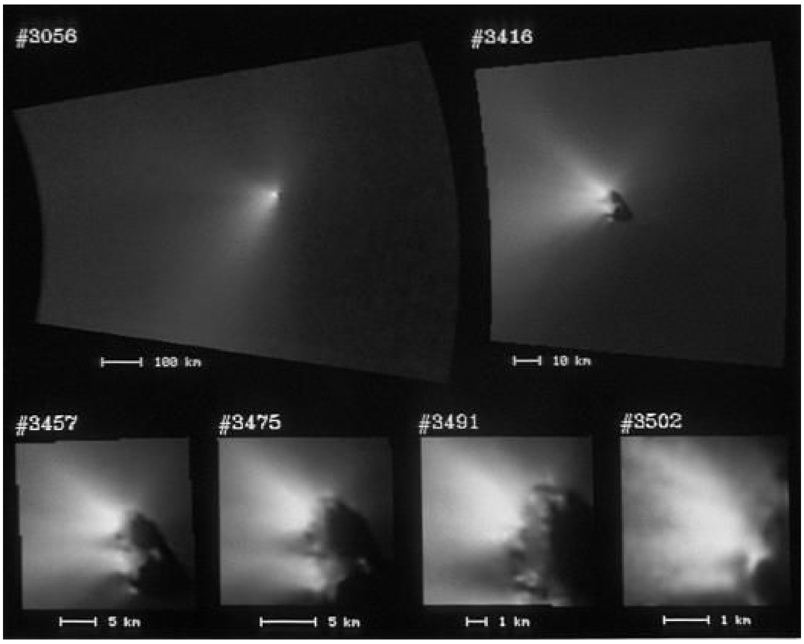

Abb. 209: Sechs Bilder des Halleyschen Kometen / *Selection of six images of comet Halley*.

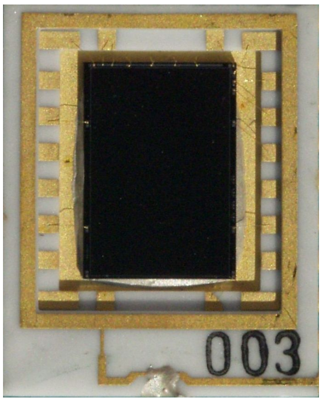

Abb. 208: HMC Max-Planck CCD / *HMC Max-Planck CCD detector*.

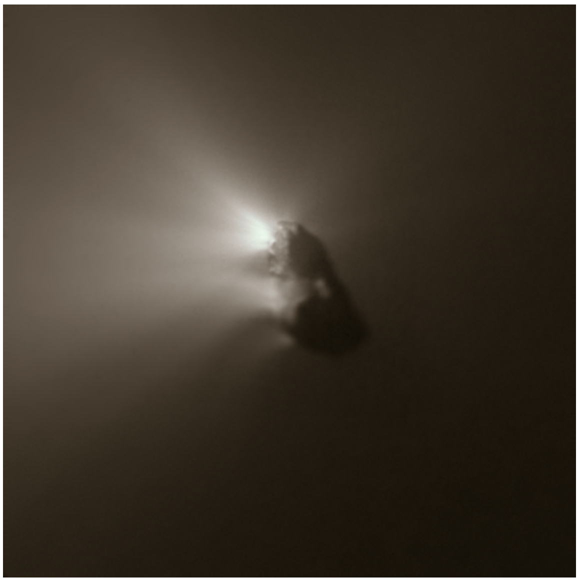

Abb. 210: Unser ‘bestes’ Bild des Kometenkerns / *Our ‘best’ image of the nucleus of comet Halley*.

Für HMC musste eine besondere Bildaufnahmetechnik entwickelt werden, um von einer rotierenden Plattform aus (1 Umdrehung in 4 s) scharfe Bilder aufnehmen zu können. Extrem kurze Belichtungszeiten bis zu 60 μs waren dazu erforderlich. Insgesamt wurden 2 CCDs eingesetzt, wobei jeder CCD in zwei getrennte Hälften geteilt war. Damit erhielten wir 4 voneinander unabhängige Bildaufnehmer, die zum Teil mit feststehenden Spektralfiltern oder einem Filterrad versehen waren.

Giotto wurde 1985 gestartet und erreichte den Kometen Halley planmäßig am 13. März 1986. HMC arbeitete perfekt und nahm innerhalb von gut zwei Stunden mehr als 2000 Bilder auf. Wegen der stark begrenzten Datenrate (100 kbit/s) konnten in der letzten Phase nur noch Teilbilder (74x74 Bildpunkte) übertragen werden. Abb. 209 zeigt 6 ausgewählte Bilder, wobei das erste Bild aus 100 000 km Entfernung zum ersten Mal den Kern eines Kometen zeigt. Abb. 210 ist unser ‘bestes’ Bild, das aus den letzten 70 Aufnahmen mit der höchsten Auflösung zusammengesetzt worden ist.

Mit HMC sind zum ersten Mal in der westlichen Welt CCDs für eine hochauflösende Kamera im Weltraum für wissenschaftliche Beobachtungen eingesetzt worden.

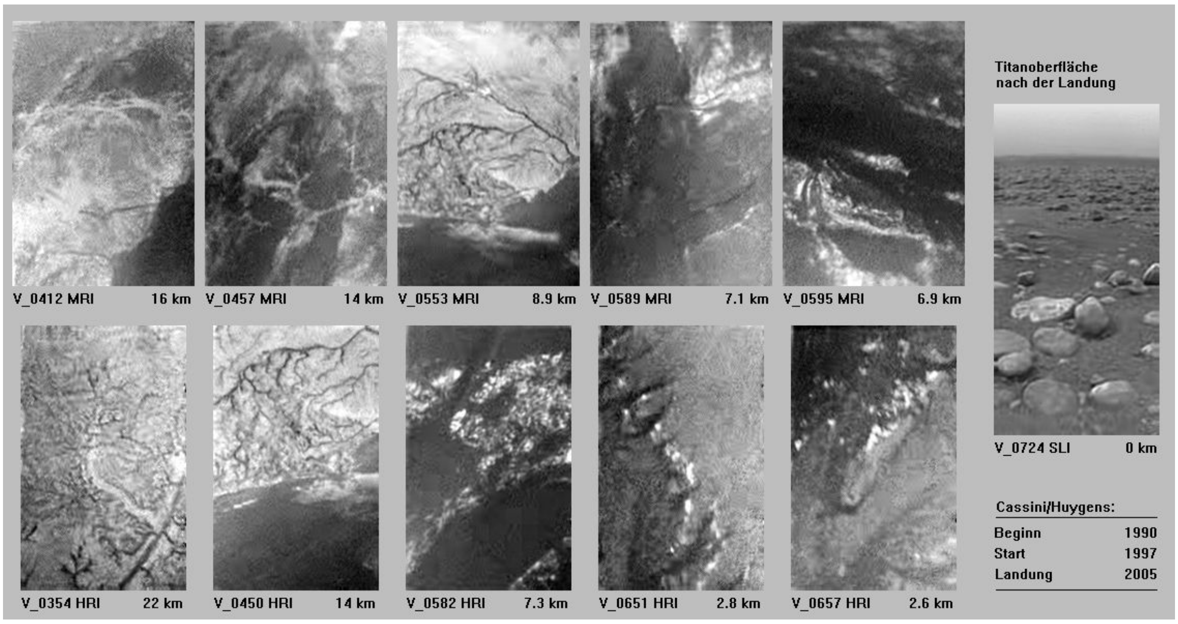

Abb. 212: Auswahl von DISR-Bildern vom Titan während des Abstiegs und nach der Landung / *Selection of DISR images from Titan taken during the descent and after landing*.

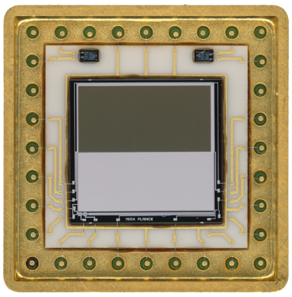

Abb. 211: DISR Max-Planck CCD / *DISR Max-Planck CCD*.

2. Die zweite CCD-Bildaufnehmer-Generation

Nach dem großen Erfolg mit HMC wurde unser Institut 1990 von einem Konsortium der University of Arizona angesprochen, die Bildaufnahmetechnik für die Descent Imager/Spectral Radiometer (DISR)-Kamera beizusteuern. Diese Kamera sollte 1997 mit der Cassini/Huygens-Sonde zum Saturn gestartet werden und 7 Jahre später auf dem Mond Titan landen, um dessen verhüllte Oberfläche zu erforschen.

Die amerikanische DISR-Kamera ist ein komplexes Instrument. Insgesamt 9 optische Pfade werden mit einem Glasfiber-Bündel auf einen CCD projiziert, um ein Minimum an Verlustleistung und Gewicht zu erreichen. Wegen der extrem hohen Kosten für die gesamte Mission und der langen Anreisezeit waren außerordentlich hohe Auflagen der NASA für die Funktionssicherheit zu erfüllen.

Ein neuer CCD wurde gebraucht. Die Wahl für die Entwicklung des Detektors fiel diesmal auf die Firma Loral in Kalifornien. Hier trafen wir wiederum auf unsere Kollegen von der NASA, die sich gerade die zweite Detektor-Generation für das Hubble Space Telescope fertigen ließen.

Der Loral Max-Planck-CCD (Abb. 211) hatte 512x256 aktive Bildpunkte und ebenso viele Bildspeicherpunkte und war speziell für das DISR-Instrument mit der begrenzten Datenrate ausgelegt. Eine eingebaute elektronische Verschluss-Funktion erübrigte den Einsatz eines störanfälligen mechanischen Verschlusses. Der CCD konnte bei Temperaturen bis -120°C betrieben werden, während die Elektronik einen halben Meter entfernt in einem beheizten Gehäuse untergebracht war. Die Entwicklung unseres CCDs war mit einigen Schwierigkeiten verbunden; insgesamt haben wir 10 Anläufe begleitet, bis die gewünschte Perfektion erreicht war.

Der Abstieg durch die Titanatmosphäre am 14. Januar 2005 verlief planmäßig. DISR konnte neben 600 Bildern eine große Anzahl von Spektren und anderen Daten übertragen. Obwohl ein vergleichbar großer Datensatz durch eine fehlerhafte Initiierung bei Cassini verloren ging, war das Projekt insgesamt ein voller Erfolg. Abb. 212 zeigt eine Auswahl von den gewonnenen Bildern aus drei verschiedenen Kamerasystemen.

1993, ein Jahr vor der Abgabe der DISR-Elektronik, kam es zu einer weiteren Beteiligung an einem Projekt mit der University of Arizona. Eine andere Gruppe hatte dort herausgefunden, dass die DISR-Bildaufnahmetechnik auch bestens für ihre geplante Mars-Stereo-Kamera (Imager for Mars Pathfinder, IMP) geeignet war. Unsere Technik war in der Lage, den CCD oben auf dem Mast (Abb. 213) über eine Kabellänge von knapp 5 m ohne Einschränkung zu bedienen. Obwohl dieses Projekt bei uns parallel zu DISR 'quasi nebenbei' abgewickelt werden musste, erwies es sich als außerordentlich erfolgreich und erfuhr nach der Landung im Jahre 1997 weltweit eine große Beachtung. Die Kamera funktionierte 3 Monate lang ohne Probleme und nahm insgesamt fast 20 000 Bilder und wissenschaftliche Daten auf. Abb. 214 zeigt das erste farbige Bild, das bereits am Abend nach der Landung veröffentlicht wurde.

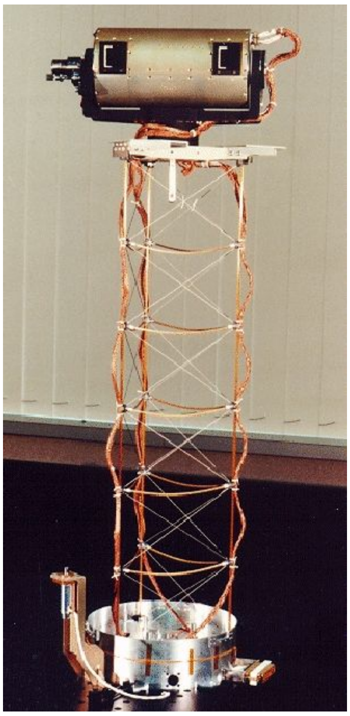

Abb. 213: Die Mars Pathfinder Camera / *The imager for Mars Pathfinder (IMP)*.

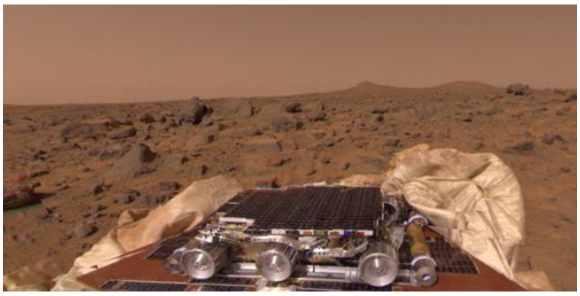

Abb. 214: Das erste Bild der Pathfinder Kamera / *The very first IMP image*.

Das CCD-Labor, in dem zwischenzeitlich bis zu 4 Mitarbeiter gearbeitet hatten, schrumpfte nun wieder auf 2 Mitarbeiter zusammen. Dennoch war es in der Lage, zwei weitere Projekte mit Kameratechnik auf

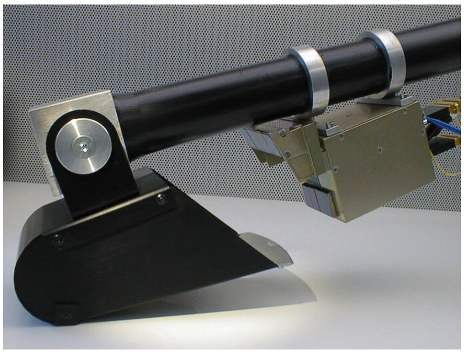

Abb. 215: Robotic Arm Camera für Polar Lander / *The Robotic Arm Camera for Polar Lander*.

der Basis des DISR-CCDs auszurüsten. 1997 wurde ein Doppelkamerasystem mit einem Leistungsbedarf von 1,2 Watt für das Mars Polar Lander-Projekt entwickelt. Ein CCD war dabei in der Robotic Arm Camera (RAC) eingebaut, die hier im Hause von H. Hartwig entwickelt worden war, während der zweite CCD wiederum für eine Stereokamera eingesetzt wurde. Abb. 215 zeigt ein Bild der RAC mit der Schaufel, die Bodenproben aus bis zu 50 cm Tiefe herausheben konnte. Mit Hilfe von spektraler Beleuchtung war die RAC in der Lage, die Bodenproben insbesondere auch auf Wasseranteile zu untersuchen. Bedauerlicherweise ist die Mission wegen eines Fehlers im Steuerprogramm der Sonde gescheitert.

1998 wurde schließlich in einer weiteren Zusammenarbeit mit der University of Arizona ein Bildaufnahmesystem für zwei Kameras des Mars Surveyor-Projekts gefertigt. Das Projekt wird nun aber erst 2007 unter dem Namen Phoenix eingesetzt.

3. Die dritte CCD-Bildaufnehmer-Generation

Ende der 90er Jahre hatte sich wiederum ein europäisches Konsortium unter der Leitung von H. U. Keller mit einem Vorschlag für eine Kamera zu einem Kometen im Rahmen des Rosetta-Projektes der ESA durchgesetzt. Das neue System besteht aus einer Weitwinkelkamera und aus einer hochauflösenden Kamera, die unabhängig voneinander betrieben werden können.

Die Technik war inzwischen fortgeschritten; im Instrument war nun ausreichend Speicherplatz vorhanden. Neue, wesentlich größere CCDs mit 2048x2048 Bildpunkten konnten damit eingesetzt werden. Die Herstellung der Detektoren wurde einer englischen Firma, E2V, übertragen. Die CCDs wurden für OSIRIS weiterentwickelt und bekamen einen besonderen Schutz gegen Überbelichtung, der es ermöglicht, auch dunkle Bereiche des Kometenkerns aufzunehmen, während andere Bildbereiche überbelichtet sind.

Abb. 216 zeigt einen OSIRIS Max-Planck CCD in seinem Transportgehäuse.

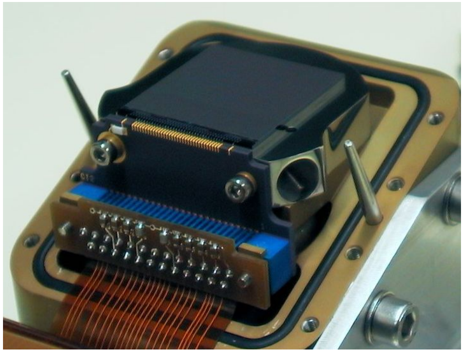

Abb. 216: Der OSIRIS CCD / *The OSIRIS CCD*.

Beide Kamerasysteme haben einen sehr hohen Dynamikbereich und sind für eine Reihe von Alternativen bei der Bildaufnahme eingerichtet. Die Sonde wurde im Jahre 2004 gestartet und wird den Kometen 67P/Churyumov-Gerasimenko erst 2014 erreichen. Während der Anreise werden die Kameras wiederholt getestet. Abb. 217 zeigt eine Aufnahme des Orion M42-Nebels.

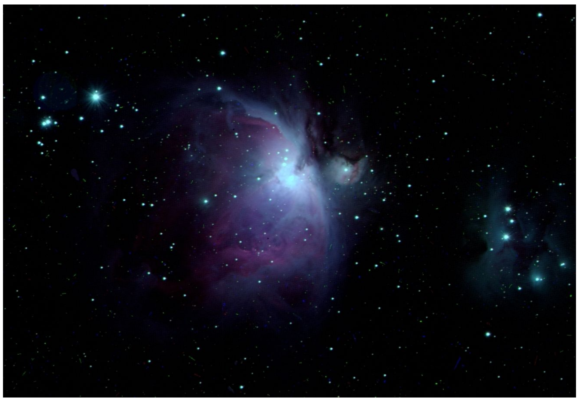

Abb. 217: Sternennebel M42 in einer Aufnahme von OSIRIS / *Orion Nebula (M42) seen by OSIRIS*.

4. Missionsbeteiligungen

Für folgende Missionen sind jeweils ein oder zwei CCD-Bildaufnehmer bereitgestellt worden:

1. ESA Giotto Mission, 1985/86, Vorbeiflug am Kometen Halley, Halley Multicolour Camera.
2. NASA/ESA Cassini/Huygens Mission zum Saturnsystem, 1997/2005, DISR auf der Huygens Probe; Landung im Januar 2005.
3. NASA Mars Pathfinder, 1996/97, Landung auf dem Mars, Imager for Mars Pathfinder (IMP).
4. NASA Mars Polar Lander, 1999, Robotic Arm Camera und Stereo Imager.
5. ESA Rosetta Mission, 2004, Rendez-vous mit einem Kometen im Jahr 2014, OSIRIS Tele- und Weitwinkelkamera.
6. NASA Phoenix Mission, 2007, Landung auf dem Mars, Robotic Arm Camera und Microscope.

5. Zusammenfassung

Zur Gründung des CCD-Labors kam es eigentlich nur deshalb, weil sich die Amerikaner aus der zunächst gemeinsam geplanten Mission zum Kometen Halley zurückgezogen hatten und das Feld damit den Europäern überließen. In der Anfangsphase haben wir die hilfreichen Gespräche mit erfahrenen Kollegen aus der Astronomie in Amerika und England gern entgegengenommen, um uns gezielt in dieses Gebiet einarbeiten zu können.

In 24 Jahren wurden im CCD-Labor insgesamt 50 CCD-Kamerasysteme gebaut, neben 12 Flugeinheiten auch die entsprechenden Ingenieur- und Testeinheiten. Es wurden dafür etwa 10 verschiedene Hybridschaltkreise entwickelt. Mit unseren Testeinrichtungen konnten wir alle entscheidenden Eigenschaften der CCDs erfassen. Da wir bei unseren Aufträgen immer mit den Entwicklungsabteilungen der Hersteller verbunden waren, waren wir stets in der Lage, unsere Ergebnisse auf höchster Ebene zu diskutieren. In mehreren Fällen hat das schließlich zu einer technologischen Weiterentwicklung bei den Herstellern geführt.

Bei der Kalibrierung und Auswertung der Daten aus unseren Kameras hat sich immer wieder gezeigt, wie vorteilhaft es ist, wenn die Bildaufnahmetechnik aus dem eigenen Hause kam und uns damit bis ins Detail bekannt war. Mit den Beteiligungen an den amerikanischen Projekten hat sich dem Institut mit verhältnismäßig geringem Aufwand der uneingeschränkte Zugang zu aktuellen Forschungsbereichen eröffnet.

Jeder CCD hatte bei uns im Labor einen numerischen Namen bekommen. Der letzte CCD mit der Nummer #244 wurde für OSIRIS eingesetzt. Mit dem Abschluss der Arbeiten für die OSIRIS-Kamera und der gleichzeitigen Umgestaltung des Instituts war es mit der verbliebenen personellen Ausstattung im CCD-Labor nicht mehr möglich, weitere Projekte zu übernehmen.

(J. R. Kramm)

Abteilung Mechanik / Department mechanics

(B. Chares)

Zu der Abteilung Mechanik gehören die Konstruktion, die Feinmechanik, die Schlosserei, der Siebdruck, bis zum Ende des Jahres 2004 die Galvanik und die Lehrwerkstatt für die Ausbildungsberufe im Industriemechaniker- und Metallbauerbereich.

Die Beteiligung unseres Institutes an mehreren laufenden oder geplanten Missionen beinhaltet auch die Entwicklung, den Bau und Test von Instrumenten oder Teilen davon. Neben direkten Missionsbeteiligungen werden Zuarbeiten für Missionsunterhaltungen, Laborexperimente und Testreihen abgedeckt. Weiterhin wird der Bereich zu Reparatur- und Instandsetzungsarbeiten heran geführt. Für die Jahre 2004 und 2005 können folgende Schwerpunkte genannt werden:

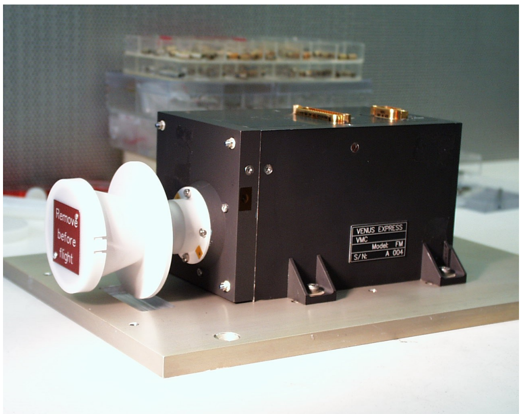

Abb. 218: Flugmodell VMC / *Flight model VMC*

Konstruktion

Unsere Konstruktionsabteilung, im Berichtszeitraum aus 5 Voll- und Teilzeitmitarbeitern bestehend, entwickelt und konstruiert mit moderner 3D-CAD Software in enger Zusammenarbeit mit den Wissenschaftlern mechanische Komponenten für laufende Projekte. Die mechanisch-konstruktive Betreuung unserer laufenden und zukünftigen Projekte gehört ebenso zur Abteilung wie die Erstellung von Graphiken für wissenschaftliche Veröffentlichungen.

Feinmechanik

In der Feinmechanik-Werkstatt wurden für ca. 18 verschiedene Experimente bzw. Missionen mechanische Arbeiten geleistet. Davon sind SUNRISE, DAWN, VMC, STEREO-SECCHI und HIFI schwerpunktmäßig zu nennen.

VMC ist mit dem erfolgreichen Start von VenusExpress im November 2005 ein großer Erfolg auch für unsere Feinmechanik-Werkstatt (Abb. 218).

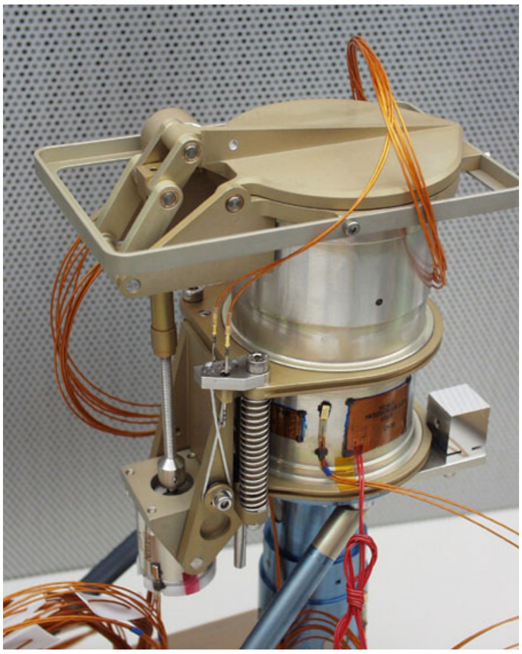

Abb. 219: DAWN Türmechanismus / *DAWN door mechanism*

Die DAWN-Kameras sind mit großer mechanischer Beteiligung aus unserer Institutswerkstatt fertig gestellt und teilweise geliefert.

Bei STEREO-SECCHI wurden Einzelteile für einen komplexen Türmechanismus gefertigt (Abb. 220).

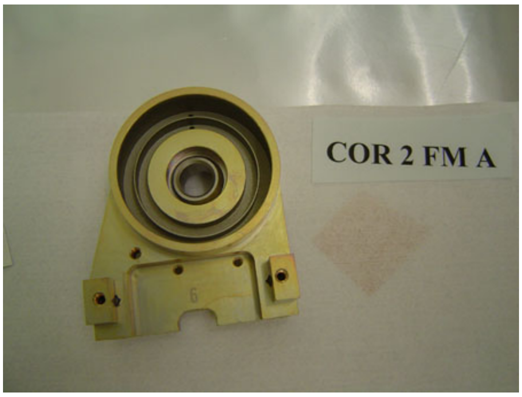

Abb. 220: Mechanisches Bauteil des SECCHI-Türmechanismus / *Mechanical part of SECCHI door mechanism*

Für sämtliche mechanische Arbeiten stehen den Mitarbeitern der Feinmechanik-Werkstatt konventionelle Bearbeitungsmaschinen sowie CNC-gesteuerte Dreh- und Fräsmaschinen zur Verfügung. Außerdem verfügt die Feinmechanik-Werkstatt über eine Erodiermaschine, mit der im Senkerodierverfahren Oberflächenstrukturen erzeugt werden können. Über eine 3D-

Messmaschine kann die Maßhaltigkeit und Qualität der Fertigung verifiziert und protokolliert werden.

Galvanik/Siebdruck

Die bis zum Ende des Jahres 2004 betriebene Galvanik war für Arbeiten in der Oberflächenveredelung tätig. Bei unseren speziellen Anforderungen handelte es sich in der Hauptsache um Funktionsbeschichtungen auf hochfesten Aluminiumknetlegierungen. Dabei ging es um spezielle elektrische oder mechanische Anforderungen an die Beschichtung. So kamen Gelbchromatieren, Vergolden, Verkupfern, Vernickeln oder Eloxieren bzw. Kombinationen der einzelnen Verfahren zum tragen (Abb. 221)

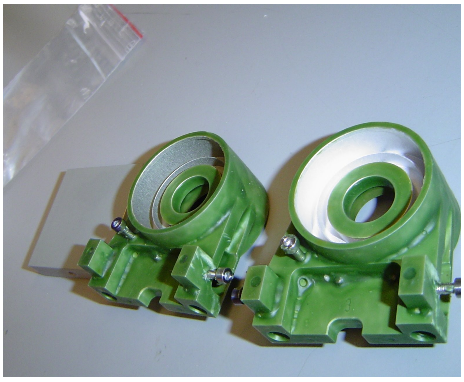

Abb. 221: Abdecklack zur Galvanikvorbereitung / *Peelable wax resist for surface treatment*

Zum derzeitigen Aufgabengebiet der Galvanik gehört auch die Herstellung von Leiterplatten, die im Ätzverfahren hergestellt werden. Zur Verfügung steht weiterhin eine Vakuum-Bedampfungsanlage für Kleinteile, mit der Beschichtungen in Gold, Silber, Aluminium, Kupfer, Chrom oder Nickel auf diverse Materialien vorgenommen werden können.

Ebenfalls in diesem Bereich steht ein Bearbeitungslaser zur Verfügung, der für Beschriftungen, Gravuren oder Zuschnitte dünner Materialien genutzt wird. Auch zum Bearbeiten von speziellen Materialien wie Keramiken wird dieser Laser verwendet.

Schlosserei

Die Aufgabe der Mitarbeiter in der Schlosserei umfassen neben den Wartungs- und Reparaturarbeiten an unseren Großgeräten auch Spezialanfertigungen für wissenschaftliche Projekte. Zu dem Wartungs- und Reparaturbereich gehören sämtliche Vakuumanlagen inklusive Peripherie. Für das Projekt SUNRISE wurde z.B. ein Transport- und Handhabungsgerät gebaut. Ebenfalls für SUNRISE wurden Hilfsgestelle für das Elektroniklabor bereitgestellt, die komfortablere Verdrahtungsarbeiten ermöglichen.

Verwaltung – Teilbereich Haustechnik / Administration – Department Physical plant

(A. Poprawa)

Die Haustechnik gehörte bis September 2005 zur Werkstatt und wurde mit dem altersbedingten Ausscheiden des Werkstattleiters der Verwaltung angegliedert.

Waren noch 2004 insgesamt 23 Mitarbeiter verschiedener Handwerksberufe beschäftigt, so waren es Ende 2005 nur noch 15. Hier zeigen sich auch die Auswirkungen des Sozialplans. Um so erfreulicher ist es, daß trotzdem ein junger Kollege unbefristet angestellt werden konnte.

Neben den traditionellen Tätigkeitsfeldern, die in jedem Institut notwendig sind, um die Infrastruktur für wissenschaftliche Forschung sicherzustellen und die bauliche Substanz zu erhalten, haben die Mitarbeiter auch bei Umbaumaßnahmen, Modellen für wissenschaftliche Experimente und der Öffentlichkeitsarbeit ihr Können unter Beweis gestellt

Besonders erwähnenswert sind hier die größeren Umbaumaßnahmen in der Kantine (Abb. 222). Hier bietet sich den Mitarbeitern jetzt ein hell und freundlich gestalteter Speisesaal und für den Nachmittagskaffee ein abgetrennter Aufenthaltsbereich. Regelmäßig finden dort Kunstausstellungen statt.

Abb. 222: Kantine / *Canteen*

Außerdem wurde das Rechenzentrum an die ständig größer werdenden Anforderung angepaßt und bietet nun mehr Gästen die Möglichkeit an den öffentlich

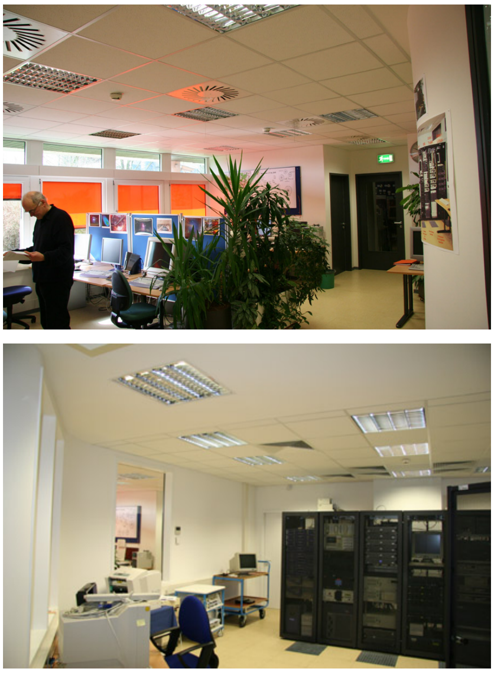

Abb. 223: Rechenzentrum / *Computer Center*

zugänglichen Stationen zu arbeiten bei gleichzeitiger Vergrößerung der Serverräume. (Abb. 223)

Die Erneuerung der Kesselanlage erfolgte zwar durch eine Fachfirma, jedoch nicht ohne umfangreiche Zuarbeiten durch die Haushandwerker wie auch bei allen anderen Maßnahmen, z.B. Niederspannungsverteiler, Brauchwasserverteilung und Klimatechnik (Abb. 224).

Abb. 224: Kesselanlage / *Domestic boiler installation*

Abb. 225: Bibliothek / *Library*

Das Laborgebäude wurde umfassend von außen betonsaniert und die alten Holzdecken wichen einer modernen Brandschutzdecke. Viele Büroräume wurden neu gestrichen, mit neuen Heizkörpern und Regalwänden ausgestattet und erhielten hohe, helle Decken erhielten (Abb. 225).

Abb. 226: Modell des Schreiner'schen Heliotrops

Eine weitere Aufgabe die in letzter Zeit verstärkt wurde ist der Modellbau für die Öffentlichkeitsarbeit. Bedingt durch die wissenschaftlichen Erfolge steigt die Nachfrage nach Ausstellungen und Führungen, und so wurden verschiedene Modelle angefertigt und im gesamten Bundesgebiet gezeigt (Abb. 226 und Abb. 227).

Abb. 227: Modell Rosetta-Orbiter

Ausbildung / Education

Rechenzentrum

Im Berichtszeitraum hat das Thema Ausbildung weiterhin eine wichtige Bedeutung eingenommen. Insgesamt haben Praktikanten im Rechenzentrum im Jahr 2004 156 und 2005 151 Praktikumswochen absolviert. Es sind teils Schüler-Praktikanten aus Haupt-, Realschulen oder Gymnasien, teils Praktikanten im Rahmen eines Fachhochschul-Studiums, die während ihres 2 bis 22 Wochen langen Aufenthalts im Institut allgemein den Betriebsalltag in einem Rechenzentrum kennen lernen oder anhand von konkreten Projekten praktische Erfahrungen für ihren späteren Beruf erwerben.
Seit dem Jahre 2002 wurde im Rechenzentrum ein Ausbildungsplatz zum Fachinformatiker für Systemintegration eingerichtet. Im Herbst 2003 hat der erste Jugendliche im Rechenzentrum seine 3-jährige Ausbildung begonnen. 2005 wurde ein weiterer Ausbildungsplatz zum Fachinformatiker geschaffen und ein zweiter Jugendlicher hat seine Arbeit aufgenommen.
(G. Monecke)

Elektroniklabor

In der Elektronik Lehrwerkstatt lernen zurzeit vier Elektroniker für Geräte und Systeme. Weiterhin werden noch zwei Industrieelektroniker Gerätetechnik ausgebildet. 2004 waren es zwei Elektroniker für Geräte und Systeme und fünf Industrieelektroniker. Im Jahr 2004 und 2005 haben je drei Industrieelektroniker ihre Gesellenprüfung mit gutem Erfolg bestanden.
(O. Matuschek)

Mechanik

In der Feinmechanik-Werkstatt und der Schlosserei am MPS wurden in den Jahren 2004 und 2005 bis zu 16 Lehrlinge gleichzeitig in den Berufen Industriemechaniker oder Metallbauer ausgebildet. Für beide Lehrberufe bestehen Lehrwerkstätten für die je ein Meister zuständig ist. Den Auszubildenden stehen sowohl herkömmliche Bearbeitungsmaschinen als auch CNC-gesteuerte Maschinen zur Verfügung und sie erhalten Grundkenntnisse in allen ihrem Berufsbild entsprechenden gängigen Metallbearbeitungsverfahren. Außerdem haben in dem Berichtszeitraum 34 Schülerpraktikanten und 5 Hochschulpraktikanten bei uns ein Praktikum absolviert.
Vor der Industrie- und Handelskammer haben folgende Mitarbeiter ihre Facharbeiterprüfung erfolgreich bestanden:
Industriemechaniker: Christian Biermann, Simon Geile, Sven Krenauer, Sebastian Poppe, Philipp Haut.
(B. Chares)

Haustechnik und Verwaltung

Im Bereich der Verwaltung wurden im Jahr 2004 insgesamt 4 Lehrlinge ausgebildet, davon 3 Kauffrauen für Bürokommunikation und ein Elektroniker für Energie- und Gebäudetechnik. Eine Kauffrau wurde wegen besonderer Leistungen in ein unbefristetes Arbeitsverhältnis übernommen.
Im Jahr 2005 wurden 5 Lehrlinge ausgebildet, davon 4 Kaufleute für Bürokommunikation und 1 Elektroniker für Energie- und Gebäudetechnik.
Hervorzuheben ist, daß wir besonderes Augenmerk auf die Integration behinderter Menschen legen und mit Hilfe des Arbeitsamtes einen behindertengerechten Ausbildungsplatz geschaffen haben und auch eine Kauffrau ausbilden.
(A. Poprawa)

VI. Personelle Gliederung / Personnel

Kollegium, wissenschaftliche Mitglieder / Board of directors, scientific members

Prof. Dr. Ulrich R. Christensen
(Geschäftsführender Direktor/Managing director)
Dr. Helmut Rosenbauer (bis 30.06.2004)
Prof. Dr. Sami K. Solanki
Prof. Dr. Vytenis M. Vasyliūnas

Leiter der Selbständigen Nachwuchsgruppe Helio- und Asteroseismologie /Head, Independent Junior Research Group of the Max Planck Society "Helio- and Asteroseismology":

Dr. Laurent Gizon

Emeritierte wissenschaftliche Mitglieder/Emeritus scientific members:

Prof. Sir Ian Axford, FRS
Prof. Dr. Tor Hagfors
Dr. Helmut Rosenbauer

Auswärtige wissenschaftliche Mitglieder/External scientific members:

Prof. Dr. Albert A. Galeev, Moskau
Prof. Dr. Johannes Geiss, Universität Bern
Prof. Dr. Karl-Heinz Glaßmeier, Technische Universität Braunschweig
Prof. Dr. Erwin Schopper, Bad Soden

Technischer Geschäftsführer/Technical Manager: Dr. Iancu Pardowitz

Wissenschaftliche und wissenschaftlich-technische Mitarbeiter/Scientific staff

Dr. Klaus-Michael Aye
Dr. Peter Barthol
Dipl.-Ing. Hartmut Bitterlich (bis 31.03.05)
Dr. Thomas Blümchen (bis 30.09.04)
Dr. Hermann Böhnhardt
Dipl.-Phys. Peter Börner (bis 31.12.05)
Dr. Reinhard Borchers (bis 31.08.05)
Dr. Volker Bothmer (bis 31.12.04)
Dr. habil. Jörg Büchner
Dr. Robert Cameron
Dr. Werner Curdt
Dr. Patrick W. Daly
Prof. Dr. Eduard Dubinin
Dr. Markus Fränz
Dr. Achim Gandorfer
Dr. Maya Garcia-Comas
Dr. Fred Goesmann
Dr. Walter Götz
Dr. Björn Grieger
Dr. Yevgen Grynko (bis 31.12.05)
Pablo Gutierrez-Marques
Dr. Paul Hartogh
Dipl.-Phys. Hermann Hartwig
Dr. Istvan Hejja (bis 28.02.05)
Dr. Martin Hilchenbach
Dr. Johann Hirzberger
Dr. Nico Hoekzema
Dr. Stubbe Hviid
Dr. Bernd Inhester
Dr. Christopher Jarchow
Prof. Dr. Klaus Jockers (bis 31.08.05)
Dr. Geraint Jones
Dr. habil. Horst Uwe Keller
Dr. Georg Kettmann
Dr. Jochen Kissel
Dr. Jens Kleimann
Dr. Jürgen Klostermeyer (bis 31.03.04)
Christian Koch
Dr. Andreas Kopp (bis 30.09.04)
Dr. Axel Korth
Dr. Jörg-Rainer Kramm
Dr. Natalie Krivova
Dr. Harald Krüger
Dr. Norbert Krupp
Dr. Michael Küppers
Dr. Andreas Lagg

Dr. Urs Mall
Dr. Wojcieck Markiewicz
Dr. Davina Markiewicz-Innes
Prof. Dr. Eckart Marsch
Dr. Alexandre Medvedev
Dr. Claudia-Veronika Meister (bis 14.04.04)
Dipl.-Math. Helmut Michels
Dr. Stefan Mühlbachler
Dr. Andreas Nathues
Dr. Erling Nielsen (bis 30.11.05)
Dr. Bernd Nikutowski
Dr. Iancu Pardowitz
Dipl.-Ing. Borut Podlipnik
Dr. Michael Richards (bis 30.11.05)
Dr. Arne K. Richter
Dr. Reinhard Roll
Dr. Markus Roth
Dr. Jon Rotvig
Prof. Dr. Konrad Sauer (bis 31.03.05)
Dr. Dieter Schmitt
Dr. Klaus Schneider (bis 31.08.05)
Dr. Udo Schühle
Prof. Dr. Manfred Schüssler
Prof. Dr. Rainer Schwenn
Dipl.-Phys. Ilse Sebastian (bis 31.12.05)
Dr. Holger Sierks
Dr. Iouri Skorov
Dipl.-Ing. Li Song
Dipl.-Ing. Istvan Szemerey
Dr. Luca Teriaca
Dr. Hellmuth Timpl
Dr. Dmitri Titov
Dipl.-Ing. Georg Tomasch
Dr. Stefan Werner (bis 30.04.04)
Dr. Johannes Wicht
Dr. Thomas Wiegelmann
Dr. Joachim Woch
Dr. Bernd Wöbke
Dr. Ursula Wüllner (bis 28.02.05)

Wissenschaftliche Stipendiaten/Postdocs

Dr. Julien Aubert (bis 31.08.04)
Dr. Regina Aznar Cuadrado
Dr. Ingo Baumann (bis 31.08.05)
Dr. Denis Belyaev (bis 26.05.05)
Dr. Juan Manuel Borrero Santiago (bis 30.11.04)
Dr. Maria Hebe Cremades Fernández (bis 18.10.05)
Dr. Borys Dabrowski
Dr. Rene Damian Duffard
Dr. Nina Elkina (bis 31.12.05)
Dr. Alberto Flandes (bis 02.08.05)
Dr. Fernando Luis Guarnieri (bis 11.07.05)
Dr. Michael Heuer
Dr. Ai Inada (bis 31.12.04)
Dr. Yuichi Ito
Dr. Jason Jackiewicz
Dr. Maxim Kramar
Dr. Hans-Günter Ludwig (bis 31.12.04)
Dr. Maria Madjarska (bis 31.10.04)
Dr. Rupali Mahajan
Dr. Marilena Mierla (bis 31.10.05)
Dr. Ana Teresa Monteiro Tomas (bis 31.12.05)
Dr. Anuschka Pauluhn (bis 29.02.04)
Dr. Pascal Petit (bis 30.11.05)
Dr. Ganna Portyankina
Dr. Oliver Preuss
Dr. Noureddine Ben Raouafi (bis 31.01.05)
Dr. Miriam Rengel
Dr. Luciano Rodriguez (bis 24.10.05)
Dr. Martin Schrinner (bis 31.10.05)
Dr. Sergey Shelyag (bis 31.01.05)
Dr. Ilya Sillin (bis 31.12.04)
Dr. Denise Aida Tortorella (bis 30.11.05)
Dr. Durgesh Kumar Tripathi (bis 17.08.05)
Dr. Luis Vieira (bis 30.11.04)
Dr. Geronimo Villanueva (bis 31.05.05)
Dr. Christian Vocks (bis 30.09.04)
Dr. Alexander Vögler
Dr. Tongjiang Wang (bis 31.12.05)
Prof. Jingsong Wang (bis 21.12.04)
Dr. Jun Zhang (bis 31.05.04)
Dr. Hong Zou (bis 20.10.05)

Doktoranden und Diplomanden/PhD students

Aleksandra Andjic (bis 14.02.05)
Laura Antonia Balmaceda
Ingo Baumann (bis 28.02.05)
Nazaret Bello Gonzalez
Monika Buske
Zhongzhou Chen (bis 12.04.04)
Chun Ming Mark Cheung
Che-yi Chuang (bis 31.01.04)
Kerstin Cierpka (bis 03.11.05)
Maria Hebe Cremades Fernández (bis 14.04.05)
Andreas Dedner (bis 31.08.04)
Yevgen Grynko (bis 31.01.05)
Michael Heuer (bis 31.03.04)
Emre Ishik
Fedor Kolesnykov (bis 31.01.05)
Maxim Kramar (bis 31.01.05)
Elena Kronberg
Takeshi Kuroda
Jiufu Lim (bis 14.11.04)
Rupali Mahajan (bis 30.04.05)
Luca Maltagliati
Lukasz Matloch
Redouane Mecheri
Marilena Mierla (bis 30.04.05)
Richard Moissl Richard
Ana Teresa Monteiro Tomas (bis 31.01.05)
Guadalupe Muñoz Martinez (bis 07.08.05)
David Orozco Suarez (bis 30.06.04)
Lucas Paganini
Evgeny Panov
Ganna Portyankina (bis 31.01.05)
Sabine Preusse (bis 31.10.05)
Aikaterini Radioti
Luciano Rodriguez (bis 10.05.05)
Elias Roussos
Markus Sailer
Ryu Saito
Bruno Sánchez-Andrade Nuño
Jean Carlo Santos
Aveek Sarkar (bis 31.07.05)
Clementina Sasso
Martin Schrinner (bis 28.02.05)
Stefan Schröder
Andrey Seleznyov (bis 31.01.05)
Alina Semenova
Sergey Shelyag (bis 31.07.04)
Rajat Mani Thomas (bis 15.03.05)
Denise Aida Tortorella (bis 05.07.05)
Iris Traulsen (bis 28.02.05)
Durgesh Kumar Tripathi (bis 31.01.05)
Martin Tschimmel
Cecilia Tubiana
Maria Usanova (bis 31.08.05)
Esa Vilenius
Geronimo Villanueva (bis 30.11.04)
Lotfi Yelles Chaouche
Vasily Zakharov

Abteilung EDV/Computing department (Leitung/Management: Dr. Iancu Pardowitz)

Andreas Blome
Michael Bruns
Peter Fahlbusch (bis 31.01.04)
Lothar Graf
Terrance Ho
Dr. Georg Kettmann
Christine Ludwieg
Helmut Michels
Godehard Monecke
Adolf Piepenbrink
Jürgen Wallbrecht

Auszubildender/Apprentice: Alexander Forsch, Daniel Maase

Laboratorien/Laboratories(Leitung/Management: Dr. Iancu Pardowitz
Sekretariat/Secretariat: Christiane Heise

Günther Auckthun
Walter Böker
Waltherus Boogaerts (bis 30.06.05)
Ulrich Bührke
Dipl.-Ing. Irene Büttner
Eberhard-Michael Clement (bis 31.12.04)
Dipl.-Ing. Arne Dannenberg
Dipl.-Ing. Werner Deutsch
Dipl.-Ing. Rainer Enge
Andreas Fischer

Dipl.-Ing. Henning Fischer
Dipl.-Ing. Dietmar Germerott
Klaus-Dieter Gräbig
Dipl.-Ing. Bianca Grauf
Manfred Güll
Olaf Hawacker (bis 31.12.04)
Dipl.-Ing. Klaus Heerlein
Heinz Günter Kellner
Martin Kolleck
Alexander Kornehl
Dipl.-Inf. Oliver Küchemann
Wolfgang Kühn
Wolfgang Kühne
Dipl.-Ing. Alexander Loose
Olaf Matuschek
Dipl.-Ing. Reinhard Meller
Markus Monecke
Dipl.-Ing. Reinhard Müller
Wolfgang Neumann (bis 31.08.04)
Jürgen Nitsch
Helga Oberländer
Dipl.-Ing. Henry Perplies
Klaus-Dieter Preschel
Waltraut Reich (bis 31.08.04)
Dipl.-Phys. Tino Riethmüller
Dipl.-Ing. Claudius Römer
Rolf Schäfer
Helmut Schild (bis 31.01.04)
Helmut Schüddekopf
Dipl.-Ing. Hartmut Sommer
Michael Sperling
Dipl.-Ing. Eckhard Steinmetz
Oliver Stenzel
Ulrich Strohmeyer (bis 31.01.05)
Christoph Stucke
Thomas Tzscheetzsch (bis 31.12.04)
Daniel Windler (bis 31.12.04)
Wolfgang Wunderlich

Werkstätten, Haustechnik, Ausbildung:/Workshops, physical plant, training

Leitung: Dipl.-Ing. Volker Thiel (bis 30.11.2005), Bernd Chares
Stellvertreter Werkstatt: Norbert Meyer
Stellvertreter Haustechnik: Horst Heise (bis 30.09.2005), Andreas Poprawa
Stellvertreter Ausbildung: Roland Mende
Sekretariat: Beatrix Hartung

Werkstatt/Workshops:

Feinmechanik: Hermann Arnemann, Hans-Joachim Gebhardt (bis 31.01.04), Ernst-Reinhold Heinrichs, Dietmar Hennecke, Detlef Jünemann, Roland Mende, Norbert Meyer, Egon Pinnecke, Werner Steinberg

Schlosserei: Hans-Joachim Heinemeier

Galvanik: Hans-Adolf Heinrichs (bis 28.02.05), Walter Wächter (bis 28.02.05)

Siebdruck/Laser: Mathias Schwarz

Haustechnik/Physical plant:

Elektro: Horst Heise (bis 30.09.05), Michael Hilz, Peter Mutio, Mario Reich, Mario Strecker

Heizung-Sanitär: Karl-Heinrich Deisel, Herbert Ellendorff (bis 30.06.04), Werner Hundertmark

Tischlerei: Helge Aue, Martin Heinrich

Gärtner: Martin Schröter, Hans-Dieter Waitz (bis 30.09.05)

Reinigung: Monika Doucet-Hitscher (bis 31.08.04), Ngow Heine, Monika Link (bis 31.12.04), Anna Macke (bis 31.12.04), Maria Müller, Birgit Podritzki (bis 31.12.04), Rosemarie Poppe, Edeltraud Rümke (bis 31.12.04), Maria Schmidt (bis 31.07.04), Heidemarie Weber (bis 31.12.04)

Küche: Johannes Kohlrautz, Sylvia Aue, Lilli Dargel, Beate Meyer

Ausbildung/Training of apprentices:

Feinmechanik: Roland Mende

Elektrotechnik: Olaf Matuschek

Auszubildende: Adamski Sascha, Christian Biermann (bis 30.04.05), André Bode, Robert Burkhardt, Albert Dargel (bis 31.05.04), Timo Effler, Fabian Ernst, Julian Fellmann (bis 31.08.04), Matthias Franke, Simon Geile (bis 30.04.05), Gregor Hadasch (bis 24.08.05), Philipp Haut (bis 30.04.05), Marius Hellmold (bis 31.07.04), Nils Henne, Martin Hildebrand, Manuel-Roland Jünemann, Stephan Kellner (bis 18.08.04), Arno Kiefert, Oliver Kliemand, Martin Koch (bis 31.08.04), Alexander Kornehl (bis 20.01.05), Till Kremser (bis 31.05.04), Sven Krenauer (bis 30.04.05), Fabian Maulhardt, Hendrik Meller, Christian Menge (bis 30.09.05), Sebastian Neumann (bis 17.09.04), David Otto, Sebastian Poppe (bis 30.04.05), Christoph Ressel, Marius Rinkleff, David Römermann, Alexander Schmidt, Peer Strogies, Nicholas Unger, Jan Hendrik Wagner, Stefan Wagner, Alex Weber, Jens Wegner, Marius Wittkowski (bis 29.06.05), Marcus Wolf, Christian Zinke (bis 30.04.04)

Dokumentation, Konstruktion/Documentation, mechanical design:

Leitung: Bernd Chares

Anita Brandt, Steffen Ebert, Angelika Hilz, Marianne Krause, Mona Wedemeier

Bibliothek/Library: Prof. Dr. Klaus Jockers (wissenschaftlicher Bibliotheksbeauftragter) (bis 31.08.2005), Dr. Bernd Inhester (seit 01.09.2005)

Inge Kraeter, Renate Meusel (bis 31.07.05), Margit Steinmetz

Öffentlichkeitsarbeit/Public relations:

Dr. Norbert Krupp, Dr. Bernd Wöbke

Redaktion der Instituts-Informationen/Editor of the institute newsletter:

Dr. Reinhard Borchers (bis 31.08.2005), Dr. Martin Hilchenbach (seit 01.09.2005)

Direktionssekretärinnen/Secretaries of the directors:

Sabine Deutsch, Susanne Kaufmann (bis 30.06.2004), Karin Peschke, Rosemarie Röttger (bis 30.06.04), Barbara Wieser

Sekretärinnen/Secretaries: Anja Behrens, Gerlinde Bierwirth, Jacqueline Bukatz, Petra Fahlbusch, Elke Hartmann, Karin Kellner (bis 30.09.05), Susanne Kaufmann, Helga Reuter, Sibylla Siebert-Rust, Ute Spilker, Margit Steinmetz, Sabine Stelzer, Andrea Vogt

Verwaltung/ Administration:	Andreas Poprawa (Verwaltungsleiter) Andrea Macke, Bernhard Bleckert (bis 31.01.04), Jürgen Bethe, Petra Fahlbusch, Roswitha Komossa, Dorothee Schreiber, Christina Thomitzek
Auszubildende/Apprentices:	Swetlana Alekseenko, Carina Huchthausen, Michaela Schmalstieg, Nadine Senger (bis 30.06.2004), Aris Thieme
Personalbüro/Personell office:	Edith Deisel, Christiane Neu
Einkauf/Goods received:	Monika Majunke (bis 31.07.04), Ilse Schwarz, Nadine Senger, Bernhard Vogt
Buchhaltung/Book-keeping:	Martina Heinemeier, Nadine Teichmann, Andrea Werner
Sonstige Dienste/Other services:	Jürgen Bethe, Renate Heitkamp (bis 30.09.05), Inge Reuter, Robert Uhde

Studentische Hilfskräfte und Praktikanten/Student assistant and traineeship:

Robert Chares (bis 15.06.04), Sven Finke (bis 31.12.04), Petra Kluth, Thilo Kröning (bis 31.08.04), Moritz Martynkewicz (bis 09.12.05), Sven Sander (bis 16.01.04), Edgar Wagner (bis 30.06.05)

VII. Wissenschaftliche Zusammenarbeit / Scientific Collaboration

Wissenschaftler, die als Gäste längere Zeit am MPS tätig waren / Scientific guests with long-term visits to MPS

(Stipendiaten der MPG, des DAAD, der DFG, der Alexander von Humboldt-Stiftung/Friedrich-Wilhelm-Bessel-Preisträger, Postdocs und Honorarempfänger/ Stipend holders of the MPG, the DAAD, the DFG, the Alexander von Humboldt Foundation/Friedrich Wilhelm Bessel Research Award and Postdocs)

Nicolas Altobelli, MPI für Kernphysik, 4. – 31. Dezember 2004. Zusammenarbeit mit Dr. N. Krupp.

Hagay Amit, Department of Earth and Planetary Sciences, John Hopkins University, Baltimore, MD, USA, 29. April – 3. Juni 2005. Zusammenarbeit mit Prof. U. Christensen und Dr. J. Wicht.

Dr. Jaime Araneda, Facultad de Ciencias Fisicas y Matematias, Universidad de Concepcion, Chile, 12. Juli – 10. August 2004 und 30. Januar – 5. März 2005. Zusammenarbeit mit Prof. E. Marsch.

Dr. Regina Aznar Cuadrado, Osservatorio Astronomico di Capodimonte, Neapel, Italien, 1. Juni 2003 – 31. Mai 2006. Zusammenarbeit mit Prof. S. K. Solanki.

Dr. K. Bamert, 17. Januar – 18. Februar 2005 und 1. – 30. September 2005. Zusammenarbeit mit Dr. M. Hilchenbach.

Dr. Ingo Baumann, 22. März – 22. September 2005. Zusammenarbeit mit Prof. S. K. Solanki.

Denis Belyaev, Space Research Institute (IKI), Moscow, Russia, 20. März – 19. Mai 2005. Zusammenarbeit mit Dr. D. Titov.

Dr. Tanyu Bonev, Institut für Astronomie der Bulgarischen Akademie der Wissenschaften, Sofia, Bulgarien, 13. Januar – 10. April 2004, 5. Oktober – 30. November 2004 und 15. März – 15. April 2005. Zusammenarbeit mit Prof. K. Jockers.

Prof. N. Borisov, Institute of Terrestrial Magnetism, Ionosphere and Radio Waves Propagation, (IZMIRAN), Russia, 1. Juni – 31. August 2005. Zusammenarbeit mit Dr. U. Mall.

Dr. Juan Manuel Borrero, 1. September – 30. November 2004. Zusammenarbeit mit Dr. A. Lagg und Prof. S. K. Solanki.

Dr. Alen Brkovic, Kiepenheuer Institut für Sonnenphysik, Freiburg, 1. Oktober – 31. Dezember 2004. Zusammenarbeit mit Prof. S. K. Solanki.

Dr. Robert Cameron, University of Sydney, Australia, 15. März 2003 – 31. Mai 2005. Zusammenarbeit mit Prof. M. Schüssler.

Dr. A. Czechowski, Space Research Center, Polish Academy of Sciences, Warsaw, Poland, 1. – 31. Januar 2004, 25. Juni – 17. Juli 2004, 18. – 31. Juli 2005 und 1. – 30. September 2005. Zusammenarbeit mit Dr. M. Hilchenbach.

Dr. Bhola N. Dwivedi, Institute of Technology, Banaras Hindu University, Varanasi, India, 17. Mai – 30. Juni 2004. Zusammenarbeit mit Dr. W. Curdt.

Dr. Nina Elkina, Keldysh Institute of the Russian Academy of Sciences, Moscow, Russia, 1. November – 21. Dezember 2004, 10. April – 10. Juli 2005 und 29. September – 31. Dezember 2005. Zusammenarbeit mit Prof. J. Büchner.

Dr. Artem Feofilov, Ludwig Maximilian Universität München, 1. Oktober – 31. Dezember 2004. Zusammenarbeit mit Dr. P. Hartogh.

Dr. Antonio Ferriz Mas, Universität Vigo, Spanien, 15. September – 20. Dezember 2005. Zusammenarbeit mit Dr. M. Schüssler.

Dr. Alberto Flandes, Departamento de investigaciones solares y planetarias, Instituto de Geofisica, & UNAM Ciudad Universitaria, Coyoacn 04510, Mexico City, Mexico, 18. Mai – 3. August 2005. Zusammenarbeit mit Dr. H. Krüger.

Dr. Andrew Fletcher, MPI für Radioastronomie, Bonn, 1. August – 30. September 2004. Zusammenarbeit mit Prof. S. K. Solanki.

Dr. S. Y. Fu, Peking University, Beijing, China, 17. Oktober – 13. November 2005. Zusammenarbeit mit Dr. A. Korth.

Dr. Yevgen Grynko, 1. Mai – 31. August 2005. Zusammenarbeit mit Prof. K. Jockers.

Dr. F. Guarnieri, INPE (Brazilian National Institute for Space Research), Sao Jose dos Campos, Brasilia, 12. Mai – 12. Juli 2005. Zusammenarbeit mit Dr. A. Korth.

Prof. H. Hiesinger, Department of Physics and Earth Sciences, Central Connecticut State University, USA, Januar 2004. Zusammenarbeit mit Dr. U. Mall.

Dr. Volkmar Holzwarth, University St. Andrews, Scotland, UK, 15. September – 17. Oktober 2005. Zusammenarbeit mit Dr. M. Schüssler.

Dr. Nikolay Ignatiev, Space Research Institute (IKI), Moscow, Russia, September/Oktober 2004; 27. März – 26. Mai 2005. Zusammenarbeit mit Dr. D. Titov.

Dr. Christoph Keller, National Solar Observatory, Tucson, AZ, USA, Friedrich-Wilhelm-Bessel-Preisträger der A. v. Humboldt-Stiftung, 8. September 2003 – 30. April 2004. Zusammenarbeit mit Dr. M. Schüssler und Prof. S. K. Solanki.

Dr. Nikolaj Kiselev, Institut für Astronomie der Nationalen V. N. Karazin Universität, Charkow, Ukraine, 1. September – 20. Dezember 2004. Zusammenarbeit mit Prof. K. Jockers.

Dr. V. Korokhin, Astron. Institute of Kharkiv, National University Ukraine, 26. Oktober – 26. November 2005. Zusammenarbeit mit Dr. U. Mall.

Dr. Irina Kulyk, Hauptobservatorium der Nationalen Akademie der Wissenschaften der Ukraine, Goloseevo bei Kiew, Ukraine, 15. April – 15. Juli 2005. Zusammenarbeit mit Prof. K. Jockers.

Dr. Hans-Günter Ludwig, Lund Observatory, Schweden, 1. September – 31. Dezember 2004. Zusammenarbeit mit Prof. S. K. Solanki.

Dr. Maria S. Madjarska-Theissen, Mullard Space Science Laboratory, Dorking, UK, 1. April – 30. Oktober 2004. Zusammenarbeit mit Prof. S. K. Solanki.

Dr. Ajay Manglik, National Geophysical Research Institute, Hyderabad, India, 30. Juni – 31. August 2005. Zusammenarbeit mit Prof. U. Christensen.

Prof. A. Otto, University of Alaska, Fairbanks, USA, 11. März – 17. April 2004, 19. Oktober – 21. November 2004, 10. Oktober – 20. November 2005. Zusammenarbeit mit Prof. J. Büchner.

Dr. Anuschka Pauluhn, International Space Science Institute, Bern, Schweiz, 1. Oktober 2003 – 29. Februar 2004. Zusammenarbeit mit Prof. S. K. Solanki.

Dr. Pascal Petit, Universität Porto, Portugal, 17. Mai 2004 – 16. Mai 2006. Zusammenarbeit mit Prof. S. K. Solanki.

Dr. Elena Petrova, Institut für Weltraumforschung der russischen Akademie der Wissenschaften, Moskau, Russland, 18. September – 16. Dezember 2005. Zusammenarbeit mit Prof. K. Jockers.

Dr. Oliver Preuß, Universität Bielefeld, 1. Januar 2005 – 31. Dezember 2007. Zusammenarbeit mit Prof. S. K. Solanki.

Prof. Zhong-Quan Qu, Yunnan Astronomical Observatory, Kunming, PR China, 30. Mai – 30. Juli 2005. Zusammenarbeit mit Prof. S. K. Solanki und Dr. A. Lagg.

Dr. Noureddine Raouafi, Observatorio Astronomico di Torino, Turin, Italien 8. Januar 2002 – 31. Januar 2005. Zusammenarbeit mit Prof. S. K. Solanki.

Dr. Anatoli Remizov, Space Science Institute (IKI) of the Russian Academy of Sciences, Moscow, Russia, 10. September – 10. Oktober 2005 und 1. Dezember 2005 – 31. März 2006. Zusammenarbeit mit Dr. H. Böhnhardt.

Dr. Matthias Rempel, High Altitude Observatory, NCAR, Boulder, USA, 5. Juni – 14. Juli 2004, 5. – 22. Dezember 2004, 2. Dezember 2005 – 16. Januar 2006. Zusammenarbeit mit Dr. M. Schüssler und Dr. L. Gizon.

Dr. Sergiy Shelyag, 15. Juli 2004 – 15. Januar 2005. Zusammenarbeit mit Prof. S. K. Solanki.

Dr. I. Silin, University of Alberta, Edmonton, Kanada, 1. Juli – 31. Dezember 2004. Zusammenarbeit mit Prof. J. Büchner

Dr. Gerd Sonnemann, Leibniz-Institut für Atmosphärenphysik, Universität Rostock, Kühlungsborn, 1. November – 16. Dezember 2005. Zusammenarbeit mit Dr. P. Hartogh.

Dr. Slawomira Szutowicz, Zentrum für Weltraumforschung der polnischen Akademie der Wissenschaften, Warschau, Polen, 16. August – 14. September 2004 und 15. Februar – 14. April 2005. Zusammenarbeit mit Prof. K. Jockers.

Dr. Luca Teriaca, Osservatorio Astrofisico di Arcetri, Florenz, Italien 1. Februar 2003 – 31. August 2005. Zusammenarbeit mit Prof. S. K. Solanki

Dr. Viktor Tishkovets, Institut für Radiophysik, Kharkov, Ukraine, 15. April – 13. Juli 2004, 20. September – 20. Dezember 2004 und 11. April – 11. Juli 2005. Zusammenarbeit mit Prof. K. Jockers.

Prof. Chuanyi Tu, Peking University, Beijing, China, 1. Januar – 31. Januar 2004, 1. November – 31. Januar 2005 und 1. Dezember – 31. Dezember 2005. Zusammenarbeit mit Prof. E. Marsch.

Dr. I. Usoskin, University Oulu, Finland, (mehrfach in 2004 und 2005) Zusammenarbeit mit Prof. S. K. Solanki und Dr. M. Schüssler.

Dr. L. E. Vieira, INPE (Brazilian National Institute for Space Research, Sao Jose dos Campos, Brasilia, 7. September – 28. November 2004. Zusammenarbeit mit Dr. A. Korth.

Dr. Alexander Vögler, 1. August 2003 – 31. Juli 2005. Zusammenarbeit mit Prof. S. K. Solanki und Prof. M. Schüssler.

Dr. Tongjiang Wang, National Astronomical Observatories, Beijing, PR China, 5. Juni 2001 – 31. Mai 2006. Zusammenarbeit mit Prof. S. K. Solanki und Dr. K. Wilhelm.

Dr. Johan Warell, Department for Astronomy and Space Physics, University of Uppsala, Sweden, 29. März – 29. April 2004. Zusammenarbeit mit Prof. U. Christensen und Dr. H. Böhnhardt.

Dr. Lidong Xia, University of Science and Technology of China, Heifei, Anhui, China, 3. August – 2. September 2004 und 29. Juli – 2. September 2005. Zusammenarbeit mit Prof. E. Marsch.

Dr. Jun Zhang, National Astronomical Observatory, Beijing, PR China, 15. September 2003 – 30. Mai 2004. Abkommen CAS/MPG, Zusammenarbeit mit Prof. S. K. Solanki und Dr. J. Woch.

Wissenschaftler, die als Gäste nur kurzzeitig am MPS tätig waren / Scientific guests with short-term visits to MPS

Dr. Nancy Ageorges, European Southern Observatory, Santiago de Chile, 13. – 25. November 2005. Zusammenarbeit mit Dr. H. Böhnhardt.

Dr. Vincenzo Andretta, Capodimonte Observatory - I.N.A.F., Naples, Italy, 17. – 29. Juni 2004. Zusammenarbeit mit Dr. Regina Aznar Cuadrado.

Dr. Aaron C. Birch, Colorado Research Associates, Boulder, CO, USA, 9. – 29. Oktober 2005. Zusammenarbeit mit Dr. L. Gizon.

Prof. Gerard Chanteur, CETP Paris, France, 11. – 23. Dezember 2005. Zusammenarbeit mit Dr. M. Fränz.

Prof. Dr. A. Eviatar, Department of Geophysics and Planetary Sciences, The Raymond and Beverly Sackler Faculty of Exact Sciences, Tel Aviv University, Ramat Aviv, Israel, 14. – 20. November 2004. Zusammenarbeit mit Prof. Dr. V. M. Vasyliūnas.

Dr. Antonio Ferriz Mas, University of Vigo, Spain, 31. Januar – 4. Februar 2005. Zusammenarbeit mit Dr. D. Schmitt.

Dr. V. M. Gubchenko, Institute of Applied Physics of the Russian Academy of Sciences, Nizhny Novgorod, Russia, 24. – 29. Oktober 2004. Zusammenarbeit mit Prof. J. Büchner.

Dr. G. Hornig, University of St. Andrews / University of Dundee, Scotland, UK, 16. – 19. März 2004 und 22. – 25. November 2005. Zusammenarbeit mit Prof. J. Büchner.

Peter Hoyng, SRON, Utrecht, NL, 1. – 5. März 2004. Zusammenarbeit mit Dr. D. Schmitt.

Dr. J. M. Jahn, Southwest Research Institute, San Antonio, TX, USA, 2 Wochen im Juni 2004. Zusammenarbeit mit Dr. A. Korth.

Dr. Frank Jenko, MPI für Plasmaphysik (IPP), Garching, 12. – 14. Januar 2005. Zusammenarbeit mit Prof. J. Büchner.

Prof. Dr. J. Kan, University of Alaska, Fairbanks, USA, 17. – 25. Mai 2005. Zusammenarbeit mit Prof. Dr. V. M. Vasyliūnas.

Dr. Ludmilla Kolokolova, University of Maryland, College Park, USA, 11. – 27. September 2005. Zusammenarbeit mit Dr. H. Böhnhardt.

Dr. Susan Lederer, University of California, San Bernardino, USA, 5. – 14. Dezember 2005. Zusammenarbeit mit Dr. H. Böhnhardt.

Hazel McAndrews, Mullard Space Science Laboratory (MSSL), Surrey, UK, 8. – 10. November 2005. Zusammenarbeit mit Dr. N. Krupp.

R. McLean, University of St. Andrews, Scotland, UK, 22. – 28. November 2004. Zusammenarbeit mit Prof. J. Büchner.

Chris Paranicas, Johns Hopkins University, Applied Physics Laboratory, USA, 8. – 12. Februar 2004. Zusammenarbeit mit Dr. N. Krupp.

Dr. Johann Reiter, Technische Universität München, Zentrum Mathematik, 12. – 16. Dezember 2005. Zusammenarbeit mit Dr. L. Gizon.

Dr. S. Savine, Space Research Institute of the Russian Academy of Sciences, Moscow, Russia, 10. – 16. Juli 2005. Zusammenarbeit mit Prof. J. Büchner.

Prof. R. Sydora, University of Alberta, Edmonton, Kanada, 19. – 21. Januar 2005. Zusammenarbeit mit Prof. J. Büchner.

Cyril Szopa, Service d'Aeronomie, Paris, France, 18. – 23. Juli 2005. Zusammenarbeit mit Dr. F. Goesmann.

Dr. GianPaolo Tozzi, INAF Arcetri Observatory, Florence, Italy, 3. – 12. November 2005. Zusammenarbeit mit Dr. H. Böhnhardt.

Dr. Andris Vaivads, Swedish Institute for Space Research, Uppsala, Sweden, 14. – 16. Oktober 2004. Zusammenarbeit mit Prof. J. Büchner.

Dr. Richard Wachter, Stanford University, Stanford, CA, USA, 18. – 21. Dezember 2005. Zusammenarbeit mit Dr. L. Gizon.

Dr. Diane Wooden, NASA Ames Research Center, Moffett Field, USA, 5. – 14. Dezember 2005. Zusammenarbeit mit Dr. H. Böhnhardt.

Prof. L. M. Zelenyi, Space Research Institute of the Russian Academy of Sciences, Moscow, Russia, 6. – 12. Mai 2005. Zusammenarbeit mit Prof. J. Büchner.

Längere Aufenthalte von Wissenschaftlern des MPS an anderen Instituten / Long-term visits of MPS scientists to other institutes

Dr. Hermann Böhnhardt, European Southern Observatory, Santiago de Chile, 10. – 20. Juli 2005.

Prof. Jörg Büchner, Fellowship of the Isaac Newton Institute for Mathematical Sciences, Cambridge, UK, 2. – 27. August 2004.

Dr. Martin Hilchenbach, Laboratoire de Phys. & Chim. de L'Environnement, Orléans, Frankreich, Juni 2004. ARC Seibersdorf Research Aerospace Technology, Seibersdorf, Austria, Dezember 2005.

Dr. Johann Hirzberger, Swedish Solar Telescope (SST), La Palma, Canary Islands, Spain, Observation campaign, 22. – 31. August 2005.

Emre Işik, School of Physics and Astronomy, University of St. Andrews, Scotland, 16. – 28. Mai 2005.

Dr. Klaus Jockers, Zentrum für Weltraumforschung der polnischen Akademie der Wissenschaften, Warschau, Polen, 21. Juli – 7. August 2004. Bulgarisches Nationalobservatorium, Rojen und Astronomisches Institut der Bulgarischen Akademie der Wissenschaften, Sofia, Bulgarien, 2. – 20. Januar 2005 und 24. November – 9. Dezember 2005.

Dr. Harald Krüger, Gaststatus am MPI für Kernphysik, Heidelberg.

Dr. Michael Küppers, ESOC, Darmstadt, 9. – 21. Januar 2005.

Takeshi Kuroda, Center for Climate System Research, University of Tokyo, Japan, 25. März – 1. April 2005, 20. – 28. September 2005, 31. Oktober – 4. November 2005.

Dr. Jon Rotvig, Department of Mathematical Sciences, Exeter, England, 25. Mai – 1. Juni 2005.

Prof. V. M. Vasyliūnas, Center for Atmospheric Research, University of Massachusetts, Lowell, USA, 26. April – 8. Mai 2004, 7. – 17. März 2005 und 10. – 19. Oktober 2005.

Dr. Thomas Wiegelmann, National Astronomical Observatory of Japan, Solar Physics Division, Tokyo, Japan, 20. Januar 2005 – 24. Februar 2005. University St. Andrews, Solar Theory Group, UK, 5. – 16. Dezember 2005.

Projekte in Zusammenarbeit mit anderen Institutionen / Projects in collaboration with other institutions

Die Art der Zusammenarbeit des MPS mit anderen Institutionen ist im einzelnen ziemlich unterschiedlich. Die folgende Aufzählung soll nur einen kurzen Überblick geben./The cooperation of MPS with other institutions is extensive and varied. The following list only provides a brief overview.

Astronomical tests of gravitation theory.- O. Preuss und S. K. Solanki in Zusammenarbeit mit F. W. Hehl (Universität Köln).

Astrophysical spectropolarimetry.- A. Gandorfer in Zusammenarbeit mit J. O. Stenflo (Institute of Astronomy, ETH Zürich, Schweiz).

BepiColombo – BELA (Laser Altimeter).- M. Hilchenbach, U. Christensen, R. Roll, H. Fischer und C. Koch in Zusammenarbeit mit N. Thomas, W. Benz, K. Gunderson, K. Seiferlin (Physikalisches Institut, Universität Bern, Schweiz); T. Spohn, E. Hauber, H. Michaelis, J. Oberst (DLR - Institut für Planetenforschung, Berlin); G. Beutler (Astronomy Institute, Universität Bern, Schweiz); C. Fallnich (Laser Zentrum Hannover); D. Giardini (Institute of Geophysics/Swiss Seismological Service, Swiss Federal Institute of Technology, (ETHZ), Zürich, Schweiz); O. Groussin (Department of Astronomy, University of Maryland, College Park, MD, USA); L. Jorda, P. Lamy (Laboratoire d'Astrophysique de Marseille, Marseille, Frankreich); L.-M. Lara, J. J. Lopez-Moreno, R. Rodrigo (Instituto de Astrofisica de Andalucia, Granada, Spanien); P. Lognonné (Département de Géophysique Spatiale et Planétaire/UMR7096-CNRS, Saint Maur des Fossé, Frankreich); D. Resendes (Instituto Superior Técnico, Universidade Técnica de Lisboa, Lisboa, Portugal).

BepiColombo — MERMAG (Magnetic Field Investigation).- U. Christensen in Zusammenarbeit mit K.-H. Glaßmeier (PI) (Institut für Geophysik und Extraterrestrische Physik, Braunschweig).

BepiColombo – MMO (Mercury Magnetospheric Orbiter).- *MPPE-MSA: Spektrometer zur Messung von geladenen und neutralen Teilchen in der Merkurmagnetosphäre (Bauphase).* N. Krupp, J. Woch, A. Loose, H. Fischer und U. Bührke in Zusammenarbeit mit D. Delcourt (Centre d'Etude Terrestre et Planetaire (CETP), Paris, Frankreich); Y. Saito (Jaxa/ISAS, Tokio, Japan).

BepiColombo – MPO (Mercury Planetary Orbiter).- *PICAM (Planetary Ion CAMera) - Detektoreinheit des Neutral and Charge Particle Analyzers SERENA (Search for Exospheric Refilling and Emitted Natural Abundances).* J. Woch, A. Loose, N. Krupp und M. Fränz in Zusammenarbeit mit S. Orsini (PI) (IFSI, Rom, Italien); K. Torkar (Co-PI) (SRI, Graz, Österreich); J.-J. Berthelier (CETP-CNRS, St Maur des Fosses, Frankreich); P. Escoubet (ESTEC, Noordwijk, Niederlande); F. Leblanc (IPSL Verrieres-Le-Buisson, Frankreich); D. Nevejans (BIRA, Brüssel, Belgien); K. Szego (KFKI, Budapest, Ungarn); O. Vaisberg (IKI, Moskau, Russland).

CASSINI – DISR.- B. Grieger und M. Küppers in Zusammenarbeit mit M. Tomasko und Mitarbeiter (Lunar and Planetary Laboratory, University of Arizona, USA).

CASSINI – MIMI/LEMMS.- *Spektrometer zur Messung von geladenen und neutralen energiereichen Teilchen in der Saturnmagnetosphäre (Datenauswertung).* N. Krupp, J. Woch und A. Lagg in Zusammenarbeit mit S. M. Krimigis, S. Livi, D. G. Mitchell (Johns Hopkins University Applied Physics Laboratory, USA); D. Hamilton (University of Maryland, USA); I. Dandouras (CESR, Toulouse, Frankreich); T. P. Armstrong (Fundamental Technologies, Kansas, USA).

CASSINI – UVIS (Ultraviolet Imaging Spectrometer), CASSINI/HUYGENS Mission.- H. U. Keller und A. Korth in Zusammenarbeit mit L. W. Esposito (PI), LASP, University of Colorado, Boulder, USA; University of Southern California, Los Angeles, USA; Jet Propulsion Laboratory, Pasadena, USA; California Institute of Technology, Pasadena, USA; Southwest Research Institute, Boulder, USA.

CCSR/NIES Martian GCM.- T. Kuroda in Zusammenarbeit mit M. Takahashi (Center for Climate System Research, University of Tokyo, Japan).

Chandrayaan-1, ISRO.- U. Mall in Zusammenarbeit mit Prof. N. Goswami (PRL, India).

Cluster II – CIS (Cluster Ion Spectrometer).- A. Korth, M. Fränz, H. Rosenbauer, V. M. Vasyliūnas und P. W. Daly in Zusammenarbeit mit H. Rème (PI), CESR, Toulouse, Frankreich; MPI Garching; Universities of New Hampshire, Washington, Seattle, Berkeley, USA; IFSI/CNR, Frascati, Italien; Lockheed, Palo Alto, USA; SISP, Kiruna, Schweden.

Cluster II – RAPID.- *Das Teilchen-Spektrometer RAPID.* Principle Investigator: P. W. Daly; Co-Investigators: U. Mall, J. Büchner, A. Korth, J. Woch, Sir Ian Axford und V. M. Vasyliūnas in Zusammenarbeit mit J. B. Blake, J. F. Fennell, J. Roeder (AC, Los Angeles, USA); Z. Y. Pu, S. Y. Fu (Beijing University, Beijing, China); T. A. Fritz, Q.-G. Zong (BU, Boston, USA); F. Gliem (IDA, Braunschweig); I. Sandahl (IRF, Kiruna, Schweden); H. Borg (Univ. Umea, Schweden); K. Kecskemety (KFKI, Budapest, Ungarn); G. D. Reeves, R.H.W. Friedel (LANL, Los Alamos, USA); D. N. Baker (LASP, Boulder, USA); M. Grande, M. Carter, C. H. Perry, J. Davies, M. Dunlop (RAL, Chilton, UK); M.G.G.T. Taylor (ESTEC, Niederlande); S. McKenna-Lawlor (SPC, Maynooth, USA); F. Søraas, K. Aarsnes, K. Oksavik (Univ. Bergen, Norwegen); K. Mursula, P. Tanskanen (Univ. Oulu, Finnland); E. T. Sarris (Univ. Thrace, Griechenland); A.T.Y. Lui (APL, USA).

Cluster Active Archive – RAPID-CAA.- *Archivierung der RAPID-Daten.* P. W. Daly und S. Mühlbachler in Zusammenarbeit mit C. H. Perry, J. Davies (RAL, Chilton, UK)).

CME driven shock wave.- B. Inhester, N.-E. Raouafi, S. K. Solanki und M. Mierla in Zusammenarbeit mit S. Manusco, C. Benna (Osservatorio Astronomico di Torino, Turin, Italien); J. P. Delaboudinière (Institut d'Astrophysique Spatiale, Orsay, Frankreich).

Computational Acoustics in a Spherical Shell.- M. Roth in Zusammenarbeit mit S. Hanasoge (Stanford University, Stanford, USA).

Coronal holes studied with UVCS.- S. K. Solanki in Zusammenarbeit mit N.-E. Raouafi (NSO, Tucson, USA).

Coronal MHD-equilibria.- T. Wiegelmann in Zusammenarbeit mit T. Neukirch (University St. Andrews, UK).

DAWN.- H. U. Keller, H. Sierks, H. Hartwig, A. Nathues und U. Christensen in Zusammenarbeit mit R. Jaumann, S. Mottola (DLR/Institut für Planetenforschung, Berlin); H. Michalik, B. Fiethe (Institut für Datentechnik und Kommunikationsnetze, Braunschweig); C. Russell, C. Raymond (University of California, Los Angeles, USA); K. C. Patel, E. Miller (Jet Propulsion Laboratory, Pasadena, USA).

Deep Impact at comet 9P/Tempel 1: Exploring the Dust Component.- H. Böhnhardt (PI) in Zusammenarbeit mit N. Ageorges, S. Bagnulo, O. Hainaut, E. Jehin, H. U. Kaeufl, F. Kerber, G. LoCurto, E. Pompei, O. Marco, F. Selmann (ESO Garching & Santiago de Chile); L. Barrera (UMCE, Santiago de Chile); T. Bonev (Univ. Sofia, Bulgarien); R. Gredel (MPI Astronomy, Heidelberg); L. Lara, J. L. Ortiz (Inst. Astrof. Andalucia, Granada, Spanien); K. Meech (Univ. Hawaii, Honolulu, USA); E. Pantin (CNRS Paris, Frankreich); H. Rauer (DLR Berlin); G. P. Tozzi (INAF Arcetri Observatory, Florence, Italien).

DFG-Schwerpunktprojekt 1115.- *Mars und die terrestrischen Planeten.* J. Kleimann in Zusammenarbeit mit A. Kopp (Theoretische Physik IV, Ruhr-Universität Bochum).

Dust from the β Pictoris disk.- N. A. Krivova und S. K. Solanki in Zusammenarbeit mit A. V. Krivov (Universität Potsdam); V. B. Titov (Universität St. Petersburg, Russland).

EUROPLANET (European Planetology Network).- *Aufbau eines Netzwerks in Europa zur Optimierung der Forschungsaktivitäten im Bereich Planeten.* N. Krupp in Zusammenarbeit mit 60 Instituten in Europa.

Galileo – EPD (Energetic Particles Detector).- *Spektrometer zur Messung von geladenen energiereichen Teilchen in der Jupitermagnetosphäre (Datenauswertung).* N. Krupp, J. Woch und A. Lagg in Zusammenarbeit mit D. J. Williams, R. McEntire (Johns Hopkins University, Applied Physics Laboratory, USA).

GBSO – Ground Based Solar Observations.- S. K. Solanki, A. Lagg, J. Hirzberger, R. Thomas, R. Aznar Cuadrado und C. Sasso in Zusammenarbeit mit M. Collados (IAC, La Laguna, Tenerife, Spanien); A. López Ariste (THEMIS, La Laguna, Tenerife, Spanien); R. Wachter (University of Stanford, California, USA); D. Fluri, N. Afram (ETH Zürich, Schweiz); K. Puschman, E. Wiehr (Institut für Astrophysik, Universität Göttingen); S. Stangl (Institut für Physik, Universität Graz, Austria).

Granulation on Alpha Centauri A and B.- S. K. Solanki in Zusammenarbeit mit C. Frutiger (ETH Zürich, Schweiz); G. Mathys (European Southern Observatory, Chile).

Helio-and asteroseismology, with applications to extrasolar planets.- S. K. Solanki in Zusammenarbeit mit L. Gizon (Stanford University, USA).

HIFI–WBS (Heterodyne Instrument for FIRST – Wideband Spectrometer).- P. Hartogh, P. Börner, C. Jarchow und M. Küppers in Zusammenarbeit mit T. de Graauw, H. J. Aarts, D. A. Beintema, J. Gao, H. Jacobs, W. Jellema, W. Luinge, P. R. Roelfsema, X. Tielens, H. van de Stadt, B. van Leeuwen, N. D. Whyborn, K. J. Wildeman (SRON, Utrecht, Niederlande); E. Van Dishoeck (Universität Leiden, Niederlande); R. Güsten, K. Menten (Max-Planck-Institut für Radioastronomie, Bonn); C. H. Honingh, K. Jacobs, R. Schieder, J. Stutzki (Universität Köln); A. Emrich (Omnisys, Göteborg, Schweden); S. Torchinsky (Chalmers, Göteborg, Schweden); M. Larsson (Universität Stockholm, Schweden); C. Rosolen (Arpeges, Observatoire de Paris, Meudon, Frankreich); G. Beaudin (LERMA, Meudon, Frankreich); E. Caux, A. Cros (CESR, Toulouse, Frankreich); P. Cais (Bordeaux Observatory, Frankreich); E. Lellouch, T. Encrenaz (DESPA, Paris, Frankreich); C. Gry (LAS Marseille, Frankreich); N. Maurun (Graal, Montpellier, Frankreich); K. Schuster (IRAM, Grenoble, Frankreich); F. Boulanger (IAS, Orsay, Frankreich); L. T. Little (Kent University, UK); T. Miller (UMIST, UK); T.J.T. Moore (Liverpool-J. Moures, UK); S. Withington (MRAO Cambridge, UK); G. J. White (QMW London, UK); R. Cerrulli, R. Orfei (IFSI Frascati, Italien); V. Natale (CAISMI Florenz, Italien); J. Martin-Pintado (OAN, Alcala, Spanien); J.D.G. Puyol (Obs. Yebes, Spanien); M. J. Sarna, R. Szczerba (Copernicus AC, Warschau, Polen); W. R. McGrath, J. C. Pearson, T. C. Gaier (JPL, Pasadena, USA); T. G. Phillips, J. Zmuidzinas (Caltech, Pasadena, USA); A. I. Harris (Maryland University, USA); E. Herbst (Ohio State University, USA); D. A. Neufeld (Johns Hopkins University, USA); N. R. Erickson (FCRAO, Amherst, MA, USA); S. Verghese (Lincoln Lab., MIT, USA); S. Kwok (Calgary University, Canada); D. A. Naylor (Lethbridge University, Canada); F. Lo (IAA Taiwan); H. Wang (NTU, Taipeh, Taiwan); P. Zimmermann (RPG, Meckenheim).

INTAS-Projekt 2003-51-4872.- *Ion and electron scales in mass and energy transfer: magnetospheric mapping, modelling and future missions.* J. Büchner in Zusammenarbeit mit Partnerteilnehmerländern: Belarus, Frankreich, Italien, Polen, Russland.

Interaction of Acoustic Waves with a Magnetic Cylinder.- L. Gizon in Zusammenarbeit mit A. C. Birch (CoRA, NorthWest Research Associates, Boulder, USA); S. Hanasoge (Stanford University, Stanford, USA).

Interball und Cluster – Data analysis.- J. Büchner in Zusammenarbeit mit L. Zelenyi, S. Savin, E. Panov (Space Research Institute of the Russian Academy of Sciences, Moskau, Russland).

Kinetische Physik des Sonnenwinds.- *Forschung auf dem Gebiet der Plasma-Beam Instabilitäten im Sonnenwind und in der Sonnenkorona. Numerische Simulationen zum Zerfall und der parametrischen Entwicklung von Alfvén Wellen großer Amplitude.* E. Marsch in Zusammenarbeit mit J. Araneda (Universität Concepcion, Chile).

Kinetic simulation techniques in space physics.- J. Büchner in Zusammenarbeit mit N. Elkina (Keldysh Institute of the Russian Academy of Sciences, Moskau, Russland).

KuaFu – "Space Weather Explorer".- R. Schwenn in Zusammenarbeit mit Chuanyi Tu (PI) (Peking University, Beijing, China).

Local Helioseismology of Small Magnetic Features.- L. Gizon und M. Roth in Zusammenarbeit mit T.L. Duvall (NASA, GSFC, Greenbelt, USA); A.C. Birch (CoRA, NorthWest Research Associates, Boulder, USA).

Magnetic fields in white dwarfs.- S. K. Solanki und C. Aznar Cuadrado in Zusammenarbeit mit S. Jordan (Universität Heidelberg); R. Napiwotzki (University of Leicester, UK); H. M. Schmid (ETH-Zürich, Schweiz); G. Mathys (European Southern Observatory, Santiago, Chile).

MAOAM (The Martian Atmosphere: Observing And Modeling).- P. Hartogh, C. Jarchow, T. Kuroda, A. Medvedev, R. Saito und G. Villanueva in Zusammenarbeit mit U. Berger, G. Sonnemann, M. Grygalashvyly (IAP Kühlungsborn); A. Feofilov, A. Kutepov (IAA München); H. Elbern (Institut für Geophysik und Meteorologie, Köln); M. Allen (JPL, Pasadena, USA); Gordon Chin (GSFC, Greenbelt, USA).

Mars Climate Simulator.- B. Grieger in Zusammenarbeit mit K. Fraedrich und Mitarbeiter (Meteorologisches Institut der Universität Hamburg); R. Greve (Institute of Low Temperature Science, Hokkaido University, Japan).

Mars Express.- Nick Hoekzema in Zusammenarbeit mit K. Gwinner, T. Roatch, H. Hofmann (DLR, Berlin); G. Neukum (FU, Berlin); A. Inada (CalTech, Los Angelos, CA, USA); L. Petrova (IKI, Moskau, Russland).

Mars Express – ASPERA-3 (Analyzer of Space Plasmas and EneRgetic Atoms).- M. Fränz, J. Woch, N. Krupp, E. Dubinin, E. Roussos, C. Martinecz und J. Kleimann in Zusammenarbeit mit R. Lundin (PI), S. Barabash (IRF, Kiruna, Schweden); D. Winningham, R. Frahm (SWRI, San Antonio, USA); P. Wurz (Universität Bern, Schweiz); A. Coates (MSSL, London, England); M. Grande (RAL, Chilton, England); J. A. Sauvaud, A. Fedorov (CESR, Toulouse, Frankreich); E. Kallio (FMI, Helsinki, Finnland); S. Orsini (IFSI, Rom, Italien); C. C. Curtis (UoA, Tuscon, USA).

Mars Express – OMEGA.- D. Titov in Zusammenarbeit mit J.-P. Bibring, Y. Langevin, B. Gondet (Institut d'Astrophysique Spatiale (IAS), Orsay, Frankreich); P. Drossart, R. Melchiorri (Observatoire de Paris, Meudon, Frankreich); N. Ignatiev (Space Research Institute (IKI), Moskau, Russland).

Mars Express – PFS.- D. Titov in Zusammenarbeit mit V. Formisano, D. Grassi (Institute of Physics of Interplanetary Space (IFSI-INAF), Rom, Italien); N. Ignatiev, A. Fedorova (Space Research Institute (IKI), Moskau, Russland); E. Lellouch, T. Fouchet, Th. Encrenaz (Observatoire de Paris, Meudon, Frankreich).

Meteorites, cosmogenic nuclides and past solar activity.- S. K. Solanki in Zusammenarbeit mit I. G. Usoskin (Sodankylä Geophysical Observatory, Finnland); C. Taricco (Universität Turin, Italien); N. Bhandari (Basic Sciences Research Institute, Ahmedabad, Indien); G. A. Kovaltsov (Ioffe Physical-Technical Institute, St. Petersburg, Russland).

MICA – Mirror Coronagraph for Argentina.- R. Schwenn in Zusammenarbeit mit Instituto de Astronomia y Fisica del Espacio (IAFE), Buenos Aires, Argentinien; Observatorio Astronomico Felix Aguilar (OAFA), Universität Juan, Argentinien; MPE, Garching.

Microflares and the solar emission distribution.- S. K. Solanki in Zusammenarbeit mit A. Pauluhn (Paul Scherrer Institut, Villingen, Schweiz).

Molecular Zeeman effect.- S. K. Solanki in Zusammenarbeit mit S. Berdyugina, D. M. Fluri (ETH Zürich, Schweiz); P. A. Braun (Universität St. Petersburg, Russland.)

Moving magnetic features.- S. K. Solanki in Zusammenarbeit mit J. Wang, J. Zhang (National Astronomical Observatories, Beijing, VR China).

Nonlinear force-free coronal magnetic fields (NLFFF-consortium).- T. Wiegelmann in Zusammenarbeit mit K. Schrijver (LMSAL, Palo Alto, USA).

Numerical simulations of coronal loop oscillations.- S. K. Solanki und T. J. Wang in Zusammenarbeit mit M. Selwa, K. Murawski (UMCS Lublin, Polen); U. Shumlak (University of Washington, Seattle, USA); G. Toth (University of Michigan, Ann Arbor, USA).

Plasmawechselwirkungen extrasolarer Planeten mit ihrem Stern.- J. Büchner in Zusammenarbeit mit U. Motschmann (Technische Universität Braunschweig).

PROBA II – LYRA (Large Yield Radiometer).- U. Schühle in Zusammanarbeit mit: J.-F. Hochedez, A. BenMoussa, D. Berghmans, A. Theissen, V. Delouille, B. Nicula, L. Wauters, R. Van der Linden, A. Zhukov, F. Clette (Royal Observatory of Belgium (ROB), Brüssel, Belgien); W. Schmutz, S. Koller, H. Roth, E. Rozanov, I. Rüedi, C. Wehrli (Physikalisch-Meteorologisches Observatorium Davos (PMOD) and World Radiation Center, Davos, Schweiz); K. Haenen, V. Mortet, Z. Remes, M. Nesládek, M. D'Olieslaeger (Institute for Materials Research, Diepenbeek, Belgien); Y. Stockman, J.-M. Defise, J.-P. Halain, P. Rochus (Centre Spatial de Liège (CSL), Angleur, Belgien); D. Gillotay, D. Fussen, M. Dominique, F. Vanhellemont (Belgian Institute for Space Aeronomy, Brüssel, Belgien); V. Slemzin, A. Mitrofanov (Lebedev Physical Institute, Moskau, Russland); D. McMullin (Naval Research Laboratory (NRL), Washington, DC, USA); M. Kretzschmar, (Istituto Fisica dello Spazio Interplanetario (IFSI), Rom, Italien); R. Petersen, M. Nesládek, M. D'Olieslaeger (IMEC, Division IMOMEC, Diepenbeek, Belgien); J. Roggen (IMEC, Louvain, Belgien); S. Koizumi (Advanced Materials Laboratory, National Institute for Materials Science, Tsukuba, Japan); H. Amano (Department of Materials Science and Engineering, Meijo University, Nagoya, Japan); A. Soltani (Institut d'Electronique, de Microélectronique et de Nanotechnologie, Villeneuve d'Ascq, Frankreich).

PROBA II – SWAP (Sun Watcher using APS Detectors).- U. Schühle in Zusammenarbeit mit D. Berghmans, J. F. Hochedez, B. Nicula, G. Lawrence, A. C. Katsyiannis, R. Van der Linden, A. Zhukov, F. Clette (Royal Observatory of Belgium, Solar Physics, Brüssel, Belgien); J. M. Defise, J. H. Lecat, P. Rochus, E. Mazy, T. Thibert (Centre Spatial de Liège, Angleur, Belgien); P. Nicolosi, M. G. Pelizzo (University of Padova, Padova, Italien); V. Slemzin (Lebedev Physical Institute, Moskau, Russland).

Quellregionen des Sonnenwindes.- *Langfristige Zusammenarbeit im Bereich der Theorie und Datenauswertung, insbesondere an den alten Helios Plasma-Daten und den aktuellen SUMER Daten.* E. Marsch in Zusammenarbeit mit C.-Y. Tu (Peking University, Beijing, China); L.-D. Xia (University of Science and Technology, Heifei, Anhui, China).

Quiet Sun magnetism.- A. Lagg und S. K. Solanki in Zusammenarbeit mit E. V. Khomenko, M. Collados, J. Trujillo Bueno, B. Ruiz Cobo, M. J. Martínez González (Instituto de Astrofisica de Canarias, Teneriffa, Spanien).

RAISE – Rapid Acquisition Imaging Spectrograph Experiment.- U. Schühle in Zusammenarbeit mit D. Hassler, D. Slater, C. DeForest, S. McIntosh (Southwest Research Institute, San Antonio, USA); T. Ayres (University of Colorado, Boulder, USA); R. Thomas (NASA GSFC, Greenbelt, USA); H. Michaelis (Institut für Planetenforschung, DLR, Berlin).

ROSETTA – CONSERT (Radio Tomography Project).- E. Nielsen und T. Hagfors in Zusammenarbeit mit Laboratoire de Planétologie, University of Grenoble, Frankreich; ESA.

ROSETTA – COSAC (PHILAE).- F. Goesmann, R. Roll in Zusammenarbeit mit F. Raulin (LISA - UMR 7583, Universités Paris 12 & Paris 7, Faculté des Sciences, Créteil, Frankreich); U. J. Meierhenrich (Université Nice-Sophia Antipolis L.C.M.B.A. et UMR 6001 CNRS, Nice, Frankreich); C. Szopa (Service d'Aéronomie (SA), UMR CNRS 7620, IPSL, Verrières le Buisson, Frankreich).

ROSETTA – COSIMA.- J. Kissel (PI bis 15. Mai 2005), M. Hilchenbach (Co-PI, PI seit 15. Mai 2005), H. Krüger (Co-I), H. Böhnhardt(Co-I) und H. Fischer (engineer) in Zusammenarbeit mit K. Altwegg (Physikalisches Institut, Universität Bern, Schweiz); B. C. Clark (Lockheed Martin Astronautics, Denver, CO, USA); L. Colangeli (Istituto Nazionale di Astrofisica - Osservatorio Astronomico di Capodimonte, Napoli, Italien); H. Cottin, F. Raulin (LISA, Universites Paris 12 & 7, Creteil Cedex, Frankreich); S. Czempiel, J. Eibl, G. Haerendel, H. Höfner, P. Parigger (MPI für extraterrestrische Physik, Garching); C. Engrand (Centre de Spectrométrie Nucléaire et de Spectrométrie de Masse (CSNSM), Orsay, Frankreich); H. M. Fehringer, R. Schulz (ESA/ESTEC, Noordwijk, Niederlande); B. Feuerbacher (DLR, Köln); M. Fomenkova (Center for Astrophysics and Space Sciences, University of California, La Jolla, CA, USA); A. Glasmachers (Universität Wuppertal, Lehrstuhl für Messtechnik, Wuppertal); J. M. Greenberg (Raymond and Beverly Sackler Laboratory for Astrophysics, Leiden, Niederlande); E. Grün (MPI für Kernphysik, Heidelberg); H. Henkel, H. von Hoerner, A. Koch (von Hoerner und Sulger, Schwetzingen); K. Hornung (Universität der Bundeswehr LRT-7, Neubiberg); E. K. Jessberger, T. Stephan (Institut für Planetologie, Münster); F. R. Krueger (Ingenieurbüro Krueger, Darmstadt); G. Kurat (Naturhistorisches Museum, Wien, Austria); Y. Langevin (Institut d'Astrophysique, Orsay, Frankreich); F. Rüdenauer (Institut für Physik, Seibersdorf, Austria); J. Rynö, J. Silén (Finnish Meteorological Institute, Helsinki, Finnland); E. R. Schmid, W. Werther (Department of Analytical and Food Chemistry, Universität Wien, Austria); W. Steiger (ARC Seibersdorf Research GmbH Business Field Aerospace Technology, Seibersdorf, Austria); L. Thirkell, R. Thomas (Laboratoire de Phys. & Chim. de L'Environnement, Orléans, Frankreich); K. Torkar (Institut für Weltraumforschung, Graz, Austria); N. G. Utterback (Consultant, Sta. Barbara, CA, USA); K. Varmuza (Institut für Verfahrenstechnik, Umwelttechnik und Techn. Biowissenschaften, TU Wien, Austria); K. P. Wanczek (Institut für Anorganische und Physikalische Chemie, Universität Bremen); E. Zinner (Laboratory for Space Sciences, Washington University, St. Louis, MO, USA); H. Zscheeg (Abbott Laboratories Vascular Devices Ltd., Beringen, Schweiz).

ROSETTA – MIRO (Mirowave Instrument for the ROSETTA-Orbiter).- P. Hartogh, W. Ip und I. Mann in Zusammenarbeit mit S. Gulkis, M. Allen, M. Frerking, M. Hofstadter, M. Janssen, T. Spilker (JPL, Pasadena, USA); D. Muhleman (Caltech, Pasadena, USA); G. Beaudin, D. Bockelee-Morvan, J. Crovisier, P. Encrenaz, T. Encrenaz, E. Lellouch (Observatoire de Paris-Meudon, Frankreich); D. Despois (Observatoire de Bordeaux, Frankreich); H. Rauer (DLR, Berlin); P. Schloerb (University of Massachusetts, Amherst, USA).

ROSETTA – OSIRIS.- H. U. Keller, H. Sierks, S. F. Hviid, R. Kramm und M. Küppers in Zusammenarbeit mit C. Barbieri, F. Angrilli (CISAS, University of Padova, Padova, Italien); P. Lamy, L. Jorda (Laboratoire d'Astrophysique de Marseille, Marseille, Frankreich); H. Rickmann (Department of Astronomy and Space Physics, Uppsala, Schweden); R. Rodrigo, L. M. Lara (Instituto de Astrofísica de Andalucía – CSIC, Granada, Spanien); D. Koschny (Research and Scientific Support Department, ESTEC, Noordwijk, Niederlande); M. F. A'Hearn (Department of Astronomy University of Maryland, USA); L. Sabau (Instituto Nacional de Técnica Aersospacial, Torrejon de Ardoz, Spanien); M. E. Bailey (Armagh Observatory College Hill, Armagh, Northern Ireland); M. A. Barucci (Observatoire de Paris, Meudon, Frankreich); J.-L. Bertaux (Service d'Aéronomie du CNRS, Verrière-le-Buisson, Frankreich); J. A. Burns (Cornell University, Ithaca, USA); M. Fulle (Osservatorio Astronomica de Trieste, Trieste, Italien); F. Gliem, H. Michalik (Institut für Datentechnik und Kommunikationsnetze, Braunschweig); W.-H. Ip (Institute of Space Science, National Central University, Chung Li, Taiwan); E. Kührt (DLR/Institut für Planetenforschung, Braunschweig); A. Sanz (Universidad Politécnica de Madrid, Madrid, Spanien); N. Thomas (Physikalisches Institut der Universität Bern, Bern, Schweiz); G. Cremonese, R. Ragazzoni (INAF, Osservatorio Astronomico, Padova, Italien).

ROSETTA – PHILAE (ROSETTA Lander).- H. Böhnhardt und R. Roll in Zusammenarbeit mit DLR Köln-Wahn; J. P. Bibring (IAS, Paris, France).

ROSETTA – RTOF/ROSINA.- *Bau der Elektronik für das Massenspektrometer RTOF (Reflection Time-of-Flight).* A. Korth und U. Mall in Zusammenarbeit mit H. Balsiger (PI), Universität Bern, Schweiz; BIRA, Brüssel, Belgien; CESR, Toulouse, Frankreich; IPSL, Saint Maur, Frankreich; IDA, Technische Universität Braunschweig; University of Michigan, Ann Arbor, MI, USA; Southwest Research Institute, San Antonio, TX, USA; Universität Giessen.

Secular evolution of solar activity.- M. Schüssler und S. K. Solanki in Zusammenarbeit mit I. Usoskin (University Oulu, Finnland); B. Kromer (Institut für Umweltphysik, Heidelberger Akademie der Wissenschaften); J. Beer (EAWAG, Dübendorf, Schweiz) und M. Korte (GeoForschungsZentrum Potsdam).

SEIS (Exomars).- U. Christensen und R. Roll in Zusammenarbeit mit P. Lognonne (IPGP, Paris, Frankreich).

Simulation der Dynamik der Sonnenkorona.- J. Büchner in Zusammenarbeit mit A. Otto (University of Alaska, Fairbanks, USA).

SMART-1 SIR.- U. Mall in Zusammenarbeit mit Prof. M. Banaszkiewicz (Polish Academy of Science, Polen).

SOFIA–GREAT (SOFIA – German Receiver for Astronomy at THz frequencies).- P. Hartogh in Zusammenarbeit mit R. Guesten, K. Menten, P. v. d. Wal (MPI für Radioastronomie, Bonn); R. Schieder, J. Stutzki (Universität Köln); H. W. Hübers (DLR-Berlin); H. P. Röser (Institut für Raumfahrtsysteme, Universität Stuttgart).

SOHO – CELIAS.- W. I. Axford, H. Grünwaldt (Lead Co-I CTOF), M. Hilchenbach (Lead Co-I STOF) und E. Marsch in Zusammenarbeit mit P. Bochsler (PI) (Physikalisches Institut, Universität Bern, Schweiz); D. Hovestadt (PI hardware phase), B. Klecker (Deputy PI), P. Laeverenz, M. Scholer (MPI für Extraterrestrische Physik, Garching); F. M. Ipavich (Lead Co-I MTOF), M. A. Coplan, G. Gloeckler, S. E. Lasley, J. A. Paquette (Department of Physics and Astronomy and IPST, University of Maryland, College Park, MD, USA); P. Bochsler (PI), H. Balsiger, A. Bürgi, J. Fischer, P. Wurz (Physikalisches Institut, Universität Bern, Schweiz); R. Wimmer-Schweingruber, Karin Bamert (Extraterrestrische Physik, University of Kiel); J. Geiss, R. Kallenbach (International Space Science Institute, Bern, Schweiz); F. Gliem (Lead Co-I DPU), K.-U. Reiche (Institut für Datentechnik und Kommunikationsnetze, TU Braunschweig); D. L. Judge, H. S. Ogawa (Space Science Center, University of Southern California, Los Angeles, CA, USA); G. G. Managadze, M. I. Verigin (Institute for Space Physics, Moskau, Russland); A. B. Galvin, H. Kucharek, M. A. Lee, Y. Litvinenko, E. Möbius (EOS, University of New Hampshire, Durham, NH, USA); M. Neugebauer (Jet Propulsion Laboratory, Pasadena, CA, USA); K. C. Hsieh (Department of Physics, University of Arizona, Tucson, AZ, USA); D. McMullin (Space Science Division, Naval Research Laboratory, Washington, DC, USA); A. Czechowski (Space Research Center, Polish Academy of Sciences, Warschau, Polen).

SOHO – LASCO (Large Angle and Spectrometric Coronagraph).- R. Schwenn und B. Inhester in Zusammenarbeit mit R. Howard (PI) (Naval Research Laboratory, Washington, USA); Laboratoire d'Astronomie Spatiale, Marseille, Frankreich; Universität Paris, Frankreich; Observatoire de Paris, Frankreich; University of Birmingham, UK.

SOHO – SUMER.- *Solar and Heliospheric Observatory – Solar Ultraviolet Measurements of Emitted Radiation.* W. Curdt, D. E. Innes, E. Marsch, U. Schühle, S. K. Solanki, T. Wang und L. Teriaca in Zusammenarbeit mit E. Landi, U. Feldman (Naval Research Laboratory (NRL), Washington, USA); P. Lemaire, A. H. Gabriel, J.-C. Vial (Institut d'Astrophysique Spatiale (IAS), Orsay, Frankreich); A. I. Poland (GSFC, Greenbelt, USA); M.C.E. Huber (Schweiz); J. Hollandt (PTB, Berlin); O. Siegmund (SSL, Berkeley, CA, USA); D. Hassler (SWRI, Boulder, USA); G. A. Doschek, U. Feldman, J. T. Mariska (NRL, Washington, USA); P. G. Judge (HAO, Boulder, USA); N. Brynildsen, M. Carlsson, P. Maltby, O. Kjeldseth-Moe (ITA, Oslo, Norwegen); P. Brekke (ESA/GSFC, Greenbelt, USA); H. P. Warren (HSCA, Cambridge, USA); B. N. Dwivedi (DAP, Varanasi, Indien); C.-Y. Tu (DG, Peking, China); H. Peter (KIS, Freiburg); J. G. Doyle (Armagh Observatory, Irland); P. Heinzel (Czech Academy); A. Pauluhn (ISSI Bern, Schweiz).

Solar Flare Telescope.- T. Wiegelmann in Zusammenarbeit mit T. Sakurai (National Astronomical Observatory, Japan).

Solar infrared spectropolarimetry.- N. Krupp, A. Lagg, S. K. Solanki und J. Woch in Zusammenarbeit mit M. Collados (Instituto de Astrofisica de Canarias, Teneriffa, Spanien).

Solar irradiance variations.- S. K. Solanki und N. Krivova in Zusammenarbeit mit Y. Unruh (Imperial College, London, UK); T. Wenzler (ETH Zürich, Schweiz).

Solar Orbiter: EUI.- U. Schühle, W. Curdt, L. Teriaca, E. Marsch und S. K. Solanki in Zusammenarbeit mit T. Apporchaux, J.-C. Vial, F. Auchere (Institut d'Astrophysique Spatiale, Paris, Frankreich); J.-F. Hochedez, A. BenMoussa (Royal Observatory of Belgium, Brüssel, Belgien); J. M. Defise (Centre Spatial de Liege, Liege, Belgien); L. Harra, J. Sun, D. Williams (Mullard Space Science Laboratories, London, UK).

Solar Orbiter: EUS.- W. Curdt, U. Schühle, L. Teriaca, E. Marsch und S. K. Solanki in Zusammenarbeit mit R. Harrison, P. R. Young, E. C. Sawyer (Rutherford Appleton Laboratory (RAL), Oxfordshire, UK); R. Thomas (GSFC, NASA, Washington, USA); L. Poletto (National Institute for the Physics of Matter, Padua, Italien); G. Tondello (University of Padua, Italien).

Solar Orbiter: VIM.- S. K. Solanki, W. Curdt, A. Gandorfer, L. Gizon, H. Hartwig, J. Hirzberger, A. Lagg, U. Schühle, G. Tomasch und J. Woch in Zusammenarbeit mit V. Martinez Pillet (Instituto de Astrofísica de Canarias, IAC, La Laguna, Spanien); T. Appourchaux (Institut d'Astrophysique Spatiale, IAS, Paris, Frankreich); M. Sigwarth, (Kiepenheuer-Institut für Sonnenphysik, KIS, Freiburg); G. Scharmer (Institute for Solar Physics, Stockholm, Schweden); M. Carlsson, (Institutt for teoretisk astrofysikk, Oslo, Norwegen).

Solare Stereoskopie.- B. Inhester in Zusammenarbeit mit ISSI Bern; T. Dudoc de Witt (CNRS, Orleans, Frankreich); A. Vouridas (NRL, Washington, USA); J.-F. Hochedez (ROB, Brüssel, Belgien); A. Llebaria (LAS, Marseille, Frankreich); J. P. Wuelser (LMSAL, Palo Alto, USA); F. Auchere (IAS, Orsay, Frankreich).

Spitzer and ESO observations of Oort Cloud Comets during their sojourns through the Solar Systems.- H. Böhnhardt in Zusammenarbeit mit N. Biver (Observatory Paris-Meudon, Frankreich); P. Ehrenfreund (University Leiden, Niederlande); D. Harker (University San Diego, USA); M. Kelley (Joint Astronomy Center, USA); S. Lederer (University San Bernardino, USA); D. Prialnik, E. Beer-Harari (University Tel Aviv, Israel); D. Wooden (PI) (NASA Ames Res. Center, Moffett Fields, USA); C. Woodward (University Minnesota, USA).

Starspots.- A. Semenova und S. K. Solanki in Zusammenarbeit mit S. Berdyugina (ETH Zürich, Schweiz).

STEREO – IMPACT/SIT.- *Bau einer Flugzeit-Elektronik für das SIT-Instrument (Suprathermal Ion Telescope).* A. Korth, U. Mall und V. M. Vasyliūnas in Zusammenarbeit mit J. Luhmann (PI), UC Berkeley Space Science Laboratory, USA; NASA GSFC, USA; California Institute of Technology, USA; University of Maryland, USA; Centre d'Etude Spatiale des Rayonnements, Frankreich; Los Alamos National Laboratory, USA; Jet Propulsion Laboratory, USA; ESA/ESTEC - European Space and Technology Center, Niederlande; CNRS Observatoire Midi-Pyrenees and Observatoire de Paris, Frankreich; University of California, Los Angeles, USA; SAIC, Science Applications, USA; International Corporation, USA; NOAA Space Environment Center, USA; University of Michigan, USA.

STEREO – SECCHI (Sun Earth Connections Coronal and Heliospheric Investigation).- R. Schwenn und B. Inhester in Zusammenarbeit mit R. Howard (PI), Naval Research Laboratory, Washington, USA; University of Michigan, USA; Applied Physics Laboratory, Johns Hopkins University, Laurel, USA; GSFC, Greenbelt, USA; Lockheed Martin Palo Alto Research Laboratory, Stanford, USA; Stanford University, Stanford, USA; Boston College, Boston, USA; Jet Propulsion Laboratory, Pasadena, USA; SAIC, San Diego, USA; Mullard Space Science Center, UK; University of Birmingham, UK; Laboratoire d'Astronomie Spatiale, Marseille, Frankreich; Universität Paris, Frankreich; Observatoire de Paris, Frankreich; Universität Lüttich, Belgien; Universität Kiel.

Structure of sunspots.- J. M. Borrero, A. Lagg, S. K. Mathew, S. K. Solanki und N. A. Krivova in Zusammenarbeit mit L. Bellot Rubio (Instituto de Astrofísica de Andalucía, Granada, Spanien); M. Collados (Instituto de Astrofisica de Canarias, Teneriffa, Spanien); H. Socas Navarro, B. Lites (High Altitude Observatory, Boulder, USA).

Structure of the solar chromosphere.- S. K. Solanki in Zusammenarbeit mit M. Loukitcheva (University St. Petersburg, Russland); S. White (University of Maryland, Greenbelt, USA); M. Carlssson (University Oslo, Norwegen).

SUNRISE.- *Ballongetragenes 1-m Sonnenteleskop für hochauflösende spektro-polarimetrische Beobachtungen der Sonnenatmosphäre.* S. K. Solanki, P. Barthol, A. Gandorfer und M. Schüssler in Zusammenarbeit mit V. Martinez-Pillet (Instituto de Astrofisica de Canarias, Teneriffa, Spanien), W. Schmidt (Kiepenheuer-Institut für Sonnenphysik, Freiburg), B. W. Lites (High Altitude Observatory, NCAR, Boulder, USA); (Lockheed Martin Solar and Astrophysical Lab, Palo Alto, USA).

Surface exploration of Kuiper Belt Objects.- H. Böhnhardt (PI) in Zusammenarbeit mit S. Bagnulo (ESO, Santiago de Chile); A. Barucci (Observatory Paris-Meudon, Frankreich); I. Belskaya (University Kharkov, Ukraine); W. Grundy (University Flagstaff, USA); T. Herbst (MPI für Astronomie, Heidelberg); L. Kolokolova (University Maryland, College Park, USA); K. Muinonen (University Helsinki, Finnland).

The YORP effect in asteroid (54509) 2000PH5.- H. Böhnhardt in Zusammenarbeit mit A. Fitzsimmons (PI), S. Lowry (University Belfast, GB); P. Pravec (Ondrejov Observatory, Slovakei).

Time-Distance Helioseismology with Data from the MDI Structure Program.- L. Gizon und M. Roth in Zusammenarbeit mit J. G. Beck (Stanford University, Stanford, USA).

Topologische Untersuchungsmethoden und Anwendungen.- J. Büchner in Zusammenarbeit mit E. Priest (University of St. Andrews, Schottland, UK).

Topology of coronal magnetic fields.- T. Wiegelmann in Zusammenarbeit mit E. Priest, R. Maclean (University St. Andrews, UK).

Ulysses – DUST.- H. Krüger (PI) und J. Kissel in Zusammenarbeit mit N. Altobelli, C. Polanskey (Jet Propulsion Laboratory, Pasadena, CA, USA); B. Anweiler, D. Linkert, G. Linkert, R. Srama (MPI für Kernphysik, Heidelberg); E. Grün (MPI für Kernphysik, Heidelberg und Hawaii Institute of Geophysics and Planetology, Honolulu, HI, USA); S. F. Dermott, B. A. Gustafson (University of Florida, Gainesville, FL, USA); A. L. Graps (INAF-Istituto di Fisica dello Spazio Interplanetario, CNR - ARTOV, Rom, Italien); D. P. Hamilton (University of Maryland, College Park, MD, USA); M. S. Hanner (Jet Propulsion Laboratory, Pasadena, CA, USA); M. Horany (Laboratory for Atmospheric and Space Physics, Univ. of Colorado, Boulder, CO, USA); M. Landgraf (ESA/ESOC, Darmstadt); B. A. Lindblad (Lund Observatory, Lund, Schweden); I. Mann (Institut für Planetologie, Universität Münster); J.A.M. McDonnell (Planetary and Space Science Research Institute, Milton Keynes, UK); G. E. Morfill (MPI für Extraterrestrische Physik, Garching); G. Schwehm (ESTEC, Noordwijk, Niederlande).

Ulysses – EPAC/GAS.- *Teilchenspektrometer zur Messung energiereicher geladener Teilchen im interplanetaren Raum und zur Messung interstellaren neutralen Heliums (Datenauswertung).* N. Krupp, J. Woch, M. Witte und M. Fränz in Zusammenarbeit mit B. Blake (Aerospace Corporation, USA); J. Quenby (Imperial College London, UK); M. Yamauchi (IRF, Schweden).

Ulysses – SWICS (Solar Wind Ion Composition Spectrometer).- L. Rodriguez, J. Woch und M. Fränz in Zusammenarbeit mit R. von Steiger (ISSI, Bern, Schweiz).

Ulysses – URAP (Jupiter's radio emission).- C. H. Barrow in Zusammenarbeit mit R. J. MacDowall, M. L. Kaiser (NASA GSFC, USA); A. Lecacheux, P. Zarka (Meudon Observatory, Frankreich).

Venus Express – ASPERA-4 (Analyzer of Space Plasmas and EneRgetic Atoms).- M. Fränz, J. Woch, N. Krupp, E. Dubinin, E. Roussos, C. Martinecz und J. Kleimann in Zusammenarbeit mit S. Barabash (PI), R. Lundin (IRF, Kiruna, Schweden); D. Winningham, R. Frahm (SWRI, San Antonio, USA); P. Wurz (Universität Bern, Schweiz); A. Coates (MSSL, London, England); M. Grande (RAL, Chilton, England); C. C. Curtis (UoA, Tuscon, USA); J. A. Sauvaud, A. Fedorov (CESR, Toulouse, Frankreich); E. Kallio (FMI, Helsinki, Finnland); S. Orsini (IFSI, Rom, Italien).

Venus Express – PFS.- D. Titov in Zusammenarbeit mit V. Formisano, D. Grassi (Institute of Physics of Interplanetary Space (IFSI-INAF), Rom, Italien); N. Ignatiev (Space Research Institute (IKI), Moskau, Russland).

Venus Express Scientific Support.- D. Titov in Zusammenarbeit mit H. Svedhem, R. Hoofs, D. Koschny, D. Meritt, D. McCoy, H. Eggel, J. Reddy (ESTEC-ESA, Noordwijk, Niederlande).

Venus Express – VIRTIS.- D. Titov in Zusammenarbeit mit P. Drossart (Observatoire de Paris, Meudon, Frankreich); G. Piccioni (Institute for Space Astrophysics (IAS-INAF), Rom, Italien).

Venus Express – VMC (Venus Monitoring Camera).- D. Titov in Zusammenarbeit mit H. Michalik, B. Fiethe, C. Dierker, B. Osterloh (Institut für Datentechnik und Kommunikationsnetze (IDA, TU Braunschweig)); R. Jaumann, Th. Behnke, Th. Roatsch, K.-D. Matz (Institut für Planetenforschung); N. Ignatiev, D. Belyaev, Yu. Nikol'sky (Space Research Institute (IKI), Moskau, Russland).

WASPAM / CAWSES.- P. Hartogh, C. Jarchow und L. Song in Zusammenarbeit mit G. Hansen (NILU, Tromsö, Norwegen); U. P. Hoppe (FFI, Kjeller, Norwegen); M. Gausa (ALOMAR, Andenes, Norwegen); U. von Zahn, F. J. Lübken, U. Berger, G. Sonnemann (IAP Kühlungsborn); G. Nedoluha, M. Stevens (NRL, Washington, USA); P. Espy (British Antarctic Survey, Cambridge, UK); Y. Kasai (NICT, Applied Research and Standards Department, Tokyo, Japan).

Projektförderungen durch das Bundesministerium für Bildung und Forschung (BMBF) und ESA / Project grants provided by BMBF and ESA

DLR: ASPERA-3 (MEX), BepiColombo (BELA), BepiColombo (MPPE-MSA), BepiColombo (PICAM/SERENA), Cassini MIMI/LEMMS, Chandrayaan-1 (SIR-2), Cluster/CAA (50%), Cluster/RAPID, DAWN, Galileo EPD im Rahmen des Projektes ULYGAL, HIFI-WBS, IDS (Interdisciplinary Study of the Outer Planets), Rosetta–COSAC, Rosetta–COSIMA, Rosetta–MIRO, Rosetta–OSIRIS, Rosetta–PHILAE, Rosetta–ROSINA/RTOF, SOHO–LASCO, SOHO–SUMER, STEREO–SECCHI, SUNRISE, Ulysses EPAC/GAS im Rahmen des Projektes ULYGAL

ESA: ASPERA-4 (VEX) (über ASTRIUM), BepiColombo–BELA, Cluster/CAA (50%), Europlanet, PROBA2/SWAP, PROBA2/LYRA, Rosetta–MIRO, Rosetta–PHILAE, Solar Orbiter, Venus Express (VMC), Venus Express Scientific Support

NASA: RAISE

JPL: DAWN

Lehrtätigkeiten / Teaching

Von Mitgliedern des MPS wurden an mehreren, inländischen und ausländischen Universitäten verschiedene Vorlesungen gehalten:/
MPS scientists have lectured at a number of German and foreign universities:

Georg-August-Universität zu Göttingen

Prof. Dr. J. Büchner
WS 2003/2004: Introduction into astrophysical plasmas and particles
SS 2004: Numerical methods for astrophysical plasmas and particles
WS 2004/2005: Astro-Plasmen und Teilchen: 1. Grundlagen
SS 2005: Mathematische Methoden der Astroplasmen und Teilchen

Prof. Dr. J. Büchner und Dr. L. Gizon
WS 2005/2006: Physikalische Grundlagen des Weltraumwetters

Prof. Dr. U. Christensen
WS 2004/2005: Einführung in die Planetologie

Prof. Dr. K. Jockers
WS 2003/2004: Lichtstreuung an Teilchen und an Regolith

SS 2004: Die Entstehung von Sonnensystemen
WS 2004/2005: Asteroiden und Kometen
SS 2005: Die Entstehung von Sonnensystemen

Prof. Dr. R. Schwenn
WS 2003/2004: Explosive Prozesse im Sonnensystem: Flares, Massenauswürfe, interplanetare Stoßwellen

Universität Bremen, Fachbereich Geowissenschaften

Dr. Björn Grieger
WS 2004/2005: 3d-Datenvisualisierung
WS 2005/2006: Geostatistik

Universität Heidelberg

Dr. Harald Krüger
SS 2004: Seminar für mittlere Semester "Das äußere Sonnensystem"
SS 2005: Seminar für mittlere Semester "Terrestrische Planeten und Asteroiden"

IMPRS Vorlesungen / IMPRS lectures

Cosmology, 2 – 5 March 2004 (Hoyng)

How to write a scientific paper, 2 March 2004 (Solanki)

Presentation skills, 3 March 2004 (Degenhardt)

How to write a grant proposal, 4 March 2004 (Glassmeier)

Data analysis and numerical methods, 18 – 21 October 2004 (Lagg, Motschmann, Schmitt, Otto)

Introduction to solar physics, 31 January – 4 February 2005 (Solanki)

Hydrodynamics, 31 January – 4 February 2005 (Ferriz Mas)

Project management, 23 – 25 May 2005 (Madauss)

Magnetospheres – Earth and outer planets, 12 – 16 September 2005 (Vasyliunas, Krupp, Daly)

Planetary atmospheres, 12 – 16 September 2005 (Titov, Grieger)

Solar System Seminar, 23 seminar days with 70 talks by students and 18 tutorial talks by guests (Schmitt)

Weitere Lehrtätigkeiten oder Kurse / Other lectures or courses

Dr. P. Hartogh
Microwave remote sensing in solar system research, Planetary Sciences Summer School, Weihai, Shandong, China, August 15 – 26, 2005.

Dr. N. Krupp
Magnetospheric Physics-Jupiter and Saturn compared to Earth, Part 1-4, Planetary Sciences Summer School, Weihai, Shandong, China, August 24, 2005.

Dr. D. Schmitt / Prof. Dr. R. Schwenn / Prof. Dr. M. Schüssler:
"Die Sonne – der unruhige Stern nebenan", mehrere Kurse am XLAB (Göttinger Experimentallabor für Junge Leute e.V.), 2004.

Prof. Dr. M. Schüssler
Schülervorträge am Hainberg-Gymnasium Göttingen (Juli 2005) und Eichsfeld-Gymnasium Duderstadt (Juli 2005).

Prof. Dr. R. Schwenn
Physics of the Heliosphere: An Introduction, Vorlesung (12 Stunden), 3rd El Leoncito Summer School of Solar Physics, San Juan, Argentinien, November 2005.

Dr. D. Titov
Lecture on Venus at the School on Space Physics, l'Aquila, Italy, July 2004.
Lectures on Venus science at the School on Space Physics, Planetary Sciences Summer School, Weihai, Shandong, China, August 15 – 26, 2005.

Mitgliedschaften in wissenschaftlichen Gremien / Memberships in scientific councils

Barrow C. H.: Fellow of the Royal Astronomical Society; International Astronomical Union (IAU) und American Astronomical Society.

Böhnhardt H.: International Astronomical Union (IAU), Commissions 15 and 51; COSPAR, Commission B und Astronomische Gesellschaft (AG).

Büchner J.: Leiter der Fachgruppe 1 "Erdnaher Weltraum" der AG Extraterrestrische Forschungen der Deutschen Physikalischen Gesellschaft; International Astronomical Union (IAU), Commission 10; COSPAR, Commission D; International Scientific Committee of the International Conferences on Space Plasma simulation (ISSS); Scientific Committee of the International School for Plasma-Astrophysics Varenna-Abastumani und Scientific Committee of the World Institute for Space Environmental Research (WISER).

Christensen U.: Advisory board / Center of Dynamics of Complex Systems, Universität Potsdam;

American Geophysical Union; Deutsche Akademie der Naturforscher Leopoldina; ESA Solar System Working Group; Executive Committee der International Association of Seismology and Physics of the Earth's Interior (IASPEI); Göttinger Akademie der Wissenschaften und Kommission für Geowissenschaftliche Hochdruckforschung der Bayerischen Akademie der Wissenschaften.

Curdt W.: German JOSO (Joint Organisation of Solar Observatories) representative und International Astronomical Union (IAU).

Daly P. W.: Cluster Science Data System, Implementation Working Group.

Fränz M.: European Geophysical Union und American Geophysical Union.

Gandorfer A.: THEMIS Scientific Advisory Council.

Grieger B.: Fakultät der International Max Planck Research School on Physical Processes in the Solar System and Beyond und Koordinator des European Planetary Network (EuroPlaNet).

Hartogh P.: Alomar Scientific Advisory Committee.

Hilchenbach M.: Solar Orbiter Payload Working Group.

Jockers K.: International Astronomical Union (IAU).

Krüger H.: Astronomische Gesellschaft und Division of Planetary Science of the American Astronomical Society.

Küppers M.: Division of Planetary Sciences of the American Astronomical Society.

Kuroda T.: The Japanese Society for Planetary Sciences.

Lagg A.: Telescope Allocation Committee (TAC): Vergabe von Beobachtungszeit an den deutschen Teleskopen auf Teneriffa.

Marsch E.: Chairman Science Definition Team der Solar Orbiter Mission der ESA (2004 – 2005) und Gutachterausschuss Extraterrestrik des DLR (seit 2001).

Rotvig J.: American Geophysical Union.

Schmitt D.: Studienkommission Physik, Universität Göttingen.

Schühle U.: ESA's "Solar Orbiter Payload Working Group".

Schüssler M.: Advisory Committee, High Altitude Observatory, NCAR, Boulder, CO, USA (bis 2005).

Schwenn R.: Science Definition Teams der NASA für die geplante Sentinel-Mission und "International Living With a Star" Working Group.

Solanki S. K.: Mitglied des wissenschaftlichen Beirats des High Altitude Observatory in Boulder, Colorado/USA, des Istituto Ricerche Solari Locarno (IRSOL) und der Gesellschaft für Wissenschaftliche Datenverarbeitung Göttingen; Stellvertretender Vorsitzender und Mitglied des Senatsausschusses des DLR; Mitglied des Berufungsausschusses und des Dreierausschusses des Senats des DLR und des Programmausschusses Extraterrestrik des DLR.

Titov D.: Vice-Chair of the ICPAE (International Committee on the Planetary Atmospheres and Evolution) und Chairman of the COSPAR Sub-commission C3.

Gutachtertätigkeiten / Review reports

Gutachtertätigkeiten für wissenschaftliche Zeitschriften/Reviews for scientific journals
(Die folgende Aufstellung soll nur eine kurze Übersicht über die Gutachtertätigkeiten von Wissenschaftlern des MPS für wissenschaftliche Zeitschriften geben. Angeführt sind die Namen der Gutachter (alphabetisch), die Zeitschriften sowie die Anzahl der in den Jahren 2004 und 2005 dafür gegebenen Gutachten./*In the following the names of the reviewers and the journals together with the total number of reviews per journal are listed.*)

Gutachter/Reviewers:

C. H. Barrow, H. Böhnhardt, J. Büchner, U. Christensen, W. Curdt, P. W. Daly, A. Gandorfer, L. Gizon, P. Hartogh, M. Hilchenbach, B. Inhester, K. Jockers, A. Korth, H. Krüger, N. Krupp, M. Küppers, U. Mall, E. Marsch, D. Schmitt, U. Schühle, R. Schwenn, S. K. Solanki, L. Teriaca, D. Titov, V. M. Vasyliūnas, J. Wicht, T. Wiegelmann, K. Wilhelm, J. Woch.

Zeitschriften/Journals:

Advances in Geosciences (2), Advances in Space Research (36), Annales Geophysicae (11), Applied Optics (1), Astra (2), Astronomy and Astrophysics (20), Astronomy and Astrophysics Letter (2), Astronomical Journal (1), Astrophysical Journal (10), Atmospheric Chemistry and Physics (ACP) (1), Canadian Journal of Physics (1), COSPAR (2), Earth, Moon and Planets (4), Earth & Planetary Science Letters (2), Geology (1), Geophysical & Astrophysical Fluid Dynamics (2), Geophysical Research Letters (18), HOB (3), Icarus (6), IEEE Transactions on Geoscience and Remote Sensing (1), IEEE Transactions on Microwave Theory and Techniques (1), Journal of Atmospheric and

Solar-Terrestrial Physics (3), Journal of Geophysical Research (33), Monthly Notices of the Royal Astronomical Society (1), Nature (7), Naturwissenschaften (1), Nonlinear Processes in Geophysics (8), Optics and Laser in Engineering (1), Physics of Plasmas (5), Physics of the Earth and Planetary Deep Interiors (2), Physical Review Letters (1), Planetary and Space Science (9), Proceedings of PRE VI Planetary Radio Emissions Workshop (3), Radio Science (1), Science (4), Solar Physics (8), Space Science Reviews (1),

Gutachtertätigkeiten anderer Art/Other types of reviews:

Böhnhardt H.: Observing Program Committee Panel C, European Southern Observatory, 2005; NASA adhoc review for the fly-by of the Stardust1 mission at comet Wild2, 2004; PhD thesis, Young-Yun Choi, Dept. of Geophysics and Planetary Sciences, University of Tel Aviv, Israel und 4 Personengutachten.

Büchner J.: Peer reviewer for: NASA (USA) (8), PPARC (UK) (2) und 2 Promotionsgutachten.

Christensen U.: Fachgutachter der DFG für Physik des Erdkörpers; Begutachtung von Projektanträgen beim DLR, Helmholtzgesellschaft, NSF, NERC, SNF und Gutachten in verschiedenen Berufungsverfahren.

Goesmann F.: Review of the gas chromatograph of the experiment Sample Analysis on Mars (SAM) of the American Mars Science Laboratory Mission (MSL)

Jockers K.: Personengutachten für Israel Science Foundation (1) und Humboldt-Stiftung (2).

Korth A.: Gutachter bei der Auswahl der Bepi-Colombo Nutzlast für den japanischen Mercury Magnetospheric Orbiter (MMO), ISAS/JAXA, Tokio, August 2004; im NASA Proposal Programm "Sun Earth Connections Geospace Supporting Research and Technology", Washington DC, USA, November 2004 und im Prüfungsausschuss für eine Doktorprüfung, Bergen, Norwegen, März 2005.

Marsch E.: Gutachten für die DFG, Forschungsprojekt, 2004; Research Proposal, FONDECYT, Santiago, Chile, 2005; The Royal Society, UK, Fellowship, 2005 und NASA GSFC, AGU Fellow, USA, 2005.

Schmitt D.: Gutachten für National Science Foundation und Deutsche Forschungsgemeinschaft.

Schüssler M.: Fachgutachter der DFG für Astronomie/Astrophysik (bis März 2004) und Gutachter für NSF (USA), ESA, EU und TU Graz.

Schwenn R.: Gutachten für Projektvorschlag beim Schweizerischen Nationalfonds.

Solanki S. K.: Gutachten für Deutsche Forschungsgemeinschaft (3); COST (1); ETH Zürich (1); MPG Projektantrag (1); Schweizerischen Nationalfonds (4); European Young Investigator Award (2); Österreichischen Wissenschaftsfonds (1) und etliche Personengutachten.

Vasyliūnas V. M.: Gutachten für AGU Books, 2004; Cambridge University Press, 2005 und Personengutachten, 2004 und 2005.

Woch J.: Gutachten für NASA (2) und PhD, Universität Oulu, Finnland.

Tätigkeiten als Convener bei wissenschaftlichen Tagungen / Converships during scientific meetings

Barrow C. H.: Sessions on "Solar System Radiophysics" at: EGU European Geosciences Union, 1st General Assembly, Nice, France, 25 – 30 April 2004; Joint AOGS 1st Annual Meeting and 2nd APHW Conference, Singapore, 5 – 9 July 2004; EGU, European Geosciences Union, 2nd General Assembly, Vienna, Austria, 24 – 29 April 2005; Joint AOGS 2nd Annual Meeting and 3rd APHW Conference, Singapore, 20 – 24 June 2005.

Böhnhardt H.: AOGS Singapore, Session 14 "Recent progress in solar system astronomy with large ground-based facilities", 20 – 24 June 2005.

Büchner J.: Co-convener "Theory and Simulation of Solar System Plasmas", European Geosciences Union, 1st General Assembly, Nice, France, 25 – 30 April 2004; Main Scientific organizer (Convener) "Reconnection at Sun and planets", Committee on Space Research (COSPAR), 35th Scientific Assembly, Paris, France, 2004; Main Scientific organizer (Convener) "Theory and Simulation of Solar System Plasmas", European Geosciences Union, 2nd General Assembly, Vienna, Austria, 24 – 29 April 2005.

Christensen U.: Co-Convener, Session "GD02/SM2/MPRG3 Core, CMB and Deep Mantle" (co-organized by MPRG & SM), European Geosciences Union, 2nd General Assembly, Vienna, Austria, 24 – 29 April 2005.

Grieger B.: Session "Terrestrial Planets, Pluto, and Satellites of Gas Giants" of the 3rd International Entry Probe Workshop in Athens, Greece, 27 June – 1 July 2005.

Hartogh P.: AOGS 1st Annual Meeting, Singapore, 5 – 9 July 2004; AOGS 2nd Annual Meeting, Singapore, 20 – 24 June 2005.

Hilchenbach M.: European Geophysical Union, Session “Solar atmosphere and solar wind”, 2004, 2005.

Krüger H.: Sitzung “Comets and Asteroids” (PS4) gemeinsam mit K. Jockers und G. Schwehm, EGU-Tagung 2005.

Krupp N.: European Geophysical Union, General Assembly: Session PS Outer Planets Plasma Physics, Nice, France, 25 – 30 April 2004; European Geophysical Union, General Assembly: Session PS Outer Planets Plasma Physics, Vienna, Austria, 24 – 29 April 2005.

Schüssler M.: Solar MHD: Theory and Observations – a High Resolution Perspective, NSO Sacramento Peak Observatory, Sunspot NM, USA, 18 – 22 July 2005.

Titov D.: Convener of the EGU Symposium “Science Investigations with Venus Express”, 2004, 2005; Convener of the AOGS Symposium “Planetary Atmospheres”, 2004.

Woch J.: 10th Scientific Assembly of IAGA, Convener, Special Session: GAIII13 “Fundamental processes: lessons from other magnetospheres”, Toulouse, France, 16 – 29 July 2005.

Organisation von Workshops / Workshop organisation

Böhnhardt H.: First Philae post-launch scientific workshop, Teistungenburg, 4. – 6. April 2005. IAU Symposium 229, “Asteroids, Comets, Meteors 2005”, Buzios, Rio de Janeiro, Brazil, 8. – 12. August 2005.

Büchner J.: DPG-AEF (Working group for extraterrestrial research) Conferences on the near Earth space, Kiel, 8. – 11. März 2004. Im Rahmen der Einsteinkonferenz der DPG, Berlin, März 2005.

Christensen U., J. Aubert, M. Buske, D. Tortorella, J. Wicht zusammen mit Prof. Hans-Peter Bunge und Prof. Heiner Igel (Institut für Allgemeine und Angewandte Geophysik, LMU München), Dr. Reinhard Boehler und Prof. Dr. Albrecht W. Hofmann (Max-Planck-Institut für Chemie, Mainz), Prof. Ulrich Hansen (Institut für Geophysik, Münster), Prof. Rainer Kind (GFZ Potsdam) und Prof. Andreas Tilgner (Institut für Geophysik, Universität Göttingen): 9th Symposium on Study of the Earth’s Deep Interior (SEDI), Garmisch-Partenkirchen, 4. – 9. Juli 2004.

Hartogh P.: Herschel HIFI Solar System Workshop, Katlenburg-Lindau, 14. – 15. Februar 2005.

Hilchenbach M.: COSIMA Workshop, Helsinki, Finnland, November 2005.

Jockers K., H. Krüger und G. Schwehm (ESTEC): PS4: Comets and Asteroids, General Assembly 2005 of European Geosciences Union.

Krupp N., E. Roussos, A. Lagg und J. Woch: Cassini MIMI Team Meeting, 21. – 22. April 2005.

Krupp N., G. H. Jones und B. Grieger: Europlanet: First Meeting of Activity N2 (Discipline Working Groups), Hotel Gesundbrunnen, Northeim, 21. – 23. November 2005.

Küppers M.: Organisation OSIRIS calibration workshops, 23. – 24. August 2004 und 16. – 17. Februar 2005.

Lagg A., D. Markiewicz-Innes und M. Schüssler: Chromospheric and Coronal Magnetic Fields (CC-MAG), MPS, Katlenburg-Lindau, 30. August – 2. September 2005.

Mall U.: Lunar Exploration – the Next Decade, 353-WE-Heraeus-Seminar, Bad Honnef, 6. – 10. Juni 2005.

Marsch E.: Deputy Organizer, “Solar Encounter, the Solar Orbiter Mission”, Session D2.4/E3.4, 35th COSPAR General Assembly, Paris, Frankreich, 18. – 25. Juli 2004.

Solanki S. K.: SOC Member of: First International Symposium on SPACE CLIMATE: Direct and Indirect Observations of Long-Term Solar Activity, Oulu, Finnland, 20. – 23. Juni 2004; IAU Symposium 226 “Coronal and Stellar Mass Ejections”, Beijing, China, 13. – 17. September 2004; Solar Variability and Earth Climate, Monte Porzio Catone, Italien, 27. Juni – 1. Juli 2005; “Chromospheric and Coronal Magnetic Fields”, Katlenburg-Lindau, 30. August – 2. September 2005.

Chromospheric and Coronal Magnetic Fields

The Max-Planck-Institut für Sonnensystemforschung hosted a workshop on magnetic fields in the solar chromosphere and corona from 30 August to 2 September, 2005 (Fig. 228). More than 100 guest scientists participated in this extremely productive meeting. The program started with a keynote lecture by Prof. E. N. Parker (Chicago University), with the title ‘The solar X-ray corona: consequence of an untidy magnetic topology’. There were sessions on measurements techniques, the coupling to the photosphere, the structure of the magnetic network and canopy, the generation and stability of magnetic structures and chromospheric/coronal seismology. The summary was given by Prof. E. R. Priest (St Andrews University).

(D. Innes, A. Lagg, S. K. Solanki)

Fig. 228: The participants

Öffentlichkeitsarbeit / Public relations

Dr. N. Krupp (Pressesprecher des MPS),Dr. B. Wöbke

Die Öffentlichkeitsarbeit am MPS erreichte in den Jahren 2004 und 2005 einen höheren Stellenwert. Dies zeigte sich sowohl in der TV- und Hörfunkpräsenz, aber auch in der Präsenz in Printmedien. Die Öffentlichkeitsarbeit am MPS beinhaltete aber auch öffentliche Vorträge, die Erich-Regener-Vortragsreihe, Ausstellungen, Institutsführungen, Pressenotizen.

TV- und Hörfunksendungen mit MPS-Beiträgen / TV- and radio coverage with MPS participation

Die Schwerpunkte der Radio- und Fersehsendungen in den Jahren 2004 und 2005 waren an den aktuellen Weltraumprojekten angelehnt. Zu Beginn 2004 gab es mehrere Sendungen über die Mission Mars Express. Im Februar und März 2004 lag der Schwerpunkt der Berichterstattung bei Rosetta (Vorberichte und Start). Einige Beiträge mit MPS-Beteiligung gab es auch zum Venustransit im Mai 2004. Einen weiteren Schwerpunkt gab es im Juli 2004 mit der Ankunft der Raumsonde Cassini am Saturn. 2005 begann spektakulär mit der Landung der Huygens-Sonde auf dem Saturnmond Titan. Die spektakulären Bilder der teilweise am MPS entwickelten Kamera wurden oft in TV-Beiträgen gezeigt oder erwähnt. Im Mai/Juni 2005 gab es einige TV-Beiträge über Sonne und Klima. Im Juli 2005 wurden Sendungen im Rahmen von Deep Impact und Beobachtungen der Rosetta-Kamera ausgestrahlt. Vorberichte und Start der Raumsonde Venus Express im September/Oktober 2005 rundeten die Berichterstattung ab.

Eine Übersicht aller uns bekannten Sendungen 2004/2005 ist in nachfolgender Tabelle 1 (siehe Seite 211) zusammengefasst.

Neue Institutsbroschüren und neuer Institutsfilm / New institute's brochures and video

Im Rahmen der Neustrukturierung und Umbenennung des Instituts wurden zwei neue Institutsbroschüren (deutsch und englisch) entworfen. Neben einer ausführlichen Version (Auflage 10.000 Stück) wurde auch eine für das Institut kostenlose Kurzbroschüre zusammen mit der JS-Gruppe (Auflage 1.000 Stück) erstellt.

Desweiteren wurde ein modular aufgebauter Institutsfilm erstellt, der zweisprachig (deutsch und englisch) auf DVD vervielfältigt wurde (Auflage 1.000 Stück mit Miniaturbroschüre).

Damit ist es nun möglich das Institut auch international darzustellen.

Tag der offenen Tür, 9. Juli 2005

Ein besonderes Highlight in der Öffentlichkeitsarbeit 2004/2005 war der Tag der offenen Tür am 9. Ju-

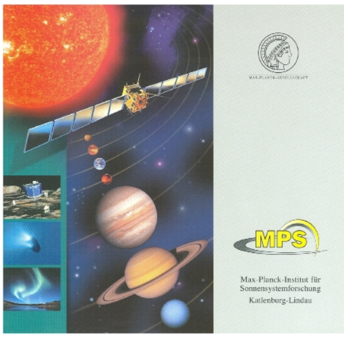

Abb. 229: Titelblatt der neuen Institutsbroschüre / Cover page of the new institute's brochure.

Abb. 230: DVD-Hülle des neuen Institutsfilms / Cover page of the new institute's DVD.

li 2005. Nach intensiver Vorbereitung von mehreren Monaten und nach überregionaler Ankündigung in Hörfunk- und Zeitungsartikeln (siehe Abb. 231) war die Resonanz mit etwa 8000 Besuchern überwältigend (siehe Luftaufnahme in Abb. 232).

Blickfang waren ein 1:1-Modell der Rosetta Raumsonde, ein 1:10-Modell einer Ariane 5-Rakete und ein 1:1-Modell der Huygens-Sonde. Mit im Programm waren außerdem:

- Vorträge
- Liveschaltung nach Chile
- Videofilme
- Führungen und Rundgänge
- Informationsstände
- ausgestellte Weltrauminstrumente
- Kinderprogramm
- Medaillenprägung
- Verpflegung
- Souvenirs

Die lokale Presse berichtete ausführlich über den sehr erfolgreichen Tag (siehe Zeitungsartikel im Göttinger Tageblatt Abb. 233).

Abb. 231: Plakat zum Tag der offenen Tür (9. Juli 2005) / Announcement of the public day (July 9, 2005)

Abb. 232: Luftaufnahme des MPS am Tag der offenen Tür (9. Juli 2005) / Aerial view of MPS on July 9, 2005 during the public day.

Pressenotizen / Press releases

Im Berichtszeitraum wurden die folgenden Pressenotizen herausgegeben:

- ESA-Mission "Rosetta" vor dem Start. 10. Februar 2004.
- Der "Dynamo der Erde" arbeitet effizienter als bisher angenommen. Max-Planck- Wissenschaftler haben bisherige Vorstellungen korrigiert, wie viel Energie benötigt wird, um das Magnetfeld der Erde zu erzeugen. 12. Mai 2004.

8000 Besucher kommen dem Weltraum näher

Riesenandrang im MPI für Sonnensystemforschung: Instrumente, Planeten, Raketen

Pathfinder-Mission zum Mars 1997: Mit 3-D-Brillen blicken Mario Döring und Thy Tran auf ein Bild der Kamera IMP. Deren Bildaufnahme-System wurde am MPS entwickelt und gebaut. Claus

Landet im Jahr 2014: Niklas und Lukas vor Philae-Modell.

Rosetta-Modell: Dr. Iancu Pardowitz erklärt Details der Sonde.

Das Interesse der Besucher war riesig: Sonnabend kamen mehr als 8000 Menschen ins Max-Planck-Institut für Sonnensystemforschung (MPS). Der Tag der offenen Tür brachte die Arbeit des Instituts und den Weltraum näher.

Rosetta ist unterwegs, um im November 2014 auf eine Bahn des Kometen Churyumow-Gerasimenko einzuschwenken. Dann wird es spannend: setzt der Lander Philae so auf, dass er wissenschaftliche Daten zur Erde senden kann? Dr. Iancu Pardowitz vom MPS erklärt bei einer Führung die Schwierigkeiten. Kaum Anziehungskraft hat der Komet. Philae ist so konstruiert, dass eine Harpune und Widerhaken an den Teleskopbeinen sich mit der Kometenoberfläche sofort verankern müssen.

Das MPS in Katlenburg-Lindau war seit 1960 an 80 erfolgreichen Weltraummissionen beteiligt. Sonne und Heliosphäre, Planeten und Kometen, Magnetosphären sind die Forschungsschwerpunkte. Dafür werden am MPS Weltrauminstrumente entwickelt und gebaut. In den Werkstätten wird vom Modell bis zum fertigen Gerät alles hergestellt.

Das 1946 gegründete Institut – damals für Ionosphärenforschung, später für Aeronomie und seit 2004 für Sonnensystemforschung – ist auch ein Ausbildungsbetrieb für durchschnittlich 26 Jugendliche. Mit Gesellen und Meistern stellten sie die Arbeit von Elektronikern, Feinmechanikern, Tischlern, Schlossern, Industriemechanikern oder Fachinformatikern vor.

Arbeit nach der Mission

„Wenn Rosetta landet, bin ich 17 Jahre alt", sagt ein Mädchen bei der Führung von Prof. Ulrich Christensen. „Und dabei ist das Projekt noch viel älter. Ende der achtziger Jahre hat die Planung für die Rosetta-Mission begonnen", erklärt Christensen. Für Weltraumforschung brauche es Zeit, langfristige Planung.

Nach einer Mission kommt die Auswertung von gewonnenen Daten. Neben Beobachtungen, Auswertungen von Bildern der Sonne oder denen der Cassini/Huygens-Mission zum Saturn und seinem Mond Titan ergänzen theoretische Arbeiten die Forschung von Wissenschaftlern, Stipendiaten und Doktoranden aus aller Welt im Institut. Ihr Ziel, Gemeinsamkeiten und Unterschiede der Planeten zu erkennen, das Wissen um Entstehung und Entwicklung des Sonnensystems zu vergrößern.

Wer sich darüber informieren wollte, konnte an einer der zahlreichen Führungen teilnehmen. Detaillierte Informationen gaben die Mitarbeiter an Infoständen und mit 14 Vorträgen, die die Reise zu Planeten und Kometen erklärten oder den Instrumentenbau für die Raumfahrt. Währenddessen konnten die jüngsten Besucher in Ruhe den Lander Philae basteln, malen oder sich am Spielbus Nomi austoben. Das Kinder-Quiz brachte Kinder und Eltern zu interessanten Stationen im Institut und mit richtigen Antworten zum Lösungswort: Rosetta. *Angela Brünjes*

Abb. 233: Ein Beispiel eines Zeitungsartikels im Göttinger Tageblatt mit Berichterstattung über den Tag der offenen Tür am MPS / Example of an article in newspapers (here Göttinger Tageblatt) reporting about the public day at MPS.

- MPAe im Wandel. Neuausrichtung der Forschung und Namensänderung des Max-Planck-Instituts für Aeronomie. 27. Mai 2004.
- Planetensonde "Cassini-Huygens" vor der Ankunft am Saturn. 3. Juni 2004.
- Otto-Hahn-Medaille für Alexander Vögler. 18. Juni 2004.
- Ein Arbeitsleben für die Weltraumforschung. Dr. Helmut Rosenbauer tritt in den Ruhestand. Neuer Institutsname ab 1. Juli 2004. 22. Juni 2004.
- Bremsmanöver Cassini. 26. Juni 2004.
- Welche Bedeutung hat die Sonne für das globale Klima? 2. August 2004.
- Der Sonnenwind sorgte für den Verlust der Mars-Atmosphäre. 23. September 2004.
- Sonne seit über 8000 Jahren nicht mehr so aktiv wie heute. 27. Oktober 2004.
- Schnappschüsse vom Titan mit deutscher Technik. 17. Januar 2005.
- Ein Pfannkuchen um Saturn. 25. Februar 2005.
- "Philae"-Arbeitstagung in Teistungenburg. 18. März 2005.
- Der Sonnenwind entsteht in koronalen Trichtern. Die ESA/NASA-Raumsonde SOHO bestimmt den Ursprung des schnellen Sonnenwinds in der Atmosphäre der Sonne. 22. April 2005.
- Max-Planck-Forscher beobachten Beschuss des Kometen Tempel. 27. Juni 2005.
- Max-Planck-Forscher beobachten Auswirkungen des Einschlags auf dem Kometen Tempel 1. Das Kamerasystem OSIRIS auf der Raumsonde ROSETTA misst dramatischen Helligkeitsanstieg. 5. Juli 2005.
- "Venus Express" – der Start steht bevor. 18. Oktober 2005.
- Organisiertes Windchaos auf dem Jupiter. Internationales Forscherteam erklärt mit neuen Computersimulationen die Entstehung der bandförmigen Windstrukturen auf dem Jupiter. 14. November 2005.
- "Huygens" enthüllt lebensfeindliche Welt auf Titan. 6. Dezember 2005.

Monatsthemen auf der MPS-Website /
Topics of the month at MPS-website

- August 2004: Erste Kometenbilder der OSIRIS-Kameras auf ROSETTA (Dr. Michael Küppers).
- Dezember 2004: OSIRIS fotografiert den Orionnebel M42 (Dr. Michael Küppers).
- Februar 2005: Cluster-Mission verlängert (Dr. Patrick Daly).
- April 2005: Plasmaströmungen in Koronalöchern folgen den koronalen Magnetfeldern (Dr. Thomas Wiegelmann).

Ausstellungsstände / Exhibition stands

Der mobile Ausstellungsstand, mit dessen Hilfe die wissenschaftliche Arbeit am Institut der Öffentlichkeit in verständlicher Form vorgestellt wird, wurde bei folgenden Anlässen ausgestellt:

- Hannover, Messe, Zukunftsinitiative "Go for High Tech" (Rosetta), 19. – 24. April 2004.
- Informationsmarkt zur Berufsfindung, Berufsbildende Schulen II, Northeim, 11. – 12. Mai 2004.
- Bonn (DLR), (Cassini/Huygens), 29. Juni 2004.
- Berlin, Ausstellung "Man & Space" im Automobil Forum Unter den Linden, (Cassini/Huygens), 6. – 8. Juli 2004.
- Lindau (MPS), (Cassini/Huygens), 14. – 31. Januar 2005.
- Informationsmarkt zur Berufsfindung, Berufsbildende Schulen II, Northeim, 26. – 27. April 2005.

- Göttingen, "2. Göttinger Astronomietage", (Verschiedenes), 10. – 11. September 2005.

Institutsführungen und Anfragen /
Institute tours and information

Im Jahr 2004 fanden 20 Führungen mit 437 Personen, im Jahr 2005 fanden 20 Führungen mit 401 Personen statt.

Weitere Veranstaltungen / Other arrangements

- Girl's Day für Schülerinnen der Klassen 5 – 10 der umliegenden Schulen (ca. 50 Teilnehmer), 22. April 2004.
- Ferienprogramm für Schüler der Gemeinde Katlenburg-Lindau: "Vakuum–Versuche mit dem leeren Raum", 20. Juli 2004.
- "Lange Nacht der Sterne" im MPS mit 391 Besuchern, 18. September 2004.
- Weihnachtsmarkt Lindau – mit mexikanischer Suppe (Pozole), 27. November 2004.
- Presseinformationsveranstaltung für Wissenschaftsjournalisten über Cassini/Huygens, 17. Dezember 2004.
- Girl's Day für Schülerinnen der Klassen 5 – 10 der umliegenden Schulen (ca. 50 Teilnehmer), 28. April 2005.
- "Tag der offenen Tür" am MPS mit ca. 8000 Besuchern, 9. Juli 2005.
- Ferienprogramm für Schüler der Gemeinde Katlenburg-Lindau: "Licht und Fa(e)rben – Mal' mir einen Regenbogen", 29. Juli 2005.
- Weihnachtsmarkt Lindau – mit spanischen Empanadas, 26. November 2005.
- Kinderveranstaltung zum Nikolaustag, 6. Dezember 2005.

Erich-Regener-Vortragsreihe /
Erich-Regener lecture series

Vorträge dieser Reihe wenden sich an in der Region wohnende Laien.

12. Februar 2004
Dieter Wagner (Kreisarchiv Göttingen): Lindau – Geschichte eines Eichsfelddorfes.

22. April 2004
Prof. Dr. Udo Backhaus (Universität Duisburg-Essen): Der Venusdurchgang am 8. Juni 2004. Die Wiederkehr eines sehr seltenen und historisch bedeutsamen astronomischen Ereignisses.

23. Juni 2004
Dr. Reinhard Roll (MPS, Katlenburg-Lindau): Der Rosetta-Lander: Ein Labor auf einem Kometen.

2. September 2004
Dr. Joachim Woch (MPS, Katlenburg-Lindau): Canyons, Wasser, Klimawandel – Europas Planetenmission Mars Express.

11. November 2004
Dr. Dörte Mehlert (Landessternwarte Heidelberg): Galaxien im jungen Universum.

2. Dezember 2004
Dipl.-Geologin Gisela Pösges (Zentrum für Rieskrater- und Impaktforschung Nördlingen): Der Impaktkrater Nördlinger Ries – ein kosmisches Ereignis formt eine einzigartige Landschaft.

17. Februar 2005
Dr. Felix Lühning (Bremen): Der Gottorfer Globus.

14. April 2005
Dr. Gerda Horneck (DLR Köln, Institut für Luft- und Raumfahrtmedizin): Astrobiologie – Ist Leben ein kosmisches Phänomen?

8. Juni 2005
Prof. Dr. Wolfhard Schlosser (Ruhr-Universität Bochum): Die Himmelsscheibe von Nebra.

8. September 2005
Monika Buske, Sabine Preusse, Martin Tschimmel (MPS, Katlenburg-Lindau): "Doktoranden und Dissertationen am MPS": 1. Riesenvulkane auf dem Mars – eine Ursache im tiefen Planeteninneren. 2. Heiße Jupiter – Planeten mit einer engen Beziehung zu ihrem Stern. 3. Wasserdampf auf dem Mars – Ergebnisse der Sonde Mars Express.

22. November 2005
Dr. Jochen Kissel (Heidelberg und MPS, Katlenburg-Lindau): Deep Impact: Triff einen Kometen und lerne daraus.

8. Dezember 2005
Dr. Wolfgang Rau (TU München): Dunkle Materie.

Öffentliche Vorträge / Public presentations

Grieger B.: Die Mission Huygens – Landung auf dem verschleierten Mond Titan. Ausstellung "Man & Space" im Automobil Forum Unter den Linden, Berlin, 8. Juli 2004.

Hilchenbach M. und R. Roll: Wiedersehen mit Rosetta. MPS, Katlenburg-Lindau, 4. März 2005.

Keller H. U. und B. Grieger: Unter den Wolken – Huygens' Blick auf Titans Oberfläche. MPS, Katlenburg-Lindau, 27. Januar 2005.

Krupp N.: Die Mission Cassini – eine Reise zum Herrn der Ringe. Ausstellung "Man & Space" im Automobil Forum Unter den Linden, Berlin, 8. Juli 2004.

Krupp N.: Ankunft am Saturn – Erste Ergebnisse der Cassini-Mission. MPS, Katlenburg-Lindau, 13. Dezember 2004.

Verschiedenes / Miscellaneous

Dr. P. W. Daly: Betreuung der Online-Veröffentlichungs- und Vortragsliste.

Habilitationen / Habilitation

Dr. Harald Krüger
Habilitation an der Universität Heidelberg, Februar 2004.

Ernennungen / Appointments

Prof. Dr. Jörg Büchner
apl Professor der Georg-August-Universität Göttingen, 5. Dezember 2005

Dr. Laurent Gizon
Chairman of HELAS Local Helioseismology Network.

Dr. Markus Roth
HELAS Project Scientist.

Prof. Dr. Sami K. Solanki
Associate Member der Royal Astronomical Society (2005).

Auszeichnungen / Awards

Prof. Dr. Jörg Büchner
Award for Achievements in Cluster Science, NASA, 24. August 2004.
Award for outstanding contributions to Cluster's exploration of Geospace, ESA, 21. September 2005.

Prof. Dr. Ulrich Christensen und Prof. Dr. Klaus Jockers
Am 31. März 2005 wurde unserem Institut als Zeichen der Anerkennung und Dankbarkeit für die langjährige Zusammenarbeit mit Kollegen des Astronomischen Institutes der Bulgarischen Akademie der Wissenschaften der Akademie-Preis verliehen. Die Auszeichnung nahmen Prof. Christensen und Prof. Jockers entgegen.

Dr. Laurent Gizon
JOSO-Preis (Joint Organisation for Solar Observations) für herausragende Arbeiten eines jungen Wissenschaftlers im Bereich der Sonnenforschung. Wurde im Rahmen des 2. Central European Solar Physics Meetings verliehen (Bairisch Kölldorf, Österreich), 25. Mai 2005.

Prof. Dr. Klaus Jockers
Marin Drinov Ehren-Medaille am Bande, überreicht von der Bulgarischen Akademie der Wissenschaften in Sofia, Bulgarien, 31. März 2005.

Dr. Martin Schrinner
Berliner-Ungewitter-Preis der Fakultät für Physik, Universität Göttingen, 2005.

Dr. Alexander Vögler
Berliner-Ungewitter-Preis der Fakultät für Physik, Universität Göttingen, Februar 2004.

Dr. Alexander Vögler
Otto-Hahn-Medaille der MPG, Juni 2004.

Dr. Johannes Wicht und Dr. Julien Aubert
Heinz-Billing-Preis, zweiter Platz, 2004.

Herausgebertätigkeiten / Editorships

Aznar Cuadrado R.: Technical editor of Living Reviews in Solar Physics.

Böhnhardt H.: Member editorial board "Earth, Moon, and Planets", Scientific journal of Springer-Kluwer Academic Publishers. Guest co-editor of special issue on the Rosetta mission, Space Science Review, to be published in 2006/2007. Co-editor, "The Kuiper Belt", book project of the University of Arizona Press to be published in 2007.

Büchner J.: Editor: "Nonlinear Processes in Geophysics", EGU-AGU journal. Editor: "Magnetic Helicity at Sun and in magnetospheres", Elsevier, 2004. Editor: "Reconnection at Sun and at planets", Elsevier, 2005.

Christensen U.: Advisory Editor: Physics of the Earth & Plantetary Interiors.

Hartogh P.: Editor: Atmospheric Chemistry and Physics (ACP). Editor: Advances in Geosciences.

Lagg A.: Proceedings of Chromospheric and Coronal Magnetic Fields, ESA Publication Division, ESA SP-596.

Mall U.: Space Weather, Lectures Notes in Physics 656, Springer-Verlag.

Marsch E.: Mitherausgeber der Zeitschrift: "Living Reviews in Solar Physics" since 2003.

Schüssler M.: Editorial Board Living Reviews in Solar Physics.

Solanki S. K.: 'Editor in chief' der elektronischen, referierten Review-Zeitschrift "Living Reviews in Solar Physics"; "Solar Physics" Editorial Board; Co-Editor (Eds. Innes, D. E., Lagg, A., Solanki, S. K., Danesy, D.): Chromospheric and Coronal Magnetic Fields, ESA SP-596, ESA Publ. Div., Noordwijk, (2005).

Direktionsberaterkreis des MPS /
„Direktionsberaterkreis" at MPS

Gewählte Mitglieder des Direktionsberaterkreises für die Amtszeit 2004 waren:
Dr. Peter Barthol (Planeten), als Ersatzmitglied *Peter Börner, Dr. Andreas Lagg (Sonne),* als Ersatzmitglied *Dr. Bernd Inhester, Michael Bruns (Zentrale Dienste),* als Ersatzmitglied *Georg Tomasch.*

Gewählte Mitglieder des Direktionsberaterkreises für die Amtszeit 2005 waren:
Dr. Fred Goesmann (Planeten), als Ersatzmitglied *Dr. Patrick Daly, Dr. Andreas Lagg (Sonne),* als Ersatzmitglied *Dr. Bernd Inhester, Dr. Peter Barthol (Zentrale Dienste),* als Ersatzmitglied *Eckhard Steinmetz.*

40 Jahre in der MPG / 40 years at MPG

- Hans-Adolf Heinrichs (20. Februar 2004)
- Renate Meusel (1. April 2005)
- Elke Hartmann (15. April 2005)
- Horst Heise (1. Oktober 2005)

25 Jahre in der MPG / 25 years at MPG

- Günter Auckthun (16. April 2004)
- Martina Heinemeier (1. September 2004)
- Bernd Wöbke (1. Januar 2005)
- Bernd Inhester (3. August 2005)
- Sabine Deutsch (25. August 2005)

Tabelle 1: **Radio und TV Berichte über das Institut**

Tag der Aufnahme	**Radio Sender**	**TV Sender**	**Sende- datum/zeit**	**Projekt Thema**
07.01.2004	NDR 1		08.00 - 11.00	Mars-Express
07.01.2004	NDR info		11.00 + 13.00	Mars-Express
07.01.2004		NDR Hallo Niedersachsen	18.00 + 19.30	Mars-Express
08.01.2004	NDR 1		07.00 + 11.00	Mars-Express
10.01.2004		NDR Hallo Niedersachsen	19.30 - 20.00	Mars-Express
12.01.2004		NDR Hallo Niedersachsen	19.30 - 20.00	Mars-Express
20.01.2004		NDR Hallo Niedersachsen	18.00 + 19.30	Mars-Express
25.01.2004	NDR 4			Radio aurora
27.01.2004		Deutsche Welle TV	22.02.04: 20.30 (dt.) 23.30 (engl.) 23.02.04: 08.30 (dt.) 11.30 (engl.) 24.02.04: 02.30 (dt.) 05.30 (engl.) 14.30 (dt.) 17.30 (engl.)	Rosetta
27.01.2004	NDR info		20.02.04: 21.05 22.02.04: 15.05	Rosetta
27.01.2004	NDR 1		20.02.04	Rosetta
16.02.2004	Norwegian station			Rosetta
17.02.2004	MDR			Rosetta
17.02.2004		NDR Hallo Niedersachsen	18. oder 19.02.04 18.00 + 19.30	Rosetta
18.02.2004	Stadtradio Göttingen		11.00 - 12.00	Mars
26.02.2004	NDR info NDR 1 live		08.00 - 11.00	Rosetta
26.02.2004		NDR Hallo Niedersachsen	18.00 + 19.30	Rosetta
26.02.2004		Göttingen TV		Rosetta
27.02.2004		NDR Hallo Niedersachsen	18.00 + 19.30	Rosetta
27.02.2004		Göttingen TV		Rosetta
02.03.2004		NDR Hallo Niedersachsen	18.00 + 19.30	Rosetta
02.03.2004	NDR 1			Rosetta
07./08.04. 2004		DLR Pressestelle	27.05.04	Rosetta
13.05.2004	Deutschlandfunk		06.06.04	Venus Transit
14.05.2004		ZDF	01.06.04	Geophysics, Dynamo
08.06.2004		ZDF Mittagsmagazin	13.00	Venus Transit
01.07.2004		ZDF Heute Journal	21.45	Cassini
02.07.2004		NDR Hallo Niedersachsen	18.00	Cassini
03.07.2004		ZDF Heute Nachrichten	19.00	Cassini
04.07.2004		ZDF Heute Nacht	00.00	Cassini
	NDR info NDR info		06.08.04: 21.05 08.08.04: 15.05	Sonne, Klima
10.09.2004	BR 2 IQ		10.09.04: 18.00	Cassini
21.10.2004	Deutscher Rundfunk Forschung Aktuell		17.12.04: 16.30	Cassini
21.10.2004	Deutschlandfunk, SWR 2		09.01.05: 16.30 10.01.05: 08.30 11.01.05: 16.30	Cassini
17.12.2004		NDR Hallo Niedersachsen	17.12.04: 18.00 + 19.30	Cassini
14.01.2004		ZDF Heute Journal	21.45	Cassini, Huygens, Keller
14.01.2005 15.01.2005		NDR Hallo Niedersachsen NDR Hallo Niedersachsen	18.00 + 19.30 19.30	Cassini, Huygens, Krupp Keller, Grieger, Küppers
15.01.2005	Deutsche Welle		23.01.05: 20.30 24.01.05: 08.30 25.01.05: 02.30 und 14.30	Huygens, Keller
21.01.2005	HR 1		06.10	Cassini, Grieger
25.01.2005	NDR 1		30.01.05: 15.10 - 16.00	Huygens, Keller, Krupp
05.02.2005	TV Berlin		16.03	Cassini, Huygens, Keller
07.02.2005	Deutschlandfunk für SWF			Cassini, Krupp, Keller

weiter. . .

Tabelle 1: Radio und TV Berichte über das Institut (*Fortsetzung*)

Tag der Aufnahme	**Radio Sender**	**TV Sender**	**Sende-datum/zeit**	**Projekt Thema**
06.04.2005	Stadtradio Göttingen			Rosetta, Böhnhardt
30.05.2005		Pro Sieben Talk	17.00 - 18.00	Sonne, Solanki
30.05.2005		SAT 1 Nachrichten	17.30	Sonne, Solanki
01.06.2005		HR Fernsehen Alle Wetter	18.20 - 18.30	Sonne, Solanki
14.06.2005	BR 2 Rundfunk		21.06.05: 18.00	Sonne, Solanki
30.06.2005	FFN			Tag der offenen Tür Krupp, Borchers
30.06.2005		Focus TV	03.07.05: 22.10	Sonne, Curdt
04.07.2005	 WDR 5 WDR 2	NDR Hallo Niedersachsen NDR DAS! ZDF Morgenmagazin RTL Nachrichten	18.00 + 19.30 18.00, 18.45 11.30 13.40	Deep Impact Christensen Keller
09.07.2005	Radio 1, Die Profis		11.40	Deep Impact
18.08.2005	SWR 1 NDR 1			Asteroid, Jockers
30.09.2005	MDR			Sonnenfinsternis, Curdt
07.10.2005		Deutsche Welle TV	23.10.05	Venus Express
09.11.2005		NDR Hallo Niedersachsen	18.00	Venus Express
09.11.2005	NDR info			Venus Express
10.11.2005		WDR, Q21	29.11.05: 21.00	Huygens

VIII. Berichte, Vorträge und Veröffentlichungen / Reports, Talks and Publications

Interne MPS-Berichte / Internal MPS reports

(W wissenschaftlicher, T technischer Bericht; M Handbuch (Manual); V Vorschlag für ein Experiment; L Manuskript für eine Vorlesung/Seminar)

(W scientific, T technical report; M manual; V experiment proposal; L lecture paper/seminar)

MPAE-W-485-04-01
Hong Zou and Erling Nielsen
Methods for Obtaining Electron Density Profiles from MARSIS Ionograms and derivation of parameters characterizing the profiles.

MPAE-W-485-04-02
Hong Zou and Erling Nielsen
Faraday rotation and MARSIS as a detector of crustal magnetic fields.

Experimentvorschläge / Proposals

Asteroseismological Determination of Stellar Rotation Axes: Implications for Stellar Radii, Stellar Rotation, and Planetary System Formation. (L. Gizon, S. Solanki, MPS). Proposal in response to COROT AO. (accepted)

BepiColombo – BepiCam: A stereo and high resolution camera for ESA's Mercury Planetary Orbiter on BepiColombo. (PI: H. Böhnhardt (MPS), MPS co-investigators: W. Boogaerts, U. Christensen, S. Hviid, J. Kramm, M. Küppers, W. Markiewicz, R. Roll, H. Sierks). Scientific instrument proposal for ESA's BepiColombo mission; the proposal was not selected

BepiColombo – IRIS: Infrared Imaging Spectrometer. (U. Mall). An instrument proposal for the planetary orbiter of the BepiColombo Mission.

BepiColombo – MERTIS-TIS: Thermal Infrared Spectrometer for ESA's BepiColombo Mission to explore, Mercury. (U. Mall).

BepiColombo – MISTER. (P. Hartogh). Proposal submitted to ESA (not selected), 2004.

BepiColombo MMO – MPPE. (Mercury Plasma/Particle Experiment) (N. Krupp, J. Woch). An instrument proposal for plasma investigations on the Magnetospheric Orbiter of the BepiColombo Mission (PI: Y. Saito, ISAS, Japan; selected).

BepiColombo MPO – SERENA. (Search for Exospheric Refilling and Emitted Natural Abundances) (J. Woch, N. Krupp). An instrument proposal for plasma and neutral gas investigations on the Planetary Orbiter of the BepiColombo Mission (PI: S. Orsini, IFSI, Italy; selected)

CAWSES. (Climate and Weather of the Sun-Earth-System)(P. Hartogh). Proposal to DFG (selected), Oktober 2005.

European ExoMars Mission: An experiment was proposed. It comprises a combined instrument of gas-chromatograph / mass-spectrometer (GC-MS) together with an Atmospheric Pressure Matrix Assisted Laser Desorption Ionisation (AP-MALDI) system. The name of the instrument is Mars Organic Molecule Anlyser (MOMA). (Fred Goesmann is the team coordinator of an international team from Germany, the United States of America, France, and The Netherlands).

European Solar Magnetism Network 3 (ESMN3): FP 6 EU Proposal. (A. Lagg). Proposals für bodengebundene Sonnenbeobachtungen (je 1 für 2004 und 2005).

Evolution of coronal magnetic fields. (T. Wiegelmann). DFG-Antrag.

HELAS: European Helio- and Asteroseismology Network. Proposal to the European Union (FP 6). (Board Members: L. Gizon, M. Roth, MPS). (granted)

Local Helioseismology of Small Magnetic Elements. (L. Gizon, MPS (Consultant) with Aaron Birch (PI), CoRA, USA). Proposal 0607604 submitted to the National Science Foundation.

NewContour: A cometary mission proposal within NASA's Discovery Program. (PI: J. Veverka (Cornell Univ., USA); co-investigator: H. Böhnhardt (MPS)). The mission was not selected.

SIR-2. A Near-Infrared Spectrometer for the Indian Chandrayaan-1 mission. (U. Mall).

Subphotospheric Dynamics of the Sun. (L. Gizon, M. Schüssler, A. Vögler, R. Cameron, MPS). Proposal to the International Space Science Institute (ISSI, Bern). (accepted)

T-Owl: A thermal and mid-infrared imager and spectrograph for the Overwhelmingly Large Telescope OWL. ESO study proposal of an astronomical instrument. (PI: R. Lenzen (MPI for Astronomy Heidelberg); collaborator: H. Böhnhardt (MPS)).

SAPPHYRE. (E. Marsch). EU Proposal, Marie Curie Actions, RTN, 2005.

Structure Formation. (E. Marsch). EU Proposal, Marie Curie Actions, RTN, 2004.

Studying the superrotation of Venus' atmosphere with a general circulation model of intermediate complexity. (B. Grieger). Proposal for the DFG Priority Program Mars and the terrestrial planets.

VESPER. (P. Hartogh). Proposal submitted to NASA (not selected), Februar 2005.

Tee-Seminare / Tea Seminars

Leitung/Organizers: Dr. P.W. Daly, Dr. B. Inhester und Dr. J. Woch (bis Ende 2004, ab 2005:) **Dr. W. Curdt, Dr. C. Jarchow und Dr. W. Markiewicz**

In den Seminaren wird von Wissenschaftlern des MPS, aber auch von Gästen in unregelmäßigen Zeitabständen über laufende Arbeiten vorgetragen.

MPS scientists, as well as guests to the Institute, report on their current work in the informal seminars.

Dr. Hardy Peter, Kiepenheuer Institut, Freiburg: Structure and dynamics of the transition zone. 22. Januar 2004.

Dr. Jochen Kissel, MPAE: Stardust-Flyby at Comet Wild – First Results of the Dust Experiment CIDA. 3. Februar 2004.

Dr. E. Wiehr, Universitäts-Sternwarte, Göttingen: Giant convection beneath sunspots: tiny flux concentrations as surface signature. 17. Februar 2004.

Dr. A. Kosovichev, Stanford University: Investigation of subphotospheric structures and flows by helioseismology. 15. März 2004.

Dr. G. Hornig, Ruhr-Universität, Bochum: Magnetic null points in the solar corona. 18. März 2004.

Dr. R. Sydora, University of Alberta, Edmonton: Gyrokinetic simulation of forced current sheet equilibria in the solar corona. 25. März 2004.

Dr. P. Petit, Centro de Astrophysica, University of Porto: Magnetism and activity of solar-type stars. 30. März 2004.

Dr. A. Otto, University of Fairbanks, Alaska: Magnetic Reconnection and Hall Physics. 1. April 2004.

Mike Stevens, Naval Research Lab, USA: Satellite Observations of the Arctic Mesospheric Cloud Mass: Measuring the Contribution from Space Shuttle Exhaust. 2. April 2004.

Dr. Mark Robinson, Center of Planetary Sciences, Northwestern University: Mercury – from Messenger to Bepi-Colombo. 21. April 2004.

Dr. Frank Bensch, Universität Bonn: (Ortho-)Water Rotational Transitions in Comets: Radiative Transfer Model and SWAS Observations. 15. Juni 2004.

Colin Barrow, MPAe: Radio Astronomy of Jupiter. 24. Juni 2004.

Dr. D. Berdichevsky, L3 GS Inc at NASA/GSFC: On the Global Nature of the Travelling Interplanetary Shock. 29. Juli 2004.

Dr. Jaime Araneda, University of Concepción, Chile: Non-linear Stability of Alfvén-Cyclotron waves: Connections to in-situ Measurements in the Fast Solar Wind. 11. August 2004.

Dr. Louise Harra, Mullard Space Science Lab, UK: EUV Imaging for Solar Orbiter. 16. August 2004.

Prof. U. Cubasch, Freie Universität Berlin: The Sun's impact on the Earth's climate: results from 3D simulations. 17. August 2004.

Prof. K. Murawski, University of Lublin, Poland: Numerical Simulations of MHD Waves in Solar Coronal Loops. 20. August 2004.

Jean-Francois Hochedez, Royal Observatory of Belgium, Brussels: The payload of PROBA-2, heralding Solar Orbiter. 26. August 2004.

Dr. A. Brkovic, Kiepenheuer Institut, Freiburg: Statistical Comparison of Blinkers and Explosive Events. 30. August 2004.

Prof. W. Kundt, Universität Bonn: All about Black Holes – have we really identified them? 15. September 2004.

Dr. J.N. Goswami, Physical Research Lab., Ahmedabad, India: Origin of the Moon and the Solar System: a matter of Chance and Destiny. 6. Oktober 2004.

Dr. A. Vaivads, Space Research Institute, Uppsala: New Results about Reconnection at the Magnetopause based on Cluster observations. 15. Oktober 2004.

Prof. Dr. A. Hady, Astronomy Dept., Faculty of Science, Cairo University: Giant Storms during the Decline Phase of Solar Cycle 21, 22, 23 & October/November Event. 19. Oktober 2004.

Dr. U. Käufl, ESO, Garching: Ground-based Observations of Comets, Planets, Exo-Planets in the Infrared – the Future has Already Started. 27. Oktober 2004.

Dr. V.M. Gubchenko, Institute of Applied Physics, Russian Academy of Sciences, Nizhny Novgorod: On a Plasma Kinetic Model of a 3D Solar Corona and Solar Wind at the Heliospheric Sheet. 28. Oktober 2004.

Prof. F. Verheest, Sterrenkundig Observatorium, Universität Gent: Linear and non-linear waves and solitons in pair plasmas. 22. November 2004.

Dr. R. McLean, University of St. Andrews: Topological Techniques and Examples of their Application in Solar Physics. 25. November 2004.

Prof. Nelson J. Schuch, National Institute of Space Research, Santa Maria, Brazil: Space and Atmospheric Sciences in the South of Brazil. 26. November 2004.

Prof. L. Strüder, Max-Planck-Institut für extraterrestrische Physik: High speed detectors from NIR to X-rays – in Heaven and on Earth. 29. November 2004.

Dr. H. Ludwig, Lund Observatory, Sweden: Hydrodynamical simulations of convection-related stellar micro-variability. 2. Dezember 2004.

Dr. L Kolokolova, Univ. of Maryland, College Park: Physical properties of cometary dust from its light scattering. 7. Dezember 2004.

Dr. Frank Jenko, MPI für Plasmaphysik (IPP), Garching: Turbulent transport – a key obstacle on the way towards fusion power. 13. Januar 2005.

Prof. R. Sydora, University of Alberta, Canada: Shear Alfvén Wave Heating: Comparing Solar and Auroral Plasmas. 20. Januar 2005.

Dr. Francis Nimmo, UCLA: Extension on Europa. 10. Februar 2005.

Thijs de Graauw, SRON, Groningen: The Heterodyne Instrument for the Far Infrared on the Herschel Space Observatory. 14. Februar 2005.

Christian Beck, Kiepenheuer-Institut, Freiburg: The magnetic properties of G-band bright points in a sunspot moat. 3. März 2005.

Eberhard Wiehr, Uni-Sternwarte Göttingen: Solar faculae – the hot counterparts of sunspots. 9. März 2005.

Elena Benevolenskaya, UC Stanford: Long-lived complexes of solar activity and connectivity in the corona. 22. März 2005.

Stephan Stellmach, Uni Münster: Dynamo in a box, toward extreme parameters. 4. April 2005.

Dr. Johann K. Hirzberger, Uni Graz: Small scale features in solar magnetic structures. 6. April 2005.

Prof. Robert Erdelyi, Sheffield University: Seismology and Dynamics of the Lower Solar Atmosphere. 15. April 2005.

Dr. Ansgar Reiners, UC Berkeley: Differential Rotation in Stars. 27. April 2005.

Dr. Christian T. Dum, MPE Garching: Beam-Plasma and Current Driven Instabilities – Test of Turbulence Theories. 12. Mai 2005.

Prof. Joseph R. Kan, University of Alaska Fairbanks: Substorm Expansion Onset and Storm Ring Current Intensification. 20. Mai 2005.

Prof. Kurt Varmuza, Technische Universität Wien: Multivariate data analysis – a useful tool in biology, chemistry and physics. 31. Mai 2005.

Alberto Flandes, Geophysics Institute of the National University of Mexico (U.N.A.M.): Dust Escape Mechanisms from Io. 8. Juni 2005.

Dr. Sven Wedemeyer-Böhm, Kiepenheuer-Institut für Sonnenphysik, Freiburg: Carbon Monoxide in the Solar Atmosphere. 16. Juni 2005.

Dr. Jason Jackiewicz, Boston College, USA: Atomic Fermion Condensates: Using “Old” Physics to Solve a New Problem. 17. Juni 2005.

Dr. Miriam Rengel, TLS Tautenburg: Searching for Embryonaric Suns. 3. August 2005.

Mag Selwa, Maria Curie-Sklodowska University, Lublin: Numerical Simulation of MHD Waves in Solar Coronal Loops. 26. August 2005.

Dr. Sergey Popel, Institute for Dynamics of Geospheres, RAS: Nano- and microscale particles in natural phenomena and strong perturbations in plasmas (recent studies at the Institute for Dynamics of Geospheres RAS). 18. Oktober 2005.

Prof. M. Ya. Marov, Keldysh Institute of Applied Mathematics, Moscow: Venus: Current Knowledge on the Eve of Venus Express. 24. November 2005.

Dr. Nancy Ageorges, European Southern Observatory, Chile: Near-IR observations with adaptive optics at ESO VLT. 24. November 2005.

Dr. Gunnar Hornig, University of Dundee, Scotland: Three-dimensional reconnection. 25. November 2005.

Dr. Fouad Guessous, Universität Marburg: Bacteriorhodopsin (BR): a biological pigment for optical data-storage and security-printing. 2. Dezember 2005.

Dr. Shaun Bloomfield, Belfast University: Observations of Magnetoacoustic Waves in the Solar Chromosphere. 6. Dezember 2005.

Dr. Joachim Schmidt, Internationale Universität Bremen: Flux Tubes in the Solar Corona. 8. Dezember 2005.

K. Sauer, MPS: Nonlinear coherent waves in space plasmas: observations and models. 14. Dezember 2005.

Johann Reiter, Technische Universität München: Measurement of High-Degree Solar Oscillations. 14. Dezember 2005.

R. Schwenn, U. Schühle, C.-Y. Tu, MPS / Peking University: Mögliche Beteiligung des MPS am 'Lyman-alpha Filtergraph Telescope' und 'Lyman-alpha Coronagraph' auf der 'Kuafu Space Weather Explorer' Mission. 20. Dezember 2005.

IMPRS Solar System Seminars / IMPRS Solar System Seminars

The Solar System Seminars (S^3) takes place every second Wednesday afternoon from 13:00 to 16:30. It consists of up to three talks by students on their PhD projects (each 20 min talk plus 10 min discussion), an extended coffee break for further discussion and a tutorial talk (60 min).

Andrey Seleznyov:
Understanding solar variability with an application to the planetary transit detection.
Maxim Kramar:
3D vector tomography for the coronal magnetic field.
Rupali Mahajan:
Evolution of north polar cap of Mars.
Hardi Peter (Freiburg):
The solar corona and its relation to stars.
21. Januar 2004.

Ingo Baumann:
Evolution of the large-scale magnetic field on the solar surface: a parameter study.
Yevgen Grynko:
The phase curve of cometary dust: observations and problem of interpretation.
Aveek Sarkar:
On the way to Karlsruhe dynamo.
4. Februar 2004.

Durgesh Tripathi:
Plasma and magnetic field dynamics of prominences in coronal mass ejections.
Luciano Rodriguez:
Signatures of magnetic clouds in the solar wind.
Marilena Mierla:
Using LASCO/C1 spectroscopy for coronal diagnostics.
Oliver Preuß (Bielefeld):
From Newtonian to metric-affine gravity: recent developments and experiments.
18. Februar 2004.

Ilya Silin:
Parallel computing using MPI and OpenMP.
Alina Semenova:
Modeling of giant starspots on the poles of rapidly rotating stars using the Doppler imaging technique.
Juan Manuel Borrero:
Serendipitous discovery of 5min oscillations in a sunspot penumbra.
Hartmut Zohm, Sibylle Günter (Garching):
Small- and large-scale instabilities in magnetically confined plasmas at low collisionality.
21. April 2004.

Ana Tomas:
Jupiter's main and secondary auroral oval.
Monika Buske:
The influence of the depth-dependence of the thermal expansivity and conductivity on the thermal evolution of the martian mantle.
Albrecht Hofmann (Mainz):
Anatomy of the Hawaiian mantle plume.
12. Mai 2004.

Sergey Shelyag:
Spectro-polarimetric diagnostics of magneto-convection simulations of solar photosphere.
Denise Tortorella:
Thermal convection in rapidly rotating spherical shells: from Boussinesq to anelastic approximation.
Guadalupe Munoz:
CMEs dynamics ... what is missing in the puzzle?
Joachim Woch:
Energetic neutral atom imaging and its application to planetary research.
26. Mai 2004.

Ryu Saito:
Improvements in the radiative transfer module of the MAOAM-GCM.
Sabine Preusse:
Puzzling extrasolar planets – The stellar component.
Jean-Mathias Grießmeier:

Puzzling extrasolar planets – The planetary component.
Hermann Opgenoorth (ESA):
ESA's solar and solar terrestrial missions – present and future.
16. Juni 2004.

Fedor Kolesnikov:
Shear instability of a helical flow around a magnetic flux tube.
Yasuhito Narita:
Waves upstream and downstream of collisionless shocks: Cluster observations.
Michael Rost:
Magnetic dust aggregation under microgravity and low magnetic field conditions.
Nazaret Bello Gonzalez:
Sunspot penumbrae: observational features.
Vasily Zakharov:
Center to limb variation diagnostics of radiation simulations of the solar photosphere.
14. Juli 2004.

Mark Cheung:
Magnetic flux emergence in the photosphere.
Laura Balmaceda:
Reconstruction of solar irradiance based on the evolution of the magnetic field.
Juan Manuel Borrero:
The fine structure of the sunspot penumbra.
Dmitry Titov:
Venus: mysteries of the forgotten planet.
3. November 2004.

Alexandra Andjic:
Analysis of short-period acoustic waves in the solar chromosphere.
Aveek Sarkar:
Simulation of the Karlsruhe dynamo experiment.
Dragos Constantinescu:
Pattern recognition with Cluster data.
Klaus Jockers:
Access to scientific literature in the times of digital data exchange.
17. November 2004.

Ganna Portyankina:
Spider patterns in the cryptic region of the Martian south polar cap.
Evgeny Panov:
Cluster observations of thin current sheets at the Earth's magnetopause.
Alexander Bößwetter:
Plasma boundaries at Mars: A 3d simulation study.
Arne Richter (Copernicus):
Online and open access publication – doubts and advantages.
1. Dezember 2004.

Katerina Radioti:
Energetic particle composition of the Jovian magnetosphere – Observations and possible interpretations.
Elena Kronberg:
Nature of substorms at Jupiter.
Martin Schrinner:
Mean-field view on geodynamo models.
Luca Teriaca:
Spectroscopy of the solar transition region and corona.
8. Dezember 2004.

Maxim Kramar:
Inversion of the magnetic field from polarimetry data of magnetically sensitive coronal ions.
Durgesh Tripathi:
Evolution of photospheric magnetic field in the source regions of coronal mass ejections.
Ingo Baumann:
Simulating the Sun's open magnetic flux using an extended flux transport model.
Pascal Petit:
Magnetic mapping of solar-type stars.
12. Januar 2005.

Hebe Cremades:
Geometrical properties of coronal mass ejections.
Sebastian Schäfer:
Searching for field line resonances: case studies from Cluster.
Rupali Mahajan:
Dynamic simulation of Martian polar caps.
Martin Tschimmel:
Water vapour on Mars – measurements by the PFS instrument on Mars Express.
9. Februar 2005.

Stefan Schröder:
Huygens' encounter with Titan.
Redouane Mecheri:
Coronal waves: Propagation and dissipation in the multi-fluid description.
Lukasz Matloch:
Modelling of mesogranulation.
Patrick Daly:
PowerWhat? Presentation techniques with pdfLaTeX.
23. Februar 2005.

Monika Buske:
Thermal evolution models for the Martian mantle and the question of an early dynamo in Mars.
Yevgen Grynko:
LASCO C3 observations of comet C/2004 F4 Bradfield.
Yasuhito Narita:
Low-frequency waves upstream and downstream of the terrestrial bow shock.

4. Mai 2005.

Nazaret Bello Gonzalez:
Polarimetric observations of sunspot penumbrae.
Julian Blanco:
Polar faculae: an introduction.
Alina Semenova:
Doppler imaging of Sigma Geminorum.
1. Juni 2005.

Ana Tomas:
Pitch angle distribution changes and their relation to global particle transport in the Jovian magnetosphere.
Ryu Saito:
Influence of the surface on the atmospheric circulation of Mars.
Ingo von Borstel:
Making planets in the lab - some small steps on a long journey.
Vasily Zakharov:
A comparative study of the contrast of solar magnetic elements in CN and CH.
15. Juni 2005.

Marilena Mierla:
Flows in the inner solar corona using LASCO/C1 data.
Guadalupe Munoz:
Dynamics of coronal mass ejections in the interplanetary medium.
Luciano Rodriguez:
Solar wind ions and energetic particles related to magnetic clouds.
29. Juni 2005.

Sabine Preusse:
"Magnetic communication" scenarios for hot Jupiters and their stars.
Jean-Mathias Griessmeier:
Exoplanetary radio emissions.
Sven Simon:
Global simulation of solar wind interaction with magnetized asteroids.
Gero Kleindienst:
ULF waves in the kronian magnetosphere.
13. Juli 2005.

Elias Roussos:
Moon-magnetosphere interactions at Saturn: Cassini MIMI/LEMMS observations.
Laura Balmaceda:
Cross-calibrated sunspot areas: an essential ingredient for irradiance models.
Evgeny Panov:
Cluster observation of perpendicular electromagnetic waves at the magnetopause.
23. November 2005.

Clementina Sasso:
Spectopolarimetry in the He I 1083.0 nm: The Paschen-Back effect influence.
Martin Tschimmel:
Atmospheric water vapour from the PFS/Mars Express observations.
Mark Cheung:
The structure of the reversed granulation in the photosphere.
7. Dezember 2005.

Instituts-Seminare / Institute seminars

Leitung: Das Kollegium

In den Institutsseminaren wird hauptsächlich über die Fortführung laufender und die Aufnahme neuer Projekte berichtet, einschließlich der finanziellen und personellen Belange.

The Institute seminars report on the status of current projects as well as presentations of future projects, including questions of financing and personnel.

F. Goesmann, M. Hilchenbach: MOMA, the Mars Organic Molecule Analyser: an instrument proposal for ExoMars. 29. November 2005.

U. Christensen, R. Roll: The Seismometer for ExoMars. 29. November 2005.

R. Schwenn, U. Schühle, C.-Y. Tu: Mögliche Beteiligung des MPS am 'Lyman-alpha Filtergraph Telescope' und 'Lyman- alpha Coronagraph' auf der 'Kuafu Space Weather Explorer' Mission. 22. Dezember 2005.

MPS-Kolloquien / MPS Colloquia

Leitung: Dr. Hermann Böhnhardt

Zu diesen Kolloquien werden meistens nur auswärtige Wissenschaftler eingeladen, um möglichst allgemein über ihr Arbeitsgebiet zu berichten.

Colloquia are usually given by external scientists invited to the Institute to report fairly broadly on their field of research.

Prof. Konrad Sauer, MPAe, Lindau: Multi-Ion Space Plasma Research: Two highlights. 4. Februar 2004.

Dr. Dominique Bockelee-Morvan, LESIA, Observatoire de Paris: Comets at radio wavelengths. 23. März 2004.

Prof. Simon White, MPA, Garching: The formation of galaxies and of larger cosmic structures. 2. April 2004.

Prof. Siegfied Franck, Potsdam Institute for Climate Impact Research (PIK): Habitable zones in extrasolar planetary systems: The search for a second Earth. 17. Juni 2004.

Dr. Frank Jenko, MPI für Plasmaphysik (IPP), Garching: Turbulent transport – a key obstacle on the way towards fusion power. 13. Januar 2005.

Prof. R. Sydora, University of Alberta, Canada: Shear Alfvén Wave Heating: Comparing Solar and Auroral Plasmas. 20. Januar 2005.

Prof. Dr. Stefan Dreizler, Universitäts-Sternwarte Göttingen: Stellar Astrophysics with MONET and SALT. 1. März 2005.

Dr. Günter Wuchterl, Universität Jena: The First Million Years of the Sun. 16. März 2005.

Prof. Friedrich Wilhelm Hehl, Universität Köln / University Columbia/Missouri: Einstein-Cartan theory and beyond – some possible experimental consequences of gravitational gauge theories. 26. April 2005.

Prof. Dr. Luann Becker, University of California, Santa Barbara, USA: Impacts, Volvanism and the Mass Extinction at the end-Permian. 2. Mai 2005.

Dr. Roland Gredel, Calar Alto Observatorium, Max-Planck-Institut für Astronomie, Heidelberg: Optical and near-infrared absorption line studies of interstellar molecules. 4. Mai 2005.

Prof. L. M. Zelenyi, Space Research Institute, Russian Academy of Sciences, Moskau: RUSSIAN SPACE PHYSICS MISSIONS: Solar System Studies 2006-2015. 10. Mai 2005.

Prof. Claus Lämmerzahl, ZARM, Universität Bremen: The Pioneer Anomaly – present status and outlook. 18. Mai 2005.

Dr. Alan Harris, DLR Berlin: Near-Earth Asteroids: Their Physical Nature and the Impact Hazard. 1. Juni 2005.

Prof. Phil Nicholson, Cornell University Ithaca, USA: Near-infrared observations of Saturn's rings and satellites with Cassini. 27. Juni 2005.

Prof. Dr. Oskar von der Lühe, Kiepenheuer Institut Freiburg: High Resolution Solar Observations with Adaptive Optics and Image Reconstruction Methods. 10. November 2005.

Dr. Mario Trieloff, Universität Heidelberg: Planetesimal formation in the early Solar System. 17. November 2005.

Dr. Jochen Kissel, MPS and Heidelberg: Deep Impact: Mission accomplished – and still learning. 23. November 2005.

Prof. Dr. Werner Schmutz, Physikalisch–Meteorologisches Observatorium Davos – World Radiation Center: UV variability of the Sun as input climate model calculation. 30. November 2005.

Dr. Diane Wooden, NASA Ames Research Center, Moffett Field, (California): Comet Dust – The story of planet formation as told by the tiniest particles. 7. Dezember 2005.

Vorträge 2004 /
Talks 2004

Betreuung der Online-Veröffentlichungs- und Vortragsliste: P. W. Daly

Amit, H., P. Olson, and U. Christensen: Core flow recovery from a numerical dynamo model. 9th Symposium on Study of the Earth's Deep Interior, Garmisch-Partenkirchen, Germany, July 4 – 9, 2004. (Poster).

Armstrong, T. P., J. W. Manweiler, N. Krupp, A. Lagg, S. Livi, S. M. Krimigis, D. G. Mitchell, and L. J. Lanzerotti: Comparison of initial Cassini/LEMMS and Voyager 1 and 2 low energy charged particle trapped radiation observations. 35th COSPAR Scientific Assembly, Paris, France, July 18 – 25, 2004.

Asikainen, T., K. Mursula, R. Friedel, and P. Daly: Statistical study of energetic particles in the cusp and the high-latitude dayside plasma sheet. 1st General Assembly of the European Geosciences Union, Nice, France, April 25 – 30, 2004.

Aubert, J.: Steady zonal flows in spherical shell fluid dynamos. 9th Symposium on Study of the Earth's Deep Interior, Garmisch-Partenkirchen, Germany, July 4 – 9, 2004.

— Zonal flows and the geodynamo. 9th Symposium on Study of the Earth's Deep Interior, Garmisch-Partenkirchen, Germany, July 4 – 9, 2004. (Poster).

Aubert, J. and J. Wicht: Axial vs. equatorial dipolar dynamo models with implications for planetary magnetic fields. Joint Assembly of the AGU, CGU, SEG, EEGS, Montreal, Canada, May 10 – 14, 2004.

Axford, W. I.: Four kinds of solar wind. 35th COSPAR Scientific Assembly, Paris, France, July 18 – 25, 2004. (Poster).

— Pico-flare heating of the quiet corona and solar wind. Joint AOGS 1st Annual Meeting and 2nd APHW Conference, Singapore, July 5 – 9, 2004. (Oral).

— The history of heliospheric research. UCR IGPP Symposium, Riverside, CA, USA, February, 2004. (Oral).

Aznar Cuadrado, R., S. K. Solanki, A. Lagg, and R. M. Thomas: Signature of current sheets as seen by TIP at VTT in the He I multiplet at 1083.0 nm. SOHO 15: Coronal Heating, St. Andrews, Scotland, UK, September 6 – 9, 2004. (Poster).

Bamert, K., R. Kallenbach, M. Hilchenbach, R. F. Wimmer-Schweingruber, and B. Klecker: Acceleration of suprathermal $^3He^{++}$ at interplanetary traveling shocks. 35th COSPAR Scientific Assembly, Paris, France, July 18 – 25, 2004. (Poster).

Barabash, S., M. Holmström, R. Lundin, H. Andersson, A. Grigoriev, O. Norberg, M. Yamauchi, K. Asamura, A. J. Coates, D. R. Linder, D. O. Kataria, C. C. Curtis, K. C. Hsieh, B. R. Sandel, A. Fedorov, E. Budnik, J.-A. Sauvaud, J.-J. Thocaven, M. Grande, M. Carter, D. H. Reading, H. Koskinen, E. Kallio, P. Riihela, W. Schmidt, T. Säles, J. Kozyra, N. Krupp, S. Livi, J. Woch, J. Luhmann, S. McKenna-Lawlor, S. Orsini, R. Cerulli-Irelli, M. Maggi, A. Mura, A. Milillo, E. Roelof, D. Williams, D. Winningham, R. Frahm, J. Scherrer, J. Sharber, P. Wurz, and P. Bochsler: The latest results on the energetic neutral atoms and plasma of Mars from the ASPERA instrument of Mars Express. 35th COSPAR Scientific Assembly, Paris, France, July 18 – 25, 2004.

Barrow, C. H.: Radio Observations of Jupiter up to Ulysses. Joint AOGS 1st Annual Meeting and 2nd APHW Conference, Singapore, July 5 – 9, 2004. (Oral).

— The hectometric radio emission (HOM), the solar wind and the Jovian aurora. 1st General Assembly of the European Geosciences Union, Nice, France, April 25 – 30, 2004.

Baumann, I.: Evolution of the large-scale magnetic field on the solar surface: a parameter study. First International Symposium on Space Climate, Oulu, Finland, June 20 – 23, 2004.

BenMoussa, A., U. Schühle, K. Haenen, M. Nesladek, and J.-F. Hochedez: Diamond detector development for LYRA, the solar VUV radiometer on board PROBA II. 9th International Workshop on Surface and Bulk Defects in CVD Diamond Films, Diepenbeek, Belgium, July 7, 2004. (Oral).

Boehnhardt, H.: Perspectives of cometary research. MPG Fachbeirat, Katlenburg-Lindau, Germany, November 8 – 9, 2004. (Oral).

— Physical properties of the most pristine solar system bodies: Transneptunian objects and Centaurs. ESO OPC Meeting, Garching, Germany, November 22, 2004. (Oral).

— ROSETTA long-term perspectives of cometary research. MPS Kuratorium Meeting, Katlenburg-Lindau, Germany, November 10, 2004. (Oral).

— The Edgeworth-Kuiper-Belt-Fridge at the edge of the planetary system. Universität Göttingen, Göttingen, Germany, June 25, 2004. (Oral).

— The ROSETTA Lander PHILAE and bioastronomy of comets. Int. Conf. Bioastronomy 2004, Reykjavik, Iceland, July 12 – 16, 2004. (Oral).

— Two images of comet 67P in 2004. OSIRIS Science Team Meeting, Katlenburg-Lindau, Germany, October 27 – 29, 2004. (Oral).

Bolton, S. J., D. Santos-Costa, M. Blanc, S. Maurice, N. Krupp, and I. Dandouras: Emissions radiated from the radiation belts of Saturn. 1st General Assembly of the European Geosciences Union, Nice, France, April 25 – 30, 2004.

Bolton, S. J., D. Santos-Costa, N. Krupp, M. K. Dougherty, E. C. Roelof, D. G. Mitchell, R. M. Thorne, and M. Blanc: Energetic proton and electron distributions in Saturn magnetosphere as revealed by Cassini/Voyager observations and proposed by models. AGU Fall Meeting, San Francisco, USA, December 13 – 17, 2004.

Bößwetter, A., T. Bagdonat, U. Motschmann, and K. Sauer: Plasma boundaries at Mars: 3D-simulation study. 1st General Assembly of the European Geosciences Union, Nice, France, April 25 – 30, 2004.

Brandt, P. C., J. Saur, D. G. Mitchell, E. C. Roelof, C. Paranicas, B. H. Mauk, S. M. Krimigis, and N. Krupp: Saturn's global ion distribution from Cassini/Inca Ena and in-situ measurements. AGU Fall Meeting, San Francisco, USA, December 13 – 17, 2004.

Büchner, J.: Consequences of the LHD instability for three-dimensional collisionless reconnection through thin current sheets (Invited lecture). Isaac Newton Institute for Mathematical Sciences, Cambridge, UK, August 20, 2004.

— Current sheet formation and reconnection due to photospheric footpoint motion and magnetic field topology. RHESSI-SOHO-TRACE workshop on flares and CMEs, Sonoma, USA, December 8 – 12, 2004, invited lecture. (Oral).

— Current sheet instabilities and reconnection – consequences for solar system plasmas. Plasma-theory-workshop of the Max-Planck-Institut für Plasmaphysik, Schloss Ringberg, Tegernsee, Germany, November 8 – 12, 2004, invited lecture. (Oral).

— Magnetic reconnection processes – SOHO, Cluster observations and models. 1st General Assembly of the European Geosciences Union, Nice, France, April 25 – 30, 2004, solicited, invited talk.

— Magnetopause stability – simulations and comparison with Cluster observations. 8th Cluster Workshop, University of New Hampshire, Durham, NH, USA, September 9 – October 1, 2004, invited. (Oral).

— Modeling of plasma instabilities in thin current sheets. International Conference on Sun-Earth Connections: Multiscale Coupling in Sun-Earth Processes, Kona, USA, February 9 – 13, 2004, invited lecture.

— Modelling the multi-scale coupling in solar reconnection. AGU Fall Meeting, San Francisco, USA, December 13 – 17, 2004. (Oral).

— Multiscale coronal structures and their links to the photosphere: SOHO observations and MHD simulations. IAU Symp. 223: Multi-Wavelength Investigations of Solar Activity, Saint Petersburg, Russia, June 14 – 19, 2004, invited lecture. (Oral).

— New results of MHD and kinetic plasma simulations of the solar atmosphere and reconnection. Colloquium, Isaac Newton Institute for Mathematical Science, Cambridge, UK, August 6, 2004. (Oral).

— Reconnection at Sun and Earth: observations and simulations. UCLA IGPP Institute Colloquium, Los Angeles, USA, February 2, 2004, invited Lecture.

— Structure formation at magnetic boundaries. 35th COSPAR Scientific Assembly, Paris, France, July 18 – 25, 2004, invited talk. (Oral).

— Structure formation in collisionless thin current sheets – PIC- and Vlasov-code simulations. Physikalisches Kolloquium der Ruhr-Universität Bochum, Bochum, Germany, September 9, 2004. (Oral).

Büchner, J., B. Nikutowski, and A. Otto: Reconnection at Sun: simulation models based on SOHO observations. 35th COSPAR Scientific Assembly, Paris, France, July 18 – 25, 2004. (Oral).

— Solar transition region reconnection. AGU Fall Meeting, San Francisco, USA, December 13 – 17, 2004.

Büchner, J., B. Nikutowski, and I. Silin: Shear-flow reconnection in the solar atmosphere. 1st General Assembly of the European Geosciences Union, Nice, France, April 25 – 30, 2004. (Poster).

Büchner, J. and I. Silin: The nonlinear instability of thin current sheets and collisionless reconnection. 1st General Assembly of the European Geosciences Union, Nice, France, April 25 – 30, 2004, solicited, invited talk.

Buske, M. and U. Christensen: Dreidimensionale Evolutionsmodelle der Mantelkonvektion im Mars.

64. Jahrestagung der Deutschen Geophysikalischen Gesellschaft, Berlin, Germany, March 8 – 12, 2004.

— Thermal evolution models for the Martian mantle. 9th Symposium on Study of the Earth's Deep Interior, Garmisch-Partenkirchen, Germany, July 4 – 9, 2004. (Poster).

Chanteur, G., R. Modolo, E. Dubinin, and A. Matthews: Simulations of the production of hydrogen and oxygen atoms in the Martian environment. 1st General Assembly of the European Geosciences Union, Nice, France, April 25 – 30, 2004.

Christensen, U.: Numerical models of the geodynamo – can they be scaled to the core? AGU Fall Meeting, San Francisco, USA, December 13 – 17, 2004, invited. (Oral).

— Numerical simulation of planetary dynamos. International Meeting on Dynamos of the Sun, Stars and Planets, Albert-Ludwigs-Universität und Kiepenheuer-Institut for Sonnenphysik, Freiburg, Germany, October 4 – 6, 2004. (Oral).

Christensen, U. and A. Tilgner: The power requirement of the geodynamo from scaling ohmic dissipation in numerical and laboratory dynamos. 1st General Assembly of the European Geosciences Union, Nice, France, April 25 – 30, 2004. (Oral).

Cortijo, S. V. S., P. Hartogh, and C. Jarchow: Microwave brightness temperature from a rough liquid surface. Joint AOGS 1st Annual Meeting and 2nd APHW Conference, Singapore, July 5 – 9, 2004, invited. (Oral).

Cremades, H., V. Bothmer, and D. Tripathi: Geometric Properties of Coronal Mass Ejections. IAU Symposium 226 on Stellar and Coronal Mass Ejections, Beijing, China, September 13 – 17, 2004. (Oral).

Cremades, H., **V. Bothmer**, and D. Tripathi: On the three-dimensional configuration of coronal mass ejections. 1st General Assembly of the European Geosciences Union, Nice, France, April 25 – 30, 2004. (Poster).

Cremades, H., V. Bothmer, and D. Tripathi: Properties of structured coronal mass ejections in solar cycle 23. 35th COSPAR Scientific Assembly, Paris, France, July 18 – 25, 2004. (Oral).

Czechowski, A., **M. Hilchenbach**, and K. C. Hsieh: Observations of energetic neutral atoms and the anomalous cosmic rays spectrum at the termination shock. 35th COSPAR Scientific Assembly, Paris, France, July 18 – 25, 2004. (Poster).

Czechowski, A., **K. Scherer**, H. J. Fahr, M. Hilchenbach, and K. C. Hsieh: Low-energy ACR in a time-dependent model of the heliosphere. 35th COSPAR Scientific Assembly, Paris, France, July 18 – 25, 2004. (Oral).

Daly, P. W.: The energetic particle spectrometer RAPID on board Cluster – a three year overview. Frühjahrstagung der DPG, Extraterrestrische Physik, Kiel, Germany, March 8 – 11, 2004. (Oral).

Daly, P. W., S. Mühlbachler, J. F. Fennell, J. B. Blake, J. Roeder, R. Friedel, G. D. Reeves, M. Grande, C. H. Perry, M. W. Dunlop, and J. Davies: Trapped, streaming and counter-streaming energetic electrons in the geomagnetic tail: Cluster/RAPID. Joint Assembly of the AGU, CGU, SEG, EEGS, Montreal, Canada, May 17 – 21, 2004. (Poster).

Dandouras, I., D. G. Mitchell, E. C. Roelof, S. M. Krimigis, P. C. Brandt, D. C. Hamilton, and N. Krupp: Energetic neutral atom emissions associated with Titan: observations during Cassini's first orbits of Saturn. AGU Fall Meeting, San Francisco, USA, December 13 – 17, 2004.

Davies, J. A., M. W. Dunlop, C. H. Perry, M. Lockwood, M. Grande, M. K. Carter, and P. W. Daly: A survey of energetic plasma observations by the RAPID experiment on Cluster. Joint Assembly of the AGU, CGU, SEG, EEGS, Montreal, Canada, May 17 – 21, 2004. (Poster).

Dubinin, E.: Instabilities as drivers of nonlinear stationary waves. ISSI Workshop: Nonlinear Plasma Waves-Solitons, Periodic Waves and Oscillitons – in Diverse Space Plasma Environments. Observations and Theory, Bern, Switzerland, March 22 – 26, 2004.

Dubinin, E. and K. Sauer: Origin of coherent wave packet emissions in space plasmas. 1st General Assembly of the European Geosciences Union, Nice, France, April 25 – 30, 2004.

Escoubet, C. P., J. M. Bosqued, J. Berchem, F. Pitout, H. Laakso, A. Masson, M. Dunlop, H. Rème, A. Fazakerley, I. Dandouras, B. Lavraud, and P. Daly: Cluster observations in the polar cusp under northward IMF-Bz. 1st General Assembly of the European Geosciences Union, Nice, France, April 25 – 30, 2004.

Fennell, J. F., J. L. Roeder, R. Friedel, M. Grande, and P. W. Daly: Electron distributions at the dusk and dawn magnetotail flanks: Cluster RAPID observations. Joint Assembly of the AGU, CGU, SEG, EEGS, Montreal, Canada, May 17 – 21, 2004. (Poster).

Fränz, M., I. Dandouras, H. Rème, A. N. Fazakerley, V. Genot, T. S. Horbury, A. Korth, and O. Moullard: Magnetosheath and solar wind instabilities observed by Cluster. 1st General Assembly of the European Geosciences Union, Nice, France, April 25 – 30, 2004. (Oral).

Friedel, R. H., S. P. Monk, M. G. Taylor, G. D. Reeves, D. Baker, P. W. Daly, M. W. Dunlop, and J. A. Davies: Energetic electron morphology in the central mid-tail plasmasheet. Joint Assembly of the AGU, CGU, SEG, EEGS, Montreal, Canada, May 17 – 21, 2004. (Oral).

Greve, R. and **B. Grieger**: Simple climate parameterizations for simulations of the recent evolution of the north polar cap of Mars. Second MATSUP Workshop, Darmstadt, Germany, March 8 – 9, 2004. (Oral).

Grieger, B.: ARCHIMEDES Mission Science Proposal. 3rd ARCHIMEDES Management Meeting, München, Germany, November 25 – 26, 2004.

— Color images from DISR. DISR Team Meeting, Tucson, AZ, USA, September 13 – 15, 2004. (Oral).

— Color images from DISR: 2. False color generation with a Kohonen Map. DISR Team Meeting, Tucson, AZ, USA, November 15 – 17, 2004. (Oral).

— Die Mission Huygens – Landung auf dem verschleierten Mond Titan. Man & Space – Momente der Faszination, Berlin, Germany, June 18 – August 29, 2004. (Oral).

— Direkt zum Mars – Die Vision der Mars Society von der Besiedelung des roten Planeten. Hannover-Messe, Hannover, Germany, April 20, 2004. (Oral).

— Plans for concerted analysis of SA and DLVS data in Lindau. DISR Team Meeting, Katlenburg-Lindau, Germany, July 28 – 30, 2004. (Oral).

— Solar Aureole Imager data assimilation. DISR Team Meeting, Goddard Space Flight Center, Greenbelt, Maryland, USA, March 22, 2004. (Oral).

— Summary of the Huygens Science Working Team Meeting #26. DISR Team Meeting, Katlenburg-Lindau, Germany, July 28 – 30, 2004. (Oral).

— Using Venus Express PFS data to simulate Venus' atmospheric dynamics with the general circulation model PUMA. PFS VEX and MEX general meeting, Frascati, Italy, September 27 – October 1, 2004. (Oral).

Grieger, B., M. Küppers, H. U. Keller, J. Wambsganß, and D. Kubas: Observing the parallax effect due to gravitational lensing with OSIRIS. OSIRIS Science Team Meeting, Katlenburg-Lindau, Germany, October 27 – 29, 2004. (Oral).

Grieger, B., R. Mahajan, J. Segschneider, and N. Ignatiev: Modeling atmosphere, ocean, and cryosphere of Earth and Earth like planets. DFG Research Conference "Earth, Water, Air and Life", Washington, DC, USA, April 4 – 6, 2004. (Poster).

Grieger, B. and S. Schröder: The visibility of Titan's surface from the descending probe. Huygens Science Working Team Meeting, Paris, France, July 26 – 27, 2004. (Oral).

Haberreiter, M., N. A. Krivova, W. Schmutz, and T. Wenzler: Reconstruction of solar UV irradiance back to 1974. 35th COSPAR Scientific Assembly, Paris, France, July 18 – 25, 2004. (Oral).

Hagfors, T.: Mars Express and the long wavelength ground penetrating radar: a dowsing rod in the search for water on Mars? The University of Natal, KwaZulu-Natal, Durban, South Africa, May 13, 2004.

— The Arecibo Observatory and its contributions to the fields of astronomy and ionospheric science. Can one hope for a similarly fruitful development with SKA, the Square Kilometer Array? The University of Natal, KwaZulu-Natal, Durban, South Africa, May 21, 2004.

Hamilton, D. C., G. Gloeckler, S. M. Krimigis, J. Dandouras, S. Livi, N. Krupp, and T. P. Armstrong: Composition and sources of suprathermal ions in Saturn's magnetosphere. AGU Fall Meeting, San Francisco, USA, December 13 – 17, 2004.

Hamilton, D. C., G. Gloeckler, S. M. Krimigis, D. G. Mitchell, J. Dandouras, S. Livi, N. Krupp, and T. P. Armstrong: Suprathermal ion composition observations during CASSINI's approach and orbit insertion at Saturn. 35th COSPAR Scientific Assembly, Paris, France, July 18 – 25, 2004.

Hartogh, P.: Chirp Transform Spectrometers versus Poly Phase Filterbanks. Future aspects of DDL developments, Chinese Academy of Sciences, Institute of Acoustics, Beijing, China, December 15 – 16, 2004. (Oral).

— General circulation- and submm radiative transfer modeling of the Martian atmosphere at MPS. Herschel Space Observatory Calibration Workshop: Models and observations of astronomical calibration sources, Lorentz Center, Leiden, Netherlands, December 1 – 3, 2004, invited. (Oral).

— HIFI science preparation. HIFI Science Preparation Meeting, Katlenburg-Lindau, Germany, May 18, 2004. (Oral).

— MAOAM and Exoplanets? GREAT and Exoplanets Meeting, DLR Adlershof/MPAE, Katlenburg-Lindau, Germany, May 13, 2004. (Oral).

— Microwave remote sensing of planetary atmospheres. Institutskolloquium, Institut für Planetenforschung, DLR, Berlin-Adlershof, May 26, 2004, invited. (Oral).

— Mikrowellenfernerkundung planetarer Atmosphären. Planetologisches Kolloquium, Institut für Planetologie, Universität Münster, Germany, April 28, 2004, invited. (Oral).

— MIME-like instrument: Chirp Transform Spectrometers for arrays? ESTEC-Meeting on Future Spaceborne Microwave Systems, Noordwijk, Netherlands, February 23, 2004. (Oral).

— Multi-channel spectrometer developments at MPS. International Conference on Submillimeter Science and Technology, Ahmedabad, India, October 13 – 15, 2004, invited. (Oral).

— Planetary Science with Herschel. The dusty and molecular universe, a prelude to HERSCHEL and ALMA, Ministere de la Recherche, Paris, France, October 27 – 29, 2004, invited. (Oral).

— VESPER MPAE contribution: CTS-development and microwave RTE modeling status. VESPER meeting, Goddard Space Flight Center, Washington, DC, USA, March 15, 2004. (Oral).

— WASPAM: Instrumental status and new scientific results. ASAC-Meeting, Andenes, Norway, September 8, 2004. (Oral).

Hartogh, P. and C. Jarchow: Submm brightness temperature modeling and retrieval calculations for the atmospheres of Mars and the giant planets in preparation of GREAT and HIFI. International Conference on Submillimeter Science and Technology, Ahmedabad, India, October 13 – 15, 2004, invited. (Oral).

— The microwave brightness of planetary atmospheres – preparatory modeling for GREAT and HIFI. International Workshop on Critical Evaluation of mm-/submm-wave Spectroscopic Data for Atmospheric Observations, Ibaraki, Japan, January 29 – 30, 2004, invited. (Oral).

Hartogh, P., C. Jarchow, G. Sonnemann, and M. Grygalashvyly: Microwave detection and quantitative GCM-analysis of the tertiary ozone maximum. Joint AOGS 1st Annual Meeting and 2nd APHW Conference, Singapore, July 5 – 9, 2004, invited. (Oral).

Hartogh, P., E. Lellouch, and C. Jarchow: HIFI-Planets guaranteed time – key project. HIFI Science Steering Commitee Meeting, Sterrewacht Leiden, Netherlands, April 18, 2004. (Oral).

Hartogh, P. and L. Song: Microwave detection of rocket exhaust plumes in the lower thermosphere. International Conference on Submillimeter Science and Technology, Ahmedabad, India, October 13 – 15, 2004, invited. (Oral).

Hartogh, P. and G. Villanueva: GREAT high resolution spectrometer and LO-box status. GREAT Consortium Meeting, Max-Planck-Institute for Radio Astronomy, Bonn, Germany, December 21, 2004. (Oral).

Heber, B., N. Krupp, L. Rodriguez, B. Blake, and H. Kunow: Ulysses COSPIN/KET and EPAC observations of Jovian electron bursts during the distant Jupiter encounter. AGU Fall Meeting, San Francisco, USA, December 13 – 17, 2004.

Heyminck, S., R. Güsten, P. van der Wal, J. Stutzki, R. Schieder, U. U. Graf, K. Jacobs, O. Sieberts, D. Rabanus, H. Röser, H. Hübers, and P. Hartogh: The SOFIA first generation instrument GREAT. Millimeter and Submillimeter Detectors for Astronomy II – Astronomical Telescopes and Instrumentation, Glasgow, Scotland, June 23 – 25, 2004. (Oral).

Hilchenbach, M.: Simulation of the landing of Rosetta-Philae on comet 67P/ Churyumov-Gerasimenko. Simpack User Meeting, Wartburg/ Eisenach, Germany, November 10, 2004. (Oral).

— Simulation of the landing of Rosetta-Philae on comet 67P/ Churyumov-Gerasimenko. Seminarvortrag, TU München, Germany, Garching, November 25, 2004. (Oral).

— Solar energetic particle events in the suprathermal energy region. 1st General Assembly of the European Geosciences Union, Nice, France, April 25 – 30, 2004. (Oral).

Hilchenbach, M., K. Bamert, B. Klecker, F. Ipavich, and R. Kallenbach: Energetic particle events in the suprathermal energy region as observed by SOHO/CELIAS/STOF. 35th COSPAR Scientific Assembly, Paris, France, July 18 – 25, 2004. (Oral).

Hilchenbach, M., K. C. Hsieh, A. Czechowski, B. Klecker, R. Kallenbach, and E. Moebius: Oberservation of energetic hydrogen and helium atoms with SOHO/CELIAS/STOF. 35th COSPAR Scientific Assembly, Paris, France, July 18 – 25, 2004. (Oral).

Hilchenbach, M. and H. Rosenbauer: Impact on a comet surface: Rosetta Lander simulations. AEF, Kiel, Germany, March 8 – 11, 2004. (Poster).

Ho, T. M., N. Thomas, D. C. Boice, T. Bonev, K. Jockers, and L. A. Soderblom: The dust coma of 10P/Borrelly. 36th Annual DPS Meeting, Luisville, KY, USA, November 8 – 12, 2004. (Oral).

— The dust coma of 19P/Borrelly. 35th COSPAR Scientific Assembly, Paris, France, July 18 – 25, 2004. (Oral).

Ignatiev, N. I., D. V. Titov, and W. J. Markiewicz: Sensitivity of the Venus Monitoring Camera observations to atmospheric and surface parameters. 1st General Assembly of the European Geosciences Union, Nice, France, April 25 – 30, 2004. (Poster).

Inada, A., N. Hoekzema, W. J. Markiewicz, H. U. Keller, K. Gwinner, J. P. Muller, H. Hoffmann, G. Neukum, and the HRSC Co-Investigator Team: Observations of Martian Clouds by High Resolution Stereo Camera (HRSC) on board Mars Express for the First Six Months. 35th COSPAR Scientific Assembly, Paris, France, July 18 – 25, 2004. (Oral).

Inada, A., N. Hoekzema, W. J. Markiewicz, H. U. Keller, G. Neukum, H. Hoffmann, and the HRSC Co-Investigator Team: Observations of Martian clouds by High Resolution Stereo Camera (HRSC) on board Mars Express for the first three months. 1st General Assembly of the European Geosciences Union, Nice, France, April 25 – 30, 2004. (Poster).

Ip, W. H., W. H. Hsu, A. Lagg, N. Krupp, J. Woch, S. Livi, T. Armstrong, and T. Krimigis: Microsignatures of satellite and ring absorption events. 35th COSPAR Scientific Assembly, Paris, France, July 18 – 25, 2004.

Jockers, K., T. Bonev, S. Szutowicz, and G. Villanueva: Gas and dust in comet 2P/Encke observed in the visual and in the submillimeter wavelength ranges. Conference devoted to the 60th anniversary of the Main Astronomical Observatory of the National Academy of Sciences of Ukraine, Astronomy in Ukraine – Past, Present and Future (MAO-2004), Kiev, Ukraine, July 15 – 17, 2004.

Jockers, K. and V. P. Tishkovets: Multiple scattering of light by densely packed random media: first results of a new approach. 83rd Annual Meeting of the Deutsche Mineralogische Gesellschaft, Aachen, Germany, September 18 – 21, 2004. (Oral).

Kallenbach, R., K. Bamert, C. W. Smith, M. Hilchenbach, and R. F. Wimmer-Schweingruber: Excitation of ion whistler waves upstream of an interplanetary traveling shock. 35th COSPAR Scientific Assembly, Paris, France, July 18 – 25, 2004. (Poster).

Keller, H. U. and Yu. V. Skorov: Gas production and nucleus evolution. Joint AOGS 1st Annual Meeting and 2nd APHW Conference, Singapore, July 5 – 9, 2004. (Oral).

Klecker, B., M. Hilchenbach, E. Moebius, M. A. Popecki, L. M. Kistler, and H. Kucharek: Strong energy dependence of the mean ionic charge of suprathermal lons in impulsive events. 1st General Assembly of the European Geosciences Union, Nice, France, April 25 – 30, 2004. (Oral).

Klecker, B., E. Moebius, M. A. Popecki, M. Hilchenbach, L. M. Kistler, and H. Kucharek: Observation of energy-dependent ionic charge states in impulsive solar energetic particle events. 35th COSPAR Scientific Assembly, Paris, France, July 18 – 25, 2004. (Oral).

Kossacki, K. J. and W. J. Markiewicz: Melting of surface water ice seasonally deposited from atmosphere in Martian gullies – can it be directly observed? 35th COSPAR Scientific Assembly, Paris, France, July 18 – 25, 2004. (Poster).

— Seasonal melting of surface water ice condensing in Martian gullies. 1st General Assembly of the European Geosciences Union, Nice, France, April 25 – 30, 2004. (Poster).

Kramar, M., B. Inhester, and **T. Wiegelmann**: Basics of vector tomography. Non-linear force free field workshop, Palo Alto, USA, May 17 – 20, 2004. (Oral).

Krivova, N. A. and **A. V. Krivov**: Large interstellar dust grains: signposts of other solar systems? Symposion zu Ehren von Dr. J. Guertler und Dr. J. Dorschner anlässlich ihrer 65. Geburtstage, Universität Jena, Germany, June 16, 2004. (Oral).

Krivova, N. A. and S. K. Solanki: Reconstruction of solar UV irradiance. 35th COSPAR Scientific Assembly, Paris, France, July 18 – 25, 2004. (Poster).

Kronberg, E., N. Krupp, A. Lagg, J. Woch, K.-H. Glassmeier, and K. K. Kurana: Substorms at Jupiter? 1st General Assembly of the European Geosciences Union, Nice, France, April 25 – 30, 2004. (Oral).

Kronberg, E., J. Woch, N. Krupp, A. Lagg, and K.-H. Glassmeier: Substorms at Jupiter? Frühjahrstagung der DPG, Extraterrestrische Physik, Kiel, Germany, March 8 – 11, 2004. (Oral).

Krüger, H.: Jovian dust streams measurements during Ulysses' 2004 distant Jupiter encounter. Joint Assembly of the AGU, CGU, SEG, EEGS, Montreal, Canada, May, 2004. (Oral).

— Staubteilchen – Boten ferner Welten. Förderverein Planetarium Göttingen, ZHG, Göttingen, Germany, December 14, 2004. (Oral).

— Staubteilchen, Boten ferner Welten. Symposium ”Die Planeten der Sonne und der fernen Sterne – Begegnung zwischen Astronomie und Geowissenschaften. Kenntnisstand und neue Ergebnisse – Wissenstransfer und Öffentlichkeitsarbeit“, Klaus Tschira Stiftung, Villa Bosch, Heidelberg, Germany, October 26, 2004. (Oral).

Krüger, H., E. Grün, and the Ulysses Dust Science Team: Jovian dust streams: first results from the Ulysses distant Jupiter encounter. EGU 1st General Assembly, Nice, France, April 25 – 30, 2004. (Oral).

Krüger, H., D. P. Hamilton, and E. Grün: Galileo in-situ dust measurements in Jupiter’s Gossamer Rings. 35th COSPAR Scientific Assembly, Paris, France, July 18 – 25, 2004. (Poster).

Krupp, N.: Ankunft am Saturn – Erste Ergebnisse der Cassini-Mission. Erich Regener Vortragsreihe, Max-Planck-Institut für Sonnensystemforschung, Katlenburg-Lindau, Germany, December 13, 2004. (Oral).

— Ankunft am Saturn – Erste Resultate der Cassini-Mission. Förderkreis Planetarium Göttingen, Vortragsreihe Faszinierendes Weltall, Universität Göttingen, Germany, November 30, 2004. (Oral).

— Die Mission Cassini – eine Reise zum Herrn der Ringe. Man & Space – Momente der Faszination, Ausstellung und Veranstaltungsreihe, Berlin, Germany, July 8, 2004.

— Energetic particles and neutrals in Saturns magnetosphere observed during Cassinis approach and orbit insertion at Saturn. The Saturn Universe: A Cassini Workshop, Capri, Italy, October 5 – 8, 2004. (Oral).

— Energetic particles in the vicinity of Titan. Titan Seminar Series Part 1, Imperial College London, UK, March 7 – 9, 2004.

— First results from Cassini on energetic particles (MIMI LEMMS and MIMI CHEMS) around flyby Ta. Titan Seminar Series Part 3, Imperial College London, UK, November 21 – 23, 2004. (Oral).

— Galileo-Highlights einer historischen Mission zum Jupiter. Frühjahrstagung der DPG, Extraterrestrische Physik, Kiel, Germany, March 8 – 11, 2004. (Oral).

— The UVIS instrument on Cassini. Titan Seminar Series Part 2, Imperial College London, UK, March 7 – 9, 2004.

Krupp, N., A. Lagg, J. Woch, S. M. Krimigis, S. Livi, D. G. Mitchell, D. C. Hamilton, T. P. Armstrong, and L. J. Lanzerotti: Energetic particles in the vicinity of Saturn: Cassini MIMI/LEMMS observations. 35th COSPAR Scientific Assembly, Paris, France, July 18 – 25, 2004.

Krupp, N., J. Woch, A. Lagg, J. Lim, S. M. Krimigis, D. G. Mitchell, E. C. Roelof, B. H. Mauk, C. Paranicas, S. Livi, T. P. Armstrong, M. K. Dougherty, W. S. Kurth, P. Louarn, I. Dandouras, and D. C. Hamilton: Structure of Saturn’s magnetosphere as revealed by energetic particles. AGU Fall Meeting, San Francisco, USA, December 13 – 17, 2004.

Kucharek, H., E. Moebius, W. Li, C. Farrugia, M. Popecki, A. Galvin, B. Klecker, M. Hilchenbach, and P. Bochsler: Injection and acceleration of interstellar helium at interplanetary shocks. 35th COSPAR Scientific Assembly, Paris, France, July 18 – 25, 2004. (Poster).

Küppers, M., G. Villanueva, and P. Hartogh: Abundance ratios and coma structure of comets 2001 Q4 (NEAT) and 2002 T7 (LINEAR). Division of Planetary Science of the AAS, Louisville, Kentucky, USA, November 8 – 12, 2004. (Oral).

Kuroda, T., M. Takahashi, N. Hashimoto, and D. Sakai: Simulation of the Martian atmosphere using a CCSR/NIES AGCM. Joint AOGS 1st Annual Meeting and 2nd APHW Conference, Singapore, July 5 – 9, 2004. (Oral).

Lagg, A.: Sample title. Stanford University, Palo Alto, CA, USA, November 22, 2004, invited.

— Stokes polarimetry in HeI 10830: magnetic field topology of an emerging flux region. Stanford University, Palo Alto, CA, USA, November 22, 2004, invited.

Lagg, A., J. Woch, N. Krupp, A. Gandorfer, and S. K. Solanki: Temporal evolution of chromospheric downflows. IAU Symp. 223: Multi-Wavelength Investigations of Solar Activity, St. Petersburg, Russia, June 14 – 19, 2004. (Poster).

Lellouch, E., P. Hartogh, and J. Crovisier: Solar-system observations with Herschel. 35th COSPAR Scientific Assembly, Paris, France, July 18 – 25, 2004. (Oral).

Limaye, S. S., W. J. Markiewicz, and D. V. Titov: Atmospheric circulation from Venus Monitoring

Camera observations. 1st General Assembly of the European Geosciences Union, Nice, France, April 25 – 30, 2004. (Poster).

Livi, S., T. P. Armstrong, P. C. Brandt, D. C. Hamilton, S. M. Krimigis, N. Krupp, B. H. Mauk, D. G. Mitchell, C. P. Paranicas, E. C. Roelof, and J. W. Manweiler: Energetic particle injections in Saturns magnetosphere. AGU Fall Meeting, San Francisco, USA, December 13 – 17, 2004.

Lorito, S., D. Schmitt, G. Consolini, P. D. Michelis, and P. Hoyng: Stochastic resonance in a bistable geodynamo model. 1st General Assembly of the European Geosciences Union, Nice, France, April 25 – 30, 2004. (Poster).

Mahajan, R. A., R. Greve, and B. Grieger: The evolution of the north polar cap of Mars – effect of dust content and ice rheology. 35th COSPAR Scientific Assembly, Paris, France, July 18 – 25, 2004. (Poster).

Maksimovic, M., I. Zouganelis, J.-Y. Chaufray, K. Issautier, E. E. Scime, J. Littleton, C. Salem, E. Marsch, H. Elliott, and D. J. McComas: Radial evolution of the electron distribution functions in the fast solar wind between 0.3 and 2 AU. 1st General Assembly of the European Geosciences Union, Nice, France, April 25 – 30, 2004. (Oral).

Markiewicz, W. J., N. M. Hoekzema, S. Hviid, A. Inada, H. U. Keller, E. Petrova, K. Gwinner, H. Hoffmann, G. Neukum, the HRSC Co-Investigator Team, and the MER Co-Investigator Team: Atmospheric optical depths from HRSC stereo images of Mars. 35th COSPAR Scientific Assembly, Paris, France, July 18 – 25, 2004. (Oral).

Markiewicz, W. J., N. M. Hoekzema, A. Inada, H. U. Keller, E. Petrova, K. Gwinner, H. Hoffmann, G. Neukum, R. Greely, C. Stauzer, the HRSC Co-Investigator Team, and the MER Co-Investigator Team: Atmospheric and variable features phenomena with HRSC on Mars Express. 35th COSPAR Scientific Assembly, Paris, France, July 18 – 25, 2004, solicited. (Oral).

Markiewicz, W. J., N. M. Hoekzema, H. U. Keller, G. Neukum, H. Hoffmann, and the HRSC Co-Investigator Team: Atmospheric and variable features phenomena with HRSC on Mars Express. 1st General Assembly of the European Geosciences Union, Nice, France, April 25 – 30, 2004. (Poster).

Markiewicz, W. J., **N. M. Hoekzema**, H. U. Keller, G. Neukum, and the HRSC Co-Investigator Team: Atmospheric optical depth from HRSC stereo images of Mars. 1st General Assembly of the European Geosciences Union, Nice, France, April 25 – 30, 2004. (Poster).

Markiewicz, W. J., H. U. Keller, D. Titov, R. Jaumann, H. Michalik, D. Crisp, L. Esposito, S. Watanabe, N. Ignatiev, and N. Thomas: Venus Monitoring Camera for Venus Express. 35th COSPAR Scientific Assembly, Paris, France, July 18 – 25, 2004. (Poster).

Markiewicz, W. J., D. Titov, H. U. Keller, R. Jaumann, H. Michalik, D. Crisp, L. Esposito, S. S. Limaye, S. Watanabe, N. Ignatiev, and N. Thomas: Venus Monitoring Camera for Venus Express. 1st General Assembly of the European Geosciences Union, Nice, France, April 25 – 30, 2004, solicited. (Oral).

Marsch, E.: Kinetic aspects of coronal heating. SOHO 15: Coronal Heating, St. Andrews, Scotland, UK, September 6 – 9, 2004, invited. (Oral).

— Kinetic effects in solar coronal heating and solar wind. Platon Network: Plasma Astrophysics of Heating, Flares and Winds, Strasbourg, France, June 24 – 25, 2004. (Oral).

— Solar Orbiter – Main goals and present status. 35th COSPAR Scientific Assembly, Paris, France, July 18 – 25, 2004, solicited. (Oral).

— Solar wind responses to the solar activity cycle. 35th COSPAR Scientific Assembly, Paris, France, July 18 – 25, 2004, solicited. (Oral).

— Turbulence and waves in the solar wind. 35th COSPAR Scientific Assembly, Paris, France, July 18 – 25, 2004, solicited. (Oral).

Marsch, E., X. Ao, and C. Tu: Zur Temperaturanisotropie des Kerns der Protonen Geschwindigkeitsverteilungsfunktion im Sonnenwind. Frühjahrstagung der DPG, Extraterrestrische Physik, Kiel, Germany, March 8 – 11, 2004.

Marsch, E. and **R. Schwenn**: Future solar and heliospheric research with Solar Orbiter. Joint AOGS 1st Annual Meeting and 2nd APHW Conference, Singapore, July 5 – 9, 2004, invited.

Marsch, E. and C.-Y. Tu: New observational results on the thermal anisotropy of the core and the differential speed of the beam of solar wind protons. 1st General Assembly of the European Geosciences Union, Nice, France, April 25 – 30, 2004. (Oral).

Marsch, E., T. Wiegelmann, and L. Xia: Coronal plasma flows and magnetic fields in solar active regions. SOHO 15: Coronal Heating, St. Andrews, Scotland, UK, September 6 – 9, 2004. (Poster).

Mazelle, C., C. Bertucci, K. Sauer, E. Dubinin, and M. Acuna: On the properties of coherent waves at the proton cyclotron frequency at Mars. 1st General Assembly of the European Geosciences Union, Nice, France, April 25 – 30, 2004.

Meister, C.-V.: Diurnal and seasonal variations of LTE radiative heating rates based on MGS/TES nadir temperature measurements. Second MATSUP Workshop, Darmstadt, Germany, March 8 – 9, 2004. (Poster).

Meister, C.-V., U. Berger, A. Feofilov, P. Hartogh, and A. Kutepov: Recent progress in the implementation of non-LTE radiation transport into the general circulation and climate model MART-ACC. Second MATSUP Workshop, Darmstadt, Germany, March 8 – 9, 2004. (Oral).

Meister, C.-V., P. Hartogh, A. Feofilov, and A. Kutepov: Non-LTE radiation transport effects in the Martian atmosphere. 1st General Assembly of the European Geosciences Union, Nice, France, April 25 – 30, 2004. (Oral).

— Non-LTE radiation transport effects in the upper atmosphere of Mars. Second MATSUP Workshop, Darmstadt, Germany, March 8 – 09, 2004. (Poster).

— Non-LTE radiation transport effects in the upper atmosphere of Mars. 35th COSPAR Scientific Assembly, Paris, France, July 18 – 25, 2004. (Poster).

Meister, C.-V., P. Hartogh, C. Jarchow, U. Berger, G. Sonnemann, and H. Elbern: Recent improvements of the general circulation and climate model of the Martian atmosphere MART-ACC. 1st General Assembly of the European Geosciences Union, Nice, France, April 25 – 30, 2004. (Poster).

Meister, C.-V., P. Hartogh, G. Sonnemann, U. Berger, A. Feofilov, A. Kutepov, and H. Elbern: Recent progress in the development of the general circulation and climate model of the Martian atmosphere MART-ACC. 35th COSPAR Scientific Assembly, Paris, France, July 18 – 25, 2004. (Oral).

Meister, C.-V. and G. Sonnemann: Plans to include a chemistry modul into MART-ACC. Second MATSUP Workshop, Darmstadt, Germany, March 8 – 9, 2004. (Poster).

Mitchell, D. G., S. M. Krimigis, B. H. Mauk, E. C. Roelof, C. P. Paranicas, P. C. Brandt, J. Dandouras, S. Livi, D. C. Hamilton, and N. Krupp: Energetic neutral atom emission during Cassini's approach and orbit insertion at Saturn: source strength and dynamics. 35th COSPAR Scientific Assembly, Paris, France, July 18 – 25, 2004.

Modolo, R., G. Chanteur, E. Dubinin, and A. Matthews: Simulations of the Martian plasma environment at solar min and solar max conditions. 1st General Assembly of the European Geosciences Union, Nice, France, April 25 – 30, 2004.

Mühlbachler, S. and **C. J. Farrugia**: A statistical investigation of dayside magnetosphere erosion showing saturation of response. AGU Fall Meeting, San Francisco, USA, December 13 – 17, 2004. (Poster).

Mühlbachler, S., R. Nakamura, W. Baumjohann, H. Noda, G. Paschmann, and J. Quinn: Convection in the near Earth tail lobe – Cluster/EDI observations 2001-2003. 8th Cluster Workshop, University of New Hampshire, Durham, NH, USA, September 9 – October 1, 2004. (Oral).

Muñoz, G., A. Lara, and R. Schwenn: Evaluation of ICME travel time models. IAU Symposium 226 on Coronal and Stellar Mass Ejections, Beijing, China, September 13 – 16, 2004. (Poster).

Narita, Y., K.-H. Glassmeier, S. Schäfer, U. Motschmann, I. Dandouras, K.-H. Fornaçon, M. Fränz, E. Georgescu, A. Korth, H. Rème, I. Richter, and K. Sauer: Dispersion relations and wave propagation in the foreshock and magnetosheath: A low-frequency picture from Cluster. 1st General Assembly of the European Geosciences Union, Nice, France, April 25 – 30, 2004. (Poster).

Neukum, G., R. Jaumann, H. Hoffmann, E. Hauber, J. Albertz, T. B. McCord, W. J. Markiewicz, and the HRSC Co-Investigator Team: The HRSC experiment on Mars Express: first results from Mars orbit. 1st General Assembly of the European Geosciences Union, Nice, France, April 25 – 30, 2004, solicited. (Oral).

Panov, E., J. Büchner, K.-H. Glassmeier, A. Korth, M. Fränz, B. Nikutowski, S. Savin, and L. M. Zelenyi: Cluster multipoint investigation of the small scale magnetopause structure. 1st General Assembly of the European Geosciences Union, Nice, France, April 25 – 30, 2004.

Panov, E., J. Büchner, A. Korth, M. Fränz, B. Nikutowski, A. Balogh, H. Rème, and M. Andre: Turbulence at the Earth's magnetopause. International workshop on turbulence in space plasmas, Italy, September 27 – October 3, 2004. (Oral).

Paranicas, C., N. Krupp, T. P. Armstrong, D. G. Mitchell, S. M. Krimigis, B. H. Mauk, E. C. Roelof, P. C. Brandt, and D. J. Williams: Charged neutral interactions inside 3 Saturn radii using Cassini MIMI data. AGU Fall Meeting, San Francisco, USA, December 13 – 17, 2004.

Paranicas, C., A. Lagg, N. Krupp, J. Woch, and B. H. Mauk: Charged particle losses near the inner Galilean satellites. Joint Assembly of the AGU, CGU, SEG, EEGS, Montreal, Canada, May 17 – 21, 2004.

Pau, J. L., C. Rivera, J. Pereiro, E. Muñoz, E. Calleja, U. Schühle, E. Frayssinet, B. Beaumont, J. P. Faurie, and P. Gibart: Nitride-based photodetectors: from visible to X-ray monotoring. European Materials Research Society Spring Meeting, Strasbourg, France, May 24 – 28, 2004. (Oral).

Perry, C. H., J. A. Davies, M. Grande, M. W. Dunlop, and P. W. Daly: Observations of heavy ions in the near-Earth environment in response to the geomagnetic storms of October/November 2003. Joint Assembly of the AGU, CGU, SEG, EEGS, Montreal, Canada, May 17 – 21, 2004. (Poster).

Petit, P.: Differential rotation of solar-type stars. Cool stars, stellar systems and the Sun 13, Hamburg, Germany, July 5 – 9, 2004. (Oral).

Petit, P. and J.-F. Donati: Dynamo processes and differential rotation in solar-type stars. SF2A-2004: Semaine de l'Astrophysique Francaise, Paris, France, June 14 – 18, 2004, invited review. (Oral).

— Magnetic mapping of solar-type stars. Cool stars, stellar systems and the Sun 13, Hamburg, Germany, July 5 – 9, 2004. (Oral).

Petit, P., J.-F. Donati, M. Aurière, V. Costa, N. Johnson, J. D. Landstreet, F. Lignières, S. Marsden, D. Mouillet, F. Paletou, N. Toqué, and G. A. Wade: Large-scale magnetic geometry of the G8 dwarf ξ Bootis A. Cool stars, stellar systems and the Sun 13, Hamburg, Germany, July 5 – 9, 2004. (Poster).

Podladchikova, E. V. and J. Büchner: Singular value decomposition of cancelling magnetic features associated with EUV bright-points. 35th COSPAR Scientific Assembly, Paris, France, July 18 – 25, 2004. (Poster).

Portyankina, G. and W. J. Markiewicz: Spider patterns in the Martian cryptic region. 1st General Assembly of the European Geosciences Union, Nice, France, April 25 – 30, 2004. (Poster).

Preusse, S., J. Büchner, and U. Motschmann: Stellar wind regimes at the orbit of close-in extrasolar planets. Workshop on Extrasolar Planets, Orsay, France, May 14, 2004. (Oral).

Preusse, S., J. Büchner, U. Motschmann, and A. Kopp: Numerical simulations of the magnetospheric interaction in extrasolar planetary systems. AEF Annual meeting, Kiel, Germany, May 8 – 11, 2004. (Poster).

Preusse, S., A. Kopp, J. Büchner, and U. Motschmann: Extrasolar planets in stellar winds. Extrasolar Planet Seminar, Institut für Geophysik und Meteorologie, Universität Köln, Germany, August 27, 2004.

— Sternwindregime von extrasolaren Planeten in kurzperiodischen Orbits. 3. Workshop Planetenbildung: Das Sonnensystem und extrasolare Planeten, Münster, Germany, October 6 – 8, 2004. (Oral).

Radioti, A., N. Krupp, J. Woch, A. Lagg, and K.-H. Glassmeier: Ion abundance ratios of the Jovian magnetosphere. 1st General Assembly of the European Geosciences Union, Nice, France, April 25 – 30, 2004. (Oral).

— Plasma composition in the Jovian magnetosphere. Frühjahrstagung der DPG, Extraterrestrische Physik, Kiel, Germany, March 8 – 11, 2004. (Poster).

— Plasma composition in the magnetosphere of Jupiter. 1st General Assembly of the European Geosciences Union, Nice, France, April 25 – 30, 2004.

Raouafi, N.-E. and S. K. Solanki: Reliability of large temperature anisotropies in the polar coronal holes. Joint AOGS 1st Annual Meeting and 2nd APHW Conference, Singapore, July 5 – 9, 2004. (Oral).

Richter, M., A. Gottwald, F. Scholze, U. Schühle, and G. Ulm: Calibration of space instrumentation with synchrotron radiation. 35th COSPAR Scientific Assembly, Paris, France, July 18 – 25, 2004. (Oral).

Richter, M., A. Gottwald, F. Scholze, U. Schühle, and G. Ulm: Instrument calibrations with synchrotron radiation. 5th TIGER Symposium, Paris, France, July 18 – 25, 2004. (Oral).

Rodriguez, L., J. Woch, N. Krupp, and M. Fränz: Eyecciones coronales de masa vistas en el espacio interplanetario. Seminar, Universidad de Alcalá, Madrid, Spain, January 29, 2004. (Oral).

Rodriguez, L., J. Woch, N. Krupp, M. Fränz, R. von Steiger, C. Cid, R. Forsyth, and K.-H. Glassmeier: Internal structure of magnetic clouds seen by Ulysses. 35th COSPAR Scientific Assembly, Paris, France, July 18 – 25, 2004. (Oral).

— Topology and internal structure of magnetic clouds inferred from Ulysses measurements. IAU Symposium 226 on Coronal and Stellar Mass Ejections, Beijing, China, September 13 – 17, 2004. (Poster).

Rodriguez, L., **J. Woch**, N. Krupp, M. Fränz, R. von Steiger, and K. H. Glassmeier: A statistical study of oxygen freezing-in temperature and energetic particles inside magnetic clouds observed by Ulysses. 1st General Assembly of the European Geosciences Union, Nice, France, April 25 – 30, 2004. (Poster).

Rotvig, J.: Compressible models of planetary cores in spherical geometry. 9th Symposium on Study of the Earth's Deep Interior, Garmisch-Partenkirchen, Germany, July 4 – 9, 2004. (Poster).

— Compressible models of planetary cores in spherical geometry. UK MHD Meeting 2004, Nice, France, May 6 – 7, 2004. (Poster).

— Multiple jets on Jupiter (and in the lab). 9th Symposium on Study of the Earth's Deep Interior, Garmisch-Partenkirchen, Germany, July 4 – 9, 2004. (Poster).

Saito, R., U. Berger, P. Hartogh, and G. Villanueva: Enhancement of the radiative transfer module: numerical experiments with different boundary conditions and comparison of modeling results with TES data. Second MATSUP Workshop, Darmstadt, Germany, March 8 – 9, 2004. (Oral).

Saito, R. and Y. Kasai: The abundance of the H_2O – O_2 complex in the Earth's atmosphere. International Workshop on Critical Evaluation of mm-submm-wave Spectroscopic Data for Atmospheric Observations, Ibaraki, Japan, January 29 – 30, 2004. (Poster).

Santos-Costa, D., S. Bolton, H. B. Garrett, N. Krupp, R. E. Sault, R. M. Thorne, and S. Levin: Radial diffusion coefficients for the transport of radiation-belt particles: a case study for protons and electrons in Jupiter's inner magnetosphere. AGU Fall Meeting, San Francisco, USA, December 13 – 17, 2004.

Sauer, K.: About the existence of stationary nonlinear waves due to kinetic effects. ISSI Workshop: Nonlinear Plasma Waves-Solitons, Periodic Waves and Oscillitons – in Diverse Space Plasma Environments. Observations and Theory, Bern, Switzerland, March 22 – 26, 2004.

— Origin of coherent large-amplitude waves in multi-ion plasmas. ISSI Workshop: Nonlinear Plasma Waves-Solitons, Periodic Waves and Oscillitons – in Diverse Space Plasma Environments. Observations and Theory, Bern, Switzerland, March 22 – 26, 2004.

— Oscillitons – origin of coherent large-amplitude waves. ISSI, International Team Meeting, Bern, Schwitzerland, May 3 – 6, 2004. (Oral).

— Solitons and oscillitons in multi-ion plasmas – origin of large-amplitude coherent waves. Alfvén 2004 Workshop on space, Beaulieu, France, April 19 – 23, 2004. (Oral).

Sauer, K. and E. Dubinin: Solitons and oscillitons as origin of coherent large-amplitude structures in beam-plasma configurations. 1st General Assembly of the European Geosciences Union, Nice, France, April 25 – 30, 2004.

— The history of the magnetic pile-up boundary at Mars. Joint AOGS 1st Annual Meeting and 2nd APHW Conference, Singapore, July 5 – 9, 2004. (Oral).

Sauer, K., E. Dubinin, and C. Mazelle: LF nonlinear waves in a beam-plasma system: application to the foreshock at Mars. 1st General Assembly of the European Geosciences Union, Nice, France, April 25 – 30, 2004.

Sauer, K., C. Mazelle, and E. Dubinin: Coherent large-amplitude waves in multi-ion plasmas originated from oscillitons: application to the foreshock of Earth and Mars. Joint AOGS 1st Annual Meeting and 2nd APHW Conference, Singapore, July 5 – 9, 2004. (Oral).

Savin, S., E. Amata, L. Zelenyi, M. Dunlop, M. Andre, P. Song, J. Büchner, P. M. E. Décréau, J. L. Rauch, and J. A. Sauvaud: Thin current sheet dynamics and sources at high-latitude magnetopause. 1st General Assembly of the European Geosciences Union, Nice, France, April 25 – 30, 2004. (Poster).

Savin, S., E. Amata, L. M. Zelenyi, M. Andre, and J. Büchner: Wave-particle interaction as a general mechanism for magnetosheath flow energy transient dissipation. 35th COSPAR Scientific Assembly, Paris, France, July 18 – 25, 2004. (Poster).

Savin, S., L. Zelenyi, E. Amata, and J. Büchner: Tracing of high latitude magnetopause by interball, polar and geotail versus MHD and gas dynamic modelling. 35th COSPAR Scientific Assembly, Paris, France, July 18 – 25, 2004. (Oral).

Savin, S., L. Zelenyi, E. Amata, G. Consolini, J. Büchner, M. Andre, S. Skalsky, J. Pickett, J. L. Rauch, and J. Blecki: Nonlinear interaction of magnetosheath flow with high-beta magnetopause. 1st General Assembly of the European Geosciences Union, Nice, France, April 25 – 30, 2004. (Oral).

Savin, S., L. Zelenyi, E. Amata, M. Dunlop, M. Andre, and J. Büchner: Dynamics of charged current sheets at high-latitude magnetopause. 35th COSPAR Scientific Assembly, Paris, France, July 18 – 25, 2004. (Oral).

Schröder, S., B. Grieger, A. Rodin, and H. U. Keller: Analyzing Huygens' DISR data: preparing for the descent into Titan's atmosphere. 35th COSPAR Scientific Assembly, Paris, France, July 18 – 25, 2004. (Poster).

Schühle, U.: Kalibrierung von weltraumgebundenen Instrumenten für die Sonnenforschung. 190. PTB-Seminar, Physikalisch-Technische Bundesanstalt, Berlin, Germany, May 18, 2004. (Oral).

Schüssler, M.: Convection and magnetic fields on the Sun. XLAB Science Camp, Göttingen, Germany, August 30, 2004. (Oral).

— Feuer und Eis: Eine Reise vom Mittelpunkt der Sonne bis nach Grönland. Lange Nacht der Sterne, MPS, Katlenburg-Lindau, Germany, September 18, 2004. (Oral).

— Flux tubes, surface magnetism, and the solar dynamo: constraints and open problems. Dynamos of the Sun, Stars & Planets, Freiburg i. Brsg., Germany, October 4 – 6, 2004. (Oral).

Schwenn, R.: Coronal mass ejections: what we have learned with SOHO? IAU Symposium 226 on Coronal and Stellar Mass Ejections, Beijing, China, September 13 – 16, 2004, invited. (Oral).

— Das neue Bild der Sonne. Vorlesungsreihe "Astronomie zum Studienanfang", Universität Göttingen, Germany, November 10, 2004.

— Early sentinels: the Helios 1 and 2 solar probes. Extended Science Definition Team for the NASA Sentinel Mission, Berkeley, USA, September 8, 2004.

— On predicting CME arrivals at Earth. Joint AOGS 1st Annual Meeting and 2nd APHW Conference, Singapore, July 5 – 9, 2004.

— Preparing for STEREO – revisit Helios! AGU Fall Meeting, San Francisco, USA, December 13 – 17, 2004, invited talk.

— Solar wind at Mercury. Joint AOGS 1st Annual Meeting and 2nd APHW Conference, Singapore, July 5 – 9, 2004, invited.

— Solar wind observations. Joint AOGS 1st Annual Meeting and 2nd APHW Conference, Singapore, July 5 – 9, 2004, invited.

— The Sun as the driver of space weather. School of Earth & Space Sciences, University of Science & Technology, Hefei, China, September 23, 2004.

— The Sun as the driver of space weather. Institute of Space Physics and Applied Technology of the Peking University, Beijing, China, September 29, 2004.

Segschneider, J., **B. Grieger**, H. U. Keller, K. F. E. Kirk, F. Lunkeit, A. Rodin, and R. Greve: The climate on Mars – observations and modelling. Second MATSUP Workshop, Darmstadt, Germany, March 8 – 9, 2004. (Oral).

Semenova, A., S. Berdyugina, S. K. Solanki, I. Ilyin, and I. Tuominen: Doppler imaging of Sigma Gem and HR1099. Cool Stars, Stellar Systems and the Sun 13, Hamburg, Germany, July 5 – 9, 2004. (Poster).

Silin, I. and J. Büchner: Coupling of waves and reconnection in guide field, magnetopause-like current sheets. AGU Fall Meeting, San Francisco, USA, December 13 – 17, 2004.

— Vlasov-code simulations of reconnection through magnetopause-like current layers. 1st General Assembly of the European Geosciences Union, Nice, France, April 25 – 30, 2004. (Oral).

— Vlasov-code simulations of reconnection through magnetopause-like current layers. 35th COSPAR Scientific Assembly, Paris, France, July 18 – 25, 2004. (Oral).

Solanki, S. K.: Die Sonne, ein Motor für globale Klimaänderungen? Planetarium, Stuttgart, Germany, October 28, 2004. (Oral).

— How is the Sun's magnetic field related to Einstein and our climate? Lublin, Poland, January 13, 2004. (Oral).

— How is the Sun's magnetic field related to Einstein and our climate? Joint Astrophysics Colloquium, MPI für Astrophysik, Garching, Germany, June 3, 2004. (Oral).

— How is the Sun's magnetic field related to Einstein and our climate? Astrophysical Seminar, Nanjing University, China, September 17, 2004. (Oral).

— How is the Sun's magnetic field related to Einstein and our climate? IMPRS Special Lecture, Max-Planck-Institut für Radioastronomie, Bonn, Germany, November 16, 2004. (Oral).

— Irradiance models. 35th COSPAR Scientific Asssembly, Paris, France, July 18 – 25, 2004. (Oral).

— Long-term solar irradiance variations: from current measurements to long-term estimates. First International Symposium on "Space Climate: Direct and Indirect Observations of Long-Term Solar Activity", Oulu, Finland, June 20 – 23, 2004. (Oral).

— Magnetic fields on the Sun and Sun-like stars. "Exploring the X-Ray Universe: Hot Plasma in Space", Mullard Space Science Laboratory, Dorking, Great Britain, June 22 – 25, 2004. (Oral).

— Solares Magnetfeld, Einstein, Klima – gibt es einen Zusammenhang? Institut für Astronomie und Geophysik, Universität Graz, Austria, May 7, 2004. (Oral).

— Sonnenaktivität, Einstein und Klima. Physikalisches Kolloquium, Universität Heidelberg, Germany, December 3, 2004.

— Structure of the solar chromosphere. IAU Symposium 223 "Multi-Wavelength Investigations of Solar Activity", St. Petersburg, Russia, June 14 – 19, 2004. (Oral).

— Was hat das Magnetfeld der Sonne mit Einstein und unser Klima zu tun? Physikalisches Kolloquium, Universität Bayreuth, Germany, December 14, 2004.

— Wie stark beeinflusst die Sonne das Klima und den derzeitigen Klimawandel? Rundgespräch der Kommission für Ökologie der Bayerischen Akademie der Wissenschaften "Klimawandel im 20. und 21. Jahrhundert – Welche Rolle spielen Kohlendioxid, Wasser und andere Treibhausgase wirklich?", München, Germany, May 17, 2004. (Oral).

Solanki, S. K. and **A. Gandorfer**: The Sun's magnetic field. Joint AOGS 1st Annual Meeting and 2nd APHW Conference, Singapore, July 5 – 9, 2004, invited review. (Oral).

Solanki, S. K. and N. A. Krivova: Irradiance models. 35th COSPAR Scientific Assembly, Paris, France, July 18 – 25, 2004. (Oral).

Solanki, S. K., A. Lagg, T. Wiegelmann, J. Woch, N. Krupp, and M. Collados: Direct detection of a current sheet in the solar atmosphere. 1st General Assembly of the European Geosciences Union, Nice, France, April 25 – 30, 2004.

Solanki, S. K., I. Usoskin, and M. Schüssler: Solar activity and climate during the last millenium. 35th COSPAR Scientific Asssembly, Paris, France, July 18 – 25, 2004. (Oral).

— Solar activity over the last 1150 years: does it correlate with climate? Cool Stars, Stellar Systems and the Sun 13, Hamburg, Germany, July 5 – 9, 2004. (Oral).

Solanki, S. K., I. Usoskin, M. Schüssler, and K. Mursula: Solar activity over the last 1150 years: does it correlate with climate? EGU 1st General Assembly, Nice, France, April 25 – 30, 2004. (Oral).

Song, L. and P. Hartogh: Analysis of the seasonal dependence of polar mesospheric water vapour trends derived from ground-based microwave measurements. Joint AOGS 1st Annual Meeting and 2nd APHW Conference, Singapore, July 5 – 9, 2004, invited. (Poster).

Song, P. and **V. M. Vasyliūnas**: Meaning of ting. AGU Fall Meeting, San Francisco, USA, December 13 – 18, 2004. (Oral).

Sonnemann, G. R., M. Grygalashvyly, P. Hartogh, and C. Jarchow: Behaviour of mesospheric ozone under nearly polar night conditions. 35th COSPAR Scientific Assembly, Paris, France, July 18 – 25, 2004. (Oral).

Teriaca, L., L. Maltagliati, A. Falchi, G. Cauzzi, and R. Falciani: Overview of an eruptive flare: from chromospheric evaporation to cooling of hot flaring loops. SOHO 15: Coronal heating, St. Andrews, Scotland, UK, September 6 – 9, 2004. (Oral).

Teriaca, L., L. Maltagliati, A. Falchi, G. Cauzzi, and R. Falciani: Overview of an eruptive flare: from chromospheric evaporation to cooling of hot flaring loops. Solar coronal loops workshop and Solar B discussion, Palermo, Italy, September 1 – 3, 2004. (Oral).

Tomás, A. T., N. Krupp, J. Woch, and K.-H. Glassmeier: Energetic electrons in the inner part of the Jovian magnetosphere and their relation to auroral emissions. Frühjahrstagung der DPG, Extraterrestrische Physik, Kiel, Germany, March 8 – 11, 2004. (Poster).

Tomás, A. T., J. Woch, N. Krupp, A. Lagg, and K.-H. Glassmeier: Energetic electrons in the inner part of the Jovian magnetosphere and their relation to auroral emissions. 1st General Assembly of the European Geosciences Union, Nice, France, April 25 – 30, 2004. (Oral).

Tortorella, D., J. Aubert, and U. Christensen: Linear study on the onset of convection in a rapidly rotating anelastic-fluid spherical shell. 9th Symposium on Study of the Earth's Deep Interior, Garmisch-Partenkirchen, Germany, July 4 – 9, 2004. (Poster).

Tripathi, D., V. Bothmer, S. K. Solanki, R. Schwenn, M. Mierla, and G. Stenborg: SOHO/EIT observation of plasma downflow in a prominence associated coronal mass ejection on 05-Mar-2005. IAU Symposium 226 on Coronal and Stellar Mass Ejections, Beijing, China, September 13 – 16, 2004. (Poster).

Vasyliūnas, V. M.: Meaning of energy transfer functions and dipolarization and the substorm current wedge. 7th International Conference on Substorms, Levi, Finland, March 22 – 26, 2004. (Poster).

— Parallel electric fields and the generalized Ohm's law. Winckler Symposium on Fast Temporal Variations in Auroral Particle Precipitation, University of Minnesota, Minneapolis, Minnesota, USA, April 21 – 23, 2004. (Poster).

— Relation between magnetic fields and electric currents in cosmic plasmas. AGU Fall Meeting, San Francisco, USA, December 13 – 18, 2004. (Oral).

— The generalized Ohm's law and the time evolution of electric fields and currents. Space Physics Seminar, Boston University, Boston, Massachusetts, USA, April 29, 2004. (Oral).

Villanueva, G., U. Berger, and P. Hartogh: Improvement of the MAOAM program code: parallel-computing capability, numerical stability and seasonal cycle. Second MATSUP Workshop, Darmstadt, Germany, March 8 – 9, 2004.

Villanueva, G. and P. Hartogh: Planetary research with the Chirp Transform Spectrometer on SOFIA. Planetary research Seminar, NASA - Goddard Space Flight Center, USA, May 12, 2004. (Oral).

Villanueva, G., P. Hartogh, and C. Jarchow: The new Chirp Transform Spectrometer on SOFIA. Joint AOGS 1st Annual Meeting and 2nd APHW Conference, Singapore, July 5 – 9, 2004, invited. (Oral).

Vögler, A.: Structure and dynamics of magnetic fields in the solar photosphere. 35th COSPAR Scientific Assembly, Paris, France, July 18 – 25, 2004. (Oral).

Vögler, A., R. H. Cameron, C. U. Keller, and M. Schüssler: Decay of a simulated bipolar field in the solar surface layers. Workshop on Magnetohydrodynamics of Stellar Interiors, Cambridge, UK, September 6 – 15, 2004.

Wagner-Gentner, A., U. Graf, R. Güsten, P. Hartogh, H. Hübers, M. Phillip, D. Rabanus, and J. Stutzki: GREAT optics. Millimeter and Submillimeter Detectors for Astronomy II – Astronomical Telescopes and Instrumentation, Glasgow, Scotland, June 23 – 25, 2004. (Poster).

Wang, T.: Oscillations and waves in coronal loops: recent results from SOHO and TRACE. 1st General Assembly of the European Geosciences Union, Nice, France, April 25 – 30, 2004. (Oral).

Wicht, J.: Paleomagnetische Interpretation simulierter magnetischer Feldumkehrungen. 64. Jahrestagung der Deutschen Geophysikalischen Gesellschaft, Berlin, Germany, March 8 – 12, 2004.

— Site dependence of reversal durations. 9th Symposium on Study of the Earth's Deep Interior, Garmisch-Partenkirchen, Germany, July 4 – 9, 2004. (Poster).

Wicht, J. and P. Olson: A spherical Couette dynamo. 9th Symposium on Study of the Earth's Deep Interior, Garmisch-Partenkirchen, Germany, July 4 – 9, 2004. (Poster).

Wiegelmann, T.: Coronal magnetic fields. Frühjahrstagung der DPG, Extraterrestrische Physik, Kiel, Germany, March 8 – 11, 2004.

— Coronal magnetic fields. Non-linear force free field workshop, Palo Alto, USA, May 17 – 20, 2004.

— Reconstruction of coronal magnetic fields. 1st General Assembly of the European Geosciences Union, Nice, France, April 25 – 30, 2004. (Oral).

Wiegelmann, T. and B. Inhester: Computing non-linear force free coronal magnetic fields: a comparison of the Wheatland method and the Grad-Rubin method. Non-linear force free field workshop, Palo Alto, USA, May 17 – 20, 2004. (Oral).

— How to use magnetic field information for coronal loop identification? Solar Image Processing Workshop II, Annapolis, Maryland, USA, November 3 – 5, 2004. (Poster).

— Reconstruction of 3D solar magnetic fields. SECCHI Team Meeting, Oxnard, CA, USA, April 15 – 16, 2004. (Oral).

— The STEREO-SECCHI 3D software package. 1st General Assembly of the European Geosciences Union, Nice, France, April 25 – 30, 2004. (Poster).

Wiegelmann, T. and S. K. Solanki: Why are coronal holes indistinguishable from the quiet Sun in transition region radiation? SOHO-15, ST. Andrews, Scotland, UK, September 6 – 9, 2004. (Oral).

Wilhelm, K.: Observations of of the Sun in the vacuum ultraviolet wavelength band from space. Joint AOGS 1st Annual Meeting and 2nd APHW Conference, Singapore, July 5 – 9, 2004. (Oral).

— Observations of ultraviolet emission lines in solar coronal holes with SOHO. Joint AOGS 1st Annual Meeting and 2nd APHW Conference, Singapore, July 5 – 9, 2004. (Oral).

— Solar VUV measurements obtained by SOHO instruments and their radiometric calibration. 35th COSPAR Scientific Assembly, Paris, France, July 18 – 25, 2004. (Oral).

Wilhelm, K., W. Curdt, T. J. Wang, and B. N. Dwivedi: Recent observations on the heating and cooling of active-region loops. Joint AOGS 1st Annual Meeting and 2nd APHW Conference, Singapore, July 5 – 9, 2004. (Oral).

Winterhalter, D., K. Sauer, E. Dubinin, and M. Kivelson: Multi-spacecraft observations of large-amplitude waves at the Earths bow shock, and possible interpretation. 1st General Assembly of the European Geosciences Union, Nice, France, April 25 – 30, 2004.

Woch, J.: Magnetospheric sources of Jupiter's aurora. 1st General Assembly of the European Geosciences Union, Nice, France, April 25 – 30, 2004.

Wu, P., T. A. Fritz, Q. Zong, and P. W. Daly: Three dimensional energetic electron distributions observed during substorms: using a new mode the L3DD data of the Cluster RAPID experiment. AGU Fall Meeting, San Francisco, USA, December 13 – 17, 2004.

Wu, P., **T. A. Fritz**, Q. Zong, J. Niehof, and P. W. Daly: A comparison of Cluster and Polar energetic particle fluxes on November 13, 2003. Joint Assembly of the AGU, CGU, SEG, EEGS, Montreal, Canada, May 17 – 21, 2004. (Oral).

Xia, L. D., **E. Marsch**, and K. Wilhelm: On the network structure in solar equatorial coronal holes. 1st General Assembly of the European Geosciences Union, Nice, France, April 25 – 30, 2004. (Oral).

Zhang, H., T. Fritz, and P. Daly: High latitude boundary observed by Cluster. Joint Assembly of the AGU, CGU, SEG, EEGS, Montreal, Canada, May 17 – 21, 2004. (Poster).

Zhang, H., Q. Zong, T. Fritz, and P. Daly: Dayside boundary layer under northward IMF: a Cluster perspective. AGU Fall Meeting, San Francisco, USA, December 13 – 17, 2004.

Zong, Q., T. Fritz, S. Fu, A. Korth, and P. Daly: Triple cusps observed by Cluster – temporal or spatial effect? Joint Assembly of the AGU, CGU, SEG, EEGS, Montreal, Canada, May 17 – 21, 2004. (Oral).

Zong, Q., T. Fritz, S. Fu, Z. Pu, D. Baker, H. Zhang, A. Lui, K. Glassmeier, A. Korth, P. Daly, A. Balogh, and H. Rème: Cluster observations of Earthward flowing plasmoid in the tail. AGU Fall Meeting, San Francisco, USA, December 13 – 17, 2004.

Vorträge 2005 /
Talks 2005

Aasnes, A., R. H. Friedel, G. Reeves, B. Lavraud, J. A. Davies, P. W. Daly, A. Balogh, and H. Rème: A survey of energetic electrons in the Earth's magnetotail. AGU Fall Meeting, San Francisco, USA, December 5 – 9, 2005.

Agarwall, J., **H. Boehnhardt**, M. Mueller, and E. Gruen: Comet 67P/Churyumov-Gerasimenko observed with ESO-WFI. General Assembly of the European Geosciences Union, Vienna, Austria, April 25 – 29, 2005. (Poster).

Armstrong, T. P., J. Manweiler, N. Krupp, A. Lagg, S. Krimigis, S. Livi, D. Mitchell, E. Roelof, C. Paranicas, and D. Hamilton: Observations of the spectrum and angular distribution of trapped protons in Saturn's inner magnetosphere: implications for sources, transport, and loss. AGU Fall Meeting, San Francisco, USA, December 5 – 9, 2005. (Oral).

Arvelius, S., M. Yamauchi, H. Nilsson, R. Lundin, H. Rème, M. B. Bavassano-Cattaneo, G. Paschmann, A. Korth, L. M. Kistler, and G. K. Parks: Statistical study of relationships between dayside high-altitude and high-latitude O+ ion outflows and geomagnetic/solar activities. Cluster and Double Star Sysmposium, ESA/ESTEC, Noordwijk, Netherlands, September 19 – 23, 2005. (Poster).

Aubert, J. and U. Christensen: Scaling properties of numerical dynamos. General Assembly of the European Geosciences Union, Vienna, Austria, April 25 – 29, 2005. (Oral).

Balmaceda, L., S. K. Solanki, and N. Krivova: A cross-calibrated time series of sunspot areas since 1874. Solar Variability and Earth Climate, Monte Porzio Catone, Italy, June 27 – July 1, 2005. (Poster).

Bamert, K., R. F. Wimmer-Schweingruber, R. Kallenbach, M. Hilchenbach, H. Kunow, R. Müller-Mellin, A. Klassen, and C. W. Smith: Spectra and composition of suprathermal and energetic ions associated with the November 2 – 6, 2003 interplanetary coronal mass ejection events: SOHO/CELIAS/HSTOF and SOHO/EPHIN data. Solar Wind 11/SOHO 16 Conference, Whistler, British Columbia, Canada, June 12 – 17, 2005. (Poster).

Bamert, K., R. F. Wimmer-Schweingruber, R. Kallenbach, M. Hilchenbach, R. Müller-Mellin, A. Klassen, and C. W. Smith: Ion acceleration and wave-particle interaction at the interplanetary shocks associated with the Halloween 2003 and the 20 January 2005 events: SOHO/HSTOF, SOHO/EPHIN, and ACE/MAG observations. AGU Fall Meeting, San Francisco, USA, December 5 – 9, 2005. (Poster).

Bamert, K., R. F. Wimmer-Schweingruber, R. Kallenbach, M. Hilchenbach, and C. W. Smith: Spectra and composition of suprathermal ions associated with the November 4 – 6, 2003 interplanetary coronal mass ejection event: SOHO/CELIAS/HSTOF data. General Assembly of the European Geosciences Union, Vienna, Austria, April 25 – 29, 2005. (Poster).

Barrow, C. H. and T. D. Carr: First observations of Jupiter's radio emission in Florida. PRE VI Planetary Radio Emissions Workshop, Graz, Austria, April 20 – 22, 2005. (Oral).

Barrow, C. H., M. L. Kaiser, and R. J. MacDowall: Radio observations of Jupiter from high jovicentric latitudes. General Assembly of the European Geosciences Union, Vienna, Austria, April 25 – 29, 2005. (Oral).

— Radio observations of the Jovian bKOM and HOM from high jovicentric latitudes by Ulysses/URAP. AOGS 2nd Annual Meeting, Singapore, June 20 – 24, 2005. (Oral).

Bavassano-Cattaneo, M. B., M. F. Marcucci, A. Retino, G. Pallocchia, H. Rème, I. Dandouras, E. Möbius, B. Klecker, C. W. Carlson, M. McCarthy, A. Korth, R. Lundin, and A. Balogh: Ion kinetic signatures during a quasi-continuous reconnection event tailward of the cusp: Cluster CIS observations. Cluster and Double Star Symposium, ESA/ESTEC, Noordwijk, Netherlands, September 19 – 23, 2005. (Poster).

Berger, U., M. Grygalashvyly, G. Sonnemann, and P. Hartogh: The chemistry-transport module of the MAOAM-GCM. Third Workshop of the Subgroup "Atmosphere and Surface Processes" of the DFG Priority Programme "Mars and the Terrestrial Planets", Darmstadt, Germany, March 10 – 11, 2005. (Oral).

Blanc, M., N. André, S. Maurice, E. Pallier, T. Gombosi, K.-C. Hansen, S. Bolton, D. Young, F. Crary, A. Coates, E. Sittler, M. Dougherty, D. Gurnett, W. Kurth, P. Louarn, T. Krimigis, D. Mitchell, I. Dandouras, N. Krupp, L. Esposito, D. Shemansky, R. Srama, S. Kempf, and MAPS investigators: The Cassini view of Saturn's magnetosphere. 37th Division of Planetary Science Meeting, Cambridge, UK, September 4 – 9, 2005. (Oral).

Boehnhardt, H.: Albedo & size estimation of solar system bodies. MPIfR-MPS Mini-Workshop, MPS Katlenburg-Lindau, Germany, February 11, 2005.

— Comet 67P/Churyumov-Gerasimenko: new results and a summary. PHILAE Experimenters Workshop, Teistungen, Germany, April 4 – 6, 2005. (Oral).

— Das ROSETTA Projekt. Lions Club, Goslar, Germany, February 17, 2005.

— Deep Impact and Rosetta: Kometenforschung heute und in 10 Jahren. Kolloquium des Förderkreises für das Planetarium in Göttingen, Göttingen, Germany, November 1, 2005. (Oral).

— Deep Impact: summary and conclusions. SESAME Science Team Meeting, Budapest, Hungary, October 12 – 14, 2005. (Oral).

— Minor bodies in the planetary system. Haereus Physics Summer School on Planetary Systems, Bad Honnef, Germany, October 17 – 21, 2005. (Oral).

— The Edgeworth-Kuiper Belt – fridge at the edge of the planetary system. Seminar, University Observatory, Göttingen, Germany, May 12, 2005. (Oral).

— The Kuiper Belt – fridge at the edge of the planetary system. Institute Seminar, Astronomical Institute of Universidad Catolica, Santiago de Chile, June 29, 2005. (Oral).

Boehnhardt, H., S. Bagnulo, A. Barucci, I. Belskaya, L. Kolokolova, and K. Muinonen: Polarimetry of Kuiper Belt objects and centaurs. IAU Symposium No. 229, Asteroids, Comets, Meteors 2005, Buzios, Rio de Janeiro, Brasil, August 7 – 12, 2005. (Poster).

Boehnhardt, H., A. Fitzsimmons, S. Lowry, P. Pravec, D. Voghroulicky, and J.-L. Margot: The YORP effect on asteroid (54509) 2000 PH5. Calar Alto Colloquium, Heidelberg, Germany, April 27 – 28, 2005. (Oral).

Boehnhardt, H., O. Hainaut, H. U. Kaeufl, H. Rauer, and the ESO Deep Impact Project Team: The Deep Impact Campaign at ESO: overview and highlights. IAU Symposium No. 229, Asteroids, Comets, Meteors 2005, Buzios, Rio de Janeiro, Brasil, August 7 – 12, 2005. (Oral).

Boehnhardt, H., H. Rauer, U. Kaeufl, E. Pantin, and G.-P. Tozzi: Deep Impact at ESO – first results. VVV Seminar, European Southern Observatory, Santiago de Chile, July 15, 2005. (Oral).

Boehnhardt, H. and the ESO Deep Impact Dust Team: The Deep Impact Campaign at ESO: dust and nucleus characterization. IAU Symposium No. 229, Asteroids, Comets, Meteors 2005, Buzios, Rio de Janeiro, Brasil, August 7 – 12, 2005. (Poster).

Bonev, T. and K. Jockers: Dynamical modeling of the dust in comet C/LINEAR (2000 WM1). IAU Symposium No. 229: Asteroids, Comets, Meteors, Buzios, Brasil, August 7 – 12, 2005. (Poster).

Büchner, J.: Anomalous resistivity due to strongly nonlinear waves. 69. Jahrestagung der Deutschen Physikalischen Gesellschaft, Fachverband Extraterrestrische Physik, Berlin, Germany, March 4 – 9, 2005. (Oral).

— Anomalous resistivity in space physics. Los Alamos Reconnection Workshop, Santa Fe, New Mexico, USA, August 8 – 12, 2005, invited talk.

— Current sheet formation and reconnection in the transition region of the solar atmosphere due to photospheric footpoint motion and pre-existing magnetic field topology. General Assembly of the European Geosciences Union, Vienna, Austria, April 25 – 29, 2005. (Oral).

— Do magnetic nulls matter in solar reconnection? Los Alamos Reconnection Workshop, Santa Fe, New Mexico, USA, August 8 – 12, 2005, invited talk.

— Kinetic plasma simulation methods. Autumn College on Plasma Physics, The Abdus International Centre for Theoretical Physics, Trieste, Italy, September 5 – 30, 2005. (Oral).

— Magnetic field geometry and topology of 3D reconnection at Sun and stars. 69. Jahrestagung der Deutschen Physikalischen Gesellschaft, Fachverband Extraterrestrische Physik, Berlin, Germany, March 4 – 9, 2005. (Oral).

— Magnetospheric boundaries: simulation results and Cluster observations. General Assembly of the European Geosciences Union, Vienna, Austria, April 25 – 29, 2005, invited talk.

— Physical modeling of solar magnetic fields and currents. Solar group seminar, Katlenburg-Lindau, Germany, November 29, 2005. (Oral).

— Plasma dynamics in the solar transition region and corona as a consequence of observed photospheric magnetic fields and flows. Kiepenheuer Institut für Sonnenphysik, Freiburg, Germany, November 3, 2005, KIS-Kolloquiumsvortrag.

— Reconnection as a major mechanism of energy release in the solar corona. European SPM-11: The Dynamic Sun: Challenges for Theory and Observations, Leuven, Belgium, September 11 – 16, 2005. (Oral).

— Resonant Wave Particle Interactions – How good is the Quasilinear Theory? Autumn College on Plasma Physics, The Abdus Salam International Centre for Theoretical Physics, Trieste, Italy, September 5 – 30, 2005, invited lecture.

— SOHO and Cluster – theory and simulation. Solar Dynamics and its Effects on the Heliosphere and Earth, Bern, Switzerland, April 18 – 22, 2005, invited talk.

— Solar coronal modelling based on observed photospheric magnetic fields and including the microphysics of reconnection. The 6th Solar-B Science Meeting, Kyoto, Japan, November 8 – 11, 2005, invited review talk.

— Space plasma simulations: achievements, problems and future horizons. Space Science Week, Moscow, Russia, October 3 – 6, 2005, invited talk.

— Vlasov code simulation. 7th International School and Symposium for Space Simulation (ISSS-7), Kyoto, Japan, March 25 – 31, 2005, invited tutorial.

— Vlasov code simulation in space physics. WISER Workshop High Performace Computing 2005, Leuven, Belgium, April 18 – 22, 2005, invited talk.

Büchner, J. and B. Nikutowski: Acceleration of the fast solar wind by reconnection. Solar Wind 11/SOHO 16 Conference, Whistler, British Columbia, Canada, June 12 – 17, 2005.

Büchner, J., B. Nikutowski, and A. Otto: Physically consistent simulation of chromospheric and coronal magnetic fields. Chromospheric and Coronal Magnetic Fields, Katlenburg-Lindau, Germany, August 30 – September 2, 2005. (Oral).

Bunce, E. J., S. W. H. Cowley, C. M. Jackman, D. M. Wright, A. J. Coates, M. K. Dougherty, W. S. Kurth, N. Krupp, and A. M. Rymer: First observation of a compression-induced hot plasma injection event in Saturn's magnetosphere: a multi-instrument comparison. General Assembly of the European Geosciences Union, Vienna, Austria, April 25 – 29, 2005. (Oral).

Cameron, R., A. Vögler, M. Schüssler, and V. Zakharov: Simulations of Solar Pores. SPM-11: The Dynamic Sun: Challenges for Theory and Observations, Leuven, Belgium, September 11 – 15, 2005.

Cao, X., Z. Pu, H. Zhang, S. Fu, C. Xiao, Q. Zong, Z. Liu, J. Cao, A. Korth, M. Frazen, C. Carr, H. Rème, and K. Glassmeier: TC-1 and Cluster observation of substorm dipolarization on September 14, 2004. AGU Fall Meeting, San Francisco, USA, December 5 – 9, 2005. (Poster).

Christensen, U.: Cassini-Huygens: Saturn und seine Monde. XXI. Weltraumphysikalisches Kolloquium, Ruhr-Universität, Bochum, Germany, November 10, 2005. (Oral).

— Die ungleichen Geschwister der Erde – Planetenforschung heute. Wissenschaft im Rathaus, Max-Planck-Institut für Physik komplexer Systeme, Dresden, Germany, October 13, 2005. (Oral).

— Magnetohydrodynamic models of planetary dynamos. Astronomisches Institut der Bulgarischen Akademie der Wissenschaften, Sofia, Bulgaria, March 31, 2005, invited. (Oral).

— Numerical modelling of the geodynamo. William Smith Meeting "The Deep Earth": The structure and evolution of the interior of our planet, London, UK, November 23 – 24, 2005, invited. (Oral).

Christensen, U. and J. Aubert: Scaling laws for dynamos in rotating spherical shells. 10th Scientific Assembly of IAGA, Toulouse, France, July 18 – 29, 2005, invited. (Oral).

— Scaling laws for dynamos in rotating spherical shells. 10th Scientific Assembly of IAGA, Toulouse, France, July 18 – 29, 2005, invited. (Oral).

Couvidat, S., A. C. Birch, and L. Gizon: Time-distance helioseismology: impact of phase-speed filters on travel-time measurements. Joint Assembly of the AGU, SEG, NABS, SPD/AAS, New Orleans, USA, May 23 – 27, 2005. (Poster).

Cremades, H. and V. Bothmer: Dimensions of structured and halo coronal mass ejections. Solar Wind 11/SOHO 16 Conference, Whistler, British Columbia, Canada, June 12 – 17, 2005. (Oral).

— Position angles of structured coronal mass ejections and their relation to streamers. IAGA 2005, Toulouse, France, July 18 – 29, 2005. (Oral).

Curdt, W., E. Landi, T.-J. Wang, and U. Feldman: Evidence for in situ heating in active region loops. Solar Wind 11/SOHO 16 Conference, Whistler, British Columbia, Canada, June 12 – 17, 2005. (Poster).

Czechowski, A., **M. Hilchenbach**, and K. Scherer: Pick-up and low energy ACR ions in a time-dependent heliosphere. General Assembly of the European Geosciences Union, Vienna, Austria, April 25 – 29, 2005. (Poster).

Dal Lago, A., L. A. Balmaceda, L. E. A. Vieira, E. Echer, F. L. Guarneri, J. Santos, M. R. da Silva,

A. de Lucas, W. D. Gonzalez, A. L. C. de Gonzalez, R. Schwenn, and N. J. Schuch: Very intense geomagnetic storms caused by the interaction between interplanetary ejecta and high speed streams. Chapman Conference on Corotating Solar Wind Streams and Recurrent Geomagnetic Activity, Manaus, Brazil, February 6 – 12, 2005. (Poster).

Daly, P. W.: Managing Cluster data. IMPRS Lecture, MPS, Katlenburg-Lindau, Germany, September 12 – 16, 2005. (Oral).

— The Cluster mission to the Earth's magnetosphere. IMPRS Lecture, MPS, Katlenburg-Lindau, Germany, September 12 – 16, 2005. (Oral).

Daly, P. W. and **S. Mühlbachler**: Cluster Active Archive – the RAPID contribution. Cluster and Double Star Symposium, ESA/ESTEC, Noordwijk, Netherlands, September 19 – 23, 2005. (Poster).

D'Amicis, R., S. Orsini, E. Antonucci, D. Telloni, S. Fineschi, A. Milillo, R. Bruno, A. M. Di Lellis, and M. Hilchenbach: Numerical results for the neutral particle detector of coronal hole-associated neutral solar wind as expected at the Solar Orbiter position. Solar Wind 11/SOHO 16 Conference, Whistler, British Columbia, Canada, June 12 – 17, 2005. (Poster).

Dandouras, I., P. Garnier, E. C. Roelof, D. G. Mitchell, P. C. Brandt, S. M. Krimigis, N. Krupp, D. C. Hamilton, and D. Toublanc: Energetic neutral atom emissions associated with Titan: first Cassini observations. General Assembly of the European Geosciences Union, Vienna, Austria, April 25 – 29, 2005. (Oral).

— Titan's and Saturn's exospheres: First MIMI energetic neutral atom observations. Joint Assembly of the AGU, SEG, NABS, SPD/AAS, New Orleans, USA, May 23 – 27, 2005. (Oral).

Dandouras, I., V. Pierrard, J. Goldstein, C. Vallat, G. K. Parks, H. Rème, M. McCarthy, L. M. Kistler, B. Klecker, A. Korth, M. B. Bavassano-Cattaneo, P. Escoubet, and A. Masson: Multipoint observations of ionic structures in the plasmasphere by Cluster–CIS and comparisons with IMAGE-EUV observations and with model simulations. Cluster and Double Star Symposium, ESA/ESTEC, Noordwijk, Netherlands, September 19 – 23, 2005. (Poster).

Delsanti, A., N. Peixinho, F. Merlin, A. Doressoundiram, H. Boehnhardt, and A. Barucci: Infrared properties of Kuiper Belt objects and centaurs. IAU Symposium No. 229, Asteroids, Comets, Meteors 2005, Buzios, Rio de Janeiro, Brasil, August 7 – 12, 2005. (Poster).

Dotto, E., S. Fornasier, A. Barucci, H. Boehnhardt, *et al.*: Jupiter Trojan Asteroids: investigation of dynamical families. IAU Symposium No. 229, Asteroids, Comets, Meteors 2005, Buzios, Rio de Janeiro, Brasil, August 7 – 12, 2005. (Poster).

Dubinin, E., M. Fränz, J. Woch, S. Barabash, R. Lundin, and the ASPERA-3 Team: Plume-like structure near the Martian wake. General Assembly of the European Geosciences Union, Vienna, Austria, April 25 – 29, 2005. (Oral).

Dubinin, E., K. Sauer, M. Maksimoviic, N. Cornilleau-Werhlin, and M. Fränz: Cluster observations of almost monochromatic whistler wave packets and the mechanism of their formation. 69. Jahrestagung der Deutschen Physikalischen Gesellschaft, Fachverband Extraterrestrische Physik, Berlin, Germany, March 4 – 9, 2005.

Dubinin, E., J. Woch, M. Fränz, N. Krupp, R. Lundin, S. Barabash, and D. Winningham: Plume-like structure near the Martian wake, ASPERA-MEX observations. 69. Jahrestagung der Deutschen Physikalischen Gesellschaft, Fachverband Extraterrestrische Physik, Berlin, Germany, March 4 – 9, 2005.

Farrugia, C. J., **M. Leitner**, H. K. Biernat, H. Matsui, R. Schwenn, H. Kucharek, K. W. Ogilvie, and R. P. Lepping: Evolution of interplanetary magnetic clouds from 0.3 AU to 1 AU: a joint Helios-Wind investigation. Solar Wind 11/SOHO 16 Conference, Whistler, British Columbia, Canada, June 12 – 17, 2005. (Poster).

Fennell, J. F., J. L. Roeder, T. L. Mulligan, A. Korth, M. Grande, and R. H. Friedel: Polar crossing and upstream of the magnetopause and bow shock. AGU Fall Meeting, San Francisco, USA, December 5 – 9, 2005. (Poster).

Flandes, A. and **H. Krüger**: CIR modulation of Jupiter dust stream detection. Dust in Planetary Systems, Kauai'i, Hawaii, USA, September 26 – 30, 2005. (Poster).

Fränz, M., E. Dubinin, S. Barabash, R. Lundin, E. Roussos, and the ASPERA-3 Team: Ion intrusion through the induced magnetospheric boundary at Mars – ASPERA-3 observations. 10th Scientific Assembly of IAGA, Toulouse, France, July 18 – 29, 2005. (Oral).

Fränz, M., E. Dubinin, J. Woch, S. Barabash, R. Lundi, and the ASPERA-3 Team: Variations of the magnetic pile-up boundary location in the Martian magnetosphere. General Assembly of the European Geosciences Union, Vienna, Austria, April 25 – 29, 2005. (Oral).

Fränz, M., E. Dubinin, J. Woch, and the ASPERA Team: Filamentary structure of neutral atoms at Mars – ASPERA observation. 1st Mars Express Science Conference,, Noordwijk, Netherlands, February 24, 2005.

Fränz, M. and J. Woch: Vulkane, Wasser, Klimawandel – Europas Planetenmission Mars Express. VHS Astronomie Reihe, VHS Buxtehude, Germany, April 14, 2005. (Oral).

Fritz, T., **Q. Zong**, D. Baker, M. Goldstein, P. Daly, S. Fu, H. Frey, A. Balogh, and H. Rème: Earthward flowing plasmoid: structure and its related auroral signature. AGU Fall Meeting, San Francisco, USA, December 5 – 9, 2005.

Fu, S.-Y., Q.-G. Zong, J. Yang, **Z.-Y. Pu**, P. W. Daly, A. Korth, and T.-L. Zhang: Preliminary study of a plasmoid event observed in the plasma sheet. Cluster and Double Star Symposium, ESA/ESTEC, Noordwijk, Netherlands, September 19 – 23, 2005. (Poster).

Gandorfer, A.: Polarimetry of the Second Solar Spectrum near the atmospheric cut-off. Solar Polarization Workshop 4, Boulder, Colorado, USA, September 20, 2005. (Oral).

— Présentation de ZIMPOL et perspectives de ce type de systèmes pour THEMIS. THEMIS réunion groupe "Polarisation", Observatoire de Paris, Paris, France, July 18, 2005, invited talk. (Oral).

— UV Polarimetry of the second solar spectrum. Chromospheric and Coronal Magnetic Fields, MPS, Katlenburg-Lindau, Germany, August 29, 2005. (Oral).

Garnier, P., I. Dandouras, E. C. Roelof, D. G. Mitchell, S. M. Krimigis, N. Krupp, D. C. Hamilton, and D. Toublanc: Titan's exosphere: MIMI energetic neutral atom observations and modelling. 10th Scientific Assembly of IAGA, Toulouse, France, July 18 – 29, 2005.

Garnier, P., I. Dandouras, D. Toublanc, D. Mitchell, T. Krimigis, N. Krupp, D. C. Hamilton, P. C. Brandt, E. Roelof, and H. J. Waite: The exosphere of Titan and its interaction with the Kronian magnetosphere: MIMI obervations and modeling. AGU Fall Meeting, San Francisco, USA, December 5 – 9, 2005.

Giang, T. T., M. Yamauchi, H. Nilsson, R. Lundin, Y. Ebihara, H. Rème, I. Dandouras, M. B. Bavassano-Cattaneo, G. Paschmann, A. Korth, L. M. Kistler, and G. K. Parks: Oxygen-proton difference of the sub-KeV ring current ion drift. Cluster and Double Star Symposium, ESA/ESTEC, Noordwijk, Netherlands, September 19 – 23, 2005. (Poster).

Gizon, L.: A short survey of helioseismology (JOSO Prize Lecture). Second Central European Solar Physics Meeting, Bairisch Koelldorf, Austria, May 19 – 21, 2005. (Oral).

— Determination of rotation axes. 9th COROT Week of ESA, ESA/ESTEC, Noordwijk, Netherlands, December 5 – 9, 2005, invited. (Oral).

— Helioseismological diagnostics of solar activity. International Workshop on Solar Activity: Exploration, Understanding and Prediction, Lund, Sweden, September 19 – 21, 2005, invited. (Oral).

— Science Requirements for Helioseismology. VIM-Solar Orbiter Team Meeting, Torréjon de Ardoz, Spain, November 15 – 18, 2005, invited. (Oral).

Gizon, L., **G. Vauclair**, S. Solanki, and S. Dreizler: Asteroseismic determination of stellar rotation axes: feasibility study for COROT additional and core programs. Second Corot-Brasil Workshop, Ubatuba, Brazil, November 2 – 6, 2005, invited. (Oral).

Goesmann, F.: The electron macroscope, a simple electron beam instrument. General Assembly of the European Geosciences Union, Vienna, Austria, April 25 – 29, 2005. (Poster).

Goesmann, F., L. Becker, P. Ehrenfreund, F. Raulin, and M. Hilchenbach: A combined GC/MS and AP-MALDI Instrument for the Detection and Identification of organic Molecules on Mars. General Assembly of the European Geosciences Union, Vienna, Austria, April 25 – 29, 2005. (Oral and poster).

Goesmann, F. and R. Roll: Long-Term in-situ monitoring of a cometary nucleus; capabilities of the COSAC instrument onboard Philae. IAU Symposium No. 229 Asteroids, Comets, Meteors, Buzois, Rio de Janeiro, Brazil, August 7 – 12, 2005. (Poster).

— Long-term in-situ monitoring of cometary outgassing; one task for the COSAC instrument onboard Philae. General Assembly of the European Geosciences Union, Vienna, Austria, April 25 – 29, 2005. (Poster).

Grieger, B.: Blurring in Titan's atmosphere. 37th Meeting of the AAS Division for Planetary Sciences, Cambridge UK, September 4 – 9, 2005. (Poster).

— Circulation of Europa's ocean. Workshop on a Future Mission to Europa and the Jovian System, Paris, France, December 12 – 13, 2005. (Oral).

— Unter den Wolken Titans – Die Huygens-Sonde lüftet den Schleier des Saturnmondes. Violauer Kometen- und Planetentagung der Vereinigung der Sternenfreunde, Violau, Germany, May 13 – 16, 2005.

Grieger, B., H. S. Griebel, and the ARCHIMEDES Science Team: ARCHIMEDES – A balloon mission to Mars led by the German Mars Society. 3rd International Planetary Probe Workshop, Athen, Greece, June 27 – July 1, 2005.

Grieger, B., R. Kramm, and H. U. Keller: Retrieving surface and atmosphere properties from Huygens/DISR images. Cassini Planning Science Group Meeting, Florence, Italy, February 28 – March 4, 2005. (Oral).

— Retrieving Titan's surface and atmosphere properties from Huygens/DISR images. DFG Priority Programme 1115 "Mars and the Terrestrial Planets", Subgroup Atmosphere and Surface Processes, Darmstadt, Germany, March 10 – 11, 2005. (Oral).

Grieger, B., R. Kramm, H. U. Keller, and the DISR Team: Retrieving atmospheric properties from Huygens/DISR images. Titan/Cassini-Huygens Workshop, Heraclion, Crete, Greece, May 30 – June 3, 2005. (Poster).

Grieger, B., D. Titov, H. U. Keller, and K. Fraedrich: Studying the superrotation of Venus' atmosphere with a general circulation model of intermediate complexity. Colloquium of the DFG Priority Program "Mars and the terrestrial planets", Berlin, Germany, August 29 – 30, 2005. (Oral).

Gulkis, S., M. Allen, C. Backus, G. Beaudin, N. Biver, D. Bockelé-Morvan, J. Crovisier, D. Despois, P. Encrenaz, M. Frerking, M. Hofstadter, P. Hartogh, W. Ip, M. Janssen, L. Kamp, T. Koch, E. Lellouch, I. Mann, D. Muhleman, H. Rauer, P. Schloerb, and T. Spilker: Remote sensing of a comet at millimeter and submillimeter wavelengths from an orbiting spacecraft. AOGS 2nd Annual Meeting, Singapore, June 20 – 24, 2005. (Oral).

Hamilton, D., M. Hill, S. Krimigis, D. Mitchell, J. Dandouras, S. Livi, N. Krupp, and T. Armstrong: Variations in ion composition in Saturn's magnetosphere and a comparison with Earth and Jupiter. Joint Assembly of the AGU, SEG, NABS, SPD/AAS, New Orleans, USA, May 23 – 27, 2005. (Oral).

Hartogh, P.: Chirp transform spectrometer development status and future prospectives. The International Workshop on Submillimeter Wave Earth Observation: Past, Present and Future, Kyoto, Japan, November 14 – 15, 2005. (Oral).

— FIR and submillimetre heterodyne spectroscopy of the giant planet's atmospheres and their moons. 39th ESLAB Symposium "Trends in Space Science and Cosmic Vision 2020", Noordwijk, Netherlands, April 19 – 21, 2005. (Poster).

— Mid atmospheric water vapour derived from ground-based cm and mm wave measurements: experiments, data and scientific results. The International Workshop on Submillimeter Wave Earth Observation: Past, Present and Future, Kyoto, Japan, November 14 – 15, 2005. (Oral).

— Performance of the new 1 GHz DDL. SAW-Meeting, Beijing, China, August 19, 2005. (Oral).

— The GREAT experiment and its application to solar system research. The International Workshop on Submillimeter Wave Earth Observation: Past, Present and Future, Kyoto, Japan, November 14 – 15, 2005. (Oral).

— The water hole – extremely low water vapour during the last two years in the winter polar mesosphere. ASAC-Meeting, Hamburg, Germany, March 13 – 14, 2005. (Oral).

Hartogh, P. and F. Bensch: Estimation of water vapour rotational ground state emissions after Deep Impact and expected signal-to-noise of the MIRO detection. MIRO Science Team Meeting, Pasadena, CA, USA, January 31 – February 2, 2005. (Oral).

Hartogh, P., U. Berger, H. Elbern, C. Jarchow, T. Kuroda, A. Kutepov, **A. S. Medvedev**, R. Saito, and G. Sonnemann: MAOAM – Present status and future plans. DFG Colloquium: Mars and the Terrestrial Plantes, Berlin, Germany, August 29 – 30, 2005. (Oral).

Hartogh, P., H. Boehnhardt, B. Grieger, M. Hilchenbach, and N. Krupp: Possible contributions of the MPS to an Europa Orbiter. Jupiter Exploration Workshop, Toulouse, France, October 11 – 12, 2005. (Oral).

Hartogh, P. and C. Jarchow: Mars as a Submm Calibrator. Herschel Calibration Workshop, Cambridge, UK, September 10, 2005. (Oral).

— Submm radiances of Titan and Europa in the HIFI bands. Herschel Solar System Science Team Meeting, Paris, France, October 2, 2005. (Oral).

Hartogh, P., C. Jarchow, N. Thomas, E. Lellouch, and T. de Graauw: Submm wave sounding of sources and sinks of water vapour in the surface bounded atmosphere of Europa. Future Mission to Europa and the Jovian System, CNES, Paris, France, December 12 – 13, 2005. (Oral).

Hartogh, P., E. Lellouch, J. Crovisier, and the Herschel Solar System Science Team: Water (and chemistry) in the solar system. Herschel Science Workshop, Utrecht, Netherlands, April 18 – 22, 2005. (Oral).

Hartogh, P. and A. Medvedev: Constraining MAOAM temperatures and winds with ground-based interferometric observations in the submm range. Submillimeter Astronomy in the era of the SMA, Cambridge, MA, USA, June 13 – 16, 2005. (Poster).

— Warmings in the polar middle atmosphere of Mars: requirements on the validation of MAOAM general circulation model simulations. AOGS 2nd Annual Meeting, Singapore, June 20 – 24, 2005. (Oral).

Hartogh, P. and G. Sonnemann: The upper stratosphere and mesosphere ozone variability: ground-based millimeter wave observations as a test bed for the MAOAM chemistry-transport module. AOGS 2nd Annual Meeting, Singapore, June 20 – 24, 2005. (Oral).

Helbert, J., E. Jessberger, J. Benkhoff, G. Arnold, M. Banaszkiewicz, A. Bischoff, M. Blecka, S. Calcutt, L. Coangeli, A. Coradini, S. Erard, S. Fonti, R. Killen, J. Knollenberg, E. Kührt, I. Mann, **U. Mall**, L. Moroz, G. Peter, M. Rataj, M. S. Robinson, T. Spohn, A. Sprague, D. Stöffler, F. Taylor, and J. Warrell: MERTIS – A thermal infrared imaging spectrometer for the Bepi-Colombo Mission. 36th Annual Lunar and Planetary Science Conference, League City, Texas, USA, March 14 – 18, 2005. (Oral).

Heyminck, S., R. Güsten, P. van der Wal, J. Stutzki, U. U. Graf, H.-W. Hübers, P. Hartogh, and H.-P. Röser: GREAT – The German first light heterodyne instrument for SOFIA. New Observing Opportunities in the Far-Infrared and Submillimeter Range – Splinter Meeting of the Annual Meeting of the Astronomische Gesellschaft (AG) The many facets of the universe – Revelations by New Instruments, Cologne, Germany, September 26 – October 1, 2005. (Oral).

Hilchenbach, M.: Analysis of cometary dust grains: a method for understanding the structure of comet nuclei? IAU Symposium No. 229, Asteroids, Comets, Meteors – ACM, Buzios, Rio de Janeiro, Brazil, August 7 – 12, 2005. (Poster).

— ENA originating from the solar wind acceleration region in the solar corona. AOGS 2nd Annual Meeting, Singapore, June 20 – 24, 2005. (Oral).

— Rosetta – Mission to a comet: organic chemistry, water and relevance for life sciences. Centro de estudos do mar, Pontal do Sul, Pontal do Parana, Brasil, August 5, 2005. (Oral).

Hilchenbach, M. and K. Bamert: Neutral solar wind: a tool for studying the solar atmosphere? General Assembly of the European Geosciences Union, Vienna, Austria, April 25 – 29, 2005. (Poster).

Hilchenbach, M., K. Bamert, and A. Czechowski: Potential observations of the solar atmosphere via in-situ measurements of the neutral solar wind. Solar Wind 11/SOHO 16 Conference, Whistler, British Columbia, Canada, June 12 – 17, 2005. (Poster).

Hilchenbach, M. and A. Czechowski: Anomalous hydrogen and helium spectra at the termination shock from energetic neutral atoms flux intensity measurements. Solar Wind 11/SOHO 16 Conference, Whistler, British Columbia, Canada, June 12 – 17, 2005. (Poster).

Hilchenbach, M., A. Czechowski, and K. Scherer: Energetic neutral atoms in a time-dependent heliosphere. Solar Wind 11/SOHO 16 Conference, Whistler, British Columbia, Canada, June 12 – 17, 2005. (Poster).

Hilchenbach, M., J. Kissel, H. Krüger, Y. Langevin, J. Silen, and L. Thirkell: Cometary dust grain in-situ analysis: COSIMA, Rosetta and future prospects . IAU Symposium No. 229, Asteroids, Comets, Meteors – ACM, Buzios, Rio de Janeiro, Brazil, August 7 – 12, 2005. (Poster).

Hilchenbach, M. and H. Krüger: Analysis of cometary dust: a means for understanding the structure of comet nuclei? AOGS 2nd Annual Meeting, Singapore, June 20 – 24, 2005. (Oral).

— Cometary dust composition: a tool for understanding the building blocks of comet nuclei? General Assembly of the European Geosciences Union, Vienna, Austria, April 25 – 29, 2005. (Poster).

Inhester, B. and T. Wiegelmann: Nonlinear force-free magnetic field extrapolations: Comparison of Grad-Rubin and Wheatland-Sturrock algorithms. STEREO/ Solar-B Science Planning Workshop, Turtle Bay, Oahu, Hawaii, USA, November 15 – 18, 2005. (Poster).

Ip, W. H., D. Kinoshita, L. N. Hau, A. Fujiwara, F. Saito, S. Yoshida, K. W. Min, A. Bhardwaj,

H. Boehnhardt, P. Hartogh, T. M. Capria, G. Cremonese, S. Orsini, A. Milillo, A. Allison, and D. Jewitt: A mission called SAPPORO. AOGS 2nd Annual Meeting, Singapore, June 20 – 24, 2005. (Oral).

Ip, W.-H., N. Krupp, J. Woch, A. Lagg, S. Livi, C. Paranicas, S. M. Krimigis, T. P. Armstrong, and J. Dandouras: Charge exchange effects in the Saturnian System. General Assembly of the European Geosciences Union, Vienna, Austria, April 25 – 29, 2005. (Oral).

Jarchow, C. and P. Hartogh: Retrieval Simulation for the MIRO Instrument on the Rosetta Orbiter. 37th annual meeting of the Division for Planetary Sciences of the American Astronomical Society, Cambridge, UK, September 4 – 9, 2005. (Poster).

Jockers, K.: Ground-based support of space missions (planets and comets) at the MPI of Solar System Research at present and in the future. First annual Europlanet N3 Meeting (Kickoff), Graz, Austria, March 9, 2005. (Oral).

— Kometenforschung im Rahmen der Zusammenarbeit zwischen dem Institut für Astronomie der BAN und dem MPI für Sonnensystemforschung. Astronomisches Institut der Bulgarischen Akademie der Wissenschaften, Sofia, Bulgarien, March 31, 2005. (Oral).

Jockers, K., N. Kiselev, T. Bonev, V. Rosenbush, N. Shakhovskoy, Yu. Efimov, D. Shakhovskoy, K. Antonyuk, and S. Kolesnikov: CCD imaging and aperture polarimetry od Comet 2P/Encke: Are there two polarimetric classes of comets? IAU Symposium No. 229: Asteroids, Comets, Meteors, Buzios, Brasil, August 7 – 12, 2005. (Poster).

Jockers, K., N. Kiselev, T. Bonev, V. Rosenbush, N. Shakhovskoy, S. Kolestnikov, Yu. Efimov, D. Shakhovskoy, and K. Antonyuk: Polarimetry of Comet 2P/Encke: two classes of comets? General Assembly of the European Geosciences Union, Vienna, Austria, April 25 – 29, 2005. (Poster).

Jockers, K., S. Szutowicz, G. Villanueva, T. Bonev, and P. Hartogh: HCN and CN in Comet 2P/Encke: a three-dimensional view on Comet Encke's outgassing. IAU Symposium No. 229: Asteroids, Comets, Meteors, Buzios, Brasil, August 7 – 12, 2005. (Oral).

— HCN and CN in Comet 2P/Encke: a threedimensional view on Comet Encke's outgassing. General Assembly of the European Geosciences Union, Vienna, Austria, April 25 – 29, 2005. (Poster).

Jockers, K., V. P. Tishkovets, E. V. Petrova, and I. V. Kulyk: Regolith on atmosphereless bodies in the solar system – ab-initio theory and ground-based astronomical observations emphasizing polarimetry. 3rd Colloquium DFG Priority Programme "Mars and the terrestrial planets", Berlin, Germany, August 29 – 30, 2005. (Poster).

Jones, G. H., A. J. Coates, S. C. Lowry, R. Sharp, A. Fitzsimmons, and C. M. Lisse: Observations of Comet 9P/Tempel around the Deep Impact collision from the Isaac Newton and UK Schmidt Telescopes. 37th Division of the Planetary Sciences Meeting, Cambridge, UK, September 4 – 9, 2005. (Poster).

Jones, G. H., E. Roussos, N. Krupp, J. Woch, A. Lagg, C. Paranicas, S. M. Krimigis, D. G. Mitchell, B. H. Mauk, W. Ip, and M. K. Dougherty: Macrosignatures of the icy moons in the inner magnetosphere of Saturn. AGU Fall Meeting, San Francisco, USA, December 5 – 9, 2005.

Kaeufl, H. U., H. Boehnhardt, N. Ageorges, S. Bagnulo, T. Bonev, Y. Fernandez, O. Hainaut, F. Kerber, *et al.*: Deep Impact at comet 9P/Tempel 1: mid-infrared observations. IAU Symposium No. 229, Asteroids, Comets, Meteors 2005, Buzios, Rio de Janeiro, Brasil, August 7 – 12, 2005. (Poster).

Kaeufl, H. U., T. Bonev, H. Boehnhardt, Y. Fernandez, and C. Lisse: Pre-impact Mid-IR and optical observations of comet 9P/Tempel 1. IAU Symposium No. 229, Asteroids, Comets, Meteors 2005, Buzios, Rio de Janeiro, Brasil, August 7 – 12, 2005. (Poster).

Kallenbach, R., K. Bamert, and M. Hilchenbach: Self-consistent adjustment of the flux of energetic ions and their injection threshold at heliospheric shocks. Solar Wind 11/SOHO 16 Conference, Whistler, British Columbia, Canada, June 12 – 17, 2005. (Poster).

Kallenbach, R., K. Bamert, M. Hilchenbach, and C. W. Smith: An extension of the quasi-linear theory on shock acceleration to low-energy ions. Solar Wind 11/SOHO 16 Conference, Whistler, British Columbia, Canada, June 12 – 17, 2005. (Poster).

Keiling, A., G. Parks, H. Rème, I. Dandouras, J. Bosqued, M. Wilber, M. McCarthy, L. Kistler, C. Mouikis, B. Klecker, A. Korth, R. Lundin, and H. Frey: Non-adiabatic bouncing ion clusters in the plasma sheet boundary layer observed by Cluster-CIS. AGU Fall Meeting, San Francisco, USA, December 5 – 9, 2005. (Poster).

Keiling, A., G. K. Parks, H. Rème, I. Dandouras, J.-M. Bosqued, M. McCarthy, E. Möbius, E. Amata, B. Klecker, A. Korth, and R. Lundin: First-ever multipoint observations of energy-dispersed ion structures in the plasma sheet boundary layer using Cluster. Cluster and Double Star Symposium, ESA/ESTEC, Noordwijk, Netherlands, September 19 – 23, 2005. (Poster).

Keller, H. U.: Comets. Planetary Sciences Summer School, Weihai, Shandong, China, August 15 – 26, 2005. (Oral).

— News from the world of Saturn. Astronomisches Kolloquium, Heidelberg, Germany, November 22, 2005. (Oral).

— Spectral investigation of the Moon with the SMART-1 Near Infrared Spectrometer SIR. Planetary Sciences Summer School, Weihai, Shandong, China, August 15 – 26, 2005. (Oral).

— The Saturn system after landing of the Huygens probe on Titan. Planetary Sciences Summer School, Weihai, Shandong, China, August 15 – 26, 2005. (Oral).

— Titan after landing of the Huygens Probe. Shanghai Astronomical Observatory, Shanghai, China, August 28, 2005. (Oral).

— Titan after landing of the Huygens probe. ISAS, The Institute of Space and Astronautical Science, Tokyo, Japan, October 5, 2005. (Oral).

— Titan after landing of the Huygens probe. Adlershofer Planetenseminar, Berlin, Germany, November 30, 2005. (Oral).

Keller, H. U., U. Christensen, A. Nathues, H. Sierks, R. Jaumann, S. Mottola, C. Russel, and the DAWN Science Team: Scientific investigations of 4 Vesta und 1 Ceres with the DAWN Framing Cameras. IAU Symposium No. 229 Asteroids, Comets, Meteors, Buzios, Rio de Janeiro, Brazil, August 7 – 12, 2005. (Poster).

Keller, H. U. and B. Grieger: Unter den Wolken – Huygens Blick auf Titans Oberfläche. Public lecture, MPS, Katlenburg-Lindau, Germany, January 27, 2005. (Oral).

Keller, H. U., B. Grieger, R. Kramm, M. Küppers, S. Schröder, Y. Skorov, M. Tomasko, and the DISR Team: Recent results of Titan achieved by Hyygens DISR. AOGS 2nd Annual Meeting, Singapore, June 20 – 24, 2005. (Oral).

Keller, H. U., M. Küppers, S. Hviid, H. Sierks, C. Barbieri, S. Fornasier, I. Bertini, L. Jorda, P. Gutierres, L. M. Lara, D. Koschny, J. Knollenberg, N. Thomas, and the OSIRIS Science Team: Deep Imapct observations by the scientific imaging system OSIRIS of the Rosetta mission. 37th Meeting of the AAS Division for Planetary Sciences, Cambridge, UK, September 4 – 9, 2005. (Oral).

Keller, H. U., M. Küppers, S. F. Hviid, H. Sierks, C. Barbieri, S. Fornasier, L. Jorda, P. J. Gutierrez, L.-M. Lara, D. Koschny, J. Knollenberg, and the OSIRIS Science Team: Deep Impact observations by the scientific imaging system OSIRIS of the Rosetta Mission. IAU Symposium No. 229 Asteroids, Comets, Meteors, Buzios, Rio de Janeiro, Brazil, August 7 – 12, 2005. (Oral).

Keller, H. U., U. Mall, and A. Nathues: SIR – NIR spectrometers for studying the lunar mineralogy. AOGS 2nd Annual Meeting, Singapore, June 20 – 24, 2005. (Oral).

— SIR-2 – NIR spectrometer for studying the lunar minerology. International Lunar Conference, Toronto, Canada, September 18 – 23, 2005. (Oral).

Keller, H. U., U. Mall, A. Nathues, and the SIR Science Team: SIR – a NIR spectrometer for studying the lunar mineralogy. 37th Meeting of the AAS Division for Planetary Sciences, Cambridge, UK, September 4 – 9, 2005. (Oral).

Keller, H. U., Y. V. Skorov, and G. N. Markelov: Kinetic simulation of gas transport near a nonspherical cometary nucleus. IAU Symposium No. 229 Asteroids, Comets, Meteors, Buzios, Rio de Janeiro, Brazil, August 7 – 12, 2005. (Oral).

Keller, H. U., M. Tomasko, and the DISR Team: Titan's surface – a close-up view. Titan/Cassini – Huygens Meeting, Heraklion, Crete, Greece, May 30 – June 3, 2005. (Oral).

Kiselev, N., S. Velichko, K. Jockers, V. Rosenbush, and S. Kikuchi: Database of comet polarimetry. IAU Symposium No. 229: Asteroids, Comets, Meteors, Buzios, Brasil, August 7 – 12, 2005. (Poster).

Kissel, J., M. Hilchenbach, **H. Krüger**, H. Fischer, C. Tubiana, *et al.*: COSIMA: a high resolution time-of-flight secondary ion mass spectrometer for cometary dust particles on its way to comet 67P/Churyumov-Gerasimenkov. Dust in Planetary Systems, Kauai'i, Hawaii, September 26 – 30, 2005. (Poster).

Klecker, B., E. Moebius, M. A. Popecki, L. M. Kistler, H. Kucharek, M. Hilchenbach, W. Dröge, and J. J. Kartavykh: Ionic charge states: a clue for the understanding of the location of the source region of solar energetic particles. General Assembly of the European Geosciences Union, Vienna, Austria, April 25 – 29, 2005. (Poster).

Klecker, B., E. Moebius, M. A. Popecki, L. M. Kistler, H. Kucharek, and M. Hilchenbach: Ionic charge states of Mg, Si and Fe in Fe-Rich solar energetic particle events. Solar Wind 11/SOHO 16 Conference, Whistler, British Columbia, Canada, June 12 – 17, 2005. (Oral).

Kleindienst, G., K. Glassmeier, M. K. Dougherty, N. Krupp, and A. S. Chris: ULF waves in the Kronian magnetosphere. AGU Fall Meeting, San Francisco, USA, December 5 – 9, 2005.

Korth, A.: Begann die Entwicklung des Lebens auf der Erde mit dem Einschlag von Kometen? Schulvortrag anlässlich der Hauptversammlung der MPG, Gymnasium an der Rostocker Heide, Röver-shagen, Germany, June 22, 2005. (Oral).

— Plasma sheet response during corotating interaction regions. Rapid Team Meeting, Beijing, China, April 11 – 14, 2005. (Oral).

— The Cluster mission and the response of the plasma sheet during high speed streams from the Sun. Dalian University of Technology, Dalian City, China, April 10, 2005. (Oral).

Korth, A., L. E. Vieira, M. Fränz, E. Echer, W. Gonzales, R. Friedel, C. G. Mouikis, and H. Rème: Plasma sheet response, observed by Cluster, due to small scale IMF Bz fluctuations in corotating high speed streams. Chapman Conference on Corotating Solar Wind Streams and Recurrent Geomagnetic Activity, Manaus, Brazil, February 6 – 12, 2005. (Oral).

Korth, A., L. E. Vieira, M. Fränz, R. Friedel, Q.-G. Zong, and H. Rème: Plasma sheet response during high speed streams. 3. Cluster Tail Workshop, Observatoire Paris-Meudon, France, March 7 – 11, 2005. (Oral).

Krimigis, S. M., D. G. Mitchell, D. C. Hamilton, N. Krupp, and I. Dandouras: Saturn's dynamical magnetosphere: energetic particles and neutrals from the magnetosphere imaging instrument MIMI on Cassini. AOGS 2nd Annual Meeting, Singapore, June 19 – 24, 2005. (Oral).

Krimigis, S. M., D. G. Mitchell, D. C. Hamilton, N. Krupp, S. Livi, E. C. Roelof, I. Dandouras, B. H. Mauk, P. C. Brandt, C. Paranicas, J. Saur, T. P. Armstrong, S. Bolton, A. F. Cheng, G. Gloeckler, M. E. Hill, K. Hsieh, W. Ip, A. Lagg, L. J. Lanzerotti, R. W. McEntire, and D. J. Williams: Saturn's dynamic magnetosphere: energetic particles and neutrals from the Magnetospheric Imaging Instrument (MIMI). Joint Assembly of the AGU, SEG, NABS, SPD/AAS, New Orleans, USA, May 23 – 27, 2005. (Oral).

Krimigis, S. M., D. G. Mitchell, D. C. Hamilton, N. Krupp, S. Livi, E. C. Roelof, J. Dandouras, B. H. Mauk, J. P. Brandt, C. Paranicas, N. Krupp, D. C. Hamilton, W. S. Kurth, P. Zarka, M. K. Dougherty, E. J. Bunce, and D. E. Shemansky: Overview of results from the Cassini magnetospheric imaging instrument (MIMI) during the first year of operations. 36th Annual Lunar and Planetary Science Conference, League City, Texas, USA, March 14 – 18, 2005. (Oral).

Krimigis, S. M., D. G. Mitchell, D. C. Hamilton, N. Krupp, S. Livi, E. C. Roelof, J. Dandouras, B. H. Mauk, J. P. Brandt, C. Paranicas, J. Saur, T. P. Armstrong, S. Bolton, A. F. Cheng, G. Gloeckler, K. C. Hsieh, W.-H. Ip, A. Lagg, L. J. Lanzerotti, R. W. McEntire, and D. J. Williams: Observations of energetic particles and neutrals at Saturn from the Cassini magnetosphere imaging instrument MIMI. General Assembly of the European Geosciences Union, Vienna, Austria, April 25 – 29, 2005. (Oral).

Krimigis, S. M., D. G. Mitchell, D. C. Hamilton, N. Krupp, S. Livi, E. C. Roelof, J. Dandouras, B. H. Mauk, P. C. Brandt, C. P. Paranicas, J. Saur, T. P. Armstrong, S. Bolton, A. F. Cheng, G. Gloeckler, M. E. Hill, K. C. Hsieh, W. H. Ip, A. Lagg, L. J. Lanzerotti, R. W. McEntire, and D. J. Williams: Dynamics of energetic particles and neutrals in Saturn's variable magnetosphere: results from the MIMI investigation. 37th Division of planetary science meeting, Cambridge, UK, September 4 – 9, 2005. (Oral).

Krivova, N.: Irradiance reconstructions – evolution of sources. SORCE-2005: Paleo Connections Between the Sun, Climate, and Culture, Durango, CO, USA, September 14 – 16, 2005. (Oral).

— Modelling of irradiance variations through atmosphere models. Solar Variability and Earth Climate, Monte Porzio Catone, Italy, June 27 – July 1, 2005. (Oral).

— Solar irradiance variations on time scales of interest for climate studies. "Physik seit Einstein", 69. Jahrestagung der Deutschen Physikalischen Gesellschaft, Berlin, Germany, March 4 – 9, 2005. (Oral).

Kronberg, E., K.-H. Glassmeier, J. Woch, N. Krupp, and A. Lagg: Why is the dynamic of the Jovian magnetosphere quasi-periodical? A possible intrinsic mechanism. General Assembly of the European Geosciences Union, Vienna, Austria, April 25 – 29, 2005. (Oral).

Kronberg, E., J. Woch, K.-H. Glassmeier, N. Krupp, and A. Lagg: Periodical substorms at Jupiter and

Earth. 10th Scientific Assembly of IAGA, Toulouse, France, July 18 – 29, 2005. (Oral).

Krüger, H.: Der Mond – Nachbar der Erde. Volkshochschule Mosbach, Binau/Baden, Germany, November 04, 2005. (Oral).

— Galileo in-situ dust measurements in Jupiter's gossamer rings. Workshop on 'Physiscs of Dusty Rings', ISSI, Bern, Switzerland, June 20 – 24, 2005. (Oral).

— Jupiter's dust disk: an astrophysical laboratory. Institute of Astronomy, Vienna, Austria, April 28, 2005. (Oral).

— Jupiter dust stream measurements from Ulysses' second Jupiter encounter. Conference on 'The Physics of Dusty Plasmas', Orleans, France, June 13 – 17, 2005. (Oral).

— Merkur und Venus; heisse Welten im inneren Sonnensystem. Volkshochschule Mosbach (Baden), Binau, Germany, June 3, 2005. (Oral).

Krüger, H., E. Grün, and the Ulysses Dust Science Team: Dust stream measurements from Ulysses' second Jupiter encounter. General Assembly of the European Geosciences Union, Vienna, Austria, April 25 – 29, 2005. (Oral).

Krüger, H., G. Linkert, D. Linkert, B. Anweiler, and E. Grün: Dust stream measurements from Ulysses' distant Jupiter flyby. Dust in Planetary Systems, Kauai'i, Hawaii, USA, September 26 – 30, 2005. (Oral).

Krüger, H., R. Moissl, D. P. Hamilton, and E. Grün: Galileo in-situ dust measurements in Jupiter's gossamer rings. Dust in Planetary Systems, Kauai'i, Hawaii, USA, September 26 – 30, 2005. (Poster).

Krupp, N.: Besuch beim Herrn der Ringe – Erste Resultate der Cassini-Mission. Westfälische Volkssternwarte und Planetarium, Recklinghausen, Germany, February 16, 2005. (Oral).

— Europlanet activity N2: Discipline Working Groups. Europlanet Kick-off Meeting and General Assembly #1, Vienna, Austria, April 24, 2005.

— Magnetospheres – Earth and outer planets, parts 1-3. IMPRS Lecture, MPS, Katlenburg-Lindau, Germany, September 12 – 16, 2005. (Oral).

— Magnetospheres of solar system bodies other than Earth. 10th Scientific Assembly of IAGA, Toulouse, France, July 18 – 29, 2005. (Oral).

— Magnetospheric Physics-Jupiter and Saturn compared to Earth, Part 1-4. Planetary Sciences Summer School, Weihai, Shandong, China, August 24, 2005. (Oral).

Krupp, N., **B. Grieger**, and A.-M. Harri: Europlanet activity N2: discipline working groups. Outcome of the First Meeting. Presentation to the European Project Officer, Brussels, Belgium, December 1 – 2, 2005. (Oral).

Krupp, N., G. Jones, E. Roussos, A. Lagg, J. Woch, D. Hamilton, and the MIMI Team: Saturn's magnetosphere near Titan's orbit. Titan Series IV, Imperial College London, UK, November 16 – 18, 2005. (Oral).

Krupp, N., **G. Jones**, E. Roussos, A. Lagg, J. Woch, D. Hamilton, and the MIMI Team: Titan's interaction (MIMI/LEMMS and MIMI/CHEMS) results. Titan Series IV, Imperial College London, UK, November 16 – 18, 2005. (Oral).

Krupp, N., H. Krüger, B. Grieger, M. Küppers, M. Fränz, and J. Wicht: Europlanet MPS. General Assembly of the European Geosciences Union, Vienna, Austria, April 25 – 29, 2005. (Poster).

Krupp, N., A. Lagg, J. Woch, G. H. Jones, E. Roussos, S. M. Krimigis, S. Livi, D. G. Mitchell, E. C. Roelof, C. Paranicas, D. C. Hamilton, T. P. Armstrong, and M. K. Dougherty: Global structure and dynamics of the Kronian magnetosphere: Cassini results. AGU Fall Meeting, San Francisco, USA, December 5 – 9, 2005. (Oral).

Krupp, N., A. Lagg, J. Woch, S. M. Krimigis, S. Livi, D. G. Mitchell, E. C. Roelof, C. Paranicas, D. C. Hamilton, T. P. Armstrong, and M. K. Dougherty: The Saturnian plasma sheet as releaved by energetic particle measurements. General Assembly of the European Geosciences Union, Vienna, Austria, April 25 – 29, 2005. (Oral).

Krupp, N., A. Lagg, J. Woch, E. Roussos, S. M. Krimigis, S. Livi, D. G. Mitchell, E. C. Roelof, C. Paranicas, J. Saur, D. C. Hamilton, T. P. Armstrong, and M. K. Dougherty: Dynamics of the Saturnian magnetosphere as revealed by energetic particle measurements: Cassini/MIMI results. 10th Scientific Assembly of IAGA, Toulouse, France, July 18 – 29, 2005. (Oral).

Krupp, N., A. Lagg, J. Woch, E. Roussos, S. M. Krimigis, S. Livi, D. G. Mitchell, E. C. Roelof, C. Paranicas, J. Saur, D. C. Hamilton, T. P. Armstrong, M. K. Dougherty, and **G. H. Jones**: The Saturnian magnetosphere as revealed by energetic particle and magnetometer measurements: Cassini results. Magnetospheres of the Outer Planets 2005, Leicester, UK, August 7 – 12, 2005. (Oral).

Kucharek, H., E. Moebius, Y. Lu, C. Smith, B. Klecker, C. Farrugia, M. Popecki, A. Galvin, M. Hilchenbach, and P. Bochsler: Sources and acceleration of energetic He+ in interplanetary space. Solar Wind 11/SOHO 16 Conference, Whistler, British Columbia, Canada, June 12 – 17, 2005. (Poster).

Kulyk, I. and K. Jockers: Ground-based photometric observations of Jupiter's inner satellites Thebe, Amalthea, and Methis at small phase angle. General Assembly of the European Geosciences Union, Vienna, Austria, April 25 – 29, 2005. (Oral).

Küppers, M., H. U. Keller, M. G. Tomasko, and the DISR Team: Investigation of the small-scale properties of Titans surface with Huygens/DISR images. Titan Cassini/Huygens Meeting, Heraklion, Greece, May 30 – June 3, 2005. (Poster).

Küppers, M., G. Villanueva, and P. Hartogh: Coma abundances in comets and clues about their formation and evolution. Asteroids, Comets, Meteors, Buzios, Brasil, August 7 – 12, 2005. (Poster).

Küppers, M., G. Villanueva, and **P. Hartogh**: Coma abundances in comets and clues about their formation and evolution. AOGS 2nd Annual Meeting, Singapore, June 20 – 24, 2005. (Poster).

Kuroda, T.: Studies of the Martian meteorology using general circulation models: radiative effects of Martian dust. AOGS 2nd Annual Meeting, Suntec, Singapore, June 20 – 24, 2005. (Oral).

Kuroda, T. and P. Hartogh: Temperature inversion during the 2001 global dust storm on Mars: observation with SWAS and modeling with MAOAM. AOGS 2nd Annual Meeting, Suntec, Singapore, June 20 – 24, 2005.

Kuroda, T., A. Medvedev, and P. Hartogh: Radiative effects of dust in the MAOAM-GCM. MATSUP Workshop, TU Darmstadt, Germany, March 10 – 11, 2005. (Oral).

Kurth, W. S., D. A. Gurnett, G. B. Hospodarsky, M. K. Dougherty, C. S. Arridge, N. A. Achilleos, N. Andre, F. J. Crary, H. J. McAndrews, K. Szego, A. M. Rymer, S. M. Krimigis, D. G. Mitchell, N. Krupp, D. C. Hamilton, and K. C. Hansen: Saturn's magnetosphere boundaries. AGU Fall Meeting, San Francisco, USA, December 5 – 9, 2005. (Oral).

Lagg, A.: Results from chromospheric magnetic field measurements. Chromospheric and Coronal Magnetic Fields, Katlenburg-Lindau, Germany, August 29, 2005.

Lagg, A., J. Woch, S. K. Solanki, and A. Gandorfer: Supersonic downflows in the vicinity of a solar pore. Solar Polarization Workshop 4, Boulder, Colorado, USA, 2005. (Oral).

Lara, L., **H. Boehnhardt**, *et al.*: Ground-based support for the DEEP IMPACT Mission to comet 9P/Tempel 1. Calar Alto Colloquium, Heidelberg, Germany, April 27 – 28, 2005. (Oral).

Leitner, M., **C. J. Farrugia**, V. A. Osherovich, J. Fainberg, H. K. Biernat, K. W. Ogilvie, and R. Schwenn: The relative distribution of the magnetic and plasma kinetic energy densities as a function of heliospheric distance. Solar Wind 11/SOHO 16 Conference, Whistler, British Columbia, Canada, June 12 – 17, 2005. (Poster).

Lellouch, E., P. Hartogh, R. Moreno, B. Bezard, N. Thomas, M. Banasciewicz, L. M. Lara, and T. D. Graauw: Sounding the chemistry and dynamics of the Jovian stratosphere at submillimeter wavelengths. Future Mission to Europa and the Jovian System, CNES, Paris, France, December 12 – 13, 2005. (Oral).

Lui, A. T. Y., Y. Zheng, A. Balogh, P. W. Daly, M. W. Dunlop, T. A. Fritz, G. Gustafsson, S. B. Mende, C. J. Owen, R. F. Pfaff, H. Rème, Y. Zhang, and Q. Zong: Magnetotail substorm features from multi-point observations. Cluster and Double Star Symposium, ESA/ESTEC, Noordwijk, Netherlands, September 19 – 23, 2005. (Oral).

Mall, U.: Near-infrared observations of the Moon. Royal Astronomical Society Meeting, London, UK, November 11, 2005. (Oral).

Mall, U., A. Nathues, and H. U. Keller: First results from the near-infrared spectrometer on SMART-1. General Assembly of the European Geosciences Union, Vienna, Austria, April 25 – 29, 2005. (Oral).

— Near-infrared investigations of the lunar far side with SIR on SMART-1. AGU Fall Meeting, San Francisco, CA, USA, December 5 – 9, 2005. (Oral).

Mall, U., A. Nathues, H. U. Keller, and the SIR-2 Science Team: SIR-2 – the NIR spectrometer for the Chandrayaan-1 Mission. 37th Meeting of the AAS Division for Planetary Sciences, Cambridge, UK, September 4 – 9, 2005. (Poster).

Marcucci, M. F., M. B. Bavassano-Cattaneo, G. Pallocchia, E. Amata, H. Rème, I. Dandouras, L. Kistler, B. Klecker, A. Korth, and A. Balogh: Cluster observations of oxygen ions at the dusk flank magnetopause during variable IMF orientation. General Assembly of the European Geosciences Union, Vienna, Austria, April 25 – 29, 2005. (Poster).

Marcucci, M. F., G. Pallocchia, M. B. Bavassano-Cattaneo, E. Amata, H. Rème, I. Dandouras, L. Kistler, B. Klecker, A. Korth, and C. M. Carr: Double star observations of accelerated flow reversals at the dayside magnetopause during by dominated IMF. Cluster and Double Star Symposium, ESA/ESTEC, Noordwijk, Netherlands, September 19 – 23, 2005. (Poster).

Marsch, E.: Importance of kinetic effects in heating the open and closed corona. Solar Wind 11/SOHO 16 Conference, Whistler, British Columbia, Canada, June 12 – 17, 2005. (Oral).

— Kinetic aspects of coronal heating. 69. Jahrestagung der Deutschen Physikalischen Gesellschaft, Fachverband Extraterrestrische Physik, Berlin, Germany, March 4 – 9, 2005. (Oral).

— Kinetic physics of the solar corona and solar wind. Seminar am MPI für Plasmaphysik, Abt. Tokomakphysik, Garching, Germany, March 17 – 18, 2005, eingeladener Seminarvortrag. (Oral).

— Kinetic Processes in the solar corona. Autumn College on Plasma Physics, The Abdus Salam International Centre for Theoretical Physics, Trieste, Italy, September 5 – 30, 2005. (Oral).

— Origin of the solar wind in coronal funnels and correlation heights of ultraviolet emission regions. 11th European Solar Physics Meeting, The Dynamic Sun: Challenges for Theory and Observations, Leuven, Belgium, September 11 – 16, 2005. (Oral).

— The science goals of Solar Orbiter from an in situ perspective. Connecting the Sun to the Earth, Royal Astronomical Society Discussion Meeting, London, UK, October 14, 2005. (Oral).

Marsch, E., C.-Y. Tu, C. Zhou, L.-D. Xia, L. Zhao, J.-X. Wang, and K. Wilhelm: Solar wind origin in coronal funnels and correlation heights of the sources of solar ultraviolet emission. Chromospheric and Coronal Magnetic Fields, Katlenburg-Lindau, Germany, August 30 – September 2, 2005. (Oral).

Marsch, E., T. Wiegelmann, and L. Xia: Coronal plasma flows and magnetic fields in solar active regions. 69. Jahrestagung der Deutschen Physikalischen Gesellschaft, Fachverband Extraterrestrische Physik, Berlin, Germany, March 4 – 9, 2005. (Oral).

Marsch, E., **T. Wiegelmann**, and L. D. Xia: Coronal plasma flows and magnetic fields in solar active regions. General Assembly of the European Geosciences Union, Vienna, Austria, April 25 – 29, 2005. (Poster).

Mauk, B. H., J. S. Saur, D. G. Mitchell, E. C. Roelof, P. C. Brandt, T. P. Armstrong, D. C. Hamilton, S. M. Krimigis, N. Krupp, S. A. Livi, J. W. Manweiler, and C. P. Paranicas: Energetic particle injections in Saturn's magnetosphere. General Assembly of the European Geosciences Union, Vienna, Austria, April 25 – 29, 2005. (Oral).

Medvedev, A., A. Feofilov, T. Kuroda, R. Saito, G. Villanueva, and P. Hartogh: Progress with the Martian General Circulation Model (GCM) MAOAM. Third Workshop of the Subgroup "Atmosphere and Surface Processes" of the DFG Priority Programme "Mars and the Terrestrial Planets", Darmstadt, Germany, March 10 – 11, 2005. (Oral).

Medvedev, A. S., A. Feofilov, T. Kuroda, R. Saito, G. Villanueva, and P. Hartogh: Progress with the Martian General Circulation Model (GCM) MAOAM. MATSUP Workshop, TU Darmstadt, Germany, March 10 – 11, 2005. (Oral).

Medvedev, A. S. and R. Saito: Wave-mean flow interactions in the atmosphere of Mars. AOGS 2nd Annual Meeting, Suntec, Singapore, June 20 – 24, 2005. (Oral).

Mitchell, D. G., P. C. Brandt, E. C. Roelof, I. M. Dandouras, S. M. Krimigis, B. H. Mauk, N. Krupp, D. C. Hamilton, W. S. Kurth, P. Zarka, M. K. Dougherty, E. J. Bunce, and D. E. Shemansky: Energetic ion acceleration in Saturn's magnetotail: substorms on Saturn? Joint Assembly of the AGU, SEG, NABS, SPD/AAS, New Orleans, USA, May 23 – 27, 2005. (Oral).

Moragas-Klostermeyer, G., R. Srama, S. Kempf, S. Helfert, M. Roy, M. Burton, N. Altobelli, V. Dikarev, H. Krüger, and E. Grün: Generated dust impact charge measurements by Cassini's dust instrument CDA. Dust in Planetary Systems, Kauai'i, Hawaii, USA, September 26 – 30, 2005. (Oral).

Mulligan, T., J. B. Blake, J. L. Roeder, J. F. Fennell, R. Friedel, and P. Daly: Non-force-free modeling of flux ropes in the plasma sheet and comparison with RAPID/Cluster high energy particle observations. General Assembly of the European Geosciences Union, Vienna, Austria, April 25 – 29, 2005. (Poster).

Mulligan, T., J. F. Fennell, J. L. Roeder, R. Friedel, T. A. Fritz, and P. W. Daly: Cluster/RAPID high energy particle observations within non-force-free flux ropes in the plasma sheet. AGU Fall Meeting, San Francisco, USA, December 5 – 9, 2005.

Neubauer, F. M., H. Backes, M. K. Dougherty, C. T. Russell, A. Wennmacher, N. Achilleos, N. Andre,

C. Arridge, C. Bertucci, G. H. Jones, K. K. Khurana, T. Knetter, and A. Law: Investigation of the 3D-magnetic field structure of the Titan interaction with the Kronian outer magnetosphere near ∼10 SLT using magnetic field data and modelling: draping boundary and polarity reversal layer. AGU Fall Meeting, San Francisco, USA, December 5 – 9, 2005.

Neubauer, F. M., H. Backes, A. Wennmacher, M. K. Dougherty, N. Achilleos, C. S.Arridge, C. Bertucci, A. Law, K. K. Khurana, C. T. Russell, N. Andre, and G. H. Jones: Titan's magnetospheric interaction: status after Cassini Titan close encounters TA, TB, T3, T4, T5. Magnetospheres of the Outer Planets 2005, Leicester, UK, August 7 – 12, 2005. (Oral).

Panov, E., **J. Büchner**, A. Korth, M. Fränz, B. Nikutowski, and K.-H. Glassmeier: Cluster observations of thin current sheets at the Earths magnetopause. 69. Jahrestagung der Deutschen Physikalischen Gesellschaft, Fachverband Extraterrestrische Physik, Berlin, Germany, March 4 – 9, 2005. (Poster).

Panov, E. V., J. Büchner, M. Fränz, A. Korth, B. Nikutowski, S. Savin, K.-H. Fornacon, I. Dandouras, and H. Rème: ROY project: simulations and extended techniques. General Assembly of the European Geosciences Union, Vienna, Austria, April 25 – 29, 2005. (Poster).

Parks, G., E. S. Lee, M. Wilber, I. Dandouras, M. Goldstein, E. Lucek, K. Maziane, C. Mazelle, C. Carr, S. Schwartz, A. Fazakerley, H. Rème, J. A. Sauvaud, J. M. Bosqued, C. Gurgiolo, W. Keith, M. B. Bavassano-Cattaneo, P. Escoubet, J. B. Cao, L. Kissler, E. Möbius, and A. Korth: Cluster and double star observations of Earth's bow shock. Cluster and Double Star Sysmposium, ESA/ESTEC, Noordwijk, Netherlands, September 19 – 23, 2005, invited. (Oral).

Peixinho, N., A. Doressoundiram, A. Barucci, I. Belskaya, H. Boehnhardt, *et al.*: Understanding the surface properties of centaurs and TNOs through visible multi-colour photometry. IAU Symposium No. 229, Asteroids, Comets, Meteors 2005, Buzios, Rio de Janeiro, Brasil, August 7 – 12, 2005. (Poster).

Perry, C. H., J. A. Davies, **M. W. Dunlop**, M. Grande, and P. W. Daly: Morphology of the energetic electrons of the magnetotail plasma sheet. General Assembly of the European Geosciences Union, Vienna, Austria, April 25 – 29, 2005. (Poster).

Preuss, O., S. Solanki, S. Jordan, and M. Haugan: An astronomical search for evidence of new physics. EPS13 "Beyond Einstein – Physics for the 21st Century", Bern, Switzerland, July, 11 – 15, 2005. (Oral).

Preusse, S., A. Kopp, J. Büchner, and U. Motschmann: Magnetic communication scenarios for close-in extrasolar planets. 10th Anniversary of 51Peg b, Paris, France, August, 25, 2005.

Preusse, S., A. Kopp, J. Büchner, and M. U.: Plasma interactions in extrasolar planetary systems. 69. Jahrestagung der Deutschen Physikalischen Gesellschaft, Fachverband Extraterrestrische Physik, Berlin, Germany, March 4 – 9, 2005. (Oral).

Pu, Z., J. Wang, M. Dunlop, X. Zhang, Y. Wei, X. Zhou, S. Fu, C. Xiao, Q. Zong, C. Carr, H. Rème, F. Pitout, A. Fazakerley, P. Daly, and Z. Liu: A conjunction FTE event of Cluster and TC1 on 04. 01. 2005: a preliminary study. Cluster and Double Star Symposium, ESA/ESTEC, Noordwijk, Netherlands, September 19 – 23, 2005. (Oral).

Pu, Z. Y., X. Cao, H. Zhang, S. Y. Fu, Q.-G. Zong, C. J. Xiao, Z. X. Liu, A. Korth, M. Frazen, M. Dunlop, C. Carr, H. Rème, I. Dandouras, R. Friedel, and G. Reeves: Multi-spacecraft observations of tailward propagation of dipolarization front during substorms. Cluster and Double Star Symposium, ESA/ESTEC, Noordwijk, Netherlands, September 19 – 23, 2005. (Poster).

Radioti, A., N. Krupp, J. Woch, A. Lagg, and K.-H. Glassmeier: Energy dependence of the Jovian ion abundance ratios. General Assembly of the European Geosciences Union, Vienna, Austria, April 25 – 29, 2005. (Oral).

Radioti, A., **N. Krupp**, J. Woch, A. Lagg, and K.-H. Glassmeier: Energy dependence of the Jovian ion abundance ratios – ion accereleration due to Alfvén waves. 10th Scientific Assembly of IAGA, Toulouse, France, July 18 – 29, 2005. (Oral).

Rauer, H., H. Boehnhardt, and the ESO Deep Impact Gas Team: The Deep Impact Campaign at ESO: observations of the gas component. IAU Symposium No. 229, Asteroids, Comets, Meteors 2005, Buzios, Rio de Janeiro, Brasil, August 7 – 12, 2005. (Poster).

Rodriguez, L., J. Woch, N. Krupp, M. Fränz, R. von Steiger, C. Cid, R. Forsyth, and K.-H. Glassmeier: Internal characteristics of magnetic clouds inferred from Ulysses measurements. General Assembly of the European Geosciences Union, Vienna, Austria, April 25 – 29, 2005. (Oral).

— Solar wind ions and energetic particles within magnetic clouds. Solar Wind 11/SOHO 16 Conference, Whistler, British Columbia, Canada, June 12 – 17, 2005. (Poster).

Rodriguez, L., J. Woch, N. Krupp, M. Fränz, R. von Steiger, C. Cid, R. Forsyth, and K.-H. Glassmeier: Solar wind ions and energetic particles within magnetic clouds. 10th Scientific Assembly of IAGA, Toulouse, France, July 18 – 29, 2005. (Oral).

Roll, R., H. Boehnhardt, F. Goesmann, M. Hilchenbach, H. Rosenbauer, J. P. Bibring, S. Espinasse, P. Goudon, J. Biele, S. Ulamec, and the PHILAE Project Team: PHILAE, the ROSETTA Lander for long-term in-situ monitoring of cometary interior. IAU Symposium No. 229 Asteroids, Comets, Meteors, Buzois, Rio de Janeiro, Brazil, August 7 – 12, 2005. (Poster).

Roth, M.: Temporal variation in the meridional circulation. International Workshop “Observations and Models of the Solar Cycle”, Berne, Switzerland, October 4 – 7, 2005. (Oral).

Rotvig, J.: Differential rotation in planetary cores. UK MHD Meeting 2005, Exeter, UK, May 26 – 27, 2005. (Oral).

— Differential rotation in planetary cores. IAGA 2005, Toulouse, France, July 18 – 29, 2005. (Oral).

Roussos, E., N. Krupp, G. H. Jones, A. Lagg, J. Woch, C. Paranicas, D. G. Mitchell, S. M. Krimigis, M. K. Dougherty, W. H. Ip, and T. P. Armstrong: Electron microsignatures from the Saturnian satellites: Cassini MIMI/LEMMS observations. AGU Fall Meeting, San Francisco, USA, December 5 – 9, 2005. (Oral).

Saito, R. and P. Hartogh: Influence of the surface on the atmospheric circulation of Mars (as revealed from the general circulation model of the Martian atmosphere MAOAM). AOGS 2nd Annual Meeting, Singapore, June 20 – 24, 2005. (Oral).

Saito, R., A. Medvedev, and P. Hartogh: LTE radiative processes in MAOAM. Third Workshop of the Subgroup “Atmosphere and Surface Processes” of the DFG Priority Programme “Mars and the Terrestrial Planets”, Darmstadt, Germany, March 10 – 11, 2005. (Oral).

Santos, J., J. Büchner, M. Alves, B. Nikutowski, and H. Zhang: Derivation of plasma flow velocities using photospheric magnetic field measurements. Chromospheric and Coronal Magnetic Fields, Katlenburg-Lindau, Germany, August 30 – September 2, 2005. (Poster).

Santos-Costa, D., S. J. Bolton, R. Sault, H. B. Garrett, R. M. Thorne, S. Levin, and N. Krupp: The Jovian synchrotron emission’s time variability and the radiation-belt electrons dynamics. AGU Fall Meeting, San Francisco, USA, December 5 – 9, 2005.

Sanz, P. S., J. L. Ortiz, H. Boehnhardt, and L. Barrera: New photometry results on TNOs and centaurs from the ESO VLT. IAU Symposium No. 229, Asteroids, Comets, Meteors 2005, Buzios, Rio de Janeiro, Brasil, August 7 – 12, 2005. (Poster).

Sarris, E. T., S. M. Krimigis, D. G. Mitchell, D. C. Hamilton, N. Krupp, C. Bertucci, and M. Dougherty: Energetic ions upstream from the Saturnian magnetosphere: Cassini/MIMI observations. General Assembly of the European Geosciences Union, Vienna, Austria, April 25 – 29, 2005. (Oral).

Sasso, C.: El Sol Nuestra Estrella. Celebración del Año Mundial de la Física en el IPN, Instituto Politécnico Nacional - México D.F., November 23, 2005.

Sasso, C., A. Lagg, and S. K. Solanki: Infrared spectropolarimetric observations at VTT in the chromospheric HeI 1083.0 nm multiplet. Turbulence and Fine Scale Structure in Solar and Astrophysical Plasmas, Castello di Montegufoni, Florence, Italy, October 3 – 7, 2005. (Oral).

Sauer, K., **E. Dubinin**, M. Fränz, and C. Mazelle: Solitary waves in ion-beam plasmas: application to Cluster foreshock observations. 69. Jahrestagung der Deutschen Physikalischen Gesellschaft, Fachverband Extraterrestrische Physik, Berlin, Germany, March 4 – 9, 2005.

Savin, S., E. Amata, M. Andre, M. Dunlop, Y. Khotyaintsev, J. Büchner, J. Blecki, and J. L. Rauch: Structure of the magnetopause at the ion gyroscale: mass and momentum transfer. 10th Scientific Assembly of IAGA, Toulouse, France, July 18 – 29, 2005. (Poster).

Savin, S., E. Amata, J. Blecki, J. Büchner, and L. Zelenyi: Minimum in magnetic field a signature or the driver of transport across magnetospheric boundaries? General Assembly of the European Geosciences Union, Vienna, Austria, April 25 – 29, 2005. (Oral).

Schlegel, K.: A brief history of lightning research. EU Research Training Network: “Coupling of Atmospheric Layers, Science Meeting”, Elounda, Crete, June 20 – 24, 2005. (Oral).

— Die Magnetosphäre der Erde. Volkshochschule, Soest, Germany, February 24, 2005. (Oral).

Schmitt, D.: Klimaveränderung – Treibhauseffekt oder Sonnenaktivität? Landesfachausschuss Umwelt der FPD, Hannover, Germany, November 12, 2005.

— Origin of solar magnetic variability. Solar Variability and Earth Climate, Monte Porzio Catone, Italy, June 27 – July 1, 2005.

Schrijver, K., **M. DeRosa**, T. Metcalf, Y. Liu, J. McTiernan, Z. Mikic, S. Régnier, M. Wheatland, and T. Wiegelmann: Non-linear force-free field modeling: model techniques, boundary conditions, hares, and hounds. Joint Assembly of the AGU, SEG, NABS, SPD/AAS, New Orleans, USA, May 23 – 27, 2005. (Oral).

Schröder, S. E., M. G. Tomasko, H. U. Keller, and the DISR Team: The reflectance spectrum of Titan's surface as determined by Huygens. 37th Meeting of the AAS Division for Planetary Sciences, Cambridge, UK, September 4 – 9, 2005. (Poster).

Schüssler, M.: Rekonstruktion der Sonnenaktivität in der Vergangenheit. Geophysikalisches Seminar, Institut für Geophysik, Univ. Göttingen, Germany, January 25, 2005.

— The solar dynamo: how much progress have we made in the last fifty years? Stellar Dynamos and Magnetic Buoyancy (A meeting in Honour of Eugene Parker), Royal Astronomical Society, London, UK, November 11, 2005, invited talk. (Oral).

Schwenn, R.: CMEs, solar wind and Sun-Earth connections: unresolved issues. 10th Scientific Assembly of IAGA, Toulouse, France, July 18 – 29, 2005, invited Reporter review in Div. IV. (Oral).

— Lessons for STEREO – learned from Helios. STEREO & Solar-B Workshop, Oahu, Hawaii, USA, November 15 – 18, 2005, invited. (Oral).

— New views of the Sun – our star. University of San Juan, Argentina, November 30, 2005, public lecture.

— SOHO als Weltraumwetterstation: Praktische Erfahrungen. 2. Nationaler Workshop zum Weltraumwetter, Neustrelitz, Germany, September 26 – 27, 2005. (Oral).

— Solar wind sources and their variations over the solar cycle. ISSI Workshop on Solar dynamics and its effects on heliosphere and Earth, Bern, Switzerland, April 18 – 23, 2005. (Oral).

— Sources of CMEs during the declining phase of the solar cycle. Chapman Conference on Corotating Solar Wind Streams and Recurrent Geomagnetic Activity, Manaus, Brazil, February 6 – 12, 2005.

— Weltraumwettermissionen in Vorbereitung: KuaFu (China), Solar Orbiter (ESA), Sentinels (NASA). 2. Nationaler Workshop zum Weltraumwetter, Neustrelitz, Germany, September 26 – 27, 2005.

Schwenn, R., **A. Dal Lago**, E. Huttunen, W. D. Gonzalez, and G. Muñoz: Improve space weather forcasting using the halo expansion speed. Solar Wind 11/SOHO 16 Conference, Whistler, British Columbia, Canada, June 12 – 17, 2005.

Schwenn, R., **A. Dal Lago**, E. Huttunen, W. D. Gonzalez, and G. Muñoz-Martinez: The association of coronal mass ejections with their effects near the Earth. Solar Wind 11/SOHO 16 Conference, Whistler, British Columbia, Canada, June 12 – 17, 2005. (Poster).

Siebertz, O., R. Schieder, C. Gal, M. Olbrich, and P. Hartogh: Acousto-optical spectrometers for THz heterodyne instruments observations. AOGS 2nd Annual Meeting, Singapore, June 20 – 24, 2005. (Oral).

Silin, I., R. Sydora, J. Büchner, A. Vaivads, and Y. Khotyaintsev: Anomalous resistivity due to nonlinear lower-hybrid drift waves. General Assembly of the European Geosciences Union, Vienna, Austria, April 25 – 29, 2005. (Poster).

Silin, I., R. Sydora, J. Büchner, A. Vaivads, and Yu. Khotyaintsev: Enhanced anomalous resistivity due to lower-hybrid drift waves, as found in Vlasov-code simulations and Cluster measurements. Canadian DASP Meeting, Edmonton, Canada, February 24 – 25, 2005. (Oral).

Skorov, Y. V., **H. U. Keller**, M. Tomasko, L. Doose, and the DISR Team: On the scattering properties of fractal tholin particle. 37th Meeting of the AAS Division for Planetary Sciences, Cambridge, UK, September 4 – 9, 2005. (Oral).

Solanki, S. K.: Der Feuerball am Himmel, unsere Sonne. Hauptversammlung des Doktorandennetzwerkes der MPG, Göttingen, Germany, November 26, 2005.

— Die Sonne – Ein Motor für das Erdklima? Olbers-Sitzung der Wittheit zu Bremen, Bremen, Germany, February 8, 2005.

— Die Sonne, ein Motor für das Erdklima? Vortragsreihe Faszinierendes Weltall des Förderkreises Planetarium Göttingen e.V., Göttingen, Germany, October 18, 2005.

— Die Sonne: ein Motor für globale Klimaänderungen? Planetarium Mannheim, Mannheim, Germany, January 21, 2005.

— Feuerball am Himmel, die Sonne. Finanzfloß 2005 der Birkmayer GmbH Sonne Neue Energie für Deutschland, München, Germany, July 28, 2005.

— Past levels of solar activity and irradiance. SORCE Meeting Paleo Connections Between the Sun, Climate, and Culture, Durango, Colorado, USA, September 14 – 16, 2005.

— Solar microscopy: unveiling the Suns basic physical processes at their intrinsic scales. 2005 ESLAB Symposium Trends in Space Science and Cosmic Vision 2020, Noordwijk, Netherlands, April 19 – 21, 2005.

— Solar variability and its possible connection with climate. Geophysikalisches Kolloquium, MPI für Meteorologie, Hamburg, Germany, December 1, 2005.

— Solar variability of possible relevance for the Earths climate. ISSI Workshop on Solar Variability and Planetary Climates, Bern, Switzerland, June 6 – 10, 2005.

— The magnetic vector mapped near the base of the solar corona using He I 10830 Å line. 4th Solar Polarization Workshop, Boulder, Colorado, USA, September 19 – 23, 2005.

— Was hat das Magnetfeld der Sonne mit Einstein und unserem Klima zu tun? Seminar, Forschungszentrum Graz der Österreichischen Akademie der Wissenschaften, Institut für Weltraumforschung, Graz, Austria, June 16, 2005.

— Was hat das Magnetfeld der Sonne mit Einstein und unserem Klima zu tun? Physikalisches Kolloquium Universität Rostock, Rostock, Germany, June 23, 2005.

Solanki, S. K. and N. A. Krivova: Irradiance modelling. IAMAS 2005, Beijing, China, August 2 – 11, 2005.

Solanki, S. K., A. Lagg, R. Aznar, D. Orozco, T. Wiegelmann, J. Woch, M. Collados, N. Krupp, and A. Gandorfer: Measuring the magnetic vector with the He I 10830 Å line: a rich new world. 4th Solar Polarization Workshop, Boulder, Colorado, USA, September 19 – 23, 2005.

Solanki, S. K. and M. Schüssler: Mechanisms of secular magnetic fields variations. Solar Variability and Earth Climate, Monte Porzio Catone, Italy, June 27 – July 1, 2005.

Song, L., P. Hartogh, and C. Jarchow: Improved remote sensing of trace constituents in the atmosphere. Scientific Assembly of the International Association of Meteorology and Atmospheric Sciences, Beijing, China, August 2 – 11, 2005. (Poster).

Sonnemann, G. R., P. Hartogh, and M. Grygalashvyly: Nonlinear response of the ozone chemistry within the stratopause and mesopause region under realistic conditions. Topical Problems of Nonlinear Wave Physics, St. Petersburg - Nizhny Novgorod, Russia, August 2 – 9, 2005. (Oral).

Spohn, T., N. Thomas, U. Christensen, J. Oberst, K. Seiferlin, H. Michaelis, M. Hilchenbach, and K. Gunderson: BELA – The BepiColombo Laser Altimeter. AGU Fall Meeting, San Francisco, USA, December 5 – 9, 2005. (Poster).

Stenzel, O. J., R. A. Mahajan, R. Greve, B. Grieger, H. U. Keller, K. Fraedrich, E. Kirk, and F. Lunkeit: Recent developments from the Mars climate simulation project. 4th MATSUP Workshop, Göttingen, Germany, March 23 – 24, 2005. (Oral).

Stenzel, O. J., R. A. Mahajan, R. Greve, B. Grieger, H. U. Keller, J. Segschneider, K. Fraedrich, F. Lunkeit, and E. Kirk: The Mars climate simulation, coupling an ice sheet model to a general circulation model. DFG Berichtskolloquium – Mars und die terrestrischen Planeten, Berlin, Germany, August 29 – 30, 2005.

Stenzel, O. J., R. A. Mahajan, R. Greve, B. Grieger, J. Segschneider, K. Fraedrich, E. Kirk, and F. Lunkeit: The Mars climate simulation, coupling an ice sheet model to a general circulation model. 3rd MATSUP Workshop, Darmstadt, Germany, March 10 – 11, 2005. (Oral).

Tang, R., X. Deng, S. Li, R. Nakamura, W. Baumjohann, T. Zhang, Z. Liu, P. Daly, H. Rème, C. Carr, and A. Balogh: Simultaneously observation of reconnection by Cluster and Double Star. AGU Fall Meeting, San Francisco, USA, December 5 – 9, 2005.

Teriaca, L.: Plumes as seen in the ultraviolet. AOGS 2nd Annual Meeting, Singapore, June 19 – 24, 2005, invited review. (Oral).

Thomas, N., W. Baumjohann, V. Dehant, E. Chassefiere, F. Leblanc, P. Drossart, E. Lellouch, E. Kallio, H. Boehnhardt, B. Grieger, P. Hartogh, H. Krueger, N. Krupp, W. Markiewicz, J. Woch, K.-H. Glassmeier, J. Oberst, T. Spohn, C. Barbieri, G. Cremonese, G.-P. Tozzi, A. Coradini, S. Orsini, D. Stam, M. Roos-Serote, R. Rodrigo, J. Lopez-Moreno, L. Lara, A. Sáchez-Lavega, J. Rojas, R. Hueso, E. García-Melendo, S. Perez-Hoyos, S. Baeza, J. Arregui, J. Legarreta, S. Barabash, J.-E. Wahlund, M. Andre, L. Blomberg, K. Altwegg, K. Gunderson, J. Horner, K. Seiferlin, P. Wurz,

M. Dougherty, M. Grande, F. W. Taylor, P. Read, P. Irwin, I. P. Wright, H. Rucker, and P. Louarn: A multi-disciplinary investigation of the Jovian system. 39th ESLAB Symposium "Trends in Space Science and Cosmic Vision 2020", Noordwijk, Netherlands, April 19 – 21, 2005. (Oral).

Tomás, A. T., J. Woch, N. Krupp, A. Lagg, and K.-H. Glassmeier: Pitch angle distribution changes and their relation to global particle transport in the case of the Jovian magnetosphere. 10th Scientific Assembly of IAGA, Toulouse, France, July 18 – 29, 2005. (Oral).

Tortorella, D.: Effects of radial dependent local Prandtl number on thermal convection in a compressible rotating spherical shell. 10th Scientific Assembly of IAGA, Toulouse, France, July 18 – 29, 2005. (Poster).

Tu, C.-Y., C. Zhou, E. Marsch, K. Wilhelm, L.-D. Xia, L. Zhao, and J.-X. Wang: Height of origin and 3-D formation scenario for the solar wind in coronal funnels. Solar Wind 11/SOHO 16 Conference, Whistler, British Columbia, Canada, June 12 – 17, 2005. (Oral).

Vasyliūnas, V. M.: Configuration of the magnetosphere. IMPRS Lecture, MPS, Katlenburg-Lindau, Germany, September 12 – 16, 2005. (Oral).

— Dynamical processes in magnetospheres. International Max Planck Research School on Physical Processes in the Solar System and Beyond, Katlenburg-Lindau, Germany, September 12 – 14, 2005. (Oral).

— Magnetosphere-Ionosphere Coupling. International Max Planck Research School on Physical Processes in the Solar System and Beyond, Katlenburg-Lindau, Germany, September 12 – 14, 2005. (Oral).

— Magnetotail twist revisited: effect on polar-cap flow. General Assembly of the European Geosciences Union, Vienna, Austria, April 25 – 29, 2005. (Oral).

— Physics of corotation in planetary magnetospheres. General Assembly of the European Geosciences Union, Vienna, Austria, April 25 – 29, 2005, invited paper. (Oral).

— Reinterpreting the Burton-McPherron-Russell equation for predicting dst. AGU Fall Meeting, San Francisco, USA, December 5 – 9, 2005. (Poster).

— Stress balance in thin current sheets: implications for pressure anisotropy in the Jovian magnetosphere. Conference on Magnetospheres of the Outer Planets, Leicester, UK, August 8 – 12, 2005. (Oral).

Veselov, M., V. Kunitsyn, S. Savin, I. Nesterov, and J. Büchner: ROY project: simulations and extended techniques. General Assembly of the European Geosciences Union, Vienna, Austria, April 25 – 29, 2005. (Poster).

Vögler, A., M. Schüssler, **S. K. Solanki**, and V. Zakharov: Simulations of magneto-convection and solar irradiance variations. ISSI Workshop on Solar Variability and Planetary Climates, Bern, Switzerland, June 6 – 10, 2005.

— Simulations of magneto-convection and solar irradiance variations. Solar Variability and Earth Climate, Monte Porzio Catone, Italy, June 27 – July 1, 2005.

Waara, M., H. Nilsson, S. Arvelius, O. Marghitu, M. Bouhram, Y. Hobara, M. Yamauchi, H. Rème, I. Dandouras, M. B. Bavassano-Cattaneo, G. Paschmann, A. Korth, L. M. Kistler, and G. K. Parks: Oxygen ion outflow observed at high altitude. Cluster and Double Star Symposium, ESA/ESTEC, Noordwijk, Netherlands, September 19 – 23, 2005. (Poster).

Wicht, J.: Computer simulations of geomagnetic reversals. Physikalisches Kolloquium, University of Alberta, Edmonton, Canada, October 14, 2005.

— Dynamics of inverse magnetic field patches in dynamo simulations. AGU Fall Meeting, San Francisco, USA, December 5 – 9, 2005, invited. (Poster).

— Geodynamo simulations, recent success, future prospects. Gordon Research Conference: The interior of the Earth, Mount Holyoke College, South Hadley, MA, USA, June 12 – 17, 2005, invited. (Oral).

— Inverse field patches, excursions, and reversals in numerical, dynamo simulations. Workshop SPP 'Geomagnetische Variationen', Bremen, Germany, January 20 – 21, 2005, invited. (Oral).

— Inverse magnetic field patches and reversals in dynamo simulations. General Assembly of the European Geosciences Union, Vienna, Austria, April 25 – 29, 2005, invited. (Oral).

Wicht, J., P. Olson, and D. Lathrop: A spherical-Couette dynamo. General Assembly of the European Geosciences Union, Vienna, Austria, April 25 – 29, 2005. (Oral).

— A super-rotating dynamo for Saturn. General Assembly of the European Geosciences Union, Vienna, Austria, April 25 – 29, 2005. (Poster).

— Numerical dynamos driven by differential rotation. 10th Scientific Assembly of IAGA, Toulouse, France, July 18 – 29, 2005. (Oral).

Wiegelmann, T.: Coronal magnetic fields. MPS Solar Seminar, Katlenburg-Lindau, Germany, June 7, 2005. (Oral).

— Coronal magnetic fields: theory and application to coronal holes, active regions, stereoscopy and tomography. Solar MHD Theory Group Seminars and Talks, St. Andrews, UK, December 14, 2005. (Oral).

— Magnetic modelling for the STEREO-mission. National Astronomical Observatory of Japan, Tokyo, Japan, January 28, 2005. (Oral).

— Magnetic modelling for the STEREO-mission. Kyoto University, Kyoto, Japan, January 31, 2005. (Oral).

— Non-linear force-free fields: I. Testruns. Non-Linear Force-Free Fields Workshop, Palo Alto, CA, USA, May 17 – 20, 2005, invited. (Oral).

— Non-linear force-free fields: II. Applications. Non-Linear Force-Free Fields Workshop, Palo Alto, CA, USA, May 17 – 20, 2005, invited. (Oral).

— Non-linear force-free magnetic fields. Chromospheric and Coronal Magnetic Fields, Katlenburg-Lindau, Germany, August 29 – September 2, 2005. (Poster).

— Nonlinear force-free modelling of coronal magnetic fields. Earth Simulator, Yokohama, Japan, February 17, 2005. (Oral).

— Nonlinear force-free modelling of coronal magnetic fields. National Astronomical Observatory of Japan, Tokyo, Japan, February 18, 2005. (Oral).

Wiegelmann, T., B. Inhester, A. Lagg, and S. K. Solanki: Magnetic modelling for the STEREO-mission. General Assembly of the European Geosciences Union, Vienna, Austria, April 25 – 29, 2005. (Oral).

Wiegelmann, T., A. Lagg, S. K. Solanki, B. Inhester, and J. Woch: Magnetic loops: a comparison of extrapolations from the photosphere with chromospheric measurements. Chromospheric and Coronal Magnetic Fields, Katlenburg-Lindau, Germany, August 29 – September 2, 2005. (Oral).

— Observational tests of coronal magnetic field models. General Assembly of the European Geosciences Union, Vienna, Austria, April 25 – 29, 2005. (Oral).

Wiegelmann, T., S. K. Solanki, L. D. Xia, and E. Marsch: The magnetic fine structure of coronal holes. General Assembly of the European Geosciences Union, Vienna, Austria, April 25 – 29, 2005. (Oral).

Wu, P., T. A. Fritz, R. S. Reed, R. Friedel, G. Reeves, D. Baker, and P. Daly: High resolution substorm energetic electrons seen in the magnetotail by all 4 Cluster satellites. AGU Fall Meeting, San Francisco, USA, December 5 – 9, 2005.

Xia, L.-D., **R. Schwenn**, A. Dal Lago, E. Huttunen, W. D. Gonzalez, and G. Muñoz: Space weather explorer – the Kuafu Mission. Solar Wind 11/SOHO 16 Conference, Whistler, British Columbia, Canada, June 12 – 17, 2005.

Xia, L.-D., R. Schwenn, E. Donavan, E. Marsch, J.-S. Wang, Y.-W. Zhang, and C.-Y. Tu: Space weather explorer – the Kuafu mission. Solar Wind 11/SOHO 16 Conference, Whistler, British Columbia, Canada, June 12 – 17, 2005. (Poster).

Xiao, C., Z. Pu, Z. Ma, X. Wang, S. Fu, T. Phan, Q. Zong, Z. Liu, K.-H. Glassmeier, A. Balogh, H. Rème, I. Dandouras, A. Korth, M. Fränz, A. Fazakerley, and C. Escoubet: Cluster measurements of fast magnetic reconnection in Earth's magnetotail. AGU Fall Meeting, San Francisco, USA, December 5 – 9, 2005. (Poster).

Xiao, C. J., Z. Y. Pu, Z. W. Ma, X. G. Wang, S. Y. Fu, T. D. Phan, Q. G. Zong, Z. X. Liu, K.-H. Glassmeier, H. Rème, A. Balogh, A. Korth, M. Fränz, and C. P. Escoubet: Cluster measurements of fast magnetic reconnection in Earth's magnetotail. Cluster and Double Star Symposium, ESA/ESTEC, Noordwijk, Netherlands, September 19 – 23, 2005. (Poster).

Zhang, H., T. Fritz, Q. Zong, P. Daly, and A. Balogh: Dayside magnetospheric boundary layer: coordinated observation by Cluster and Double Star. AGU Fall Meeting, San Francisco, USA, December 5 – 9, 2005.

Zhang, H., Z. Pu, X. Cao, S. Fu, C. Xiao, Q. Zong, Z. Liu, J. Cao, A. Korth, M. Frazen, C. Carr, H. Rème, and K.-H. Glassmeier: Magnetic flux pileup and magnetic field dipolarization during substorm. AGU Fall Meeting, San Francisco, USA, December 5 – 9, 2005. (Poster).

Zhao, J. and L. Gizon: Do supergranules tend to align in the north-south direction? Joint Assembly of the AGU, SEG, NABS, SPD/AAS, New Orleans, USA, May 23 – 27, 2005. (Oral).

Zong, Q., T. Fritz, D. Baker, S. Fu, L. Xie, P. Daly, A. Balogh, and H. Rème: Energetic particle modulation by ULF waves in the inner magnetosphere.

AGU Fall Meeting, San Francisco, USA, December 5 – 9, 2005.

Zong, Q.-G., T. A. Fritz, M. Dunlop, Z. Y. Pu, C. P. Escoubet, Y. Bogdanova, H. Laakso, H. Rème, A. N. Fazakerley, and P. Daly: Cluster/Double Star observations of cusp oscillations. General Assembly of the European Geosciences Union, Vienna, Austria, April 25 – 29, 2005. (Poster).

Veröffentlichungen 2004 / Publications 2004

Altobelli, N., H. Krüger, R. Moissl, M. Landgraf, and E. Grün: Influence of wall impacts on the Ulysses dust detector in modelling the interstellar dust flux. Planet. Space Sci. **52**, 1287–1295 (2004), doi:10.1016/j.pss.2004.07.022.

Altwegg, K., A. Jäckel, H. Balsiger, E. Arijs, J.-J. Berthelier, S. Fuselier, F. Gliem, T. Gombosi, A. Korth, and H. Rème: ROSINA's scientific perspective at Churyumov-Gerasimenko. Astrophys. Space Sci. **311**, 257–270 (2004).

Aubert, J. and J. Wicht: Axial vs. equatorial dipolar dynamo models with implications for planetary magnetic fields. Earth and Planetary Science Letters **221**, 409–419 (2004), doi:10.1016/S0012-821X(04)00102-5.

Aznar Cuadrado, R., S. Jordan, R. Napiwotzki, H. M. Schmid, S. K. Solanki, and G. Mathys: Discovery of kilogauss magnetic fields in three DA white dwarfs. Astron. & Astrophys. **423**, 1081–1094 (2004), doi:10.1051/0004-6361:20040355.

Aznar Cuadrado, R., S. K. Solanki, A. Lagg, and R. M. Thomas: Signature of current sheets as seen by TIP at VTT in the HeI multiplet at 1083.0 nm. In: Proc. SOHO 15 'Coronal Heating', eds. R. W. Walsh, J. Ireland, D. Danesy, and B. Fleck, ESA SP-575, pp. 593–596, ESA Publ. Div., Noordwijk (2004).

Balmaceda, L. A., W. D. Gonzalez, E. Echer, J. C. Santos, L. E. A. Vieira, A. D. Lago, F. L. Guarnieri, and A. L. C. Gonzalez: The solar origins of the sun-earth connection events on April 1999 and February 2000. Braz. J. Phys. **34**, 1745–1747 (2004).

Bamert, K., R. Kallenbach, N. F. Ness, C. W. Smith, T. Terasawa, M. Hilchenbach, R. F. Wimmer-Schweingruber, and B. Klecker: Hydromagnetic Wave Excitation Upstream of an Interplanetary Traveling Shock. Astrophys. J. **601**, L99–L102 (2004a), doi:10.1086/381962.

Bamert, K., R. Wimmer-Schweingruber, R. Kallenbach, M. Hilchenbach, and B. Klecker: Suprathermal ions of solar and interstellar origin associated with the April 912, 2001, CMEs. Adv. Space Res. **34**, 161–165 (2004b), doi:10.1016/j.asr.2003.01.036.

Basilevsky, A. T., H. U. Keller, A. Nathues, U. Mall, H. Hiesinger, and M. Rosiek: Scientific objectives and selection of targets for the SMART-1 Infrared Spectrometer (SIR). Planet. Space Sci. **52**, 1261–1285 (2004), doi:10.1016/j.pss.2004.09.002.

Baumann, I., D. Schmitt, M. Schüssler, and S. K. Solanki: Evolution of the large-scale magnetic field on the solar surface: a parameter study. Astron. & Astrophys. **426**, 1075–1091 (2004), doi:10.1051/0004-6361:20048024.

BenMoussa, A., J.-F. Hochedez, W. K. Schmutz, U. Schühle, M. Nesládek, Y. Stockman, U. Kroth, M. Richter, A. Theissen, Z. Remes, K. Haenen, V. Mortet, S. Koller, J. P. Halain, R. Petersen, M. Dominique, and M. D'Olieslaeger: Solar-blind diamond detectors for LYRA, the solar VUV radiometer on board PROBA II. Experimental Astronomy **16**, 141–148 (2004a).

BenMoussa, A., U. Schühle, K. Haenen, M. Nesladek, S. Koizumi, and J. F. Hochedez: PIN diamond detector development for LYRA, the solar VUV radiometer on board PROBA II. Phys. Status Solidi A **201**, 2536–2541 (2004b).

de Bergh, C., H. Boehnhardt, A. Barucci, A. Lazzarin, S. Fornasier, J. Romon-Martin, G. P. Tozzi, A. Doressoundiram, and E. Dotto: Aqueous altered silicates at the surface of two Plutinos? Astron. & Astrophys. **416**, 791–798 (2004), doi:10.1051/0004-6361:20031727.

Bertelsen, P., W. Goetz, M. B. Madsen, K. M. Kinch, S. F. Hviid, J. M. Knudsen, H. P. Gunnlaugsson, J. Merrison, P. Nornberg, S. W. Squyres, J. F. Bell, K. E. Herkenhoff, S. Gorevan, A. S. Yen, T. Myrick, G. Klingelhöfer, R. Rieder, and R. Gellert: Magnetic Properties Experiments on the Mars exploration Rover Spirit at Gusev crater. Science **305**, 827–829 (2004), doi:10.1126/science.1100112.

Bertucci, C., C. Mazelle, D. H. Crider, D. L. Mitchell, K. Sauer, M. H. Acuna, J. E. P. Connerney, R. P. Lin, N. F. Ness, and D. Winterhalter: MGS MAG/ER observations at the magnetic pileup boundary of Mars: draping enhancement and low frequency waves. Adv. Space Res. **33**, 1938–1944 (2004), doi:10.1016/j.asr.2003.04.054.

Bewsher, D., D. Brown, D. Innes, and C. Parnell: Probability analysis of coincident blinkers and explosive events. In: Proc. SOHO 15 - Coronal heating, eds. R. W. Walsh, J. Ireland, D. Danesy, and B. Fleck, ESA SP-575, pp. 465–470, ESA Publ. Div., Noordwijk (2004).

Boattini, A., G. D'Abramo, G. Scholl, H. Hainaut, H. Boehnhardt, R. West, M. Carpino, G. Hahn, R. Michelsen, G. Forti, P. Pravec, G. P. Valsecchi, and D. J. Asher: Near-Earth asteroid search and follow-up beyond the 22nd magnitude: A pilot program with ESO telescopes. Astron. & Astrophys. **418**, 743–750 (2004), doi:10.1051/0004-6361:20034428.

Boehnhardt, H.: Split comets. In: Comets II, eds. M. C. Festou, H.-U. Keller, and H. A. Weaver, The University of Arizona Press, Tucson, USA (2004).

Boehnhardt, H., S. Bagnulo, K. Muinonen, A. Barucci, L. Kolokolova, E. Dotto, and G. P. Tozzi: Surface characterization of 28978 Ixion (2001 KX76). Astron. & Astrophys. **415**, L21–L25 (2004), doi: 10.1051/0004-6361:20040005.

Bogdanova, Y. V., B. Klecker, G. Paschmann, L. M. Kistler, C. Mouikis, E. Moebius, H. Rème, J. M. Bosqued, I. Dandouras, J. A. Sauvaud, N. Cornilleau-Wehrlin, H. Laakso, A. Korth, M. B. Bavassano-Cattaneo, M. F. Marcucci, T. Phan, C. Carlson, G. Parks, J. P. McFadden, M. McCarthy, and R. Lundin: Investigation of the source region of ionospheric oxygen outflow in the cleft/cusp using multi-spacecraft observations by CIS onboard Cluster. Adv. Space Res. **34**, 2459–2464 (2004), doi:10.1016/j.asr.2004.02.014.

Borrero, J. M., S. K. Solanki, L. R. Bellot Rubio, A. Lagg, and S. K. Mathew: On the fine structure of sunspot penumbrae – I. A quantitative comparison of two semiempirical models with implications for the Evershed effect. Astron. & Astrophys. **422**, 1093–1104 (2004), doi:10.1051/0004-6361: 20041001.

Bosinger, T., G. C. Hussey, C. Haldoupis, and K. Schlegel: Auroral E-region electron density height profile modification by electric field driven vertical plasma transport: some evidence in EISCAT CP-1 data statistics. Ann. Geophys. **22**, 901–910 (2004).

Bößwetter, A., T. Bagdonat, U. Motschmann, and K. Sauer: Plasma boundaries at Mars: a 3-D simulation study. Ann. Geophys. **22**, 4363–4379 (2004).

Bothmer, V.: The solar and interplanetary causes of space storms in solar cycle 23. IEEE Trans. Plasma Sci. **32**, 1411–1414 (2004).

Brownlee, D. E., F. Horz, R. L. Newburn, M. Zolensky, T. C. Duxbury, S. Sandford, Z. Sekanina, P. Tsou, M. S. Hanner, B. C. Clark, S. F. Green, and J. Kissel: Surface of young Jupiter family Comet 81P/Wild 2: View from the Stardust spacecraft. Science **304**, 1764–1769 (2004), doi:10.1126/science.1097899.

Bruls, J. H. M. J. and S. K. Solanki: Apparent solar radius variations — The influence of magnetic network and plage. Astron. & Astrophys. **427**, 735–743 (2004), doi:10.1051/0004-6361:20041311.

Brynildsen, N., P. Maltby, O. Kjeldseth-Moe, and K. Wilhelm: Dual flows with supersonic velocities in the sunspot transition region. Astrophys. J. **612**, 1193–1195 (2004), doi:10.1086/422838.

Büchner, J., B. Nikutowski, and A. Otto: Coronal heating by transition region reconnection. In: Proc. of the SOHO15 "Coronal Heating" Workshop, 6-9 September 2004, eds. J. Ireland and R. W. Walsh, ESA SP-575, pp. 23–28, ESA Publ. Div., Noordwijk (2004a).

— Magnetic coupling of photosphere and corona: MHD simulation for multi-wavelength observations. In: Multi-Wavelength Investigations of Solar Activity, eds. A. V. Stepanov, E. E. Benevolenskaya, and A. G. Kosovichev, no. 223 in Proceedings IAU Symposium, pp. 353–356, Cambridge University Press, Cambridge, UK (2004b), doi:10. 1017/S174392130400612X.

Buratti, B. J., D. T. Britt, L. A. Soderblom, M. D. Hicks, D. C. Boice, R. H. Brown, R. Meier, R. M. Nelson, J. Oberst, T. C. Owen, A. S. Rivkin, B. R. Sandel, S. A. Stern, N. Thomas, and R. V. Yelle: 9969 Braille: Deep Space 1 infrared spectroscopy, geometric albedo, and classification. Icarus **167**, 129–135 (2004), doi:10.1016/j.icarus.2003.06.002.

Cameron, R., M. Schüssler, and A. Vögler: The Sun - a ball of electrically well-conducting gas. inSIDE - Innovatives Supercomputing **2**, 4–5 (2004a).

Cameron, R., A. Vögler, and M. Schüssler: Simulation of solar magneto-convection. In: High Performance Computing in Science and Engineering: Transactions of the Second Joint HLRB and KONWIHR Result and Reviewing Workshop, eds. S. Wagner, W. Hanke, A. Bode, and F. Durst, pp. 431–442, Springer, Berlin (2004b).

Cameron, R., A. Vögler, S. Shelyag, and M. Schüssler: The Decay of a Simulated Pore. In: The Solar-B Mission and the Forefront of Solar Physics, eds. T. Sakurai and T. Sekii, ASP Conf. Ser. 325, pp. 57–62 (2004c).

Chen, J. S., P. Hoffmann, M. Zecha, and J. Röttger: On the relationship between aspect sensitivity, wave activity, and multiple scattering centers of mesosphere summer echoes: a case study using coherent radar imaging. Ann. Geophys. **22**, 807–817 (2004).

Christensen, U. R. and A. Tilgner: Power requirement of the geodynamo from ohmic losses in numerical and laboratory dynamos. Nature **429**, 169–171 (2004).

Costa, A. and G. Stenborg: Characterization of intensity variations along Fe XIV coronal loops — A case study. Solar Phys. **222**, 229–245 (2004), doi: 10.1023/B:SOLA.0000043570.97010.b7.

Cremades, H. and V. Bothmer: On the three-dimensional configuration of coronal mass ejections. Astron. & Astrophys. **422**, 307–322 (2004), doi:10.1051/0004-6361:20035776.

Curdt, W., E. Landi, and U. Feldman: The SUMER spectral atlas of solar coronal features. Astron. & Astrophys. **427**, 1045–1054 (2004), doi:10.1051/0004-6361:20041278.

Curdt, W., E. Landi, and U. Feldman: The SUMER spectral atlas of solar coronal features. Astron. & Astrophys. **427**, 1045–1054 (2004), doi:10.1051/0004-6361:20041278.

Curdt, W., T. J. Wang, B. N. Dwivedi, B. Kliem, and I. E. Dammasch: SUMER observations of heating and cooling of coronal loops. In: Proc. of SOHO 13 – Waves, Oscillations and Small-Scale Transient Events in the Solar Atmosphere: A Joint View from SOHO and TRACE, ed. H. Lacoste, ESA SP-547, pp. 333–336, ESA Publ. Div., Noordwijk (2004).

Czechowski, A., K. Hsieh, M. Hilchenbach, J. Kota, and A. Shaw: Anomalous helium ions as the source of energetic helium atoms in the outer heliosphere. Adv. Space Res. **34**, 104–108 (2004), doi:10.1016/j.asr.2003.03.054.

Dal Lago, A., L. E. A. Vieira, E. Echer, W. D. Gonzalez, A. L. C. De Gonzalez, F. L. Guarnieri, N. J. Schuch, and R. Schwenn: Comparison between halo CME expansion speeds observed on the Sun, the related shock transit speeds to earth and corresponding ejecta speeds at 1 AU. Solar Phys. **222**, 323–328 (2004), doi:10.1023/B:SOLA.0000043566.21049.82.

Defise, J. M., D. Berghmans, J. F. Hochedez, J. H. Lecat, E. Mazy, P. Rochus, T. Thibert, P. Nicolosi, M. G. Pelizzo, U. Schühle, R. A. M. Van der Linden, and A. N. Zhukov: SWAP: Sun Watcher using APS detector on-board PROBA-2, a new EUV off-axis telescope on a technology demonstration platform. In: Telescopes and Instrumentation for Solar Astrophysics, eds. S. Fineschi and M. Gummin, vol. 5171, pp. 143–153, SPIE - International Society for Optical Engineering (2004), doi:10.1117/12.516510.

Delsanti, A., O. Hainaut, E. Jourddeuil, K. J. Meech, H. Boehnhardt, and L. Barrera: Simultaneous visible and near-IR photometric study of Kuiper Belt Object surfaces with the ESO Very Large Telescopes. Astron. & Astrophys. **417**, 1145–1158 (2004), doi:10.1051/0004-6361:20034182.

Djuth, F. T., B. Isham, M. T. Rietveld, T. Hagfors, and C. La Hoz: First 100 ms of HF modification at Tromso, Norway. J. Geophys. Res. **109**, A11307 (2004), doi:10.1029/2003JA010236.

Dubinin, E., K. Sauer, and J. F. McKenzie: Nonlinear stationary waves and solitons in ion beam-plasma configuration. J. Geophys. Res. **109**, A02208 (2004), doi:10.1029/2003JA010283.

Esposito, L. W., C. A. Barth, J. E. Colwell, G. M. Lawrence, W. E. McClintock, A. I. F. Stewart, H. U. Keller, A. Korth, H. Lauche, M. C. Festou, A. L. Lane, C. J. Hansen, J. N. Maki, R. A. West, H. Jahn, R. Reulke, K. Warlich, D. E. Shemansky, and Y. L. Yung: The Cassini ultraviolet imaging spectrograph investigation. Space Sci. Rev. **115**, 299–361 (2004), doi:10.1007/s11214-004-1455-8.

Feldman, U., I. E. Dammasch, E. Landi, and G. A. Doschek: Observations indicating that $\approx 1 \times 10^7$ K solar flare plasmas may be produced in situ from $\approx 1 \times 10^6$ K coronal plasma. Astrophys. J. **609**, 439–451 (2004a), doi:10.1086/420964.

Feldman, U., E. Landi, and W. Curdt: Newly identified forbidden transitions within the ground configuration of ions of very low abundance P, Cl, K, and Co. Astrophys. J. **607**, 1039–1045 (2004b), doi:10.1086/383532.

Fornasier, S., A. Doressoundiram, G. P. Tozzi, A. Barucci, H. Boehnhardt, C. de Bergh, A. Delsanti, J. Davies, and E. Dotto: ESO Large Program on physical studies of Transneptunian Objects and Centaurs: Final results of the visible spectrophotometric observations. Astron. & Astrophys. **421**, 353–363 (2004a), doi:10.1051/0004-6361:20041221.

Fornasier, S., E. Dotto, F. Marzari, A. Barucci, H. Boehnhardt, O. Hainaut, and C. de Bergh: Visible spectroscopic and photometric survey of L5 Trojans: Investigation of dynamical families. Icarus **172**, 221–232 (2004b), doi:10.1016/j.icarus.2004.06.015.

Frolov, V. L., E. N. Sergeev, G. P. Komrakov, P. Stubbe, B. Thide, M. Waldenvik, E. Veszelei, and T. B. Leyser: Ponderomotive narrow continuum (NCp) component in stimulated electromagnetic emission spectra. J. Geophys. Res. **109**, A07304 (2004), doi:10.1029/2001JA005063.

Frutos-Alfaro, F., A. Korth, M. Fränz, C. G. Mouikis, L. M. Kistler, B. Klecker, H. Rème, I. Dandouras, J. M. Bosqued, J. A. Sauvaud, E. Möbius, H. Kucharek, J. P. McFadden, C. W. Carlson, E. Amata, and R. Lundin: Cluster mission and data analysis for the March 2001 magnetic storm. Geofisica International **43**, 217–223 (2004).

Gandorfer, A. M., H. P. Povel, P. Steiner, F. Aebersold, U. Egger, A. Feller, D. Gisler, S. Hagenbuch, and J. O. Stenflo: Solar polarimetry in the near UV with the Zurich Imaging Polarimeter ZIMPOL II. Astron. & Astrophys. **422**, 703–708 (2004a), doi: 10.1051/0004-6361:20040254.

Gandorfer, A. M., S. K. Solanki, M. Schüssler, W. Curdt, B. W. Lites, V. Martínez Pillet, W. Schmidt, A. M. Title, and the Sunrise Team: SUNRISE: High resolution UV/VIS observations of the Sun from the stratosphere. In: Astronomical Telescopes and Instrumentation - The Industrial Revolution in Astronomy, ed. J. M. Oschmann, *Proceedings of SPIE*, vol. 5489, pp. 732–741, SPIE, Bellingham (2004b).

Gizon, L. and S. K. Solanki: Measuring stellar differential rotation with asteroseismology. Solar Phys. **220**, 169–184 (2004), doi:10.1023/B:SOLA.0000031378.29215.0c.

Glassmeier, K. H., J. Vogt, A. Stadelmann, and S. Buchert: Concerning long-term geomagnetic variations and space climatology. Ann. Geophys. **22**, 3669–3677 (2004).

Goesmann, F.: The Electron Macroscope. In: Proceedings of the 37th ESLAB symposium, "Tools and technologies for future planetary exploration", Noordwijk, The Netherlands, 2-4 Dec. 2003, vol. 543, pp. 183–186 (2004).

Goesmann, F. and M. Hilchenbach: The gas-chromatograph mass-spectrometer (GC-MS), an instrument for in-situ measurements of volatiles in planetary atmospheres and lithospheres. In: Proc. 37th ESLAB Symposium Tools and Technologies for Future Planetary Exploration, ed. B. Battrick, ESA SP-543, pp. 151–158, ESA Publ. Div., Noordwijk (2004).

Gömöry, P., J. Rybak, A. Kucera, W. Curdt, and H. Wöhl: Dynamics of the quiet upper solar atmosphere in the network. In: Proc. SOHO 15 - Coronal heating, eds. R. W. Walsh, J. Ireland, D. Danesy, and B. Fleck, ESA SP-575, pp. 400–404, ESA Publ. Div., Noordwijk (2004).

Grach, S. M., Yu. E. Men'kova, and P. Stubbe: On the penetration of upper hybrid waves into a plasma depletion. Adv. Space Res. **34**, 2428–2432 (2004), doi:10.1016/j.asr.2004.03.014.

Greve, R., R. A. Mahajan, J. Segschneider, and B. Grieger: Evolution of the north-polar cap of Mars: A modelling study. Planet. Space Sci. **52**, 775–787 (2004), doi:10.1016/j.pss.2004.03.007.

Grieger, B., N. I. Ignatiev, N. M. Hoekzema, and H. U. Keller: Indication of a near surface cloud layer on Venus from reanalysis of Venera 13/14 spectrophotometer data. In: Proc. Int. Workshop 'Planetary Probe Atmospheric Entry and Descent Trajectory Analysis and Science', ESA SP-544, pp. 63–70, ESA Publ. Div., Noordwijk (2004a).

Grieger, B., J. Segschneider, H. U. Keller, A. V. Rodin, F. Lunkeit, E. Kirk, and K. Fraedrich: Simulating Titan's tropospheric circulation with the Portable University Model of the Atmosphere. Adv. Space Res. **34**, 1650–1654 (2004b), doi:10.1016/j.asr.2003.08.079.

Grydeland, T., E. M. Blixt, U. P. Løvhaug, T. Hagfors, C. La Hoz, and T. S. Trondsen: Interferometric radar observations of filamented structures due to plasma instabilities and their relation to dynamic auroral rays. Ann. Geophys. **22**, 1115–1132 (2004).

Grynko, Y., K. Jockers, and R. Schwenn: The phase curve of cometary dust: Observations of comet 96P/Machholz 1 at large phase angle with the SOHO LASCO C3 coronagraph. Astron. & Astrophys. **427**, 755–761 (2004), doi:10.1051/0004-6361:20047131.

Guzik, T. G., J. H. Adams, H. S. Ahn, G. Bashindzhagyan, J. Chang, M. Christl, A. R. Fazely, O. Ganel, D. Granger, R. Gunasingha, Y. J. Han, J. B. Isbert, H. J. Kim, K. C. Kim, S. K. Kim, E. Kouznetsov, M. Panasyuk, A. Panov, B. Price, G. Samsonov, W. K. H. Schmidt, E. S. Seo, R. Sina, N. Sokolskaya, M. Stewart, A. Voronin, J. Z. Wang, J. P. Wefel, J. Wu, and V. Zatsepin: The ATIC Long Duration Balloon project. Adv. Space Res. **33**, 1763–1770 (2004), doi:10.1016/j.asr.2003.05.018.

Hanlon, P. G., M. K. Dougherty, N. Krupp, K. C. Hansen, F. J. Crary, D. T. Young, and G. Tóth: Dual spacecraft observations of a compression event within the Jovian magnetosphere: Signatures of externally triggered supercorotation? J. Geophys. Res. **109**, A09S09 (2004), doi:10.1029/2003JA010116.

Hartogh, P.: Microwave investigation of planets. In: Proceedings of the 37th ESLAB Symposium "Tools and Technologies for Future Planetary Exploration", ed. B. Battrick, ESA SP-543, pp. 65–72, ESA Publ. Div., Noordwijk (2004).

Hartogh, P. and C. Jarchow: The microwave brightness of planetary atmospheres—preparatory modeling for GREAT and HIFI. In: Proceedings of the International Workshop on Critical Evaluation of mm-/submm-wave Spectroscopic Data for Atmospheric Observations, January 29-30, 2004, Ibaraki, Japan, eds. T. Amano, Y. Kasai, and T. Manabe, pp. 75–78, Communications Research Laboratory (2004).

Hartogh, P., C. Jarchow, G. R. Sonnemann, and M. Grygalashvyly: On the spatiotemporal behaviour of ozone within the upper mesosphere/mesopause region under nearly polar night conditions. J. Geophys. Res. **109**, D18303 (2004), doi:10.1029/2004JD004576.

Herkenhoff, K. E., S. W. Squyres, R. Arvidson, D. S. Bass, J. F. Bell, P. Bertelsen, N. A. Cabrol, L. Gaddis, A. G. Hayes, S. F. Hviid, J. R. Johnson, K. M. Kinch, M. B. Madsen, J. N. Maki, S. M. McLennan, H. Y. McSween, J. W. Rice, M. Sims, P. H. Smith, L. A. Soderblom, N. Spanovich, R. Sullivan, and A. Wang: Textures of the soils and rocks at Gusev crater from Spirit's Microscopic Imager. Science **305**, 824–826 (2004a), doi:10.1126/science.1100015.

Herkenhoff, K. E., S. W. Squyres, R. Arvidson, D. S. Bass, J. F. Bell, P. Bertelsen, B. L. Ehlmann, W. Farrand, L. Gaddis, R. Greeley, J. Grotzinger, A. G. Hayes, S. F. Hviid, J. R. Johnson, B. Jolliff, K. M. Kinch, A. H. Knoll, M. B. Madsen, J. N. Maki, S. M. McLennan, H. Y. McSween, D. W. Ming, J. W. Rice, L. Richter, M. Sims, P. H. Smith, L. A. Soderblom, N. Spanovich, R. Sullivan, S. Thompson, T. Wdowiak, C. Weitz, and P. Whelley: Evidence from Opportunity's microscopic imager for water on Meridiani Planum. Science **306**, 1727–1730 (2004b), doi:10.1126/science.1105286.

Hilchenbach, M.: Ion mobility spectrometry: An analytical separation tool for planetary exploration. In: Proc. 37th ESLAB Symposium Tools and Technologies for Future Planetary Exploration, ed. B. Battrick, ESA SP-543, pp. 175–178, ESA Publ. Div., Noordwijk (2004a).

— Remote sensing of the Lunar or Asteroid surfaces via pick-up ions in the solar wind downward direction. In: Proc. 37th ESLAB Symposium Tools and Technologies for Future Planetary Exploration, ed. B. Battrick, ESA SP-543, pp. 55–58, ESA Publ. Div., Noordwijk (2004b).

Hilchenbach, M., B. Chares, and H. Rosenbauer: First contact with a comet surface: Rosetta lander simulations. In: The new Rosetta targets: Oberservations, simulations and instrument performances, eds. L. Colangeli, E. Epifani, and P. Palumbo, *Astrophysics and space science libary*, vol. 311, pp. 289–296, Kluwer Academic Publishers, Dordrecht Boston London (2004).

Hilchenbach, M. and H. Rosenbauer: Mission Philae - Mit Mechanik zu den Anfängen des Sonnensystems. Kultur & Technik **4**, 18–21 (2004).

Holter, Ø., P. Galopeau, A. Roux, S. Perraut, A. Pedersen, A. Korth, and T. Bösinger: Two satellite study of substorm expansion near geosynchronous orbit. Ann. Geophys. **22**, 4299–4310 (2004).

Hsieh, K. C., J. Kota, A. Czechowski, M. Hilchenbach, and A. Shaw: Studying the heliosphere in energetic neutral H and He atoms above 30 keV/amu. In: Physics of the Outer Heliosphere, 8-13 February, 2004 in Riverside, California, eds. V. Florinski, N. V. Pogorelov, and G. P. Zank, *AIP Conference Proceedings,*, vol. 719, pp. 64–69, American Institute of Physics, Melville, NY (2004a).

Hsieh, K. C., T. H. Zurbuchen, J. Orr, G. Gloeckler, and M. Hilchenbach: A collimator design for monitoring heliospheric energetic neutral atoms at 1 AU. Adv. Space Res. **34**, 213–218 (2004b), doi:10.1016/j.asr.2003.02.056.

Huang, Z. Y., Z. Y. Pu, C. J. Xiao, Q. G. Zong, S. Y. Fu, L. Xie, Q. Q. Shi, J. B. Cao, Z. X. Liu, C. Shen, J. K. Shi, L. Lu, N. Q. Wang, T. Chen, T. Fritz, K. H. Glassmeier, P. Daly, and H. Rème: Multiple flux rope events at the high-latitude magnetopause: Cluster/RAPID observations on January 26, 2001. Chinese J. Geophys. **47**, 197–206 (2004).

Innes, D. and T.-J. Wang: SUMER observations of active region loop dynamics. In: Proc. SOHO 15 - Coronal heating, eds. R. W. Walsh, J. Ireland, D. Danesy, and B. Fleck, ESA SP-575, pp. 553–556, ESA Publ. Div., Noordwijk (2004a).

Innes, D. E.: Transition region dynamics. In: Proc. of SOHO 13 – Waves, Oscillations and Small-Scale Transient Events in the Solar Atmosphere: A Joint View from SOHO and TRACE, ed. H. Lacoste, ESA SP-547, pp. 215–221, ESA Publ. Div., Noordwijk (2004).

Innes, D. E. and T. J. Wang: Observations of sunward flows in the 21 April 2002 postflare super-arcade. In: Proc. of SOHO 13 – Waves, Oscillations and Small-Scale Transient Events in the Solar Atmosphere: A Joint View from SOHO and TRACE, ed. H. Lacoste, ESA SP-547, pp. 479–482, ESA Publ. Div., Noordwijk (2004b).

Ip, W. H. and A. Kopp: Mercury's Birkeland current system. Adv. Space Res. **33**, 2172–2175 (2004), doi:10.1016/S0273-1177(03)00444-7.

Ip, W. H., A. Kopp, and J. H. Hu: On the star-magnetosphere interaction of close-in exoplanets. Astrophys. J. **602**, L53–L56 (2004), doi:10.1086/382274.

Jiang, J. H., B. Wang, K. Goya, K. Hocke, S. D. Eckermann, J. Ma, D. L. Wu, and W. G. Read: Geographical distribution and interseasonal variability of tropical deep convection: UARS MLS observations and analyses. J. Geophys. Res. **109**, D03111 (2004), doi:10.1029/2003JD003756.

Joko, S., H. Nilsson, R. Lundin, B. Popielawska, H. Rème, M.-B. Bavassano-Cattaneo, G. Paschmann, A. Korth, L. M. Kistler, and G. K. Parks: Shell-like configuration in O^+ ion velocity distribution at high altitudes in the dayside magnetosphere observed by Cluster/CIS. Ann. Geophys. **22**, 2473–2483 (2004).

Kaasalainen, M., P. Pravec, Y. N. Krugly, L. Sarounova, J. Torppa, J. Virtanen, S. Kaasalainen, A. Erikson, A. Nathues, J. Durech, M. Wolf, J. S. V. Lagerros, M. Lindgren, C. I. Lagerkvist, R. Koff, J. Davies, R. Mann, P. Kusnirak, N. M. Gaftonyuk, V. G. Shevchenko, V. G. Chiorny, and I. N. Belskaya: Photometry and models of eight near-Earth Asteroids. Icarus **167**, 178–196 (2004), doi:10.1016/j.icarus.2003.09.012.

Kallenbach, R., K. Bamert, R. Wimmer-Schweingruber, B. Klecker, and M. Hilchenbach: Probing diffusion parameters of suprathermal ions near heliospheric shocks. Adv. Space Res. **34**, 157–160 (2004a), doi:10.1016/j.asr.2003.03.067.

Kallenbach, R., M. Hilchenbach, S. V. Chalov, and K. Bamert: On the origin of energetic neutral atoms detected by the SOHO/CELIAS/HSTOF sensor. In: Physics of the Outer Heliosphere, 8-13 February, 2004 in Riverside, California, eds. V. Florinski, N. V. Pogorelov, and G. P. Zank, *AIP Conference Proceedings,*, vol. 719, pp. 229–236, American Institute of Physics, Melville, NY (2004b).

Keiling, A., A. Rème, I. Dandouras, J. M. Bosqued, V. Sergeev, J.-A. Sauvaud, C. Jacquey, B. Lavraud, P. Louarn, T. Moreau, C. Vallat, C. P. Escoubet, G. K. Parks, M. McCarthy, E. Möbius, E. Amata, B. Klecker, A. Korth, R. Lundin, P. Daly, and Q.-G. Zong: New properties of energy-dispersed ions in the plasma sheet boundary layer observed by Cluster. J. Geophys. Res. **109**, A05215 (2004a), doi: 10.1029/2003JA010277.

Keiling, A., H. Rème, I. Dandouras, J. M. Bosqued, G. K. Parks, M. McCarthy, L. Kistler, E. Amata, B. Klecker, A. Korth, and R. Lundin: Transient ion beamlet injections into spatially separated PSBL flux tubes observed by Cluster-CIS. Geophys. Res. Lett. **31**, L12804 (2004b), doi:10.1029/2004GL020192.

Keiling, A., H. Rème, I. Dandouras, J. M. Bosqued, V. Sergeev, J.-A. Sauvaud, C. Jacquey, B. Lavraud, P. Louarn, T. Moreau, C. Vallat, C. P. Escoubet, G. K. Parks, M. McCarthy, E. Möbius, E. Amata, B. Klecker, A. Korth, R. Lundin, P. Daly, and Q.-G. Zong: New properties of energy-dispersed ions in the plasma sheetboundary layer observed by Cluster. J. Geophys. Res. **109**, A05215 (2004c), doi: 10.1029/2003JA010277.

Keller, C. U., M. Schüssler, A. Vögler, and V. Zakharov: On the origin of solar faculae. Astrophys. J. **607**, L59–L62 (2004), doi:10.1086/421553.

Kempf., S., R. Srama, N. Altobelli, S. Auer, V. Tschernjawski, J. Bradley, M. E. Burton, S. Helfert, T. V. Johnson, H. Krüger, G. Moragas-Klostermeyer, and E. Grün: Cassini between Earth and asteroid belt: first in-situ charge measurements of interplanetary grains. Icarus **171**, 317–335 (2004), doi:10.1016/j.icarus.2004.05.017.

Khomenko, E. V., S. Shelyag, S. K. Solanki, A. Vögler, and M. Schüssler: Stokes diagnostics of magneto-convection. Profile shapes and asymmetries. In: Multi-Wavelength Investigations of Solar Activity, Proc. IAU Symp. 223, eds. A. V. Stepanov, E. E. Benevolenskaya, and A. G. Kosovichev, pp. 635–636, University Press, Cambridge (2004).

Khurana, K. K., V. M. Vasyliūnas, B. H. Mauk, L. Frank, B. Paterson, M. G. Kivelson, N. Krupp, J. Woch, A. Lagg, and B. Kurth: The configuration of Jupiter's magnetosphere. In: Jupiter: The Planet, Satellites and Magnetosphere, eds. F. Bagenal, T. Dowling, and W. McKinnon, Cambridge Planetary Science, chap. 24, pp. 593–616, Cambridge University Press (2004).

Kigure, H., Y. Uchida, M. Nakamura, S. Hirose, and R. Cameron: Distribution of Faraday rotation measure in jets from active galactic nuclei. I. Predictions from our sweeping magnetic twist model. Astrophys. J. **600**, 88–95 (2004a), doi:10.1086/379759.

— Distribution of Faraday rotation measure in jets from Active Galactic Nuclei. II. Prediction from our sweeping magnetic twist model for the wiggled parts of active galactic nucleus jets and tails. Astrophys. J. **608**, 119–135 (2004b), doi:10.1086/386538.

Kiselev, N. N., K. Jockers, and T. Bonev: CCD imaging polarimetry of Comet 2P/Encke. Icarus **168**, 385–391 (2004), doi:10.1016/j.icarus.2003.12.012.

Kissel, J., F. R. Krueger, J. Silén, and B. C. Clark: The Cometary and Interstellar Dust Analyzer at Comet 81P/Wild 2. Science **304**, 1774–1776 (2004), doi: 10.1126/science.1098836.

Klein, V., J. Popp, N. Tarcea, M. Schmitt, W. Kiefer, S. Hofer, T. Stuffler, M. Hilchenbach, D. Doyle, and M. Dieckmann: Remote raman spectroscopy as a prospective tool for planetary surfaces. J. Raman Spectrosc. **35**, 433–440 (2004).

Kolesnikov, F., M. Bünte, D. Schmitt, and M. Schüssler: Kelvin-Helmholtz and shear instability of a helical flow around a magnetic flux tube. Astron. & Astrophys. **420**, 737–749 (2004), doi:10.1051/0004-6361:20041040.

Korth, A., M. Fränz, Q.-G. Zong, T. A. Fritz, J.-A. Sauvaud, H. Rème, I. Dandouras, R. Friedel, C. G. Mouikis, L. M. Kistler, E. Möbius, M. F. Marcucci, M. Wilber, G. Parks, A. Keiling, R. Lundin, and P. W. Daly: Ion injections at auroral latitude during the March 31, 2001 magnetic storm observed by Cluster. Geophys. Res. Lett. **31**, L20806 (2004), doi:10.1029/2004GL020356.

Kossacki, K. J. and W. J. Markiewicz: Seasonal melting of surface water ice condensing in martian gullies. Icarus **171**, 272–283 (2004), doi:10.1016/j.icarus.2004.05.018.

Kramm, J. R., H. U. Keller, R. Müller, D. Germerott, and G. Tomasch: A Marconi CCD42-40 with antiblooming - Experiences with the OSIRIS CCDs for the ROSETTA mission. In: Scientific detectors for astronomy - The beginning of a new era, eds. P. Amico, J. W. Beletic, and J. E. Beletic, pp. 131–135, Kluwer Academic Press, Dordrecht, The Netherlands (2004).

Krimigis, S. M., D. G. Mitchell, D. C. Hamilton, S. Livi, J. Dandouras, S. Jaskulek, T. P. Armstrong, A. F. Cheng, G. Gloeckler, K. C. Hsieh, W.-H. Ip, E. P. Keath, E. Kirsch, N. Krupp, L. J. Lanzerotti, B. H. Mauk, R. W. McEntire, E. C. Roelof, B. E. Tossman, B. Wilken, and D. J. Williams: Magnetosphere Imaging Instrument (MIMI) on the Cassini Mission to Saturn/Titan. Space Sci. Rev. **114**, 233–329 (2004), doi:10.1007/s11214-004-1410-8.

Krivov, A. V., N. A. Krivova, S. K. Solanki, and V. B. Titov: Towards understanding the β Pictoris dust stream. Astron. & Astrophys. **417**, 341–352 (2004), doi:10.1051/0004-6361:20034379.

Krivova, N. A. and S. K. Solanki: Effect of spatial resolution on estimating the Sun's magnetic flux. Astron. & Astrophys. **417**, 1125–1132 (2004a), doi: 10.1051/0004-6361:20040022.

— Solar variability and global warming: A statistical comparison since 1850. Adv. Space Res. **34**, 361–364 (2004b), doi:10.1016/j.asr.2003.02.051.

Krueger, F. R., W. Werther, J. Kissel, and E. R. Schmid: Assignment of quinone derivatives as the main compound class composing 'interstellar' grains based on both polarity ions detected by the "Cometary and Interstellar Dust Analyser" WIDA) onboard the spacecraft STARDUST. Rapid Commun. Mass Spectrom. **18**, 103–111 (2004).

Krueger, H.: Jupiter's Dust Disc: An Astrophysical Laboratory. In: Reviews in Modern Astronomy, ed. R. Schielicke, vol. 16, pp. 111–128, Wiley (2004).

Krüger, H.: Raumsonde Ulysses untersucht erneut Staub vom Jupiter. Sterne und Weltraum **42**, 16–17 (2004).

Krüger, H., M. Horányi, A. V. Krivov, and A. L. Graps: Jovian Dust: Streams, Clouds and Rings. In: Jupiter: Planet, Satellites & Magnetosphere, ed. T. D. Fran Bagenal, Bill McKinnon, chap. 10, pp. 219–240, Cambridge University Press, Cambridge, U. K. (2004).

Krupp, N.: Besuch beim Herrn der Ringe. MaxPlanck-Forschung **1/2004**, 46–49 (2004a).

— Visiting the Lord of the Rings. MaxPlanckResearch **2**, 46–49 (2004b).

Krupp, N., V. M. Vasyliūnas, J. Woch, A. Lagg, K. K. Khurana, M. G. Kivelson, B. H. Mauk, E. C. Roelof, D. J. Williams, S. M. Krimigis, W. S. Kurth, L. A. Frank, and W. R. Paterson: The Dynamics of the Jovian magnetosphere. In: Jupiter: The Planet, Satellites and Magnetosphere, eds. F. Bagenal, T. Dowling, and W. McKinnon, Cambridge Planetary Science, chap. 25, pp. 617–638, Cambridge University Press (2004a).

Krupp, N., J. Woch, A. Lagg, S. Livi, D. G. Mitchell, S. M. Krimigis, M. K. Dougherty, P. G. Hanlon, T. P. Armstrong, and S. A. Espinosa: Energetic particle observations in the vicinity of Jupiter: Cassini MIMI/LEMMS results. J. Geophys. Res. **109**, A09S10 (2004b), doi:10.1029/2003JA010111.

Kulyk, I. and K. Jockers: Ground-based photometric observations of Jupiter's inner satellites Thebe, Amalthea, and Metis at small phase angles. Icarus **170**, 24–34 (2004), doi:10.1016/j.icarus.2004.03.008.

Kulyk, I., K. Jockers, T. Credner, and T. Bonev: The wavelength dependence of the monochromatic extinction coefficient for the observatory on Terskol Peak. Kinematika i Fizika Nebesnykh Tel **20**, 372–378 (2004).

Kutzner, C. and U. R. Christensen: Simulated geomagnetic reversals and preferred virtual geomagnetic pole paths. Geophys. J. Int. **157**, 1105–1118 (2004), doi:10.1111/j.1365-246X.2004.02309.x.

Lagg, A., J. Woch, N. Krupp, A. Gandorfer, and S. K. Solanki: Temporal evolution of chromospheric downflows. In: Multi-Wavelength Investigations of Solar Activity, Proc. IAU Symp. 223, eds. A. V. Stepanov, E. E. Benevolenskaya, and A. G. Kosovichev, pp. 279–280, University Press, Cambridge (2004a).

Lagg, A., J. Woch, N. Krupp, and S. K. Solanki: Retrieval of the full magnetic vector with the He I multiplet at 1083 nm. Maps of an emerging flux region. Astron. & Astrophys. **414**, 1109–1120 (2004b), doi: 10.1051/0004-6361:20031643.

Lara, L. M., R. Rodrigo, G. P. Tozzi, H. Boehnhardt, and P. Leisy: The spectrum of Comet C/1999 H1 (Lee) between 0.6 and 1 micron. Astron. & Astrophys. **420**, 371–382 (2004a), doi:10.1051/0004-6361:20034214.

Lara, L. M., G. P. Tozzi, H. Boehnhardt, M. D'Martino, and R. Schulz: Gas and Dust in Comet C/2000 WM1 during its closest approach to Earth: Optical imaging and long-slit spectroscopy. Astron. & Astrophys. **422**, 717–729 (2004b), doi:10.1051/0004-6361:20040159.

Lemaire, P., P. Gouttebroze, J.-C. Vial, W. Curdt, U. Schühle, and K. Wilhelm: Flare observation of the Sun as a star by SUMER/SOHO in the hydrogen Lyman continuum. Astron. & Astrophys. **418**, 737–742 (2004), doi:10.1051/0004-6361:20034405.

Loukitcheva, M., S. K. Solanki, M. Carlsson, and R. F. Stein: Millimeter observations and chromospheric dynamics. Astron. & Astrophys. **419**, 747–756 (2004a), doi:10.1051/0004-6361:20034159.

Loukitcheva, M. A., S. K. Solanki, and S. White: The solar chromosphere as seen in high-resolution millimeter observations. In: Multi-Wavelength Investigations of Solar Activity, Proc. IAU Symp. 223, eds. A. V. Stepanov, E. E. Benevolenskaya, and A. G. Kosovichev, pp. 643–644, University Press, Cambridge (2004b).

Lübken, F. J., M. Zecha, J. Hoffner, and J. Röttger: Temperatures, polar mesosphere summer echoes, and noctilucent clouds over Spitsbergen (78 degrees N). J. Geophys. Res. **109**, D11203 (2004), doi: 10.1029/2003JD004247.

Lundin, R., S. Barabash, H. Andersson, M. Holmström, A. Grigoriev, M. Yamauchi, J.-A. Sauvaud, A. Fedorov, E. Budnik, J.-J. Thovacen, D. Winningham, R. Frahm, J. Scherrer, J. Sharber, K. Asamura, H. Hayakawa, A. Coates, D. R. Linder, C. Curtis, K. C. Hsieh, B. R. Sandel, M. Grande, M. Carter, D. H. Reading, H. Koskinen, E. Kallio, P. Riihela, W. Schmidt, T. Täles, J. Kozyra, N. Krupp, J. Woch, J. Luhmann, S. McKenna-Lawler, R. Cerulli-Irelli, S. Orsini, M. Maggi, A. Mura, A. Milillo, E. Roelof, D. Williams, S. Livi, P. Brandt, P. Wurz, and P. Boechsler: Solar Wind-Induced Atmospheric Erosion at Mars: First Results from ASPERA-3 on Mars Express. Science **305**, 1933–1936 (2004), doi: 10.1126/science.1101860.

Marcucci, M. F., M. B. Bavassano-Cattaneo, G. Pallocchia, E. Amata, R. Bruno, A. M. Di Lellis, V. Formisano, H. Rème, J. M. Bosqued, I. Dandouras, J. A. Sauvaud, L. M. Kistler, E. Moebius, B. Klecker, C. W. Carlson, G. K. Parks, M. McCarthy, A. Korth, R. Lundin, and A. Balogh: Energetic magnetospheric oxygen in the magnetosheath and its response to IMF orientation: Cluster observations. J. Geophys. Res. **109**, A07203 (2004), doi: 10.1029/2003JA010312.

Marsch, E.: Kinetic aspects of coronal heating. In: Proceedings of the SOHO 15 Workshop - Coronal Heating, St. Andrews, Scotland, 6-9 September 2004, eds. R. W. Walsh, J. Ireland, D. Danesy, and B. Fleck, ESA SP-575, ESA Publ. Div., Noordwijk (2004a).

— Waves and turbulence in the solar corona. In: The Sun and the Heliosphere as an Integrated System, eds. G. Poletto and S. T. Suess, *Astrophysics and Space Science Library*, vol. 317, pp. 283–317, Kluwer Academic Publishers, Dordrecht, The Netherlands (2004b).

— Waves in the solar corona. In: Stars as Suns: Activity, Evolution and Planets, eds. A. K. Dupree and A. O. Benz, *IAU Symposium*, vol. 219, pp. 449–460, Astronomical Society of the Pacific, USA (2004c).

Marsch, E., X.-Z. Ao, and C.-Y. Tu: On the temperature anisotropy of the core part of the proton velocity distribution function in the solar wind. J. Geophys. Res. **109**, A04102 (2004a), doi:10.1029/2003JA010330.

Marsch, E., T. Wiegelmann, and L. D. Xia: Coronal plasma flows and magnetic fields in solar active regions Combined observations from SOHO and NSO/Kitt Peak. Astron. & Astrophys. **428**, 629–645 (2004b), doi:10.1051/0004-6361:20041060.

Mathew, S. K., S. K. Solanki, A. Lagg, M. Collados, J. M. Borrero, and S. Berdyugina: Thermal-magnetic relation in a sunspot and a map of its Wilson depression. Astron. & Astrophys. **422**, 693–701 (2004), doi:10.1051/0004-6361:20040136.

Mauk, B. H., D. G. Mitchell, R. W. McEntire, C. P. Paranicas, E. C. Roelof, D. J. Williams, S. M. Krimigis, and A. Lagg: Energetic ion characteristics and neutral gas interactions in Jupiter's magnetosphere. J. Geophys. Res. **109**, A09S12 (2004), doi: 10.1029/2003JA010270.

Mazelle, C., D. Winterhalter, K. Sauer, J. G. Trotignon, M. H. Acuña, K. Baumgärtel, C. Bertucci, D. A. Brain, S. H. Brecht, M. Delva, E. Dubinin, M. Øieroset, and J. Slavin: Bow shock and upstream phenomena at Mars. Space Sci. Rev. **111**, 115–181 (2004), doi: 10.1023/B:SPAC.0000032717.98679.d0.

McKenzie, J. F.: Nonlinear stationary waves of the ion-cyclotron-acoustic type: solitons and spiky waveforms. J. Plasma Phys. **70**, 533–541 (2004).

McKenzie, J. F., E. Dubinin, K. Sauer, and T. B. Doyle: The application of the constants of motion to nonlinear stationary waves in complex plasmas: a unified fluid dynamic viewpoint. J. Plasma Phys. **70**, 431–462 (2004a).

McKenzie, J. F., F. Verheest, T. B. Doyle, and M. A. Hellberg: Compressive and rarefactive ion-acoustic solitons in bi-ion plasmas. Phys. Plasmas **11**, 1762–1769 (2004b).

McKenzie, J. R. and T. B. Doyle: Trans-sonic cusped shaped, periodic waves and solitary waves of the electrostatic ion-cyclotron type. Nonlin. Proc. Geophys. **11**, 421–425 (2004).

McMullin, D. R., M. Bzowski, E. Möbius, A. Pauluhn, R. Skoug, W. T. Thompson, M. Witte, R. von Steiger, D. Rucinski, D. Judge, M. Banaszkiewicz, and R. Lallement: Heliospheric conditions that affect the interstellar gas inside the heliosphere. Astron. & Astrophys. **426**, 885–895 (2004), doi:10.1051/0004-6361:20047147.

Meziane, K., C. Mazelle, M. Wilber, D. LeQuéau, J. P. Eastwood, H. Rème, I. Dandouras, J. A. Sauvaud, J. M. Bosqued, G. K. Parks, L. M. Kistler, M. McCarthy, B. Klecker, A. Korth, M.-B. Bavassano-Cattaneo, R. Lundin, and A. Balogh: Bow shock specularly reflected ions in the presence of low-frequency electromagnetic waves: a case study. Ann. Geophys. **22**, 2325–2335 (2004a).

Meziane, K., M. Wilber, C. Mazelle, D. LeQuéau, H. Kucharek, E. A. Lucek, H. Rème, A. M. Hamza, J. A. Sauvaud, J. M. Bosqued, I. Dandouras, G. K. Parks, M. McCarthy, B. Klecker, A. Korth, M. B. Bavassano-Cattaneo, and R. N. Lundin: Simultaneous observations of field-aligned beams and gyrating ions in the terrestrial foreshock. J. Geophys. Res. **109**, A05107 (2004b), doi:10.1029/2003JA010374.

Möbius, E., M. Bzowski, S. Chalov, H. J. Fahr, G. Gloeckler, V. Izmodenov, R. Kallenbach, R. Lallement, D. McMullin, H. Noda, M. Oka, A. Pauluhn, J. Raymond, D. Rucinski, R. Skoug, T. Terasawa, W. Thompson, J. Vallerga, R. von Steiger, and M. Witte: Synopsis of the interstellar He parameters from combined neutral gas, pickup ion and UV scattering observations and related consequences. Astron. & Astrophys. **426**, 897–907 (2004), doi:10.1051/0004-6361:20035834.

Nagy, A. F., D. Winterhalter, K. Sauer, T. E. Cravens, S. Brecht, C. Mazelle, D. Crider, E. Kallio, A. Zakharov, E. Dubinin, M. Verigin, G. Kotova, W. I. Axford, C. Bertucci, and J. G. Trotignon: The plasma environment of Mars. Space Sci. Rev. **111**, 33–114 (2004), doi:10.1023/B:SPAC.0000032718.47512.92.

Narita, Y., K.-H. Glassmeier, S. Schäfer, U. Motschmann, M. Fränz, I. Dandouras, K.-H. Fornaçon, E. Georgescu, A. Korth, H. Rème, and I. Richter: Alfvén waves in the foreshock propagating upstream in the plasma rest frame: statistics from Cluster observations. Ann. Geophys. **22**, 2315–2323 (2004).

Nielsen, E.: Mars Express and MARSIS. Space Sci. Rev. **111**, 245–262 (2004a), doi:10.1023/B:SPAC.0000032712.05204.5e.

— Mean velocities measured with the double pulse technique. Ann. Geophys. **22**, 3531–3536 (2004b).

Nielsen, E., F. Honary, and M. Grill: Time resolution of cosmic noise observations with a correlation experiment. Ann. Geophys. **22**, 1687–1689 (2004).

Nilsson, H., S. Joko, R. Lundin, H. Rème, J. A. Sauvaud, I. Dandouras, A. Balogh, C. Carr, L. M. Kistler, B. Klecker, C. W. Carlson, M. B. Bavassano-Cattaneo, and A. Korth: The structure of high altitude O^+ energization and outflow: a case study. Ann. Geophys. **22**, 2497–2506 (2004).

Ning, Z., D. E. Innes, and S. K. Solanki: Dynamic behaviors of the quiet Sun seen by SUMER. In: Proc. SOHO 13 'Waves, Oscillations and Small-Scale Transient Events in the Solar Atmosphere: A Joint View from SOHO and TRACE', ed. H. Lacoste, ESA SP-547, pp. 297–302, ESA Publ. Div., Noordwijk (2004a).

— Line profile characteristics of solar explosive event bursts. Astron. & Astrophys. **419**, 1141–1148 (2004b), doi:10.1051/0004-6361:20034499.

Pau, J. L., O. Hainout, C. Rivera, E. Muñoz, E. Calleja, J. F. Hochedez, F. Omnès, U. Schühle, and P. Lemaire: Fabrication and characterisation of AlGaN photodetectors for applications in the

EUV/XUV ranges. In: Proceedings Conferencia de Dispositivos Electrónicos (2004a).

Pau, J. L., C. Rivera, E. Muñoz, E. Calleja, U. Schühle, E. Frayssinet, B. Beaumont, J. P. Faurie, and P. Gibart: Response of ultra-low dislocation density GaN photodetectors in the near- and vacuum-ultraviolet. J. Appl. Phys. **95**, 8275–8279 (2004b), doi:10.1063/1.1748855.

Pau, J. L., C. Rivera, J. Pereiro, E. Muñoz, E. Calleja, U. Schühle, E. Frayssinet, B. Beaumont, J. P. Faurie, and P. Gibart: Nitride-based photodetectors: from visible to X-ray monitoring. Superlattices Microstruct. **36**, 807–814 (2004c), doi:10.1016/j.spmi.2004.09.037.

Pauluhn, A. and S. K. Solanki: Radiance emission by flaring activity. In: Proc. SOHO 13 'Waves, Oscillations and Small-Scale Transient Events in the Solar Atmosphere: A Joint View from SOHO and TRACE', ed. H. Lacoste, ESA SP-547, pp. 323–328, ESA Publ. Div., Noordwijk (2004a).

— Small-Scale flares as the cause of quiet Sun EUV emission. In: Proc. SOHO 15 'Coronal Heating', eds. R. W. Walsh, J. Ireland, D. Danesy, and B. Fleck, ESA SP-575, pp. 501–506, ESA Publ. Div., Noordwijk (2004b).

Peixinho, N., H. Boehnhardt, I. Belskaya, A. Doressoundiram, A. Barucci, and A. Delsanti: ESO Large Program and Centaurs and TNOS: Visible colors - final results. Icarus **170**, 153–166 (2004), doi:10.1016/j.icarus.2004.03.004.

Petit, P. and J.-F. Donati: Dynamo processes and differential rotation in solar-type stars. In: SF2A-2004: Semaine de l'Astrophysique Francaise, meeting held in Paris, France, June 14-18, 2004, eds. F. Combes, D. Barret, T. Contini, F. Meynadier, and L. Pagani, Conference Series, EDP-Sciences (2004).

Petrova, E. V., V. P. Tishkovets, and K. Jockers: Polarization of Light Scattered by Solar System Bodies and the Aggregate Model of Dust Particles. Solar System Research **38**, 309–324 (2004), doi:10.1023/B:SOLS.0000037466.32514.fe.

Popp, J., N. Tarcea, L. Baciu, N. Thomas, C. Cockell, H. W. G. Edwards, J. Gomez-Elvira, M. Hilchenbach, R. Hochleitner, S. Hofer, V. Hoffmann, B. Hofmann, E. K. Jessberger, W. Kiefer, J. Martinez-Frias, S. Maurice, F. R. Pérez, M. Schmitt, G. Simon, F. Sobron, W. Weigand, J. A. Whitby, and P. Wurz: Extended Miras: The instrumental approach for the search of traces of extinct and extant life on Mars, instrument setup. In: Proc. 37th ESLAB Symposium Tools and Technologies for Future Planetary Exploration, ed. B. Battrick, ESA SP-543, pp. 147–150, ESA Publ. Div., Noordwijk (2004a).

Popp, J., N. Tarcea, N. Thomas, C. Cockell, H. W. G. Edwards, J. Gomez-Elvira, M. Hilchenbach, R. Hochleitner, S. Hofer, V. Hoffmann, B. Hofmann, E. K. Jessberger, W. Kiefer, J. Martinez-Frias, S. Maurice, F. Rull Pérez, M. Schmitt, G. Simon, F. Sobron, W. Weigand, J. A. Whitby, and P. Wurz: EXTENDED-MIRAS: the instrumental approach for the search of traces of extinct and extant life on Mars, measuring scenario. In: Proceedings of the Third European Workshop on Exo-Astrobiology, 18-20 November 2003, Madrid, Spain, eds. R. A. Harris and L. Ouwehand, ESA SP-545, pp. 131–134, ESA Publ. Div., Noordwijk (2004b).

Preuss, O., M. P. Haugan, S. K. Solanki, and S. Jordan: An astronomical search for evidence of new physics: Limits on gravity-induced birefringence from the magnetic white dwarf RE J0317-853. Phys. Rev. D **70**, 067101 (2004a), doi:10.1103/PhysRevD.70.067101.

Preuss, O., M. Schüssler, V. Holzwarth, and S. K. Solanki: Distribution of magnetically confined circumstellar matter in oblique rotators. Astron. & Astrophys. **417**, 987–992 (2004b), doi:10.1051/0004-6361:20034525.

Raouafi, N.-E., S. Mancuso, S. K. Solanki, B. Inhester, M. Mierla, G. Stenborg, J. P. Delaboudiniere, and C. Benna: Shock wave driven by an expanding system of loops. Astron. & Astrophys. **424**, 1039–1048 (2004a), doi:10.1051/0004-6361:20040083.

Raouafi, N.-E., S. Manusco, S. K. Solanki, B. Inhester, C. Benna, J. P. Delaboudinière, G. Stenborg, and M. Mierla: Interpretation of the coronal EUV signature of the CME event on June 27 1999. In: Proc. SOHO 13 'Waves, Oscillations and Small-Scale Transient Events in the Solar Atmosphere: A Joint View from SOHO and TRACE', ed. H. Lacoste, ESA SP-547, pp. 317–322, ESA Publ. Div., Noordwijk (2004b).

Raouafi, N.-E. and S. K. Solanki: Effect of the electron density stratification on off-limb OVI line profiles: How large is the velocity distribution anisotropy in the solar corona? Astron. & Astrophys. **427**, 725–733 (2004a), doi:10.1051/0004-6361:20041203.

— Effect of the electron density stratification on the off-limb O VI line profiles. In: Multi-Wavelength Investigations of Solar Activity, Proc. IAU Symp. 223, eds. A. V. Stepanov, E. E. Benevolenskaya, and

A. G. Kosovichev, pp. 481–482, University Press, Cambridge (2004b).

— Effect of the line-of-sight integration on the profiles of coronal lines. In: Proc. SOHO 13 'Waves, Oscillations and Small-Scale Transient Events in the Solar Atmosphere: A Joint View from SOHO and TRACE', ed. H. Lacoste, ESA SP-547, pp. 401–406, ESA Publ. Div., Noordwijk (2004c).

— Sensitivity of solar off-limb line profiles to electron density stratification and the velocity distribution anisotropy. In: Proc. SOHO 15 'Coronal Heating', eds. R. W. Walsh, J. Ireland, D. Danesy, and B. Fleck, ESA SP-575, pp. 170–175, ESA Publ. Div., Noordwijk (2004d).

Reinisch, B. W., X. Huang, P. Song, J. L. Green, S. F. Fung, V. M. Vasyliūnas, D. L. Gallagher, and B. R. Sandel: Plasmaspheric mass loss and refilling as a result of a magnetic storm. J. Geophys. Res. **109**, A01202 (2004), doi:10.1029/2003JA009948.

Rochus, P. L., J.-M. Defise, J.-P. Halain, C. A. Jamar, E. Mazy, L. Rossi, T. Thibert, F. Clette, P. Cugnon, D. Berghmans, J.-F. Hochedez, J.-P. Delaboudiniere, F. Auchere, R. Mercier, M.-F. Ravet, F. Delmotte, M. Idir, U. Schühle, V. Bothmer, S. Fineschi, R. A. Howard, J. D. Moses, and J. S. Newmark: MAGRITTE: an instrument suite for the solar atmospheric imaging assembly (AIA) aboard the Solar Dynamics Observatory. In: Telescopes and Instrumentation for Solar Astrophysics, eds. S. Fineschi and M. Gummin, vol. 5171, pp. 53–64, SPIE - International Society for Optical Engineering (2004), doi:10.1117/12.503964.

Rodriguez, L., J. Woch, N. Krupp, M. Fränz, R. von Steiger, R. Forsyth, D. Reisenfeld, and K.-H. Glassmeier: A statistical study of oxygen freezing-in temperature and energetic particles inside magnetic clouds observed by Ulysses. J. Geophys. Res. **109**, A01108 (2004), doi:10.1029/2003JA010156.

Rosell-Melé, A., E. Bard, K.-C. Emeis, B. Grieger, C. Hewitt, P. J. Müller, and R. R. Schneider: Sea surface temperature anomalies in the oceans at the LGM estimated from the alkenone-$U_{37}^{K'}$ index: comparison with GCMs. Geophys. Res. Lett. **31**, L03208 (2004), doi:10.1029/2003GL018151.

Russell, C. T., A. Coradini, U. Christensen, M. C. De Sanctis, W. C. Feldman, R. Jaumann, H. U. Keller, A. S. Konopliv, T. B. McCord, L. A. McFadden, H. Y. McSween, S. Mottola, G. Neukum, C. M. Pieters, T. H. Prettyman, C. A. Raymond, D. E. Smith, M. V. Sykes, B. G. Williams, J. Wise, and M. T. Zuber: Dawn: A journey in space and time. Planet. Space Sci. **52**, 465–489 (2004), doi: 10.1016/j.pss.2003.06.013.

Rybak, J., A. Kucera, W. Curdt, and H. Wöhl: Observational evidences for heating of the solar corona by nanoflares in the network derived from the transition region spectral lines. In: Proc. SOHO 15 - Coronal heating, eds. R. W. Walsh, J. Ireland, D. Danesy, and B. Fleck, ESA SP-575, pp. 529–534, ESA Publ. Div., Noordwijk (2004a).

Rybak, J., A. Kucera, W. Curdt, and H. Wöhl: On relations among the calibrated parameters of the transition region spectral line. In: Proc. of SOHO 13 – Waves, Oscillations and Small-Scale Transient Events in the Solar Atmosphere: A Joint View from SOHO and TRACE, ed. H. Lacoste, ESA SP-547, pp. 311–315, ESA Publ. Div., Noordwijk (2004b).

Saito, R. and Y. Kasai: The abundance of the H_2O-O_2 complex in the Earth's atmosphere. In: Proceedings of the International Workshop on Critical Evaluation of mm-/submm-wave Spectroscopic Data for Atmospheric Observations, eds. T. Amano, Y. Kasai, and T. Manabe, Communication Research Laboratory Publication Series, Communication Research Laboratory, Ibaraki University, Ibaraki, Japan (2004).

Saul, L., E. Möbius, C. W. Smith, P. Bochsler, H. Grünwaldt, B. Klecker, and F. Ipavich: Observational evidence of pitch angle isotropization by IMF waves. Geophys. Res. Lett. **31**, L05811 (2004), doi: 10.1029/2003GL019014.

Sauvaud, J. A., P. Louarn, G. Fruit, H. Stenuit, C. Vallat, J. Dandouras, H. Rème, M. André, A. Balogh, M. Dunlop, L. Kistler, E. Möbius, C. Mouikis, B. Klecker, G. K. Parks, J. McFadden, C. Carlson, F. Marcucci, G. Pallocchia, R. Lundin, A. Korth, and M. McCarthy: Case studies of the dynamics of ionospheric ions in the Earth's magnetotail. J. Geophys. Res. **109**, A01212 (2004), doi:10.1029/2003JA009996.

Savin, S., L. Zelenyi, S. Romanov, I. Sandahl, J. Pickett, E. Amata, L. Avanov, J. Blecki, E. Budnik, J. Büchner, C. Cattell, G. Consolini, J. Fedder, S. Fuselier, H. Kawano, B. Nikutowski, C. T. Russell, and K. Stasiewicz: Magnetosheath-cusp interface. Ann. Geophys. **22**, 183–212 (2004a).

Savin, S. P., L. M. Zelenyi, E. Amata, J. Büchner, J. Blecki, S. I. Klimov, B. Nikutowski, J. L. Rauch, S. A. Romanov, A. A. Skalsky, P. Song, and K. Stasiewicz: Dynamic interaction of a plasma flow with the hot boundary of the geomagnetic trap. JETP Lett. **79**, 368–371 (2004b).

Schühle, U., J.-F. Hochedez, J. L. Pau, C. Rivera, E. Muñoz, J. Alvarez, J.-P. Kleider, P. Lemaire, *T. Appourchaux, B. Fleck, A. Peacock, M. Richter, U. Kroth, A. Gottwald, M. C. Castex, A. Deneuville, P. Muret, M. Nesladek, F. Omnès, J. John, and C. Van Hoof*: Development of imaging arrays for solar UV observations based on wide band gap materials. In: Telescopes and Instrumentation for Solar Astrophysics, eds. S. Fineschi and M. Gummin, *Proceedings of the International Society of Optical Engineering (SPIE)*, vol. 5171, pp. 231–238, SPIE - International Society of Optical Engineering (2004), doi:10.1117/12.507730.

Schulz, R., J. A. Stüwe, and H. Boehnhardt: Rosetta target Comet 67P/Churyumov-Gerasimenko: Post-perihelion gas and dust production rates. Astron. & Astrophys. **422**, L19–L21 (2004), doi:10.1051/0004-6361:20040190.

Schüssler, M. and D. Schmitt: Does the butterfly diagram indicate a solar flux-transport dynamo? Astron. & Astrophys. **421**, 349–351 (2004a), doi:10.1051/0004-6361:20041302.

— Theoretical models of solar magnetic variability. In: Solar Variability and its Effect on Climate, ed. J. Pap, Geophysical Monograph 141, p. 33, American Geophysical Union (2004b).

Schütz, O., H. Boehnhardt, E. Pantin, M. Sterzik, S. Els, J. Hahn, and Th. Henning: A search for circumstellar dust disks with ADONIS. Astron. & Astrophys. **424**, 613–618 (2004), doi:10.1051/0004-6361:20034215.

Seleznyov, A. D., N. A. Krivova, and S. K. Solanki: Understanding solar variability as groundwork for planet transit detection. In: Stars as Suns: Activity, Evolution, and Planets, eds. A. K. Dupree and A. O. Benz, *IAU Symposium*, vol. 219, pp. CD–815–CD–819, Cambridge Univ. Press (2004).

Selwa, M., K. Murawski, and S. K. Solanki: Excitation and damping of slow magnetosonic standing waves in a solar coronal loop. In: Proc. SOHO 15 'Coronal Heating', eds. R. W. Walsh, J. Ireland, D. Danesy, and B. Fleck, ESA SP-575, pp. 91–96, ESA Publ. Div., Noordwijk (2004).

Shelyag, S., M. Schüssler, S. K. Solanki, S. Berdyugina, and A. Vögler: G-band spectral synthesis and diagnostics of simulated solar magneto-convection. Astron. & Astrophys. **427**, 335–343 (2004), doi:10.1051/0004-6361:20040471.

Sicard, A., S. Bourdarie, N. Krupp, A. Lagg, D. Boscher, D. Santos-Costa, E. Gerard, P. Galopeau, S. Bolton, R. Sault, and D. J. Williams: Long-term dynamics of the inner Jovian electron radiation belts. Adv. Space Res. **33**, 2039–2044 (2004), doi:10.1016/j.asr.2003.04.053.

Skorov, Yu. V., G. N. Markelov, and H. U. Keller: Direct statistical simulation of the near-surface layers of the cometary atmosphere. I. A spherical nucleus. Solar System Research **38**, 455–475 (2004), doi:10.1007/s11208-005-0017-2.

Solanki, S. K.: Magnetic coupling and topological changes. In: Proc. SOHO 13 'Waves, Oscillations and Small-Scale Transient Events in the Solar Atmosphere: A Joint View from SOHO and TRACE', ed. H. Lacoste, ESA SP-547, pp. 155–162, ESA Publ. Div., Noordwijk (2004a).

— Structure of the solar chromosphere. In: Multi-Wavelength Investigations of Solar Activity, Proc. IAU Symp. 223, eds. A. V. Stepanov, E. E. Benevolenskaya, and A. G. Kosovichev, pp. 195–202, University Press, Cambridge (2004b).

— The magnetic field from the solar interior to the heliosphere. In: The Sun and the Heliosphere as an Integrated System, eds. G. Poletto and S. T. Suess, pp. 373–395, Kluwer, Dordrecht (2004c).

Solanki, S. K. and N. A. Krivova: Solar irradiance variations: From current measurements to long-term estimates. Solar Phys. **224**, 197–208 (2004), doi:10.1007/s11207-005-6499-8.

Solanki, S. K., O. Preuss, M. Haugan, A. Gandorfer, H. P. Povel, P. Steiner, K. Stucki, P. N. Bernasconi, and D. Soltau: Solar constraints on new couplings between electromagnetism and gravity. Phys. Rev. D **69**, 062001 (2004a), doi:10.1103/PhysRevD.69.062001.

Solanki, S. K. and M. Schüssler: Small-Scale solar magnetic elements: simulations and observations. In: The Solar-B Mission and the Forefront of Solar Physics, eds. T. Sakurai and T. Sekii, *ASP Conference Series*, vol. 325, pp. 105–113 (2004), iSBN 1-58381-1187-7.

Solanki, S. K. and Y. C. Unruh: Spot sizes on Sun-like stars. Mon. Not. Roy. Astron. Soc. **348**, 307–315 (2004), doi:10.1111/j.1365-2966.2004.07368.x.

Solanki, S. K., I. G. Usoskin, B. Kromer, M. Schüssler, and J. Beer: Unusual activity of the Sun during recent decades compared to the previous 11,000 years. Nature **431**, 1084–1087 (2004b).

Squyres, S. W., R. E. Arvidson, J. F. Bell, J. Brückner, N. A. Cabrol, W. Calvin, M. H. Carr, P. R. Christensen, B. C. Clark, L. Crumpler, D. J. Des Marais, C. d'Uston, T. Economou, J. Farmer, W. Farrand, W. Folkner, M. Golombek, S. Gorevan, J. A. Grant, R. Greeley, J. Grotzinger, L. Haskin, K. E. Herkenhoff, S. Hviid, J. Johnson, G. Klingelhöfer, *A. Knoll, G. Landis, M. Lemmon, R. Li, M. B. Madsen, M. C. Malin, S. M. McLennan, H. Y. McSween, D. W. Ming, J. Moersch, R. V. Morris, T. Parker, J. W. Rice, L. Richter, R. Rieder, M. Sims, M. Smith, P. Smith, L. A. Soderblom, R. Sullivan, H. Wänke, T. Wdowiak, M. Wolff, and A. Yen*: The Spirit Rover's Athena Science Investigation at Gusev Crater, Mars. Science **305**, 794–799 (2004a), doi:10.1126/science.3050794.

Squyres, S. W., R. E. Arvidson, J. F. Bell, J. Brückner, N. A. Cabrol, W. Calvin, M. H. Carr, P. R. Christensen, B. C. Clark, L. Crumpter, D. J. Des Marais, C. d'Uston, T. Economou, J. Farmer, W. Farrand, W. Folkner, M. Golombek, S. Gorevan, J. A. Grant, R. Greeley, J. Grotzinger, L. Haskin, K. E. Herkenhoff, S. Hviid, J. Johnson, G. Klingelhöfer, A. H. Knoll, G. Landis, M. Lemmon, R. Li, M. B. Madsen, M. C. Malin, S. M. McLennan, H. Y. McSween, D. W. Ming, J. Moersch, R. V. Morris, T. Parker, J. W. Rice, L. Richter, R. Rieder, M. Sims, M. Smith, P. Smith, L. A. Soderblom, R. Sutlivan, H. Wänke, T. Wdowiak, M. Wolff, and A. Yen: The Opportunity Rover's Athena science investigation at Meridiani Planum, Mars. Science **306**, 1698–1703 (2004b), doi:10.1126/science.1106171.

Srama, R., T. J. Ahrens, N. Altobelli, S. Auer, J. G. Bradley, M. Burton, V. V. Dikarev, T. Economou, H. Fechtig, M. Görlich, M. Grande, A. L. Graps, E. Grün, O. Havnes, S. Helfert, M. Horányi, E. Igenbergs, E. K. Jeßberger, T. V. Johnson, S. Kempf, A. V. Krivov, H. Krüger, G. Moragas-Klostermeyer, P. Lamy, M. Landgraf, D. Linkert, G. Linkert, F. Lura, A. Mocker-Ahlreep, J. A. M. McDonnell, D. Möhlmann, G. E. Morfill, M. Müller, M. Roy, G. Schäfer, G. H. Schlotzhauer, G. H. Schwehm, F. Spahn, M. Stübig, J. Svestka, V. Tschernjawski, A. J. Tuzzolino, R. Wäsch, and H. A. Zook: The Cassini Cosmic Dust Analyzer. Space Sci. Rev. **114**, 455–471 (2004a), doi:10.1007/s11214-004-1435-z.

Srama, R., M. Rachev, A. Srovig, S. Kempf, G. Moragas-Klostermeyer, H. Krüger, S. Auer, A. Glasmachers, and E. Grün: Dust Astronomy with a dust telescope. In: Proceedings of 37th ESLAB Symposium 'Tools and Technologies for future planetary exploration', Noordwijk, The Netherlands, 2-4 December 2003, ESA SP-543, pp. 73–78, ESA Publ. Div., Noordwijk (2004b).

Stenborg, G., M. Rovira, and R. Schwenn: Observacione de la corona solar. Ciencia hoy **14**, 20–29 (2004).

Stolle, C., N. Jakowski, K. Schlegel, and M. Rietveld: Comparison of high latitude electron density profiles obtained with the GPS radio occultation technique and EISCAT measurementss. Ann. Geophys. **22**, 2015–2022 (2004).

Taylor, M. G. G. T., M. W. Dunlop, B. Lavraud, A. Vontrat-Reberac, C. J. Owen, P. Décréau, P. Trávníček, R. C. Elphic, R. H. W. Friedel, J. P. Dewhurst, Y. Wang, A. Fazakerley, A. Balogh, H. Rème, and P. W. Daly: Cluster observations of a complex high-altitude cusp passage during highly variable IMF. Ann. Geophys. **22**, 3707–3719 (2004a).

Taylor, M. G. G. T., R. H. W. Friedel, G. D. Reeves, M. W. Dunlop, T. A. Fritz, P. W. Daly, and A. Balogh: Multisatellite measurements of electron phase space density gradients in the Earth's inner and outer magnetosphere. J. Geophys. Res. **109**, A05220 (2004b), doi:10.1029/2003JA010294.

Teriaca, L., D. Banerjee, A. Falchi, J. G. Doyle, and M. S. Madjarska: Transition region small-scale dynamics as seen by SUMER on SOHO. Astron. & Astrophys. **427**, 1065–1074 (2004a), doi:10.1051/0004-6361:20040503.

Teriaca, L., L. Maltagliati, A. Falchi, R. Falciani, and G. Cauzzi: Overview of an eruptive flare: from chromospheric evaporation to cooling of hot flaring loops. In: Proc. SOHO 15 - Coronal heating, eds. R. W. Walsh, J. Ireland, D. Danesy, and B. Fleck, ESA SP-575, pp. 265–270, ESA Publ. Div., Noordwijk (2004b).

Thomas, N., B. S. Lüthi, S. F. Hviid, H. U. Keller, W. J. Markiewicz, T. Blümchen, A. T. Basilevsky, P. H. Smith, R. Tanner, C. Oquest, R. Reynolds, J.-L. Josset, S. Beauvivre, B. Hofmann, P. Rüffer, and C. T. Pillinger: The microscope for Beagle 2. Planet. Space Sci. **52**, 853–866 (2004), doi:10.1016/j.pss.2004.02.008.

Tishkovets, V. P., E. V. Petrova, and K. Jockers: Optical properties of aggregate particles comparable in size to the wavelength. J. Quant. Spectrosc. Radiat. Transf. **86**, 241–265 (2004).

Tomás, A., J. Woch, N. Krupp, A. Lagg, K.-H. Glassmeier, M. K. Dougherty, and P. G. Hanlon: Changes of the energetic particles characteristics in the inner part of the Jovian magnetosphere: a topological study. Planet. Space Sci. **52**, 491–498 (2004a), doi:10.1016/j.pss.2003.06.011.

Tomás, A. T., J. Woch, N. Krupp, A. Lagg, K.-H. Glassmeier, and W. S. Kurth: Energetic electrons in the inner part of the Jovian magnetosphere and their relation to auroral emissions. J. Geophys. Res. **109**, A06203 (2004b), doi:10.1029/2004JA010405.

Tomasz, F., J. Rybak, A. Kucera, W. Curdt, and H. Wöhl: SUMER/SOHO and TRACE study of the transition region blinker. In: Proc. of SOHO 13 – Waves, Oscillations and Small-Scale Transient Events in the Solar Atmosphere: A Joint View from SOHO and TRACE, ed. H. Lacoste, ESA SP-547, pp. 307–309, ESA Publ. Div., Noordwijk (2004).

Tozzi, G. P., L. M. Lara, L. Kolokolova, H. Boehnhardt, J. Licandro, and R. Schulz: Sublimating components in the coma of Comet C/2000 WM1 (LINEAR). Astron. & Astrophys. **424**, 325–330 (2004), doi:10.1051/0004-6361:20035893.

Tripathi, D., V. Bothmer, and H. Cremades: The basic characteristics of EUV post-eruptive arcades and their role as tracers of coronal mass ejection source regions. Astron. & Astrophys. **422**, 337–349 (2004a), doi:10.1051/0004-6361:20035815.

Tripathi, D., V. Bothmer, S. K. Solanki, R. Schwenn, M. Mierla, and G. Stenborg: Plasma dynamics of a prominence associated coronal mass ejection. In: Multi-Wavelength Investigations of Solar Activity, Proc. IAU Symp. 223, eds. A. V. Stepanov, E. E. Benevolenskaya, and A. G. Kosovichev, pp. 401–402, University Press, Cambridge (2004b).

Tsou, P., D. E. Brownlee, J. D. Anderson, S. Bhaskaran, A. R. Cheuvront, B. C. Clark, T. Duxbury, T. Economou, S. F. Green, M. S. Hanner, F. Horz, J. Kissel, J. A. M. McDonnell, R. L. Newburn, R. E. Ryan, S. A. Sandford, Z. Sekanina, A. J. Tuzzolino, J. M. Vellinga, and M. E. Zolensky: Stardust encounters comet 81P Wild 2. J. Geophys. Res. **109**, E12S01 (2004), doi:10.1029/2004JE002317.

Tsurutani, B., A. Mannucci, B. Iijima, M. A. Abdu, J. H. A. Sobral, W. Gonzalez, F. Guarnieri, T. Tsuda, A. Saito, K. Yumoto, B. Fejer, T. J. Fuller-Rowell, J. Kozyra, J. C. Foster, A. Coster, and V. M. Vasyliūnas: Global dayside ionospheric uplift and enhancement associated with interplanetary electric fields. J. Geophys. Res. **109**, A08302 (2004a), doi:10.1029/2003JA010342.

Tsurutani, B. T., W. D. Gonzalez, X. Y. Zhou, R. P. Lepping, and V. Bothmer: Properties of slow magnetic clouds. J. Atmos. Solar-Terr. Phys. **66**, 147–151 (2004b), doi:10.1016/j.jastp.2003.09.007.

Tu, C.-Y., E. Marsch, and Z.-R. Qin: Dependence of the proton beam drift velocity on the proton core plasma beta in the solar wind. J. Geophys. Res. **109**, A05101 (2004), doi:10.1029/2004JA010391.

Usoskin, I. G., K. Mursula, S. K. Solanki, M. Schüssler, and K. Alanko: Reconstruction of solar activity for the last millenium using ^{10}Be data. Astron. & Astrophys. **413**, 745–751 (2004a), doi:10.1051/0004-6361:20031533.

Usoskin, I. G., S. K. Solanki, M. Schüssler, and K. Mursala: Comment on "Millennium scale sunspot number reconstruction: Evidence for an unusually active Sun since the 1940s" - Reply. Phys. Rev. Lett. **92**, 199002 (2004b), doi:10.1103/PhysRevLett.92.199002.

Uspensky, M., A. Koustov, P. Janhunen, E. Nielsen, K. Kauristie, O. Amm, R. Pellinen, H. Opgenoorth, and R. Pirjola: STARE velocities: 2. Evening westward electron flow. Ann. Geophys. **22**, 1077–1091 (2004).

Vasyliūnas, V. M.: Comment on 'The superposition of rotating and stationary magnetic sources: implications for the auroral region' [Phys. Plasmas 10, 2971 (2003)]. Phys. Plasmas **11**, 1738–1739 (2004a).

— Comparative magnetospheres: lessons for Earth. Adv. Space Res. **33**, 2113–2120 (2004b), doi:10.1016/j.asr.2003.04.051.

Verheest, F., T. Cattaert, E. Dubinin, K. Sauer, and J. F. McKenzie: Whistler oscillitons revisited: the role of charge neutrality? Nonlin. Proc. Geophys. **11**, 447–452 (2004).

Verigin, M. I., J. Slavin, A. Szabo, G. A. Kotova, A. P. Remizov, H. Rosenbauer, S. Livi, K. Szego, M. Tatrallyay, K. Schwingenschuh, and T. L. Zhang: Unusually distant bow shock encounters at Mars: Analysis of March 24, 1989 event. Space Sci. Rev. **111**, 233–243 (2004), doi:10.1023/B:SPAC.0000032713.86796.d1.

Veselovsky, I. S., M. I. Panasyuk, S. I. Avdyushin, G. A. Bazilevskaya, A. V. Belov, S. A. Bogachev, V. M. Bogod, A. V. Bogomolov, V. Bothmer, K. A. Boyarchuk, E. V. Vashenyuk, V. I. Vlasov, A. A. Gnezdilov, R. V. Gorgutsa, V. V. Grechnev, Y. I. Denisov, A. V. Dmitriev, M. Dryer, Y. I. Yermolaev, E. A. Eroshenko, G. A. Zherebtsov, I. A. Zhitnik, A. N. Zhukov, G. N. Zastenker, L. M. Zelenyi, M. A. Zeldovich, G. S. Ivanov-Kholodnyi, A. P. Ignat'ev, V. N. Ishkov, O. P. Kolomiytsev, I. A. Krasheninnikov, K. Kudela, B. M. Kuzhevsky, S. V. Kuzin, V. D. Kuznetsov, S. N. Kuznetsov, V. G. Kurt, L. L. Lazutin, L. N. Leshchenko, M. L. Litvak, Y. I. Logachev, G. Lawrence, A. K. Markeev, V. S. Makhmutov, A. V. Mitrofanov, I. G. Mitrofanov, O. V. Morozov, I. N. Myagkova, A. A. Nusinov, S. N. Oparin, O. A. Panasenco, A. A. Pertsov, A. A. Petrukovich, A. N. Podorolsky, E. P. Romashets, S. I. Svertilov, P. M. Svidsky, A. K. Svirzhevskaya, N. S. Svirzhevsky, V. A. Slemzin, Z. Smith, I. I. Sobel'man, D. E. Sobolev, *Y. I. Stozhkov, A. V. Suvorova, N. K. Sukhodrev, I. P. Tindo, S. K. Tokhchukova, V. V. Fomichev, I. V. Chashey, I. M. Chertok, V. L. Shishov, B. Y. Yushkov, O. S. Yakovchouk, and V. G. Yanke*: Solar and heliospheric phenomena in October-November 2003: Causes and effects. Cosmic Research **42**, 435–488 (2004), doi:10.1023/B:COSM.0000046229.24716.02.

Vögler, A.: Effects of non-grey radiative transfer on 3D simulations of solar magneto-convection. Astron. & Astrophys. **421**, 755–762 (2004a), doi:10.1051/0004-6361:20047044.

— Simulating radiative magneto-convection in the solar photosphere. In: The Sun and Planetary Systems - Paradigms for the Universe, ed. R. E. Schielicke, no. 17 in Reviews in Modern Astronomy, pp. 69–85 (2004b).

Vögler, A., J. H. M. J. Bruls, and M. Schüssler: Approximations for non-grey radiative transfer in numerical simulations of the solar photosphere. Astron. & Astrophys. **421**, 741–754 (2004), doi:10.1051/0004-6361:20047043.

Wang, D. Y., G. P. Stiller, T. von Clarmann, H. Fischer, M. Lopez-Puertas, B. Funke, N. Glatthor, U. Grabowski, M. Höpfner, S. Kellmann, M. Kiefer, A. Linden, G. M. Tsidu, M. Milz, T. Steck, J. H. Jiang, C. O. Ao, G. Manney, K. Hocke, D. L. Wu, L. J. Romans, J. Wickert, and T. Schmidt: Cross-validation of MIPAS/ENVISAT and GPS-RO/CHAMP temperature profiles. J. Geophys. Res. **109**, D19311 (2004a), doi:10.1029/2004JD004963.

Wang, J.-S. and E. Nielsen: Evidence for topographic effects on the Martian ionosphere. Planet. Space Sci. **52**, 881–886 (2004a), doi:10.1016/j.pss.2004.01.008.

— Solar wind modulation of the Martian ionosphere observed by MARS Global Surveyor. Ann. Geophys. **22**, 2277–2281 (2004b).

Wang, T. J.: Overview of recent results in observations. In: Proc. of SOHO 13 – Waves, Oscillations and Small-Scale Transient Events in the Solar Atmosphere: A Joint View from SOHO and TRACE, ed. H. Lacoste, ESA SP-547, pp. 417–426, ESA Publ. Div., Noordwijk (2004).

Wang, T. J. and S. K. Solanki: Vertical oscillations of a coronal loop observed by TRACE. Astron. & Astrophys. **421**, L33–L36 (2004), doi:10.1051/0004-6361:20040186.

Wang, T. J., S. K. Solanki, W. Curdt, and D. E. Innes: Overview of slow mode oscillations in hot coronal loops observed by SUMER. In: Stars as Suns: Activity, Evolution, and Planets, eds. A. K. Dupree and A. O. Benz, *IAU Symposium*, vol. 219, pp. CD–712–CD–716, Cambridge Univ. Press (2004b).

Wehry, A., H. Krüger, and E. Grün: Analysis of Ulysses data: Radiation pressure effects of dust particles. Astron. & Astrophys. **419**, 1169–1174 (2004), doi:10.1051/0004-6361:20035613.

Wenzler, T., S. K. Solanki, N. A. Krivova, and D. M. Fluri: Comparison between KPVT/SPM and SOHO/MDI magnetograms with an application to solar irradiance reconstructions. Astron. & Astrophys. **427**, 1031–1043 (2004), doi:10.1051/0004-6361:20041313.

Werner, S., H. U. Keller, A. Korth, and H. Lauche: UVIS/HDAC Lyman-alpha observations of the geocorona during Cassini's Earth swingby compared to model prediction. Adv. Space Res. **34**, 1647–1649 (2004), doi:10.1016/j.asr.2003.03.074.

Wicht, J. and P. Olson: A detailed study of the polarity reversal mechanism in a numerical dynamo model. Geochemistry Geophysics Geosystems **5**, Q03H10 (2004), doi:10.1029/2003GC000602.

Wiegelmann, T.: Optimization code with weighting function for the reconstruction of coronal magnetic fields. Solar Phys. **219**, 87–108 (2004), doi:10.1023/B:SOLA.0000021799.39465.36.

Wiegelmann, T. and S. K. Solanki: Similarities and differences between coronal holes and the quiet sun: are loop statistics the key? Solar Phys. **225**, 227–247 (2004a), doi:10.1007/s11207-004-3747-2.

— Why are coronal holes indistinguishable from the quiet sun in transition region radiation? In: Proc. SOHO 15 'Coronal Heating', eds. R. W. Walsh, J. Ireland, D. Danesy, and B. Fleck, ESA SP-575, pp. 35–40, ESA Publ. Div., Noordwijk (2004b).

Wilber, M., E. Lee, G. K. Parks, K. Meziane, C. W. Carlson, J. P. McFadden, H. Rème, I. Dandouras, J.-A. Sauvaud, J.-M. Bosqued, L. Kistler, E. Möbius, M. McCarthy, A. Korth, B. Klecker, M.-B. Bavassano-Cattaneo, R. Lundin, and E. Lucek: Cluster observations of velocity space-restricted ion distributions near the plasma sheet. Geophys. Res. Lett. **31**, L24802 (2004), doi:10.1029/2004GL020265.

Wilhelm, K., B. N. Dwivedi, E. Marsch, and U. Feldman: Observations of the Sun at vacuum-ultraviolet wavelengths from space. Part I: Concepts and instrumentation. Space Sci. Rev. **111**, 415–480 (2004a), doi:10.1023/B:SPAC.0000032695.27525.54.

Wilhelm, K., B. N. Dwivedi, and L. Teriaca: On the widths of the Mg X lines near 60 nm in the corona. Astron. & Astrophys. **415**, 1133–1139 (2004b), doi: 10.1051/0004-6361:20034234.

Wilhelm, K. and W. Kalkofen: Observations of the solar chromosphere with SUMER. In: Proc. of SOHO 13 – Waves, Oscillations and Small-Scale Transient Events in the Solar Atmosphere: A Joint View from SOHO and TRACE, ed. H. Lacoste, ESA SP-547, pp. 137–138, ESA Publ. Div., Noordwijk (2004).

Witte, M.: Kinetic parameters of interstellar neutral helium - Review of results obtained during one solar cycle with the Ulysses/GAS-instrument. Astron. & Astrophys. **426**, 835–844 (2004), doi:10.1051/0004-6361:20035956.

Witte, M., M. Banaszkiewicz, H. Rosenbauer, and D. McMullin: Kinetic parameters of interstellar neutral helium: updated results from the ULYSSES/GAS-instrument. Adv. Space Res. **34**, 61–65 (2004), doi:10.1016/j.asr.2003.01.037.

Woch, J., N. Krupp, A. Lagg, and A. Tomás: The structure and dynamics of the Jovian energetic particle distribution. Adv. Space Res. **33**, 2030–2038 (2004), doi:10.1016/j.asr.2003.04.050.

Xia, L. D. and E. Marsch: Observational constraints on ion acceleration by waves in coronal holes. In: Proc. of SOHO 13 – Waves, Oscillations and Small-Scale Transient Events in the Solar Atmosphere: A Joint View from SOHO and TRACE, ed. H. Lacoste, ESA SP-547, pp. 387–390, ESA Publ. Div., Noordwijk (2004).

Xia, L. D., E. Marsch, and K. Wilhelm: On the network structures in solar equatorial coronal holes — Observations of SUMER and MDI on SOHO. Astron. & Astrophys. **424**, 1025–1037 (2004a), doi: 10.1051/0004-6361:20047027.

— Topological changes of the magnetic network as seen in different UV/EUV emission lines. In: Proc. of SOHO 13 – Waves, Oscillations and Small-Scale Transient Events in the Solar Atmosphere: A Joint View from SOHO and TRACE, ed. H. Lacoste, ESA SP-547, pp. 169–174, ESA Publ. Div., Noordwijk (2004b).

Young, D. T., F. J. Crary, J. E. Nordholt, F. Bagenal, D. Boice, J. L. Burch, A. Eviatar, R. Goldstein, J. J. Hanley, D. R. Lawrence, D. J. McComas, R. Meier, D. Reisenfeld, K. Sauer, and R. C. Wiens: Solar wind interaction with comet 19P/Borelly. Icarus **167**, 80–88 (2004), doi:10.1016/j.icarus.2003.09.011.

von Zahn, U., G. Baumgarten, U. Berger, J. Fiedler, and P. Hartogh: Noctilucent clouds and the mesospheric water vapour: the past decade. Atmos. Chem. Phys. **4**, 2449–2464 (2004a).

von Zahn, U., U. Berger, J. Fielder, and P. Hartogh: Noctilucent clouds and the mesospheric water vapour: the past decade. Atmos. Chem. Phys. Discuss. **4**, 3045–3076 (2004b).

Zatsepin, V. I., J. H. Adams, H. S. Ahn, G. I. Bashindzhagyan, K. E. Batkov, J. Chang, M. Christl, A. R. Fazely, O. Ganel, R. M. Gunasingha, T. G. Guzik, J. Isbert, K. C. Kim, E. N. Kouznetsov, M. I. Panasyuk, A. D. Panov, W. K. H. Schmidt, E. S. Seo, N. V. Sokolskaya, J. Z. Wang, J. P. Wefel, and J. Wu: The silicon matrix as a charge detector in the ATIC experiment. Nucl. Instr. Methods Phys. A **524**, 195–207 (2004).

Zong, Q.-G., T. A. Fritz, Z. Y. Pu, S. Y. Fu, D. N. Baker, H. Zhang, A. T. Lui, I. Vogiatzis, K.-H. Glassmeier, A. Korth, P. W. Daly, A. Balogh, and H. Rème: Cluster observations of Earthward flowing plasmoid in the tail. Geophys. Res. Lett. **31**, L18803 (2004a), doi:10.1029/2004GL020692.

Zong, Q.-G., T. A. Fritz, H. Spence, K. Oksavik, Z.-Y. Pu, A. Korth, and P. W. Daly: Energetic particle sounding of the magnetopause: A contribution by Cluster/RAPID. J. Geophys. Res. **109**, A04207 (2004b), doi:10.1029/2003JA009929.

Zong, Q.-G., T. A. Fritz, H. Zhang, A. Korth, P. W. Daly, M. W. Dunlop, K.-H. Glassmeier, H. Rème, and A. Balogh: Triple cusps observed by Cluster—Temporal or spatial effect? Geophys. Res. Lett. **31**, L09810 (2004c), doi:10.1029/2003GL019128.

Zou, H. and E. Nielsen: Faraday rotation and MARSIS as a detector of crustal magnetic field. MPAE Report MPAe-W-485-04-02, Max-Planck-Institut für Aeronomie, Katlenburg-Lindau, Germany (2004a).

— Methods for obtaining electron density profiles from MARSIS ionograms and derivation of parameters characterizing the profiles. MPAE Report MPAe-W-485-04-01, Max-Planck-Institut für Aeronomie, Katlenburg-Lindau, Germany (2004b).

Veröffentlichungen 2005 / Publications 2005

A'Hearn, M. F., M. J. S. Belton, W. A. Delamere, J. Kissel, K. P. Klaasen, L. A. McFadden, K. J. Meech, H. J. Melosh, P. H. Schultz, J. M. Sunshine, P. C. Thomas, J. Veverka, D. K. Yeomans, M. W. Baca, I. Busko, C. J. Crockett, S. M. Collins, M. Desnoyer, C. A. Eberhardy, C. M. Ernst, T. L. Farnham, L. Feaga, O. Groussin, D. Hampton, S. I. Ipatov, J. Y. Li, D. Lindler, C. M. Lisse, N. Mastrodemos, W. M. Owen, J. E. Richardson, D. D. Wellnitz, and R. L. White: Deep Impact: Excavating comet Tempel 1. Science **310**, 258–264 (2005), doi:10.1126/science.1118923.

Altobelli, N., S. Kempf, H. Krüger, M. Landgraf, M. Roy, and E. Grün: Interstellar dust flux measurements by the Galileo dust instrument between the orbits of Venus and Mars. J. Geophys. Res. **110**, A07 102 (2005a), doi:10.1029/2004JA010772.

Altobelli, N., S. Kempf, H. Krüger, M. Landgraf, R. Srama, and E. Grün: In-situ monitoring of interstellar dust in the inner solar system. In: The Spectral Energy Distributions of Gas-Rich Galaxies: Confronting Models with Data, eds. R. Tuffs and C. Popescu, *AIP conference series*, vol. 761, pp. 149–155 (2005b), Heidelberg, October 2004.

Arvelius, S., M. Yamauchi, H. Nilsson, R. Lundin, Y. Hobara, H. Rème, M. B. Bavassano-Cattaneo, G. Paschmann, A. Korth, L. M. Kistler, and G. K. Parks: Statistics of high-altitude and high-latitude O^+ ion outflows observed by Cluster/CIS. Ann. Geophys. **23**, 1909–1916 (2005).

Aubert, J.: Steady zonal flows in spherical shell dynamos. J. Fluid Mech. **542**, 53–67 (2005), doi: 10.1017/S0022112005006129.

Auchere, F., J. W. Cook, J. S. Newmark, D. R. McMullin, R. von Steiger, and M. Witte: Model of the all-sky HeII 30.4 nm solar Flux. Adv. Space Res. **35**, 388–392 (2005a), doi:10.1016/j.asr.2005.02.036.

— The Heliospheric HeII 30.4 nm Solar Flux During Cycle 23. Astrophys. J. **625**, 1036–1044 (2005b).

Aznar Cuadrado, R., S. Jordan, R. Napiwotzki, H. M. Schmid, S. K. Solanki, and G. Mathys: Kilo-Gauss magnetic fields in three DA white dwarfs. In: 14th European Workshop on White Dwarfs, eds. D. Koester and S. Moehler, *Astron. Soc. Pacific Conf. Ser.*, vol. 334, pp. 159–164 (2005).

Aznar Cuadrado, R., S. K. Solanki, and A. Lagg: Supersonic downflows in the solar chromosphere are very common. In: Proceedings of the International Scientific Conference on Chromospheric and Coronal Magnetic Fields, eds. D. E. Innes, A. Lagg, S. K. Solanki, and D. Danesy, ESA SP-596, ESA Publ. Div., Noordwijk (2005).

Balmaceda, L., S. K. Solanki, and N. Krivova: A cross-calibrated sunspot areas time series since 1874. Memorie della Societa Astronomica Italiana **76**, 929–932 (2005).

Barnes, J. R., A. Collier Cameron, J.-F. Donati, D. J. James, S. C. Marsden, and P. Petit: The dependence of differential rotation on temperature and rotation. Mon. Not. Roy. Astron. Soc. **357**, L1 (2005).

Baumann, I.: Magnetic Flux Transport on the Sun. Doktorarbeit, Universität Göttingen (2005).

Baumann, I., D. Schmitt, and M. Schüssler: A necessary extension of the flux transport model. Memorie della Societa Astronomica Italiana **76**, 933–936 (2005).

Baumann, I. and S. K. Solanki: On the size distribution of sunspot groups in the Greenwich sunspot record 1874-1976. Astron. & Astrophys. **443**, 1061–1066 (2005), doi:10.1051/0004-6361:20053415.

Baumgärtel, K., K. Sauer, and E. Dubinin: Kinetic slow mode-type solitons. Nonlin. Proc. Geophys. **12**, 291–298 (2005).

Belton, M. J., K. J. Meech, M. F. A'Hearn, O. Groussin, L. Mcfadden, C. Lisse, Y. R. Fernandez, J. Pittichova, H. Hsieh, J. Kissel, K. Klaasen, P. Lamy, D. Prialnik, J. Sunshine, P. Thomas, and I. Toth: Deep impact: Working properties for the target nucleus - Comet 9P/Tempel 1. Space Sci. Rev. **117**, 137–160 (2005), doi:10.1007/s11214-005-3389-1.

Berdyugina, S. V., P. A. Braun, D. M. Fluri, and S. K. Solanki: The molecular Zeeman effect and diagnostics of solar and stellar magnetic fields. III. Theoretical spectral patterns in the Paschen-Back regime. Astron. & Astrophys. **444**, 947–960 (2005), doi: 10.1051/0004-6361:20053806.

Bewsher, D., D. E. Innes, C. E. Parnell, and D. S. Brown: Comparison of blinkers and explosive events: A case study. Astron. & Astrophys. **432**, 307–317 (2005), doi:10.1051/0004-6361:20041171.

Birn, J., K. Galsgaard, M. Hesse, M. Hoshino, J. Huba, G. Lapenta, P. L. Pritchett, K. Schindler, L. Yin, J. Büchner, T. Neukirch, and E. R. Priest: Forced magnetic reconnection. Geophys. Res. Lett. **32**, L06105 (2005), doi:10.1029/2004GL022058.

Blixt, E. M., T. Grydeland, N. Ivchenko, T. Hagfors, C. La Hoz, B. S. Lanchester, U. P. Løvhaug, and T. S. Trondsen: Dynamic rayed aurora and enhanced ion-acoustic radar echoes. Ann. Geophys. **23**, 3–11 (2005).

Borisov, N. and E. Nielsen: Excitation of plasma waves by unstable photoelectron and thermal electron populations on closed magnetic field lines in the Martian ionosphere. Ann. Geophys. **23**, 1249–1258 (2005).

Borrero, J. M., A. Lagg, S. K. Solanki, and M. Collados: On the fine structure of the sunspot penumbrae. II The nature of the Evershed flow. Astron. & Astrophys. **436**, 333–345 (2005), doi:10.1051/0004-6361:20042553.

Büchner, J.: Vlasov code simulation in space physics. In: 7th International School/Symposium for Space Simulations, eds. Y. Omura and H. Usui (2005).

Büchner, J. and B. Nikutowski: Acceleration of the fast solar wind by reconnection. In: Proceedings of the Solar Wind 11/SOHO 16 Conference, 12-17 June 2005, Whistler, Canada, eds. B. Fleck and T. H. Zurbuchen, ESA SP-592, pp. 141–146, ESA Publ. Div., Noordwijk (2005).

Büchner, J. and B. Nikutowski: Physically consistent simulation of chromospheric and coronal magnetic fields. In: Proc. of the International Scientific Conference "Chromospheric and Coronal Magnetic Fields",Lindau, August 30 – September 2, 2005, ESA SP-596, ESA Publ. Div., Noordwijk (2005).

Büchner, J., B. Nikutowski, and A. Otto: Plasma acceleration due to transition region reconnection. In: Particle acceleration in astrophysical plasmas: Geospace and beyond, eds. J. L. Horwitz, J. D. Perez, R. D. Preece, and J. Queenby, *Geophysical Monographs*, vol. 156, pp. 161–170, American Geophysical Union (2005).

Bunce, E. J., S. W. H. Cowley, D. M. Wright, A. J. Coates, M. K. Dougherty, N. Krupp, W. S. Kurth, and A. M. Rymer: In situ observations of a solar wind compression-induced hot plasma injection in Saturn's tail. Geophys. Res. Lett. **32**, L20S04 (2005), doi:10.1029/2005GL022888.

Büsching, I., A. Kopp, M. Pohl, R. Schlickeiser, C. Perrot, and I. Grenier: Cosmic-ray propagation properties for an origin in supernova remnants. Astrophys. J. **619**, 314–326 (2005), doi:10.1086/426537.

Cai, H. T., S. Y. Ma, and K. Schlegel: Climatologic characteristics of high-latitude ionosphere - EISCAT observations and comparison with the IRI model. Chinese J. Geophys. **48**, 471–479 (2005).

Cameron, R. and D. Galloway: The structure of small-scale magnetic flux tubes. Mon. Not. Roy. Astron. Soc. **358**, 1025–1035 (2005), doi:10.1111/j.1365-2966.2005.08840.x.

Cameron, R., A. Vögler, M. Schüssler, and V. Zakharov: Simulations of solar pores. In: Proceedings of the 11th European Solar Physics Meeting — The Dynamic Sun: Challenges for Theory and Observations, 11-16 September 2005, eds. D. Danesy, S. Poedts, A. De Groof, and J. Andries, ESA SP-600, ESA Publ. Div., Noordwijk (2005), on CD.

Curdt, W., E. Landi, T. Wang, and U. Feldman: In-situ heating in active region loops . Hvar. Obs. Bull. **29**, 157–165 (2005a).

Curdt, W., E. Landi, T.-J. Wang, and U. Feldman: Evidence for in situ heating in active region loops. In: Proceedings of the Solar Wind 11/SOHO 16 Conference, 12-17 June 2005, Whistler, Canada, eds. B. Fleck and T. H. Zurbuchen, ESA SP-592, pp. 475–478, ESA Publ. Div., Noordwijk (2005b).

Czechowski, A., M. Hilchenbach, and K. C. Hsieh: Heliospheric energetic neutral atoms as a means to determine the anomalous cosmic ray spectrum at the termination shock. Astron. & Astrophys. **431**, 1061–1068 (2005), doi:10.1051/0004-6361:20041417.

Dandouras, I., V. Pierrard, J. Goldstein, C. Vallat, G. K. Parks, H. Rème, C. Gouillart, F. Sevestre, M. McCarthy, L. M. Kistler, B. Klecker, A. Korth, M. B. Bavassano-Cattaneo, P. Escoubet, and A. Masson: Multipoint Observations of Ionic Structures in the Plasmasphere by CLUSTER—CIS and Comparisons With IMAGE-EUV Observations and With Model Simulations. In: Inner Magnetosphere Interactions: New Perspectives from Imaging, eds. J. Burch, M. Schulz, and H. Spence, *Geohpysical Monograph*, vol. 159, pp. 23–54, American Geophysical Union, Washington (2005), doi:10.1029/159GM03.

Davies, J. A., M. Grande, C. H. Perry, M. W. Dunlop, M. K. Carter, J. B. Blake, J. F. Fennell, P. W. Daly, R. H. W. Friedel, and T. A. Fritz: Energetic electron observations of magnetospheric boundaries using the imaging electron spectrometers on Cluster and Polar. Adv. Space Res. **36**, 1916–1921 (2005), doi:10.1016/j.asr.2004.01.028.

Deng, X. H., R. X. Tang, R. Nakamura, W. Baumjohann, T. L. Zhang, P. W. Daly, H. Rème, C. M. Carr, A. Balogh, Z. X. Liu, and J. F. Wang: Observation of reconnection pulses by Cluster and Double Star. Ann. Geophys. **23**, 2921–2927 (2005).

Doressoundiram, A., M. A. Barucci, G. P. Tozzi, F. Poulet, H. Boehnhardt, C. de Bergh, and N. Peixinho: Spectral characteristics and modeling of the Transneptunian object (55565) 2002 AW_{197} and the Centaurs (55576) 2002 GB_{10} and (83982) 2002 GO_9: ESO Large Program on TNOs and Centaurs. Planet. Space Sci. **53**, 1501–1509 (2005), doi: 10.1016/j.pss.2004.11.007.

Doyle, J. G., J. Giannikakis, L. D. Xia, and M. S. Madjarska: Line broadening of EUV lines across the solar limb: A spicule contribution? Astron. & Astrophys. **431**, L17–L20 (2005), doi:10.1051/0004-6361:200400137.

Dubinin, E., K. Sauer, and J. F. McKenzie: Differential ion streaming in the solar wind as an equilibrium state. J. Geophys. Res. **110**, A07101 (2005a), doi:10.1029/2004JA010826.

— Nonlinear inertial and kinetic Alfvèn waves. J. Geophys. Res. **110**, A10S04 (2005b), doi:10.1029/2004JA010770.

Emerich, C., P. Lemaire, J.-C. Vial, W. Curdt, U. Schühle, and K. Wilhelm: A new relation between the central spectral solar H I Lyman α irradiance and the line irradiance measured by SUMER/SOHO during the cycle 23. Icarus **178**, 429–433 (2005), doi:10.1016/j.icarus.2005.05.002.

Encrenaz, T., R. Melchiorri, T. Fouchet, P. Drossart, E. Lellouch, B. Gondet, J. P. Bibring, Y. Langevin, D. Titov, N. Ignatiev, and F. Forget: A mapping of Martian water sublimation during early northern summer using OMEGA/Mars Express. Astron. & Astrophys. **441**, L9–L12 (2005), doi:10.1051/0004-6361:200500171.

Esposito, L. W., J. E. Colwell, K. Larsen, W. E. McClintock, A. I. F. Stewart, J. T. Hallett, D. E. Shemansky, J. M. Ajello, C. J. Hansen, A. R. Hendrix, R. A. West, H. U. Keller, A. Korth, W. R. Pryor, R. Reulke, and Y. L. Yung: Ultraviolet imaging spectroscopy shows an active Saturnian system. Science **307**, 1251–1255 (2005), doi:10.1126/science.1105606.

Farrugia, C. J., M. Leitner, H. K. Biernat, R. Schwenn, K. W. Ogilvie, H. Matsui, H. Kucharek, V. K. Jordanova, and R. P. Lepping: Evolution of interplanetary magnetic clouds from 0.3 AU to 1 AU: A joint Helios-Wind investigation. In: Connecting Sun And Heliosphere, Proceedings of the Conference Solar Wind 11 - SOHO 16, eds. B. Fleck and T. H. Zurbuchen, ESA SP-592, pp. 723 – 726, ESA Publ. Div., Noordwijk (2005).

Feldstein, Y. I., A. E. Levitin, J. U. Kozyra, B. T. Tsurutani, A. Prigancova, L. Alperovich, W. D. Gonzalez, U. Mall, I. I. Alexeev, L. I. Gromova, and L. A. Dremukhina: Self-consistent modeling of the large-scale distortions in the geomagnetic field during the 24-27 September 1998 major magnetic storm. J. Geophys. Res. **110**, A11214 (2005), doi: 10.1029/2004JA010584.

Fernandez, J. R., R. D. Palmer, P. B. Chilson, I. Haggstrom, and M. T. Rietveld: Range imaging observations of PMSE using the EISCAT VHF radar: Phase calibration and first results. Ann. Geophys. **23**, 207–220 (2005).

Fernández, M. H. C.: Three-dimensional configuration and evolution of coronal mass ejections. Doktorarbeit, TU Braunschweig (2005).

Frutiger, C., S. K. Solanki, and G. Mathys: Fundamental parameters and granulation properties of Alpha Centauri A and B obtained from inversions of their spectra. Astron. & Astrophys. **444**, 549–559 (2005), doi:10.1051/0004-6361:20053534.

Fu, S. Y., Q. G. Zong, Z. Y. Pu, C. J. Xiao, A. Korth, P. Daly, and H. Rème: Energetic Particles Observed in the CUSP Region During a Storm Recovery Phase. Surveys in Geophysics **26**, 241–254 (2005), doi:10.1007/s10712-005-1881-5.

Gandorfer, A.: The Second Solar Spectrum - A high spectral resolution polarimetric survey of scattering polarization near the solar limb in graphical representation. Voll III: 3160 Angstroems to 3915 Angstroems. vdf, Zurich (2005).

Ganel, O., J. H. Adams, H. S. Ahn, J. Ampe, G. Bashindzhagyan, G. Case, J. Chang, S. Ellison, A. Fazely, R. Gould, D. Granger, R. Gunasingha, T. G. Guzik, Y. J. Han, J. Isbert, H. J. Kim, K. C. Kim, S. K. Kim, Y. Kwon, M. Panasyuk, A. Panov, B. Price, G. Samsonov, W. K. H. Schmidt, M. Sen, E. S. Seo, R. Sina, N. Sokolskaya, M. Stewart, A. Voronin, D. Wagner, J. Z. Wang, J. P. Wefel, J. Wu, and V. Zatsepin: Beam tests of the balloon-borne ATIC experiment. Nucl. Instr. Methods Phys. A **552**, 409–419 (2005), doi:10.1016/j.nima.2005.06.081.

García-Alvarez, D., C. M. Johns-Krull, J. G. Doyle, I. Ugarte-Urra, M. S. Madjarska, and C. J. Butler: Optical and EUV observations of solar flare kernels. Astron. & Astrophys. **444**, 593–603 (2005), doi:10.1051/0004-6361:20053708.

Gizon, L.: Am Puls der Sonne. MaxPlanckForschung **3**, 48–54 (2005a).

— The Pulse of the Sun. MaxPlanckResearch **4**, 48–54 (2005b).

Gizon, L. and A. C. Birch: Local Helioseismology. Living Rev. Solar Phys. **2**, 6 (2005).

Goesmann, F., H. Rosenbauer, R. Roll, and H. Boehnhardt: COSAC onboard Philae: a bioastronomy experiment for the short-period comet 67P/Churyumov-Gerasimenko. Astrobiology **5, No.5**, 622–631 (2005).

Goetz, W., P. Bertelsen, C. S. Binau, H. P. Gunnlaugsson, S. F. Hviid, K. M. Kinch, D. E. Madsen, M. B. Madsen, M. Olsen, R. Gellert, G. Klingelhofer, D. W. Ming, R. V. Morris, R. Rieder, D. S. Rodionov, P. A. de Souza, C. Schroder, S. W. Squyres, T. Wdowiak, and A. Yen: Indication of drier periods on Mars from the chemistry and mineralogy of atmospheric dust. Nature **436**, 62–65 (2005), doi: 10.1038/nature03807.

Gömöry, P., J. Rybak, A. Kucera, W. Curdt, and H. Wöhl: Variability and dynamics of the outer atmospheric layers in the quiet solar network. Hvar Obs. Bull. **29**, 71–78 (2005).

Gonzalez, W. D. and E. Echer: A study on the peak Dst and peak negative Bz relationship during intense geomagnetic storms. Geophys. Res. Lett. **32**, L18103 (2005), doi:10.1029/2005GL023486.

Gottwald, A., M. Richter, G. Ulm, and U. Schühle: Stability of vacuum-ultraviolet radiometric transfer standards: electron cyclotron resonance versus hollow cathode source. Rev. Sci. Inst. **76**, 023101 (2005), doi:10.1063/1.1835051.

Greve, R. and R. A. Mahajan: Influence of ice rheology and dust content on the dynamics of the north-polar cap of Mars. Icarus **174**, 475–485 (2005), doi: 10.1016/j.icarus.2004.07.031.

Grieger, B.: Shading under Titan's sky. Planet. Space Sci. **53**, 577–585 (2005), doi:10.1016/j.pss.2004.04.003.

Grün, E., R. Srama, H. Krüger, S. Kempf, V. Dikarev, S. Helfert, and G. Moragas-Klostermeyer: 2002 Kuiper Prize Lecture: Dust Astronomy. Icarus **174**, 1–14 (2005), doi:10.1016/j.icarus.2004.09.010.

Grynko, Y.: Light scattering by cometary dust particles with sizes large compared to the wavelength of light. Doktorarbeit, Universität Göttingen (2005).

Gurnett, D. A., D. L. Kirchner, R. L. Huff, D. D. Morgan, A. M. Persoon, F. Duru, E. Nielsen, A. Safaeinili, J. J. Plaut, and G. Picardi: Radar soundings of the ionosphere of Mars. Science **310**, 1929–1933 (2005), doi:10.1126/science.1121868.

Haberreiter, M., N. A. Krivova, W. Schmutz, and T. Wenzler: Reconstruction of the solar UV irradiance back to 1974. Adv. Space Res. **35**, 365–369 (2005), doi:10.1016/j.asr.2005.04.039.

Haldoupis, C., T. Ogawa, K. Schlegel, J. A. Koehler, and T. Ono: Is there a plasma density gradient role on the generation of short scale Farley-Buneman waves? Ann. Geophys. **23**, 3323–3337 (2005).

Hartogh, P., A. S. Medvedev, T. Kuroda, R. Saito, G. Villanueva, A. G. Feofilov, A. A. Kutepov, and U. Berger: Description and climatology of a new general circulation model of the Martian atmosphere. J. Geophys. Res. **110**, E11008 (2005), doi: 10.1029/2005JE002498.

Heber, B., A. Kopp, H. Fichtner, and S. E. S. Ferreira: On the determination of energy spectra of MeV electrons by the Ulysses COSPIN/KET. Adv. Space Res. **35**, 605–610 (2005), doi:10.1016/j.asr.2005.01.054.

Heimpel, M., J. Aurnou, and J. Wicht: Simulation of equatorial and high-latitude jets on Jupiter in a deep convection model. Nature **438**, 193–196 (2005), doi:10.1038/nature04208.

Heuer, M.: Kinetische Plasmaprozesse und Welle-Teilchen-Wechselwirkungen von Ionen im schnellen Sonnenwind. Doktorarbeit, Universität Göttingen (2005), summa cum laude.

Hilchenbach, M., K. Bamert, and A. Czechowski: Potential Observations of the Solar Atmosphere via In-Situ Measurements of the Neutral Solar Wind. In: Proceedings of the Solar Wind 11/SOHO 16 Conference, 12-17 June 2005, Whistler, Canada, eds. B. Fleck and T. H. Zurbuchen, ESA SP-592, pp. 673–676 (2005a).

Hilchenbach, M. and A. Czechowski: Anomalous hydrogen and helium spectra at the termination shock from energetic neutral atoms flux intensity measurements. In: Proceedings of the Solar Wind 11/SOHO 16 Conference, 12-17 June 2005, Whistler, Canada, eds. B. Fleck and T. H. Zurbuchen, ESA SP-592, pp. 413–416 (2005).

Hilchenbach, M., A. Czechowski, and K. Scherer: Energetic neutral atoms in a time-dependent heliosphere. In: Proceedings of the Solar Wind 11/SOHO 16 Conference, 12-17 June 2005, Whistler, Canada, eds. B. Fleck and T. H. Zurbuchen, ESA SP-592, pp. 417–420 (2005b).

Hirzberger, J., S. Stangl, K. Gersin, J. Jurčák, K. G. Puschmann, and M. Sobotka: The structure of a penumbral connection between solar pores. Astron. & Astrophys. **442**, 1079–1086 (2005), doi:10.1051/0004-6361:20053257.

Huttunen, K. E. J., R. Schwenn, V. Bothmer, and H. E. J. Koskinen: Properties and geoeffectiveness of magnetic clouds in the rising, maximum and early declining phases of solar cycle 23. Ann. Geophys. **23**, 625–641 (2005).

Innes, D. E., A. Lagg, S. K. Solanki, and D. Danesy (eds.): Chromospheric and Coronal Magnetic Fields, ESA SP-596, ESA Publ. Div., Noordwijk (2005).

Isham, B., T. Hagfors, B. Khudukon, R. Yu. Yurik, E. D. Tereshchenko, M. T. Rietveld, V. Belyey, M. Grill, C. La Hoz, A. Brekke, and C. Heinselman: An interferometer experiment to explore the aspect angle dependence of stimulated electromagnetic emission spectra. Ann. Geophys. **23**, 55–74 (2005).

Jockers, K., N. Kiselev, T. Bonev, V. Rosenbush, N. Shakhovskoy, S. Kolesnikov, Yu. Efimov, D. Shakhovskoy, and K. Antonyuk: CCD imaging and aperture polarimetry of comet 2P/Encke: are there two polarimetric classes of comets? Astron. & Astrophys. **441**, 773–782 (2005a), doi:10.1051/0004-6361:20053348.

Jockers, K., S. Szutowicz, G. Villanueva, N. Kiselev, T. Bonev, and P. Hartogh: Gas and dust in Comet 2P/Encke observed in the visual and submillimeter wavelength ranges. In: Proceedings of the MAO-2004 Conference, Kinematics and Physics of Celestial Bodies, ed. Y. S. Yatskiv, vol. Suppl.Ser. N5, pp. 458–464 (2005b).

Kaeufl, H.-U., N. Ageorges, S. Bagnulo, L. Barrera, H. Boehnhardt, et al.: Deep Impact at ESO Telescopes. The ESO Messenger **121**, 11–16 (2005).

Kallenbach, R., K. Bamert, and M. Hilchenbach: Self-consistent adjustment of the flux of energetic ions and their injection threshold at the solar wind termination shock. In: Proceedings of the Solar Wind 11/SOHO 16 Conference, 12-17 June 2005, Whistler, Canada, eds. B. Fleck and T. H. Zurbuchen, ESA SP-592, pp. 433–436 (2005a).

Kallenbach, R., K. Bamert, M. Hilchenbach, and C. W. Smith: Excitation of proton cyclotron waves at interplanetary travelling shocks: ACE/MAG and SOHO/CELIAS observations. In: Proceedings of the Solar Wind 11/SOHO 16 Conference, 12-17 June 2005, Whistler, Canada, eds. B. Fleck and T. H. Zurbuchen, ESA SP-592, pp. 429–432 (2005b).

— Observations of Turbulence near Interplanetary Travelling Shocks. In: The Physics of Collisionless Shocks: 4th Annual IGPP International Astrophysics Conference, eds. G. Li, G. P. Zank, and C. T. Russell, *AIP Conference Proceedings*, vol. 781, pp. 129–134, AIP (2005c).

Kallenbach, R., M. Hilchenbach, S. V. Chalov, J. A. Le Roux, and K. Bamert: On the injection problem at the solar wind termination shock. Astron. & Astrophys. **439**, 1–22 (2005d), doi:10.1051/0004-6361:20052874.

Keiling, A., G. K. Parks, H. Rème, I. Dandouras, J. M. Bosqued, M. Wilber, M. McCarthy, C. Mouikis, E. Amata, B. Klecker, A. Korth, R. Lundin, and H. U. Frey: Bouncing ion clusters in the plasma sheet boundary layer observed by Cluster-CIS. J. Geophys. Res. **110**, A09207 (2005), doi:10.1029/2004JA010497.

Keller, H. U., L. Jorda, M. Küppers, P. J. Gutierrez, S. F. Hviid, J. Knollenberg, L.-M. Lara, H. Sierks, C. Barbieri, P. Lamy, H. Rickman, and R. Rodrigo: Deep Impact Observations by OSIRIS Onboard the Rosetta Spacecraft. Science **310**, 281–283 (2005), doi:10.1126/science.1119020.

Khomenko, E. V., M. J. Martinez Gonzalez, M. Collados, A. Vögler, S. K. Solanki, B. Ruiz Cobo, and C. Beck: Magnetic flux in the internetwork quiet Sun. Astron. & Astrophys. **436**, L27–L30 (2005a), doi:10.1051/0004-6361:200500114.

Khomenko, E. V., S. Shelyag, S. K. Solanki, and A. Vögler: Stokes diagnostics of simulations of magnetoconvection of mixed-polarity quiet-Sun regions. Astron. & Astrophys. **442**, 1059–1078 (2005b), doi:10.1051/0004-6361:20052958.

Kistler, L. M., C. Mouikis, E. Möbius, B. Klecker, J. A. Sauvaud, H. Rème, A. Korth, M. F. Marcucci, R. Lundin, G. K. Parks, and A. Balogh: Contribution of nonadiabatic ions to the cross-tail current in an O^+ dominated thin current sheet. J. Geophys. Res. **110**, A06213 (2005), doi:10.1029/2004JA010653.

Klecker, B., E. Moebius, M. A. Popecki, L. M. Kistler, H. Kucharek, and M. Hilchenbach: Ionic Charge States of Mg, Si and Fe in Fe-Rich Solar Energetic Particle Events. In: Proceedings of the Solar Wind 11/SOHO 16 Conference, 12-17 June 2005, Whistler, Canada, eds. B. Fleck and T. H. Zurbuchen, ESA SP-592, pp. 77–80 (2005).

Kramar, M.: A feasibility study of the use of vector tomography for the reconstruction of the coronal magnetic field. Doktorarbeit, Universität Göttingen (2005).

Kramar, M., B. Inhester, and S. K. Solanki: On the tomography reconstruction of the coronal magnetic field from coronal Hanle/Zeeman observations. In:

Proceedings of the International Scientific Conference on Chromospheric and Coronal Magnetic Fields, eds. D. Innes, A. Lagg, S. K. Solanki, and D. Danesy, ESA SP-596, ESA Publ. Div., Noordwijk (2005).

Krimigis, S. M., D. G. Mitchell, D. C. Hamilton, N. Krupp, S. Livi, E. C. Roelof, J. Dandouras, T. P. Armstrong, B. H. Mauk, C. Paranicas, P. C. Brandt, S. J. Bolton, A. F. Cheng, T. Choo, G. Gloeckler, J. Hayes, K. C. Hsieh, W.-H. Ip, S. Jaskulek, E. P. Keath, E. Kirsch, M. Kusterer, A. Lagg, L. J. Lanzerotti, D. LaVallee, J. Manweiler, R. W. McEntire, W. Rasmuss, J. Saur, F. S. Turner, D. J. Williams, and J. Woch: Dynamics of Saturn's Magnetosphere from the Magnetospheric Imaging Instrument During Cassini's Orbital Insertion. Science **307**, 1270–1273 (2005a), doi:10.1126/science.1105978.

Krimigis, S. M., D. G. Mitchell, D. C. Hamilton, N. Krupp, S. Livi, E. C. Roelof, J. Dandouras, B. H. Mauk, J. P. Brandt, C. Paranicas, J. Saur, T. P. Armsrong, S. Bolton, A. F. Cheng, G. Gloeckler, K. C. Hsieh, W.-H. Ip, A. Lagg, L. J. Lanzerotti, R. W. McEntire, and D. J. Williams: Overview of Results from the Cassini Magnetospheric Imaging Instrument (MIMI) During the First Year of Operations. In: 36th Annual Lunar and Planetary Science Conference, p. 1361 (2005b).

Krivova, N. A. and S. K. Solanki: Modelling of irradiance variations through atmosphere models. Memorie della Societa Astronomica Italiana **76**, 834–841 (2005a).

— Reconstruction of solar UV irradiance. Adv. Space Res. **35**, 361–364 (2005b), doi:10.1016/j.asr.2004.12.027.

Kronberg, E., J. Woch, N. Krupp, A. Lagg, K. K. Khurana, and K.-H. Glassmeier: Mass release at Jupiter: Substorm-like processes in the Jovian magnetotail. J. Geophys. Res. **110**, A03211 (2005), doi:10.1029/2004JA010777.

Krüger, H., R. J. Forsyth, A. L. Graps, and E. Grün: Electromagnetically interacting dust streams during Ulysses' Second Jupiter Encounter. In: New vistas in dusty plasmas, eds. L. Boufendi, M. Mikikian, and P. K. Shukla, *AIP conference proceedings*, vol. 799, pp. 157–160 (2005a).

Krüger, H., G. Linkert, D. Linkert, R. Moissl, and E. Grün: Galileo long-term dust monitoring in the Jovian magnetosphere. Planet. Space Sci. **53**, 1109–1120 (2005b), doi:10.1016/j.pss.2005.04.009.

Krupp, N.: Energetic particles in the magnetosphere of Saturn and a comparison with Jupiter. Space Sci. Rev. **116**, 345–369 (2005), doi:10.1007/s11214-005-1961-3.

Krupp, N., A. Lagg, J. Woch, S. M. Krimigis, S. Livi, D. G. Mitchell, E. C. Roelof, C. Paranicas, B. H. Mauk, D. C. Hamilton, T. P. Armstrong, and M. K. Dougherty: The Saturnian plasma sheet as revealed by energetic particle measurements. Geophys. Res. Lett. **32**, L20S03 (2005), doi:10.1029/2005GL022829.

Kuo, F. S. and J. Röttger: Horizontal wavelength of gravity waves in the lower atmosphere measured by the SOUSY Svalbard Radar. Chin. J. Phys. **43**, 464–480 (2005).

Küppers, M., I. Bertini, S. Fornasier, P. J. Gutierrez, S. F. Hviid, L. Jorda, H. U. Keller, J. Knollenberg, D. Koschny, R. Kramm, L.-M. Lara, H. Sierks, N. Thomas, C. Barbieri, P. Lamy, H. Rickman, R. Rodrigo, and the OSIRIS team: A large dust/ice ratio in the nucleus of comet 9P/Tempel 1 . Nature **437**, 987–990 (2005), doi:10.1038/nature04236.

Kuroda, T., N. Hashimoto, D. Sakai, and M. Takahashi: Simulation of the Martian atmosphere using a CCSR/NIES AGCM. J. Meteorol. Soc. Jpn. **83**, 1–19 (2005), doi:10.2151/jmsj.83.1.

Lagerkvist, C. I., L. Moroz, A. Nathues, A. Erikson, F. Lahulla, O. Karlsson, and M. Dahlgren: A study of Cybele asteroids — II. Spectral properties of Cybele asteroids. Astron. & Astrophys. **432**, 349–354 (2005), doi:10.1051/0004-6361:20041152.

Lagg, A.: Results from Chromospheric Magnetic Field Measurements. In: Proceedings of the International Scientific Conference "Chromospheric and Coronal Magnetic Fields", eds. D. E. Innes, A. Lagg, S. K. Solanki, and D. Danesy, ESA SP-596, ESA Publ. Div., Noordwijk (2005).

Lavraud, B., H. Rème, M. W. Dunlop, J.-M. Bosqued, I. Dandouras, J.-A. Sauvaud, A. Keiling, T. D. Phan, R. Lundin, P. J. Cargill, C. P. Escoubet, C. W. Carlson, J. P. McFadden, G. K. Parks, E. Möbius, L. M. Kistler, E. Amata, M.-B. Bavassano-Cattaneo, A. Korth, B. Klecker, and A. Balogh: Cluster observes the high-altitude cusp region. Surveys in Geophysics **26**, 135–175 (2005), doi:10.1007/s10712-005-1875-3.

Leitner, M., C. J. Farrugia, H. K. Biernat, R. Torbert, N. V. Erkaev, K. W. Ogilvie, and R. Schwenn: On the thickness of the sheath of magnetic clouds in the inner heliosphere: a Helios - Wind investigation. In: Connecting Sun And Heliosphere, Proceedings of the Conference Solar Wind 11 - SOHO 16, eds. B. Fleck and T. H. Zurbuchen, ESA SP-592, pp. 739 – 742 (2005a).

Leitner, M., C. J. Farrugia, V. A. Osherovich, J. Fainberg, H. K. Biernat, K. W. Ogilvie, R. Schwenn, and R. Torbert: The relative distribution of the magnetic and plasma kinetic energy densities in the inner heliosphere ($<$ 1 AU). In: Connecting Sun And Heliosphere, Proceedings of the Conference Solar Wind 11 - SOHO 16, eds. B. Fleck and T. H. Zurbuchen, ESA SP-592 (2005b).

Lemaire, P., C. Emerich, J.-C. Vial, W. Curdt, U. Schühle, and K. Wilhelm: Variation of the full Sun hydrogen Lyman profiles through solar cycle 23. Adv. Space Res. **35**, 384–387 (2005), doi: 10.1016/j.asr.2004.11.004.

Lorito, S., D. Schmitt, G. Consolini, and P. D. Michelis: Stochastic resonance in a bistable geodynamo model. Astronomische Nachrichten **326**, 227–230 (2005), doi:10.1002/asna.200410381.

Mahajan, R. A.: Modelling Martian Polar Caps. Doktorarbeit, Universität Göttingen (2005).

Maksimovic, M., I. Zouganelis, J.-Y. Chaufray, K. Issautier, E. E. Scime, J. E. Littleton, E. Marsch, D. J. McComas, C. Salem, R. P. Lin, and H. Elliott: Radial evolution of the electron distribution functions in the fast solar wind between 0.3 and 1.5 AU. J. Geophys. Res. **110**, A09104 (2005), doi: 10.1029/2005JA011119.

Marsch, E.: Importance of kinetic effects in heating the open and closed corona. In: Proceedings of the Solar Wind 11/SOHO 16 Conference, 12-17 June 2005, Whistler, Canada, eds. B. Fleck and T. H. Zurbuchen, ESA SP-592, pp. 191–198, ESA Publ. Div., Noordwijk (2005a).

— The relativistic energy spectrum of hydrogen. Annalen der Physik **14**, 324–343 (2005b), doi:10.1002/andp.200410137.

Marsch, E., R. Marsden, R. Harrison, R. Wimmer-Schweingruber, and B. Fleck: Solar Orbiter—mission profile, main goals and present status. Adv. Space Res. **36**, 1360–1366 (2005), doi:10.1016/j.asr.2004.11.012.

Marsden, S. C., S. V. Berdyugina, J. F. Donati, J. A. Eaton, M. H. Williamson, I. Ilyin, D. A. Fischer, M. Muñoz, H. Isaacson, M. I. Ratner, M. Semel, P. Petit, and B. D. Carter: A sun in the spectroscopic binary IM Pegasi, the guide star for the Gravity Probe B mission. Astrophys. J. **634**, L173–L176 (2005), doi:10.1086/498941.

Mauas, P. J. D., V. Andretta, A. Falchi, R. Falciani, L. Teriaca, and G. Cauzzi: Helium line formation and abundance in a solar active region. Astrophys. J. **619**, 604–612 (2005), doi:10.1086/426428.

Mauk, B. H., J. Saur, D. G. Mitchell, E. C. Roelof, P. C. Brandt, T. P. Armstrong, D. C. Hamilton, S. M. Krimigis, N. Krupp, S. A. Livi, J. W. Manweiler, and C. P. Paranicas: Energetic particle injections in Saturn's magnetosphere. Geophys. Res. Lett. **32**, L14S05 (2005), doi:10.1029/2005GL022485.

McKenzie, J. F., E. M. Dubinin, and K. Sauer: Relativistic whistler oscillitons - do they exist? Nonlin. Proc. Geophys. **12**, 425–431 (2005).

McKenzie, J. F. and T. Hagfors: Parametric resonances revisited: comparison with kinetic description. J. Plasma Phys. **71**, 579–587 (2005), doi: 10.1017/S0022377804003381.

Mecheri, R. and E. Marsch: Beam-instabilities in a coronal funnel within the multi-fluid description. In: Proceedings of the 11th European Solar Physics Meeting — The Dynamic Sun: Challenges for Theory and Observations, 11-16 September 2005, eds. D. Danesy, S. Poedts, A. De Groof, and J. Andries, ESA SP-600, ESA Publ. Div., Noordwijk (2005a), on CD.

— Coronal waves: propagation in the multi-fluid description. In: Discussion Meeting Issue "MHD waves and oscillations in the solar plasma", The Royal Society, London, UK (2005b), doi:10.1098/rsta.2005.1716.

Meech, K. J., N. Ageorges, M. F. A'Hearn, C. Arpigny, A. Ates, J. Aycock, S. Bagnulo, J. Bailey, R. Barber, L. Barrera, R. Barrena, J. M. Bauer, M. J. S. Belton, F. Bensch, B. Bhattacharya, N. Biver, G. Blake, D. Bocklee-Morvan, H. Boehnhardt, B. P. Bonev, T. Bonev, et al.: Deep Impact: Observations from a worldwide Earth-based campaign. Science **310**, 265–269 (2005), doi:10.1126/science.1118978.

Mendoza-Torres, J. E., J. P. Torres-Papqui, and K. Wilhelm: Explosive events in the solar atmosphere seen in extreme-ultraviolet emission lines. Astron. & Astrophys. **431**, 339–344 (2005), doi:10.1051/0004-6361:20041299.

Mierla, M., R. Schwenn, L. Teriaca, G. Stenborg, and B. Podlipnik: Using LASCO-C1 spectroscopy for coronal diagnostics. Adv. Space Res. **35**, 2199–2203 (2005), doi:10.1016/j.asr.2005.04.031.

Mierla, M. C.: On the Dynamics of the Solar Corona. Doktorarbeit, Universität Göttingen (2005).

Mitchell, D. G., P. C. Brandt, E. C. Roelof, J. Dandouras, S. M. Krimigis, B. H. Mauk, C. P. Paranicas, N. Krupp, D. C. Hamilton, W. S. Kurth, P. Zarka, M. K. Dougherty, E. J. Bunce, and

D. E. Shemansky: Energetic ion acceleration in Saturn's magnetotail: Substorms at Saturn? Geophys. Res. Lett. **32**, L20S01 (2005), doi:10.1029/2005GL022647.

Modolo, R., G. M. Chanteur, E. Dubinin, and A. P. Matthews: Influence of the solar EUV flux on the Martian plasma environment. Ann. Geophys. **23**, 433–444 (2005).

Mühlbachler, S., C. J. Farrugia, J. Raeder, H. K. Biernat, and R. B. Torbert: A statistical investigation of dayside magnetosphere erosion showing saturation of response. J. Geophys. Res. **110**, A11207 (2005), doi:10.1029/2005JA011177.

Murray, J. B., J.-P. Muller, G. Neukum, S. C. Werner, E. Hauber, W. J. Markiewicz, J. W. Head, III, B. H. Foing, D. Page, K. L. Mitchell, G. Portyankina, and the HRSC Co-Investigator Team: Evidence from HRSC Mars Express for a frozen sea close to Mars' equator. In: Proceedings of the 36th Annual Lunar and Planetary Science Conference, March 14-18, 2005, League City, Texas, 1741 (2005a).

— Evidence from the Mars Express High Resolution Stereo Camera for a frozen sea close to Mars' equator. Nature **434**, 352–356 (2005b), doi:10.1038/nature03379.

Mursula, K., R. Kerttula, T. Asikainen, R. Friedel, A. Vaivads, F. Søraas, M. Grande, M. Carter, P. W. Daly, T. A. Fritz, J. F. Fennell, and A. Balogh: Cluster/RAPID energetic electron observations at the dayside magnetospheric boundary. Adv. Space Res. **36**, 1904–1908 (2005), doi:10.1016/j.asr.2004.03.021.

Nathues, A., S. Mottola, M. Kaasalainen, and G. Neukum: Spectral study of the Eunomia asteroid family—I. Eunomia. Icarus **175**, 452–463 (2005), doi:10.1016/j.icarus.2004.12.013.

Ning, Z. J. and M. D. Ding: Chromospheric Internetwork Oscillations at Various Locations of the Quiet Sun. Chinese Journal of Astronomy & Astrophysics **5**, 273–284 (2005).

Orozco Suarez, D., A. Lagg, and S. K. Solanki: Photospheric and chromospheric magnetic structure of a sunspot. In: Proceedings of the International Scientific Conference on Chromospheric and Coronal Magnetic Fields, eds. D. E. Innes, A. Lagg, S. K. Solanki, and D. Danesy, ESA SP-596, ESA Publ. Div., Noordwijk (2005).

Paranicas, C., D. G. Mitchell, S. Livi, S. M. Krimigis, E. Roussos, N. Krupp, J. Woch, A. Lagg, J. Saur, and F. S. Turner: Evidence of Enceladus and Tethys microsignatures. Geophys. Res. Lett. **32**, L20101 (2005), doi:10.1029/2005GL024072.

Petit, P., J. F. Donati, M. Auriere, J. D. Landstreet, F. Lignieres, S. Marsden, D. Mouillet, F. Paletou, N. Toque, and G. A. Wade: Large-scale magnetic field of the G8 dwarf ξ Bootis A. Mon. Not. Roy. Astron. Soc. **361**, 837–849 (2005a), doi:10.1111/j.1365-2966.2005.09207.x.

Petit, P., J.-F. Donati, M. Jardine, and A. Collier Cameron: Prominence mapping of the RS CVn system HR 1099. In: Coronal and Stellar Mass Ejections, IAU Symposium Proceedings of the International Astronomical Union No. 226, eds. K. Dere, J. Wang, and Y. Yan, pp. 511–512, IAU, Cambridge University Press (2005b), doi:10.1017/S1743921305001158.

Picardi, G., P. J. Jeffrey, D. Biccari, O. Bombaci, D. Calabrese, M. Cartacci, A. Cicchetti, S. M. Clifford, P. Edenhofer, W. M. Farrell, C. Federico, A. Frigeri, D. A. Gurnett, T. Hagfors, E. Heggy, A. Herique, R. L. Huff, A. B. Ivanov, W. T. K. Johnson, R. L. Jordan, D. L. Kirchner, W. Kofman, C. J. Leuschen, E. Niesen, R. Orosei, E. Pettinelli, R. J. Phillips, D. Plettemeier, A. Safaeinili, R. Seu, E. R. Stofan, G. Vannaroni, T. R. Watters, and E. Zampolini: Radar soundings of the subsurface of Mars. Science **310**, 1925–1928 (2005), doi:10.1126/science.1122165.

Popescu, M. D., D. Banerjee, E. O'Shea, J. G. Doyle, and L. D. Xia: Very long period activity at the base of solar wind streams. Astron. & Astrophys. **442**, 1087–1090 (2005), doi:10.1051/0004-6361:20053714.

Portyankina, G.: Atmosphere-surface vapor exchange and ices in the Martian polar regions. Doktorarbeit, Universität Göttingen (2005).

Preuss, O., S. Jordan, M. P. Haugan, and S. K. Solanki: Constraining gravitational theories by observing magnetic white dwarfs. In: 14th European Workshop on White Dwarfs, eds. D. Koester and S. Moehler, *Astron. Soc. Pacific Conf. Ser.*, vol. 334, pp. 265–268 (2005).

Preuss, O., S. K. Solanki, M. P. Haugan, and S. Jordan: Gravity-induced birefringence within the framework of Poincaré gauge theory. Phys. Rev. D **72**, 042 001 (2005), doi:10.1103/PhysRevD.72.042001.

Preusse, S.: Szenarien der Plasmawechselwirkung in kurzperiodischen extrasolaren Planetensystemen. Doktorarbeit, Technische Universität Braunschweig (2005).

Preusse, S., A. Kopp, J. Büchner, and U. Motschmann: Magnetic communication scenarios for close-in extrasolar planets. In: Status and prospects for hot Jupiter studies, Haute Provence Observatory Colloquium, August 22-25, 2005, pp. 1–8 (2005a).

Preusse, S., A. Kopp, J. Büchner, and U. Motschmann: Stellar wind regimes of close-in extrasolar planets. Astron. & Astrophys. **434**, 1191–1200 (2005b), doi: 10.1051/0004-6361:20041680.

Pryor, W. R., A. Ian, F. Stewart, L. W. Esposito, W. E. McClintock, J. E. Colwell, A. J. Jouchoux, A. J. Steffl, D. E. Shemansky, J. M. Ajello, R. A. West, C. J. Hansen, B. T. Tsurutani, W. S. Kurth, G. B. Hospodarsky, D. A. Gurnett, K. C. Hansen, J. H. Waite, Jr., F. J. Crary, D. T. Young, N. Krupp, J. T. Clarke, D. Grodent, and M. K. Dougherty: Cassini UVIS observations of Jupiter's auroral variability. Icarus **178**, 312–326 (2005), doi:10.1016/j.icarus. 2005.05.021.

Pu, Z. Y., Q.-G. Zong, T. A. Fritz, C. J. Xiao, Z. Y. Huang, S. Y. Fu, Q. Q. Shi, M. W. Dunlop, K.-H. Glassmeier, A. Balogh, P. Daly, H. Rème, J. Dandouras, J. B. Cao, Z. X. Liu, C. Shen, and J. K. Shi: Multiple Flux Rope Events at the High-Latitude Magnetopause: Cluster/RAPID Observation on 26 January, 2001. Surveys in Geophysics **26**, 193–214 (2005), doi:10.1007/s10712-005-1878-0.

Radioti, A., N. Krupp, J. Woch, A. Lagg, K.-H. Glassmeier, and L. Waldrop: Ion abundance ratios in the Jovian magnetosphere. J. Geophys. Res. **110**, A07225 (2005), doi:10.1029/2004JA010775.

Raouafi, N.-E., S. Manusco, S. K. Solanki, B. Inhester, M. Mierla, G. Stenborg, J. P. Delaboudinière, and C. Benna: Shock wave driven by an expanding system of loops. In: Coronal and Stellar Mass Ejections, Proc. IAU Symp. 226, eds. K. P. Dere, J. Wang, and Y. Yan, pp. 127–128, Cambridge University Press (2005), doi:10.1017/ S1743921305000323.

Rème, H., I. Dandouras, C. Aoustin, J. M. Bosqued, J. A. Sauvaud, C. Vallat, P. Escoubet, J. B. Cao, J. Shi, M. B. Bavassano-Cattaneo, G. K. Parks, C. W. Carlson, Z. Pu, B. Klecker, E. Moebius, L. Kistler, A. Korth, and R. Lundin: The HIA instrument on board the Tan Ce 1 Double Star near-equatorial spacecraft and its first results. Ann. Geophys. **23**, 2757–2774 (2005).

Retinò, A., M. B. Bavassano-Cattaneo, M. F. Marcucci, A. Vaivads, M. André, Y. Khotyaintsev, T. Phan, G. Pallocchia, H. Rème, E. Möbius, B. Klecker, C. W. Carlson, M. McCarthy, A. Korth, R. Lundin, and A. Balogh: Cluster multispacecraft observations at the high-latitude duskside magnetopause: implications for continuous and component magnetic reconnection. Ann. Geophys. **23**, 461–473 (2005).

Rodriguez, L., J. Woch, N. Krupp, M. Fränz, R. von Steiger, C. Cid, R. Forsyth, and K.-H. Glaßmeier: Bidirectional proton flows and comparison of freezing-in temperatures in ICMEs and magnetic clouds. In: Coronal and Stellar Mass Ejections, IAU Symposium Proceedings of the International Astronomical Union No. 226, eds. K. Dere, J. Wang, and Y. Yan, pp. 420–427, IAU, Cambridge University Press (2005), doi:10.1017/S1743921305000967.

Romboli, L. R.: Internal characteristics of magnetic clouds and interplanetary coronal mass ejections. Doktorarbeit, TU Braunschweig (2005).

Rosenbush, V. K., N. N. Kiselev, V. G. Shevchenko, K. Jockers, N. M. Shakhovskoy, and Y. S. Efimov: Polarization and brightness opposition effects for the E-type Asteroid 64 Angelina. Icarus **178**, 222–234 (2005), doi:10.1016/j.icarus.2005.04.008.

Roussos, E., N. Krupp, J. Woch, A. Lagg, G. H. Jones, C. Paranicas, D. G. Mitchell, S. Livi, S. M. Krimigis, M. K. Dougherty, T. Armstrong, W.-H. Ip, and U. Motschmann: Low energy electron microsignatures at the orbit of Tethys: Cassini MIMI/LEMMS observations. Geophys. Res. Lett. **32**, L24107 (2005), doi:10.1029/2005GL024084.

Ruan, P., S. Y. Fu, Q.-G. Zong, Z. Y. Pu, X. Cao, W. L. Liu, X. Z. Zhou, and P. W. Daly: Ion composition variations in the plasma sheet observed by Cluster/RAPID. Geophys. Res. Lett. **32**, L01105 (2005), doi:10.1029/2004GL021266.

Ryabchikova, T., G. A. Wade, M. Auriere, S. Bagnulo, J. F. Donati, S. V. Jeffers, N. Johnson, J. D. Landstreet, F. Lignieres, T. Lueftinger, S. Marsden, D. Mouillet, F. Paletou, P. Petit, P. Reegen, J. Silvester, S. Strasser, and N. Toque: Rotational periods of four roAp stars. Astron. & Astrophys. **429**, L55–L58 (2005), doi:10.1051/0004-6361:200400112.

Sasso, C., A. Lagg, and S. K. Solanki: Influence of the Paschen-Back effect on the Stokes profiles of the HE 10830 Å triplet. In: Proceedings of the International Scientific Conference on Chromospheric and Coronal Magnetic Fields, eds. D. E. Innes, A. Lagg, S. K. Solanki, and D. Danesy, ESA SP-596, ESA Publ. Div., Noordwijk (2005).

Sauer, K., M. Fränz, E. Dubinin, C. Mazelle, A. Korth, H. Rème, I. Dandouras, and K.-H. Glassmeier: Upstream gyrating ion events: Cluster observations and simulations. In: The Physics of Collisionless

Shocks, *AIP Conference Proceedings*, vol. 781, pp. 146–150 (2005).

Savin, S., A. Skalsky, L. Zelenyi, L. Avanov, N. Borodkova, S. Klimov, V. Lutsenko, E. Panov, S. Romanov, V. Smirnov, Yu. Yermolaev, P. Song, E. Amata, G. Consolini, T. A. Fritz, J. Büchner, B. Nikutowski, J. Blecki, C. Farrugia, N. Maynard, J. Pickett, J. A. Sauvaud, J. L. Rauch, J. G. Trotignon, Y. Khotyaintsev, and K. Stasiewicz: Magnetosheath Interaction with the High Latitude Magnetopause. Surveys in Geophysics **26**, 95–133 (2005a), doi: 10.1007/s10712-005-1874-4.

Savin, S., L. Zelenyi, E. Amata, J. Büchner, B. Nikutowski, and E. Panov: Magnetosheath interaction with high latitude magnetopause: dynamic flow chaotization. Planet. Space Sci. **53**, 133–140 (2005b), doi:10.1016/j.pss.2004.09.037.

Schlegel, K.: Space Weather effects in the upper atmosphere: High latitudes. In: Space Weather: The Physics behind a slogan, eds. K. Scherer, H. Fichtner, B. Heber, and U. Mall, Lecture Notes in Physics, Springer, Berlin, Heidelberg (2005).

Schlegel, K., H. Lühr, J.-P. St.-Maurice, G. Crowley, and C. Hackert: Thermospheric density structures over the polar reagions observed with CHAMP. Ann. Geophys. **23**, 1659–1672 (2005).

Schmitt, D.: Origin of solar magnetic variability. Memorie della Societa Astronomica Italiana **76**, 773–780 (2005).

Schrinner, M.: Mean-field view on geodynamo models. Doktorarbeit, Universität Göttingen (2005), summa cum laude.

Schrinner, M., K.-H. Rädler, D. Schmitt, M. Rheinhardt, and U. Christensen: Mean-field view on magnetoconvection and dynamo models. In: Proceedings of the Joint 15th Riga and 6th pamir International Conference, vol. I, pp. 85–88 (2005a).

Schrinner, M., K.-H. Rädler, D. Schmitt, M. Rheinhardt, and U. Christensen: Mean-field view on rotating magnetoconvection and a geodynamo model. Astronomische Nachrichten **326**, 245–249 (2005b), doi:10.1002/asna.200410384.

Schüssler, M.: Flux tubes, surface magnetism, and the solar dynamo: constraints and open problems. Astron. Nachr./AN **326**, 194–204 (2005a), doi:10.1002/asna.200410376.

— Is there a phase constraint for solar dynamo models? Astron. & Astrophys. **439**, 749–750 (2005b), doi:10.1051/0004-6361:20053459.

— The Sun and its restless magnetic field. In: Space weather: the physics behind a slogan, eds. K. Scherer, H. Fichtner, B. Heber, and U. Mall, pp. 23–50, Springer, Berlin/Heidelberg/New York (2005c).

Schüssler, M., J. H. M. J. Bruls, A. Vögler, and P. Vollmöller: Simulation of solar radiative magneto-convection. In: Analysis and Numerics for Conservation Laws, ed. G. Warnecke, pp. 107–136, Springer Verlag, Berlin (2005).

Schüssler, M. and M. Rempel: The dynamical disconnection of sunspots from their magnetic roots. Astron. & Astrophys. **441**, 337–346 (2005), doi: 10.1051/0004-6361:20052962.

Schwenn, R.: Solar Wind and Interplanetary Magnetic Field. In: Geophysics and Geochemistry, from Encyclopedia of Life Support Systems (EOLSS), Eolss Publishers, Oxford, UK (2005a).

— What have we learned with SOHO. In: Coronal and Stellar Mass Ejections, IAU Symposium Proceedings of the International Astronomical Union No. 226, eds. K. Dere, J. Wang, and Y. Yan, pp. 19–20, IAU, Cambridge University Press (2005b), doi:10.1017/S1743921305001158.

Schwenn, R., A. Dal Lago, E. Huttunen, and W. D. Gonzalez: The association of coronal mass ejections with their effects near the Earth. Ann. Geophys. **23**, 1033–1059 (2005).

Segschneider, J., B. Grieger, H. U. Keller, F. Lunkeit, E. Kirk, K. Fraedrich, A. Rodin, and R. Greve: Response of the intermediate complexity Mars Climate Simulator to different obliquity angles. Planet. Space Sci. **53**, 659–670 (2005), doi:10.1016/j.pss.2004.10.003.

Seidelmann, P. K., B. A. Archinal, M. F. A'Hearn, D. P. Cruikshank, J. L. Hilton, H. U. Keller, J. Oberst, J. L. Simon, P. Stooke, D. J. Tholen, and P. C. Thomas: Report of the IAU/IAG Working Group on Cartographic Coordinates and Rotational Elements: 2003. Celest. Mech. Dyn. Astron. **91**, 203–215 (2005), doi:10.1007/s10569-004-3115-4.

Selwa, M., K. Murawski, and S. K. Solanki: Excitation and damping of slow magnetosonic standing waves in a solar coronal loop. Astron. & Astrophys. **436**, 701–709 (2005a), doi:10.1051/0004-6361:20042319.

Selwa, M., K. Murawski, S. K. Solanki, T. J. . Wang, and G. Tóth: Numerical simulations of vertical oscillations of a solar coronal loop. Astron. & Astrophys. **440**, 385–390 (2005b), doi:10.1051/0004-6361:20053121.

Selwa, M., K. Murawski, S. K. Solanki, T. J. Wang, and U. Shumlak: Impulsive generation of vertical oscillations of a solar coronal arcade loop. In: Proceedings of the International Scientific Conference on Chromospheric and Coronal Magnetic Fields, eds. D. E. Innes, A. Lagg, S. K. Solanki, and D. Danesy, ESA SP-596, ESA Publ. Div., Noordwijk (2005c).

Shkuratov, Y. G. and Y. S. Grynko: Light scattering by media composed of semitransparent particles of different shapes in ray optics approximation: consequences for spectroscopy, photometry, and polarimetry of planetary regoliths. Icarus **173**, 16–28 (2005), doi:10.1016/j.icarus.2003.12.022.

Silin, I. and J. Büchner: Small-scale reconnection due to lower-hybrid drift instability in current sheets with sheared fields. Phys. Plasmas **12**, 012320 (2005), doi:10.1063/1.1830015.

Silin, I., J. Büchner, and A. Vaivads: Anomalous resistivity due to nonlinear lower-hybrid drift waves. Phys. Plasmas **12**, 062902 (2005), doi:10.1063/1.1927096.

Sokolskaya, N. V., J. H. Adams, H. S. Ahn, K. E. Batkov, G. L. Bashindzhagyan, J. Z. Wang, J. P. Wefel, J. Wu, O. Ganel, T. G. Guzik, R. M. Gunasingha, V. I. Zatsepin, J. Isbert, K. C. Kim, M. Christl, E. N. Kouznetsov, M. I. Panasyuk, A. D. Panov, E. S. Seo, A. R. Fazely, J. Chang, and W. K. H. Schmidt: Albedo in the ATIC experiment: Measurements and simulations. Phys. Atom. Nuclei **68**, 1176–1182 (2005), doi:10.1134/1.1992573.

Solanki, S. K.: Wie stark beeinflusst die Sonne das Klima und den derzeitigen Klimawandel? In: Klimawandel im 20. und 21. Jahrhundert, ed. B. A. der Wissenschaften, *Rundgespräche der Kommission für Ökologie*, vol. 28, pp. 111–121, Verlag Dr. Friedrich Pfeil, München (2005).

Solanki, S. K., N. A. Krivova, and T. Wenzler: Irradiance models. Adv. Space Res. **35**, 376–383 (2005a), doi:10.1016/j.asr.2004.12.077.

Solanki, S. K. and M. Schüssler: Mechanisms of secular magnetic field variations. Mem. S.A.It. **76**, 781–788 (2005).

Solanki, S. K. and M. Schüssler: Small-scale solar magnetic elements: simulations and observations. In: The Solar-B Mission and the Forefront of Solar Physics, eds. T. Sakurai and T. Sekii, *ASP Conference Series*, vol. 325, pp. 105–114, Astronomical Society of the Pacific, San Francisco (2005).

Solanki, S. K., I. G. Usoskin, B. Kromer, M. Schüssler, and J. Beer: How unusual is today's solar activity? (reply). Nature **436**, E4–E5 (2005b), doi:10.1038/nature04046.

Song, P., V. M. Vasyliūnas, and L. Ma: A three-fluid model of solar wind-magnetosphere-ionosphere-thermosphere coupling. In: Multiscale Coupling of Sun-Earth Processes, eds. A. T. Y. Lui, Y. Kamide, and G. Consolini, pp. 447–456, Elsevier, Amsterdam, The Netherlands (2005a).

— Solar wind-magnetosphere-ionosphere coupling: Neutral atmosphere effects on signal propagation. J. Geophys. Res. **110**, A09309 (2005b), doi:10.1029/2005JA011139.

Sonnemann, G. R., P. Hartogh, and M. Grygalashvyly: Nonlinear response of the ozone chemistry within the stratopause and mesopause region under realistic conditions. In: Proc. Int. Symp.: Topical Problems of Nonlinear wave Physics, NWP-2005 (2005).

Sremcevic, M., A. V. Krivov, H. Krüger, and F. Spahn: Impact-generated dust clouds around planetary satellites: model versus Galileo data. Planet. Space Sci. **53**, 625–641 (2005), doi:10.1016/j.pss.2004.10.001.

Stenzel, O. J. and J. S. von Storch: The effect of orography on the global atmospheric angular momentum and the general circulation. Meteorol. Zeitschrift **14**, 387–393 (2005).

Teriaca, L., U. Schühle, S. K. Solanki, W. Curdt, and E. Marsch: The dynamics of the lower transition region as inferred from the hydrogen Lyman-α line radiance. In: Proceedings of the 11th European Solar Physics Meeting — The Dynamic Sun: Challenges for Theory and Observations, 11-16 September 2005, eds. D. Danesy, S. Poedts, A. De Groof, and J. Andries, ESA SP-600, ESA Publ. Div., Noordwijk (2005a), on CD.

Teriaca, L., U. Schühle, S. K. Solanki, W. Curdt, and E. Marsch: The structure of the lower transition region as inferred from the hydrogen Lyman-α line radiance. In: Proceedings of the International Scientific Conference on Chromospheric and Coronal Magnetic Fields, eds. D. E. Innes, A. Lagg, S. K. Solanki, and D. Danesy, ESA SP-596, ESA Publ. Div., Noordwijk (2005b).

Thomas, N., W. Baumjohann, V. Dehant, E. Chassefiere, F. Leblanc, P. Drossart, E. Lellouch, E. Kallio, H. Boehnhardt, B. Grieger, P. Hartogh, H. Krueger, N. Krupp, W. Markiewicz, J. Woch, K.-H. Glassmeier, J. Oberst, T. Spohn, C. Barbieri, G. Cremonese, G.-P. Tozzi, A. Coradini, S. Orsini, D. Stam, M. Roos-Serote, R. Rodrigo, J. Lopez-Moreno, L. Lara, A. Sáchez-Lavega, J. Rojas, R. Hueso, E. García-Melendo, S. Perez-Hoyos, *S. Baeza, J. Arregui, J. Legarreta, S. Barabash, J.-E. Wahlund, M. Andre, L. Blomberg, K. Altwegg, K. Gunderson, J. Horner, K. Seiferlin, P. Wurz, M. Dougherty, M. Grande, F. W. Taylor, P. Read, P. Irwin, I. P. Wright, H. Rucker, and P. Louarn*: A multi-disciplinary investigation of the Jovian system. In: Proceedings of the 39th ESLAB Symposium, Trends in Space Science and Cosmic Vision 2020, ed. A. G. F. Favata, J. Sanz-Forcada, ESA SP-588, pp. 225–231, ESA Publ. Div., Noordwijk (2005).

Tomás, A. T. M.: Energetic particles in the Jovian magnetosphere and their relation to auroral emissions. Doktorarbeit, TU Braunschweig (2005).

Tomasko, M. G., A. Archinal, T. Becker, B. Bezard, M. Bushroe, M. Combes, D. Cook, A. Coustenis, C. de Bergh, L. E. Dafoe, L. Doose, S. Doute, A. Eibl, S. Engel, F. Gliem, B. Grieger, K. Holso, E. Howington-Kraus, E. Karkoschka, H. U. Keller, R. Kirk, R. Kramm, M. Küppers, P. Lanagan, E. Lellouch, M. Lemmon, J. Lunine, E. McFarlane, J. Moores, G. M. Prout, B. Rizk, M. Rosiek, P. Rueffer, S. E. Schröder, B. Schmitt, C. See, P. Smith, L. Soderblom, N. Thomas, and R. West: Rain, winds and haze during Huygens probe's descent to Titan's surface. Nature **438**, 765–778 (2005), doi: 10.1038/nature04126.

Tomasz, F., J. Rybak, A. Kucera, W. Curdt, and H. Wöhl: Influence of transition region blinker on the surrounding chromospheric and coronal plasma. Hvar Obs. Bull. **29**, 197–204 (2005).

Tortorella, D. A.: Numerical studies of thermal and compressible convection in rotating spherical shells: an application to the giant planets. Doktorarbeit, Universität Göttingen (2005).

Trattner, K. J., S. A. Fuselier, T. K. Yeoman, C. Carlson, W. K. Peterson, A. Korth, H. Rème, J. A. Sauvaud, and N. Dubouloz: Spatial and temporal cusp structures observed by multiple spacecraft and ground based observations. Surveys in Geophysics **26**, 281–305 (2005), doi:10.1007/s10712-005-1883-3.

Tripathi, D., V. Bothmer, S. K. Solanki, R. Schwenn, M. Mierla, and G. Stenborg: SOHO/EIT observation of a coronal inflow. In: Coronal and Stellar Mass Ejections, Proc. IAU Symp. 226, eds. K. P. Dere, J. Wang, and Y. Yan, pp. 133–134, Cambridge University Press, Cambridge (2005), doi: 10.1017/S1743921305000359.

Tripathi, D. K.: EUV and coronagraphic observations of coronal mass ejections. Doktorarbeit, Universität Göttingen (2005).

Tu, C.-Y., C. Zhou, E. Marsch, K. Wilhelm, L.-D. Xia, L. Zhao, and J.-X. Wang: The height of solar wind origin in coronal funnels and a 3-D scenario for solar wind formation. In: Proceedings of the Solar Wind 11/SOHO 16 Conference, 12-17 June 2005, Whistler, Canada, eds. B. Fleck and T. H. Zurbuchen, ESA SP-592, pp. 131–134, ESA Publ. Div., Noordwijk (2005a).

Tu, C.-Y., C. Zhou, E. Marsch, K. Wilhelm, L. Zhao, L.-D. Xia, and J.-X. Wang: Correlation heights of the sources of solar ultraviolet emission lines in a quiet-sun region. Astrophys. J. **624**, L133–L136 (2005b), doi:10.1086/430520.

Tu, C.-Y., C. Zhou, E. Marsch, L.-D. Xia, L. Zhao, J.-X. Wang, and K. Wilhelm: Solar wind origin in coronal funnels. Science **308**, 519–523 (2005c), doi: 10.1126/science.1109447.

Ugarte-Urra, I., J. G. Doyle, R. W. Walsh, and M. S. Madjarska: Electron density along a coronal loop observed with CDS/SOHO. Astron. & Astrophys. **439**, 351–359 (2005), doi:10.1051/0004-6361:20042560.

Usoskin, I. G., M. Schüssler, S. K. Solanki, and K. Mursula: Solar activity, cosmic rays and Earth's temperature: A millenium-scale comparison. J. Geophys. Res. **110**, A10 102 (2005a), doi:10.1029/2004JA010946.

— Solar activity over the last 1150 years: does it correlate with climate? In: Proc. The 13th Cambridge Workshop on Cool Stars, Stellar Systems and the Sun, eds. F. Favata, G. A. J. Hussain, and B. Battrick, ESA SP-560, pp. 19–22, ESA Publ. Div., Noordwijk (2005b).

Uspensky, M., A. Koustov, V. Sofieva, O. Amm, K. Kauristie, W. Schmidt, E. Nielsen, T. Pulkkinen, R. Pellinen, S. Milan, and R. Pirjola: Multipulse and double-pulse velocities of Scandinavian Twin Auroral Radar Experiment (STARE) echoes. Radio Sci. **40**, RS3008 (2005), doi:10.1029/2004RS003151.

Vainchtein, D. L., J. Büchner, A. I. Neishtadt, and L. M. Zelenyi: Quasiadiabatic description of nonlinear particle dynamics in typical magnetotail configurations. Nonlin. Proc. Geophys. **12**, 101–115 (2005).

Vasyliūnas, V. M.: Relation between magnetic fields and electric currents in plasma. Ann. Geophys. **23**, 2589–2597 (2005a).

— Time evolution of electric fields and currents and the generalized Ohm's law. Ann. Geophys. **23**, 1347–1354 (2005b).

Vasyliūnas, V. M. and P. Song: Meaning of ionospheric Joule heating. J. Geophys. Res. **110**, A02301 (2005), doi:10.1029/2004JA010615.

Villanueva, G. and P. Hartogh: The high resolution chirp transform spectrometer for the SOFIA-GREAT instrument. Experimental Astronomy pp. 225–231 (2005), doi:10.1007/s10686-005-9004-3.

Vogiatzis, I. I., T. A. Fritz, Q.-G. Zong, D. N. Baker, E. T. Sarris, and P. W. Daly: Fine-time energetic electron behavior observed by Cluster/RAPID in the magnetotail associated with X-line formation and subsequent current disruption. Ann. Geophys. **23**, 2265–2280 (2005).

Vögler, A.: On the effect of photospheric magnetic fields on solar surface brightness: Results of radiative MHD simulations. Memorie della Societa Astronomica Italiana **76**, 842–849 (2005).

Vögler, A., S. Shelyag, M. Schüssler, F. Cattaneo, T. Emonet, and T. Linde: Simulations of magneto-convection in the solar photosphere: Equations, methods and results of the MURaM code. Astron. & Astrophys. **429**, 335–351 (2005), doi:10.1051/0004-6361:20041507.

Waldrop, L. S., T. A. Fritz, M. G. Kivelson, K. Khurana, N. Krupp, and A. Lagg: Jovian plasma sheet morphology: particle and field observations by the Galileo spacecraft. Planet. Space Sci. **53**, 681–692 (2005), doi:10.1016/j.pss.2004.11.003.

Wang, T. J., S. K. Solanki, D. E. Innes, and W. Curdt: Initiation of hot coronal loop oscillations: Spectral features. Astron. & Astrophys. **435**, 753–764 (2005), doi:10.1051/0004-6361:20052680.

Webb, G. M., J. F. McKenzie, E. Dubinin, and K. Sauer: Hamiltonian approach to nonlinear travelling whistler waves. In: The Physics of collisionless shocks, eds. G. Li, G. Zank, and C. T. Russell, 4th Annual IGPP International Astrophysics Conference, p. 141, Palm Springs, USA (2005a).

Webb, G. M., J. F. McKenzie, E. M. Dubinin, and K. Sauer: Hamiltonian formulation of nonlinear travelling Whistler waves. Nonlin. Proc. Geophys. **12**, 643–660 (2005b).

Wenzler, T., S. K. Solanki, and N. A. Krivova: Can surface magnetic fields reproduce solar irradiance variations in cycles 22 and 23? Astron. & Astrophys. **432**, 1057–1061 (2005), doi:10.1051/0004-6361:20041956.

Wicht, J.: Palaeomagnetic interpretation of dynamo simulations. Geophys. J. Int. **162**, 371–380 (2005), doi:10.1111/j.1365-246X.2005.02665.x.

Wicht, J. and J. Aubert: Dynamos in Action. GWDG-Bericht **68**, 49–66 (2005).

Wiegelmann, T.: Non-Linear Force-Free Magnetic Fields. In: Proceedings of the International Scientific Conference on Chromospheric and Coronal Magnetic Fields, eds. D. E. Innes, A. Lagg, S. K. Solanki, and D. Danesy, ESA SP-596, ESA Publ. Div., Noordwijk (2005).

Wiegelmann, T., B. Inhester, A. Lagg, and S. K. Solanki: How to use magnetic field information for coronal loop identification. Solar Phys. **228**, 67–78 (2005a), doi:10.1007/s11207-005-2511-6.

Wiegelmann, T., A. Lagg, S. K. Solanki, B. Inhester, and J. Woch: Comparing magnetic field extrapolations with measurements of magnetic loops. Astron. & Astrophys. **433**, 701–705 (2005b), doi:10.1051/0004-6361:20042421.

— Magnetic loops: A comparison of extrapolations from the photosphere with chromospheric measurements. In: Proceedings of the International Scientific Conference on Chromospheric and Coronal Magnetic Fields, eds. D. E. Innes, A. Lagg, S. K. Solanki, and D. Danesy, ESA SP-596, ESA Publ. Div., Noordwijk (2005c).

Wiegelmann, T., L. D. Xia, and E. Marsch: Links between magnetic fields and plasma flows in a coronal hole. Astron. & Astrophys. **432**, L1–L4 (2005d), doi:10.1051/0004-6361:200500029.

Wild, J. A., S. E. Milan, S. W. H. Cowley, J. M. Bosqued, H. Rème, T. Nagai, S. Kokubun, Y. Saito, T. Mukai, J. A. Davies, B. M. A. Cooling, A. Balogh, and P. W. Daly: Simultaneous in-situ observations of the signatures of dayside reconnection at the high- and low-latitude magnetopause. Ann. Geophys. **23**, 445–460 (2005).

Wilhelm, K., A. Fludra, L. Teriaca, R. A. Harrison, B. N. Dwivedi, and C. D. Pike: The widths of vacuum-ultraviolet spectral lines in the equatorial solar corona observed with CDS and SUMER. Astron. & Astrophys. **435**, 733–741 (2005a), doi:10.1051/0004-6361:20042460.

Wilhelm, K., U. Schühle, W. Curdt, M. Hilchenbach, E. Marsch, P. Lemaire, J.-L. Bertaux, S. D. Jordan, and U. Feldman: On the nature of the unidentified solar emission near 117 nm. Astron. & Astrophys. **439**, 701–711 (2005b), doi:10.1051/0004-6361:20042580.

Willis, M., M. J. Burchell, T. J. Ahrens, H. Krüger, and E. Grün: Decreased values of cosmic dust number density estimates in the solar system. Icarus **176**, 440–452 (2005), doi:10.1016/j.icarus.2005.02.018.

Xia, L. D., M. D. Popescu, Y. Chen, and J. G. Doyle: On the connection between the disk and limb events observed by SOHO. In: Proceedings of the Solar Wind 11/SOHO 16 Conference, 12-17 June 2005, Whistler, Canada, eds. B. Fleck and T. H. Zurbuchen, ESA SP-592, pp. 575–578, ESA Publ. Div., Noordwijk (2005a).

Xia, L. D., M. D. Popescu, J. G. Doyle, and J. Giannikakis: Time series study of EUV spicules observed by SUMER/SOHO. Astron. & Astrophys. **438**, 1115–1122 (2005b), doi:10.1051/0004-6361:20042579.

Xiao, C. J., Z. Y. Pu, Y. Wei, Z. X. Liu, C. M. Carr, T. L. Zhang, K.-H. Glassmeier, H. Rème, I. Dandouras, and P. Daly: Multiple flux rope events at the magnetopause observations by TC-1 on 18 March 2004. Ann. Geophys. **23**, 2897–2901 (2005).

Yang, J., S. Y. Fu, W. L. Liu, P. Ruan, Z. Y. Pu, P. Daly, and Y. F. Wang: Spatial distribution of energetic ion compositions in the plasma sheet observed by Cluster/RAPID. Chinese J. Geophys. **48**, 1226–1232 (2005), in Chinese.

Yao, L., S. L. Liu, S. P. Jin, Z. X. Liu, J. K. Shi, A. Balogh, H. Rème, and P. W. Daly: A study of orientation and motion of flux transfer events observed at the high-latitude dayside magnetopause. Chinese J. Geophys. **48**, 1217–1225 (2005), in Chinese.

Zakharov, V., A. Gandorfer, S. K. Solanki, and M. Löfdahl: A comparative study of the contrast of solar magnetic elements in CN and CH. Astron. & Astrophys. **437**, L43–L46 (2005), doi:10.1051/0004-6361:200500135.

Zhang, H., T. A. Fritz, Q.-G. Zong, and P. W. Daly: Stagnant exterior cusp region as viewed by energetic electrons and ions: A statistical study using Cluster Research with Adaptive Particle Imaging Detectors (RAPID) data. J. Geophys. Res. **110**, A05211 (2005), doi:10.1029/2004JA010562.

Zhang, J., J. Woch, and S. K. Solanki: Polar Coronal holes during solar cycles 22 and 23. Chin. J. Astron. Astrophys. **5**, 531–538 (2005).

Zong, Q. G., T. A. Fritz, A. Korth, P. W. Daly, M. Dunlop, A. Balogh, J. F. Fennell, J. D. Sullivan, R. W. H. Friedel, and H. Rème: Energetic Electrons as a Field Line Topology Tracer in the High Latitude Boundary/Cusp Region: Cluster RAPID Observations. Surveys in Geophysics **26**, 215–240 (2005a), doi:10.1007/s10712-005-1879-z.

Zong, Q.-G., T. A. Fritz, H. Spence, H. U. Frey, S. B. Mende, A. Korth, and P. W. Daly: Reverse convection and cusp proton aurora: Cluster, Polar and Image observation. Adv. Space Res. **36**, 1779–1784 (2005b), doi:10.1016/j.asr.2004.09.023.

Zong, Q.-G., T. A. Fritz, H. Spence, H. Zhang, Z. Y. Huang, Z. Y. Pu, K.-H. Glassmeier, A. Korth, P. W. Daly, A. Balogh, and H. Rème: Plasmoid in the high latitude boundary/cusp region observed by Cluster. Geophys. Res. Lett. **32**, L01101 (2005c), doi:10.1029/2004GL020960.

Zou, H., J.-S. Wang, and E. Nielsen: Effect of the seasonal variations in the lower atmosphere on the altitude of the ionospheric main peak at Mars. J. Geophys. Res. **110**, A09311 (2005), doi:10.1029/2004JA010963.

Max-Planck-Institut für
Sonnensystemforschung
Max-Planck-Straße 2
37191 Katlenburg-Lindau
Tel: 05556-979-0
Fax: 05556-979-240
E-Mail: presseinfo@mps.mpg.de